ENVIRONMENTAL IMPACTS OF PESTICIDES: ENVIRONMENTAL FATE, ECOTOXICOLOGY, RISK ASSESSMENT, AND REMEDIATION

EDITED BY: Liangang Mao, Yue Geng, Jiehong Guo, Mazhar Iqbal Zafar and Yanhua Wang

PUBLISHED IN: Frontiers in Environmental Science

frontiers Research Topics

ISSN 1664-8714
ISBN 978-2-83250-722-3
DOI 10.3389/978-2-83250-722-3

About Frontiers

Frontiers is more than just an open-access publisher of scholarly articles: it is a pioneering approach to the world of academia, radically improving the way scholarly research is managed. The grand vision of Frontiers is a world where all people have an equal opportunity to seek, share and generate knowledge. Frontiers provides immediate and permanent online open access to all its publications, but this alone is not enough to realize our grand goals.

Frontiers Journal Series

The Frontiers Journal Series is a multi-tier and interdisciplinary set of open-access, online journals, promising a paradigm shift from the current review, selection and dissemination processes in academic publishing. All Frontiers journals are driven by researchers for researchers; therefore, they constitute a service to the scholarly community. At the same time, the Frontiers Journal Series operates on a revolutionary invention, the tiered publishing system, initially addressing specific communities of scholars, and gradually climbing up to broader public understanding, thus serving the interests of the lay society, too.

Dedication to Quality

Each Frontiers article is a landmark of the highest quality, thanks to genuinely collaborative interactions between authors and review editors, who include some of the world's best academicians. Research must be certified by peers before entering a stream of knowledge that may eventually reach the public - and shape society; therefore, Frontiers only applies the most rigorous and unbiased reviews.
Frontiers revolutionizes research publishing by freely delivering the most outstanding research, evaluated with no bias from both the academic and social point of view. By applying the most advanced information technologies, Frontiers is catapulting scholarly publishing into a new generation.

What are Frontiers Research Topics?

Frontiers Research Topics are very popular trademarks of the Frontiers Journals Series: they are collections of at least ten articles, all centered on a particular subject. With their unique mix of varied contributions from Original Research to Review Articles, Frontiers Research Topics unify the most influential researchers, the latest key findings and historical advances in a hot research area! Find out more on how to host your own Frontiers Research Topic or contribute to one as an author by contacting the Frontiers Editorial Office: frontiersin.org/about/contact

ENVIRONMENTAL IMPACTS OF PESTICIDES: ENVIRONMENTAL FATE, ECOTOXICOLOGY, RISK ASSESSMENT, AND REMEDIATION

Topic Editors:
Liangang Mao, Institute of Plant Protection, Chinese Academy of Agricultural Sciences, China
Yue Geng, Agro-Environmental Protection Institute, Ministry of Agriculture and Rural Affairs, China
Jiehong Guo, University of Minnesota Twin Cities, United States
Mazhar Iqbal Zafar, Quaid-i-Azam University, Pakistan
Yanhua Wang, Zhejiang Academy of Agricultural Sciences, China

Citation: Mao, L., Geng, Y., Guo, J., Zafar, M. I., Wang, Y., eds. (2022). Environmental Impacts of Pesticides: Environmental Fate, Ecotoxicology, Risk Assessment, and Remediation. Lausanne: Frontiers Media SA.
doi: 10.3389/978-2-83250-722-3

Table of Contents

frontiers | Frontiers in Environmental Science

TYPE Editorial
PUBLISHED 24 October 2022
DOI 10.3389/fenvs.2022.1065958

OPEN ACCESS

EDITED AND REVIEWED BY
Oladele Ogunseitan,
University of California, Irvine,
United States

*CORRESPONDENCE
Liangang Mao,
maoliangang@126.com

SPECIALTY SECTION
This article was submitted to Toxicology, Pollution and the Environment, a section of the journal Frontiers in Environmental Science

RECEIVED 10 October 2022
ACCEPTED 12 October 2022
PUBLISHED 24 October 2022

CITATION
Mao L, Geng Y, Guo J, Zafar MI and Wang Y (2022), Editorial: Environmental impacts of pesticides: Environmental fate, ecotoxicology, risk assessment, and remediation.
Front. Environ. Sci. 10:1065958.
doi: 10.3389/fenvs.2022.1065958

Editorial: Environmental impacts of pesticides: Environmental fate, ecotoxicology, risk assessment, and remediation

Liangang Mao[1]*, Yue Geng[2], Jiehong Guo[3], Mazhar Iqbal Zafar[4] and Yanhua Wang[5]

[1]State Key Laboratory for Biology of Plant Disease and Insect Pests, Institute of Plant Protection, Chinese Academy of Agricultural Sciences, Beijing, China, [2]Agro-Environmental Protection Institute, Ministry of Agriculture and Rural Affairs, Tianjin, China, [3]Masonic Cancer Center, University of Minnesota Minneapolis, MN, United States, [4]Department of Environmental Sciences, Faculty of Biological Sciences, Quaid-i-Azam University, Islamabad, Pakistan, [5]State Key Laboratory for Managing Biotic and Chemical Threats to the Quality and Safety of Agro-Products, Institute of Agro-Product Safety and Nutrition, Zhejiang Academy of Agricultural Sciences, Hangzhou, China

KEYWORDS

environmental fate, ecotoxicology, risk assessment, remediation, pesticide, combined pollution, toxicity

Editorial on the Research Topic
Environmental impacts of pesticides: Environmental fate, ecotoxicology, risk assessment, and remediation

Introduction

In the past few decades, conventional agriculture has relied heavily on the use of pesticides (including insecticides, fungicides, and herbicides etc.) for controlling pest species and enhancing crop yields (Carvalho, 2006; Dhananjayan et al., 2020; Washuck et al., 2022). However, the large-scale application of pesticides can pose a serious threat to various non-target organisms, for example, bees, birds, silkworms, earthworms, natural parasitic and predatory organisms, fishes, algae, daphnia, amphibians, etc (Stanley et al., 2016; Kenko et al., 2022). Studies on the environmental fate, toxic effects, and environmental risk of pesticides, and the combined effects of pesticides and other environmental and agricultural contaminants (e.g., heavy metals, pharmaceutical and personal care products (PPCPs), and microplastics) have attracted increasing attention in recent years (Zhou et al., 2004; Chen et al., 2015; Picó et al., 2020). Potential remediation methods and technologies for pesticides and pesticide-contaminant combinations have also been developed rapidly (Sun et al., 2018; Zhang et al., 2020).

In this Research Topic, we set up a Research Topic of *Environmental impacts of pesticides: Environmental fate, ecotoxicology, risk assessment and remediation*, which not only covers pesticides but also the combinations of pesticides and other kind of contaminants (e.g., heavy

metals, PPCPs, and microplastics etc.). The following themes are included in this Research Topic: (a) Environmental fate including how pesticides enter the air, soil, and aquatic environment after being applied to agricultural crops; (b) Ecotoxicity: pesticide effects on non-target organisms, individually or in combination with other contaminants; (c) Mechanisms of interaction of pesticides and pesticide mixtures on non-target organisms; (d) Environmental risk assessment of pesticides and pesticide mixtures on non-target organisms and aquatic ecosystem; (e) Technologies and techniques that can be utilized to effectively remediate pesticide contamination and reduce the environmental risks.

Even though a lot of progresses have been made in investigating the environmental impacts of pesticides, there are still knowledge gaps exist in above themes and the goal of our Research Topic is to fill those gaps. We finally accepted and published 16 papers authored by 99 researchers from nine countries, including China, United States, Pakistan, Norway, Egypt, Saudi Arabia, the Netherlands, Kazakhstan, and Canada.

Highlights from Publications Featured in this Research Topic are as follows.

Environmental fate of pesticides and its residues in crops

Yu et al. investigated the dissipation behavior of fungicide difenoconazole in paddy sediment system under different field conditions following the application of biogas residues. Commelin et al. reported the overlooked environmental risk of overland transport of 31 pesticides in the particulate phase, which generally lasted over long period time when applied on agriculture on sloping lands. Yu et al. monitored the exposure of propiconazole in water and soil from rice–crab co-cultured fields.

In the study of Wang et al., the disappearance behavior, residue distribution and dietary risk assessment of kresoxim-Methyl in banana (*Musa nana* Lour.) was investigated based on a modified QuEChERS procedure using HPLC-MS/MS. In the research of Fan and Li, residues, dissipation and dietary risk assessment of two fungicides oxadixyl and cymoxanil in cucumber was analyzed based on a QuEChERS method using UPLC-MS/MS under greenhouse and open field conditions.

Pesticide ecotoxicology/toxicology on non-target organisms and resistance monitoring

In the study by Zhou et al., the sensory behaviors of thermotaxis, avoidance of copper ion, chemotaxis to NaCl, and chemotaxis to diacetyl were investigated in nematodes (*Caenorhabditis elegans*) exposed to six insecticides (dinotefuran, thiamethoxam, thiacloprid, nitenpyram, acetamiprid, and sulfoxaflor) in the range of micrograms per liter (μg/L). Li et al. investigated the environmental impact of trifluralin on soil microbial communities and functions in a 3-month greenhouse experiment. Yu et al. evaluated the acute toxicity, sub-chronic toxicity, and bioaccumulation of propiconazole to *Eriocheir sinensis* in the rice–crab co-culture fields. Pochron et al. found that exposure to glyphosate, the herbicidal ingredient in Roundup products Roundup Ready-to-Use III, offered no nutritional benefit, but increased movement speed and decreased body mass in earthworms (*Eisenia fetida*). According to the research of Massoud et al., low doses of malathion exposure increased several enzyme activities and caused multiple histopathological changes on Wister male rats (*Rattus norvegicus*) after 24-h and/or 21-days treatment, implying the chronic toxicity of environmental residue malathion to animals and human.

In the research of Riaz et al., the frequency of pyrethroid insecticide resistance gene kdr (knockdown resistance) in housefly populations of District Jhang, Pakistan was investigated. In the study of Wang et al., levels of resistance to cyantraniliprole in whiteflies (*Bemisia tabaci*) with 18 field-sampled populations across China were measured.

Pesticide contamination remediation techniques and technologies

Massoud et al. synthesized a zinc oxide nanocatalyst and obtained the most effective process ($ZnO(s)/H_2O_2/UV$) for detoxification of some highly toxic insecticides (dimethoate and methomyl) in an aquatic system. Wang et al. prepared a montmorillonite–biochar composite (MMT/BC) and demonstrated that MMT/BC has higher removal capacity of atrazine in aqueous solution compared to raw biochar (BC). In the study of Aziz et al., the constructed wetland with the bacterial–plant consortium showed its potential to biodegrade insecticide chlorpyrifos and its major metabolites. Tussipkan and Manabayeva reviewed the genetic diversity of alfalfa (*Medicago Sativa* L.), and transgenic alfalfa plants for enhanced phytoremediation of persistent organic pollutants (POPs), petroleum and heavy metals. Khalid et al. examined the effect of sewage sludge-amended soil on growth, enzyme activities, and genotoxicity in earthworms (*Pheretima posthuma*) and demonstrated that wheat straw and biochar ameliorated the toxic effects of sewage sludge in earthworms.

Future research

Overall, the Research Topic of published articles and reviews in this Research Topic already advanced our

understanding of environmental fate, ecotoxicology, risk assessment and remediation of pesticides. Nevertheless, great challenges still exist in computational toxicology for predicting environment risk of pesticides and in understanding the "cocktail effect" of pesticides and their combination with other environmental and agricultural contaminants (e.g., heavy metals, PPCPs, and microplastics). More research on those fields is warranted.

Author contributions

This editorial draft was written by LM. All authors revised and contributed to the article and approved the submitted version. LM, YG, JG, MZ, and YW as guest topic editors have worked extensively on the call for submissions, and edited the manuscripts submitted to this Research Topic.

Funding

This Research Topic was supported by the National Key R&D Program of China (2021YFD1700300).

Acknowledgments

We thank all authors and reviewers for their contributions, as well as the Journal Committee for providing the opportunity to establish the Research Topic.

Conflict of interest

The authors declare that the research was conducted in the absence of any commercial or financial relationships that could be construed as a potential conflict of interest.

Publisher's note

References

Carvalho, F. P. (2006). Agriculture, pesticides, food security and food safety. *Environ. Sci. policy* 9 (7-8), 685–692. doi:10.1016/j.envsci.2006.08.002

Chen, C., Wang, Y., Qian, Y., Zhao, X., and Wang, Q. (2015). The synergistic toxicity of the multiple chemical mixtures: Implications for risk assessment in the terrestrial environment. *Environ. Int.* 77, 95–105. doi:10.1016/j.envint.2015.01.014

Dhananjayan, V., Jayakumar, S., and Ravichandran, B. (2020). "Conventional methods of pesticide application in agricultural field and fate of the pesticides in the environment and human health," in *Controlled release of pesticides for sustainable agriculture*. Editors K. R., R.S. Thomas and T. Volova, (Cham: Springer). doi:10.1007/978-3-030-23396-9_1

Kenko, D. B. N., Ngameni, N. T., and Kamta, P. N. (2022). Environmental assessment of the influence of pesticides on non-target arthropods using PRIMET, a pesticide hazard model, in the Tiko municipality, Southwest Cameroon. *Chemosphere* 308, 136578. doi:10.1016/j.chemosphere.2022.136578

Picó, Y., Alvarez-Ruiz, R., Alfarhan, A. H., El-Sheikh, M. A., Alshahrani, H. O., and Barceló, D. (2020). Pharmaceuticals, pesticides, personal care products and microplastics contamination assessment of Al-Hassa irrigation network (Saudi Arabia) and its shallow lakes. *Sci. Total Environ.* 701, 135021. doi:10.1016/j.scitotenv.2019.135021

Stanley, J., Preetha, G., and Stanley, J. (2016). *Pesticide toxicity to non-target organisms*, 502. Berlin, Germany: Springer.

Sun, S., Sidhu, V., Rong, Y., and Zheng, Y. (2018). Pesticide pollution in agricultural soils and sustainable remediation methods: A review. *Curr. Pollut. Rep.* 4 (3), 240–250. doi:10.1007/s40726-018-0092-x

Washuck, N., Hanson, M., and Prosser, R. (2022). Yield to the data: Some perspective on crop productivity and pesticides. *Pest Manag. Sci.* 78 (5), 1765–1771. doi:10.1002/ps.6782

Zhang, H., Yuan, X., Xiong, T., Wang, H., and Jiang, L. (2020). Bioremediation of co-contaminated soil with heavy metals and pesticides: Influence factors, mechanisms and evaluation methods. *Chem. Eng. J.* 398, 125657. doi:10.1016/j.cej.2020.125657

Zhou, Q., Cheng, Y., Zhang, Q., and Liang, J. (2004). Quantitative analyses of relationships between ecotoxicological effects and combined pollution. *Sci. China Ser. C* 47, 332–339. doi:10.1360/03yc0042

frontiers in Environmental Science

ORIGINAL RESEARCH
published: 03 February 2022
doi: 10.3389/fenvs.2021.806456

Frequency of Pyrethroid Insecticide Resistance *kdr* Gene and Its Associated Enzyme Modulation in Housefly, *Musca domestica* L. Populations From Jhang, Pakistan

Bushra Riaz[1], Muhammad Kashif Zahoor[1], Kausar Malik[2], Aftab Ahmad[3], Humara Naz Majeed[4], Farhat Jabeen[5], Muhammad Zulhussnain[1] and Kanwal Ranian[1]*

[1]Entomology Lab, Department of Zoology, Government College University, Faisalabad, Pakistan, [2]Centre of Excellence in Molecular Biology, University of the Punjab, Lahore, Pakistan, [3]Centre of Department of Biochemistry/US-Pakistan Center for Advance Studies in Agriculture and Food Security (USPCAS-AFS), University of Agriculture Faisalabad, Faisalabad, Pakistan, [4]Department of Biochemistry, Government College Women University, Faisalabad, Pakistan, [5]Department of Zoology, Government College University, Faisalabad, Pakistan

OPEN ACCESS

Edited by:
Mazhar Iqbal Zafar, Quaid-i-Azam University, Pakistan

Reviewed by:
Renata Da Rosa, State University of Londrina, Brazil
Sofia Khalid, Fatima Jinnah Women University, Pakistan

***Correspondence:**
Muhammad Kashif Zahoor
kashif.zahoor@gcuf.edu.pk

Specialty section:
This article was submitted to Toxicology, Pollution and the Environment, a section of the journal Frontiers in Environmental Science

Received: *31 October 2021*
Accepted: *15 December 2021*
Published: *03 February 2022*

Citation:
Riaz B, Kashif Zahoor M, Malik K, Ahmad A, Majeed HN, Jabeen F, Zulhussnain M and Ranian K (2022) Frequency of Pyrethroid Insecticide Resistance kdr *Gene and Its Associated Enzyme Modulation in Housefly,* Musca domestica *L. Populations From Jhang, Pakistan. Front. Environ. Sci. 9:806456. doi: 10.3389/fenvs.2021.806456*

Housefly, *Musca domestica*, is considered responsible for transmitting a wide variety of human and veterinary diseases. Mostly, insecticides are being used for their control and more commonly, pyrethroid insecticides worldwide. However, resistance has been reported against various pyrethroid insecticides. Houseflies become resistant by two major mechanisms, i.e., target site insensitivity through knockdown resistance gene mutation (*kdr*) and enzyme detoxification. Thus, the current study was designed to monitor the frequency of pyrethroid resistance gene *kdr* in housefly populations of District Jhang. The flies were collected from seven sampling sites and then reared in the lab for molecular and biochemical assays. The amplification of template DNA was performed for knockdown resistance gene through the outer primers *kdr1* and *kdr4*, and the inner primers *kdr1* and *kdr2* using PASA (PCR Amplification of Specific Alleles) method which specifically amplify the domain-II of *kdr* gene. Three populations were found homozygous susceptible (+/+; 42.85%), whereas two populations were found genetically homozygous resistant (–/–; 28.57%) which are insensitive to pyrethroid insecticides. Similarly, two populations were found heterozygous (+/–; 28.57%) for *kdr* suggesting thereby that at least 1/4th homozygous-resistant (–/–) housefly populations with insensitivity to pyrethroids would be produced in the future keeping in view the Mendelian ratio. Biochemical assay showed that homozygous-resistant populations had increased activity of Acetylcholinesterase (AChE), α-Carboxylesterases (α-Carboxyl), β-Carboxylesterase (β-Carboxyl), Alkaline Phosphatase (AkP), and Acidic Phosphatase (AcP) enzymes. In addition, heterozygous populations also showed increased activities of these enzymes. The current results would not only help avoid the indiscriminate load of insecticides onto the environment but also serve as a hallmark for the management of housefly populations in target areas in the future.

Keywords: pyrethroids, *kdr*, PASA, resistant, susceptible and enzyme inhibition

INTRODUCTION

Housefly is considered a major insect pest of animals as well as humans mainly due to its high rate of fecundity (Brown et al., 1995). It reduces the level of livestock activities through annoyance, upsetting animals during their times of feeding and resting, and also induces potential transmission of various pathogens (Cheeke, 2005; Forster et al., 2009). Manure and organic waste produced by overpopulated human beings in urban and rural areas as well provides feeding and breeding sites to these houseflies, thus causing dramatic increase in housefly population at these sites (Khamesipour et al., 2018).

Because of high fecundity, it poses serious concern of control. Although flies do not bite, they act as vectors of various pathogens i.e., virus, bacteria, fungi, protozoa, and nematodes. More than hundred pathogens are reported wherein houseflies serve as vectors (Khamesipour et al., 2018). Flies pick up pathogens from detritus, waste, and the other resources of sludge and then transfer vomits through their body parts, faeces, and contaminated mouth parts to humans, poultry, and various animals. The pathogens usually transferred by houseflies are *Pseudomonas*, *Shigela*, *Salmonella*, *Staphylococcus*, *Campylobacter*, *Escherichia coli*, *Enterococcu*, *Klebsiella*, *Campylobacter*, *Acinetobacter*, *Trichuris*, *Chlamydia*, and *Strongyloides* larvae, *Entrobious vermicularis* causing typhoid fever, food poisoning, tuberculosis, dysentery, opthalmic, anthrax, and infestation by parasitic worms (Khamesipour et al., 2018; Iqbal et al., 2014; Lord and Boston, 1904).

Increase in housefly population results in increase in nuisance in poultry farms, ultimately affecting the egg production of chickens. In addition, quality and appearance of eggs are compromised due to fly faeces (Howard and Wall, 1996). Different control measures are being used worldwide viz. avoidance to build-up of fly population through cleanliness, screening, waste management, etc. But chemical control remains the last and ultimate option. It has been established that chemical control of disease-causing vectors has become difficult because of their resistance toward chemicals. Since the instant reaction by pest control practitioners is to increase in dosage, which results in increased resistance level and contamination of the environment (Khamesipour et al., 2018; Abbas et al., 2014; Shono et al., 2004; Feyereisen, 1995; Kjaersgaard, et al., 2015). Physiologically, through resistance insects show certain characteristics such as decrease in uptake of insecticides, increase in detoxification, and alternation in target sites (Casida, 2016). Subsequently, metabolic resistance against insecticides also exists which increases mixed-function oxidase (MFO), glutathione S-transferase (GST) activity, alters esterases, and DDT dehydrochlorinase activities (Panini et al., 2016). Change in esterase level has been known as the mechanism of pyrethroid resistance in household insects such as mosquitoes and houseflies *Musca domestica* L. (Ahn et al., 1992).

Non-metabolic resistance factor was first documented conferring as rapid paralytic knock down and severe activity of Pyrethroids and DDT in housefly, *Musca domestica* in 1951 (Busvine, 1951). The mechanism is currently named as *kdr* (knockdown resistance) (Martins and Valle, 2012). Voltage Gated Sodium Channel (VGSC) is reported as the main target site of pyrethroid insecticides and is vital for electrical signaling within the nervous system. But insensitivity at this site is conferred by means of mutation in VGSC which serves as a primary mechanism of resistance against pyrethroids. The kdr mutation in sodium channel gene is caused due to a substitution of amino acids residue of Leucine to phenylalanine (L1014F) and has been associated with resistance in houseflies. Subsequent studies showed that resistant flies had alleles such as CYP6D1 and Vssc1 that contribute to resistance against permethrin and pyrethroids (Liu and Pridgeon, 2002; Rinkevich et al., 2006; Scott et al., 2013). It has been reported in United Arab Emirates that housefly populations causing detoxification as well as L1014F replacement of sodium channels suggest that there should be implication of management program for resistance against pyrethroids (Al-Deeb, 2014).

In Pakistan, chemical pesticides were consistently used for the control of housefly and vast research work has been done for its chemical control. However, to our knowledge, there is no molecular work or any reports available on the frequency of pyrethroid insecticide resistance for *kdr* alleles. Therefore, the current study was designed to investigate the frequency of pyrethroid insecticide resistance *kdr* allele in housefly population from different locations of District Jhang, Punjab, Pakistan.

MATERIALS AND METHODS

Collection of Houseflies

The collection of adult houseflies was undertaken from seven different sampling sites from District Jhang viz. Civil lines, 18-hazari, Head trimu, Nawaz chowk, Malhumorr, Sattelite town, and Haveli bahadur shah during 2017–18 (**Figure 2**).

Bioassays for Susceptibility/Resistance Against Pyrethroid Insecticides in Housefly Populations

The collected flies were reared in Entomology Lab of Department of Zoology, Government College University Faisalabad, on artificial diet under optimum conditions in 40 cm × 25 cm × 30 cm cages covered with mesh screen having cloth sleeves at their opening described by Keiding and Arevad (1964). Houseflies were maintained in cages with sugar-soaked cotton wool in small-sized beakers. Full fat fresh milk was also provided, soaked in cotton wool and wheat bran with yeast-moistened water and dry milk after emergence of flies to increase the production of eggs. Flies take about 10 days to complete their life cycle; food was changed after an interval of 2–3 days depending on the number of larvae. Bioassays were conducted at temperature 25 ± 2°C, 60 ± 5% relative humidity, and 12:12 (L/D) photoperiod. The collected fly samples from each respective site were pooled and used for mortality bioassays and molecular as well as biochemical assays. The lab strain considered as reference strain was used as control.

The insecticides used were of analytical standards and purified chromatographically above 90% purity level. Stock solution of 1 mM was prepared and kept in acetone. Insecticides used in bioassays included Lambda-cyhalothrin, Deltamethrin, Cypermethrin, Chlorpyrifos, and Tetramethrin. All of these chemicals were applied with respect to technical material diluted to the required concentration in Acetone.

A completely randomized experimental design was used. Five concentrations (2.5, 5, 10, 20, and 40 ppm) of each insecticide were prepared and replicated for three times. Approximately 60 flies were used in each concentration causing >0% and <100% mortality. In case of each treatment fresh dilution was used from the already-prepared stock solution. Mortality levels were assessed at 24, 48, and 72 h of exposure to insecticides. Mortality in control groups was also noted to obtain the corrected mortality according to Abbot's formula (Abbot, 1925). Ataxic individuals considered died (Khan et al., 2014).

$$P = \frac{T - C}{100 - C} \times 100$$

Here P is the % corrected mortality, C is the % mortality in the nontreated group, and T is the % mortality in the treated group.

Evaluation of Resistance of Pyrethroid Insecticides in *Musca domestica* Populations

For the evaluation of resistance, three generations of *M. domestica* pooled sample from District Jhang were reared. The adult mortality had been recorded after 72 h; the flies that remained alive were allowed to complete their three generations. Twenty adult flies were used to evaluate the resistance after 48 h feeding on the corresponding pyrethroid insecticides. Mortality data were recorded after 48 h of insecticide treatment on the emerged flies of the F1 and F2 (parental) generations (Sultana et al., 2016).

The number of emerging flies was recorded after 2 weeks and, meanwhile, the mortality was calculated. The resistance level was measured in each succeeding generation to evaluate the increase in the level of resistance following the protocol of Singh and Prakash (2013). The resistance ratios (Resistant/Susceptible) were estimated by dividing the LD50 for resistant strain with the LD50 for the Lab/reference strain.

PCR Amplification of Specific Alleles for *Kdr* Alleles

The TNE buffer method was used for the extraction of DNA (Ashraf et al., 2016; Zahoor et al., 2017). PASA was performed as described by Huang et al. (2004) using two outer allele-specific primers *kdr1*, 5′-AAGGATCGCTTCAAGG-3′and *kdr4*, 5′-TTCACCCAGTTCTTAAAACGAG-3′of 10 pmol and two inner primers *kdr2*, 5′-TCGTGATCGGCAATT-3′ *kdr3*, 5′-GTCAACTTACCACAAG-3′ of 40 pmol. The PCR reaction included 2 μL of genomic DNA, 10 pmol of each outer primer and 40 pmol of each inner primer, 12.5 μL *Taq* PCR Master Mixture, and 8.5 μL filtered nuclease-free water. Initial denaturation for 2 min followed by 40 cycles was performed at 95°C, 45 s at 94°C, 30 and 90 s and a final step extension for 10 min at 72°C. Each PCR reaction also included a negative control to avoid any contamination in reaction. The PCR amplified fragments were analyzed through electrophoresis on 1.5% agarose gel stained with Ethidium bromide and visualized under UV light documentation system. *kdr1* and *kdr4* primers amplified control fragment of 480 bp. *kdr1* and *kdr3* primers amplified susceptible allele fragment of 200 bp, whereas *kdr2* and *kdr4* primers amplified the fragment of 280 bp for *kdr* type (resistant) allele. The *kdr* mutation was identified by using direct DNA sequencing of voltage-gated sodium channels gene (kdr gene) (Eurofins scientific INC).

Enzyme Assay

Preparation of Whole-Body Homogenate

For enzyme assay adult houseflies were washed properly with distilled water and then dried with bloating paper. Flies were homogenized with ice-cold 20 mM sodium phosphate buffer (pH 7.0) with the help of Teflon hand homogenizer and then homogenate was centrifuged at 8,000 rpm at 4°C for 20 min. The solutions prepared for homogenization were kept at 4°C before use. The homogenates were then stored on ice for further use (Younes et al., 2011).

Estimation of Acetyl Cholinesterase Activity

For 50 μL of homogenate, addition of 50 μL of 2.6 mM acetylcholine chloride and 1 ml of 20 Mm sodium phosphate buffer (pH7.0) was made. Incubation was then performed at 25°C for 5 min. To stop the reaction, 400 μL of 0.3% fast blue B salt was added. The OD value was recorded at 405 nm (Younes et al., 2011).

Estimation of Carboxyl Esterase Activity

For 50 μL homogenate, 1 ml of 20 Mm PBS (pH 7.0) and 50 μL of each α-naphthyl acetate and β-naphthyl acetate were added individually. The prepared solutions were incubated for 20 min at 30°C. After the incubation, 400 μL of 0.3% freshly prepared fast blue B salt in 3.3% SDS was added to stop the enzymatic reaction, and allowed to develop color for 15 min at 2°C. The OD values were recorded at 430 and 590 nm for α-carboxyl esterase and β-carboxyl esterase, respectively (Younes et al., 2011).

Estimation of Acid and Alkaline Phosphatases Activity

For 50 μL of homogenate, 50 μL of 50 mM PBS (pH 7.0) and 100 μL of 20 mM p-nitro phenyl phosphate were added to estimate the activity of acid phosphatase activity. For alkaline phosphatases activity 50 μL homogenate was mixed with 50 μL of 50 mM Tris HCl buffer (pH9.0) and 100 μL of 20 mM p-nitrophenyl phosphate. Both the solutions were incubated at 37°C for 15 min and the reaction was stopped by adding 0.5M NaOH solution. The OD values were then recorded at 440 nm (Younes et al., 2011).

$$\text{Percent Enzyme inhibition} = \frac{\text{OD of control flies} - \text{OD of tretaed flies}}{\text{OD of control flies}} \times 100$$

TABLE 1 | Mean mortality of housefly (*Musca domestica* L.) larvae after 72 h of exposure to 30% concentration of insecticides.

Code	Conc. (ppm)	F value	df	*p* value	Mean mortality with different time intervals		
					24 h	48 h	72 h
1	2.5	0.095	2	0.910	23.889 ± 5.77350[a]	21.6667 ± 1.6667[a]	22.8205 ± 1.6667[a]
	5	1.546	2	0.287	28.889 ± 5.0000[a]	28.333 ± 1.6667[a]	21.1538 ± 2.8867[a]
	10	0.082	2	0.923	33.889 ± 7.63763[a]	31.667 ± 3.333[a]	31.1538 ± 2.8867[a]
	20	1.762	2	0.507	38.889 ± 2.88675[a]	43.333 ± 1.6667[a]	41.1538 ± 2.8876[a]
	40	4.321	2	0.069	43.889 ± 2.88675[a]	51.667 ± 1.6667[a]	46.1538 ± 0.0002[a]
2	2.5	0.322	2	0.737	2.6471 ± 2.88675[a]	8.333 ± 10.1379[a]	16.667 ± 15.2752
	5	0.410	2	0.681	7.3529 ± 2.88675[a]	18.333 ± 10.379[a]	6.6667 ± 14.2401[a]
	10	0.873	2	0.465	14.0196 ± 3.333[a]	26.667 ± 11.5470	8.333 ± 12.58306[a]
	20	2.671	2	0.148	29.0196 ± 1.6666[a]	43.333 ± 7.2648[a]	28.33 ± 5.000[a]
	40	1.061	2	0.403	49.0196 ± 14.813	51.6667 ± 7.6376	33.333 ± 0.0002[a]
3	2.5	180.4	2	0.001	38.8095 ± 4.4095[a]	37.8205 ± 4.409[a]	56.667 ± 3.333[b]
	5	1.061	2	0.403	49.0196 ± 14.813[a]	51.6667 ± 7.637[a]	33.333 ± 0.02[a]
	10	125.7	2	0.000	55.4762 ± 1.6666[a]	44.4872 ± 1.666[b]	51.6667 ± 1.6667[c]
	20	913.7	2	0.000	57.1429 ± 0.0002[a]	42.8205 ± 3.333[b]	50.000 ± 0.000[c]
	40	372.1	2	0.000	57.1429 ± 0.0000[a]	44.4872 ± 1.666[b]	50.000 ± 0.002[c]
4	2.5	200.3	2	0.000	1.66667 ± 1.6667[a]	16.6667 ± 1.666[b]	45.1515 ± 1.6668[c]
	5	209.4	2	0.001	10.000 ± 0.0000[a]	33.33 ± 2.88675[b]	36.8182 ± 0.0002[c]
	10	42.89	2	0.002	16.667 ± 1.6666[a]	6.6667 ± 2.8867[a]	23.4848 ± 4.4095[b]
	20	48.06	2	0.000	15.000 ± 0.0000[a]	13.333 ± 1.6667[a]	18.4848 ± 4.4095[b]
	40	27.02	2	0.001	30.000 ± 2.88675[a]	28.333 ± 1.6666[a]	9.8485 ± 1.6667[b]
5	2.5	5.018	2	0.052	4.7368 ± 0.000[a]	5.4684 ± 1.4787[ab]	13.5714 ± 6.9375[c]
	5	47.78	2	0.000	8.0702 ± 1.6667[a]	0.6863 ± 1.6667[b]	14.5238 ± 1.6667[c]
	10	55.47	2	0.002	6.4035 ± 1.6667[a]	6.4035 ± 1.6667[a]	16.1905 ± 1.6666[b]
	20	16.397	2	0.004	9.7368 ± 2.88675[a]	9.7368 ± 2.88675[a]	7.8571 ± 2.88675[b]
	40	8.699	2	0.017	14.7368 ± 2.8867	9.0196 ± 2.8867[ab]	2.8571 ± 2.88675[b]

**Means sharing the same letter within each treatment is not statistically different.*

1: Lambda-cyalothrin; 2: Deltamethrin; 3: Chlorpyrifos; 4: Cypermethrin; 5: Tetramethrin.

Statistical Analysis

The recorded data were corrected by using Abbott's formula (Abbot, 1925) and subjected to the evaluation of variance (ANOVA) using Statistica 13.0 for Windows. Post hoc testing was also carried out using the Tukey HSD test. A significant level of 5% was taken into consideration for all statistical tests. A value of $p < 0.05$ was considered statistically significant. The fingerprints were observed in a UV high-clarity fluorescent machine and their images were saved using the SynGene Gel credentials method.

RESULTS

Bioassays for Susceptibility/Resistance in Housefly Populations

To evaluate the resistance against insecticides lab strain of *Musca domestica* was treated with five insecticides Lambda cyhalothrin, deltamethrin, chlorpyrifos, cypermethrin, and tetramethrin, having used different concentrations viz. 2.5, 5, 10, 20, and 40% at exposure times of 24, 48, and 72 h, respectively. The maximum percentage mortality percentage of Lambda cyhalothrin was found at a concentration of 40 ppm (51.6%) after 48 h and 20 ppm (46.15%) after 72 h followed by 20 ppm concentration. It was found that the mortality was increased with increase in concentrations but not decreased with exposure time; moreover, low mortality was found at lower concentrations. Similar results were found with Deltamethrin; maximum mortality percentage was found at 40 ppm (51.6%) after 48 h and 49.01% after 24 h, respectively. Highest mortality rate was observed in case of Chlorpyrifos. Flies showed lowest resistance against Chlorpyrifos. At 20 ppm concentration mortality rate was found 57.1, 42.8, and 50% after 24, 48, and 72 h, respectively. Highest mortality percent (57.1%) was observed at 40 ppm concentration after 24 h. With Cypermethrin, mortality rate was found decreased with increase in exposure time (30, 28, and 9.8%) at 40 ppm after 24, 48, and 72 h, respectively. Tetramethrin showed least mortality among all tested insecticides. Overall, highest mortality rate (57.1429%) was observed at 40% concentration of Chlorpyrifos, and least mortality (14.7368%) was observed in case of Tetramethrin at same concentrations (**Table 1**). The observed mortality rate was Chlorpyrifos > Lambda Cyhalothrin > Deltamethrin > Cypermethrin > Tetramethrin.

Evaluation of Resistance of Pyrethroid Insecticides in *Musca domestica* Populations

The toxicity of four pyrethroid insecticides and resistance ratios of three generations of houseflies was recorded based on their LD_{50}values. It is to mention here that Chlorpyrifos was found with high mortality, hereby conferring lowest resistance. Hence, it was not further studied for the evaluation of resistance. The flies with higher LD_{50} values were considered resistant in successive generations. Low level of resistance was found against Lambda Cyhalothrin when compared with Cypermethrin, Deltamethrin, and Permethrin (**Table 2**). Resistance ratios (RR) ranged between

TABLE 2 | Evaluation of resistance of pyrethroid insecticides in *Musca domestica* from district Jhang.

Insecticide	Fn	LD50 µg/µL	95% CL	Slope ± S.E	$\chi 2$ (df)	RR
Cypermethrin (1.5% EC)	F1	28.469	24.3618 ± 34.407	0.0336 ± 0.0042	35.974(3)	1.1058
	F2	31.702	27.068 ± 38.6413	0.0324 ± 0.0043	39.201(3)	1.1784
	F3	36.237	30.0452 ± 43.3310	0.0321 ± 0.0043	40.446(3)	1.224
Deltamethrin (1.5% EC)	F1	41.812	32.8007 ± 61.2903	0.02053 ± 0.0042	3.3701(3)	1.033
	F2	43.283	34.219 ± 62.4279	0.02148 ± 0.0044	3.4138(3)	1.183
	F3	49.618	38.7502 ± 73.8780	0.2108 ± 0.0042	7.1525(3)	1.183
Tetramethrin (0.5% WP)	F1	57.258	43.697 ± 90.8373	0.2005 ± 0.0043	5.7721(3)	1.298
	F2	74.264	53.9657 ± 139.532	0.0180 ± 0.0047	2.3846(3)	1.257
	F3	84.137	60.001 ± 164.703	0.1960 ± 0.00547	2.3847(3)	1.462
LambdaCyalothrin (50% EC)	F1	48.736	40.8495 ± 62.4573	0.3172 ± 0.00481	1.1787(3)	0.976
	F2	46.539	41.1142 ± 57.7611	0.3992 ± 0.0051	1.4689(3)	0.975
	F3	45.152	42.318 ± 53.330	0.0574 ± 0.0072	8.9446(3)	0.947

Mean sharing the same letter within each treatment is not statistically different.

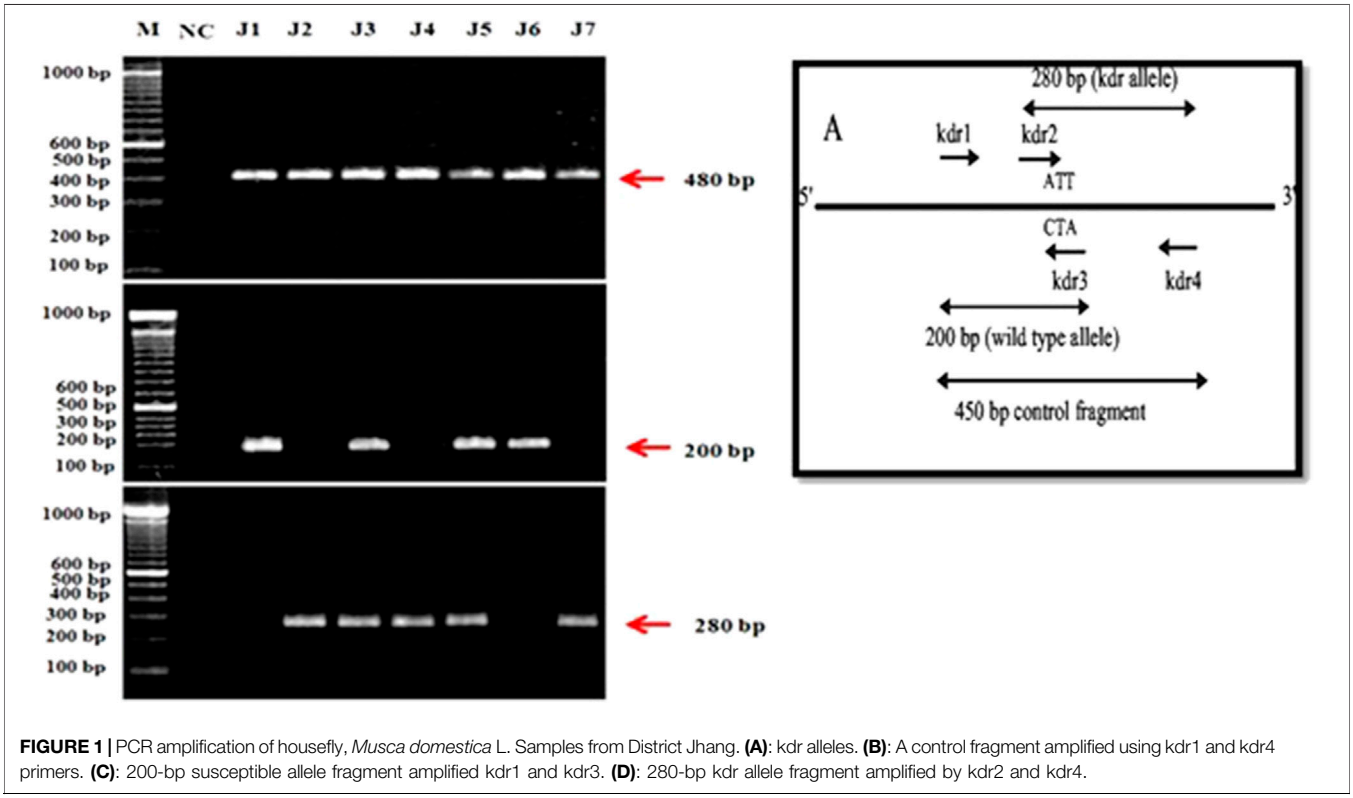

FIGURE 1 | PCR amplification of housefly, *Musca domestica* L. Samples from District Jhang. **(A)**: kdr alleles. **(B)**: A control fragment amplified using kdr1 and kdr4 primers. **(C)**: 200-bp susceptible allele fragment amplified kdr1 and kdr3. **(D)**: 280-bp kdr allele fragment amplified by kdr2 and kdr4.

0.947 and 0.976 in case of Lambda Cyhalothrin. With Deltamethrin and Cypermethrin, moderate level of resistance (RR) was found with a range between 1.033–1.183 and 1.1058–1.224, respectively. Maximum resistance was found in Tetramethrin with RR ranging between 1.257 and 1.462. Nevertheless, a reduction in % age mortality was also observed in successive generations for Permethrin, Deltamethrin, and Cypermethrin (**Table 2**).

Molecular Assay

The four *kdr* primers designed by macrogen company were used for PASA (PCR Amplification of Specific Alleles) following the protocol of Huang et al. (2004). *Kdr1* and *kdr4* amplified fragment of 480 bp, *kdr1* and *kdr3* amplified 200 bp susceptible allelic fragments while *kdr2* and *kdr4* amplified 280 bp *kdr* type allelic fragments in the domain-II of *kdr* gene. *Kdr5*, *kdr7*, and *kdr9* were also used as control during optimization to evaluate whether gene was actually amplified or not. Three populations were found homozygous susceptible (+/+; 42.85%), whereas two populations were found genetically homozygous resistant (−/−; 28.57%) which are insensitive to pyrethroid insecticides. Similarly, two populations were found heterozygous (+/−; 28.57%) for *kdr*. Hence, following the Mendelian ratio in future generation, at least 1/4th

TABLE 3 | Effect of insecticides on the percent enzyme inhibition in *Musca domestica* L. from District Jhang.

Sr#	Location	AchE	AkP	AcP	α-Carboxyl	β-Carboxyl
		df = 13, F = 1.569, *p* = 1.54	**df = 13, F = 16.28, *p* = 0.00**	**df = 13, F = 10.699, *p* = 0.000**	**df = 6, F = 5.826, *p* = <0.05**	**df = 6, F = 13.82, *p* = <0.05**
1	Control	11.13 ± 1.192	33.113 ± 17.351	31.101 ± 2.165	10.0221 ± 1.1321	9.301 ± 1.151
2	Civil lines	22.313 ± 4.754	132.266 ± 15.46	109.31 ± 7.892	19.59 ± 2.42	13.47 ± 3.77
3	18-Hazari	12.419 ± 1.232	40.341 ± 20.545	38.050 ± 3.989	11.989 ± 1.342	5.95 ± 2.14
4	Head Trimu	20.414 ± 3.302	105.531 ± 8.765	98.664 ± 3.1432	18.365 ± 2.02	16.15 ± 4.09
5	Nawaz Chowk	19.333 ± 2.375	10.066 ± 1.396	22.0667 ± 1.209	19.40 ± 1.15326	18.04 ± 2.96
6	Malhumorr	23.256 ± 3.206	99.342 ± 3.209	85.302 ± 1.546	25.146 ± 0.908	20.324 ± 2.203
7	Sattelite Town	29.434 ± 5.203	149.08 ± 15.434	125.250 ± 2.343	32.402 ± 1.208	28.43 ± 2.14
8	Haveli Bahadur	13.598 ± 1.202	69.245 ± 22.540	26.162 ± 2.1265	13.780 ± 2.375	11.69 ± 1.99

AChE = acetylcholineesterase, AcP = acidic phosphatase, AkP = alkaline phosphatase, α-Carboxyl = α-Carboxylesterases and β-Carboxyl = β-Carboxylesterases.
Means sharing the same letter within each treatment is not statistically different.

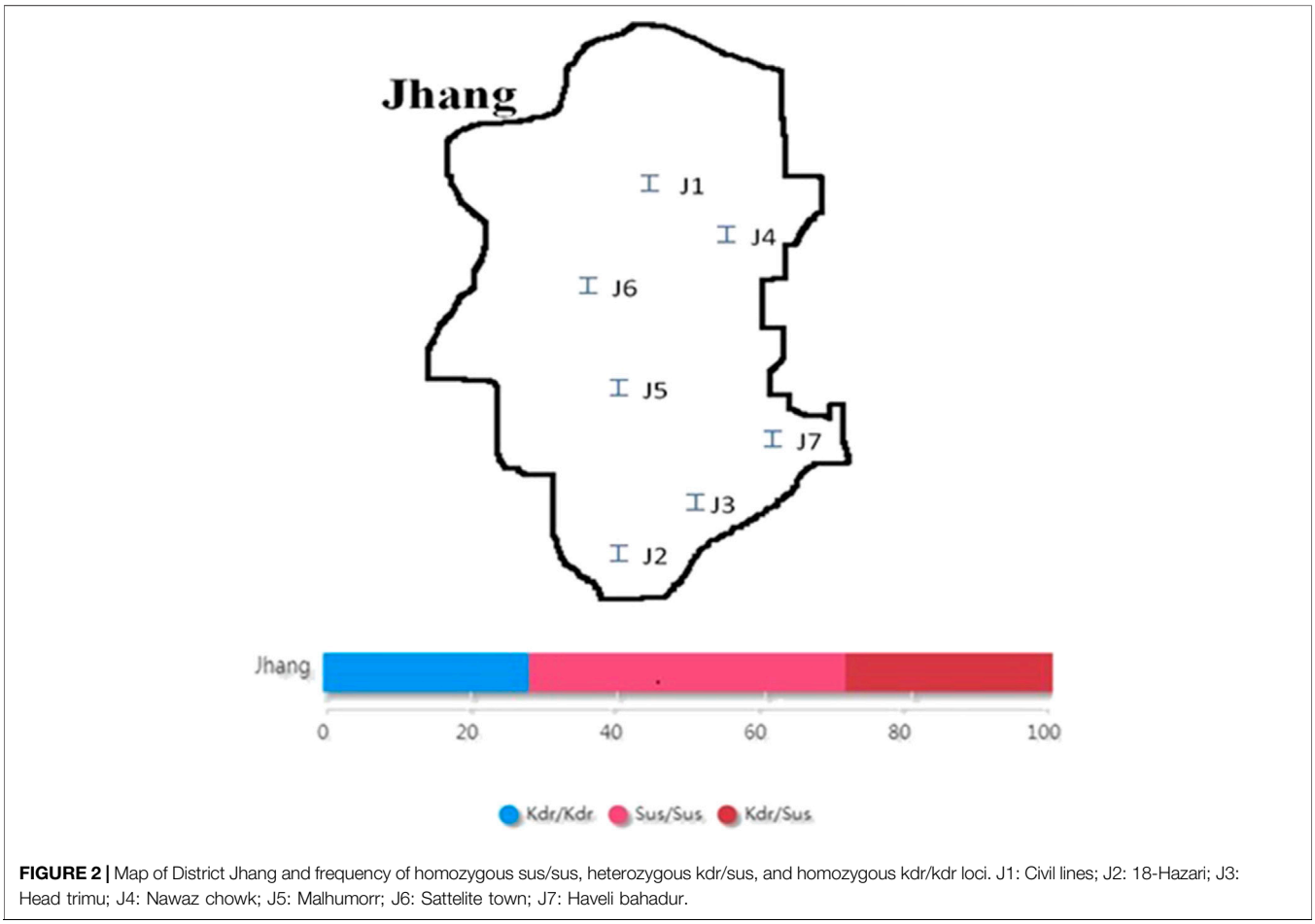

FIGURE 2 | Map of District Jhang and frequency of homozygous sus/sus, heterozygous kdr/sus, and homozygous kdr/kdr loci. J1: Civil lines; J2: 18-Hazari; J3: Head trimu; J4: Nawaz chowk; J5: Malhumorr; J6: Sattelite town; J7: Haveli bahadur.

homozygous resistant (−/−) housefly populations would be produced which would increase the insensitivity to pyrethroid insecticides (**Figure 1**). The mutation was identified at position 1014 on domain II of transmembrane six of sodium channels.

Enzyme Assay

The effect of insecticides on the activity of Acetylcholine Esterase (AchE), Carboxylesterase (α- Carboxylesterases and β-Carboxylesterases), Acidic Phosphatase (AcP), Alkaline Phosphatases (AkP) is shown in **Table 2**. Maximum percent inhibition of AChE was observed in satellite town (29.434%) followed by Malhumor (23.256%). Low level of inhibition of AChE was shown by Haveli Bahadur Shah (13.598%). Maximum percent inhibition of AkP was observed in satellite town (149.08%) followed by civil lines (132.2664%), whereas very low percent inhibition was found

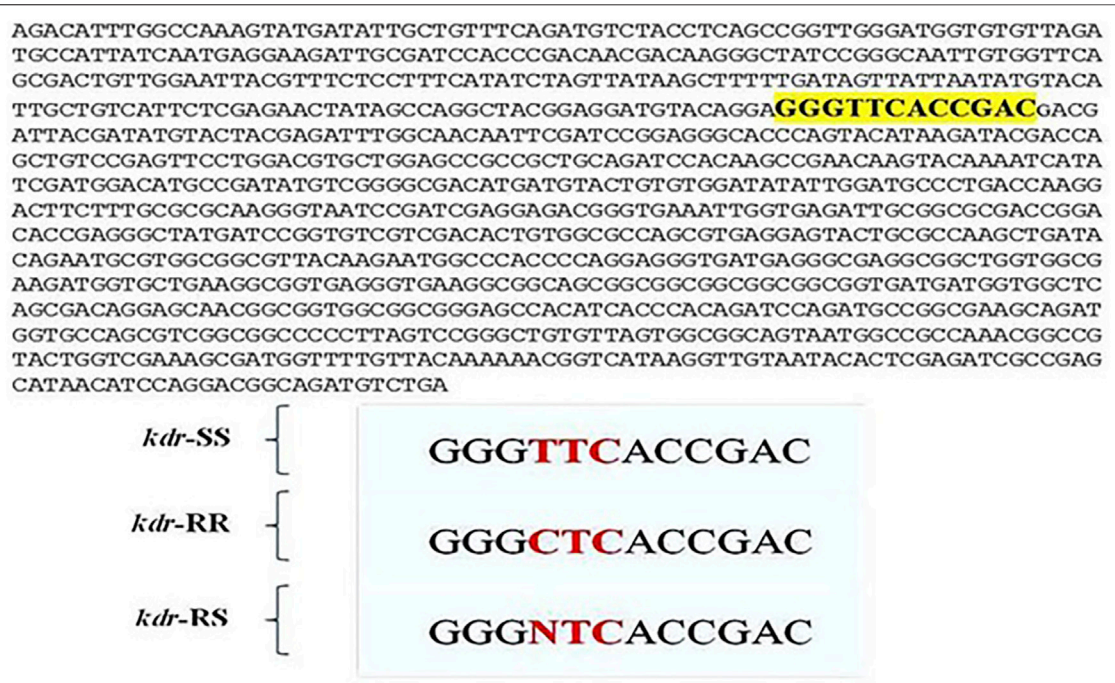

FIGURE 3 | Kdr mutation in housefly *Musca domestica* L. population from district Jhang. Lower panel: The mutation was identified from collected samples of housefly, *Musca domestica* L. at position 1014 in domain II of transmembrane six of sodium channels. Three kinds of sequences were obtained viz. *kdr* homozygous resistant (*kdr*-RR), *kdr* homozygous susceptible (*kdr*-SS), and *kdr* resistant (*kdr*-RS).

in 18-Hazari (40.341%). Similarly, maximum percent inhibition of AcP was found in satellite town (125.250%) followed by civil lines (109.31%). Low level of inhibition of AcP was found in samples from Nawaz chowk (22.067%). Maximum percent inhibition of α- Carboxylesterases was shown by satellite town (32.4%) followed by Malhumor (25.14%), whereas low level of inhibition of α- Carboxyl was found in 18-Hazari (11.98%). Similarly, maximum percent inhibition of β-Carboxylesterases was observed in Satellite town (28.43%) followed by Malhumor (20.32%), whereas very low level of inhibition was found in 18-Hazari (5.95%). Overall, the percentage inhibition of Alkaline Phosphatases (AkP) and Acidic Phosphatase (AcP) was found high as compared with Acetylcholinesterase (AChE) and Carboxylesterase (α- Carboxyl and β-Carboxyl) activity (**Table 3**).

DISCUSSION

During the present study, adult housefly (*Musca domestica* L.) was collected from seven different locations of Jhang, Punjab, Pakistan first to investigate the level of resistance against commercially used pyrethroid insecticides through bioassays and then to molecular genotyping of kdr mutation through PASA to reveal the frequency of *kdr* allele in field populations of housefly (*kdr/kdr*, *kdr/sus*, *sus/sus*). The flies were further used to find out the underlying modulation in the enzymatic activity due to pyrethroid resistance.

The percentage mortality of *Musca domestica*. L was recorded using five different concentrations of five insecticides with time exposure of 24 h, 48, and 72 h. It was recorded that with the increase in concentration of insecticides the mortality rate was also increased. Another factor that correlates with mortality is time exposure. It was already reported that prolonged exposure gave high mortality (Sultana et al., 2016 and 2019). Although all the other insecticides caused maximum mortality at exposure time of 72 h, Tetramethrin (2.85%) and Cypermethrin (9.84%) had decreased mortality when exposure time was increased. In addition, low level of resistance was found against Lambda Cyhalothrin when compared with Cypermethrin, Deltamethrin, and Permethrin consistent to our previous studies (Ranian et al., 2021). With Deltamethrin and Cypermethrin moderate level of resistance (RR) was found, whereas maximum resistance was found with Tetramethrin (Singh and Prakash, 2013).

In agreement with the molecular studies regarding *kdr* mutation by Huang et al. (2004), the *kdr* mutation was genotyped by allele-specific PCR (PASA) which revealed that this allele was present in the tested populations. The findings showed three types of genotypes with amplification of 280 bp homozygous-resistant allelic fragment (*kdr/kdr*). Some of the flies showed heterozygous genotype with amplification of two allelic fragments 280 bp for *kdr* and 200 bp or homozygous susceptible allelic fragment of 200 bp. The results were in agreement with the findings of Huang et al. (2004). It is to mention here that PASA did not work in true sense; rather the results were reproduced in separate PCR reactions. The

confirmation of L1014F mutation in housefly provides us with evidence that *Kdr*-type resistance is present in flies (**Figure 3**). The changes in sequences reinforced the importance of conservation of Leucine residue in transmembrane six of domain II of sodium channels protein conferring the target site insensitivity against pyrethroid group of insecticides as discussed by Eleftherianos et al. (2008).

Two locations viz. Civil lines and Satellite town were found homozygous resistant (*kdr/kdr*) for housefly populations, whereas Head trimu and Malhumorr were found homozygous susceptible (*sus/sus*). Three sampling sites viz. 18-Hazari, Nawaz chowk, and Haveli bahadur shah were found heterozygous for kdr (*kdr/sus*). The percentage of heterozygous genotype (*kdr/sus*) was higher as compared with homozygous genotypes. Maybe, heterozygotes have fitness advantage through a pleiotropic effect as discussed by Foster et al. (2004). The other possibility is that susceptible strains could migrate infrequently into the population in that area. The percentage of homozygous-resistant genotype was 28% and that of homozygous-susceptible sus/sus genotype was 43%, whereas maximum percentage was found for heterozygous *kdr/sus* genotype as 29% (**Figure 2**).

The enzymatic activity of fly populations revealed modulation in activity level when compared with Lab strain. It has been described that enzymatic activity contributes to resistance against pyrethroids (Eleftherianos et al., 2008). In the present study, the metabolic enzyme activity of homozygous-resistant (*kdr/kdr*), homozygous-susceptible (*sus/sus*), and heterozygous (*kdr/sus*) samples varied among different populations. According to Qin et al. (2014) in the absence of mutation at the target sites the metabolic detoxification becomes the major resistance mechanism. Hence, the enzymatic activity changes to counter the effect of employed insecticides (Sawicki, 1978; Eleftherianos et al., 2008).

The main objective to relate biochemical assay of Lab strain with field populations was to notice the changes in detoxification enzyme levels when exposed to pyrethroid insecticides. The current findings of enzyme assay of field strains while comparing with the molecular assay revealed that percent inhibition of Acetylcholinesterase (AchE), Carboxylesterase (α-Carboxylesterases and β-Carboxylesterases), Alkaline phosphatase (AkP), and Acidic phosphatase (AcP) had increased with increase in resistance (*kdr/kdr*) and decreased with increase in susceptibility (*sus/sus*). In addition, the Alkaline phosphatases (AkP) and Acidic phosphatases (AcP) activity increased more as compared with Acetylcholine Esterase (AchE) and Carboxylesterase. The results of the present study could be helpful in the strategic development of proactive management plans of *Musca domestica* L. in Jhang, Pakistan and the analysis of resistance will be helpful in the future to devise a targeted control strategy against population of housefly.

CONCLUSION

It was concluded that Tetramethrin had maximum resistance and Lambda Cyhalothrin had low level of resistance, whereas Deltamethrin and Cypermethrin showed moderate level of resistance in housefly populations from Jhang. Based on the molecular data of *kdr* alleles, two sites Civil lines and Satellite town had pyrethroid-resistant flies. Overall, three populations were found homozygous susceptible (+/+) and two populations were found heterozygous (+/−) for *kdr*. Keeping in view the simple Mendelian genetics, heterozygous for mutation lead towards homozygous *kdr* mutants, thus, increasing thereby the frequency of resistant strains in a given area. The sodium channels containing the Leucine to Phenylalanine mutation are less sensitive to the toxic effect of pyrethroid group of insecticides. It was also concluded that Acetylcholinesterase (AChE), Acid Phosphatase (AcP), Alkaline Phosphatase (AkP) had been increased in resistant housefly populations. The study helps reveal that a combination of chemicals could be a better choice rather than using pyrethroid insecticide individually. Thus, despite having molecular approaches, being rather costly, the enzyme assays would simply be used as a marker to check the susceptibility level of housefly samples from a given area.

DATA AVAILABILITY STATEMENT

The original contributions presented in the study are included in the article/supplementary material, further inquiries can be directed to the corresponding author.

AUTHOR CONTRIBUTIONS

BR designed and performed the experiments, analyzed the data, and wrote the manuscript. MK supervised and helped in designing the experiments, statistical analysis of data and approved the final manuscript. MZ and KR helped in designing and performing the experiments and arrangement of data. AA, KM, HM, and FJ reviewed and finalized the manuscript and provided the guidance in preparing manuscript.

REFERENCES

Abbas, N., Khan, H. A. A., and Shad, S. A. (2014). Cross-resistance, Genetics, and Realized Heritability of Resistance to Fipronil in the House Fly, *Musca domestica* (Diptera: Muscidae): a Potential Vector for Disease Transmission. *Parasitol. Res.* 113 (4), 1343–1352. doi:10.1007/s00436-014-3773-4

Abbott, W. S. (1925). A Method of Computing the Effectiveness of an Insecticide. *J. Econ. Entomol.* 18 (2), 265–267. doi:10.1093/jee/18.2.265a

Ahn, Y. J., Funaki, E., and Motoyama, N. (1992). "Mechanisms of Resistance to Pyrethroids and DDT in a Japanese Strain of the Housefly," in *Neurotox'91*. (Dordrecht: Springer), 257–269.

Al-Deeb, M. A. (2014). Pyrethroid Insecticide Resistance Kdr Gene in the House Fly, *Musca domestica* (Diptera: Muscidae), in the United Arab Emirates. *As* 05 (14), 1522–1526. doi:10.4236/as.2014.514163

Ashraf, H. M., Zahoor, M. K., Nasir, S., Majeed, H. N., and Zahoor, S. (2016). Genetic Analysis of *Aedes aegypti* Using Random Amplified Polymorphic DNA (RAPD) Markers from Dengue Outbreaks in Pakistan. *J. Arthropod Borne Dis.* 10 (4), 546–559.

Brown, J. K., Frohlich, D. R., and Rosell, R. C. (1995). The Sweetpotato or Silverleaf Whiteflies: Biotypes of Bemisia Tabaci or a Species Complex? *Annu. Rev. Entomol.* 40 (1), 511–534. doi:10.1146/annurev.en.40.010195.002455

Busvine, J. R. (1951). Mechanism of Resistance to Insecticide in Houseflies. *Nature* 168, 193–195. doi:10.1038/168193a0

Casida, J. E. (2016). Unexpected Metabolic Reactions and Secondary Targets of Pesticide Action. *J. Agric. Food Chem.* 64 (22), 4471–4477. doi:10.1021/acs.jafc.6b01564

Cheeke, P. R. (2005). *Applied Animal Nutrition: Feeds and Feeding (No. 636.085 C414a Ej. 1 025345)*. Pearson Prentice Hall.

Eleftherianos, I., Foster, S. P., Williamson, M. S., and Denholm, I. (2008). Characterization of the M918T Sodium Channel Gene Mutation Associated with strong Resistance to Pyrethroid Insecticides in the Peach-Potato Aphid, *Myzus persicae* (Sulzer). *Bull. Entomol. Res.* 98 (2), 183–191. doi:10.1017/s0007485307005524

Feyereisen, R. (1995). Molecular Biology of Insecticide Resistance. *Toxicol. Lett.* 82-83, 83–90. doi:10.1016/0378-4274(95)03470-6

Förster, M., Klimpel, S., and Sievert, K. (2009). The House Fly (*Musca domestica)* as a Potential Vector of Metazoan Parasites Caught in a Pig-Pen in Germany. *Vet. Parasitol.* 160 (1), 163–167. doi:10.1016/j.vetpar.2008.10.087

Foster, K. R., Shaulsky, G., Strassmann, J. E., Queller, D. C., and Thompson, C. R. L. (2004). Pleiotropy as a Mechanism to Stabilize Cooperation. *Nature* 431 (7009), 693–696. doi:10.1038/nature02894

Howard, Z. R., O'Bryan, C. A., Crandall, P. G., and Ricke, S. C. (2012). Salmonella Enteritidis in Shell Eggs: Current Issues and Prospects for Control. *Food Res. Int.* 45 (2), 755–764. doi:10.1016/j.foodres.2011.04.030

Howard, J., and Wall, R. (1996). Autosterilization of the House Fly, *Musca domestica* (Diptera: Muscidae) in Poultry Houses in North-East India. *Bull. Entomol. Res.* 86 (4), 363–367.

Huang, J., Kristensen, M., Qiao, C.-l., and Jespersen, J. B. (2004). Frequency of Kdr Gene in House Fly Field Populations: Correlation of Pyrethroid Resistance and Kdr Frequency. *J. Econ. Entomol.* 97 (3), 1036–1041. doi:10.1093/jee/97.3.1036

Iqbal, W., Malik, M. F., Sarwar, M. K., Azam, I., Iram, N., and Rashda, A. (2014). Role of Housefly (*Musca domestica*, Diptera; Muscidae) as a Disease Vector; a Review. *J. Entomol. Zoolog. Stud.* 2 (2), 159–163.

Keiding, J., and Arevad, K. (1964). Procedure and Equipment for Rearing a Large Number of Housefly Strains. *Bull. World Health Organ.* 31 (4), 527–528.

Khamesipour, F., Lankarani, K. B., Honarvar, B., and Kwenti, T. E. (2018). A Systematic Review of Human Pathogens Carried by the Housefly (*Musca domestica* L.). *BMC Public Health* 18 (1), 1049. doi:10.1186/s12889-018-5934-3

Khan, H., Abbas, N., Shad, S. A., and Afzal, M. B. S. (2014). Genetics and Realized Heritability of Resistance to Imidacloprid in a Poultry Population of House Fly, *Musca domestica* L. (Diptera: Muscidae) from Pakistan. *Pestic. Biochem. Physiol.* 114, 38–43. doi:10.1016/j.pestbp.2014.07.005

Kjaersgaard, A., Blanckenhorn, W. U., Pertoldi, C., Loeschcke, V., Kaufmann, C., Hald, B., et al. (2015). Plasticity in Behavioural Responses and Resistance to Temperature Stress in. *Musca domesticaAnimal Behav.* 99, 123–130. doi:10.1016/j.anbehav.2014.11.003

Liu, N., and Pridgeon, J. W. (2002). Metabolic Detoxication and the Kdr Mutation in Pyrethroid Resistant House Flies, *Musca domestica* (L.). *Pestic. Biochem. Physiol.* 73 (3), 157–163. doi:10.1016/s0048-3575(02)00101-3

Lord, F. T. (1904). Flies and Tuberculosis. *Bost. Med. & Surg. J.* 151 (24), 651–654.

Martins, A. J., and Valle, D. (2012). The Pyrethroid Knockdown Resistance. *Insecticides-Basic Other Appl.* 17, 38.

Panini, M., Manicardi, G. C., Moores, G. D., and Mazzoni, E. (2016). An Overview of the Main Pathways of Metabolic Resistance in Insects. *Invertebrate Survival J.* 13 (1), 326–335. doi:10.25431/1824-307X/isj.v13i1.326-335

Qin, Q., Li, Y., Zhong, D., Zhou, N., Chang, X., Li, C., et al. (2014). Insecticide Resistance of Anopheles Sinensis and an. Vagus in Hainan Island, a Malaria-Endemic Area of China. *Parasites Vectors* 7 (1), 92. doi:10.1186/1756-3305-7-92

Ranian, K., Zahoor, M. K., Zahoor, M. A., Rizvi, H., Rasul, A., Majeed, H. N., et al. (2021). Evaluation of Resistance to Some Pyrethroid and Organophosphate Insecticides and Their Underlying Impact on the Activity of Esterases and Phosphatases in House Fly, *Musca domestica* (Diptera: Muscidae). *Polish J. Environ. Stud.* 30 (1), 327–336. doi:10.15244/pjoes/96240

Rinkevich, F. D., Zhang, L., Hamm, R. L., Brady, S. G., Lazzaro, B. P., and Scott, J. G. (2006). Frequencies of the Pyrethroid Resistance Alleles of Vssc1 and CYP6D1 in House Flies from the Eastern United States. *Insect Mol. Biol.* 15 (2), 157–167. doi:10.1111/j.1365-2583.2006.00620.x

Sawicki, R. M. (1978). Unusual Response of DDT-Resistant Houseflies to Carbinol Analogues of DDT. *Nature* 275 (5679), 443–444. doi:10.1038/275443a0

Scott, J. G., Leichter, C. A., Rinkevihc, F. D., Harris, S. A., Su, C., Aberegg, L. C., et al. (2013). Insecticide Resistance in House Flies from the United States: Resistance Levels and Frequency of Pyrethroid Resistance Alleles. *Pestic. Biochem. Physiol.* 107 (3), 377–384. doi:10.1016/j.pestbp.2013.10.006

Shono, T., Zhang, L., and Scott, J. G. (2004). Indoxacarb Resistance in the House Fly, *Musca domestica*. *Pestic. Biochem. Physiol.* 80 (2), 106–112. doi:10.1016/j.pestbp.2004.06.004

Singh, S., and Prakash, S. (2013). Development of Resistance in *Tribolium castaneum*, Herbst (Coleoptera: Tenebrionidae) towards Deltamethrin in Laboratory. *Int. J. Scientific Res. Publications* 3 (8), 1–4.

Sultana, K., Zahoor, M. K., Sagheer, M., Nasir, S., Zahoor, M. A., Jabeen, F., et al. (2016). Insecticidal Activity of weed Plants, *Euphorbia Prostrata* and *Chenopodiastrum Murale* against Stored Grain Insect Pest Trogoderma Granarium Everts, 1898 (Coleoptera: Dermestidae). *Turkish J. Entomol.* 40 (3), 291–301. doi:10.16970/ted.19938

Younes, M. W., Othman, S. E., Elkersh, M. A., Youssef, N. S., and Omar, G. A. (2011). Effect of Seven Plant Oils on Some Biochemicalparameters in Khapra Beetle *Trogoderma Granarius* Everts (Coleoptera: Dermestidae). *Egypt. J. Exp. Biol.* 7 (1), 53–61.

Zahoor, M. K., Batool, F., Nasir, S., Rasool, B., Jabeen, F., Zahoor, S., et al. (2017). Population Dynamics and Genetic Homogeneity in Natural Populations of *Drosophila melanogaster* from Faisalabad, Pakistan. *Iran J. Sci. Technol. Trans. Sci.* 41 (2), 277–285. doi:10.1007/s40995-017-0267-0

Conflict of Interest: The authors declare that the research was conducted in the absence of any commercial or financial relationships that could be construed as a potential conflict of interest.

Publisher's Note: All claims expressed in this article are solely those of the authors and do not necessarily represent those of their affiliated organizations, or those of the publisher, the editors and the reviewers. Any product that may be evaluated in this article, or claim that may be made by its manufacturer, is not guaranteed or endorsed by the publisher.

frontiers in Environmental Science

ORIGINAL RESEARCH
published: 04 March 2022
doi: 10.3389/fenvs.2022.813871

Trifluralin Impacts Soil Microbial Community and Functions

Shuang Li[1], Pengqiang Du[1], Xiaohu Wu[2], Hairong He[3], Lin Zhou[1]*, Fengshou Dong[2], Xingang Liu[2] and Yongquan Zheng[2]**

[1]College of Plant Protection, Henan Agricultural University, Zhengzhou, China, [2]State Key Laboratory for Biology of Plant Diseases and Insect Pests, Institute of Plant Protection, Chinese Academy of Agricultural Sciences, Beijing, China, [3]College of Pharmacy, Henan University of Chinese Medicine, Zhengzhou, China

A 3-month experiment was designed to research the impact of trifluralin (TFL) on soil microbial communities and functions under the condition of greenhouse. In this work, silty loam from Langfang was treated with three doses of TFL (1,260, 12,600, and 126,000 g ha^{-1}) and incubated for 90 days. The half-lives of TFL were 15–23 days in all cases. The bacterial and fungal diversities and community structures were impacted by TFL. The bacterial functions of chemoheterotrophy and sulfur oxidation were decreased shortly, but the hydrocarbon degradation ability was significantly increased in the results of functional annotation of prokaryotic taxa (FAPROTAX). For the predicted results of Tax4Fun, amino acid (arginine and proline) metabolism and ABC transporter were decreased significantly, while nitrogen metabolism and ribosome translation were significantly increased. In conclusion, this work aids us to understand the risk of TFL in soil more comprehensively.

Keywords: trifluralin, soil microbe, community structure, bacterial function, fungal function

OPEN ACCESS

Edited by:
Yue Geng,
Ministry of Agriculture and Rural Affairs, China

Reviewed by:
Xiangwei Wu,
Anhui Agricultural University, China
Xuesheng Li,
Guangxi University, China

****Correspondence:***
Pengqiang Du
dupengq@163.com
Lin Zhou
zhoulinhenau@163.com
Yongquan Zheng
zhengyongquan@ippcaas.cn

Specialty section:
This article was submitted to Toxicology, Pollution and the Environment, a section of the journal Frontiers in Environmental Science

Received: *12 November 2021*
Accepted: *14 February 2022*
Published: *04 March 2022*

Citation:
Li S, Du P, Wu X, He H, Zhou L, Dong F, Liu X and Zheng Y (2022) Trifluralin Impacts Soil Microbial Community and Functions. Front. Environ. Sci. 10:813871. doi: 10.3389/fenvs.2022.813871

INTRODUCTION

Trifluralin (TFL, 2,6-dinitro-N, N-di-n-propyl-4-trifluoromethylaniline) is a fluorine-containing selective pre-emergence dinitroaniline herbicide, which is mainly used to control monocotyledonous weeds and annual broadleaf weeds, such as barnyard grass, *Eragrostis cilianensis*, crabgrass, setaria, and goosegrass (Nyporko et al., 2002; Zhu and Chen, 2003; Soltani et al., 2010; Perez-Moreno et al., 2014). It is an important herbicide in China, and there are 167 products that have been registered by 2021. The herbicidal mechanism of TFL is to inhibit the polymerization of tubulin and tissue development, inhibit meristem cell division, destroy cells, and inhibit photosynthesis to make weeds die (Nyporko et al., 2002; Chen et al., 2021). According to the research of Bansal (2011), most pesticides will get into the soil, especially for herbicides. TFL showed a long half-life in soil (Triantafyllidis et al., 2010; Du et al., 2018; Lu et al., 2019), and that was potentially harmful to soil life (Bezchlebová et al., 2007; Merlini et al., 2012; Wang et al., 2016).

Soil harbors thousands of microorganisms. They are the fundamental of soil functions and ecosystem balance, for example, maintaining plant growth and reproduction, removing harmful pollution, protecting groundwater, and fixing carbon (Zhao, 2008; Shu et al., 2016). However, the influenced soil microorganisms and impacted soil functions by pesticide have been proven by some researchers (Ju et al., 2016; Du et al., 2018; Fang et al., 2020). In the study by Ju, under the stress of myclobutanil, the abundance of bacteria, fungi, N-related gene (nifH and amoA), soil basal respiration, and microbial biomass carbon were impacted (Ju et al., 2016). Fang et al. (2020) reported that chloropicrin influenced bacterial abundance, community structure, and soil functions. In addition, in the study of Du et al. (2018), the authors reported that TFL influenced the biomass and

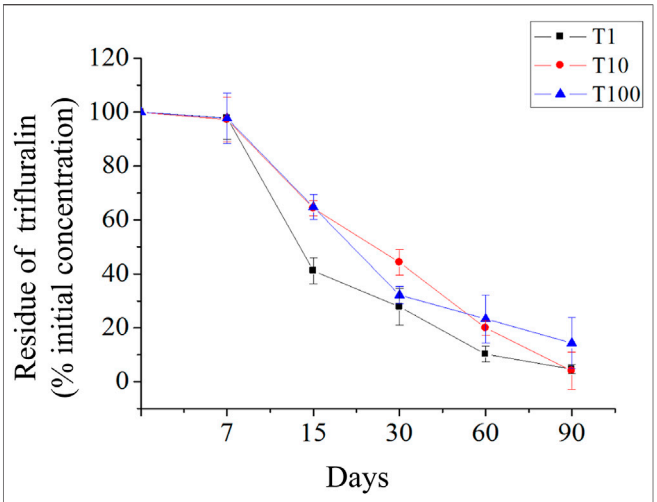

FIGURE 1 | Dynamics of trifluralin degradation in soil. The concentration of trifluralin is expressed as the % of the initial concentration for sampling date.

the ecology of soil microorganisms, and the N cycling is also influenced. However, the previous research of Du et al. (2018) was limited as it was an indoor experiment without plants and the functions only focused on N cycling.

Thus, in order to get close to the actual situation and better understand the impact on soil ecology and functions, we designed a 3-month experiment in greenhouse to evaluate the impact of TFL on bacterial and fungal ecotoxicology and the related functions. The focuses of this work were to evaluate the following questions: 1) the impact of TFL on the soil microbial community structure and 2) evaluate the influence on soil functions in greenhouse. This work can help us to deeply understand the impact of TFL on soil microbiome and their functions in greenhouse.

MATERIALS AND METHODS

Soil, Experimental Design, and Sample Collection

The soil was collected from the Langfang experimental site of the Chinese Academy of Agricultural Sciences and classified as silty loam according to the particle size of each soil. The soil was filtered by a 2-mm sieve, and the physical and chemical properties of the soil were 18 g of organic matter kg^{-1}, 74.9 mg of available phosphorus kg^{-1}, an electric conductivity of 95.8 us cm^{-1}, and a pH of 7.07. After that, the soil was placed in a 40 × 60 × 20 plastic basket, and the soil depth was 15 cm. Each basket contained 45 kg soil. There were some holes at the bottom of the plastic basket, and the diameter of each hole was 1 cm and the distance between every two holes was 5 cm. The soybean seed used was Zhonghuang 37. In each basket, 10 seeds were planted, and the sowing depth was 3–5 cm. The purity of TFL was 98.4%, which was bought from Beijing Qinchengyixin Technology Development Co., Ltd., (Beijing, China). There were three doses of TFL: T1 was the recommended dose of 1,260 g ha^{-1} in the field (0.03024 g for each basket), and T10 and T100 were 10 and 100 times of the recommended dose, respectively. The mother liquor was prepared with 1 ml acetone (0.03024 g for each basket for T1, 0.3024 g for each basket for T10, and 3.024 g for each basket for T100), and Tween 80 was added according to 0.5% of the mother liquor volume. After that, mother liquor was sprayed with 500 ml water in a hand-held sprayer. The control treatment has also been prepared and sprayed with 500 ml water. Each treatment was repeated three times. A 3-cm diameter soil sample was used to collect five samples in each plastic basket using a diagonal sampling method at days 7, 15, 30, 60, and 90. The sampling depth was 0–10 cm. The sampling site in basket was 3 cm away from the root. A part of each sample was used for the residual analysis of trifluralin, and the rest of the soil was stored at −80°C for DNA analysis.

TABLE 1 | Kinetic parameters of trifluralin degradation in soil at three different concentrations.

Parameters	Treatment		
	T1	T10	T100
A	0.838	3.43	79.15
k_1	0.0467	0.0295	0.03822
B	0.025	0.4052	0.1
k_2	0	0.0295	0
$t_{1/2}$ (d)	15	23	21
r^2	0.93	0.98	0.96

Trifluralin degradation in soil was described by bi-exponential kinetic model: $PC(t) = A \times exp(-k_1 \times t) + B \times exp(-k_2 \times t)$, *where PC is the concentration at time t; A and B are constants; and* k_1 *and* k_2 *are the dissipation kinetic constants of the first and second components;* $t_{1/2}$ *is the half-life of the initial trifluralin concentration. T1: 1,260 g* ha^{-1}, *T10: 12,600 g* ha^{-1}, *T100: 12,600 g* ha^{-1}.

Trifluralin Extraction and Detection

The procedure of TFL residue analysis was performed according to Du et al. (2018). Briefly, 5.0 g soil samples were extracted by 20 ml acetone. The extracted samples were detected by Agilent GC 7890A (Agilent Technologies, Santa Clara, CA, United States) gas chromatography equipped with an electron capture detector. The carrier gas for gas chromatography was helium, and the flow rate was 1 ml min^{-1}; the injection volume was 1 μl, without the shunt injection; the temperature of the injector was 250°C, and the initial temperature of the column was 150°C for 2 min, then the temperature of 20°C min^{-1} was increased to 280°C and held for 2 min. The electron capture detector temperature was 300°C.

DNA Extraction

A MoBio PowerSoil DNA Isolation Kit (Mo Bio Laboratories, Carlsbad, CA, United States) was used to extract soil DNA. In total, 1% agarose gel electrophoresis was used to assess the extraction effect, and the DNA concentrations were measured by NanoDrop 1000 spectrophotometry.

NGS of Bacterial and Fungal Communities

A GeneAmp 9700 PCR machine (Applied Biosystems, Waltham, MA, United States) was used to amplify the 16S rDNA V3V4 region gene and ITS hypervariable region gene. The pair of primers used for 16S rRNA were 341F (5′-CCTACGGGAGGC

TABLE 2 | Shannon diversity index of bacteria and fungi in soil with different treatments and days.

Diversity	Dosages	Days after application				
		7 days	15 days	30 days	60 days	90 days
Bacteria	CK	6.87 ± 0.05a	6.87 ± 0.09a	7.05 ± 0.12a	7.11 ± 0.05a	7.08 ± 0.06a
	T1	6.92 ± 0.11a	7.07 ± 0.03bc	7.04 ± 0.13a	7.12 ± 0.01a	7.04 ± 0.10a
	T10	6.98 ± 0.05a	6.99 ± 0.050b	7.07 ± 0.08a	7.09 ± 0.01a	7.00 ± 0.06a
	T100	7.00 ± 0.02a	7.12 ± 0.03c	7.13 ± 0.02a	7.14 ± 0.03a	7.00 ± 0.04a
Fungi	CK	3.24 ± 0.11a	3.26 ± 0.15a	3.32 ± 0.13a	2.78 ± 0.85a	3.21 ± 0.13b
	T1	3.27 ± 0.11a	3.33 ± 0.05a	3.44 ± 0.06a	3.47 ± 0.18a	3.53 ± 0.08b
	T10	3.16 ± 0.29a	3.26 ± 0.28a	3.32 ± 0.10a	3.18 ± 0.11a	2.49 ± 0.41a
	T100	3.37 ± 0.08a	3.41 ± 0.21a	3.44 ± 0.13a	3.47 ± 0.10a	3.50 ± 0.06b

Mean values (n = 3) S.E. Different letters indicate significant difference (p < 0.05, Duncan's test).

AGCAG-3′) and 806R (5′-GGACTACNNGGGTATCTAAT-3′) (Yu et al., 2005), and for the ITS rRNA gene, ITS3_KYO2 (5′-GCATCGATGAAGAACGCAGC-3′) and ITS4 (5′-ATATGTAGGATGAAGAACGYAGYRAA-3′) (Tian et al., 2017) were used. PCR products were tested by gel electrophoresis and purified using the Qiagen PCR Purification Kit (Qiagen, Hilden, Germany). Then, a Qubit 3.0 fluorometer was used to determine the concentration of PCR products. At last, Illumina HiSeq 4000 (Santiago, CA, United States of America) was used to sequence the qualified library, and the reading length was PE250.

Bioinformatics

Quantitative analysis of microbial ecology was used to operate procedures to process raw reads. The following rules were used to filter raw reads: the reads with >10% unknown nucleotides or <80% of the total number of nucleotides with the mass value >20 were removed. According to the overlapping relationship, the filtered reads were spliced into tags according to >10 bp overlapping and <2% mismatch rate. After removing the chimeric sequences, the reads of each sample were flattened, and then the sequences with similarity ≥97% were clustered into the same operational taxon by UPARSE (Edgar, 2013). The representative sequences of each operational taxon were selected and compared with the RDP database for species annotation. The Shannon Weiner index was used to calculate diversity. The Bray–Curtis distance was used to visualize beta diversity differences using principal component analysis (PCoA). Functions which related to the metabolism have been predicted by Tax4Fun (Aßhauer et al., 2015). Functional annotation of prokaryotic taxa (FAPROTAX) has been used to evaluate the impact on element cycling (Louca et al., 2016). FUNGuild has been used to predict the functions of fungi (Nguyen et al., 2016).

Data Analyses

One-way ANOVA and correlation analysis of the diversity of bacteria and fungi were performed using SAS statistical software version 9.2 (SAS Institute Inc., Cary, NC, United States). The significant differences of bacterial and fungal diversities between different treatments were tested using Fisher's least significant difference test, and a 5% level was set ($p < 0.05$). The α diversity index was used to represent the diversity of bacteria and fungi in soil.

RESULTS

TFL Degradation

The degradation dynamics of TFL in the soil was described by a bi-exponential kinetic model: $PC(t) = A \times \exp(-k_1 \times t) + B \times \exp(-k_2 \times t)$, where PC is the concentration at time t; A and B are constants; and k_1 and k_2 are the dissipation kinetic constants of the first and second components, respectively (**Figure 1**, **Table 1**). The initial depositions were 0.80, 7.87, and 81.87 mg kg^{-1}. After incubation, it was reduced to 95.26, 95.92, and 85.62% for T1, T10, and T100 treatments, with half-lives of 15, 23, and 21 days, respectively, in greenhouse. It was not detected in the control samples.

Bacterial and Fungal Profiles in Response to TFL

After quality filtering, we obtained 2,882,931 effective bacterial sequences, and they were clustered into 7,168 bacterial OTUs. The bacterial diversity is shown in **Table 2**, and it was just significantly increased at day 15 in all TFL treatments. The PCoA plot based on Bray–Curtis distance was used to analyze and compare the bacterial communities at the OTU level (**Figure 2A**). In the plot, control and T1 could be separated from others at days 15, 30, and 60.

After quality filtering, we obtained 4,270,144 effective fungal sequences, and they were clustered into 7,168 fungal OTUs. The fungal diversity is shown in **Table 2**, and it was slightly increased in T1 and T100 at day 90. The PCoA plot was used to analyze and compare fungal communities at the OTU level (**Figure 2B**). In the plot, T10 and T100 were separated from other treatments at days 7, 15, and 30.

Impact of the Functions Related to Element Cycling

The functions of element cycling were predicted by FAPROTAX and are shown in **Figure 3**. Predatory or exoparasitic was increased in T10 and T100 treatments at day 7, but it was decreased in T1 and T10 treatments at day 60. Chemoheterotrophy and aerobic chemoheterotrophy were decreased by TFL at day 15, except for chemoheterotrophy in

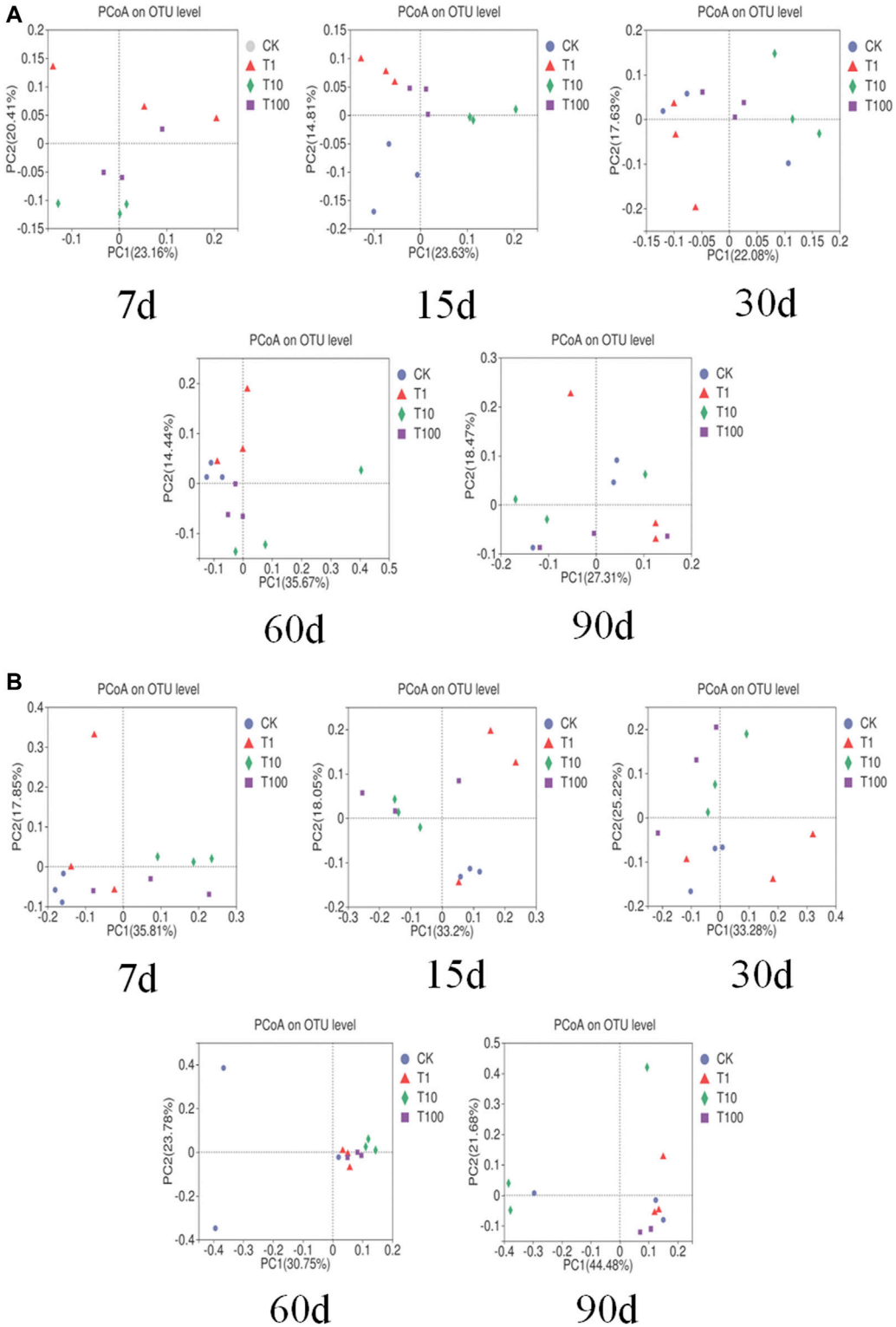

FIGURE 2 | PCoA of bacteria and fungi in soil-based on Bary-Curtis short. **(A)** is bacteria PCoA, **(B)** for the fungus PCoA.

T100 treatments. Aliphatic non-methane hydrocarbon degradation was significantly increased in T100 treatment at day 30. Hydrocarbon degradation and aliphatic non-methane hydrocarbon degradation were significantly increased in T100 treatments at day 60. The dark oxidation of sulfur compounds was decreased in all TFL treatments at day 60. Nitrification and

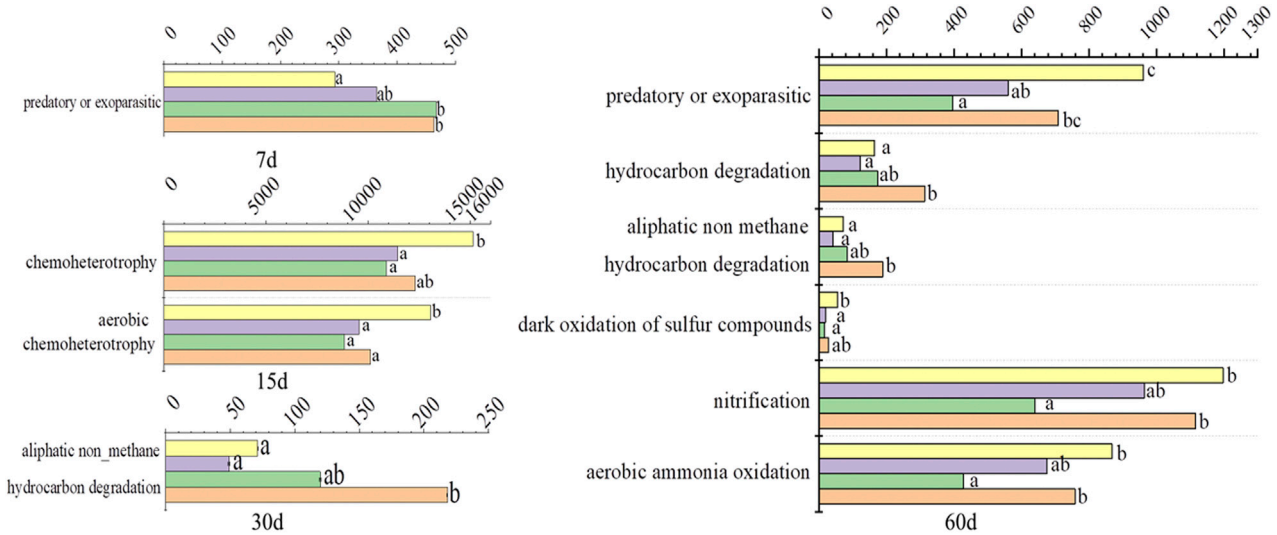

FIGURE 3 | Bacterial functions predicted by FAPROTAX. Letters "a" and "b" on the right of the columns mean significance of difference ($p < 0.05$).

aerobic ammonia oxidation were significantly decreased in T10 treatment at day 60.

Effect of Trifluralin on Pathways

According to the OTU results of 16S rRNA sequencing, the Tax4Fun database was used for function prediction analysis. The most abundant 25 pathways are listed in **Figure 4**. The metabolism of the flagellar assembly was significantly increased from day 30 to day 60 in T10 and T100 treatments, but it was just increased at days 7 and 15 in T10. The ABC transporters, and arginine and proline metabolism were significantly decreased in T10 and T100 from day 7 to day 60, except for ABC transporters at day 60. The ribosomal translation was significantly increased from days 7 to 60 in all TFL treatments, except for T1 at day 15. Nitrogen metabolism was increased by TFL from days 30 to 60. Porphyrin and chlorophyll metabolisms were increased in T100 treatment at day 15, and increased in all TFL treatments at day 60.

Impacted Fungal Functions

Based on the results of FUNGuild, the influenced functions are shown in **Figure 5**. The function which related to plant-pathogen was decreased by TFL in T10 and T100 treatments at day 15. Litter saprotroph was just significantly increased in T1 treatment at day 60.

DISCUSSION

Soil microorganisms play an important role in the Earth's ecosystem, such as the mineralization of organic matter, the circulation of organic carbon and nitrogen, and maintaining soil health. In the modern agricultural system, the herbicide is necessary to control herbs. But herbicide influences soil microbiome ecology and soil functions, which has been verified by some researchers (Pampulha et al., 2010; Zabaloy et al., 2012; Petric et al., 2014; Jiang et al., 2019; Jiang et al., 2020; Pertile et al., 2021). TFL is a widely used herbicide for soybean, and Du et al. (2018) have evaluated the impact of TFL on soil ecology and N cycling. However, there were some limitations, for example, the scale of the experiment was small and they did not evaluate other soil functions. In order to make the data closer to actual agricultural production, we performed this study to evaluate the influence of TFL on soil ecology and functions under greenhouse conditions and planting soybean.

Compared with the previous study (Du et al., 2018), TFL degraded faster in greenhouse. One possible reason was that the greenhouse was a semi-open environment and some TFL has been dissipated by light (Le Person et al., 2007). In addition, there were too much soil in the basket that may induce species in deep soil to communicate with upper soil and promote TFL degradation. The TFL residue in soil in greenhouse also had impact on soil ecology and functions. The increased bacterial diversity suggested that the responses of TFL to diverse species were different. However, this result was opposite from the findings in the indoor experiment of Du et al. (2018), and the most possible reason may be due to the bigger scale of the experiment and higher biological communication. The increased effect of bacterial diversity was also detected in soils contaminated with thiamethoxam (Wu et al., 2020). In addition, the influenced bacterial diversity indicated that bacterial ecology has been seriously disturbed. Therefore, the soil functions were also impacted, which have been proven in this study. The effect of various species to pesticides is different, and it has been proven by Forlani et al. (1995). The changed bacterial community structures in this work were the indirect reflections of different effects of bacterial species on TFL. Similarly, Du et al. (2021) also reported that bacterial diversity and community were influenced by mesosulfuron-methyl in the indoor experiments. Furthermore, the influenced bacterial diversity and community were also

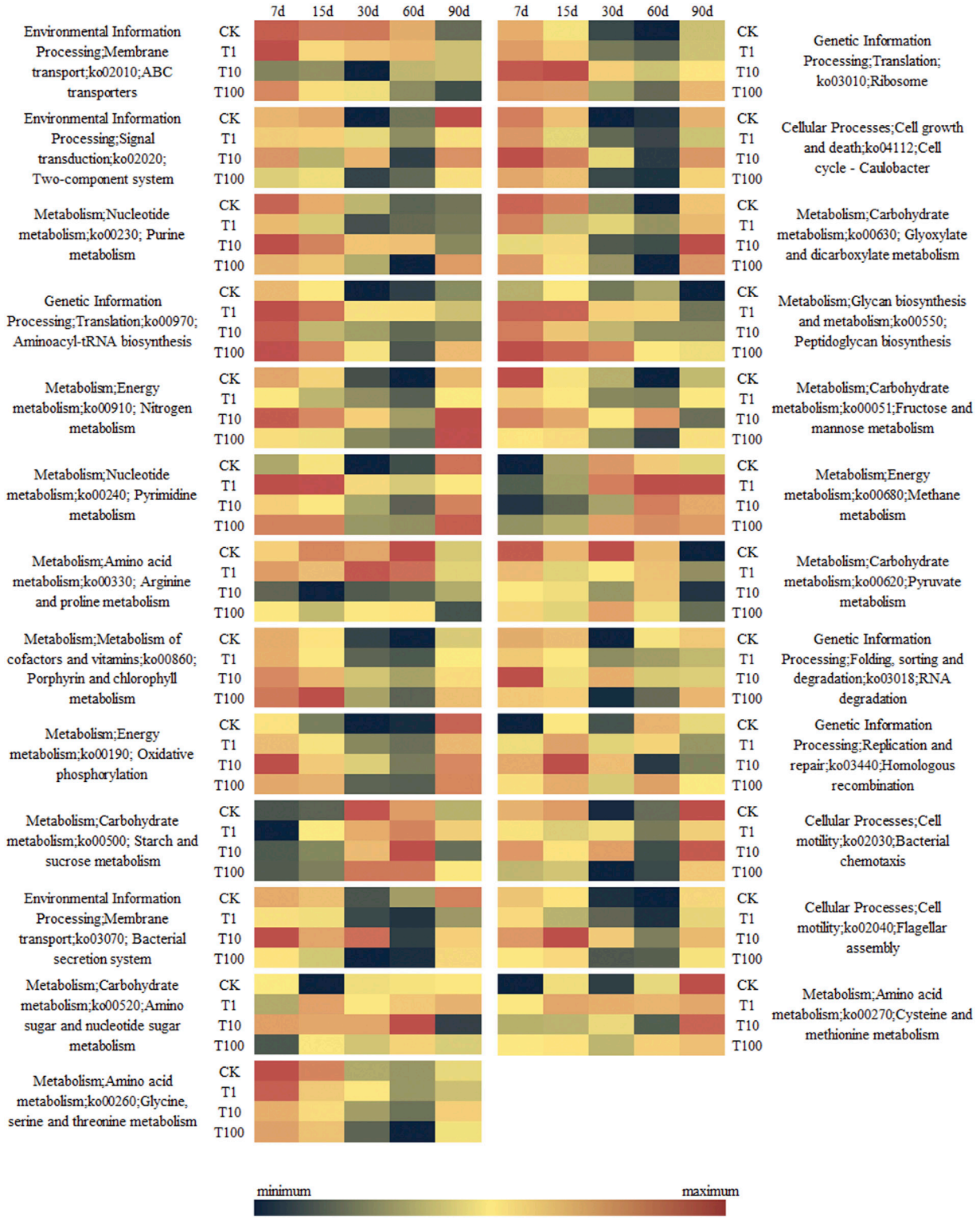

FIGURE 4 | Heatmap of pathways predicted by Tax4Fun.

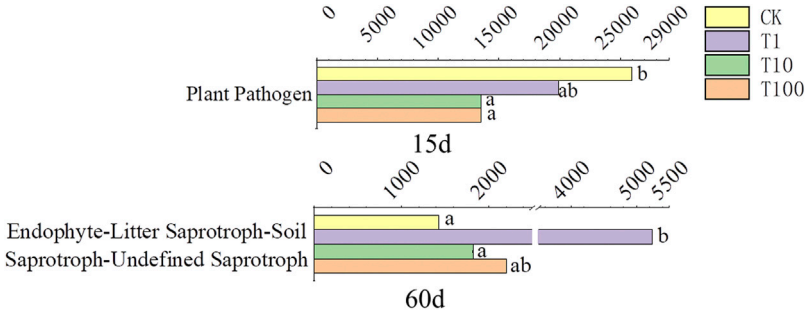

FIGURE 5 | Fungal functions predicted by FUNGuild. Letters "a" and "b" on the right of the columns mean significance of difference ($p < 0.05$).

observed in the studies of Herath et al. (2017). In addition to its direct effect on bacteria, TFL significantly decreased the diversity of fungi in T10 treatments that coincide with the results of the indoor experiment (Du et al., 2018). Clomazone also showed a decreased effect on the fungal diversity (Wu et al., 2020). The influenced fungal diversity also implied that the ecology and functions of fungi have been impacted. Compared with the fungal PCoA plot in the indoor experiments, the fungal community was slightly influenced, which suggested that the fungal community was more sensitive to TFL in the pot experiments.

Soil microbiota, the base of soil functions, is important in substance and energy exchange, ecological equilibrium maintains, soil fertility increase, and plant growth promotion (Wächtershäuser, 1990; Wardle et al., 2004; Falkowski et al., 2008; Lehtovirta-Morley et al., 2011). The influenced soil microbial ecology in this study suggested that soil functions were influenced. FAPROTAX and Tax4Fun were used to evaluate the functions which were mediated by bacteria. For the results of FAPROTAX, the hydrocarbon degradation ability was the most influenced ability. The aliphatic non-methane hydrocarbon and hydrocarbon degradation pathways were increased, suggesting that the related bacteria were acclimated by TFL and increased the hydrocarbon degradation ability. For the results of Tax4Fun, the ABC transporters decreased, suggesting that the ability of transmembrane transport was inhibited by TFL, which will influence most metabolism. In addition, the influenced amino acid (arginine and proline) and nitrogen metabolism suggested that N cycling has been influenced. The influenced fungal functions of saprotroph suggested that the decomposition process of soil has been influenced.

CONCLUSION

This study performed a pot experiment to explore the effect of TFL on soil microbial ecology and functions. In general, under the treatment of TFL, the bacterial diversity was increased and the fungal diversity was decreased. The bacterial and fungal communities were slightly influenced. Soil functions about hydrocarbon degradation, transmembrane transport, amino acid metabolism, and ribosomal translation were also influenced after TFL exposure. In addition, microbiome connections are also influenced by TFL. Therefore, TFL also showed influence on soil ecology and functions in the pot experiments.

DATA AVAILABILITY STATEMENT

The raw data supporting the conclusions of this article will be made available by the authors, without undue reservation.

AUTHOR CONTRIBUTIONS

SL: conceptualization and writing—original draft. PD: methodology, data curation, and writing—review and editing. XW: conceptualization and methodology. HH: formal analysis and writing—review and editing. LZ: supervision and writing—review and editing. FD: writing—original draft and data curation. XL: supervision. YZ: supervision, writing—review and editing, and supervision.

REFERENCES

Aßhauer, K. P., Wemheuer, B., Daniel, R., and Meinicke, P. (2015). Tax4Fun: Tax4Fun: Predicting Functional Profiles from Metagenomic 16S rRNA Data. *Bioinformatics* 31, 2882–2884. doi:10.1093/bioinformatics/btv287

Bansal, O. P. (2011). Fate of Pesticides in the Environment. *J. Indian Chem. Soc.* 88 (10), 1525–1532. doi:10.1016/j.fct.2018.01.034

Bezchlebová, J., Černohlávková, J., Lána, J., Sochová, I., Kobetičová, K., and Hofman, J. (2007). Effects of Toxaphene on Soil Organisms. *Ecotoxicology Environ. Saf.* 68 (3), 326–334. doi:10.1016/j.ecoenv.2007.05.009

Chen, J., Yu, Q., Patterson, E., Sayer, C., and Powles, S. (2021). Dinitroaniline Herbicide Resistance and Mechanisms in Weeds. *Front. Plant Sci.* 12, 634018. doi:10.3389/fpls.2021.634018

Du, P., He, H., Wu, X., Xu, J., Dong, F., Liu, X., et al. (2021). Mesosulfuron-methyl Influenced Biodegradability Potential and N Transformation of Soil. *J. Hazard. Mater.* 416, 125770. doi:10.1016/j.jhazmat.2021.125770

Du, P., Wu, X., Xu, J., Dong, F., Liu, X., and Zheng, Y. (2018). Effects of Trifluralin on the Soil Microbial Community and Functional Groups Involved in Nitrogen Cycling. *J. Hazard. Mater.* 353, 204–213. doi:10.1016/j.jhazmat.2018.04.012

Edgar, R. C. (2013). UPARSE: Highly Accurate OTU Sequences from Microbial Amplicon Reads. *Nat. Methods* 10 (10), 996–998. doi:10.1038/nmeth.2604

Falkowski, P. G., Fenchel, T., and Delong, E. F. (2008). The Microbial Engines that Drive Earth's Biogeochemical Cycles. *Science* 320 (5879), 1034–1039. doi:10.1126/science.1153213

Fang, W., Song, Z., Tao, S., Zhang, D., Huang, B., Ren, L., et al. (2020). Biochar Mitigates the Negative Effect of Chloropicrin Fumigation on Beneficial Soil Microorganisms. *Sci. Total Environ.* 738, 139880. doi:10.1016/j.scitotenv.2020.139880

Forlani, G., Mantelli, M., Branzoni, M., Nielsen, E., and Favilli, F. (1995). Differential Sensitivity of Plant-Associated Bacteria to Sulfonylurea and Imidazolinone Herbicides. *Plant Soil* 176 (2), 243–253. doi:10.1007/BF00011788

Herath, H. M. L. I., Moldrup, P., Jonge, L. W. d., Nicolaisen, M., Norgaard, T., Arthur, E., et al. (2017). Clay-to-Carbon Ratio Controls the Effect of Herbicide Application on Soil Bacterial Richness and Diversity in a Loamy Field. *Water Air Soil Pollut.* 228, 3. doi:10.1007/s11270-016-3175-6

Jiang, R., Wang, M., Chen, W., Li, X., Balseiro-Romero, M., and Baveye, P. C. (2019). Ecological Risk of Combined Pollution on Soil Ecosystem Functions: Insight from the Functional Sensitivity and Stability. *Environ. Pollut.* 255 (Pt 1), 113184. doi:10.1016/j.envpol.2019.113184

Jiang, R., Wang, M., Chen, W., Li, X., and Balseiro-Romero, M. (2020). Changes in the Integrated Functional Stability of Microbial Community under Chemical Stresses and the Impacting Factors in Field Soils. *Ecol. Indicators* 110, 105919. doi:10.1016/j.ecolind.2019.105919

Ju, C., Xu, J., Wu, X., Dong, F., Liu, X., and Zheng, Y. (2016). Effects of Myclobutanil on Soil Microbial Biomass, Respiration, and Soil Nitrogen Transformations. *Environ. Pollut.* 208, 811–820. doi:10.1016/j.envpol.2015.11.003

Le Person, A., Mellouki, A., Muñoz, A., Borras, E., Martin-Reviejo, M., and Wirtz, K. (2007). Trifluralin: Photolysis under Sunlight Conditions and Reaction with HO Radicals. *Chemosphere* 67 (2), 376–383. doi:10.1016/j.chemosphere.2006.09.023

Lehtovirta-Morley, L. E., Stoecker, K., Vilcinskas, A., Prosser, J. I., and Nicol, G. W. (2011). Cultivation of an Obligate Acidophilic Ammonia Oxidizer from a Nitrifying Acid Soil. *Proc. Natl. Acad. Sci.* 108 (38), 15892–15897. doi:10.1073/pnas.1107196108

Louca, S., Parfrey, L. W., and Doebeli, M. (2016). Decoupling Function and Taxonomy in the Global Ocean Microbiome. *Science* 353 (6305), 1272–1277. doi:10.1126/science.aaf4507

Lu, W., Li, L., Li, S., and Zhao, N. (2019). Toxicity and Field Efficacy of Water-Soluble Fluraline Nanocrystals on sunflower. *Plant Prot.* 45 (03), 237–240+248. doi:10.16688/j.zwbh.2018220

Merlini, V. V., Nogarol, L. R., Marin-Morales, M. A., and Fontanetti, C. S. J. M. R. (2012). Toxicity of Trifluralin Herbicide in a Representative of the Edaphic Fauna: Histopathology of the Midgut of Rhinocricus Padbergi (Diplopoda). *Microsc. Res. Tech.* 75 (10), 1361–1369. doi:10.1002/jemt.22075

Nguyen, N. H., Song, Z., Bates, S. T., Branco, S., Tedersoo, L., Menke, J., et al. (2016). FUNGuild: An Open Annotation Tool for Parsing Fungal Community Datasets by Ecological Guild. *Fungal Ecol.* 20, 241–248. doi:10.1016/j.funeco.2015.06.006

Nyporko, A. Y., Yemets, A. I., Klimkina, L. A., and Blume, Y. B. (2002). Sensitivity of Eleusine Indica Callus to Trifluralin and Amiprophosmethyl in Correlation with the Binding of These Compounds to Tubulin. *Russ. J. Plant Physiol.* 49 (3), 413–418. doi:10.1023/a:1015561523131

Pampulha, M. E., Ferreira, M. A., and Oliveira, A. (2010). Effects of a Phosphinothricin Based Herbicide on Selected Groups of Soil Microorganisms. *J. Basic Microbiol.* 47 (4), 325–331. doi:10.1002/jobm.200610274

Perez-Moreno, L., Castaneda-Cabrera, C., Ramos-Tapia, M., and Tafoya-Razo, J. A. (2014). CONTROL QUÍMICO PREEMERGENTE DE LA MALEZA EN TOMATE DE CÁSCARA. *Interciencia* 39 (6), 422–427. Available at: https://www.interciencia.net/wpcontent/uploads/2017/11/422-c-P%C3%89REZMORENO-6.pdf.

Pertile, M., Sousa, R. M. S., Mendes, L. W., Antunes, J. E. L., Oliveira, L. M. d. S., de Araujo, F. F., et al. (2021). Response of Soil Bacterial Communities to the Application of the Herbicides Imazethapyr and Flumyzin. *Eur. J. Soil Biol.* 102, 103252. doi:10.1016/j.ejsobi.2020.103252

Petric, I., Friedel, I., Vasileiadis, S., Martin-Laurent, F., Djuric, S., and Bru, D. (2014). A Tiered Assessment Approach Based on Standardized Methods to Estimate the Impact of Nicosulfuron on the Abundance and Function of the Soil Microbial Community. *Soil Biol. Biochem.* 75, 282–291. doi:10.1016/j.soilbio.2014.04.022

Shu, Q., Gao, Y., Liu, Y., Wang, Y., and Bao, G. (2016). Calculating Ecological Value of Land Use in the Coastal Areas of Jiangsu Province. *J. Geo-Information Sci.* 18 (6), 787–796. doi:10.3724/SP.J.1047.2016.00787

Soltani, N., Nurse, R. E., Van Eerd, L. L., Vyn, R. J., Shropshire, C., and Sikkema, P. H. (2010). Weed Control, Environmental Impact and Profitability with Trifluralin Plus Reduced Doses of Imazethapyr in Dry Bean. *Crop Prot.* 29 (4), 364–368. doi:10.1016/j.cropro.2009.07.011

Tian, X., Yang, T., He, J., Chu, Q., Jia, X., and Huang, J. (2017). Fungal Community and Cellulose-Degrading Genes in the Composting Process of Chinese Medicinal Herbal Residues. *Bioresour. Techn.* 241, 374–383. doi:10.1016/j.biortech.2017.05.116

Triantafyllidis, V., Manos, S., Hela, D., Manos, G., and Konstantinou, I. (2010). Persistence of Trifluralin in Soil of Oilseed Rape fields in Western Greece. *Int. J. Environ. Anal. Chem.* 90 (3-6), 344–356. doi:10.1080/03067310903094495

Wächtershäuser, G. (1990). Evolution of the First Metabolic Cycles. *Proc. Natl. Acad. Sci.* 87 (1), 200–204. doi:10.1073/pnas.87.1.200

Wang, Y., Cang, T., Yu, R., Wu, S., Liu, X., Chen, C., et al. (2016). Joint Acute Toxicity of the Herbicide Butachlor and Three Insecticides to the Terrestrial Earthworm, Eisenia fetida. *Environ. Sci. Pollut. Res.* 23 (12), 11766–11776. doi:10.1007/s11356-016-6347-4

Wardle, D. A., Bardgett, R. D., Klironomos, J. N., Setälä, H., van der Putten, W. H., and Wall, D. H. (2004). Ecological Linkages between Aboveground and Belowground Biota. *Science* 304 (5677), 1629–1633. doi:10.1126/science.1094875

Wu, C., Wang, Z., Ma, Y., Luo, J., and She, D. (2020). Influence of the Neonicotinoid Insecticide Thiamethoxam on Soil Bacterial Community Composition and Metabolic Function. *J. Hazard. Mater.* 405, 124275. doi:10.1016/j.jhazmat.2020.124275

Yu, Y., Lee, C., and Hwang, S. (2005). Analysis of Community Structures in Anaerobic Processes Using a Quantitative Real-Time PCR Method. *Water Sci. Technol.* 52 (1-2), 85–91. doi:10.2166/wst.2005.0502

Zabaloy, M. C., Gómez, E., Garland, J. L., and Gómez, M. A. (2012). Assessment of Microbial Community Function and Structure in Soil Microcosms Exposed to Glyphosate. *Appl. Soil Ecol.* 61, 333–339. doi:10.1016/j.apsoil.2011.12.004

Zhao, Q. (2008). Improve Understanding of Soil, the Innovative Modern Soil Science. *Acta Pedologica Sinica* 45 (05), 771–777. doi:10.3321/j.issn:0564-3929.2008.05.002

Zhu, W., and Chen, C. (2003). Effect of 48% Fluralin Emulsion Soil Treatment on Control of Grass Weeds. *Hubei Agric. Sci.* 3, 57–58. doi:10.3969/j.issn.0439-8114.2003.03.024

Conflict of Interest: The authors declare that the research was conducted in the absence of any commercial or financial relationships that could be construed as a potential conflict of interest.

Publisher's Note: All claims expressed in this article are solely those of the authors and do not necessarily represent those of their affiliated organizations, or those of the publisher, the editors, and the reviewers. Any product that may be evaluated in this article, or claim that may be made by its manufacturer, is not guaranteed or endorsed by the publisher.

frontiers in Environmental Science

REVIEW
published: 04 March 2022
doi: 10.3389/fenvs.2022.828257

Alfalfa (*Medicago Sativa* L.): Genotypic Diversity and Transgenic Alfalfa for Phytoremediation

Dilnur Tussipkan[1] *and Shuga A. Manabayeva*[1,2]*

[1]*Plant Genetic Engineering Laboratory, National Center for Biotechnology (NCB), Nur-Sultan, Kazakhstan,* [2]*L.N.Gumilyov Eurasian National University, Nur-Sultan, Kazakhstan*

Soil contamination caused by industrial and agricultural activities is an environmental problem that poses a serious risk to human health and the ecosystem. Persistent organic pollutants (POPs) are organic chemicals that persist in the environment for long periods because of their high resistance to photolytic, chemical, and biological degradation. Besides POPs, high concentrations of non-essential heavy metals and metalloids, such as arsenic, cadmium, and lead, are increasingly becoming a problem worldwide. Remediation strategies for organic and inorganic pollutants in the environment have received global attention. For organic or inorganic contaminants, phytoremediation is the strategy of choice because of a green technology that uses plants and solar energy to clean hyper-accumulated toxic pollutants from the environment. Some plant species have a high capacity to grow and survive in elevated levels of contaminants. With a long cultivation history and adaptability to a wide range of territories, alfalfa has not only widely been used for animal feed and a medicinal herb but is also an ideal natural resource and model plant for remediation of contaminated soils, offering a variety of elite characteristics. This review provides, firstly, abundant genomic information on the genetic diversity and population structure of alfalfa. Secondly, we focused on the transgenic alfalfa plants for enhanced phytoremediation of POPs, such as atrazine, polychlorinated biphenyl (PCB), and trichloroethylene (TCE), as well as phytoremediation of petroleum and heavy metals. Thirdly, the future perspective of enhancement of phytoremediation efficiency was discussed in depth. This review is intended to provide a comprehensive overview of the phytoremediation capabilities of transgenic alfalfa plants, presenting fundamental information for future research studies for enhancing phytoremediation efficiency.

Keywords: alfalfa (*Medicago sativa* L.), genotypic diversity, phytoremediation, POPs, petroleum, heavy metals

OPEN ACCESS

Edited by:
Liangang Mao,
Institute of Plant Protection (CAAS), China

Reviewed by:
Vineet Kumar,
National Environmental Engineering Research Institute (CSIR), India
Neerja Srivastava,
Chhatrapati Shahu Ji Maharaj University, India

***Correspondence:**
Shuga A. Manabayeva
manabayeva@biocenter.kz

Specialty section:
This article was submitted to Toxicology, Pollution and the Environment, a section of the journal Frontiers in Environmental Science

Received: *03 December 2021*
Accepted: *25 January 2022*
Published: *04 March 2022*

Citation:
Tussipkan D and Manabayeva SA (2022) Alfalfa (Medicago Sativa L.): Genotypic Diversity and Transgenic Alfalfa for Phytoremediation. Front. Environ. Sci. 10:828257. doi: 10.3389/fenvs.2022.828257

INTRODUCTION

Alfalfa and Core Collections Worldwide

Alfalfa (*Medicago sativa* L.) belongs to the *Fabaceae* family, *Trifolieae* tribe (Rhouma et al., 2017), and *Medicago* genus and includes several diploid alfalfa (2n = 2x = 16) with a small genome size of 550 Mbp and autotetraploid cultivated alfalfa (2n = 4x = 32) with a genome size of 800–1,000 Mbp (Blondon et al., 1994; Havananda et al., 2011). This plant grows and develops well at 22°C–30°C. Under sufficient humidity, it can also survive at 37°C–42°C. Moreover, it is characterized by high cold tolerance, ranging from −15°C to −30°C (Stepanova et al., 2016). Alfalfa has been suggested to have

two feasible origins based on its abundant diversity. One is in the Asian Minor, including Northwestern Iran, highlands of Armenia, Georgia, and Eastern Turkey, and the other is in Central Asia, including Kazakhstan, Uzbekistan, and Afghanistan (Wang and Şakiroğlu, 2021). Unfortunately, it is difficult to determine its precise origins.

Nowadays, alfalfa has been grown in approximately 30 million hectares of hay, silage, and pasture areas globally (Hawkins and Yu 2018). More than 21 thousand *Medicago sativa* L. accessions are reported from 37 country collections worldwide, and the major germplasm banks of alfalfa accessions are in the United States (4,771 accessions), followed by Australia (3,843 accessions), the Russian Federation (3,647 accessions), the United Kingdom (1,085 accessions), and Italy (989 accessions) (reviewed in (Irish and Greene 2021). Detailed accession-associated passport information on 1966 accessions is given in the online platform of the Genesys database (https://www.genesys-pgr.org/) It is important to study the genotypic diversity of alfalfa due to the large ecological distribution and demographic expansion of the species and the abundant germplasm collection.

GENOTYPIC DIVERSITY OF ALFALFA

Genetic Diversity and Population Structure of Alfalfa

Many studies over the last decade have investigated the genetic diversity of alfalfa assessed by genetic markers [reviewed in (Li and Brummer, 2012; Hawkins and Yu 2018)]. Here we concentrate on research from 2018 onwards. The genetic diversity and population structure of six alfalfa cultivars from the United States were evaluated by amplifying SSR markers with 312 discernible alleles from the whole genome (Yin et al., 2018). Twenty wild alfalfa germplasms from the Xinjiang province of China were analyzed for genetic diversity by six pairs of random amplified polymorphic DNA (RAPD) and six pairs of inter-simple sequence repeat (ISSR) markers (Ma et al., 2018). The genetic diversity among 242 worldwide alfalfa accessions was studied using 102 simple sequence repeat (SSR) primers; it was found to consist of 471 alleles distributed on eight chromosomes (He H et al., 2019). Seventy-seven alfalfa genotypes from Brazil were explored using 10 SSR markers with 54 alleles (dos Santos et al., 2020). Inter-retrotransposon-amplified polymorphism (IRAP) markers have been used to assess alfalfa's genetic diversity (Badr et al., 2020). Twelve Iranian genotypes were studied based on seed storage proteins patterns (Kakaei and Ahmadian 2021), while the genetic diversity of 25 Russian alfalfa cultivars was examined by sequence-related amplified polymorphism (SRAP) markers (Shamustakimova et al., 2021). In 2020, the phylogenetic and evolutionary analyses of diploid alfalfa had been done by 793.2 Mb genome sequencing, comprising 47,202 annotated protein-coding genes (Li et al., 2020). Worldwide, 162 autotetraploid alfalfa germplasms comprising 3.92 Mb of contig length covered 50% of the genome, and 49,165 annotated genes (Shen et al., 2020) have undergone phylogenetic and evolutionary analyses. The comparative and evolutionary analyses in these two research studies revealed that *Medicago sativa* L. diverged from *Medicago truncatula* approximately 5.2–8 million years ago (Li et al., 2020; Shen et al., 2020). Altogether, 220 global alfalfa core germplasms from China, Turkey, other Asian regions, America, and a mixed group from Europe and America were sequenced and characterized for their population structure, kinship, and population differentiation. In addition to these analyses, 875,023 high-quality SNPs, 350 common candidate genetic regions, and 686 genes were identified (Chen et al., 2021). Based on the results of these studies, alfalfa has a very high genetic diversity arising from a long history of cultivation and domestication.

ALFALFA FOR PHYTOREMEDIATION

With its long cultivation history and adaptability to a wide range of territories, alfalfa has been commonly used for animal feed (Biazzi et al., 2020). It has also been utilized as a medicinal herb since it is a good source of vitamins (A, C, E, and K), protein, and minerals such as calcium, potassium, phosphorus, and iron (for overview see https://www.webmd.com/vitamins/ai/ingredientmono-19/alfalfa). Apart from these uses, alfalfa is an ideal natural resource and model plant for remediation of contaminated soils, offering a variety of elite characteristics, including a highly productive biomass, drought tolerance, a fast-growing and prosperous root system, and availability in large amounts over several months of the year (Ren et al., 2018). Wild-type alfalfa has been used for phytoremediation of soils contaminated with heavy metals (Ju et al., 2020; He et al., 2021; Wang X et al., 2021) and organic pollutants (Chekol and Vough 2001).

The genetic engineering of plants is one of the advances in the field of phytoremediation, overcoming many of the obstacles of traditional phytoremediation (Aken et al., 2010; Rylott et al., 2015). The primary reason for the need to use transgenic plants for phytoremediation is that plants lack the necessary enzymatic machinery, which is involved in bacteria or mammals. Some of the genes or traits manipulated in transgenic plants for improved tolerance and phytoremediation potential are summarized by (Cherian and Oliveira 2005). Alternatively, the transgenic approach involves the incorporation of specific and useful genes into alfalfa to improve the traits of interest (Kumar 2011). In this review, we focus on the transgenic alfalfa plants for enhanced phytoremediation of POPs, such as atrazine, PCB and TCE, and petroleum and heavy metals (**Table 1**).

Phytoremediation for Removing Persistent Organic Pollutants

Persistent organic pollutants (POPs) are toxic organic chemicals that possess a combination of physical and chemical properties. They can persist in the environment for long periods because of high resistance to photolytic, chemical, and biological degradation (Mamirova et al., 2019). The 12 initial POPs, including pesticides, industrial chemicals, and by-products,

TABLE 1 | Transgenic alfalfa plants for enhancement of phytoremediation efficiency

Target plant	Gene (s)	Source	POPs and polluted environment	Class of POPs	Experimental condition	Result	Transgene effects	References
							Type of phytoremediation	
Bacterial genes transformed to alfalfa for phytoremediation								
Alfalfa (*Medicago sativa* L.)	*atzA* (modified according to plant codon usage)	Bacteria (*Pseudomonas* sp. strain ADP)	Atrazine – contamination	Atrazine – POPs, organic pesticides, herbicides	Laboratory experiment	Able to tolerate high concentration of atrazine and dechlorinated atrazine to hydroxyatrazine in leaves, stems, and roots	Phytodegradation	Wang et al. (2005)
Alfalfa (*Medicago sativa* L.)	*rhlA* (rhamnosyltransferase) gene	Bacteria (*Pseudomonas aeruginosa*)	Petroleum (rhamnolipids) contamination	Rhamnolipids	Laboratory experiment	Transgenic alfalfa expressing the *rhlA* gene and combined with microorganism increased the efficiency of oil degradation to 71 and 86%, respectively	Rhizodegradation	Stepanova et al. (2016)
Alfalfa (*Medicago sativa* L.)	*BphC.B* (2,3-dihydroxybiphenyl-1,2-dioxygenase) gene	Bacteria	Polychlorinated biphenyls (PCBs) and 2,4-dichlorophenol (2,4-DCP) mixed contamination	PCB – organichlorin	Laboratory experiment	Showed significantly higher biomass tolerance index, removal efficiency, and dissipation rates in deferent single and mixed contaminant concentrations of PCB and 2,4-dichlorophenol (2,4-DCP)	Phytodegradation	Wang et al. (2015)
Alfalfa (*Medicago sativa* L.)	*BphC*	Bacteria	tri-PCBs (PCB 16/PCB 32 and PCB 31/PCB 28) and tetra-PCB (PCB 49)	PCB – organichlorin	Laboratory experiment	Highest removal rate (33–81%) was observed for TAA treatment, followed by TA, WA, and NP (control) treatment	Phytodegradation	Ren et al. (2016)
Alfalfa (*Medicago sativa* L.)	*BphC*	Bacteria	PCB 5/2 and 4-DCP complex contaminant	PCB – organichlorin	Laboratory experiment	Showed highly cross-tolerant PCB and 4-DCP complex contamination	Phytodegradation	Ren et al. (2018)
Mammalian genes transformed to alfalfa for phytoremediation								
Alfalfa (*Medicago sativa* L.)	*GST* (Glutathione S-transferase) and human *CYP2E1* genes	Human	Cadmium (Cd) and trichloroethylene (TCE) mixed contamination	Cd – heavy metal; TCE – industrial chemical, organicchlorin, hexachlorobenzene	Laboratory experiment	Exhibited strong resistance towards the mixtures of Cd and TCE.	Phytodegradation	Zhang and Liu (2011)
Alfalfa (*Medicago sativa* L.)	*GST* and Human *CYP2E*1	Human	Mercury (Hg) and trichloroethylene (TCE) mixed contamination	Hg – heavy metal; TCE – industrial chemical, organicchlorin, hexachlorobenzene	Laboratory experiment	Able to grow and sustain growth at high concentrations of Hg/TCE with more fresh weight and longer root system	Phytodegradation	Zhang et al. (2013)
Overexpression of plant genes in alfalfa for phytoremediation								
Alfalfa (*Medicago sativa* L.)	ATP sulfurylase gene	*Arabidopsis thaliana*	Heavy metal	Heavy metal	Laboratory experiment	Transgenic alfalfa plants improved heavy metal tolerance and metal accumulation ability in the root and shoot tissues compared with non-transgenic plants	Accumulation	Kumar et al. (2019)

were listed in the Stockholm Convention (http://chm.pops.int/TheConvention/ThePOPs/ListingofPOPs/tabid/2509/Default.aspx). POPs are distributed in soil, sediments, air, and water. The five countries that use the most pesticides are China, the United States, Argentina, Thailand, and Brazil (Tarla et al., 2020). According to the official data of the Ministry of Agriculture of the Republic of Kazakhstan, 2,054 and 1,396 L of pesticides were used for non-agricultural purposes (weed control on roadsides) in 2018 and 2019, respectively (https://ipen.org/sites/default/files/documents/final_en_kazakhstan_hhp_report_summary_18_may_2020_0.pdf.). However, Nurzhanova et al. (2011) reported the total amount of obsolete pesticides in two regions (Almaty and Akmola) of Kazakhstan in 2011 to be 388.6 tons (Nurzhanova et al., 2011). A thorough analysis of the foci of pollution with POP pesticides and the development of methods for the remediation of contaminated areas is one of the key areas of the Kazakhstan Republic strategic development plan (Mamirova et al., 2019).

Climate change has the potential of affecting the behavior and distribution of organic pollutants, including POPs. Direct effects of climate change, like temperature increase, modification of wind and precipitation patterns, sea-level rise, snow, and ice cover, may alter the partitioning of POPs among the environmental compartments (Dalla Valle et al., 2007). The regular remediation strategies of POPs, comprising physical, chemical, and biological methods, have drawn considerable international attention over the past several decades because of such limitations as the cost-intensive, lower efficiency, and negative effects on natural habitats (Cherian and Oliveira 2005). Among these strategies, bioremediation and phytoremediation can be considered to be cost-effective, environmentally suitable, and appropriate for public acceptance (Ren et al., 2018). Bioremediation is a process used to clean up the contaminated environment, including water, soil, and subsurface materials, by microorganisms to detoxify and degrade the target pollutants. In this review, phytoremediation is examined in detail.

The term "phytoremediation" emerged in scientific research in the 1990s (Raskin et al., 1994; Salt et al., 1995) and refers to a green biotechnology using plants, associated microorganisms, and solar energy to clean hyper-accumulated toxic pollutants from the environment (Cobbett and Meagher 2002; Wu et al., 2015) and metabolize or transform them into less toxic metabolites (Cherian and Oliveira 2005). For example, the uptake and translocated processing of organic pollutants involve three detoxification stages. The first stage comprises conversion or transformation of the chemical compounds (oxidations by cytochrome P450 monooxygenases; reduction by dehydrogenases; and hydrolysis by esterases). The second stage is the conjugation to glutathione or sugars by glutathione-S-transferases or glycosyltransferases, leading to conjugated and frequently fewer toxic metabolites. The final stage is the compartmentation of these compounds in plant vacuoles or bound to the cell wall and lignin by the mechanism of ATP- or proton-dependent transporters or exocytosis (Schäffner et al., 2002; Cherian and Oliveira 2005). Phytoremediation is a better alternative approach that is appropriate for *in situ* degradation of pollutants over a large area and is cost-effective compared with the other methods. Besides these advantages, phytoremediation could support the creation of habitats for animals, promote biodiversity, reduce soil erosion by wind or water, help speed the restoration of damaged ecosystems, and supply nutrients for rhizosphere bacteria, allowing the growth and maintenance of a microbial community (Kumar et al., 2019).

Five special types of phytoremediation have been defined for removing POPs from the environment: 1) Phytodegradation, degrading organic pollutants in the soil or within the plant tissue through specific enzymes that the plant roots secrete; 2) Phytovolatilization, taking up pollutants from the soil or water and releasing them into the atmosphere through plant transpiration; 3) Phytostabilization, focusing mainly on soil pollutants near the roots, resulting in a reduction of soil erosion; 4) Phytoextraction, using the ability of plants or algae to remove contaminants from soil or water and concentrating them above ground in the plant biomass; 5) Phytostimulation, removing dangerous organic contaminants from soil using organisms within the rhizosphere (Nwoko 2010; Mishra et al., 2020) (**Figure 1**).

BACTERIAL GENES TRANSFORMED TO ALFALFA FOR PHYTOREMEDIATION

In the past 20 years, many pollutant-degrading bacteria have been isolated and characterized from polluted soils and reported to be capable of bioremediation or phytoremediation in various environments affected by different pollutants. The bacteria-associated plants exhibit contaminant degradation, growth-promoting activities, and carbon sequestration (Deng and Cao 2017). The role of bacteria in phytoremediation and some research examples on use of degradative bacteria for phytoremediation of heavy metals and organic compounds has been disclosed in several reviews (Kong and Glick 2017a; Kong and Glick 2017b; Mamirova et al., 2019; He et al., 2020; Tarla et al., 2020; Alkorta and Garbisu 2021; Basit et al., 2021; Girolkar et al., 2021; González Henao and Ghneim-Herrera 2021; Nedjimi 2021; Sharma 2021; Song et al., 2021; Gajić et al., 2022). González Henao and Ghneim-Herrera (2021), for instance, analyzed 85 research articles published over the past 15 years, which included a total of 62 bacterial genera, comprising 424 bacterial strains associated with 50 plant species in their systematic review article, which was published in Frontiers in Environmental Science in 2021. In this systematic review, *Agrobacterium*, *Bacillus*, *Klebsiella*, *Enterobacter*, *Microbacterium*, *Pseudomonas*, *Rhodococcus*, and *Mesorhizobium* were identified as the most commonly evaluated genera having crucial molecular mechanisms associated with plant growth promotion. In particular, *Klebsiella* and *Enterobacter* were considered as the best potential candidates for bioremediation and bacteria-assisted phytoremediation strategies in contaminated soil (González Henao and Ghneim-Herrera 2021). *Rhodococcus* is another genus famous for its ability to catabolize a wide range of organic compounds, including alkanes, cycloalkanes, and various aromatic hydrocarbons (Shevtsov et al., 2013).

Here, we summarize some studies not included in these reviews. Mello et al. (2020) noted that the plants inoculated with endophytic

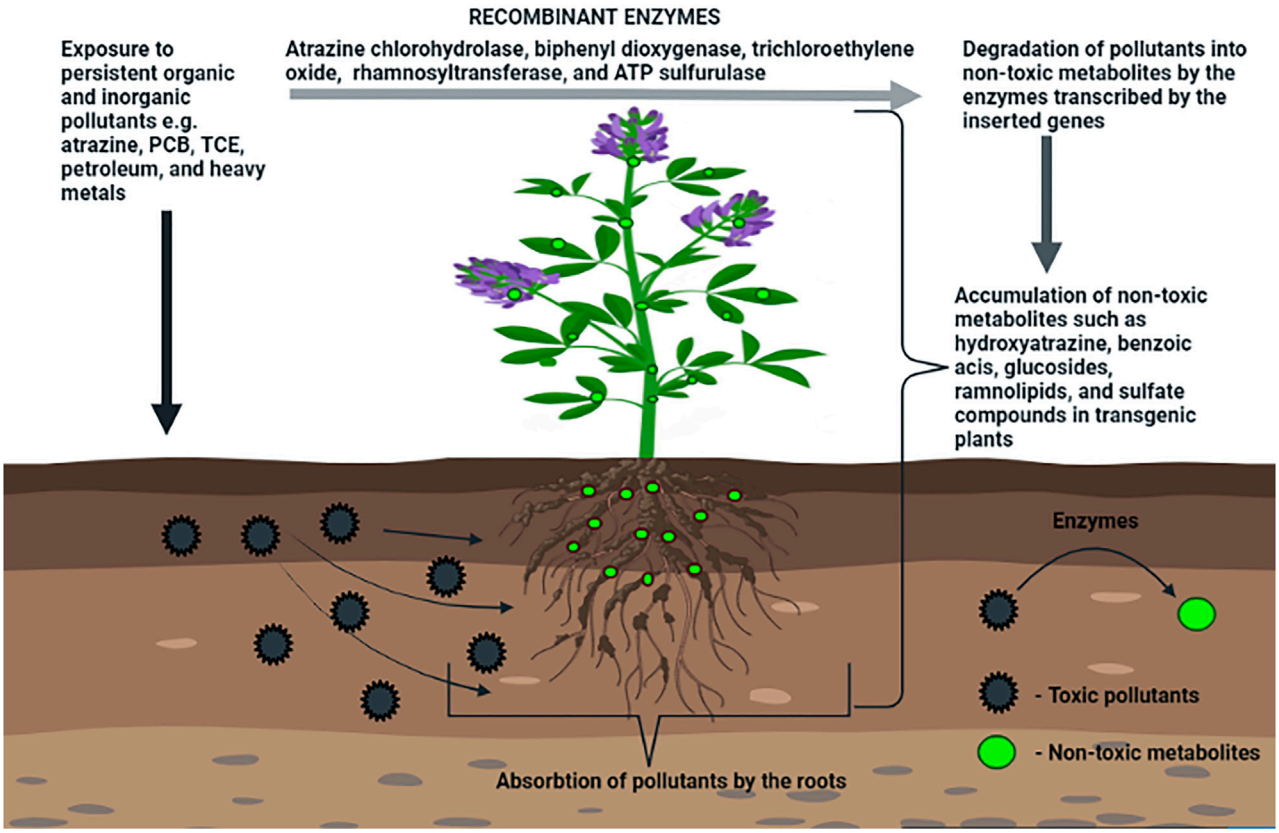

FIGURE 1 | Schematic representation of phytoremediation strategies by transgenic alfalfa plants. Phytoremediation processes by transgenic plants include phytoaccumulation (plants take up persistent organic and inorganic pollutants with soil water and store the contaminants in their tissues) and phytodegradation (metabolism of contaminants within plants due to expression of transgenes). The phytotoxic effects of atrazine, polychlorinated biphenyl (PCB), and petroleum are overcome by expressing the bacterial genes *AtzA, bphC, B,* and *rhlA*. Expression of mammalian genes *CYP2E1* and *GST* enhance degradation of trichloroethylene (TCE). Overexpression of plant gene *ATPS* improves heavy metal tolerance. Degradation of pollutants into non-toxic metabolites occurs by the enzymes transcribed by the inserted genes.

bacteria, including *Acinetobacter baumannii* BacI43, *Enterobacter* sp. BacI14, *Klebsiella pneumoniae* BacI20, *Pseudomonas* sp. BacI7, *Pseudomonas* sp. BacI38, and *Serratia marcescens* BacI56, had increased mercury volatilization and bioaccumulation in plant tissues. Anees et al. (2020) reported increased efficiency of Na phytoremediation by *Pseudomonas*, *Sanguibacter*, *Bacillus*, and *Bacillus* species. In the study of Yang et al. (2020), *Spartina alterniflora*-associated rhizo- and endobacterial communities showed resistance against at least one of the tested heavy metal ions. Mesa-Marín et al. (2020) reported that *S. ramosissima* was able to accumulate high concentrations of heavy metals, including arsenic, cadmium, copper, nickel, lead, and zinc. Silambarasan et al. (2020) revealed the feasibility of using the *Pseudomonas citronellolis* strain SLP6 to enhance phytostabilization of Cu-contaminated saline soils. The application of the *B. altitudinis* strain KP-14 remarkably increased the bio-parameters of *M. xgiganteus* cultivated on V, Cr, Mn, Ni, Cu, Zn, Sr, and Pb-contaminated soils and impacted phytoremediation parameters such as bioconcentration and translocation factors (Pidlisnyuk et al., 2020).

Bacteria-associated phytoremediation is used for heavy metals, as mentioned above, and is also used for organic compounds. In the study of Nurzhanova et al. (2021), *Bacillus vallismortis* and *Bacillus aryabhattai* were reported to have a high capability for utilization of dichlorodiphenyldichloroethylene (DDE). The biochemical and genomic characterization of 16 glyphosate-tolerant bacterial strains were described by Massot et al. (2021). As a result, they noted that *L. corniculatus* in combination with *O. haematophilum* can be adopted for phytoremediation of glyphosate on agricultural soils. These studies indicated that many microorganisms have the potential to degrade toxic compounds and are ideal candidates for bioremediation of various pollutants. The next goal of scientific research was the transgenic expression of bacterial genes on different plant species to improve phytoremediation efficiency.

Transgenic Alfalfa Plants Expressing Bacterial Atrazine Chlorohydrolase (*AtzA*) Gene for Phytoremediation

Atrazine (2-chloro-4-ethylamino-6-isopropylamino-1, 3, 5-triazine, molecular formula as C_8H_{14} ClN $_5$), a herbicide belonging to the triazine class, has been used worldwide for over 50 years as a chemical herbicide (Ye et al., 2016) for weed control due to its good weeding effect and low price (He Q et al., 2019). The annual use of atrazine globally is 70,000–90,000 tons. This herbicide induces oxidative stress, inflammation, mitochondrial dysfunction, and apoptosis in exposed cells. It also passes through biological barriers such as the blood–brain barrier and the blood–testis barrier (Sadeghnia et al., 2021). Studies aimed at removal of atrazine from the environment are important due to its stable structure, difficult degradation, long residence time in the environment, and toxicity to organisms and human beings. The advantages and disadvantages of various methods of atrazine degradation, including physicochemical, chemical, biological, and material-microbial-integrated aspects, were systematically reviewed recently by (He H et al., 2019).

Atrazine is degraded and mineralized to produce 15 metabolites or to remain chemically intact in soil. Among these identified metabolites, the four major ones are desethylatrazine, deisopropylatrazine, didealkylatrazine, and hydroxyatrazine (Houjayfa et al., 2020).

Atrazine catabolism is initiated by a plasmid-borne *atzA* gene encoding atrazine chlorohydrolase. It is the first enzyme that was discovered and purified from the soil organism *Pseudomonas* sp. strain ADP in the early 1990s (Souza et al., 1996). It catalyzes atrazine to hydroxyatrazine, which is a non-herbicidal, non-toxic, more strongly sorbed form (Wang et al., 2005). The open reading frame for chlorohydrolase was determined by sequencing to 1,419 nucleotides and encoding a 473-amino acid protein with a predicted subunit molecular weight of 52,421 (Souza et al., 1996).

The first transgenic alfalfa plants for phytoremediation were described together with tobacco and *Arabidopsis* plants expressing a codon-optimized *atzA* gene from *Pseudomonas* sp. strain ADP by Wang et al. (2005). The results showed that the transgenic alfalfa, tobacco, and *Arabidopsis* plants were not only able to survive and grow in the presence of atrazine up to 15 μg/ml in MS medium but could also dechlorinate atrazine to hydroxyatrazine up to 98.6% in leaves, stems, and roots (Wang et al., 2005).

Besides transgenic alfalfa plants, transgenic tobacco expressing *Pseudomonas sp. atzA* (Wang et al., 2010), transgenic rice (*Oryza sativa*) (Inui and Ohkawa 2005; Kawahigashi et al., 2005; Kawahigashi et al., 2006; Kawahigashi et al., 2008), and potato (Inui and Ohkawa 2005) expressing human *CYP1A1, CYP2B6,* or *CYP2C19*, potato expressing rat *CYP1A1* (Yamada et al., 2002), *Brassica juncea* overexpressing *Brassica juncea* γ-Glutamycysteine synthetase (γ-*ECS*, *GS*) gene, and *Nicotiana tabaccum* and *Medicago sativa* expressing *p-atzAa* gene (Wang et al., 2005) were used for the phytoremediation of atrazine and other herbicides, insecticides, and industrial chemicals.

Transgenic Alfalfa Plants Expressing Biphenyl Dioxygenase (*bphC, B*) Gene for Phytoremediation of Polychlorinated Biphenyl Contamination

PCBs are organic chemicals of chlorinated hydrocarbons. PCB has been applied for industrial and agricultural purposes since 1930 because of its unique physical and chemical properties. The production of PCB was stopped around the late 1970s to the early 1980s worldwide because of its high toxicity and negative impact on fauna, flora, and human health. The efficiency of bioremediation of PCB-polluted objects depends strongly on degree of pollution (Vasil'eva and Strizhakova 2007).

Biphenyl dioxygenase is the first enzyme of the bacterial catabolic pathway involved in the degradation of polychlorinated biphenyls; it catalyzes the ring cleavage reaction of 2,3-dihydroxybiphenyl into 2-hydroxy-6-oxo-6-phenyl-hexa-2,4-dienoic acid. In 2015, Wang et al. generated transgenic alfalfa plants expressing 2, 3-dihydroxybiphenyl-1, 2-dioxygenase gene (*bphC, B*) from bacteria to degrade PCB, 2,4-dichlorophenol (2,4-DCP), and mixed contamination of PCB 5/2,4-DCP. Their results showed that, firstly, the transgenic lines expressing *bphC* and *bphB* genes had a higher fresh weight with 34% higher tolerance index and higher dissipation rates of PCBs in root and shoot in a hydroponic medium containing 0.075 mg/L PCBs at the seeding stage. Secondly, the bphC, bphB transgenic lines had significantly higher biomass and tolerance index and showed 98.8% removal efficiency in 25 mg/L 2,4-DCP treatment after 144 h. Thirdly, the bphC, bphB transgenic lines were able to sustain growth in PCB 5/2,4-DCP mixed contaminants at a concentration up to 120/50 mg/L, whereas wild-type alfalfa plants could scarcely survive in a 40/10 mg/L concentration (Wang et al., 2015).

Apart from PCBs, biphenyl dioxygenase can catalyze the oxygenation of many persistent xenobiotics such as polyaromatic hydrocarbons (PAHs), chlorodibenzofurans, and chlorodioxins (Wackett et al., 2002). Various biphenyl dioxygenase genes have been characterized and cloned in different bacterium strains (Erickson and Mondello 1992; Taira et al., 1992; Sylvestre et al., 1996). The possibility of cloning of the *bphC* gene encoding 2,3-dihydroxybiphenyl-1,2-dioxygenase, from the *Comamonas testosteroni* B-356 and *Pandoraea pnomenusa* B-356, was demonstrated by Novakova et al. (2009), Novakova et al. (2010) for the production of transgenic tobacco plants to remediate of PCBs. However, only the transgenic expression of the targeted gene was reported; the remediation efficiency for PCB was not tested (Novakova et al., 2009; Novakova et al., 2010).

Low water solubility is one of the major limitations in bioremediation processes of PCBs (Wang et al., 2014). Therefore, it is known that the solubilization of high-chlorinated PCBs using biosurfactants is an effective and eco-friendly approach. For example, biosurfactant AlnA protein from *Acinetobacter radioresistens* was first used to enhance the solubility and bioavailability of PCB in soil (Wang et al., 2014). Thereafter, in 2016, Ren et al. described some crucial physiological traits and PCB remediation efficiency under four

treatments, i.e. transgenic alfalfa plants expressing *bphC* gene with the combination of biosurfactant AlnA protein (TAA treatment), transgenic alfalfa (TA), wild-type alfalfa (WT), and unplanted soil (NP) for PCB-contaminated soil. The highest removal rate (33%–81%) was observed for TAA treatment, followed by TA, WA, and NP (control) treatments (Ren et al., 2016). In 2018, Ren et al. described the transgenic alfalfa plant tolerance to the combination of PCB 5 and 2,4-DCP. The tested transgenic alfalfa plant exhibited strong resistance up to 120/50 mg/L of PCB 5/2, 4-DCP complex contaminants without any visual evidence of damage. Higher remediation efficiency was observed in the use of transgenic alfalfa plants with the combination of recombinant AlnA protein than in the transgenic alfalfa mutants (Ren et al., 2018). In both studies of Ren et al, the microbial community composition of contaminated soil was analyzed, and it showed a different distribution of the phylum and genus of microorganisms. These results suggest that the detected abundance of indigenous microorganisms by transgenic alfalfa plants with the combination of biosurfactant AlnA protein increases PCB degradation (Ren et al., 2016; Ren et al., 2018).

Transgenic Alfalfa Plants Expressing Rhamnosyltransferase (*rhlA*) Gene for Phytoremediation of Petroleum Contamination

Petroleum hydrocarbons are highly toxic to the environment because of their inherent properties like solubility, volatility, and biodegradability (Hatami et al., 2019). However, the low water solubility and dissolution rate of oil products negatively affect the biodegradation efficiency of oil. The main method for phytoremediation of oil-polluted soil is rhizodegradation. In this context, oil is known to be effectively utilized not only by bacteria but also by fungi. Therefore, most studies focus on assessing the influence of petroleum remediation with the most frequent bacterial species of *Pseudomonas fluorescens* (Gutiérrez et al., 2020), *Pseudomonas aeruginosa* (Wang et al., 2017; Dobler et al., 2020; Varjani et al., 2020; Varjani and Upasani 2021), and *Bacillus subtilis* (Montagnolli et al., 2015; Chen et al., 2017; Wang et al., 2019), and some fungi, including *Candida* and *Yarrowia,* have a great potential for phytoremediation (Salam et al., 2017; Cecchi et al., 2021). Some review studies recommend the use of fungi for petroleum phytoremediation since fungi are capable of utilizing a wider spectrum of hydrocarbons, element cycling, bioweathering, and mycogenic mineral formation (Deng and Cao 2017).

Rhamnolipids, glycolipid biosurfactants produced by various bacterial species such as *Pseudomonas* sp. and *Burkholderia* sp. can enhance the bioavailability of oil and are therefore widely applied for crude oil biodegradation (Chong and Li 2017). The chemical structure of different identified rhamnolipids and their microbial origins and roles have been thoroughly discussed by Abdel-Mawgoud et al. (Abdel-Mawgoud et al., 2010). Due to the antimicrobial properties of rhamnolipids, they have potential applications in crop protection to confer immunity against fungal and bacterial pathogens [for an extensive review, see (Crouzet et al., 2020)]. Rhamnolipids are well known to also protect plants from harmful effects of metals (Singh and Cameotra 2013; Ayangbenro and Babalola 2018).

Rhamnolipid biosynthesis is regulated exclusively by key enzymes such as RhlA, RhlB, and RhlC, which are found in *Pseudomonas* sp. and *Burkholderia* sp (Zheng et al., 2015; Chong and Li 2017). Early in 1994, the necessity of the *RhiR* gene, which encodes rhamnosyltransferase, for rhamnolipid biosynthesis, was confirmed clearly by Ochsner et al. (1994). In their study, a single open reading frame of the *RhiR* gene, which regulated rhamnolipid biosynthesis from the strain PG201 of *P. aeruginosa,* was cloned into a rhamnolipid-deficient mutant strain (65E12) of *P. aeruginosa* (Ochsner et al., 1994). The results of this research provided a platform for use of genes encoding rhamnosyltransferase to enhance phytoremediation of petroleum-contaminated soil. Therefore, the transgenic expression of rhamnosyltransferase genes in different plant species for increased phytoremediation capacity of the oil has been investigated extensively. For example, Stepanova et al. (2016) evaluated the rationale for using transgenic alfalfa plants expressing the *rhlA* gene encoding rhamnosyltransferase from *Pseudomonas aeruginosa* and combined with *Candida maltosa* for remediation of oil-polluted soil. They identified increasing efficiency of oil degradation of up to 86%, whereas 71% oil degradation was observed by using transgenic alfalfa expressing the *rhlA* gene without the combination (Stepanova et al., 2016). Similarly, transgenic *Arabidopsis thaliana* and *Nicotiana tabacum* expressing *RhlA* and *RhlB* genes from *Pseudomonas* sp. showed tolerance to crude oil and several metals, and higher degradation efficiency was obtained with oil hydrocarbons (27%) than with the wild type (2%) (Brychkova et al., 2004).

MAMMALIAN GENES TRANSFORMED TO ALFALFA FOR PHYTOREMEDIATION

Cytochrome P450s are a family of monooxygenases that catalyze the oxidation and metabolism of a diverse range of xenobiotics and endogenous compounds (Shankar and Mehendale 2014; Cook et al., 2016). CYP450s enzymes are found in all kingdoms of life: animals (over 13,000), plants (over 16,000), fungi (more than 85,000), and bacteria (more than 62,000) (Lamb et al., 2009; Nelson 2018). In 2009, David Nelson created a platform named "The Cytochrome P450 Homepage", which provides information on evolutionary schemes of 11,512 CYPs, confirming that members of CYP families and subfamilies were from common ancestors (Nelson 2009) (http://drnelson.utmem.edu/CytochromeP450.html). Therefore, in 2018, more than 300,000 CYP450s sequences in plants, vertebrates, fungi, bacteria, and prokaryotic have been mined and collected, and more than 41,000 CYP sequences have been sorted into clans, families, and subfamilies in preparation for naming by BLAST searches (Nelson 2018). In plants, CYP450s can catalyze more than 20 types of reactions in primary and secondary metabolism (Mizutani 2012; Shang and Huang 2020; Wang H et al., 2021). The database of 181 plant P450s was constructed based on sequences, structures, and functions (PCPD: http://p450.biodesign.ac.cn/) (Wang et al., 2015). The role of mammalian cytochrome P450s in the metabolism of xenobiotics has been investigated in much more detail than plant CYPs.

Overexpression of mammalian genes in appropriate plant species results in effective phytoremediation by enhancing the metabolic activities of the plant.

Transgenic Alfalfa Plant Co-expressing Human *CYP2E1* and *GST* Genes for Phytoremediation of Trichloroethylene (TCE) Contamination

Trichloroethylene (TCE) is a non-flammable, sweet-smelling, colorless, and chlorinated organic compound that has been used extensively as an industrial solvent and degreaser (Dumas et al., 2018). It is the most common halogenated organic pollutant in the environment. As shown by Li *et* al. (2019), the high concentration of TCE (greater than 10 mg/kg) negatively affects the carbon and nitrogen cycling and metabolism of soil microorganisms. As a result, soil quality declines and soil decomposition of organic matter and cycling of mineral nutrients are inhibited (Li et al., 2019).

Phytoremediation of TCE can be accomplished using transgenic plants expressing mammalian genes. For instance, one of the key enzymes in mammalian metabolism *CYP2E1* co-expressed with *glutathione S-transferase* (*GST*) gene in transgenic alfalfa plants showed healthy growth in the coexistence of TCE (0.2 mmol/L) and CdSO 4 (0.15 mmol/L) compared with the transgenic alfalfa plants expressing a single gene (GST or CYP2E1) and the non-transgenic control plants (Zhang and Liu 2011). In 2013, the same study was done on enhancing remediation of mixed mercury (Hg) and TCE by the transgenic alfalfa plants co-expressing *GST* and human *P450 2E1*. The result showed that the transgenic alfalfa plants were able to grow in up to 50/500 μM Hg/TCE and sustain growth at concentrations of 20/200 μM of Hg/TCE mixed-contaminated MS medium, accumulating Hg/TCE from 2.6- to 4.2-fold more than the non-transgenic plants. Additionally, the transgenic alfalfa plants had 3.0-fold more fresh weight at 40/400 μM Hg/TCE soil treatment and longer roots at 20/200 μM Hg/TCE soil treatment than non-transgenic plants in mixed-contaminated soil (Zhang et al., 2013).

In the past decade, the *CYP2E1* gene has been introduced into various plants, including tobacco, poplar, *Sesbania grandiflora*, and *Arabidopsis* thaliana plants, for phytoremediation of different contaminations, including TCE (Doty et al., 2000; Doty et al., 2007; James et al., 2008; Legault et al., 2017), and DDT (Mouhamad et al., 2012).

As discussed earlier, GSTs are a group of small proteins (200–250 amino acids) (Gao et al., 2020) that are critical for certain life processes, as well as for detoxication and toxification mechanisms of pharmaceuticals and environmental pollutants (Nebert and Vasiliou 2004). The *GST* gene has been introduced in various plants, including tobacco to enhance polyaromatic hydrocarbon degradation (Dixit et al., 2011) and *Arabidopsis* to enhance trichlorophenol degradation (Su et al., 2012). Besides phytoremediation purposes, some studies have indicated that silencing or overexpression of the *GST* gene in various plants significantly increased resistance to different stressors (reviewed in (Kumar and Trivedi 2018).

OVEREXPRESSION OF PLANT GENES IN ALFALFA FOR PHYTOREMEDIATION

Transgenic Alfalfa Plants Overexpressing *Arabidopsis* ATP Sulfurylase Gene for Phytoremediation of Heavy Metal Contamination

High concentrations of non-essential heavy metals and metalloids (arsenic, cadmium, and lead) are a threat to fauna and flora, even to human health (González Henao and Ghneim-Herrera 2021). ATP sulfurylase is the first and key enzyme in the sulfate assimilation pathway in plants. Four *ATPS* genes (*ATPS1, -2, -3,* and *-4*) are present in both chloroplasts and the cytosol of *Arabidopsis* leaves (Bohrer et al., 2015). The study of Kumar et al. (2019) demonstrated that transgenic alfalfa plants expressing ATP sulfurylase gene from *Arabidopsis* improved heavy metal (cadmium, vanadium, nickel, copper, and lead) tolerance and metal accumulation ability in the root and shoot tissues compared with non-transgenic plants. Some studies have shown that overexpression of the ATP sulfurylase gene in Indian mustard plants (*Brassica juncea* L) led to a higher tolerance and accumulation of Se (Pilon-Smits et al., 1999; LeDuc et al., 2006), As(III), As(V), Cd, Cu, Hg, and Zn (Wangeline et al., 2004).

DISCUSSION AND FUTURE PROSPECTS

Improvement of the Use of Local Plant Species for Phytoremediation

Numerous plant species have been identified for the purpose of phytoremediation [reviewed in (Cherian and Oliveira 2005)]. However, the phytoremediation process is limited by seasonal and local climatic conditions. There are some studies on the use of local plant species for phytoremediation of crude oil (Ho and Juan 2018; Abbaspour et al., 2020), industrial wastewater (Al-Thani and Yasseen 2020), and metal contamination (Hu et al., 2020). Nurzhanova et al. (2013) have provided a list of 17 pesticide-tolerant plants, including biannual plant sp *E. canadensis*, *B. vulgaris*, *O. acanthium, A. absinthium*, *A. cylindrica*, and *R. confertus,* and *A. annua*, *X. strumarium*, *K. scoparia*, *K. sieversiana*, *A. tricolor*, *S. dulcamara,* and *A. artemisifoli* from the Karasajsk district of Almaty oblast in Kazakhstan (Nurzhanova et al., 2013). It is important to identify readily available local plant species for effective phytoremediation of different organic and inorganic pollutants in the local conditions.

Phytoremediation Process Needs to Establish a Healthy Soil Ecosystem

The purpose of phytoremediation is not only to clean the polluted environment but also to establish a healthy soil ecosystem based on restoring the aboveground vegetation and stability of the underground soil microbial community composition. On this topic, Ren and his team have published significant studies, as outlined above, and provide a good protocol for future researchers. Alfalfa has been proposed as an ideal candidate for effective remediation approaches (Ren et al., 2016; Ren et al., 2018).

Metabolism of Pollutants in Plant Cells to Inert Forms Is Most Desirable

There are several requirements for plants used for successful phytoremediation. First, a well-developed root system is necessary. Second, the plants must produce sufficient biomass to remediate widespread high concentrations of pollutants in the field. Third, the plants must have the ability to metabolize and immobilize the pollutants. Fourth, the plants used in phytoremediation should be widely used in agricultural practice that allows repeated planting and harvesting (Paz-Alberto 2013; Eapen and D'Souza 2005). In this case, one limitation with some forms of phytoremediation is that plants can move pollutants from the ground and transpire them unaltered into the air.

To meet the abovementioned requirements: first, a better understanding is needed of the mechanisms underlying organic and inorganic pollutant accumulation and tolerance of plants. Second, utilization of plant-associated bacteria must be enhanced. Third, transgenic plants expressing bacterial and mammalian genes capable of degrading different pollutants must be generated. Fourth, transgenic plants together with microorganisms and biosurfactant to increase phytoremediation efficiency should be used.

The Main Problem Is Mixed Contamination of the Environment

One of the main problems with remediation of the contaminated environment is that there is generally contamination with multiple chemicals, often including both heavy metals and organic compounds (Olaniran et al., 2013). Most soil remediation strategies are adjusted to "focus on" single contaminant systems. It is essential to use an effective remediation method to clean up mixed contaminated areas.

Solutions to these problems: first, the combination of plants and microorganisms is nowadays often recommended for mixed contaminated soils. Second, the plants that contain genes enabling them to remediate a wider range of pollutants are desirable. The use of transgenic plants co-expressing desirable genes can be used in a variety of ways to increase the effectiveness of phytoremediation. For example, the utilization of transgenic alfalfa plants co-expressing human CYP2E1 and *GST* genes for phytoremediation of Hg/TCE contaminations yielded positive results compared with non-transgenic plants or transgenic alfalfa plants expressing a single gene (GST or CYP2E1) (Zhang and Liu 2011; Zhang et al., 2013).

The Field Experiment of Transgenic Plants for Phytoremediation Must Be Extended

To our knowledge, most studies on phytoremediation, especially on transgenic plants, have been done only in the laboratory, not in field conditions. There are many challenges to using phytoremediation successfully under natural conditions. The process of creating transgenic plants and adaptation in field conditions requires much time and labor. For example, Legault et al. (2017) spent 6 years on the field study of transgenic poplar expressing cytochrome P450 2E1 to enhance degradation of TCE. Phytoremediation in field conditions requires large areas, and the transgenic plants are limited in number. Another challenge is that while transgenic plants bring favorable advantages to phytoremediation, there are many concerns regarding human health and environmental sustainability (Gunarathne et al., 2019). Thus, appropriate political management and investigation of the status of transgenic plants for wide growth in polluted areas are needed.

Identification of Unique Genes From Hyperaccumulators and Introduction of These Key Genes Into Suitable Plant Species

About 400 plant species considered hyperaccumulators that can accumulate high concentrations of pollutants through their root system are being applied in phytoremediation. However, traditional hyperaccumulators require an extensive period, even years, for remediation of polluted areas. Besides this, there are other potential limitations of phytoremediation such as incomplete metabolism, toxic metabolites, and lower detoxification capacity (Gunarathne et al., 2019). However, the identification and proof of unique genes from the hyperaccumulators and transferring them to fast-growing species have been shown to be highly beneficial by the advanced transgenic technologies. In this case, alfalfa is a model legume for creating transgenic lines.

Genome Editing Plants for Phytoremediation

Genome editing systems, such as CRISPR/Cas, have been used for trait improvement of tubers, fibers, and cereal crops (Gao et al., 2017; Liu et al., 2021; Tussipkan and Manabayeva 2021). To our knowledge, there are few studies on using the CRISPR/Cas9 system for the enhancement of phytoremediation efficiency. Despite the genome sequence of alfalfa (*Medicago sativa* L.) being known, no genome-edited alfalfa plants used for phytoremediation have been obtained. Thus, it is an important research task to find and knock out sensitive genes by the CRISPR/Cas system to enhance the phytoremediation efficiency of alfalfa. Knocking out sensitive genes has a great significance in trait improvement for crops. Tang et al. (2017) and Yang et al. (2019) reported that knocking out the metal transporter gene *OsNramp5* using the CRISPR/Cas9 system showed low Cd accumulation in rice. (Tang et al., 2017; Yang et al., 2019).

AUTHOR CONTRIBUTIONS

TD and MS wrote the manuscript together. All authors contributed to the article and approved the submitted version.

FUNDING

This work is supported by a grant from the Ministry of Education and Science of the Republic of Kazakhstan (grant number: AP09260362).

REFERENCES

Abbaspour, A., Zohrabi, F., Dorostkar, V., Faz, A., and Acosta, J. A., (2020). Remediation of an Oil-Contaminated Soil by Two Native Plants Treated with Biochar and Mycorrhizae. *J. Environ. Manage.* 254, 109755. doi:10.1016/j.jenvman.2019.109755

Abdel-Mawgoud, A. M., Lépine, F., and Déziel, E. (2010). Rhamnolipids: Diversity of Structures, Microbial Origins and Roles. *Appl. Microbiol. Biotechnol.* 86 (5), 1323–1336. doi:10.1007/s00253-010-2498-2

Aken, B. V., Correa, P. A., and Schnoor, J. L. (2010). Phytoremediation of Polychlorinated Biphenyls: New Trends and Promises. *Environ. Sci. Technol.* 44 (8), 2767–2776. doi:10.1021/es902514d

Al-Thani, R. F., and Yasseen, B. T. (2020). Phytoremediation of Polluted Soils and Waters by Native Qatari Plants: Future Perspectives. *Environ. Pollut.* 259, 113694. doi:10.1016/j.envpol.2019.113694

Alkorta, I., and Garbisu, C. (2021). Reflections and Insights on the Evolution of the Biological Remediation of Contaminated Soils. *Front. Environ. Sci.* 9, 734628. doi:10.3389/fenvs.2021.734628

Anees, M., Qayyum, A., Jamil, M., Rehman, F. u., Abid, M., Malik, M. S., et al. (2020). Role of Halotolerant and Chitinolytic Bacteria in Phytoremediation of saline Soil Using Spinach Plant. *Int. J. phytoremediation.* 22 (6), 653–661. doi:10.1080/15226514.2019.1707160

Ayangbenro, A., and Babalola, O. (2018). Metal(loid) Bioremediation: Strategies Employed by Microbial Polymers. *Sustainability.* 10, 3028. doi:10.3390/su10093028

Badr, A., El-Sherif, N., Aly, S., Ibrahim, S. D., and Ibrahim, M. (2020). Genetic Diversity Among Selected Medicago Sativa Cultivars Using Inter-retrotransposon-amplified Polymorphism, Chloroplast DNA Barcodes and Morpho-Agronomic Trait Analyses. *Plants.* 9 (8), 995. doi:10.3390/plants9080995

Basit, A., Shah, S. T., Ullah, I., Muntha, S. T., and Mohamed, H. I. (2021). Microbe-assisted Phytoremediation of Environmental Pollutants and Energy Recycling in Sustainable Agriculture. *Arch. Microbiol.* 203 (10), 5859–5885. doi:10.1007/s00203-021-02576-0

Biazzi, E., Nelson, N., Pecetti, L., and Annicchiarico, P. (2020). "GBS-based Genome-wide Association and Genomic Selection for Alfalfa (Medicago Sativa) Forage Quality Improvement," in *The Model Legume Medicago Truncatula*, 923–927. doi:10.1002/9781119409144.ch118

Blondon, F., Marie, D., Brown, S., and Adam, K. (1994). Genome Size and Base Composition in Medicago Sativa and M. Truncatula Species. *Genome.* 37 (2), 264. doi:10.1139/g94-037

Bohrer, A. S., Yoshimoto, N., Ai, S., Rykulski, N., Saito, K., and Takahashi, H. (2015). Alternative Translational Initiation of ATP Sulfurylase Underlying Dual Localization of Sulfate Assimilation Pathways in Plastids and Cytosol in Arabidopsis thaliana. *Front. Plant Sci.* 5, 750. doi:10.3389/fpls.2014.00750

Brychkova, G. G., Sorokin, A. P., and Kartel, N. A. (2004). Bioremediation with Ecologically Safe Plants. *NATO Science Series. Ser.* 1, 147–158.

Cecchi, G., Cutroneo, L., Di Piazza, S., Besio, G., Capello, M., and Zotti, M. (2021). Port Sediments: Problem or Resource? A Review Concerning the Treatment and Decontamination of Port Sediments by Fungi and Bacteria. *Microorganisms.* 9 (6), 1279. doi:10.3390/microorganisms9061279

Chekol, T., and Vough, L. (2001). A Study of the Use of Alfalfa (Medicago Sativa L.) for the Phytoremediation of Organic Contaminants in Soil. *Remediation J.* 11, 89–101. doi:10.1002/rem.1017

Chen, L., He, F., Long, R., Zhang, F., Li, M., Wang, Z., et al. (2021). A Global Alfalfa Diversity Panel Reveals Genomic Selection Signatures in Chinese Varieties and Genomic Associations with Root Development. *J. Integr. Plant Biol.* 63 (11), 1937–1951. doi:10.1111/jipb.13172

Chen, Q., Li, J., Liu, M., Sun, H., and Bao, M. (2017). Study on the Biodegradation of Crude Oil by Free and Immobilized Bacterial Consortium in marine Environment. *PLoS One.* 12 (3), e0174445. doi:10.1371/journal.pone.0174445

Cherian, S., and Oliveira, M. M. (2005). Transgenic Plants in Phytoremediation: Recent Advances and New Possibilities. *Environ. Sci. Techn.* 39 (24), 9377–9390. doi:10.1021/es051134l

Chong, H., and Li, Q. (2017). Microbial Production of Rhamnolipids: Opportunities, Challenges and Strategies. *Microb. Cel Factories.* 16 (1), 137. doi:10.1186/s12934-017-0753-2

Cobbett, C. S., and Meagher, R. B. (2002). Arabidopsis and the Genetic Potential for the Phytoremediation of Toxic Elemental and Organic Pollutants. *Arabidopsis Book.* 1, e0032. doi:10.1199/tab.0032

Cook, D. J., Finnigan, J. D., Cook, K., Black, G. W., and Charnock, S. J. (2016). "Chapter Five - Cytochromes P450: History, Classes, Catalytic Mechanism, and Industrial Application," in *Advances in Protein Chemistry and Structural Biology*. Editor C. Z. Christov (Academic Press), 105–126. doi:10.1016/bs.apcsb.2016.07.003

Crouzet, J., Arguelles-Arias, A., Dhondt-Cordelier, S., Cordelier, S., Pršić, J., Hoff, G., et al. (2020). Biosurfactants in Plant Protection against Diseases: Rhamnolipids and Lipopeptides Case Study. *Front. Bioeng. Biotechnol.* 8, 1014. doi:10.3389/fbioe.2020.01014

Dalla Valle, M., Codato, E., and Marcomini, A. (2007). Climate Change Influence on POPs Distribution and Fate: A Case Study. *Chemospher* 67 (7), 1287–1295. doi:10.1016/j.chemosphere.2006.12.028

Deng, Z., and Cao, L. (2017). Fungal Endophytes and Their Interactions with Plants in Phytoremediation: A Review. *Chemosphere.* 168, 1100–1106. doi:10.1016/j.chemosphere.2016.10.097

Dixit, P., Mukherjee, P. K., Sherkhane, P. D., Kale, S. P., and Eapen, S. (2011). Enhanced Tolerance and Remediation of Anthracene by Transgenic Tobacco Plants Expressing a Fungal Glutathione Transferase Gene. *J. Hazard. Mater.* 192 (1), 270–276. doi:10.1016/j.jhazmat.2011.05.018

Dobler, L., Ferraz, H. C., Araujo de Castilho, L. V., Sangenito, L. S., Pasqualino, I. P., Souza Dos Santos, A. L., et al. (2020). Environmentally Friendly Rhamnolipid Production for Petroleum Remediation. *Chemosphere.* 252, 126349. doi:10.1016/j.chemosphere.2020.126349

dos Santos, I. G., Rocha, J. d., Vigna, B. B., Damião Cruz, C., Ferreira, R., Basigalup, D. H., et al. (2020). Exploring the Diversity of Alfalfa within Brazil for Tropical Production. *Euphytica.* 216 (5), 72. doi:10.1007/s10681-020-02606-w

Doty, S., James, C., Moore, A., Vajzovic, A., Singleton, G., Ma, C., et al. (2007). Enhanced Phytoremediation of Volatile Environmental Pollutants with Transgenic Trees. *Proc. Natl. Acad. Sci. U. S. A.* 104, 16816–16821. doi:10.1073/pnas.0703276104

Doty, S. L., Shang, T. Q., Wilson, A. M., Tangen, J., Westergreen, A. D., Newman, L. A., et al. (2000). Enhanced Metabolism of Halogenated Hydrocarbons in Transgenic Plants Containing Mammalian Cytochrome P450 2E1. *Proc. Natl. Acad. Sci. U. S. A.* 97 (12), 6287–6291. doi:10.1073/pnas.97.12.6287

Dumas, O., Despreaux, T., Perros, F., Lau, E., Pascal, A., Humbert, M., et al. (2018). Respiratory Effects of Trichloroethylene. *Respir. Med.* 134, 47–53. doi:10.1016/j.rmed.2017.11.021

Eapen, S., and D'Souza, S. F. (2005). Prospects of Genetic Engineering of Plants for Phytoremediation of Toxic Metals. *Biotechnol. Adv.* 23 (2), 97–114. doi:10.1016/j.biotechadv.2004.10.001

Erickson, B. D., and Mondello, F. J. (1992). Nucleotide Sequencing and Transcriptional Mapping of the Genes Encoding Biphenyl Dioxygenase, a Multicomponent Polychlorinated-Biphenyl-Degrading Enzyme in Pseudomonas Strain LB400. *J. Bacteriol.* 174 (9), 2903–2912. doi:10.1128/jb.174.9.2903-2912.1992

Gajić, G., Mitrović, M., and Pavlović, Pa. (2022). "Chapter 12 - Phytobial Remediation by Bacteria and Fungi," in *Assisted Phytoremediation*. Editor V. Pandey (Elsevier), 285–344.

Gao, J. J., Zhang, L., He Peng, R., Wang, B., and QuanYao, H. (2020). Recombinant Expression of Thermosynechococcus Elongatus BP-1 Glutathione S-Transferase in Arabidopsis thaliana : an Efficient Tool for Phytoremediation of Thiocyanate. *Biotechnol. Biotechnological Equipment.* 34 (1), 494–505. doi:10.1080/13102818.2020.1779127

Gao, W., Lu, L., Tian, X., Xu, F., Liu, J., Singh, P. K., et al. (2017). Genome Editing in Cotton with the CRISPR/Cas9 System. *Front. Plant Sci.* 8, 1364. doi:10.3389/fpls.2017.01364

Girolkar, S., Thawale, P., and Juwarkar, A. (2021). "Chapter 12 - Bacteria-Assisted Phytoremediation of Heavy Metals and Organic Pollutants: Challenges and Future Prospects," in *Bioremediation for Environmental Sustainability*. Editors V. Kumar, G. Saxena, and M. P. Shah (Elsevier), 247–267. doi:10.1016/b978-0-12-820318-7.00012-5

González Henao, S., and Ghneim-Herrera, T. (2021). Heavy Metals in Soils and the Remediation Potential of Bacteria Associated with the Plant Microbiome. *Front. Environ. Sci.* 9 (15), 604216. doi:10.3389/fenvs.2021.604216

Gunarathne, V., Mayakaduwa, S., Ashiq, A., Ranjani Weerakoon, S., Biswas, J. K., and Vithanage, M. (2019). "Chapter 5 - Transgenic Plants: Benefits, Applications, and Potential Risks in Phytoremediation," in *Transgenic Plant Technology for Remediation of Toxic Metals and Metalloids*. Editor M. Vara Prasad (Academic Press), 89–102. doi:10.1016/b978-0-12-814389-6.00005-5

Gutiérrez, E. J., Abraham, M. D. R., Baltazar, J. C., Vázquez, G., Delgadillo, E., and Tirado, D. (2020). Pseudomonas Fluorescens: A Bioaugmentation Strategy for Oil-Contaminated and Nutrient-Poor Soil. *Int. J. Environ. Res. Public Health.* 17 (19), 6959. doi:10.3390/ijerph17196959

Hatami, E., Ali, A., and Dorostkar, V. (2019). Phytoremediation of a Petroleum-Polluted Soil by Native Plant Species in Lorestan Province, Iran. *Environ. Sci. Pollut. Res.* 26 (24), 24323–24330. doi:10.1007/s11356-018-1297-7

Havananda, T., Brummer, C., and Doyle, J. (2011). Complex Patterns of Autopolyploid Evolution in Alfalfa and allies(Medicago Sativa; Leguminosae). *Am. J. Bot.* 98, 1633–1646. doi:10.3732/ajb.1000318

Hawkins, C., and Yu, L-X. (2018). Recent Progress in Alfalfa (Medicago Sativa L.) Genomics and Genomic Selection. *Crop J.* 6 (6), 565–575. doi:10.1016/j.cj.2018.01.006

He, H., Wu, M., Su, R., Zhang, Z., Chang, C., Qi, P., et al. (2021). Strong Phosphorus (P)-zinc (Zn) Interactions in a Calcareous Soil-Alfalfa System Suggest that Rational P Fertilization Should Be Considered for Zn Biofortification on Zn-Deficient Soils and Phytoremediation of Zn-Contaminated Soils. *Plant and Soil.* 461 (1), 119–134. doi:10.1007/s11104-020-04793-w

He, H., Liu, Y., You, S., Liu, J., Xiao, H., and Tu, Z. (2019). A Review on Recent Treatment Technology for Herbicide Atrazine in Contaminated Environment. *Int. J. Environ. Res. Public Health.* 16 (24), 5129. doi:10.3390/ijerph16245129

He, Q., Li, Y. Y., Liu, Y. L., Li, Z. P., Sun, S. S., and Zhan, Q. W. (2019). Genetic Diversity in the Worldwide Alfalfa Germplasm Assessed through SSR Markers. *Int. J. Agric. Biol.* 22 (5), 1205–1210. doi:10.17957/IJAB/15.1188

He, W., Megharaj, M., Wu, C-Y., Subashchandrabose, S. R., and Dai, C-C. (2020). Endophyte-assisted Phytoremediation: Mechanisms and Current Application Strategies for Soil Mixed Pollutants. *Crit. Rev. Biotechnol.* 40 (1), 31–45. doi:10.1080/07388551.2019.1675582

Ho, D., and Juan, A. (2018). "Phytoremediation of Crude Oil-Contaminated Soil with Local Plant Species," in 11th Curtin University Technology, Science and Engineering (CUTSE) International Conference.

Houjayfa, O. M., Noubissié, E., and Ngassoum, M. B. (2020). Mobility Studies of Atrazine in the Soil-Plant System in Two Cameroonian Vegetables Amaranthus hybridus and Corchorus Olitorius. *Environ. Sustainability Indicators.* 6, 100036. doi:10.1016/j.indic.2020.100036

Hu, Z., Wang, Y., Fang, Z., Shi, G., Lou, L., Ren, K., et al. (2020). Italian Ryegrass–rice Rotation System for Biomass Production and Cadmium Removal from Contaminated Paddy fields. *J. Soils Sediments.* 20 (2), 874–882. doi:10.1007/s11368-019-02470-9

Inui, H., and Ohkawa, H. (2005). Herbicide Resistance in Transgenic Plants with Mammalian P450 Monooxygenase Genes. *Pest Manag. Sci.* 61 (3), 286–291. doi:10.1002/ps.1012

Irish, B. M., and Greene, S L. (2021). "Germplasm Collection, Genetic Resources, and Gene Pools in Alfalfa," in *The Alfalfa Genome*. Editors L-Xi. Yu and C. Kole (Cham: Springer International Publishing), 43–64. doi:10.1007/978-3-030-74466-3_4

James, C. A., Xin, G., Doty, S. L., and Strand, S. E. (2008). Degradation of Low Molecular Weight Volatile Organic Compounds by Plants Genetically Modified with Mammalian Cytochrome P450 2E1. *Environ. Sci. Technol.* 42 (1), 289–293. doi:10.1021/es071197z

Ju, W., Liu, L, Jin, X., Duan, C., Cui, Y., Wang, J, et al. (2020). Co-inoculation Effect of Plant-Growth-Promoting Rhizobacteria and Rhizobium on EDDS Assisted Phytoremediation of Cu Contaminated Soils. *Chemosphere.* 254, 126724. doi:10.1016/j.chemosphere.2020.126724

Kakaei, M., and Ahmadian, S. (2021). Genetic Diversity Study of Some Iranian Alfalfa Genotypes Based on Seed Storage Proteins Patterns. *Iranian J. Sci. Technol. Trans. A: Sci.* 45 (4), 1223–1228. doi:10.1007/s40995-021-01142-z

Kawahigashi, H., Hirose, S., Ohkawa, H., and Ohkawa, Y. (2006). Phytoremediation of the Herbicides Atrazine and Metolachlor by Transgenic rice Plants Expressing Human CYP1A1, CYP2B6, and CYP2C19. *J. Agric. Food Chem.* 54 (8), 2985–2991. doi:10.1021/jf052610u

Kawahigashi, H., Hirose, S., Ohkawa, H., and Ohkawa, Y. (2005). Transgenic rice Plants Expressing Human CYP1A1 Remediate the Triazine Herbicides Atrazine and Simazine. *J. Agric. Food Chem.* 53 (22), 8557–8564. doi:10.1021/jf051370f

Kawahigashi, H., Hirose, S., Ohkawa, H., and Ohkawa, Y. (2008). Transgenic rice Plants Expressing Human P450 Genes Involved in Xenobiotic Metabolism for Phytoremediation. *J. Mol. Microbiol. Biotechnol.* 15 (2-3), 212–219. doi:10.1159/000121332

Kong, Z., and Glick, B. R. (2017a). "Chapter Two - the Role of Plant Growth-Promoting Bacteria in Metal Phytoremediation," in *Advances in Microbial Physiology*. Editor R. K. Poole (Academic Press), 97–132. doi:10.1016/bs.ampbs.2017.04.001

Kong, Z., and Glick, B. R. (2017b). The Role of Bacteria in Phytoremediation. *Applied Bioengineering.*, 327–353. doi:10.1002/9783527800599.ch11

Kumar, S. (2011). Biotechnological Advancements in Alfalfa Improvement. *J. Appl. Genet.* 52 (2), 111–124. doi:10.1007/s13353-011-0028-2

Kumar, S., and Trivedi, P. K. (2018). Glutathione S-Transferases: Role in Combating Abiotic Stresses Including Arsenic Detoxification in Plants. *Front. Plant Sci.* 9, 751. doi:10.3389/fpls.2018.00751

Kumar, V., AlMomin, S., Al-Shatti, A., Al-Aqeel, H., Al-Salameen, F., Shajan, A. B., et al. (2019). Enhancement of Heavy Metal Tolerance and Accumulation Efficiency by Expressing Arabidopsis ATP Sulfurylase Gene in Alfalfa. *Int. J. Phytoremediation.* 21 (11), 1112–1121. doi:10.1080/15226514.2019.1606784

Lamb, D. C., Lei, L., Warrilow, A. G., Lepesheva, G. I., Mullins, J. G., Waterman, M. R., et al. (2009). The First Virally Encoded Cytochrome P450. *J. Virol.* 83 (16), 8266–8269. doi:10.1128/JVI.00289-09

LeDuc, D., AbdelSamie, M., Montes-Bayón, M., Wu, C., Reisinger, S., and Terry, N. (2006). Overexpressing Both ATP Sulfurylase and Selenocysteine Methyltransferase Enhances Selenium Phytoremediation Traits in Indian Mustard. *Environ. Pollut. (Barking, Essex).* 144, 70–76. doi:10.1016/j.envpol.2006.01.008

Legault, E. K., James, C. A., Stewart, K., Muiznieks, I., Doty, S. L., and Strand, S. E. (2017). A Field Trial of TCE Phytoremediation by Genetically Modified Poplars Expressing Cytochrome P450 2E1. *Environ. Sci. Technol.* 51 (11), 6090–6099. doi:10.1021/acs.est.5b04758

Li, A., Liu, A, Du, X., Chen, J-Y., Yin, M., Hu, H-Y., et al. (2020). A Chromosome-Scale Genome Assembly of a Diploid Alfalfa, the Progenitor of Autotetraploid Alfalfa. *Hortic. Res.* 7 (1), 194. doi:10.1038/s41438-020-00417-7

Li, P., Zhang, Y., Meng, Q., Liu, Y., Tuyiringire, D., Chen, Z., et al. (2019). Effects of Trichloroethylene Stress on the Microbiological Characteristics of Mollisol. *Ecotoxicology Environ. Saf.* 184, 109595. doi:10.1016/j.ecoenv.2019.109595

Li, X, and Brummer, E. C. (2012). Applied Genetics and Genomics in Alfalfa Breeding. *Agronomy.* 2 (1), 40–61. doi:10.3390/agronomy2010040

Liu, Q., Fan, Y., Zhang, J., Liu, H., Rahman, S., Islam, S., et al. (2021). Application of CRISPR/Cas9 in Crop Quality Improvement. *Int. J. Mol. Sci.* 22 (8), 4206. doi:10.3390/ijms22084206

Ma, J. X., Yan, Z., Zhang, J, Feng, Q., Wang, T., and Lu, X. (2018). Analysis of Genetic Diversity of 20 Wild Alfalfa Germplasms in Xinjiang with RAPD and ISSR Markers. *J. Yunnan Agric. Univ.* 33 (4), 577–587.

Mamirova, A., Nurzhanova, A., and Pidlisnyuk, V. (2019). Pop Pesticides and Reclamation Methods (Review). *REPORTS.* 6, 21–34. doi:10.32014/2019.2518-1483.164

Massot, F., Gkorezis, P., Van Hamme, J., Marino, D., Trifunovic, B., Vukovic, G., et al. (2021). Isolation, Biochemical and Genomic Characterization of Glyphosate Tolerant Bacteria to Perform Microbe-Assisted Phytoremediation. *Front. Microbiol.* 11, 3506. doi:10.3389/fmicb.2020.598507

Mello, I, Targanski, S., and Pietro-Souza, W. (2020). Endophytic Bacteria Stimulate Mercury Phytoremediation by Modulating its Bioaccumulation and Volatilization. *Ecotoxicology Environ. Saf.* 202, 110818. doi:10.1016/j.ecoenv.2020.110818

Mesa-Marín, J, Pérez-Romero, J. A., Redondo-Gómez, S., Pajuelo, E., Rodríguez-Llorente, I. D., and Mateos-Naranjo, E. (2020). Impact of Plant Growth Promoting Bacteria on Salicornia ramosissima Ecophysiology and Heavy Metal Phytoremediation Capacity in Estuarine Soils. *Front. Microbiol.* 11, 553018. doi:10.3389/fmicb.2020.553018

Mishra, S., Kumar, P., and Singh, R. (2020). "3 - Transgenic Plants in Phytoremediation of Organic Pollutants," in *Bioremediation of Pollutants*. Editors V. C. Pandey and V. Singh (Elsevier), 39–56. doi:10.1016/b978-0-12-819025-8.00003-x

Mizutani, M. (2012). Impacts of Diversification of Cytochrome P450 on Plant Metabolism. *Biol. Pharm. Bull.* 35 (6), 824–832. doi:10.1248/bpb.35.824

Montagnolli, R. N., Lopes, P. R., and Bidoia, E. D. (2015). Assessing Bacillus Subtilis Biosurfactant Effects on the Biodegradation of Petroleum Products. *Environ. Monit. Assess.* 187 (1), 4116. doi:10.1007/s10661-014-4116-8

Mouhamad, R., Ghanem, I., AlOrfi, M., Ibrahim, K., Ali, N., and Al-Daoude, A. (2012). Phytoremediation of Trichloroethylene and Dichlorodiphenyltrichloroethane-Polluted Water Using Transgenic Sesbania Grandiflora and Arabidopsis thaliana Plants Harboring Rabbit Cytochrome P450 2E1. *Int. J. Phytoremediation.* 14 (7), 656–668. doi:10.1080/15226514.2011.619232

Nebert, D. W., and Vasiliou, V. (2004). Analysis of the Glutathione S-Transferase (GST) Gene Family. *Hum. Genomics.* 1 (6), 460–464. doi:10.1186/1479-7364-1-6-460

Nedjimi, B. (2021). Phytoremediation: a Sustainable Environmental Technology for Heavy Metals Decontamination. *SN Appl. Sci.* 3 (3), 286. doi:10.1007/s42452-021-04301-4

Nelson, D. R. (2009). The Cytochrome P450 Homepage. *Hum. Genomics.* 4 (1), 59–65. doi:10.1186/1479-7364-4-1-59

Nelson, D. R. (2018). Cytochrome P450 Diversity in the Tree of Life. *Biochim. Biophys. Acta Proteins Proteom.* 1866 (1), 141–154. doi:10.1016/j.bbapap.2017.05.003

Novakova, M., Mackova, M., Antosova, Z., Viktorova, J., Szekeres, M., Demnerova, K., et al. (2010). Cloning the Bacterial bphC Gene into Nicotiana Tabacum to Improve the Efficiency of Phytoremediation of Polychlorinated Biphenyls. *Bioeng. Bugs.* 1 (6), 419–423. doi:10.4161/bbug.1.6.12723

Novakova, M., Mackova, M., Chrastilova, Z., Viktorova, J., Szekeres, M., Demnerova, K., et al. (2009). Cloning the Bacterial bphC Gene into Nicotiana Tabacum to Improve the Efficiency of PCB Phytoremediation. *Biotechnol. Bioeng.* 102 (1), 29–37. doi:10.1002/bit.22038

Nurzhanova, A., Kalugin, S., and Zhambakin, K. (2013). Obsolete Pesticides and Application of Colonizing Plant Species for Remediation of Contaminated Soil in Kazakhstan. *Environ. Sci. Pollut. Res.* 20 (4), 2054–2063. doi:10.1007/s11356-012-1111-x

Nurzhanova, A., Mukasheva, T., Berzhanova, R., Kalugin, S., Omirbekova, A., and Mikolasch, A. (2021). Optimization of Microbial Assisted Phytoremediation of Soils Contaminated with Pesticides. *Int. J. Phytoremediation.* 23 (5), 482–491. doi:10.1080/15226514.2020.1825330

Nurzhanova, A., Zhambakin, K., Rakhimbayev, I., Sedlovskiy, A., and Kalugin, S. (2011). Obsolete Pesticides and Phytoremediation of Polluted Soil in Kazakhstan. *J. Life Sci.* 5 (7), 12.

Nwoko, C. O. (2010). Trends in Phytoremediation of Toxic Elemental and Organic Pollutants. *Afr. J. Biotechnol.* 9 (37), 6010–6016. doi:10.5897/AJB09.061

Ochsner, U. A., Koch, A. K., Fiechter, A., and Reiser, J. (1994). Isolation and Characterization of a Regulatory Gene Affecting Rhamnolipid Biosurfactant Synthesis in Pseudomonas aeruginosa. *J. Bacteriol.* 176 (7), 2044–2054. doi:10.1128/jb.176.7.2044-2054.1994

Olaniran, A. O., Balgobind, A., and Balakrishna, P. (2013). Bioavailability of Heavy Metals in Soil: Impact on Microbial Biodegradation of Organic Compounds and Possible Improvement Strategies. *Int. J. Mol. Sci.* 14 (5), 10197–10228. doi:10.3390/ijms140510197

Paz-Alberto, A. (2013). Phytoremediation: A Green Technology to Remove Environmental Pollutants. *Am. J. Clim. Change* 2, 71–86. doi:10.4236/ajcc.2013.21008

Pidlisnyuk, V., Mamirova, A., Kumar, P., Shapoval, P., Trögl, J., and Nurzhanova, A. (2020). Potential Role of Plant Growth-Promoting Bacteria in Miscanthus X Giganteus Phytotechnology Applied to the Trace Elements Contaminated Soils. *Int. Biodeterioration Biodegradation* 155, 105103. doi:10.1016/j.ibiod.2020.105103

Pilon-Smits, E. A., Hwang, S., Mel Lytle, C., Zhu, Y., Tai, J. C., Bravo, R. C., et al. (1999). Overexpression of ATP Sulfurylase in Indian Mustard Leads to Increased Selenate Uptake, Reduction, and Tolerance. *Plant Physiol.* 119 (1), 123–132. doi:10.1104/pp.119.1.123

Raskin, I., Nanda Kumar, P. B. A., Dushenkov, S., and Salt, D. E. (1994). Bioconcentration of Heavy Metals by Plants. *Curr. Opin. Biotechnol.* 5 (3), 285–290. doi:10.1016/0958-1669(94)90030-2

Ren, H., Wan, Y., and Zhao, Y. (2018). "Phytoremediation of Polychlorinated Biphenyl-Contaminated Soil by Transgenic Alfalfa Associated Bioemulsifier AlnA," in *Twenty Years of Research and Development on Soil Pollution and Remediation in China*. Editors Y. Luo and C. Tu (Singapore: Springer Singapore), 645–653. doi:10.1007/978-981-10-6029-8_39

Ren, H., Su, Y., Zhang, J., Pan, H., Chen, B., and Wang, Y. (2016). Recombinant Protein, AlnA, Combined with Transgenic Alfalfa Remediates Polychlorinated Biphenyl-Contaminated Soils: Efficiency and Rhizosphere Microbial Community Response. *Biotechnol. Lett.* 38 (11), 1893–1901. doi:10.1007/s10529-016-2169-1

Rhouma, H., Taski-Ajdukovic, K., Zitouna, N., Dorra, S., Milic, D., and Trifi-Farah, N. (2017). Assessment of the Genetic Variation in Alfalfa Genotypes Using SRAP Markers for Breeding Purposes. *Chilean J. Agric. Res.* 77, 332–339. doi:10.4067/S0718-58392017000400332

Rylott, E. L., Johnston, E. J., and Bruce, N. C. (2015). Harnessing Microbial Gene Pools to Remediate Persistent Organic Pollutants Using Genetically Modified Plants—A Viable Technology. *J. Exp. Bot.* 66 (21), 6519–6533. doi:10.1093/jxb/erv384

Sadeghnia, H., Shahba, S., and Ebrahimzadeh-Bideskan, A. (2021). Atrazine Neural and Reproductive Toxicity. *Toxin Rev.*, 1–14. doi:10.1080/15569543.2021.1966637

Salam, J. A., Hatha, M. A. A., and Das, N. (2017). Microbial-enhanced Lindane Removal by Sugarcane (Saccharum Officinarum) in Doped Soil-Applications in Phytoremediation and Bioaugmentation. *J. Environ. Manage.* 193, 394–399. doi:10.1016/j.jenvman.2017.02.006

Salt, D. E., Blaylock, M., Kumar, N. P., Dushenkov, V., Ensley, B. D., Chet, I., et al. (1995). Phytoremediation: A Novel Strategy for the Removal of Toxic Metals from the Environment Using Plants. *Bio/Technology.* 13 (5), 468–474. doi:10.1038/nbt0595-468

Schäffner, A., Messner, B., Langebartels, C., and Sandermann, H. (2002). Genes and Enzymes for In-Planta Phytoremediation of Air, Water and Soil. *Acta Biotechnologica.* 22, 141–151. doi:10.1002/1521-3846(200205)22:1/2<141::AID-ABIO141>3.0.CO;2-7

Shamustakimova, A. O., Mavlyutov, Y. M., and Klimenko, I. A. (2021). Application of SRAP Markers for DNA Identification of Russian Alfalfa Cultivars. *Russ. J. Genet.* 57 (5), 540–547. doi:10.1134/S1022795421050112

Shang, Yi., and Huang, S. (2020). Engineering Plant Cytochrome P450s for Enhanced Synthesis of Natural Products: Past Achievements and Future Perspectives. *Plant Commun.* 1 (1), 100012. doi:10.1016/j.xplc.2019.100012

Shankar, K., and Mehendale, H. M. (2014). "Cytochrome P450," in *Encyclopedia of Toxicology*. Editor P. Wexler. Third Edition (Oxford: Academic Press), 1125–1127. doi:10.1016/b978-0-12-386454-3.00299-2

Sharma, P. (2021). Efficiency of Bacteria and Bacterial Assisted Phytoremediation of Heavy Metals: An Update. *Bioresour. Techn.* 328, 124835. doi:10.1016/j.biortech.2021.124835

Shen, C., Du, H., Chen, Z., Lu, H., Zhu, F., Chen, H., et al. (2020). The Chromosome-Level Genome Sequence of the Autotetraploid Alfalfa and Resequencing of Core Germplasms Provide Genomic Resources for Alfalfa Research. *Mol. Plant* 13 (9), 1250–1261. doi:10.1016/j.molp.2020.07.003

Shevtsov, A., Tarlykov, P., Zholdybayeva, E., Momynkulov, D., Sarsenova, A., Moldagulova, N., et al. (2013). Draft Genome Sequence of Rhodococcus Erythropolis DN1, a Crude Oil Biodegrader. *Genome Announcements* 1 (5), e00846-13. doi:10.1128/genomeA.00846-13

Silambarasan, S., Peter, L., Valentine, A., Cornejo, P., and Kannan, V. (2020). Pseudomonas Citronellolis Strain SLP6 Enhances the Phytoremediation Efficiency of Helianthus Annuus in Copper Contaminated Soils under Salinity Stress. *Plant and Soil* 457 (1), 241–253. doi:10.1007/s11104-020-04734-7

Singh, A., and Cameotra, S. (2013). Rhamnolipids Production by Multi-Metal-Resistant and Plant-Growth-Promoting Rhizobacteria. *Appl. Biochem. Biotechnol.* 170, 1038–1056. doi:10.1007/s12010-013-0244-9

Song, Y., Shahir, S, and Abd Manan, F. (2021). Bacterial Inoculant-Assisted Phytoremediation of Heavy Metal-Contaminated Soil: Inoculant Development and the Inoculation Effects. *Biologia* 76 (9), 2675–2685. doi:10.1007/s11756-021-00804-y

Souza, M., Sadowsky, M., and Lawrence, W. (1996). Atrazine Chlorohydrolase from Pseudomonas Sp. Strain ADP: Gene Sequence, Enzyme Purification, and Protein Characterization. *J. Bacteriol.* 178, 4894–4900. doi:10.1128/jb.178.16.4894-4900.1996

Stepanova, A. Yu., Orlova, E. V., Teteshonok, D. V., and Dolgikh, Y. I. (2016). Obtaining Transgenic Alfalfa Plants for Improved Phytoremediation of

Petroleum-Contaminated Soils. *Russ. J. Genet. Appl. Res.* 6 (6), 705–711. doi:10.1134/S2079059716060083

Su, Z. H., Xu, Z. S., Peng, R. H., Tian, Y. S., Zhao, W., Han, H. J., et al. (2012). Phytoremediation of Trichlorophenol by Phase II Metabolism in Transgenic Arabidopsis Overexpressing a Populus Glucosyltransferase. *Environ. Sci. Technol.* 46 (7), 4016–4024. doi:10.1021/es203753b

Sylvestre, M., Sirois, M., Hurtubise, Y., Bergeron, J., Ahmad, D., Shareck, F., et al. (1996). Sequencing of Comamonas Testosteroni Strain B-356-Biphenyl/chlorobiphenyl Dioxygenase Genes: Evolutionary Relationships Among Gram-Negative Bacterial Biphenyl Dioxygenases. *Gene* 174 (2), 195–202. doi:10.1016/0378-1119(96)00039-x

Taira, K., Hirose, J., Hayashida, S., and Furukawa, K. (1992). Analysis of Bph Operon from the Polychlorinated Biphenyl-Degrading Strain of Pseudomonas pseudoalcaligenes KF707. *J. Biol. Chem.* 267 (7), 4844–4853. doi:10.1016/s0021-9258(18)42908-0

Tang, L., Mao, B., Li, Y., Lv, Q., Zhang, L., Chen, C., et al. (2017). Knockout of OsNramp5 Using the CRISPR/Cas9 System Produces Low Cd-Accumulating Indica rice without Compromising Yield. *Scientific Rep.* 7 (1), 1–12. doi:10.1038/s41598-017-14832-9

Tarla, D. N., Davis, L. C., Nurzhanova, A., and Pidlisnyuk, V. (2020). Phytoremediation and Bioremediation of Pesticide-Contaminated Soil. *Appl. Sci.* 10 (4), 1217. doi:10.3390/app10041217

Tussipkan, D., and Manabayeva, S. A. (2021). Employing CRISPR/Cas Technology for the Improvement of Potato and Other Tuber Crops. *Front. Plant Sci.* 12, 747476. doi:10.3389/fpls.2021.747476

Varjani, S., and Upasani, V. N. (2021). Bioaugmentation of Pseudomonas aeruginosa NCIM 5514 – A Novel Oily Waste Degrader for Treatment of Petroleum Hydrocarbons. *Bioresour. Techn.* 319, 124240. doi:10.1016/j.biortech.2020.124240

Varjani, S., Upasani, V. N., and Pandey, A. (2020). Bioremediation of Oily Sludge Polluted Soil Employing a Novel Strain of Pseudomonas aeruginosa and Phytotoxicity of Petroleum Hydrocarbons for Seed Germination. *Sci. Total Environ.* 737, 139766. doi:10.1016/j.scitotenv.2020.139766

Vasil'eva, G. K., and Strizhakova, E. R. (2007). Bioremediation of Soils and Sediments Polluted by Polychlorinated Biphenyls. *Mikrobiologiia* 76 (6), 725–741.

Wackett, L. M., Sadowsky, B. M., and Shapir, N. (2002). Biodegradation of Atrazine and Related s-triazine Compounds: From Enzymes to Field Studies. *Appl. Microbiol. Biotechnol.* 58 (11), 39–45. doi:10.1007/s00253-001-0862-y

Wang, D., Lin, J., Lin, J., Wang, W., and Li, S. (2019). Biodegradation of Petroleum Hydrocarbons by Bacillus Subtilis BL-27, a Strain with Weak Hydrophobicity. *Molecules* 24 (17), 3021. doi:10.3390/molecules24173021

Wang, H., Chen, X., Xing, X., Hao, X., and Chen, D. (2010). Transgenic Tobacco Plants Expressing atzA Exhibit Resistance and strong Ability to Degrade Atrazine. *Plant Cel Rep* 29 (12), 1391–1399. doi:10.1007/s00299-010-0924-7

Wang, J. D., Li, X. X., and Qu, C. T. (2017). Exploration of Up-Regulated Key Proteins in Pseudomonas Aeruginosa for High-Efficiency Petroleum Degradation by Proteomic Analysis. *Curr. Microbiol.* 74 (10), 1178–1184. doi:10.1007/s00284-017-1302-2

Wang, L., Samac, D. A., Shapir, N., Wackett, L. P., Vance, C. P., Olszewski, N. E., et al. (2005). Biodegradation of Atrazine in Transgenic Plants Expressing a Modified Bacterial Atrazine Chlorohydrolase (atzA) Gene. *Plant Biotechnol. J.* 3 (5), 475–486. doi:10.1111/j.1467-7652.2005.00138.x

Wang, H., Wang, Q., Liu, Y., Liao, X., Chu, H., Chang, H., et al. (2021). PCPD: Plant Cytochrome P450 Database and Web-Based Tools for Structural Construction and Ligand Docking. *Synth. Syst. Biotechnol.* 6 (2), 102–109. doi:10.1016/j.synbio.2021.04.004

Wang, X., de Souza, M. F., Li, H., Filip, M., Tack, G., Yong Sik, O., et al. (2021). Zn Phytoextraction and Recycling of Alfalfa Biomass as Potential Zn-Biofortified Feed Crop. *Sci. Total Environ.* 760, 143424. doi:10.1016/j.scitotenv.2020.143424

Wang, Y., Ren, H., Pan, H., Liu, J., and Zhang, L. (2015). Enhanced Tolerance and Remediation to Mixed Contaminates of PCBs and 2,4-DCP by Transgenic Alfalfa Plants Expressing the 2,3-Dihydroxybiphenyl-1,2-Dioxygenase. *J. Hazard. Mater.* 286, 269–275. doi:10.1016/j.jhazmat.2014.12.049

Wang, Y., Wang, C., Ren, H., Jia, B., and Zhang, L. (2014). Effectiveness of Recombinant Protein AlnA in Enhancing the Extractability of Polychlorinated Biphenyls from Contaminated Soils. *J. Hazard. Mater.* 279, 67–74. doi:10.1016/j.jhazmat.2014.06.063

Wang, Z., and Şakiroğlu, M. (2021). "The Direct Diploid Progenitor of Autotetraploid Alfalfa," in *The Alfalfa GenomeLong-Xi Yu and Chittaranjan Kole* (Cham: Springer International Publishing), 29–42. doi:10.1007/978-3-030-74466-3_3

Wangeline, A., Burkhead, J., Hale, K., Lindblom, S., Terry, N., and Pilon-Smits, E. (2004). Overexpression of ATP Sulfurylase in Indian Mustard: Effects on Tolerance and Accumulation of Twelve Metals. *J. Environ. Qual.* 33, 54–60. doi:10.2134/jeq2004.5400

Wu, Z., Bañuelos, G. S., Lin, Z-Q., Liu, Y., Yuan, L., Yin, X., et al. (2015). Biofortification and Phytoremediation of Selenium in China. *Front. Plant Sci.* 6, 136. doi:10.3389/fpls.2015.00136

Yamada, T., Ishige, T., Shiota, N., Inui, H., Ohkawa, H., and Ohkawa, Y. (2002). Enhancement of Metabolizing Herbicides in Young Tubers of Transgenic Potato Plants with the Rat CYP1A1 Gene. *Theor. Appl. Genet.* 105 (4), 515–520. doi:10.1007/s00122-002-0961-x

Yang, C-h., Zhang, Y., and Huang, C-f. (2019). Reduction in Cadmium Accumulation in Japonica rice Grains by CRISPR/Cas9-mediated Editing of OsNRAMP5. *J. Integr. Agric.* 18 (3), 688–697. doi:10.1016/s2095-3119(18)61904-5

Yang, Y., Ding, J., Chi, Y., and Yuan, J. (2020). Characterization of Bacterial Communities Associated with the Exotic and Heavy Metal Tolerant Wetland Plant Spartina Alterniflora. *Scientific Rep.* 10 (1), 1–11. doi:10.1038/s41598-020-75041-5

Ye, J. Y., Zhang, J. B., Gao, J. G., Li, H. T., Liang, D., and Liu, R. M. (2016). Isolation and Characterization of Atrazine-Degrading Strain Shewanella Sp. YJY4 from Cornfield Soil. *Lett. Appl. Microbiol.* 63 (1), 45–52. doi:10.1111/lam.12584

Yin, S., Wang, Y., and Nan, Z. (2018). Genetic Diversity Studies of Alfalfa Germplasm (Medicago Sativa L. Subsp Sativa) of United States Origin Using Microsatellite Analysis. *Legume Res.* 41 (2), 202–207. doi:10.18805/LR-358

Zhang, Y., Liu, J., Zhou, Y., Gong, T., Wang, J., and Ge, Y. (2013). Enhanced Phytoremediation of Mixed Heavy Metal (Mercury)-organic Pollutants (Trichloroethylene) with Transgenic Alfalfa Co-expressing Glutathione S-Transferase and Human P450 2E1. *J. Hazard. Mater.* 260, 1100–1107. doi:10.1016/j.jhazmat.2013.06.065

Zhang, Y., and Liu, J. (2011). Transgenic Alfalfa Plants Co-expressing Glutathione S-Transferase (GST) and Human CYP2E1 Show Enhanced Resistance to Mixed Contaminates of Heavy Metals and Organic Pollutants. *J. Hazard. Mater.* 189 (1), 357–362. doi:10.1016/j.jhazmat.2011.02.042

Zheng, T., Xu, Y. S., Yong, X. Y., Li, B., Yin, D., Cheng, Q. W., et al. (2015). Endogenously Enhanced Biosurfactant Production Promotes Electricity Generation from Microbial Fuel Cells. *Bioresour. Technol.* 197, 416–421. doi:10.1016/j.biortech.2015.08.136

Conflict of Interest: The authors declare that the research was conducted in the absence of any commercial or financial relationships that could be construed as a potential conflict of interest.

Publisher's Note: All claims expressed in this article are solely those of the authors and do not necessarily represent those of their affiliated organizations, or those of the publisher, the editors and the reviewers. Any product that may be evaluated in this article, or claim that may be made by its manufacturer, is not guaranteed or endorsed by the publisher.

frontiers in Environmental Science

ORIGINAL RESEARCH
published: 08 March 2022
doi: 10.3389/fenvs.2022.848348

Residue Monitoring of Propiconazole in the Rice–Crab Co-Culture Field and its Toxicity and Bioaccumulation to *Eriocheir sinensis*

Lina Yu[1,2], Changsheng Li[3], Yuting Zhang[1], Xuanjun Guo[1], Niannian Cao[1], Shuxin Guo[1], Sijia Wu[1], Xuefeng Li[1] and Sen Pang[1]**

[1]Department of Applied Chemistry, College of Science, China Agricultural University, Beijing, China, [2]Solid Waste and Chemicals Management Center, Ministry of Ecology and Environment, Beijing, China, [3]College of Agronomy and Biotechnology, China Agricultural University, Beijing, China

Rice–crab co-culture is a high-benefit eco-breeding pattern that has been extensively developed in many regions of China. However, little attention has been paid to the safety of pesticides used to control rice pests in the crab–rice co-culture system. This study monitored the actual residue levels of propiconazole in water and soil of rice–crab co-culture fields and evaluated the acute toxicity, subchronic toxicity, and bioaccumulation of propiconazole to *Eriocheir sinensis*. We observed that the residue level of propiconazole in paddy soil was higher than that in paddy water within 42-day field monitoring. Propiconazole demonstrated a low acute toxicity (96 h-LC_{50} > 100 mg/L) to *E. sinensis* and exhibited no obvious adverse impact on the growth of *E. sinensis* after exposure to 500 μg/L, which was 10 times the actual residual concentration of propiconazole in the crab–rice co-culture field. The highest bioaccumulation of propiconazole was obtained from gills, followed by the hepatopancreas and meat. These results will contribute to the guidance of scientific utilization of pesticides in the crab–rice co-culture field.

Keywords: propiconazole, Chinese mitten crab, acute toxicity, subchronic toxicity, tissue-specific bioaccumulation

OPEN ACCESS

Edited by:
Yue Geng,
Ministry of Agriculture and Rural Affairs, China

Reviewed by:
Josef Velíšek,
University of South Bohemia, Czechia
Jason T. Magnuson,
University of California, Riverside, United States

****Correspondence:***
Xuefeng Li
91030@cau.edu.cn
Sen Pang
pangsen7812@cau.edu.cn

Specialty section:
This article was submitted to Toxicology, Pollution and the Environment, a section of the journal Frontiers in Environmental Science

Received: *04 January 2022*
Accepted: *14 February 2022*
Published: *08 March 2022*

Citation:
Yu L, Li C, Zhang Y, Guo X, Cao N, Guo S, Wu S, Li X and Pang S (2022) Residue Monitoring of Propiconazole in the Rice–Crab Co-Culture Field and its Toxicity and Bioaccumulation to Eriocheir sinensis. Front. Environ. Sci. 10:848348. doi: 10.3389/fenvs.2022.848348

INTRODUCTION

Food shortage has become an urgent problem to be solved because of the rapid growth of population and limited water and soil resources (Bashir et al., 2020; Xu et al., 2021; Zhang et al., 2021). As one of the important staple foods, rice (*Oryza sativa L.*) feeds roughly half of the global population (Fageria, 2007; Liu et al., 2018). However, rice production systems have been identified as a major sector wasting available water resources, consuming up to 90 percent of irrigation water in Asia. Thus, improving the utilization of land and water resources in the rice production system is still a lacking demand (Bashir et al., 2020).

The co-culture of rice and aquatic animals has a history of more than 2,000 years in China (Wang et al., 2021). It has been considered a strategy to improve the utilization of land and water resources in paddy fields to provide both grains and aquatic animal protein products to humans (Zhang et al., 2021). The Chinese mitten crab (*Eriocheir sinensis*) is native to the coastal rivers and estuaries of the Yellow Sea. It is an important freshwater aquaculture species in China because of its rapid growth, strong fertility, and high nutritional values (Shen et al., 2017; Hong et al., 2019), with an annual output of over 770,000 tons (BFMA, 2020). Driven by huge economic benefits, *E. sinensis* has been

developing rapidly in China in recent years and contains a variety of farming models. Rice–crab co-culture is a high-benefit eco-breeding pattern that has been extensively developed in many regions of China, especially in Liaoning Province (Yan et al., 2014). Panjin city, Liaoning Province, a representative area for cultivating crabs in paddy fields, has a rice–crab co-culture area of about 45,300 ha, accounting for 43.27% of the city's rice-planting area.

However, there are still some problems to be solved in the rice–crab co-culture system, especially the safety issues of pesticides to biological resources, for e.g., *E. sinensis*, when they were applied to control rice diseases, pests, and weeds. Although the crabs could eliminate some weeds and pests in the field to achieve the effect of biological pest control, there is no evidence that crabs can effectively control rice diseases. Therefore, in order to avoid rice yield reduction caused by diseases, fungicides have to be used to control rice diseases in rice–crab co-culture fields. Propiconazole was first registered in 1981 by the United States Environmental Protection Agency (EPA) in applications against a broad range of fungal diseases (Souders et al., 2019). The fungicide acts via demethylation of the C14 in ergosterol biosynthesis, an event that disrupts fungal cell wall integrity, effectively impeding further fungal growth (Johansen et al., 2007). Propiconazole is widely used in China to control rice diseases, and more than 150 formulations containing propiconazole have been registered for the control of rice diseases by the Ministry of Agriculture and Rural Affairs of China. However, propiconazole is frequently detected in the aquatic environment. Battaglin et al. detected propiconazole residues in 13% of 29 rivers in 13 states of the United States with a maximum concentration of 1.15 μg/L (Battaglin et al., 2010). Similarly, in Belgium, propiconazole was detected in surface water samples collected from 16 locations and ranged from 1.9 to 178.3 ng/L in effluent from waste water treatment plants (Van De Steene et al., 2010). Propiconazole has been found to have potential effects on aquatic invertebrate crabs, such as *Mysidopsis bahia* (28 days reproduction NOEC = 0.114 mg/L) (European Food Safety Authority, 2017). In addition, the long half-life (DT50) of propiconazole in the environment makes it more vital to investigate the long-term influence on the related biological resources and environment. Edwards et al. reported that propiconazole showed a DT50 value of 99–116 days in agricultural practices (Edwards et al., 2016). DT50 of propiconazole in the water/sediment system was 561 days according to the European Food Safety Authority (European Food Safety Authority, 2017). Therefore, it is necessary to study whether propiconazole has potential adverse effects on *E. sinensis* in the rice–crab co-culture system. Although propiconazole belongs to medium bioaccumulation chemicals, indicated by the bioconcentration factor (BCF) of 180 in fish (European Food Safety Authority, 2017), whether or not propiconazole can accumulate in *E. sinensis*, enter, and affect human health through the food chain is still unknown.

In the present study, the residue level of propiconazole in water and soil of rice–crab co-culture fields was monitored. In addition, the acute toxicity, subchronic toxicity, and bioaccumulation of propiconazole to *E. sinensis* were evaluated. The purpose was to quantify the potential adverse effects of propiconazole on the Chinese mitten crab based on the actual residual amount of propiconazole in the rice and crab co-culture fields and to provide guidance for the scientific use of propiconazole in the rice and crab co-culture system.

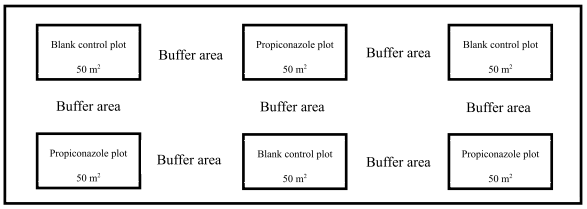

FIGURE 1 | Field experiment plot map.

MATERIALS AND METHODS

Chemical Material

95% propiconazole was purchased from Yunxin (Beijing) Agricultural Technology Co., Ltd. Stock solution of propiconazole exposure was prepared in dimethyl sulfoxide. The 25% propiconazole emulsifiable concentrate (EC) and propiconazole stock standard solutions of 100 mg/L in acetone were supplied by the College of Science, China Agricultural University. Dimethyl sulfoxide (purity 99.7%) and Tween 80 were purchased from J&K Scientific Ltd.

Field Experiment

One rice–crab co-culture field located in Panjin, China, was selected for this study. The experimental plots were 50 m^2 and consisted of a control site and propiconazole treatment site. Each treatment was conducted in three plots, with a 50-m^2 plot separating each site, acting as a buffer between locations. The map of the field experiment plot is shown in **Figure 1**.

25% propiconazole EC was sprayed evenly in the aforementioned experiment plots using a SeeSa SX-MD16E-2 backpack sprayer at an active ingredient dose of 45 g a. i/ha. The paddy water and soil samples were collected from each plot at 10 intervals up to 42 days after propiconazole application, i.e., 0 days (2 h), 1, 3, 5, 7, 10, 14, 21, 30, and 42 days. At each sampling date, at least 1 kg of soil (pooled sub-samples from randomly ten points) and 2000 ml of water (pooled sub-samples from 10 random locations) were taken and stored frozen (−20°C) until analysis.

Acute Toxicity

The acute toxicity of propiconazole to juvenile crabs was determined under static-renewal conditions. Crabs were exposed to a nominal concentration of 100 mg a. i./L for 96 h, alongside a dilution water control and solvent control (1.0×10^{-2} mg/L dimethyl sulfoxide+1.0×10^{-4} mg/L Tween 80). Each test concentration was replicated three times. Glass fish tanks with a capacity of 60 L were used for the exposure operation. Each tank contained 50 L of exposure solutions and 10 crabs. The

whole exposure solutions were replaced daily. Mortalities and visible abnormalities (individuals not dead but unresponsive to touching the periopods and eyestalk were considered abnormal) were recorded daily. During the acute toxicity experiment, crabs were not fed, and dead individuals were removed immediately from the tank.

Subchronic Toxicity

Juvenile crabs, after being weighed, were exposed to two sublethal concentrations (0.05 and 0.50 mg/L) of propiconazole dissolved in water under static-renewal conditions for 28 days. In total, ten crabs in each group without replicate were exposed to glass tanks containing 50 L blank control, solvent control (5.0×10^{-5}mg/L dimethyl sulfoxide+5.0×10^{-7}mg/L Tween 80), and propiconazole solution. The exposure solutions were prepared as described in the acute toxicity test. The control group was fed with excess feed as a reference to ensure that adequate nutrients were available. The whole test solutions were replaced daily. The crabs were examined daily during the test period. Any mortalities or the number of molting was recorded. At the end of the test, all surviving crabs were weighed as wet weights (blotted dry).

Bioaccumulation Test

In total, sixty crabs (ca. 35~40 g) of each treatment group were exposed to 0.05 and 0.50 mg/L of propiconazole for 42 days. Solution preparation, exposure operation, and feeding patterns remained consistent with subchronic experiments. Uneaten food and feces were siphoned daily from the test chambers shortly after feeding (30 min to 1 hour).

In total, four crabs were sampled on each occasion, i.e., 0 days (2 h), 1, 2, 3, 5, 7, 10, 14, 21, 28, 35, and 42 days. The gill, meat, and hepatopancreas of each crab were collected and homogenized by steel balls and stored frozen (−20°C) until analysis.

Chemical Analysis of Propiconazole in Soil, Water, and Crab Tissues

Preparation of the Water Sample

For preparation of the water sample, 10 ml of the water sample was transferred into a 50-ml centrifuge tube, and 10 ml acetonitrile and 3 g sodium chloride were added. The solution was vortexed for 5 min and subsequently centrifuged at 3800 r/min for 5 min. The organic layer was transferred to a 1-ml EP tube containing 30 mg of PSA and 100 mg of anhydrous magnesium sulfate. After vortex and centrifugation, the supernatant was filtered through a 0.22-μm membrane filter into an autosampling vial and analyzed by LC–MS/MS.

Preparation of the Soil Sample

An additional 10 ml of water was added during sample extraction, with further preparation of samples following the same procedures as described for water sample analysis.

Preparation of Crab Tissues

For preparation of crab tissues, 1.0 g of thawed gills was added to a 15-ml stoppered centrifuge tube, followed by 5 ml of acetonitrile and 3 g of sodium chloride. It was shaken vigorously for 5 min and then centrifuged at 3,800 rpm for 5 min, and one milliliter of the supernatant was added to an EP tube containing 50 mg C18 and 100 mg anhydrous magnesium sulfate. After vortex and centrifugation, the supernatant was tested by passing through a 0.22-μm filter membrane. The samples of crab meat and hepatopancreas were processed as for crab gills.

Apparatus

All samples were detected by LC–MS/MS of Shimadzu. The ion source was electrospray ionization (ESI), and Agilent Poroshell 120EC-C_{18} (2.7 μm × 2.1 mm × 50 mm) was employed at room temperature. The flow rate of acetonitrile/H_2O (0.1%HCOOH) = 70/30 (V/V) was 0.2 ml min^{-1}. MRM was selected as the detection mode in triple-quadrupole mass spectrometry. The relevant parameters and the limit of detection of this method are listed in **Table 1**.

Data Analysis

Statistical analyses were conducted using SPSS software (Version 20.0, SPSS Inc., Chicago, IL, United States). Data normality and homogeneity of variance were validated using the Kolmogorov–Smirnov and Levene's tests, respectively. Significant differences between the control and exposure groups were evaluated using Dunnett's one-way analysis of variance (ANOVA) with a statistical significance threshold of $p < 0.05$.

RESULTS

Residues of Propiconazole in Water and Soil

As shown in **Figure 2**, the concentrations of propiconazole in paddy water decreased significantly during the initial 10 days of application. The peak concentration was approximately 0.005 mg/L for propiconazole, and they then remained relatively constant from 10 to 42 days.

The measured concentrations of propiconazole in soil were presented in **Figure 3**. The levels of soil residues of propiconazole peaks on the third day (~0.05 mg/kg) after application, then reduced and fluctuated around 0.01 mg/kg during the rest of the test period.

Toxicity Results

No mortality or abnormal behaviors of juvenile crabs were observed after exposed to propiconazole (100 mg/L) for 96 h, indicating that the acute toxicity of propiconazole to *E. sinensis* is low.

The growth effect on juvenile crabs by propiconazole at concentrations of 0.05 and 0.50 mg/L was also evaluated. For a 28-day exposure, no mortality or molting was observed among the test organisms. The average weight growth rates for the 0–28 days period range from 13.7 to 15.7% (**Figure 4**), and there was no significantly statistical difference between the treatment groups and the control ones.

Bioconcentration in Crab Tissues

The highest bioaccumulation of propiconazole was detected in gills, followed by the hepatopancreas and muscle (**Figures 5–7**).

TABLE 1 | Mass spectrometric parameters.

Pesticide	Retention time (min)	Precursor ion	Product ion	Collision energy (eV)
Propiconazole	1.8	406	337 251*	–15 –25

Asterisk is used for quantitative analysis.

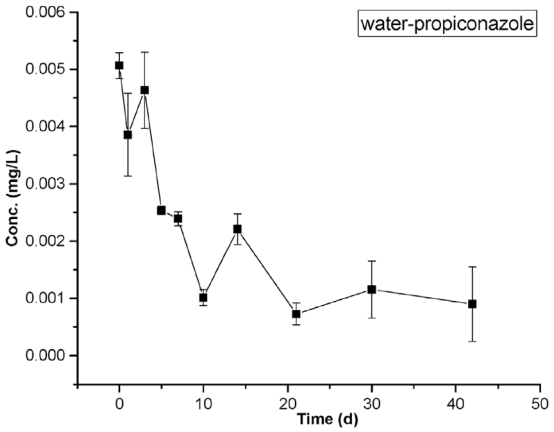

FIGURE 2 | Measured concentrations of propiconazole in water from the rice–crab co-culture field plot. The values of means ± standard error, SE, are given.

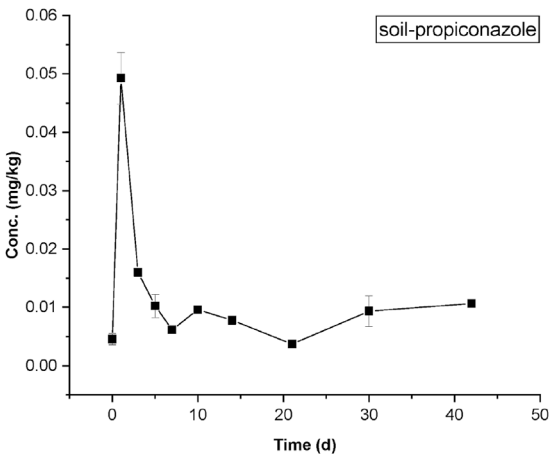

FIGURE 3 | Measured concentrations of propiconazole in soil from the rice–crab co-culture field plot. The values of means ± standard error, SE, are given.

The bioconcentration of propiconazole in the gills showed a time-dependent increase but did not reach a steady state during the 42-day test period (**Figure 5**). When crabs were exposed to propiconazole for 14 days, the bioaccumulation in the muscles reached a peak and then decreased to a steady state (**Figure 6**). The bioconcentration of propiconazole in the hepatopancreas fluctuated during the 42-day exposure period (**Figure 7**).

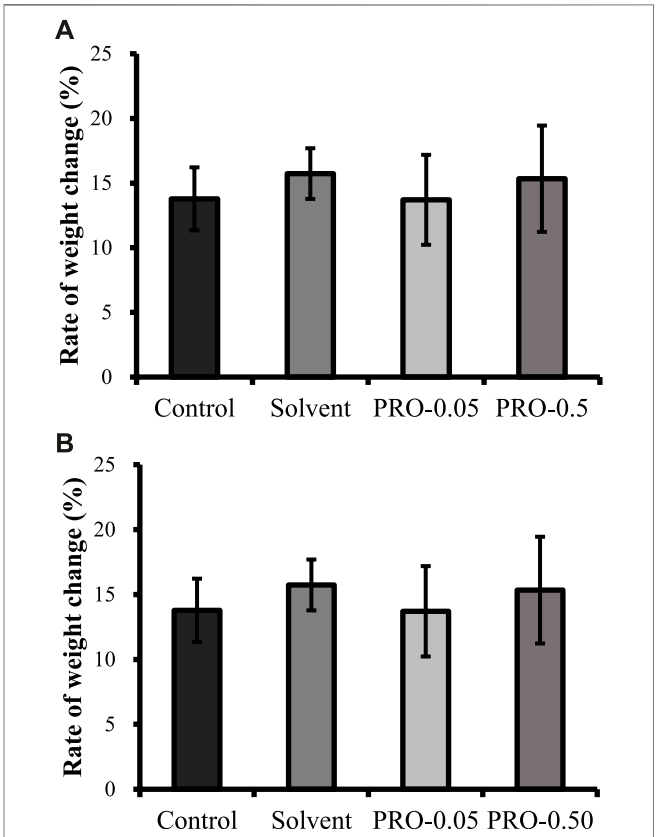

FIGURE 4 | Average weight growth rates of juvenile crabs over the 0–28 days period. Note: Control = blank control, Solvent = solvent control, PRO-0.05 = 0.05 mg/L propiconazole, and PRO-0.50 = 0.50 mg/L propiconazole. The values of means ± standard error, SE, are given.

DISCUSSION

It is reported that the effective utilization rate of pesticides was only about 40% in China (Shuqin and Fang, 2018), which means that about 60% of propiconazole will enter the paddy water and soil after it is used in paddy fields. Considering the long half-life of propiconazole in water and sediments, *E. sinensis* raised in rice fields may be exposed to high doses of propiconazole in long terms, which may harm the health of *E. sinensis* and cause economic losses. Therefore, this study first monitored the dissipation of propiconazole in the rice–crab co-culture field. The dissipation dynamics of propiconazole in the rice–crab co-culture field in Panjin City, Liaoning Province, was consistent with that of triazole fungicide difenoconazole in rice fields in Guangxi and Hubei reported by Wang et al. (2012).

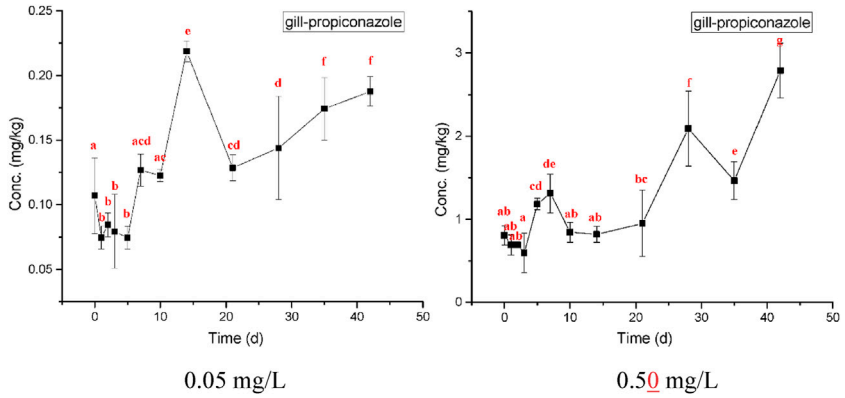

FIGURE 5 | Measured concentrations of propiconazole in crab gills at concentrations of 0.05 and 0.50 mg/L over 42 days exposure. The values of means ± standard error, SE, are given. Different lowercase letters denote significant differences ($p < 0.05$).

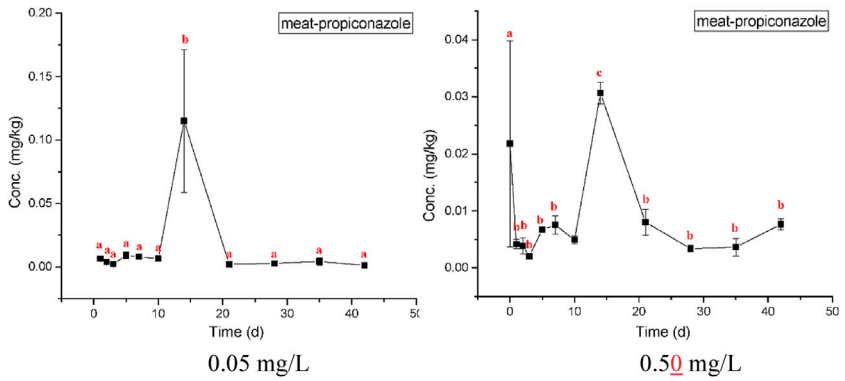

FIGURE 6 | Measured concentrations of propiconazole in crab meat at concentrations of 0.05 and 0.50 mg/L over 42 days exposure. The values of means ± standard error, SE, are given. Different lowercase letters denote significant differences ($p < 0.05$).

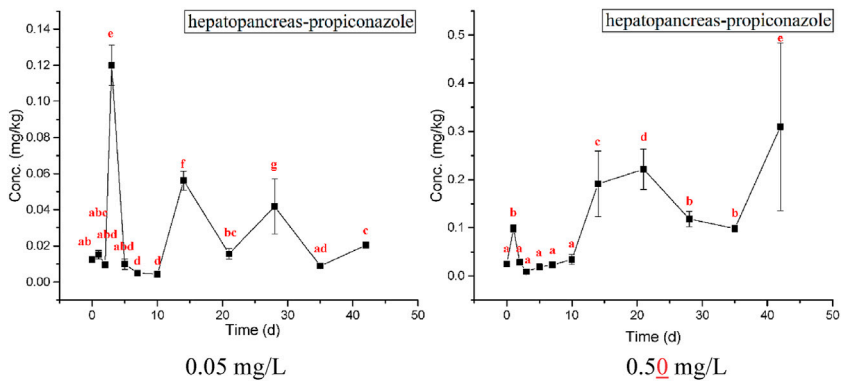

FIGURE 7 | Measured concentrations of propiconazole in the crab hepatopancreas at concentrations of 0.05 and 0.50 mg/L over 42 days exposure. The values of means ± standard error, SE, are given. Different lowercase letters denote significant differences ($p < 0.05$).

The studies on the acute toxicity of pesticides to *E. sinensis* are currently mostly focused on the evaluation of the toxicity of insecticides, while there are relatively few studies on the toxicity of fungicides and herbicides. It has been reported that the organophosphorus insecticides phoxim, chlorpyrifos, triazophos, and organochlorine insecticide endosulfan were

highly toxic to *E. sinensis*, while insecticides such as imidacloprid and avermectin were less toxic to *E. sinensis* (Li et al., 2013; Chen et al., 2014; Lu et al., 2020). Different formulations of diafenthiuron have also been found to have different toxicity to *E. sinensis*. The 96 h-LC_{50} of diafenthiuron suspension concentrate (SC) was 42.55 mg/L, while the toxicity of emulsifiable concentrate (EC) is relatively higher due to the adjuvant, 96 h-LC_{50}, was 24.66 mg/L (Gao et al., 2010). Compared with insecticides, fungicides have relatively low toxicity to *E. sinensis*. Our results demonstrated that propiconazole is a low-toxic chemical to *E. sinensis*. Similar results were also reported by Zhang (Zhang et al., 2014). Considering that the residual level of propiconazole in the field is unlikely to reach 100 mg/L, there is no risk of acute lethality to *E. sinensis* after propiconazole is applied in the rice–crab co-cultivation field.

Since propiconazole has a long half-life in the environment, evaluating its acute toxicity alone is not enough to predict its safety to *E. sinensis*. It has been reported that some environmental pollutants have an impact on the growth and development of *E. sinensis*. For example, *E. sinensis* was exposed to chronic copper solution for 21 days, which significantly affects the weight gain of *E. sinensis* (Bu et al., 2022). A similar growth inhibition result of mercury chloride on *E. sinensis* has also been reported (Zhao et al., 2009). Our subchronic toxicity test results found that when *E. sinensis* was exposed to two doses of the highest residue in the field and 10 times the highest residue, propiconazole did not affect the growth of *E. sinensis*. However, whether propiconazole has adverse effects on the biochemical indicators of *E. sinensis* needs further study. Previous studies have shown that the antioxidant enzyme activities of rainbow trout were induced after long-term exposure to propiconazole (Li et al., 2010). In addition, propiconazole can also induce hypopigmentation, disrupt mitochondrial bioenergetics, and can alter locomotor activity in zebrafish (Souders et al., 2019). Therefore, more biochemical and genetic studies are needed to clarify the potential harm of propiconazole to *E. sinensis*.

The pesticides absorbed by organisms from the surrounding environment may accumulate in the body to amplify its biological effects and may also be transmitted through the food chain, thereby adversely affecting high-level organisms. Triazole fungicides have been reported to have the risk of bioaccumulation in organisms. For instance, tebuconazole, hexaconazole, and myclobutanil have been demonstrated to accumulate in zebrafish (Andreu-Sanchez et al., 2012; Wang et al., 2015; Liu et al., 2016; Pang et al., 2020). Rainbow trout can be accumulated with a variety of triazole fungicides including bromuconazole, cyproconazole, metconazole, myclobutanil, penconazole, propiconazole, tebuconazole, tetraconazole, and triadimefon (Konwick et al., 2006). The present bioconcentration study showed that the gill and hepatopancreas of *E. sinensis* could be the most susceptible parts where propiconazole accumulated in. *E. sinensis* is one of the most popular seasonal autumn foods in China. Thus, the potential health risk induced by consuming *E. sinensis* should be concerned. No maximum residue levels (MRLs) of propiconazole have been applied to fish, fish products, and any other marine and freshwater food products. Therefore, MRLs which applied to products of amphibians and reptiles were referred to, i.e., 0.01 mg/kg for propiconazole [Reg (EU) 2021/155]. Measured residues of propiconazole in the gill and hepatopancreas rather than meat in the laboratory study exceeded the EU MRLs. The gill tissues of *E. sinensis* were inedible, but the hepatopancreas was the most favorable tissues to be consumed. In regard to health risk, the reference values of acceptable daily intake (ADI) and acute reference dose (ARfD) were established by the European Commission for propiconazole [ADI 0.04 mg/kg bw/d, ARfD 0.1 mg/kg bw; Reg (EU) 2018/1865]. Considering the limited intake of the hepatopancreas and meat during a specific season, the possibility that adverse health effects occurred to consumers due to propiconazole residues was very low.

In conclusion, it was safe for *E. sinensis* in the rice–crab co-culture field to apply propiconazole based on normal agronomic practices. However, due to the persistence of propiconazole in the environment and its bioaccumulation in crab tissues, excessive use of propiconazole in the rice–crab co-culture field system should be avoided. In addition, the mechanism of differential bioaccumulation of propiconazole in different tissues of *E. sinensis* needed further investigations.

DATA AVAILABILITY STATEMENT

The raw data supporting the conclusion of this article will be made available by the authors, without undue reservation.

AUTHOR CONTRIBUTIONS

XL and SP contributed to the conception and design of the study. CL organized the database. LY, CL, YZ, XG, NC, SG, and SW performed the experiment and statistical analysis. LY wrote the first draft of the manuscript. CL and SP wrote the sections of the manuscript. All authors contributed to manuscript revision and read and approved the submitted version.

ACKNOWLEDGMENTS

The authors acknowledge technical support from Professor Yongqiang Ma of the Department of Applied Chemistry, College of Science, China Agriculture University.

REFERENCES

Andreu-Sanchez, O., Paraiba, L. C., Jonsson, C. M., and Carrasco, J. M. (2012). Acute Toxicity and Bioconcentration of Fungicide Tebuconazole in Zebrafish (*Danio rerio*). *Environ. Toxicol.* 27 (2), 109–116. doi:10.1002/tox.20618

Bashir, M. A., Liu, J., Geng, Y., Wang, H., Pan, J., Zhang, D., et al. (2020). Co-Culture of Rice and Aquatic Animals: An Integrated System to Achieve Production and Environmental Sustainability. *J. Clean. Prod.* 249, 119310. doi:10.1016/j.jclepro.2019.119310

Battaglin, W. A., Sandstrom, M. W., Kuivila, K. M., Kolpin, D. W., and Meyer, M. T. (2010). Occurrence of Azoxystrobin, Propiconazole, and Selected Other Fungicides in US Streams, 2005–2006. *Water Air Soil Pollut.* 218 (1-4), 307–322. doi:10.1007/s11270-010-0643-2

BFMA (2020). *China Fishery Statistical Yearbook*. Beijing: China Agriculture Press.

Bu, X., Song, Y., Pan, J., Wang, X., Qin, C., Jia, Y., et al. (2022). Toxicity of Chronic Copper Exposure on Chinese Mitten Crab (Eriocheir Sinensis) and Mitigation of its Adverse Impact by Myo-Inositol. *Aquaculture* 547, 737511. doi:10.1016/j.aquaculture.2021.737511

Chen, S., Chen, M., Song, Y., Zhou, J., and Shan, Z. (2014). Toxic Effects of Two Organic Pesticides on Eriocheir Sinensis. *Environ. Sci. Technol.* 37 (9), 5–14. doi:10.3969/j.issn.1003-6504.2014.09.002

Edwards, P. G., Murphy, T. M., and Lydy, M. J. (2016). Fate and Transport of Agriculturally Applied Fungicidal Compounds, Azoxystrobin and Propiconazole. *Chemosphere* 146, 450–457. doi:10.1016/j.chemosphere.2015.11.116

European Food Safety Authority (2017). Conclusion on the Peer Review of the Pesticide Risk Assessment of the Active Substance Propiconazole. *EFSA J.* 15 (7), 4887. doi:10.2903/j.efsa.2017.4887

Fageria, N. K. (2007). Yield Physiology of Rice. *J. Plant. Nutr.* 30 (6), 843–879. doi:10.1080/15226510701374831

Gao, Y. N., Shan, Z. J., and Cheng, Y. (2010). Risk Assessment of Diafenthiuron to Three Species of Aquatic Organisms. *J. Ecol. Rural Environ.* 26 (5), 487–491. doi:10.3969/j.issn.1673-4831.2010.05.016

Hong, Y. H., Huang, Y., Yan, G. W., Pan, C., and Zhang, J. L. (2019). Antioxidative Status, Immunological Responses, and Heat Shock Protein Expression in Hepatopancreas of Chinese Mitten Crab, Eriocheir Sinensis under the Exposure of Glyphosate. *Fish Shellfish Immunol.* 86, 840–845. doi:10.1016/j.fsi.2018.12.020

Johansen, N. S., Moen, L. H., and Egaas, E. (2007). Sterol Demethylation Inhibitor Fungicides as Disruptors of Insect Development and Inducers of Glutathione S-Transferase Activities in Mamestra Brassicae. *Comp. Biochem. Physiol. C Toxicol. Pharmacol.* 145 (3), 473–483. doi:10.1016/j.cbpc.2007.02.004

Konwick, B. J., Garrison, A. W., Avants, J. K., and Fisk, A. T. (2006). Bioaccumulation and Biotransformation of Chiral Triazole Fungicides in Rainbow trout (*Oncorhynchus mykiss*). *Aquat. Toxicol.* 80 (4), 372–381. doi:10.1016/j.aquatox.2006.10.003

Li, Z. H., Zlabek, V., Grabic, R., Li, P., Machova, J., Velisek, J., et al. (2010). Effects of Exposure to Sublethal Propiconazole on Intestine-Related Biochemical Responses in Rainbow trout, *Oncorhynchus mykiss*. *Chem. Biol. Interact* 185 (3), 241–246. doi:10.1016/j.cbi.2010.02.040

Li, H., Song, W. H., Li, W. K., Fu, L. J., Yao, F. X., Hu, Z. Y., et al. (2013). Acute Toxicity of Three Pesticides to Juvenile Chinese Mitten Crab (Eriocheir Sinensis). *Chin. J. Fish.* 26 (6), 44–47. doi:10.3969/j.issn.1005-3832.2013.06.010

Liu, N., Dong, F., Xu, J., Liu, X., and Zheng, Y. (2016). Chiral Bioaccumulation Behavior of Tebuconazole in the Zebrafish (*Danio rerio*). *Ecotoxicol. Environ. Saf.* 126, 78–84. doi:10.1016/j.ecoenv.2015.12.007

Liu, J., Liu, H. B., Liu, R., Mostofa, A., Zhai, L. M., Lu, H. M., et al. (2018). "Water Quality in Irrigated Paddy Systems," in *Irrigation in Agroecosystems*. Editor G. Ondrasek (London, United Kingdom: Intech Open).

Lu, J., Zhang, J., Wang, P., Qing, H., and Zhou, G. (2020). Toxicity and Safety Evaluation of Two Pesticides against Red Swamp Crayfish *Procambarus clarkii* and Chinese Mitten Crab Eriocheir Sinensis. *Fish. Sci.* 39 (6), 908–914. doi:10.16378/j.cnki.1003-1111.2020.06.016

Pang, S., Guo, M., Zhang, X., Yu, L., Zhang, Z., Huang, L., et al. (2020). Myclobutanil Developmental Toxicity, Bioconcentration and Sex Specific Response in Cholesterol in Zebrafish (Denio Rerio). *Chemosphere* 242, 125209. doi:10.1016/j.chemosphere.2019.125209

Shen, H. S., Zang, Y., Song, K., Ma, Y. C., Dai, T. H., and Serwadda, A. (2017). A Meta-Transcriptomics Survey Reveals Changes in the Microbiota of the Chinese Mitten Crab Eriocheir Sinensis Infected with Hepatopancreatic Necrosis Disease. *Front. Microbiol.* 8, e732. doi:10.3389/fmicb.2017.00732

Shuqin, J., and Fang, Z. (2018). Zero Growth of Chemical Fertilizer and Pesticide Use: China's Objectives, Progress and Challenges. *J. Resour. Ecol.* 9, 50–58. doi:10.5814/j.issn.1674-764x.2018.01.006

Souders, C. L., 2nd, Xavier, P., Perez-Rodriguez, V., Ector, N., Zhang, J. L., and Martyniuk, C. J. (2019). Sub-lethal Effects of the Triazole Fungicide Propiconazole on Zebrafish (*Danio rerio*) Development, Oxidative Respiration, and Larval Locomotor Activity. *Neurotoxicol. Teratol.* 74, 106809. doi:10.1016/j.ntt.2019.106809

Van De Steene, J. C., Stove, C. P., and Lambert, W. E. (2010). A Field Study on 8 Pharmaceuticals and 1 Pesticide in Belgium: Removal Rates in Waste Water Treatment Plants and Occurrence in Surface Water. *Sci. Total Environ.* 408 (16), 3448–3453. doi:10.1016/j.scitotenv.2010.04.037

Wang, K., Wu, J. X., and Zhang, H. Y. (2012). Dissipation of Difenoconazole in rice, Paddy Soil, and Paddy Water under Field Conditions. *Ecotoxicol. Environ. Saf.* 86, 111–115. doi:10.1016/j.ecoenv.2012.08.026

Wang, Y., Xu, L., Li, D., Teng, M., Zhang, R., Zhou, Z., et al. (2015). Enantioselective Bioaccumulation of Hexaconazole and its Toxic Effects in Adult Zebrafish (*Danio rerio*). *Chemosphere* 138, 798–805. doi:10.1016/j.chemosphere.2015.08.015

Wang, Q., Yu, K., Ni, X., and Zhang, H. (2021). Development Process and Technical Trend of Integrated rice-fishing Cultivation. *China Rice* 27 (4), 88–91. doi:10.3969/j.issn.1006-8082.2021.04.018

Xu, Q., Liu, T., Guo, H., Dou, Z., Gao, H., and Zhang, H. (2021). Conversion from rice–wheat Rotation to rice–crayfish Coculture Increases Net Ecosystem Service Values in Hung-Tse Lake Area, east China. *J. Clean. Prod.* 319, 128883. doi:10.1016/j.jclepro.2021.128883

Yan, Y., Liu, M. D., Yang, D., Zhang, W., An, H., Wang, Y. J., et al. (2014). Effect of Different Rice-Crab Coculture Modes on Soil Carbohydrates. *J. Integr. Agric.* 13 (3), 641–647. doi:10.1016/S2095-3119(13)60722-4

Zhang, G., Zhou, J., Jiang, J., Kong, D., Tian, F., Cheng, Y., et al. (2014). Impact of Propiconazole on Aquatic Organisms in Pond Water Adjacent to Paddy Field. *Pestic. Sci. Admin* 35 (4), 36–40. doi:10.3969/j.issn.1002-5480.2014.04.008

Zhang, Y., Chen, M., Zhao, Y. Y., Zhang, A. Y., Peng, D. H., Lu, F., et al. (2021). Destruction of the Soil Microbial Ecological Environment Caused by the Over-utilization of the rice-crayfish Co-cropping Pattern. *Sci. Total Environ.* 788, 147794. doi:10.1016/j.scitotenv.2021.147794

Zhao, Y., Wang, X., Yu, Y., and Wu, J. (2009). Effect of Mercury Chloride for Survival, Growth and Molt of Juveniles of the Chinses Mitten Crab Eriocheir Sinensis. *Acta Sci. Natural. U Nankaien.* 2009 (3), 53–57.

Conflict of Interest: The authors declare that the research was conducted in the absence of any commercial or financial relationships that could be construed as a potential conflict of interest.

Publisher's Note: All claims expressed in this article are solely those of the authors and do not necessarily represent those of their affiliated organizations, or those of the publisher, the editors, and the reviewers. Any product that may be evaluated in this article, or claim that may be made by its manufacturer, is not guaranteed or endorsed by the publisher.

frontiers in Environmental Science

ORIGINAL RESEARCH
published: 14 March 2022
doi: 10.3389/fenvs.2022.814438

Effects of Biogas Residues on Dissipation of Difenoconazole in Paddy Sediment System Under Field Conditions

*Lina Yu[1,2], Yong Wen[3], Xuhui Luo[4], Yun Xiang[3], Xufeng Yuan[5], Sen Pang[1], Xiaodong Ma[1] and Xuefeng Li[1]**

[1]Department of Applied Chemistry, College of Sciences, China Agricultural University, Beijing, China, [2]Solid Waste and Chemicals Management Center, Ministry of Ecology and Environment, Beijing, China, [3]South China Institute of Environmental Sciences, Ministry of Ecology and Environment, Guangzhou, China, [4]Agricultural Ecology Institute, Fujian Academy of Agricultural Sciences, Fuzhou, China, [5]College of Agronomy and Biotechnology, China Agriculture University, Beijing, China*

Little is known about whether the application of biogas residues in rice fields will affect the degradation of pesticides. This study investigated the dissipation behavior of the fungicide difenoconazole in paddy water and sediment after the application of a chemical fertilizer or biogas residues. The results showed that the application of biogas residues changes the dissipation of difenoconazole in both paddy water and sediment. The half-lives of difenoconazole in paddy water and sediment with biogas residues were 0.50 and 10.09 days, respectively, while the half-lives of difenoconazole in paddy water and sediment with chemical fertilizer were only 0.22 and 4.64 days, respectively. After biogas residues were applied in a paddy field, no significant changes in pH value of paddy water and sediment and soil microorganisms were observed, but soil organic matter decreased by 30%. The above studies suggest that biogas residues may affect the dissipation of pesticides in paddy field water and sediments, which provides a new focus on the scientific and rational use of biogas residues as organic fertilizer in rice fields.

Keywords: difenoconazole, biogas residues, dissipation, paddy water, paddy sediment, paddy soil

OPEN ACCESS

Edited by:
Yue Geng,
Ministry of Agriculture and Rural Affairs, China

Reviewed by:
Germán Giácoman Vallejos,
Universidad Autónoma de Yucatán, Mexico
Chuanjiang Tao,
Ministry of Agriculture and Rural Affairs, China

****Correspondence:***
Xuefeng Li
91030@cau.edu.cn

Specialty section:
This article was submitted to Toxicology, Pollution, and the Environment, a section of the journal Frontiers in Environmental Science

Received: *13 November 2021*
Accepted: *20 January 2022*
Published: *14 March 2022*

Citation:
Yu L, Wen Y, Luo X, Xiang Y, Yuan X, Pang S, Ma X and Li X (2022) Effects of Biogas Residues on Dissipation of Difenoconazole in Paddy Sediment System Under Field Conditions. Front. Environ. Sci. 10:814438. doi: 10.3389/fenvs.2022.814438

INTRODUCTION

Pesticides are routinely used in integrated farm management programs to reduce possible losses. Pesticides undergo transformations in the environment when applied to crops. Despite beneficial effects on the global food supply and in maximizing the economic gain from agricultural activities, the use of pesticides can also cause environmental problems (Morrissey et al., 2015; Barron et al., 2017; Della Rossa et al., 2017; Souza et al., 2019). These persistent agrochemicals often cause health hazards to nontarget organisms, including animals and humans.

Azoles are versatile fungicides widely used to control fungal infestations in crops. Triazole fungicides are commonly used in agricultural systems against the main diseases of crops (Zubrod et al., 2019). Difenoconazole, the second molecule of triazole fungicide family to be released in the market, was developed by Switzerland Syngenta Corporation (Chowdhary and Meis, 2018). As a systemic sterol demethylation inhibitor (DMI), difenoconazole has a high ability to interfere with the mycelial growth and inhibit the spore germination of pathogens that ultimately results in inhibiting fungal growth. Difenoconazole is extensively used in a wide range of crops in many countries for its

good control of various fungal diseases (Wang et al., 2008). However, the strong hydrophobicity and high bioaccumulation of difenoconazole may lead to undesirable side effects on ecological environment and human health (Chen et al., 2021b). Difenoconazole has been identified to show high toxicity to aquatic organisms such as *Daphnia magna* (Reproduction NOEC = 0.0056 mg a.s./L) according to the European Food Safety Authority (EFSA, 2011). Our previous study with zebrafish indicated that difenoconazole was able to cause hatching inhibition, abnormal spontaneous movement, slow heart rate, growth regression, and morphological deformities (Mu et al., 2013). Difenoconazole has been used as the main fungicide to control rice diseases for many years, which has a greater opportunity to contact and contaminate the water environment. Therefore, it has become important to check the dissipation behavior of difenoconazole in a paddy field environment.

Previous studies have investigated the dissipation of difenoconazole in rice, paddy water, and sediment (Wang et al., 2012). Considering that pesticide dissipation behavior in the open field is usually related to soil properties and microorganisms in the soil, the influence of different fertilizers on the dissipation dynamics of difenoconazole remains to be further investigated. Anaerobic digestion (AD) has been widely applied in the treatment of various wastes because of its ability to degrade organic solid wastes and generate biogas as renewable energy (de França et al., 2021; Tayibi et al., 2021). As a byproduct of AD, biogas residues is rich in nitrogen, phosphorus, and organic matter and could be used as organic fertilizer (Terhoeven-Urselmans et al., 2009; Tambone et al., 2010; Liu et al., 2011; Ohdoi et al., 2013; Riva et al., 2016; Abelenda et al., 2021), which can sustainably replace inorganic fertilizer (Akhiar et al., 2017; Sigurnjak et al., 2017). Many studies have been carried out to investigate biogas residues as an alternative to chemical fertilizer to improve paddy soil fertility (Ohdoi et al., 2013). The effect of biogas residue application on soil properties has been widely reported in the literature (Odlare et al., 2014; de França et al., 2021; Jurgutis et al., 2021). Therefore, it is of great significance to investigate the influence of biogas residue application on the dissipation dynamics of pesticides in paddy fields.

The present study was performed in open rice fields in Guangze, Fujian Province, China. The purpose was to investigate the effect of biogas residues on the dissipation behavior of difenoconazole in paddy fields.

MATERIALS AND METHODS

Chemical material

Difenoconazole (25%) emulsifiable concentrate (EC) and difenoconazole stock standard solutions of 100 mg/L in acetone were supplied by the College of Science, China Agricultural University.

Biogas residues and chemical fertilizer

Biogas residues were produced during the anaerobic digestion from a biogas plant fed with pig dung, which is located in Guangze, Fujian Province, China. The basic properties of biogas residues from biogas plant fed with pig dung are shown in **Table 1**.

TABLE 1 | The basic properties of biogas residues from pig biogas plant Unit: mg/L.

TN	700.1 ± 15.2	Ca	3.59 ± 0.06	Pb	0.0060 ± 0.0007
NH_4^+–N	363.5 ± 6.1	Mg	2.00 ± 0.11	Cd	0.0005 ± 0.0001
NO_3^-–N	ND	Na	3.75 ± 0.04	Cr	0.0034 ± 0.0009
TP	4.13 ± 0.13	Fe	0.0199 ± 0.0028	As	0.012 ± 0.0017
TK	16.01 ± 0.14	Cu	0.0755 ± 0.0056	Mn	0.0275 ± 0.002
		Zn	0.0035 ± 0.0004	Hg	ND

Note. Chemical fertilizer mainly contains nitrogen, phosphorus, and potassium, and the proportion of N, P_2O_5, and K_2O is 12%, 5%, and 7%, respectively.

Field experiment

Field experiments were performed in Guangze, Fujian Province, China, in 2020. Two different treatments were chemical fertilizer treatment and biogas residue treatment (biogas residue total nitrogen input was 153.75 kg/ha equivalent to chemical fertilizer). Nitrogen input was 97.5 kg/ha before rice transplanting on June 1, 2020, and nitrogen input was 56.25 kg/ha after manuring on July 7, 2020, both with chemical fertilizer treatment and biogas residue treatment. Nitrogen content of chemical fertilizer is about 12%; therefore, rice transplantation was made, and after manuring, chemical fertilizer input was 813 and 469.5 kg/ha, separately. Nitrogen content of biogas residues is about 0.04%; therefore, after rice transplantation and manuring, biogas residue input was 243.75 and 139.09 t/ha, separately. The total experiment plot was 300 m^2 (Each plot was 50 m^2, and chemical fertilizer treatment and biogas residues treatment were repeated three times, respectively). A buffer area of 50 m^2 was used to separate the plots of different treatments.

Difenoconazole EC (25%) was sprayed evenly in the above two experiment plots using a SeeSa SX-MD16E-2 backpack sprayer at an active ingredient dose of 45 g a.i./ha. Paddy sediment was collected randomly using a sealing bag from the bottom mud surface to measure difenoconazole concentration. Paddy water was collected randomly using plastic bottles and then mixed in plastic containers to measure difenoconazole concentration. Paddy water and sediment samples were collected from each plot at 2 h (August 31, 2020), 1 day (September 1, 2020), 3 days (September 3, 2020), 7 days (September 7, 2020), 14 days (September 12, 2020), and 21 days (September 21, 2020) after difenoconazole application. Paddy soil was collected randomly using a soil auger to a depth of 10 cm from the land surface to measure pH value and soil organic matter, and soil microorganisms and soil samples were collected from each plot on May 24 and October 26, 2020. Five sediment, water, and soil samples were taken from each plot. All samples were stored at −20°C until analyzed within 1 month.

Preparation of water sample

Water sample (5 ml) was transferred into a 50-ml centrifuge tube, and 10 ml of ethyl acetate was added. The solution was vortexed for 2 min and subsequently centrifuged at 4,000 r/min for 5 min.

TABLE 2 | Mass spectrometric parameters.

Mass spectrometric parameter pesticide	Retention time (min)	Prec ion	Prod ion (CE)	Collision energy
Difenoconazole	1.8	406	337 251*	15 25

Asterisk was used for quantitative analysis.

The supernatant ethyl acetate layer was transferred into a 50-ml heart-shaped bottle. Ethyl acetate (10 ml) was added to the water sample again, and the above extraction operation was repeated once. The supernatant ethyl acetate in the heart-shaped bottle was vacuum evaporated to dryness. The residue was then dissolved with 1 ml of acetonitrile and then filtered through a 0.22-μm membrane filter into an autosampler vial and analyzed by LC–MS.

Preparation of sediment sample

Homogenized sediment sample (2 g) was transferred into a 50-ml centrifuge tube, and then 5 ml of HPLC-grade water and 10 ml of ethyl acetate were added. Further preparation of these samples was the same as for the water samples described above.

Apparatus

All samples were detected by LC-MS/MS of Shimadzu. The ion source was electrospray ionization (ESI), and Agilent POROSHELL 120EC-C_{18} (2.7 μm × 2.1 mm × 50 mm) was employed at room temperature. The flow rate of acetonitrile/H_2O (0.1%HCOOH) = 70/30 (V/V) was 0.2 ml·min^{-1}. Selected multiple reaction monitoring (MRM) as the detection mode in triple-quadrupole mass spectrometry. The relevant parameters and the limit of detection of this method are shown in **Table 2**.

Measurement of pH value, soil organic matter, and soil microorganisms

The pH of paddy water was measured directly using a calibrated pH meter. The pH of paddy soil is measured according to the following operations: 20 g of naturally dried soil was transferred into a 250-ml Erlenmeyer flask, and 100 ml of deionized water was added. The solution was shaken for 30 min and subsequently placed overnight. The supernatant layer was transferred into a beaker and measured using a calibrated pH meter. The pH measurement of paddy water and soil was repeated three times.

The soil organic matter assay was performed as described. Naturally dried soil (0.5 g) passing a 0.5-mm-diameter sieve was transferred into a glass beaker and 5 ml of $K_2Cr_2O_7$ (0.8 mol/L) was added. The solution was thoroughly mixed, and 5 ml of concentrated sulfuric acid was added then heated to 185°C–190°C. The solution was kept boiling for 5 min and was made to undergo static cool down. O-phenanthrolin indicator (three to four drops) was added to the cooled solution and titrated with $FeSO_4$ (0.2 mol/L) until the solution turns brown red. The blank test was carried out with silica instead of soil samples.

Soil microorganisms were analyzed using Illumina miseq platform (Chen et al., 2021a). DNA from different samples was extracted using the E.Z.N.A.® Soil DNA Kit (Omega Bio-tek, Norcross, GA, USA) according to the instructions of the manufacturer. Primers 338F (5′-ACT CCT ACG GGA GGC AGC AG-3′) and 806R (5′-GGA CTA CHV GGG TWT CTA AT-3′) were designed to amplify the V3–V4 region gene (Fadrosh et al., 2014). PCR amplification was performed in a total volume of 20 μl of reaction mixture containing 10 ng of template DNA, 4 μl of 5*FastPfu buffer, 2 μl of dNTPs (2.5 mM), 0.8 μl of each primer (5 μM), 0.4 μl of FastPfu polymerase, and PCR-grade water to adjust the volume. PCR amplification conditions were 30 s at 95°C, 30 s at 55°C, and 30 s at 72°C (27 cycles) (ABI GeneAmp® 9700).

The PCR products were confirmed with 2% agarose gel electrophoresis. The PCR products were purified by AxyPrep DNA Gel Extraction Kit (Axygen Biosciences, Union City, CA, USA) and quantified by QuantiFluor™-ST (Promega, USA).

The PE 2*300 library was constructed from purified amplified fragments according to standard operating procedure of Illumina MiSeq (Illumina, San Diego, CA, USA).

In brief: 1) connect the "Y"-shaped joint; 2) remove the self-connecting segment by magnetic bead screening; 3) enrichment of templates by PCR amplification; 4) denature to produce single-stranded DNA fragments by NaOH. Sequencing was performed using Illumina Miseq PE300.

Trimmomatic software was used for quality control of original sequences, and FLASH software was used as a splicing tool: 1) 50 bp was used as the removal criterion, and base back-end sequences with average mass value lower than 20 were subtracted; 2) when sequences on both ends are splicing, the maximum error ratio between overlap is 0.2, and the length should be greater than 10 bp; 3) barcode was accurately matched, and the number of base mismatches of primers was ≤2.

The UPARSE software (version 7.1) http://drive5.com/uparse/ was used for OTU sequence clustering (similarity ≥97%) at the same time removing the single sequence and chimeras. RDP classifier (http://rdp.cme.msu.edu/) was used to make species classification annotation for each sequence and compared with the Silva database (SSU123). The threshold of comparison was 70%.

Statistical analysis

The dissipation of difenoconazole has been generally expressed in terms of DT_{50}, i.e., the time after which 50% of the difenoconazole has disappeared. DT_{50} values were obtained by fitting first-order kinetics to observe degradation patterns, expressed by the equation: $C = C_0\ e^{-kt}$, where C is the chemical concentration at time t (d), C_0 is the initial concentration, and k is the first-order rate constant (d^{-1}), which is independent of C and C_0. The DT_{50} of difenoconazole was calculated using Hoskins formula ($DT_{50} = \ln 2\ k^{-1}$) for each location (Hoskins, 1961).

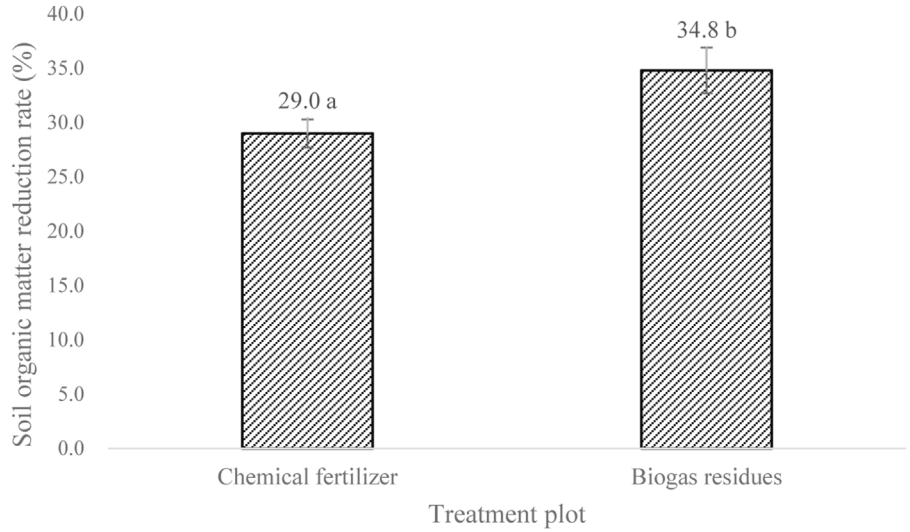

FIGURE 1 | Paddy soil organic matter reduction rate. Error bar is S.D. ($N = 3$). Different lowercase letters denote significant differences ($p < 0.05$), analyzed by ANOVA followed by Duncan multiple comparison test.

Soil organic matter (%) = $[(V_0-V) \times C \times 0.003 \times 1.724 \times f]/W \times 100\%$where, C is the molar concentration of $FeSO_4$ (mol/L), V0 is the volume of the $FeSO_4$ solution consumed by the blank test (ml), V is the volume of the $FeSO_4$ solution consumed by the soil sample test (ml), 0.003 is the molar mass of a quarter of a carbon atom (g/mol) and factor of equivalence (1 L/1,000 ml), 1.724 is the empirical coefficient of converting soil organic carbon into soil organic matter, f is the oxidation correction coefficient (f = 1.1), and W is the dry weight of the tested soil sample (g).

RESULTS

Results of pH, soil organic matter, and soil microorganisms

There was no obvious change in pH of paddy water and sediment before and after fertilizer application with pH around 6.0. However, significant changes in soil organic matter were observed between the two treatment plots with chemical fertilizer and biogas residues. The soil organic matter decreased by 29% in the chemical fertilizer treatment plot, while a higher reduction rate of 34.8% in the soil organic matter was observed in biogas residue treatment plot (**Figure 1**), indicating that under nitrogen equivalent condition, the application of chemical fertilizer contains more phosphorus and potassium to preserve soil fertility, while there is less nutrient content in biogas residues, and the paddy rice absorbed more from the soil, leading to more decrease in organic matter in biogas residue treatment. Zhang (2017) indicated that fertilizers provide nutrients for agriculture system and increase soil fertility.

There was also a slight difference in the species of soil microorganisms between the two treatment plots (**Figure 2**). The main dominant phyla were Proteobacteria, Chloroflexi, Acidobacteriota, and Actinobacteriota, indicating that the application of biogas residues has no effect on the diversity of soil microorganisms.

Dissipation of difenoconazole in paddy water and sediment

The results of difenoconazole dissipation in paddy water are shown in **Figure 3**. The initial concentrations of difenoconazole were 3.177 μg/L in chemical fertilizer treatment plot and 2.575 μg/L in biogas residue treatment plot, respectively. The dissipation dynamics of difenoconazole in paddy water could be described by the first-order kinetic equation: $C = 3.1770e^{-3.1915t}$ (chemical fertilizer treatment plot) and $C = 2.5537e^{-1.3868t}$ (biogas residue treatment plot), respectively. The dissipation half-life (DT_{50}) of difenoconazole calculated from the regression equation was 0.22 day (chemical fertilizer treatment plot) and 0.50 day (biogas residue treatment plot), respectively.

Figure 4 shows the dissipation results for difenoconazole in paddy sediment. The initial residues in sediment were 0.796 μg/kg in chemical fertilizer treatment plot and 2.145 μg/kg in biogas residue treatment plot, respectively. A sharp increase in difenoconazole residue occurred from 2 h to 1 day in both treatment plots. After reaching peak in 1 day, a gradual degradation of difenoconazole was observed in accordance with first-order kinetics. The dissipation dynamics of difenoconazole in paddy soil could be described by the equations: $C = 2.4804e^{-0.1495x}$ (chemical fertilizer treatment plot) and $C = 2.9403e^{-0.0687x}$ (biogas residue treatment plot), respectively. The DT_{50} of difenoconazole in paddy soil were 4.64 days (chemical fertilizer treatment plot) and 10.09 days (biogas residues treatment plot), respectively.

DISCUSSION

As an important agricultural production material, the pesticides benefit a lot in increasing the agricultural production. However, the current pesticide utilization rate in China is only about 40%, and about 60% of pesticides enter the environment (Shuqin and

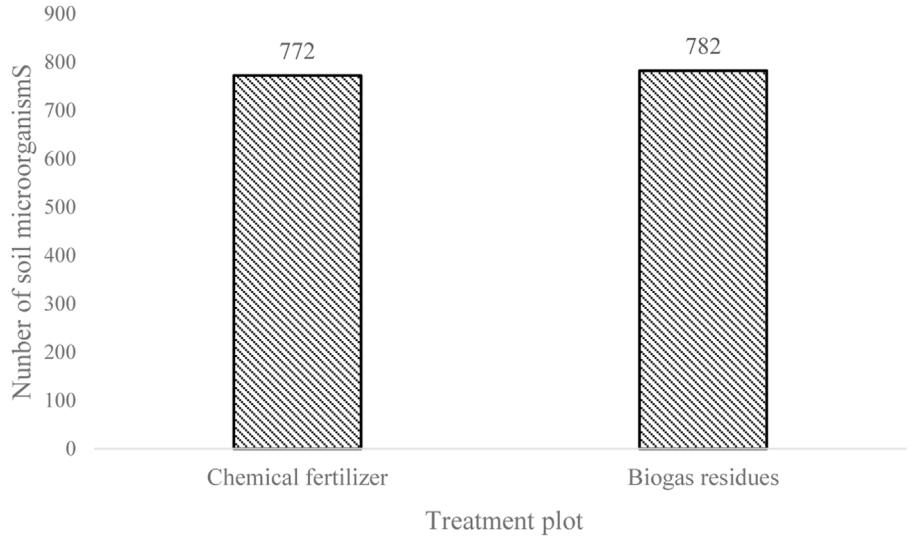

FIGURE 2 | Number of soil microorganisms in paddy soil.

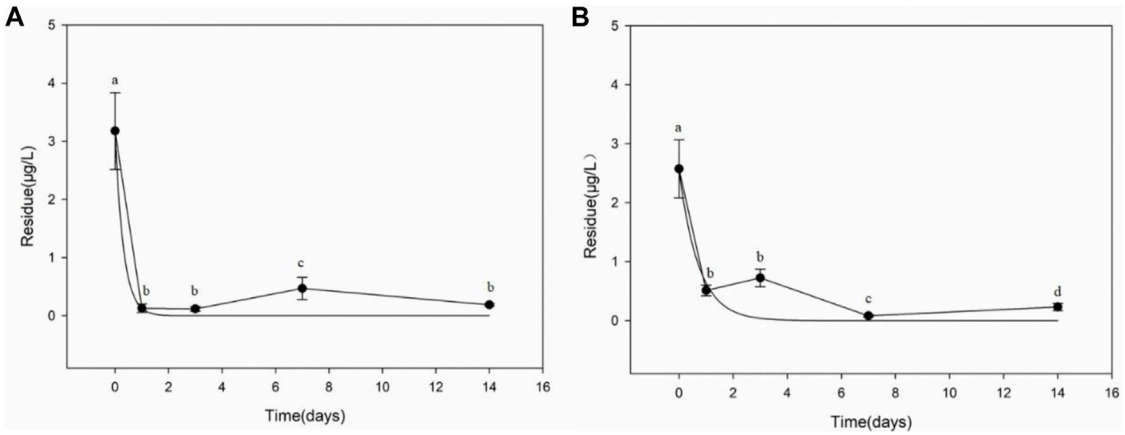

FIGURE 3 | Dissipation of difenoconazole in paddy water. **(A)** Chemical fertilizer treatment plot. **(B)** Biogas residue treatment plot. Error bar is S.D. (N = 3). Different lowercase letters denote significant differences ($p < 0.05$), analyzed by ANOVA followed by Duncan multiple comparison test.

Fang, 2018), which may pose a threat to the ecological environment. Therefore, the rapid degradation of pesticides after entering the environment is very important to environmental safety. The current research on the negative impact of biogas residues on the environment mainly focuses on heavy metal and antibiotic pollution (Pu et al., 2018; Xu et al., 2019; Liu et al., 2020; Tang et al., 2020; He et al., 2021; Lu et al., 2021). Relatively, little is known whether biogas residues have an impact on pesticide degradation after being used as fertilizer in farmland. It has been reported that the application of biogas residues can significantly improve the physical and chemical properties of soil (Zhu et al., 2012; Wang et al., 2016). However, the dissipation behavior of pesticides in the environment is usually related to soil properties, such as pH, soil organic matter, and soil microorganisms. Therefore, the effect of biogas residues applied in farmland on pesticide dissipation behavior needs further investigation.

In the present paper, we investigate the dissipation behavior of the difenoconazole in rice fields applied with chemical fertilizer or biogas residues. Pesticides can be adsorbed and degraded by organic matter that contains microorganisms (Godeau et al., 2021), which makes it more important to investigate the changes in the organic matter and microorganisms, and their roles in the effect of pesticide dissipation. We observed longer DT50 of difenoconazole in paddy sediment and water in rice fields applied with biogas residues than with chemical fertilizers, in accordance with the severe decrease in organic matter after treatment with biogas residues (**Figure 1**). Although biogas residues did not change the species of

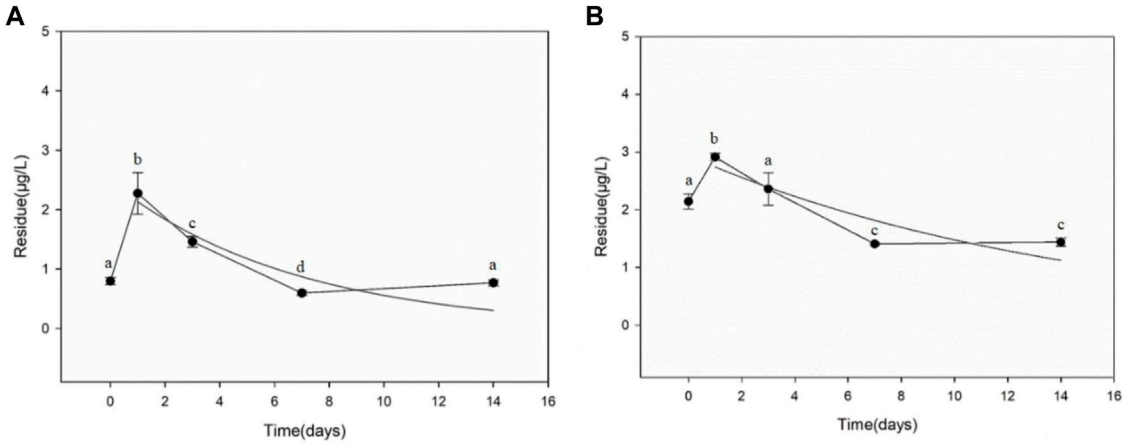

FIGURE 4 | Dissipation of difenoconazole in paddy sediment. **(A)** Chemical fertilizer treatment plot. **(B)** Biogas residue treatment plot. Error bar is S.D. ($N = 3$). Different lowercase letters denote significant differences ($p < 0.05$), analyzed by ANOVA followed by Duncan multiple comparison test.

microorganisms in paddy sediment (**Figure 2**), we speculate that biogas residues may affect the degradation ability of soil microorganisms to difenoconazole. Since the ability of soil microorganisms to degrade pesticides is related to the content of organic matter that contains energy and nutrient supplies for microorganisms in soil, which influences the microbial activities (Holatko et al., 2021). The decline in soil organic matter in paddy field with biogas residues may not provide sufficient carbon source and energy for soil microorganisms, resulting in the decline of soil microbial activities, and thus, their ability to degrade difenoconazole is also reduced. Another possibility of longer DT50 of difenoconazole with biogas residues is that slow biodegradation of difenoconazole may occur under certain conditions. In water–sediment systems, slow degradation from the system was reported; half-life is 8 months. Meanwhile, difenoconazole contains chromophores, which may be susceptible to direct photolysis by sunlight (Environmental Abiotic Degradation[1]). Grain yield with biogas residues is 8,158.05 kg/ha, 7.5% higher than 7,590.6 kg/ha of chemical fertilizers. Moreover, biogas residues contain microelements, such as calcium, magnesium, iron, etc., which help crops grow more flourishing than chemical fertilizers. We observed that rice crops with biogas residues are more flourishing than with chemical fertilizers, which may block the light to impact photodecomposition. Therefore, we speculate that DT50 of difenoconazole is longer with biogas residues than with chemical fertilizers could be photolysis.

CONCLUSION

As organic fertilizer, biogas residues can replace chemical fertilizers to provide nutrients for crops. However, our research found that biogas residues may affect the dissipation of the fungicide difenoconazole in rice fields. Difenoconazole has a longer half-life in paddy water and sediment where biogas residues were applied. This study provides a new focus on the scientific and rational use of biogas residues as organic fertilizer in rice field.

DATA AVAILABILITY STATEMENT

The datasets presented in this study can be found in online repositories. The name of the repository and accession number can be found below: National Center for Biotechnology Information (NCBI) BioProject, https://www.ncbi.nlm.nih.gov/bioproject/, PRJNA795026.

AUTHOR CONTRIBUTIONS

Investigation: LY, YW, YX, and XY. Methodology: XM and XY. Data curation: XM, XLu, and YX. Conceptualization: LY, XM, and SP. Writing–original draft: LY and XM. Writing, reviewing, and editing: LY, SP, and XM. Formal analysis: YW; SP, and YX. Supervision: XLi. Funding acquisition: XLi.

FUNDING

This work was supported by Zero-Waste City Pilots of Guangze County to evaluate "Zero-Waste Agriculture" performance on research on the establishment of breeding and planting circular ecological agriculture model and environmental risk.

ACKNOWLEDGMENTS

The authors acknowledge the technical support from Dr. Changsheng Li of the College of Agronomy and Biotechnology, China Agriculture University.

[1]https://pubchem.ncbi.nlm.nih.gov/compound/86173#section<Environmental-Fate-Exposure-Summary

REFERENCES

Abelenda, A. M., Semple, K. T., Lag-Brotons, A. J., Herbert, B. M. J., Aggidis, G., and Aiouache, F. (2021). Kinetic Study of the Stabilization of an Agro-Industrial Digestate by Adding wood Fly Ash. *Chem. Eng. J. Adv.* 7, 100127. doi:10.1016/j.ceja.2021.100127

Akhiar, A., Battimelli, A., Torrijos, M., and Carrere, H. (2017). Comprehensive Characterization of the Liquid Fraction of Digestates from Full-Scale Anaerobic Co-digestion. *Waste Manage.* 59, 118–128. doi:10.1016/j.wasman.2016.11.005

Barron, M. G., Ashurova, Z. J., Kukaniev, M. A., Avloev, H. K., Khaidarov, K. K., Jamshedov, J. N., et al. (2017). Residues of Organochlorine Pesticides in Surface Soil and Raw Foods from Rural Areas of the Republic of Tajikistan. *Environ. Pollut.* 224, 494–502. doi:10.1016/j.envpol.2017.02.031

Chen, M., Qin, Y., Deng, F., Zhou, H., Wang, R., Li, P., et al. (2021a). Illumina MiSeq Sequencing Reveals Microbial Community Succession in Salted Peppers with Different Salinity during Preservation. *Food Res. Int.* 143, 110234. doi:10.1016/j.foodres.2021.110234

Chen, S., Cai, L., Zhang, H., Zhang, Q., Song, J., Zhang, Z., et al. (2021b). Deposition Distribution, Metabolism Characteristics, and Reduced Application Dose of Difenoconazole in the Open Field and Greenhouse Pepper Ecosystem. *Agric. Ecosyst. Environ.* 313, 107370. doi:10.1016/j.agee.2021.107370

Chowdhary, A., and Meis, J. F. (2018). Emergence of Azole Resistant Aspergillus fumigatus and One Health: Time to Implement Environmental Stewardship. *Environ. Microbiol.* 20 (4), 1299–1301. doi:10.1111/1462-2920.14055

de França, A. A., von Tucher, S., and Schmidhalter, U. (2021). Effects of Combined Application of Acidified Biogas Slurry and Chemical Fertilizer on Crop Production and N Soil Fertility. *Eur. J. Agron.* 123, 126224. doi:10.1016/j.eja.2020.126224

Della Rossa, P., Jannoyer, M., Mottes, C., Plet, J., Bazizi, A., Arnaud, L., et al. (2017). Linking Current River Pollution to Historical Pesticide Use: Insights for Territorial Management? *Sci. Total Environ.* 574, 1232–1242. doi:10.1016/j.scitotenv.2016.07.065

EFSA (2011). *Conclusion on the Peer Review of the Pesticide Risk Assessment of the Active Substance Difenoconazole*. Parma, Italy: European Food Safety Authority.

Fadrosh, D. W., Ma, B., Gajer, P., Sengamalay, N., Ott, S., Brotman, R. M., et al. (2014). An Improved Dual-Indexing Approach for Multiplexed 16S rRNA Gene Sequencing on the Illumina MiSeq Platform. *Microbiome* 2 (1), 6. doi:10.1186/2049-2618-2-6

Godeau, C., Morin-Crini, N., Staelens, J.-N., Martel, B., Rocchi, S., Chanet, G., et al. (2021). Adsorption of a Triazole Antifungal Agent, Difenoconazole, on Soils from a Cereal Farm: Protective Effect of Hemp Felt. *Environ. Tech. Innovation* 22, 101394. doi:10.1016/j.eti.2021.101394

He, L., Zhu, Q., Wang, Y., Chen, C., He, M., and Tan, F. (2021). Irrigating Digestate to Improve Cadmium Phytoremediation Potential of Pennisetum Hybridum. *Chemosphere* 279, 130592. doi:10.1016/j.chemosphere.2021.130592

Holatko, J., Hammerschmiedt, T., Kintl, A., Danish, S., Skarpa, P., Latal, O., et al. (2021). Effect of Carbon-Enriched Digestate on the Microbial Soil Activity. *Plos One* 16 (7), e0252262. doi:10.1371/journal.pone.0252262

Hoskins, W. M. (1961). Mathematical Treatment of the Rate of Loss of Pesticide Residues. FAO. *Plant Prot. Bull.* 9, 163–168.

Jurgutis, L., Šlepetienė, A., Amalevičiūtė-Volungė, K., Volungevičius, J., and Šlepetys, J. (2021). The Effect of Digestate Fertilisation on Grass Biogas Yield and Soil Properties in Field-Biomass-Biogas-Field Renewable Energy Production Approach in Lithuania. *Biomass and Bioenergy* 153, 106211. doi:10.1016/j.biombioe.2021.106211

Liu, C., Chen, Y., Li, X., Zhang, Y., Ye, J., Huang, H., et al. (2020). Temporal Effects of Repeated Application of Biogas Slurry on Soil Antibiotic Resistance Genes and Their Potential Bacterial Hosts. *Environ. Pollut.* 258, 113652. doi:10.1016/j.envpol.2019.113652

Liu, W. K., Yang, Q. C., Du, L. F., Cheng, R. F., and Zhou, W. L. (2011). Nutrient Supplementation Increased Growth and Nitrate Concentration of Lettuce Cultivated Hydroponically with Biogas Slurry. *Acta Agriculturae Scand. Section B - Soil Plant Sci.* 61 (5), 391–394. doi:10.1080/09064710.2010.482539

Lu, Y., Li, J., Meng, J., Zhang, J., Zhuang, H., Zheng, G., et al. (2021). Long-term Biogas Slurry Application Increased Antibiotics Accumulation and Antibiotic Resistance Genes (ARGs) Spread in Agricultural Soils with Different Properties. *Sci. Total Environ.* 759, 143473. doi:10.1016/j.scitotenv.2020.143473

Morrissey, C. A., Mineau, P., Devries, J. H., Sanchez-Bayo, F., Liess, M., Cavallaro, M. C., et al. (2015). Neonicotinoid Contamination of Global Surface Waters and Associated Risk to Aquatic Invertebrates: a Review. *Environ. Int.* 74, 291–303. doi:10.1016/j.envint.2014.10.024

Mu, X., Pang, S., Sun, X., Gao, J., Chen, J., Chen, X., et al. (2013). Evaluation of Acute and Developmental Effects of Difenoconazole via Multiple Stage Zebrafish Assays. *Environ. Pollut.* 175, 147–157. doi:10.1016/j.envpol.2012.12.029

Odlare, M., Pell, M., Arthurson, J. V., Abubaker, J., and Nehrenheim, E. (2014). Combined mineral N and Organic Waste Fertilization - Effects on Crop Growth and Soil Properties. *J. Agric. Sci.* 152 (1), 134–145. doi:10.1017/S0021859612001050

Ohdoi, K., Miyahara, S., Iwashita, K., Umeda, M., Shimizu, H., Nakashima, H., et al. (2013). Optimization of Fertilizer Application Schedule: Utilization of Digestate after Anaerobic Digestion as Liquid Fertilizer. *IFAC Proc. Volumes* 46 (4), 317–322. doi:10.3182/20130327-3-jp-3017.00072

Pu, C., Liu, H., Ding, G., Sun, Y., Yu, X., Chen, J., et al. (2018). Impact of Direct Application of Biogas Slurry and Residue in fields: *In Situ* Analysis of Antibiotic Resistance Genes from Pig Manure to fields. *J. Hazard. Mater.* 344, 441–449. doi:10.1016/j.jhazmat.2017.10.031

Riva, C., Orzi, V., Carozzi, M., Acutis, M., Boccasile, G., Lonati, S., et al. (2016). Short-term Experiments in Using Digestate Products as Substitutes for mineral (N) Fertilizer: Agronomic Performance, Odours, and Ammonia Emission Impacts. *Sci. Total Environ.* 547, 206–214. doi:10.1016/j.scitotenv.2015.12.156

Shuqin, J., and Fang, Z. (2018). Zero Growth of Chemical Fertilizer and Pesticide Use: China's Objectives, Progress and Challenges. *J. Resour. Ecol.* 9 (sp1), 50–58. doi:10.5814/j.issn.1674-764x.2018.01.006

Sigurnjak, I., Vaneeckhaute, C., Michels, E., Ryckaert, B., Ghekiere, G., Tack, F. M. G., et al. (2017). Fertilizer Performance of Liquid Fraction of Digestate as Synthetic Nitrogen Substitute in Silage maize Cultivation for Three Consecutive Years. *Sci. Total Environ.* 599-600, 1885–1894. doi:10.1016/j.scitotenv.2017.05.120

Souza, L. P., Faroni, L. R. D. A., Heleno, F. F., Pinto, F. G., Queiroz, M. E. L. R., and Prates, L. H. F. (2019). Difenoconazole and Linuron Dissipation Kinetics in Carrots under Open-Field Conditions. *Ecotoxicology Environ. Saf.* 168, 479–485. doi:10.1016/j.ecoenv.2018.10.070

Tambone, F., Scaglia, B., D'Imporzano, G., Schievano, A., Orzi, V., Salati, S., et al. (2010). Assessing Amendment and Fertilizing Properties of Digestates from Anaerobic Digestion through a Comparative Study with Digested Sludge and Compost. *Chemosphere* 81 (5), 577–583. doi:10.1016/j.chemosphere.2010.08.034

Tang, Y., Wang, L., Carswell, A., Misselbrook, T., Shen, J., and Han, J. (2020). Fate and Transfer of Heavy Metals Following Repeated Biogas Slurry Application in a rice-wheat Crop Rotation. *J. Environ. Manage.* 270, 110938. doi:10.1016/j.jenvman.2020.110938

Tayibi, S., Monlau, F., Marias, F., Thevenin, N., Jimenez, R., Oukarroum, A., et al. (2021). Industrial Symbiosis of Anaerobic Digestion and Pyrolysis: Performances and Agricultural Interest of Coupling Biochar and Liquid Digestate. *Sci. Total Environ.* 793, 148461. doi:10.1016/j.scitotenv.2021.148461

Terhoeven-Urselmans, T., Scheller, E., Raubuch, M., Ludwig, B., and Joergensen, R. G. (2009). CO2 Evolution and N Mineralization after Biogas Slurry Application in the Field and its Yield Effects on spring Barley. *Appl. Soil Ecol.* 42 (3), 297–302. doi:10.1016/j.apsoil.2009.05.012

Wang, K., Wu, J. X., and Zhang, H. Y. (2012). Dissipation of Difenoconazole in rice, Paddy Soil, and Paddy Water under Field Conditions. *Ecotoxicology Environ. Saf.* 86, 111–115. doi:10.1016/j.ecoenv.2012.08.026

Wang, Y. Q., Han, W. B., Zhao, Y. Z., Chen, H., Wang, Y. X., and Hu, S. L. (2016). Effects of Biogas Slurry on Soil Physical and Chemical Properties. *J. Anhui Agr Sci.* 44 (1), 193–195. doi:10.3969/j.issn.0517-6611.2016.01.064

Wang, Z. H., Yang, T., Qin, D. M., Gong, Y., and Ji, Y. (2008). Determination and Dynamics of Difenoconazole Residues in Chinese Cabbage and Soil. *Chin. Chem. Lett.* 19 (8), 969–972. doi:10.1016/j.cclet.2008.04.028

Xu, Z.-M., Wang, Z., Gao, Q., Wang, L.-L., Chen, L.-L., Li, Q.-G., et al. (2019). Influence of Irrigation with Microalgae-Treated Biogas Slurry on Agronomic Trait, Nutritional Quality, Oxidation Resistance, and Nitrate and Heavy Metal Residues in Chinese Cabbage. *J. Environ. Manage.* 244, 453–461. doi:10.1016/j.jenvman.2019.04.058

Zhang, F. S. (2017). Scientific Understanding of the Role of Fertilizers. *China Agr Technol. Ext* 33 (1), 16–19. doi:10.3969/j.issn.1002-381X.2017.01.005

Zhu, Y. L., Na, W., Xi, D. B., and Zhao, X. Y. (2012). Effects of Application of Biogas Slurry of Pig Dung on Physical and Chemical Properties of Soil. *J. Anhui Agr Sci.* 40 (31), 15202–15203. doi:10.3969/j.issn.0517-6611.2012.31.043

Zubrod, J. P., Bundschuh, M., Arts, G., Brühl, C. A., Imfeld, G., Knäbel, A., et al. (2019). Fungicides: An Overlooked Pesticide Class? *Environ. Sci. Technol.* 53 (7), 3347–3365. doi:10.1021/acs.est.8b04392

Conflict of Interest: The authors declare that the research was conducted in the absence of any commercial or financial relationships that could be construed as a potential conflict of interest.

Publisher's Note: All claims expressed in this article are solely those of the authors and do not necessarily represent those of their affiliated organizations, or those of the publisher, the editors, and the reviewers. Any product that may be evaluated in this article, or claim that may be made by its manufacturer, is not guaranteed nor endorsed by the publisher.

frontiers in Environmental Science

ORIGINAL RESEARCH
published: 23 March 2022
doi: 10.3389/fenvs.2022.807290

Advanced Oxidation Processes Using Zinc Oxide Nanocatalyst for Detoxification of Some Highly Toxic Insecticides in an Aquatic System Combined With Improving Water Quality Parameters

Ahmed Massoud[1], Ibrahim El-Mehasseb[2], Moustafa Saad Allah[1], Ehab Kotb Elmahallawy[3], Khalaf F. Alsharif[4], Mohamed S. Ahmed[5] and Aly Soliman Derbalah[1]*

[1]*Pesticides Chemistry and Toxicology Department, Faculty of Agriculture, Kafr-El-Sheikh University, Kafr El Sheikh, Egypt,* [2]*Nanotechnology Center, Chemistry Department, Faculty of Science, Kafr-El-Sheikh University, Kafr El Sheikh, Egypt,* [3]*Department of Zoonoses, Faculty of Veterinary Medicine, Sohag University, Sohag, Egypt,* [4]*Department of Clinical Laboratory Sciences, College of Applied Medical Sciences, Taif University, Taif, Saudi Arabia,* [5]*Department of Pathology, Faculty of Veterinary Medicine, Kafrelsheikh University, Kafr El sheikh, Egypt*

OPEN ACCESS

Edited by:
Mazhar Iqbal Zafar, Quaid-i-Azam University, Pakistan

Reviewed by:
Mohamed Hassaan, National Institute of Oceanography and Fisheries (NIOF), Egypt
Muhammad Bilal Khan Niazi, National University of Sciences and Technology (NUST), Pakistan

***Correspondence:**
Ehab Kotb Elmahallawy
eehaa@unileon.es

Specialty section:
This article was submitted to Toxicology, Pollution and the Environment, a section of the journal Frontiers in Environmental Science

Received: *02 November 2021*
Accepted: *22 February 2022*
Published: *23 March 2022*

Citation:
Massoud A, El-Mehasseb I, Saad Allah M, Elmahallawy EK, Alsharif KF, S. Ahmed M and Derbalah AS (2022) Advanced Oxidation Processes Using Zinc Oxide Nanocatalyst for Detoxification of Some Highly Toxic Insecticides in an Aquatic System Combined With Improving Water Quality Parameters. Front. Environ. Sci. 10:807290. doi: 10.3389/fenvs.2022.807290

Pesticides are among the major organic pollutants, and their random extensive applications threaten human health and ecosystems. Clearly, detoxification of toxic insecticides from the aquatic system remains a global priority. In the present study, a zinc oxide nanocatalyst was synthesized with suitable properties to achieve complete degradation of some insecticides (dimethoate and methomyl) from aqueous media. The ZnO catalyst was used in normal and in nano-size as a part of an advanced oxidation process in the presence of H_2O_2 and UV rays. The complete detoxification of the tested pesticides after treatment with the most effective process (ZnO(s)/H_2O_2/UV) was then examined by exploring the biochemical and histopathological changes in the liver and kidneys of treated rats compared to the control. The effect of water treatment by ZnO (nano)/H_2O_2/UV on the water quality parameters of treated water was also investigated. Interestingly, the present study reported that the degradation rates of the investigated insecticides were faster using the nano-sized ZnO catalyst than the regular ZnO catalyst. In this respect, complete decomposition of the tested insecticides (100%) under the ZnO(s)/H_2O_2/UV system was achieved after 320 min of irradiation. The half-lives of the tested insecticides under ZnO(c)/H_2O_2/UV were 43.86 and 36.28 for dimethoate and methomyl, respectively, while under the ZnO(c)/H_2O_2/UV system, the half-live values were 27.72 and 19.52 min for dimethoate and methomyl, respectively. On the other hand, there were no significant changes in the biochemical and histological parameters of rats treated with remediated water when compared to the control group. The treatment of water by zinc oxide nanocatalyst improved the quality of water parameters. Collectively, advanced oxidation processes using ZnO nanocatalyst can be considered as a promising treatment technology for the complete detoxification of methomyl and dimethoate in water. However, further research is warranted for the identification of the potential breakdown products.

Keywords: degradation, insecticides, toxicity, light, nanocatalyst, water

INTRODUCTION

Nowadays, Egypt is facing and suffering from two huge problems. The first one is the Renaissance Dam in Ethiopia which might cause a shortage in water supply and reduce Egypt's share of the Nile water by 14.5 billion cubic meters, which can irrigate three million Fadden (Chronicles, 2013). The second problem is environmental pollution in general, and particularly, agrochemical pollutants in surface water through the intensive use of pesticides and fertilizers (Derbalah and Ismail, 2013; Derbalah et al., 2014; Dahshan et al., 2016; Abbassy, 2018; Abdelrazek, 2019; Eissa et al., 2020; Eissa et al., 2021). The pollution of surface water and wastewater has increased sharply, and it constitutes a major problem due to the extensive use of these substances (Evgenidou et al., 2007). Monitoring of pesticides in surface water showed the presence of organochlorines, and organophosphorus and carbamate insecticides in water resources in the Kafr El Sheikh Governorate (Massoud et al., 2011; Ismail et al., 2015). Dimethoate is considered to be a priority pollutant in water; first, due to the wide range of usage of this insecticide against different pests, and second, its high toxicity (Lasram et al., 2009). Insecticide residues have been detected in drinking water sources, and the development of viable methods for their removal is a global priority (Derbalah et al., 2014; Ismail et al., 2015). Methomyl is a widely used carbamate pesticide characterized by its high toxicity and can cause great damage when polluted to the environment due to its high solubility in water (57.9 g/L at 25°C) (Tomlin, 2003). Methomyl can easily contaminate both ground and surface water as a result of its low affinity for absorption by surface soil (Strathmann and Stone, 2002). It should be stressed that conventional physicochemical techniques, such as adsorption, flocculation, reverse osmosis, and extraction, merely transfer the organic contaminants from one phase to another without destroying them (Pasieczna-Patkowska et al., 2010; Zhang et al., 2012). Also, the classical biological treatment has proven to be inefficient for decomposing ROPs because of their complex molecular structure, high toxicity, and poor biodegradability (van der Werf, 1996; Kümmerer et al., 2000; de Lima et al., 2007). Therefore, alternative advanced technologies such as advanced oxidation processes are required for the effective removal of pesticides from water. Taken into account, heterogeneous photocatalysis with a semiconducting photocatalyst has recently emerged as an advanced oxidation process in the environmental decontamination method suitable for the treatment of water, aqueous wastes, and wastewater (Mills and Le Hunte, 1997; Andreozzi et al., 1999; Hyung and Kim, 2009). Nanostructured semiconductors such as zinc oxide (ZnO) and titanium dioxide (TiO_2) are potential candidates for the mineralization of toxic organic compounds and hazardous inorganic constituent (Curri et al., 2003), owing to their strong oxidizing ability, that is, the hydroxyl radical (OH). Zinc oxide is a semi-conductive material that can be fabricated with various morphological forms in normal and nanoscale sizes (Kumari et al., 2010). Furthermore, zinc oxide is environmentally friendly and does not have harmful effects on living organisms (Ismail et al., 2015). Fabrication of ZnO in nanostructures can change its properties including the surface area and light absorbance (Derbalah et al., 2019). Therefore, zinc oxide nanocatalyst can be used very efficiently to eliminate pesticide residues from water compared to commercial ones (Baruah et al., 2012; Derbalah et al., 2014; Derbalah et al., 2016; Derbalah et al., 2019). However, after the remediation of pesticide residues in water, a toxicity assessment is needed to directly assess the potential hazard of original pollutants and their metabolites (Derbalah, 2009). Treating pesticide residues in water using advanced oxidation methods to break them down remains inaccurate because sometimes the decomposition products of pesticides are more toxic than the pesticides themselves. Interestingly, toxicity testing is widely used to determine the potential toxicity of a particular compound or a sample of water on biological organisms along with measuring its prevalence. In contrast to a chemical analysis, toxicity testing can detect toxic compounds on the basis of their biological activity without requiring prior knowledge about the toxic substance itself. Clearly, toxicity testing offers many advantages over a chemical analysis which requires prior knowledge of toxic substances (Leusch and Chapman, 2011).

The use of an acetylcholinesterase (AChE) biosensor seems to be the most appropriate technique for unambiguous determination of toxicity of water samples and wastewater at different stages of organophosphorus and carbamate degradation processes. The main advantages of AChE bioassays include their selective sensitivity to organophosphates toxic photoproducts and prompt response, which enable online monitoring and control of photodegradation processes (Simonian et al., 2001; Kralj et al., 2007). Fundamental, physical, and chemical water quality parameters reflect the operational status of water/wastewater treatment processes (Van Vooren et al., 2001), and therefore are important for any remediation technology, not only for the complete removal of pollutants from water but also to determine the effect of the method on the water quality parameters.

The present study attempts to synthesize ZnO (nano-size) with good properties combined with evaluating its efficiency, compared to its commercial size (natural size) apart from the advanced oxidation processes, in the presence of H_2O_2 and light for the total decomposition of dimethoate and methomyl in water. The present study also aimed to confirm the complete detoxification of insecticide-contaminated water after treating it with the most effective treatment (ZnO(s)/H_2O_2/UV) with respect to altering several biochemical parameters and reporting histopathological changes in the treated liver and kidneys of rats compared to untreated control. The effect of water treatment by ZnO (nano)/H_2O_2/UV on the water quality parameters of treated water was also investigated.

MATERIALS AND METHODS

Chemicals

Dimethoate and methomyl (99.5% purity) were obtained from the Central Laboratory for Pesticides, Agriculture Research Centre, Giza, Egypt. Meanwhile, zinc oxide (ZnO, 99% purity)

was obtained from the Oxford Laboratories Pvt. Ltd., Mumbai, India. Hydrogen peroxide solution (H_2O_2) [50% (w/v)] was obtained from Piochem, Cairo, Egypt. Zinc acetate dihydrate [$Zn(CH_3COO)_2{\cdot}2H_2O$, 99.5% purity] was obtained from Loba Chemie Pvt. Ltd., Mumbai, India. Triethylamine (TEA) [$(C_2H_5)_3N$, 99% purity] was obtained from Alpha Chemika, Mumbai, India. Ethyl alcohol (ethanol, C_2H_5OH, 95% purity) was obtained from Piochem, Cairo, Egypt. Zinc nitrate hexahydrate [$Zn(NO_3)_2{\cdot}6H_2O$, 99% purity] was obtained from Winlab, India.

Synthesis of ZnO Nonacatalyst

Zinc acetate dihydrate ($ZnAc2.2H_2O$) and a capping agent (triethanolamine TEA) were mixed at a molar ratio of 5:3 in ethanol, typically with 3.2926 g of zinc acetate dihydrate and 1.255 ml of triethylamine. The mixed solution was stirred for 60 min at 50–60 °C in a condensation system until gaining a cloudy white appearance, indicating the growth of ZnO nanoparticles. The solution was then centrifuged for 10 min to separate the precipitate from the ethanol layer. The ethanol portion was removed by decantation, and the precipitate was washed with ethanol and dried under vacuum (El-Kemary et al., 2010). Then the precipitate was dried at 50°C and calcined at 400°C for 4 h to obtain a white powder of ZnO nanoparticles. Physical characterizations of the synthesized and commercial ZnO were performed using scanning electron microscopy (SEM; JEOL Ltd., Tokyo, Japan; JSM 6510) and transmission electron microscopy (TEM; JEOL; JEM-2100). A Rigaku-D/max 2500 diffractometer (Rigaku, Tokyo, Japan) with Cu-Kα radiation (λ = 0.15418 nm) was used to measure X-ray diffraction (XRD) for crystallization identification solid diffuse reflectance. The UV-Vis spectroscopy technique was employed to characterize the electronic structure of ZnO nanoparticles.

Photocatalytic Degradation of Tested Insecticides in Water

This experiment was designed to evaluate the efficiency of the advanced oxidation processes for the removal of dimethoate and methomyl from water using zinc oxide in either normal (commercial) or nano (synthesized) size mixed with H_2O_2 in the presence of UV light. The test solution was made by pouring 50 ml distilled water into a 100 ml flask, and then adding the required amount of dimethoate or methomyl that achieves a final concentration of 5 mg/L in a final volume of 100 ml while stirring the solution. Then the amount of zinc oxide required to prepare a concentration of 300 mg/L in a final volume of 100 ml was carefully added to the flask and shaken (Derbalah et al., 2014; Ismail et al., 2015; Derbalah et al., 2016). After that, the amount of hydrogen peroxide required to achieve a concentration of 20 mg/L in a final volume of 100 ml is then added (Derbalah and Ismail, 2013; Derbalah et al., 2014; Ismail et al., 2015; Derbalah et al., 2016). Using distilled water, the final volume of the solution in the flask was set at 100 ml. The pH of the solution was then adjusted to 7 using a Jenway pH/mV/temperature meter, Model 3510, which is considered the optimum pH for the zinc oxide catalyst (Ahmad et al., 2022). The solution was left in the dark for 30 min to ensure maximum pesticide adsorption on the ZnO surface. The dimethoate or methomyl solution was then exposed to UV light from 19 cm away (Laoufi NA, 2009). The solutions of the irradiated samples were removed at regular intervals (0, 10, 20, 40, 60, 80, 160, 320, and 360 min) for an HPLC analysis after the irradiation started (Derbalah, 2009). A blank experiment was carried out in the absence of light to assess abiotic loss of dimethoate or methomyl, as previously mentioned (Hansson et al., 2012). All of the experiments were carried out three times, with the average results being reported.

HPLC Analysis

The irradiated samples were analyzed directly by an HPLC system. For dimethoate, a mixture of acetonitrile and distilled water (60:40) was used as the mobile phase under the isocratic elution mode. The flow rate of the mobile phase was maintained at 1 ml min^{-1} and the column type used was (i.d. 4.6 mm; length 250 mm) filled with Wakosil-II 5 C18–100 (Wako). The used detector was UV at a wavelength of 210 nm, and the retention time was 3.30 min (Evgenidou et al., 2006). For the methomyl analysis, a mixture of acetonitrile and distilled water (20:80) was used as the mobile phase in the isocratic elution mode. The flow rate of the mobile phase was then maintained at 0.7 ml min^{-1}. The HPLC system used a Zorbax C8 column (250 mm × 4.6 mm × 5 µm) with a UV detector at a wavelength of 231 nm and a retention time of 3.84 min (Tamimi et al., 2008). The degradation efficiency (%) was calculated as follows (**Eq. 1**):

$$\text{Efficiency}\,(\%) = [\,(C_0 - C)/C_0\,] \times 100 \rightarrow \quad (1)$$

where C_0 is the initial concentration of insecticide, and C is the concentration of insecticide after photoirradiation (Rahmayeni et al., 2015).

To determine the degradation rate, plots of the natural log of the concentration over time were made. The degradation rate constant (slope), k, was calculated from the first-order rate equation (**Eq. 2**), as follows:

$$C_t = C_0 e^{-kt} \rightarrow \quad (2)$$

where C_t represents the concentration of the insecticide at time t, C_0 represents the initial concentration, and k is the degradation rate constant. When the concentration falls to 50% of its initial concentration, the half-life ($t_{1/2}$) was estimated as shown in **Eq. 3** (Monkiedje and Spiteller, 2005).

$$t_{1/2} = 0.693/K \rightarrow \quad (3)$$

Toxicity Test

Ethical Statement

The ethical approval of the present study was performed according to the ethical standards of the Faculty of Veterinary Medicine, Kafrelsheikh University, Egypt, which complies with

all relevant Egyptian legislations. The ethical approval code number of the study is KFS-2019/4.

Treatment of Rats

Adult Wister male rats (Sprague Dawley) 8 weeks of age and 80–100 g in weight obtained from the Faculty of Veterinary Medicine, Kafrelsheikh University were used. Rats were housed in polypropylene cages under standard conditions with free access to drinking water and food. The rats were kept in a temperature-controlled room for 12 h (Korsrud et al., 1972) with 12-h light and dark cycles. The rats were given a standard diet, as described (Korsrud et al., 1972). Before treatment, rats were left for 2 weeks during feeding for adaptation. The toxicity protocol used in this study states the following: 1 ml water containing dimethoate or methomyl after being treated with ZnO(s)/H_2O_2/UV) for six hours was injected as oral dose to the rats once, and then they were kept under observation for 28 days before carrying out biochemical and histopathological tests. All water samples after remediation with ZnO(s)/H_2O_2/UV were stored for 1 week in a clean brown glass in refrigerator until administration to rats. The dose of the used insecticides given to the treated rats if no degradation was induced was equal to 500 μg/kg body weight. Rats were administered with the dose by using an injection syringe with a ball in the front to prevent the occurrence of bleeding or injury to the animal. The animals were divided into four groups (six rats of each). Two groups were orally administered one time with 1 ml of water contaminated with methomyl and dimethoate after remediation (6 h) with ZnO(s)/H_2O_2/UV. The third group was orally administered one time with 1 ml water containing ZnO(s)/H_2O_2 without insecticides. The fourth group of rats was treated with pure water only and considered as the control. After 28 days of oral administration, biochemical and histopathological tests were carried out to confirm the complete detoxification of insecticides in the treated water and to assess the toxicity of ZnO(s)/H_2O_2 without the tested insecticides relative to control. The animals were observed for clinical signs of toxicity (macroscopic investigation) once a day throughout the entire observation period, and the effects were observed in all six animals. All animal studies were approved by our Institutional Animal Ethics Committee.

Biochemical Assays

Blood samples were centrifuged at 4,500 rounds per minute (rpm) for 20 min, and the serum was collected for determination of the enzymatic activity. The colorimetric methods of Waber and Dtsch (1966), Schirmeister (1964), Reitman (1957), and Habig (1974) were used for determining the level of acetylcholinesterase, glutamic-pyruvic transaminase (GPT), glutamic-oxaloacetic transaminase (GOT), and glutathione-s-transferase (GST), respectively, using the kits.

Histopathological Examination

All rats were anesthetized and sacrificed before performing the postmortem examination, and all lesions were recorded. Specimens from the liver and kidneys were collected and maintained in neutral buffered formalin (10%) for histopathological examination (Derbalah and Ismail, 2013; Ismail et al., 2015). The specimens were then dehydrated in ascending grades of alcohols, cleared in xylene, embedded in paraffin wax, sectioned at 4 μm, stained with hematoxylin and eosin (HE) stains, and examined by a light microscope (Bancroft et al., 2013).

Water Quality Parameters Assessment

An experiment was carried out to assess the effect of ZnO (nano)/H_2O_2/UV treatment on the water quality parameters of treated fresh and drainage waters. Water samples were collected in pre-cleaned polyethylene bottles from the Al-Gharbiya main drain (drainage water) and the River Nile at Fowa (fresh water). After collection, the samples were immediately placed in dark boxes and processed within 6 h of collection. The samples were divided into two parts after filtration. The first was kept without treatment, and the second was treated with the ZnO (nano)/H_2O_2/UV system, as mentioned before. The treated and untreated water samples underwent a water quality analysis to evaluate the effects of ZnO (nano)/H_2O_2/UV on the water quality. The water samples were analyzed for their major physicochemical water quality parameters, such as pH, electrical conductivity (EC), total dissolved solids (TDS), chemical oxygen demand (COD), sulfate (SO_4^{2-}), and biological oxygen demand (BOD), according to the method described (AMERICAN PUBLIC HEALTH ASSOCIATION 2005), at the Water Pollution Control Department, National Research Centre, Dokki, Giza, Egypt. All experiments were repeated three times, and the average values are reported.

RESULTS AND DISCUSSION

Characterization of Commercial and Fabricated ZnO

Figure 1 shows typical scanning electron images of synthesized and commercial ZnO. Results indicate that the shape of the synthesized ZnO is spherical with a diameter in the range of 30–49 nm (**Figure 1A**). The commercial ZnO (**Figure 1B**) appears as randomly oriented hexagonal prisms with the diameter ranging from 34 to 119 nm and with length ranging from 169 to 399 nm. Additional studies on the structures of synthesized and commercial ZnO were conducted using transmission electron microscopy.

Figure 2A shows transmission electron microscopy (TEM) images of the synthesized ZnO(s). This image shows that the shape of most of these particles is spherical with small amount of hexagonal diameters. The diameter of the synthesized ZnO(s) lies in the range of 12.48–26.12 nm. **Figure 2B** reflects the shape of the commercial ZnO which appears as nanorods (nanowire) with hexagonal diameters in the range of 30–83.87 nm with length in the range of 70.96–406.45 nm. **Figure 3A** shows the XRD diffraction pattern of ZnO nanoparticles. The peaks are indexed as 31.4° (100), 34.54° (002), 35.90° (101), 56.27° (110), 62.54° (103), and 67.64° (112), respectively. All diffraction peaks of the sample correspond to the characteristic hexagonal wurtzite structure of ZnO nanoparticles (Joint Committee on Powder

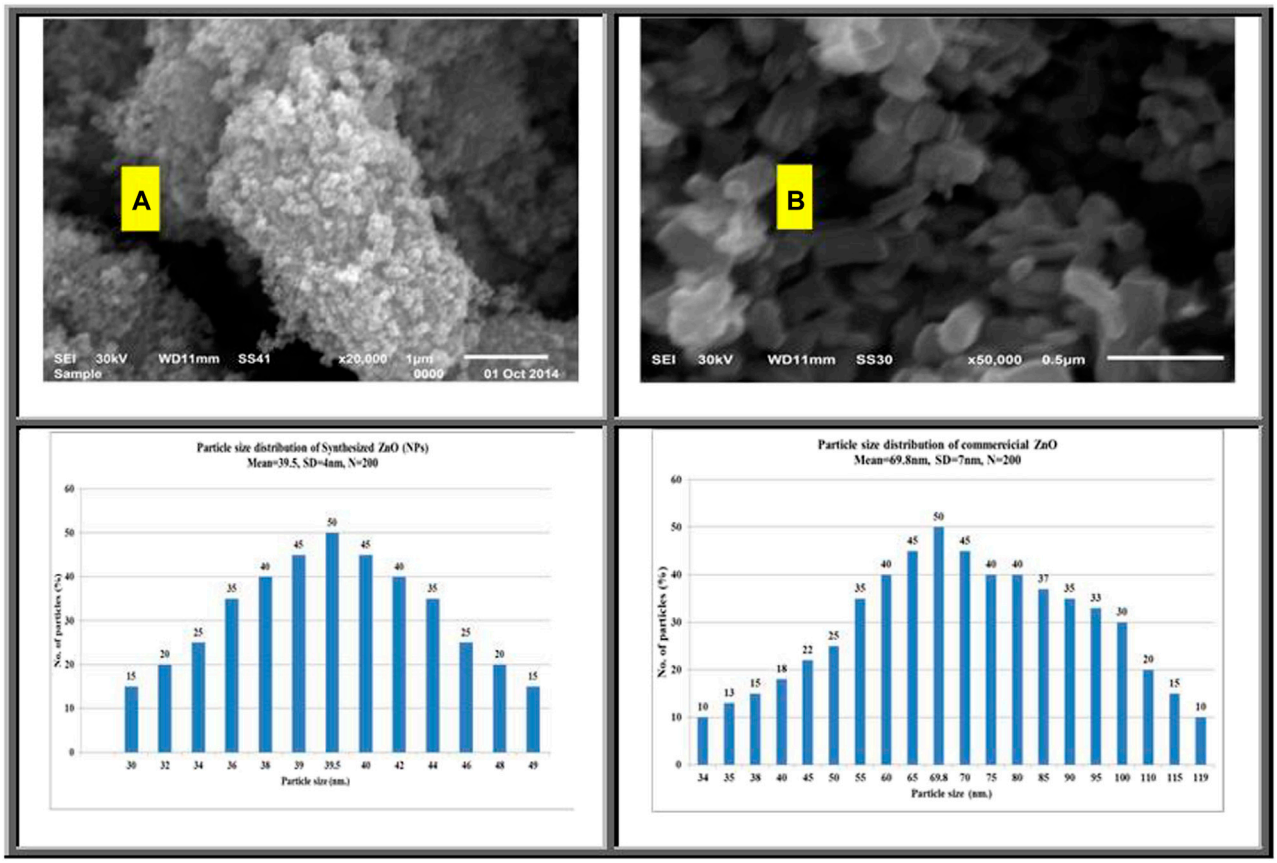

FIGURE 1 | SEM image and particle size distribution of the synthesized **(A)** and commercial **(B)** ZnO.

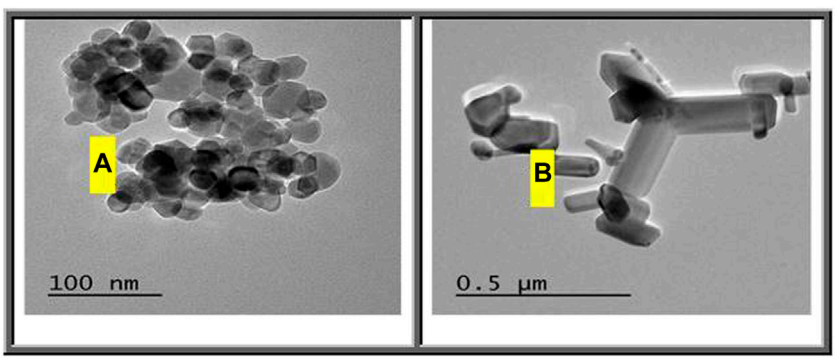

FIGURE 2 | TEM image of the synthesized **(A)** and commercial **(B)** ZnO.

Diffraction Standards (2000); diffraction data file). Similar X-ray diffraction patterns were reported by Pung et al. (2012) and Chena et al. (Chena). The average particle size of ZnO nanoparticles was found to be in the range of 34–39.7 nm using the Scherer equation (Culity, 1987). The diffraction patterns corresponding to impurities were found to be absent. This proves that pure ZnO nanoparticles were as-synthesized. However, the XRD patterns of the nanoparticles are considerably broadened due to the very small size of these particles. The strong and narrow diffraction peaks indicated that the product has good crystallinity (Samuel, 2009). The X-ray diffraction pattern of the dried commercial ZnO is shown in **Figure 2B**. The peaks are centered at 31.82° (100), 34.54° (002), 36.42° (101), 47.22° (102), 56.29° (110), 62.57° (103), and 67.66° (112), respectively. Calculation of the particle size by the Debye–Sheerer equation revealed that the average of the commercial ZnO ranges from

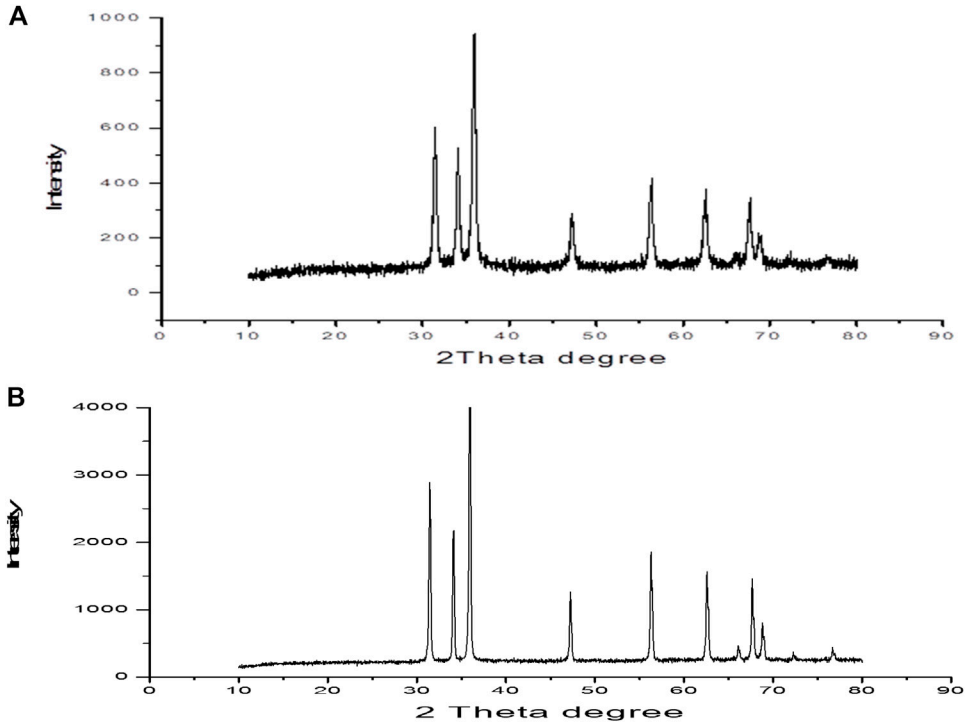

FIGURE 3 | XRD patterns of the fabricated and commercial ZnO.

61.66 to 75.8 nm. **Figures 4A,B** show FTIR spectra of the as-synthesized ZnO (NPs). Infrared studies were carried out in order to ascertain the purity and nature of the metal nanoparticles. Metal oxides generally give absorption bands in the fingerprint region, that is, below 1,000 cm^{-1}, which arises from inter-atomic vibrations. The peaks observed in **Figure 4A** at 3455 and 1,083 cm^{-1} are may be due to O-H stretching and deformation, respectively, assigned to the water adsorption on the metal surface. The peaks at 1634 and 537 cm^{-1} correspond with Zn-O stretching and deformation vibration, respectively. The metal–oxygen frequencies observed for the respective metal oxides are in accordance with literature values (Markova-Deneva, 2010). Parthasarathi and Thilagavathi (2011) reported that similar FTIR spectra were observed in ZnO nanoparticles in their investigation. **Figure 4B** shows the observed peaks of the as-received commercial ZnO (nanoparticles); two peaks at 3441 and 1,089 cm^{-1} could be due to O-H stretching and deformation, respectively, assigned to the adsorbed water on the metal surface. The peaks at 1631 and 537 cm^{-1} correspond with Zn-O stretching and deformation vibration, respectively.

The room temperature and UV-Vis absorption spectra of an aqueous solution semiconductor ZnO for as-synthesized and as-received were measured and are shown in **Figures 5A,B**. ZnO particles were dispersed in deionized water with a suitable concentration, and then the solution was used to perform the UV-Vis measurement. The spectrum shows an absorption peak of the as-synthesized ZnO at a wavelength of 368.5 nm, **Figure 5A**, and at 376.2 nm, **Figure 5B**, of the as-received ZnO which can be assigned to the intrinsic band gap absorption of ZnO due to transition of electrons from the valence band to the conduction band (Yu et al., 2006). The band gap energy (E) was calculated as per the literature report using the following equation (Hoffmann et al., 1995):

$$\text{Band gap energy (E)} = hc \rightarrow \quad (4)$$

where h is Plank's constant (6.625×10^{-34} Js), c is the speed of light (3.0×108 m/s), and λ is the wavelength (m). According to this equation, the band gap of the synthesized ZnO is 3.36 eV, while the band gap of the as-received ZnO is 3.29 eV. The wide band gap energy of semiconductor nanoparticles is more reactive in a photocatalytic degradation of the organic pollutants (Dhal et al., 2015).

Photocatalytic Degradation of Dimethoate

The ZnO(s)/H_2O_2/UV system afforded the complete (100%) degradation of the tested insecticides (dimethoate and methomyl), followed by the ZnO(c)/H2O2/UV system, after 320 min of irradiation (**Figure 6**). The half-lives of methomyl were 35.36 and 19.52 under the ZnO(c)/H_2O_2/UV and ZnO(s)/H_2O_2/UV systems, respectively (**Table 1**). The half-lives of dimethoate were 44.14 and 26.25 min under the ZnO(c)/H_2O_2/UV and ZnO(s)/H_2O_2/UV systems, respectively (**Table 1**). The degradation of the tested insecticides under dark conditions using different systems was negligible than degradation under light conditions (data not published). Photocatalytic degradation by a

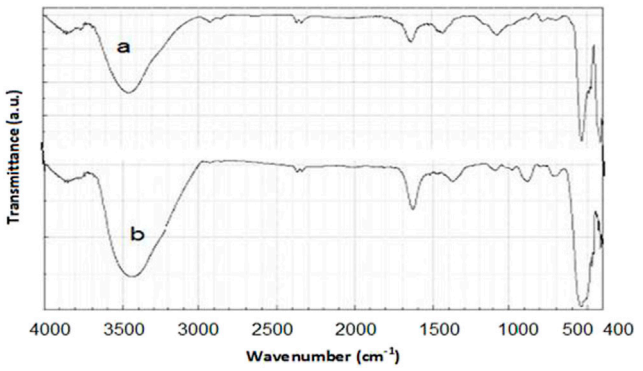

FIGURE 4 | FTIR spectroscopy of **(A)** synthesized and **(B)** commercial ZnO.

semiconducting nanocatalyst is mainly considered as a potential and effective technology for the mineralization of pesticides into environmentally friendly compounds. In addition, nanoparticles have emerged as a sustainable alternative to conventional bulk materials, as robust, high surface area, heterogeneous photocatalysts and catalyst supports. In this study, the degradation rate of dimethoate and methomyl was greatly enhanced by irradiation under ZnO(s)/H_2O_2/UV relative to ZnO(c)/H_2O_2/UV. This is may be due to the fact that stabilized nanoparticles offer a much greater surface area in a small particle size and reactivity, which leads to a higher generation rate of hydroxyl radicals relative to the normal particles (Dhal et al., 2015) and subsequently a higher degradation rate of organic pollutants. Our present results of photodegradation of dimethoate are in harmony with the finding of many researchers (Tamimi et al., 2008; Massoud et al., 2011; Juang and Chen, 2014), who reported that the total disappearance of the dimethoate parent compound and other organophosphorus insecticides degraded was more than 90% by using the advanced oxidation processes system (photocatalysts in normal and nano-size) under UV radiation.

In this study, dimethoate and methomyl were highly degraded by ZnO, possibly because zinc oxide is very reactive, the surface active sites are easily accessible to the substrate molecules, and diffusional resistance, which lead to the high generation of hydroxyl radicals by this system. The high hydroxyl radical generation rate is due to many reasons. The first reason is the ability of the ZnO semiconductor to act as a sensitizer in the presence of light and consequently enhance the photodegradation of methomyl or dimethoate. When the energy irradiating the conduction band is a greater than the band gap, valence band electrons are promoted to the conduction band, leaving a hole behind (**Eq. 5**). These electron (e-cb)–hole (h + vb) pairs can either recombine (**Eq. 6**) or interact separately with other molecules. Holes in the ZnO valence band can oxidize adsorbed water or hydroxide ions to produce •OH radicals (**Eq. 7**). Electrons in the conduction band on the catalyst surface can reduce molecular oxygen to the superoxide anion (**Eq. 8**). This radical may form hydrogen peroxide or hydroperoxy radicals (•OOH) (**Eqs 9**, **10**). The second reason involves the addition of a hydrogen oxidant, which can enhance the degradation of the tested insecticides by acting as an electron acceptor, consequently promoting change separation and producing •OH radicals, according to **Eqs 11**, **12** (El-Kemary et al., 2010). After that, the hydroxyl radicals, which have a high degradation ability, attack methomyl or dimethoate to form intermediate products. These intermediates react with more hydroxyl radicals until methomyl or dimethoate is mineralized to CO_2 and H_2O (**Eq. 13**) (Hoffmann et al., 1995; Kaneco et al., 2007).

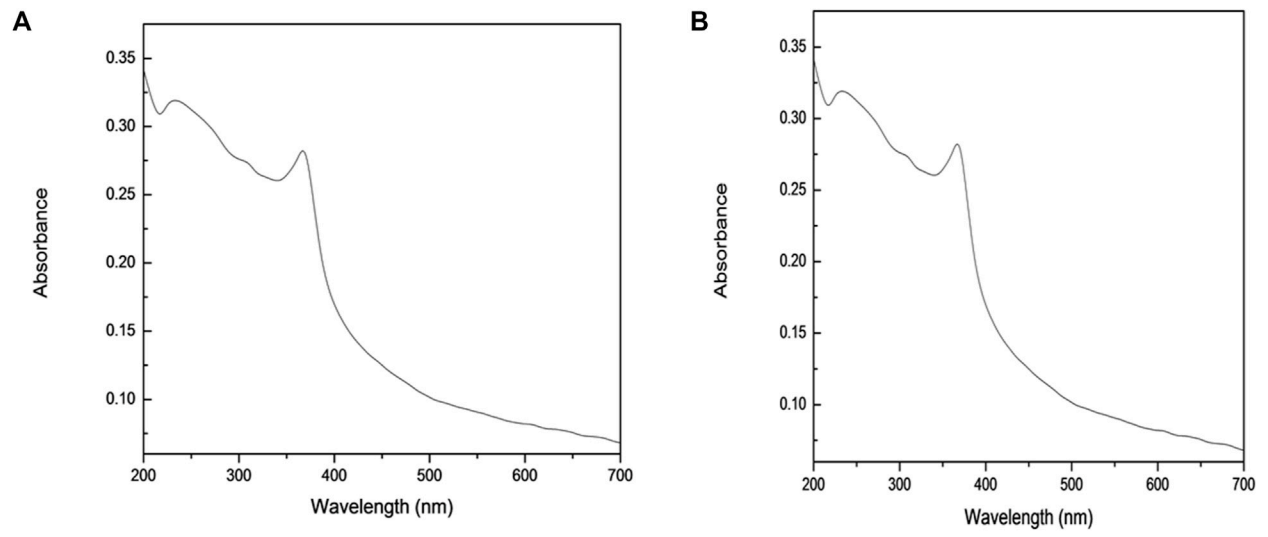

FIGURE 5 | UV-Vis absorption spectra of an aqueous solution of **(A)** synthesized and **(B)** commercial ZnO.

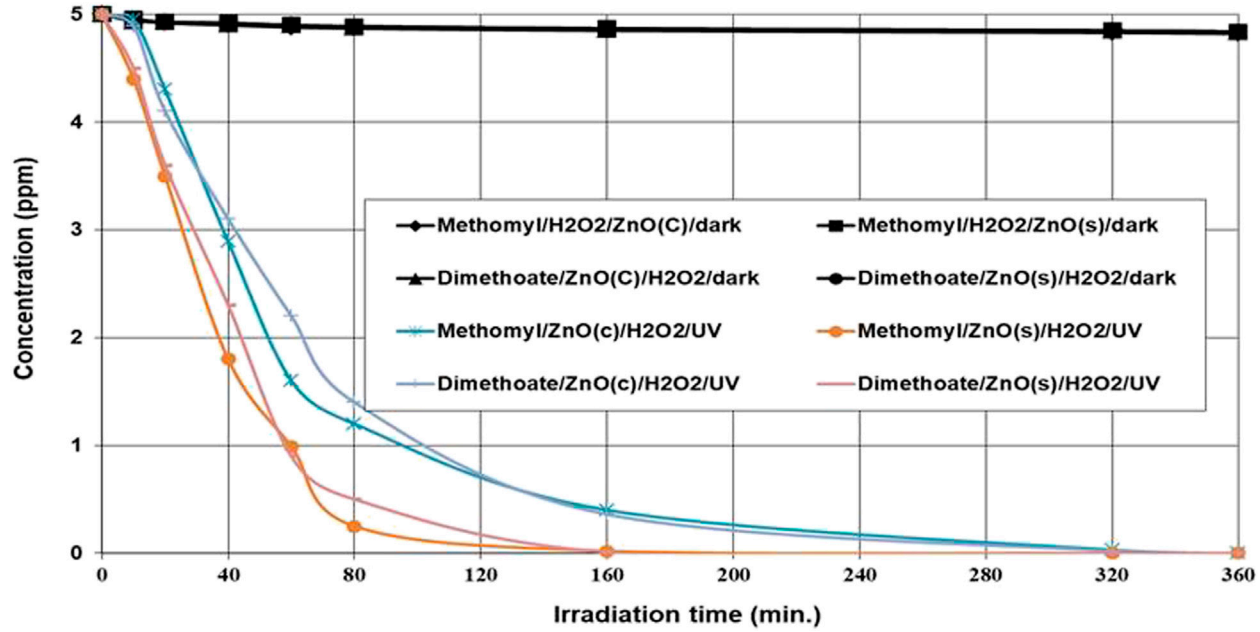

FIGURE 6 | Photocatalytic degradation of dimethoate and methomyl at an initial concentration of 5 ppm under ZnO(s)/H_2O_2/UV and ZnO(c)/H_2O_2/UV systems.

TABLE 1 | Calculated degradation rate constant and half-life values of dimethoate and methomyl under ZnO(c)/H_2O_2/UV and ZnO(s)/H_2O_2/UV systems.

Treatments	Degradation rate constant (min^{-1})	Half-life ($t_{1/2}$) (min)	R^2
Dimethoate			
ZnO(c)/H_2O_2/UV	0.0157 ± 0.001	44.14 ± 0.42	0.97
ZnO(S)/H_2O_2/UV	0.0264 ± 0.002	26.25 ± 0.25	0.91
Methomyl			
ZnO(c)/H_2O_2/UV	0.0196 ± 0.001	35.36 ± 0.53	0.97
ZnO(s)/H_2O_2/UV	0.0362 ± 0.002	19.14 ± 0.58	0.95

$$ZnO + h\upsilon \rightarrow ZnO(e_{-cb}/h_{+vb}) \rightarrow e_{-cb} + h_{+vb} \quad (5)$$

$$e_{-cb} + h_{+vb} \rightarrow \text{heat} \quad (6)$$

$$h_{+vb} + OH^- (\text{or } H_2O)\text{ads} \rightarrow \bullet OH(+H^+) \quad (7)$$

$$e_{-cb} + O_2 \rightarrow \bullet O_2^- \quad (8)$$

$$\bullet O_2^- + H_2O + H^+ \rightarrow H_2O_2 + O_2, \quad (9)$$

$$\bullet O_2^- + H^+ \rightarrow \bullet OOH \quad (10)$$

$$H_2O_2 + h\nu \rightarrow 2^{\cdot}OH \quad (11)$$

$$H_2O_2 + O_2^- \rightarrow OH^- + {}^{\cdot}OH \quad (12)$$

$$\bullet OH(\text{or} \bullet OOH) + \text{pesticide} \rightarrow \text{Oxidative products} + CO_2 + H_2O \quad (13)$$

Advanced oxidation processes, especially those with nanocatalysts (Massoud et al., 2021), are promising remediation technologies for removing dimethoate or methomyl from water resources and are suitable for highly contaminated water, such as drainage or wastewater, due to the faster degradation rate *via* its great degradation power relative to bioremediation, which takes a long time, requires special environmental conditions, and is limited to biodegradable compounds (Derbalah et al., 2014). Although nanomaterials present seemingly limitless possibilities, they bring new challenges to understanding, predicting, and managing potential safety and health risks to workers. However, more research is needed to determine the key physical and chemical characteristics of nanoparticles that determine their hazard potential (Dhal et al., 2015).

Toxicity Assessment

Biochemical Parameters

The complete detoxification of the tested insecticides in water samples treated with the most effective treatments ZnO(s)/H_2O_2/UV was confirmed by measuring the effect of these treated samples on some biochemical parameters (AChE, GPT, GOT, and GST) relative to control in treated rats. The results showed that there were no significant differences in cholinesterase, GPT, GOT, and GST levels in the rats treated with water samples after remediation when compared to control (**Table 2**). Moreover, the

TABLE 2 | Effect of ZnO(nano)/H_2O_2/UV with and without dimethoate and methomyl on the activity of some biochemical parameters in rats.

Treatment	AChE	GPT	GOT	GST
Control	$0.911 \times 10^{-1} \pm 0.001^a$	51.79 ± 0.013^a	0.0113 ± 0.001^a	19.040 ± 0.680^a
D/ZnO (s)/H_2O_2/UV	$0.912 \times 10^{-1} \pm 0.001^a$	51.81 ± 0.299^a	0.0114 ± 0.001^a	19.050 ± 0.627^a
M./ZnO(s)/H_2O_2/UV	$0.912 \times 10^{-1} \pm 0.001^a$	51.80 ± 0.935^a	0.0112 ± 0.001^a	19.071 ± 1.381^a
ZnO(s)/H_2O_2	$0.912 \times 10^{-1} \pm 0.001^a$	51.78 ± 0.935^a	0.0113 ± 0.001^a	19.040 ± 0.613^a

Statistical comparisons were made among treatments within a single column.
M = methomyl; D = dimethoate; a mean there is no significant difference between the means.

effect of ZnO(s)/H_2O_2 itself without the tested insecticides on the same biochemical parameters to reflect its safety showed no significant differences in all biochemical parameters when compared to control.

The Histopathological Changes

The complete detoxification of dimethoate and methomyl in water treated with ZnO(s)/H_2O_2/UV was confirmed with respect to histopathological changes in the liver and kidneys of treated rats compared to untreated control ones. Liver of control rats showed basic features of hepatic lobule with centrally located central vein, and the hepatocytes were arranged in cords separated from each other by small blood spaces called hepatic sinusoids and the portal area containing the bile duct, hepatic artery, and portal vein (**Figure 7A**). The liver of rats treated with water contaminated with dimethoate after remediation with ZnO(s)/H_2O_2/UV showed focal accumulation of mononuclear inflammatory cell infiltration in the portal area accompanied with moderate hepatocellular cytoplasmic vacuolation (**Figure 7B**). Meanwhile, liver of rats treated with water contaminated with methomyl after remediation with ZnO(s)/H_2O_2/UV showed slight hepatocellular degeneration and sinusoidal congestion (**Figure 7C**). Liver of rats treated with water containing ZnO(s)/H_2O_2/UV without any insecticides showed mild vacuolation in the cytoplasm of the hepatocytes (**Figure 7D**). The kidneys of control rats showed normal cortex and medulla. The cortex is composed of glomerular tuft of capillaries surrounded by Bowman's capsule forming glomeruli which are dispersed throughout, along with the proximal and distal convoluted tubules. The medulla is composed mainly of collecting ducts and loop of Henle (**Figure 8A**). Kidneys of rats treated with water contaminated with dimethoate after remediation with ZnO(s)/H_2O_2/UV showed slight to moderate changes in the form of focal interstitial nephritis with focal accumulation of mononuclear inflammatory cells in between and round the degenerated renal tubules with slight tubular dilatation. Tubular basophilia, with basophilic tubules accompanied with few single-cell necrosis, was also observed in the abovementioned lesion (**Figure 8B**). Kidneys of rats treated with water contaminated with methomyl after remediation with ZnO(s)/H_2O_2/UV showed mild interstitial mononuclear cell infiltration and slight congestion of the intertubular blood vessels as well as slight tubular dilatation (**Figure 8C**). Kidneys of rats treated with water containing ZnO(s)/H_2O_2/UV alone without dimethoate or methomyl showed almost the same histologic structure like that of the control group, except the observed slight renal tubule dilatation (**Figure 8D**).

The total detoxification of pesticide-contaminated water after remediation is considered a limiting factor in the evaluation of the efficacy of any remediation technologies. Treated water samples after remediation had no significant effect on the activity of the measured biochemical parameters and histology in the kidney or liver of treated rats when compared to the control which implies that dimethoate or methomyl and their toxic metabolites were completely detoxified (Kralj et al., 2007). Also, the results confirmed that the ZnO nanocatalyst chemical was safe for human health (Derbalah and Ismail, 2013; Ismail et al., 2015). The results showed that the toxicity of treated water, including organic pollutants and advanced oxidation intermediates, was negative, and it can be considered as the key factor to evaluate the applicability of AOPs to improve water quality parameters (Abd El-Gawad, 2008). Advanced oxidation processes, especially using nanocatalysts, are promising remediation technologies for removing dimethoate or methomyl from water sources. Advanced oxidation processes, especially using nanocatalysts, can be a more suitable remediation technology for water contaminated with high concentration, such as drainage or wastewater, due to its faster degradation rate *via* its great degradation power than bioremediation that takes a long time, needs special environmental conditions, and is limited to those compounds that are biodegradable (Borm and Müller-Schulte, 2006).

It is well known that histopathological alterations are considered a rapid method to estimate the effects of irritants and chemicals in various tissues and organs, especially the in the liver and kidneys (Dutta et al., 1993; Bernet et al., 1999). To evaluate the efficacy of different tested remediation techniques in removing dimethoate and methomyl from fresh water, a toxicity assessment was carried out with respect to the biochemical parameters and the histopathological changes in rats. Exposure to dimethoate and methomyl can cause different histopathological changes in the liver and kidneys (Wafa et al., 2011). The changes in the liver and kidneys associated with dimethoate and methomyl have been attributed to their induced oxidative stress, lipid peroxidation, and the resultant free radical accumulation (El-Demerdash et al., 2013). In the present study, there were no significant but only mild alterations in the liver and kidneys of rats treated with fabricated nanoparticles. Treated rats with dimethoate or methomyl after remediation showed moderate hepatocellular cytoplasmic vacuolation and a focal inflammatory reaction in the portal area in the liver; focal interstitial nephritis, degenerated renal tubules, and tubular basophilia of renal tubules lining the epithelium which are considered as mild retrogressive degenerative changes indicate non-harmful effects of

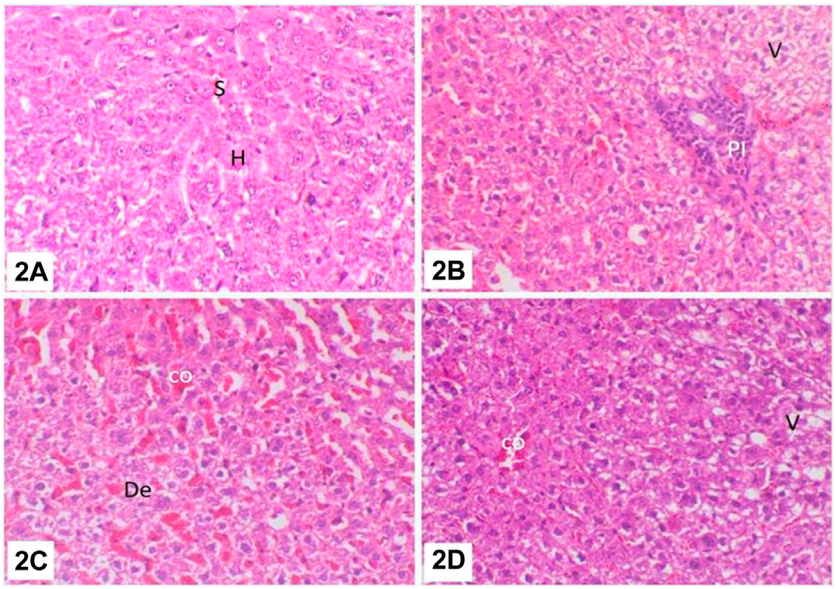

FIGURE 7 | (A) Liver of control untreated rats: hepatic sinusoid (S) and hepatocytes (H); **(B)** liver of rats treated with water contaminated with dimethoate after remediation with ZnO(s)/H_2O_2/UV: hepatocellular vacuolar degeneration (V) and portal mononuclear cell infiltration (PI); **(C)** liver of rats treated with water contaminated with methomyl after remediation with ZnO(s)/H_2O_2/UV: sinusoidal congestion (co) and hepatocellular degeneration (De); **(D)** liver of rats treated with water containing ZnO (s)/H_2O_2 without any insecticides: hepatocellular vacuolar degeneration (V) and sinusoidal congestion (co).

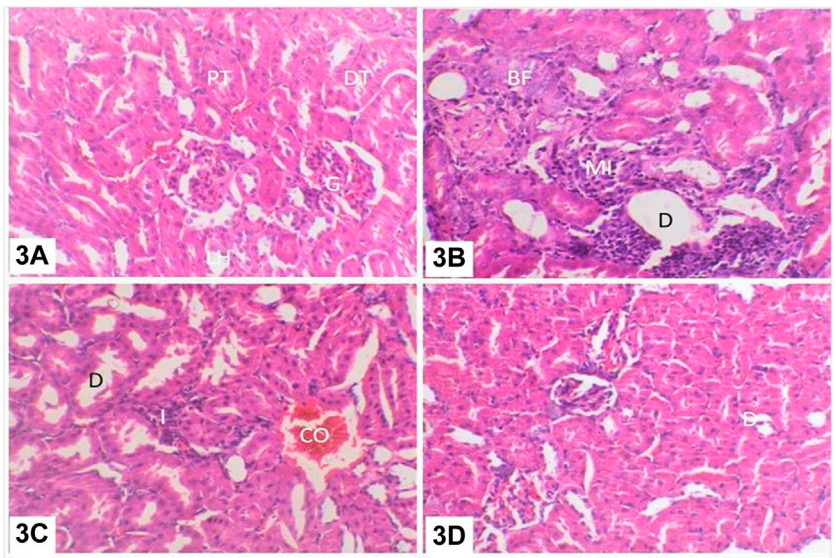

FIGURE 8 | (A) Kidneys of control rats: glomerulus (G), proximal convoluted tubules (PT), and distal convoluted tubules (DT); **(B)** kidneys of rats treated with water contaminated with dimethoate after remediation with ZnO(s)/H_2O_2/UV: intertubular mononuclear cell infiltration (MI), renal casts (RC), tubular dilatation (D), and tubular basophilia (BF); **(C)** kidneys of rats treated with water contaminated with methomyl after remediation with ZnO(s)/H2O2/UV: tubular dilatation (D) and venous congestion (CO); **(D)** kidneys of rats treated with water containing ZnO (s)/H_2O_2 without any insecticides: tubular dilatation (D).

dimethoate or methomyl after remediation in comparison with the toxic effect of the exposure to dimethoate and methomyl on the liver and kidneys without remediation as described by Sharma et al. (2005), and it can be considered as an adaptive physiological response attempting to limit cell damage that could occur by toxic insecticides or its metabolites. The inflammatory reaction observed in the liver and kidneys of rats treated with water contaminated with methomyl after remediation with ZnO(s)/H_2O_2/UV is considered a defensive response of the tissues against the oxidative stress-induced injury imposed by methomyl (Rahm

TABLE 3 | Physiochemical parameters of the drainage and fresh water before and after treatment with ZnO(nano)/H_2O_2/UV.

Parameters	Al-Gharbiya main drain before	Al-Gharbiya main drain after	Standard parameters	River Nile Before	River Nile after	Standard Parameters
pH	6.3 ± 0.12	7.2 ± 0.14	6–8 (WHO)	7.5 ± 0.12	7.9 ± 0.16	6–9
TDS	431 ± 3.25	520 ± 2.45	2000 (mg/l)	270 ± 1.25	253 ± 2.23	1,200 mg/L
EC	738 ± 2.45	863 ± 3.26	1000 mg/L (WHO)	450 ± 2.56	460 ± 3.11	2000 mg/L
COD	4530 ± 8.45	231 ± 1.78	80–150 (WHO)	839 ± 3.45	80.21 ± 1.11	150 (WHO)
BOD	97.2 ± 1.22	18.31 ± 1.01	60–100 (WHO)	320 ± 1.47	11 ± 0.33	15<
SO_4	20 ± 0.45	25 ± 1.31	250 (Egypt 2007)	7.10 ± 0.14	8.7 ± 0.24	250< (Egypt 2007)

et al., 2017). Tubular basophilia is considered a feature of renal regenerative changes, and tubules lined by cells with basophilic cytoplasm exhibit increased replication rate than tubules lined by epithelial cells with normal eosinophilic appearance (Peter et al., 1986). This condition may be considered as renal tubule cell regeneration after various forms of tubular epithelial cell injury, as seen in coagulate necrosis induced by nephrotoxic chemicals such as mercuric chloride or hexachlorobutadine (Konishi and Ward, 1989) or secondary to the vascular damage, probably through ischemia and/or ischemia/reperfusion (Tochitani et al., 2016), or it can be considered as a sign of compensatory tubular hyperplasia (Descotes et al., 1996). The obtained results indicated low toxicity of ZnO nanocatalyst on the liver and kidneys, as reported (Mebert et al., 2017), and therefore, this verify the safety in the use of ZnO(s)/H_2O_2/UV in remediation of water for human health. It could be concluded that nanocatalyst itself did not induce any significant toxicity on treated rats with respect to biochemical and histological alterations in the treated rats. It is very important to note that toxicity testing in this study is insufficient to assess the safety of treated water for humans because exposure time was limited, exposure conditions did not take into account variability between species, and the measured end points were limited. In addition, this study focused on the disappearance and crash of parent compounds but not mineralization. It is also clear that complete detoxification of the compounds under study and their breakdown products has been confirmed, but the breakdown products have not been identified. Therefore, further studies are needed to determine the potential breakdown and to identify the main physical and chemical properties of nanoparticles that determine their potential hazards.

Effect of ZnO (nano)/H_2O_2/UV on Water Quality Parameters

In the present study, the effect of the photocatalytic oxidation of the tested insecticides in water using ZnO (nano)/H_2O_2/UV on the quality parameters of different treated water resources (fresh and drainage waters) was investigated. The data revealed that water examined from different sources after treatment showed considerable variations with respect to their physical characteristics. Al-Gharbiya main drain water was characterized by an increase in pH from 6.3 to 7.2, while the pH changed in the River Nile water at Fowa from 7.5 to 7.9 after treatment with the ZnO (nano)/H2O2/UV system, as shown in **Table 3**. The EC of the Al-Gharbiya main drain water increased from 738 to 863 μs, while that of River Nile water at Fowa increased from 450 to 460 μs after treatment with the ZnO (nano)/H_2O_2/UV system. The TDS increased from 431 to 520 mg/L and from 270 to 253 mg/L in the Al-Gharbiya main drain water and River Nile water at Fowa, respectively, after treatment with the ZnO (nano)/H_2O_2/UV system. The EC and TDS were found to be higher in the Al-Gharbiya main drain water and the River Nile water at Fowa after treatment. However, the TDS and EC after treatment were still low compared with the tolerance limit of drinking water (1,200 ppm) and drainage water (2000 ppm). The measured chemical water quality parameters varied in the examined water from different sources (**Table 3**). The COD of the Al-Gharbiya main drain water greatly decreased from 4530 to 231 mg/L, while that of the River Nile water at Fowa decreased from 839 to 80.0 mg/L after treatment, as shown in. The BOD of River Nile water at Fowa and Al-Gharbiya main drain water was reduced from 320 to 11 and from 97.2 to 18.31, respectively, after treatment, as shown in . The SO_4 level of Al-Gharbiya main drain water slightly increased from 20 to 25 mg/L, while that of River Nile water at Fowa increased from 7.10 to 8.7 mg/L after treatment, as shown in .

Emerging contaminants in wastewater effluents and drinking water influents have become a cause for concern in terms of potential impacts on human health. The application of advanced oxidation processes to improve water quality has been effectively demonstrated, with ever-increasing applications worldwide (Gilmour, 2012). Depending on the characteristics of the wastewater, many contamination criteria or standards, such as COD, BOD, total organic carbon (TOC), and TSS, are defined by the quality of the wastewater (Gupta et al., 2009). The ability of any method to treat wastewater is usually quantified by the decrease in the level of one or more of the water quality parameters mentioned before.

In this study, the measured water chemical quality parameters in both types of water were reduced after treatment with ZnO (nano)/H_2O_2/UV to levels lower than the tolerance limit of drinking and drainage water (wastewater), according to Egyptian Government Law 48 (Egyptian Association Of Environmental Affair Law 48, 1982). Additionally, the physical water quality parameters after remediation with ZnO (thin film)/H2O2/UV showed that the pH, EC, and TDS of the water samples from all sources varied within the permissible limits (Gupta et al., 2009). Therefore, the used photochemical method [ZnO (nano thin film)/H_2O_2/UV] is effective for pollutant

removal and improving the water quality parameters. The reduction of the COD resulted from the reduction of the TOC in water, which may be due to the treatment of water with the ZnO (thin film)/H2O2/UV system leading to the degradation and mineralization of organic compounds and subsequently reducing the COD (Hansson et al., 2012). Finally, we conclude that the measured water quality parameters (pH, EC, TDS, BOD, and COD) were improved in both types of water after treatment with ZnO (nano thin film)/H_2O_2/UV. The SO_4^{2-} levels were increased, possibly due to the efficiency of water treatment with ZnO (thin film)/H_2O_2/UV, which led to the mineralization of organic compounds (such as dimethoate) to their inorganic salts (Tomašević et al., 2007). An analysis of the physical water quality parameters showed that the pH, EC, and TDS varied within the permissible limits in all sources (Gupta et al., 2009) and were in compliance with Egyptian Government Law 48 (Egyptian Association of Environmental Affair Law 48). Taken into account, TDS and EC are considered to be indicators of the total amount of mobile charged ions, including minerals, salts, or metals, dissolved in a given volume of water; therefore, the increase in their levels after treatment may be due to mineralization of the organic compounds of the tested insecticide to its inorganic salts by ZnO (nano)/H_2O_2/UV.

CONCLUSION

Given the abovementioned information, AOPs could be a promising strategy for complete detoxification of the tested insecticides in contaminated water, especially using ZnO nanocatalysts. Detoxification testing (biochemical and histological tests), by exposing the treated water to a sensitive target, is an expressive procedure for the complete removal of pesticide toxicity from the treated water compared to relying on fully degraded pesticides. With this in mind, a pesticide can be completely destroyed, but its decomposition products can be more toxic than the compound itself, which illustrates the importance of fully evaluating detoxification. The water quality analysis confirmed that the used remediation method besides its efficacy in insecticides removal has also improved water quality parameters.

DATA AVAILABILITY STATEMENT

The original contributions presented in the study are included in the article/Supplementary Material, further inquiries can be directed to the corresponding author.

ETHICS STATEMENT

The animal study was reviewed and approved by the ethical standards of Ethics Committee of the Faculty of Veterinary Medicine, Kafrelsheikh University, Egypt, which complies with all relevant Egyptian legislations. The ethical approval code number of the study is KFS-2019/4.

AUTHOR CONTRIBUTIONS

Conceptualization: AM, IE-M, MUS, MHS, KA, EE, and AD. Data curation: MUS and MHS. Formal analysis: IE-M, MUS, AD, and MHS. Funding acquisition: MUS and MHS. Investigation: AM, AD, IE-M, MUS, and EE. Methodology: AM, IE-M, MUS, and AD. Project administration: AM and IE-M. Resources: MHS. Software: EE. Supervision: AM, AD, KA, and EE. Validation: AM, AD, and EE. Visualization: AM, EE, and AD. Writing—original draft: IE-M, MUS, MHS, KA, EE, and AD. Writing—review and editing: AM, MHS, EE, and AD. All authors have read and agreed to the published version of the manuscript.

FUNDING

This work was supported in a part by the Taif University Researchers Supporting Program (project number: TURSP-2020/153), Taif University, Saudi Arabia.

ACKNOWLEDGMENTS

The authors would like to thank all who contributed to conduct this study and supported it.

REFERENCES

Abbassy, M. M. S. (2018). Distribution Pattern of Persistent Organic Pollutants in Aquatic Ecosystem at the Rosetta Nile branch Estuary into the Mediterranean Sea, North of Delta, Egypt. *Mar. Pollut. Bull.* 131, 115–121. doi:10.1016/j.marpolbul.2018.03.049

Abd El-Gawad, H. A. (2008). Destruction of Toxic Organic (Phenol) Compounds Using Advanced Oxidation Process. *Sci. Bull. Fac. Engin. Ain Shams Univ.* 43 (3), 1–10. doi:10.21608/fjard.2008.197483

Abdelrazek, S. (2019). Monitoring Irrigation Water Pollution of Nile Delta of Egypt with Heavy Metals. *Alexandria Sci. Exchange J.* 40 (July-September), 441–450. doi:10.21608/asejaiqjsae.2019.50350

Ahmad, M., Abbas, G., Tanveer, M., and Zubair, M. (2022). ZnO and TiO2 Assisted Photocatalytic Degradation of Butachlor in Aqueous Solution under Visible Light. *Eng. Proc.* 12 (1), 77. doi:10.3390/engproc2021012077

Alves de Lima, R. O., Bazo, A. P., Salvadori, D. M., Rech, C. M., de Palma Oliveira, D., and de Aragão Umbuzeiro, G. (2007). Mutagenic and Carcinogenic Potential of a Textile Azo Dye Processing Plant Effluent that Impacts a Drinking Water Source. *Mutat. Res.* 626 (1-2), 53–60. doi:10.1016/j.mrgentox.2006.08.002

American Public Health Association (APHA) (2005). Standard Methods for the Examination of Water and Wastewater (21st ed.). Washington, DC: American Public Health Association.

Andreozzi, R., Caprio, V., Insola, A., and Marotta, R. (1999). Advanced Oxidation Processes (AOP) for Water Purification and Recovery. *Catal. Today* 53 (1), 51–59. doi:10.1016/s0920-5861(99)00102-9

Bancroft, J. D., Layton, C., and Suvarna, S. K. (2013). *Bancroft's Theory and Practice of Histological Techniques*. 7th Ed. Churchill Livingstone, Elsevier, 151.

Baruah, S., K. Pal, S., and Dutta, J. (2012). Nanostructured Zinc Oxide for Water Treatment. *Nanoasia* 2 (2), 90–102. doi:10.2174/2210681211202020090

Bernet, D., Schmidt, H., Meier, W., Burkhardt-Holm, P., and Wahli, T. (1999). Histopathology in Fish: Proposal for a Protocol to Assess Aquatic Pollution. *J. Fish. Dis.* 22 (1), 25–34. doi:10.1046/j.1365-2761.1999.00134.x

Borm, P. J., and Müller-Schulte, D. (2006). Nanoparticles in Drug Delivery and Environmental Exposure: Same Size, Same Risks?

Chronicles, E. (2013). *Group of the Nile Basin: Cairo UniversityVs Report on EthiopiaVs Great Renaissance Dam* (Retrieved April 2, 2016).

Culity, B. D. (1987). *Elements of X-ray Diffraction*. 2nd ed. USA: Addison-Wesley.

Curri, M., Comparelli, R., Cozzoli, P., Mascolo, G., and Agostiano, A. (2003). Colloidal Oxide Nanoparticles for the Photocatalytic Degradation of Organic Dye. *Mater. Sci. Eng. C* 23 (1-2), 285–289. doi:10.1016/s0928-4931(02)00250-3

Dahshan, H., Megahed, A. M., Abd-Elall, A. M., Abd-El-Kader, M. A., Nabawy, E., and Elbana, M. H. (2016). Monitoring of Pesticides Water Pollution-The Egyptian River Nile. *J. Environ. Health Sci. Eng.* 14 (1), 15–19. doi:10.1186/s40201-016-0259-6

Derbalah, A. (2009). Chemical Remediation of Carbofuran Insecticide in Aquatic System by Advanced Oxidation Processes. *J. Agric. Res. Kafr Elsheikh Univ.* 35 (1), 308–327.

Derbalah, A., Ismail, A., Hamza, A., and Shaheen, S. (2014). Monitoring and Remediation of Organochlorine Residues in Water. *Water Environ. Res.* 86 (7), 584–593. doi:10.2175/106143014x13975035525221

Derbalah, A., and Ismail, A. (2013). Remediation Technologies of Diazinon and Malathion Residues in Aquatic System. *Environ. Prot. Eng.* 39 (3). doi:10.37190/epe130310

Derbalah, A., Ismail, A., and Shaheen, S. (2016). The Presence of Organophosphorus Pesticides in Wastewater and its Remediation Technologies. *Environ. Eng. Manag. J. (Eemj)* 15 (8). doi:10.30638/eemj.2016.190

Derbalah, A., Sunday, M., Chidya, R., Jadoon, W., and Sakugawa, H. (2019). Kinetics of Photocatalytic Removal of Imidacloprid from Water by Advanced Oxidation Processes with Respect to Nanotechnology. *J. Water Health* 17 (2), 254–265. doi:10.2166/wh.2019.259

Descotes, G., Pinard, D., Gallas, J.-F., Penacchio, E., Blot, C., and Moreau, C. (1996). Extension of the 4-week Safety Study for Detecting Immune System Impairment Appears Not Necessary: Example of Cyclosporin A in Rats. *Toxicology* 112 (3), 245–256. doi:10.1016/0300-483x(96)03407-5

Dhal, J. P., Mishra, B. G., and Hota, G. (2015). Hydrothermal Synthesis and Enhanced Photocatalytic Activity of Ternary Fe2O3/ZnFe2O4/ZnO Nanocomposite through cascade Electron Transfer. *RSC Adv.* 5 (71), 58072–58083. doi:10.1039/c5ra05894e

Dutta, H. M., Adhikari, S., Singh, N. K., Roy, P. K., and Munshi, J. S. (1993). Histopathological Changes Induced by Malathion in the Liver of a Freshwater Catfish, Heteropneustes Fossilis (Bloch). *Bull. Environ. Contam. Toxicol.* 51 (6), 895–900. doi:10.1007/BF00198287

Egyptian Association Of Environmental Affair Law 48 (1982). *N.-., Permissible Values for Wastes in River Nile and Law 4.* Cairo: Law of the Environmental Protection.

Eissa, F., Al-Sisi, M., and Ghanem, K. (2021). Occurrence, Human Health, and Ecotoxicological Risk Assessment of Pesticides in Surface Waters of the River Nile's Rosetta Branch, Egypt. *Environ. Sci. Pollut. Res.* 28 (39), 55511–55525. doi:10.1007/s11356-021-14911-5

Eissa, F., Ghanem, K., and Al-Sisi, M. (2020). Occurrence and Human Health Risks of Pesticides and Antibiotics in Nile tilapia along the Rosetta Nile branch, Egypt. *Toxicol. Rep.* 7, 1640–1646. doi:10.1016/j.toxrep.2020.03.004

El-Demerdash, F., Dewer, Y., ElMazoudy, R. H., and Attia, A. A. (2013). Kidney Antioxidant Status, Biochemical Parameters and Histopathological Changes Induced by Methomyl in CD-1 Mice. *Exp. Toxicologic Pathol.* 65 (6), 897–901. doi:10.1016/j.etp.2013.01.002

El-Kemary, M., El-Shamy, H., and El-Mehasseb, I. (2010). Photocatalytic Degradation of Ciprofloxacin Drug in Water Using ZnO Nanoparticles. *J. Lumin.* 130 (12), 2327–2331. doi:10.1016/j.jlumin.2010.07.013

Evgenidou, E., Konstantinou, I., Fytianos, K., and Albanis, T. (2006). Study of the Removal of Dichlorvos and Dimethoate in a Titanium Dioxide Mediated Photocatalytic Process through the Examination of Intermediates and the Reaction Mechanism. *J. Hazard. Mater.* 137 (2), 1056–1064. doi:10.1016/j.jhazmat.2006.03.042

Evgenidou, E., Konstantinou, I., Fytianos, K., and Poulios, I. (2007). Oxidation of Two Organophosphorous Insecticides by the Photo-Assisted Fenton Reaction. *Water Res.* 41 (9), 2015–2027. doi:10.1016/j.watres.2007.01.027

Gilmour, C. R. (2012). *Water Treatment Using Advanced Oxidation Processes: Application Perspectives*.

Gupta, D., Sunita, S. J., and Saharan, J. (2009). Physiochemical Analysis of Ground Water of Selected Area of Kaithal City (Haryana) India. *Researcher* 1 (2), 1–5.

Habig, W. H. (1974). Glutathione-S-Transferase UV Method. *J. Biol. Chem.* 249, 7130–7139. doi:10.1016/s0021-9258(19)42083-8

Hansson, H., Kaczala, F., Marques, M., and Hogland, W. (20122012). Photo-Fenton and Fenton Oxidation of Recalcitrant Industrial Wastewater Using Nanoscale Zero-Valent Iron. *Int. J. Photoenergy*. doi:10.1155/2012/531076

Hoffmann, M. R., Martin, S. T., Choi, W., and Bahnemann, D. W. (1995). Environmental Applications of Semiconductor Photocatalysis. *Chem. Rev.* 95 (1), 69–96. doi:10.1021/cr00033a004

Hyung, H., and Kim, J.-H. (2009). Dispersion of C60 in Natural Water and Removal by Conventional Drinking Water Treatment Processes. *Water Res.* 43 (9), 2463–2470. doi:10.1016/j.watres.2009.03.011

Ismail, A., Derbalah, A., and Shaheen, S. (2015). Monitoring and Remediation Technologies of Organochlorine Pesticides in Drainage Water. *Polish J. Chem. Technol.* 17 (1), 115–122. doi:10.1515/pjct-2015-0017

Joint Committee on powder diffraction standards (2000). Diffraction Data File, N.-.

Juang, R.-S., and Chen, C.-H. (2014). Comparative Study on Photocatalytic Degradation of Methomyl and Parathion over UV-Irradiated TiO2 Particles in Aqueous Solutions. *J. Taiwan Inst. Chem. Eng.* 45 (3), 989–995. doi:10.1016/j.jtice.2013.09.025

Kaneco, S., Katsumata, H., Suzuki, T., Funasaka, T., and Kiyohisa, K. (2007). Solar Photocatalytic Degradation of Endocrine Disruptor Di-n-butyl Phthalate in Aqueous Solution Using Zinc Oxide. *Bull. Catal. Soc. India* 6 (3), 22–33.

Konishi, N., and Ward, J. (1989). Increased Levels of DNA Synthesis in Hyperplastic Renal Tubules of Aging Nephropathy in Female F344/NCr Rats. *Vet. Pathol.* 26 (1), 6–10. doi:10.1177/030098588902600102

Korsrud, G. O., Grice, H. C., and McLaughlan, J. M. (1972). Sensitivity of Several Serum Enzymes in Detecting Carbon Tetrachloride-Induced Liver Damage in Rats. *Toxicol. Appl. Pharmacol.* 22 (3), 474–483. doi:10.1016/0041-008x(72)90255-4

Kralj, M. B., Franko, M., and Trebše, P. (2007). Photodegradation of Organophosphorus Insecticides–Investigations of Products and Their Toxicity Using Gas Chromatography–Mass Spectrometry and AChE-thermal Lens Spectrometric Bioassay. *Chemosphere* 67 (1), 99–107. doi:10.1016/j.chemosphere.2006.09.039

Kumari, L., Li, W., Vannoy, C. H., Leblanc, R. M., and Wang, D. (2010). Zinc Oxide Micro-and Nanoparticles: Synthesis, Structure and Optical Properties. *Mater. Res. Bull.* 45 (2), 190–196. doi:10.1016/j.materresbull.2009.09.021

Kümmerer, K., Al-Ahmad, A., and Mersch-Sundermann, V. (2000). Biodegradability of Some Antibiotics, Elimination of the Genotoxicity and Affection of Wastewater Bacteria in a Simple Test. *Chemosphere* 40 (7), 701–710. doi:10.1016/s0045-6535(99)00439-7

Laoufi Na, B. F. (2009). "Photocatalytic Oxidation of Methomyl on an Immobilized Particle TiO2 Layer," in The 11th International Conference on Environmental Science and Technology (China, Crete, Greece, 671–687.

Lasram, M. M., Annabi, A. B., El Elj, N., Selmi, S., Kamoun, A., El-Fazaa, S., et al. (2009). Metabolic Disorders of Acute Exposure to Malathion in Adult Wistar Rats. *J. Hazard. Mater.* 163 (2-3), 1052–1055. doi:10.1016/j.jhazmat.2008.07.059

Leusch, F., and Chapman, H. (2011). *The Role of Toxicity Testing in Identifying Toxic Substances: A Framework for Identification of Suspected Toxic Compounds in Water*. Canberra, Australia: Griffith University.

Markova-Deneva, I. (2010). Infrared Spectroscopy Investigation of Metallic Nanoparticles Based on Copper, Cobalt, and Nickel Synthesized through Borohydride Reduction Method. *J. Univ. Chem. Tech. Metall.* 45 (4), 351–378.

Massoud, A., Derbalah, A., El-Mehasseb, I., Allah, M. S., Ahmed, M. S., Albrakati, A., et al. (2021). Photocatalytic Detoxification of Some Insecticides in Aqueous Media Using TiO2 Nanocatalyst. *Int. J. Environ. Res. Public Health* 18 (17), 9278. doi:10.3390/ijerph18179278

Massoud, A. S. D. A. H., El-Fakhrany, I. I., and Allah, M. S. S. (2011). Toxicological Effects of Organosphorus Insecticides and Remediation Technologies of its Residues in Aquatic System B. Dimethoate. *J. Agric. Res. Kafer El-sheikh Univ.* 37, 516–533.

Mebert, A. M., Baglole, C. J., Desimone, M. F., and Maysinger, D. (2017). Nanoengineered Silica: Properties, Applications and Toxicity. *Food Chem. Toxicol.* 109, 753–770. doi:10.1016/j.fct.2017.05.054

Mills, A., and Le Hunte, S. (1997). An Overview of Semiconductor Photocatalysis. *J. Photochem. Photobiol. A: Chem.* 108 (1), 1–35. doi:10.1016/s1010-6030(97)00118-4

Monkiedje, A., and Spiteller, M. (2005). Degradation of Metalaxyl and Mefenoxam and Effects on the Microbiological Properties of Tropical and Temperate Soils. *Int. J. Environ. Res. Public Health* 2 (2), 272–285. doi:10.3390/ijerph2005020011

Parthasarathi, V., and Thilagavathi, G. (2011). Synthesis and Characterization of Zinc Oxide Nanopartilce and its Application on Fabrics for Microbe Resistant Defence Clothing. *Int. J. Pharm. Pharm. Sci.* 3 (4), 392–398.

Pasieczna-Patkowska, S., Czech, B., Ryczkowski, J., and Patkowski, J. (2010). Removal of Recalcitrant Pollutants from Wastewater. *Appl. Surf. Sci.* 256 (17), 5434–5438. doi:10.1016/j.apsusc.2009.12.132

Peter, C., Burk, J., and Vanzwieten, M. (1986). Spontaneous Nephropatheis in Rats. *Toxicol. Pathol.* 14, 91–100. doi:10.1177/019262338601400111

Pung, S.-Y., Lee, W.-P., and Aziz, A. (2012). Kinetic Study of Organic Dye Degradation Using ZnO Particles with Different Morphologies as a Photocatalyst. *Int. J. Inorg. Chem.* 2012, 1–9. doi:10.1155/2012/608183

Rahm, M., Atty, Y. A., Rahman, M. A., and Sabry, M. (2017). Structural Changes Induced by Gibberellic Acid in the Renal Cortex of Adult Male Albino Rats. *MOJ Anat. Physiol.* 3, 00080. doi:10.15406/mojap.2017.03.00080

Rahmayeni, D. A., Stiadi, Y., Jamarun, N., and Emriadi, A. S. (2015). Preparation, Characterization of ZnO/CoFe 2 O 4 Magnetic Nanocomposites and Activity Evaluation under Solar Light Irradiation. *J. Chem. Pharm. Res.* 7 (9S), 139–146.

Reitman, S. F. (1957). Glutamic – Pyruvate Transaminase Assay by Colorimetric Method. *Am. J. Clin. Path* 28, 56. doi:10.1093/ajcp/28.1.56

Samuel, M. S. B. L. a. K. C. G. (2009). Optical Properties of ZnO Nanoparticles. *Acad. Rev.* XVI (No. 1 & 2 SB), 57–65pp.

Schirmeister, J. (1964). Determination of Creatinine Level. *Deutsche Medizinische Wochenschrift* 89, 1940–1947. doi:10.1055/s-0028-1111251

Sharma, Y., Bashir, S., Irshad, M., Nag, T., and Dogra, T. (2005). Dimethoate-induced Effects on Antioxidant Status of Liver and Brain of Rats Following Subchronic Exposure. *Toxicology* 215 (3), 173–181. doi:10.1016/j.tox.2005.06.029

Simonian, A., Efremenko, E., and Wild, J. (2001). Discriminative Detection of Neurotoxins in Multi-Component Samples. *Analytica Chim. Acta* 444 (2), 179–186. doi:10.1016/s0003-2670(01)01099-6

Strathmann, T. J., and Stone, A. T. (2002). Reduction of the Pesticides Oxamyl and Methomyl by FeII: Effect of pH and Inorganic Ligands. *Environ. Sci. Technol.* 36 (4), 653–661. doi:10.1021/es011029l

Tamimi, M., Qourzal, S., Barka, N., Assabbane, A., and Ait-Ichou, Y. (2008). Methomyl Degradation in Aqueous Solutions by Fenton's Reagent and the Photo-Fenton System. *Sep. Purif. Tech.* 61 (1), 103–108. doi:10.1016/j.seppur.2007.09.017

Tochitani, T., Mori, M., Matsuda, K., Kouchi, M., Fujii, Y., and Matsumoto, I. (2016). Histopathological Characteristics of Renal Changes in Humanrenin-Angiotensinogen Double Transgenic Rats. *J. toxicologic Pathol.* 29 (2), 125–129. doi:10.1293/tox.2015-0055

Tomašević, A., Bošković, G., Mijin, D., and Kiss, E. E. (2007). Decomposition of Methomyl over Supported Iron Catalysts. *React. Kinetics Catal. Lett.* 91 (1), 53–59. doi:10.1007/s11144-007-5094-4

Tomlin, C. D. (2003). *The Pesticide Manual*. Thirteenth Edition. Alton: BCPC Publications, 650.

van der Werf, H. M. (1996). Assessing the Impact of Pesticides on the Environment. *Agric. Ecosyst. Environ.* 60 (2-3), 81–96. doi:10.1016/s0167-8809(96)01096-1

Van Vooren, L., Van De Steene, M., Ottoy, J.-P., and Vanrolleghem, P. (2001). Automatic Buffer Capacity Model Building for the Purpose of Water Quality Monitoring. *Water Sci. Technol.* 43 (7), 105–113. doi:10.2166/wst.2001.0400

Waber, H., and Dtsch, M. (1966). Cholinestrase Kinetic Colorimetric Method. *Dtsch. Med. Wschr* 91, 1927.

Wafa, T., Amel, N., Issam, C., Imed, C., Abdelhedi, M., and Mohamed, H. (2011). Subacute Effects of 2, 4-dichlorophenoxyacetic Herbicide on Antioxidant Defense System and Lipid Peroxidation in Rat Erythrocytes. *Pestic. Biochem. Physiol.* 99 (3), 256–264. doi:10.1016/j.pestbp.2011.01.004

Yu, H., Yu, J., Cheng, B., and Zhou, M. (2006). Effects of Hydrothermal post-treatment on Microstructures and Morphology of Titanate Nanoribbons. *J. Solid State. Chem.* 179 (2), 349–354. doi:10.1016/j.jssc.2005.10.024

Zhang, Z., Wu, H., Yuan, Y., Fang, Y., and Jin, L. (2012). Development of a Novel Capillary Array Photocatalytic Reactor and Application for Degradation of Azo Dye. *Chem. Eng. J.* 184, 9–15. doi:10.1016/j.cej.2011.02.057

Conflict of Interest: The authors declare that the research was conducted in the absence of any commercial or financial relationships that could be construed as a potential conflict of interest.

frontiers in Environmental Science

ORIGINAL RESEARCH
published: 24 March 2022
doi: 10.3389/fenvs.2022.859356

Sensory Disturbance by Six Insecticides in the Range of μg/L in *Caenorhabditis elegans*

Rong Zhou[1,2†], *Yue Yu*[1,2†], *Weidong Zhang*[1], *Dayong Wang*[3], *Yanan Bai*[1,2], *Yixuan Wang*[1,2] *and Yuanqing Bu*[1,2,4*]

[1]Nanjing Institute of Environmental Science, Ministry of Ecology and Environment, Nanjing, China, [2]State Environmental Protection Key Laboratory of Pesticide Environmental Assessment and Pollution Control, Nanjing, China, [3]Medical School, Southeast University, Nanjing, China, [4]Jiangsu Collaborative Innovation Center of Atmospheric Environment and Equipment Technology, Nanjing University of Information Science and Technology, Nanjing, China

Using *Caenorhabditis elegans* as an animal model, the possible toxic effects of six insecticides (dinotefuran, thiamethoxam, thiacloprid, nitenpyram, acetamiprid, and sulfoxaflor) commonly used in agriculture on sensory perception were examined. The sensory behaviors of thermotaxis, avoidance of copper ion, chemotaxis to NaCl, and chemotaxis to diacetyl were measured to investigate the damage on sensory perceptions in nematodes exposed to the examined insecticides in the range of micrograms per liter (μg/L). Exposure to dinotefuran, thiamethoxam, thiacloprid, nitenpyram, acetamiprid, or sulfoxaflor at concentrations of 10–100 μg/L resulted in severe deficits in sensory perceptions to temperature, copper ion, NaCl, and diacetyl. The relative neurotoxicity of the six insecticides examined to *C. elegans* were shown as dinotefuran > thiamethoxam > thiacloprid > nitenpyram > acetamiprid > sulfoxaflor. Moreover, post-treatment with the antioxidant ascorbate effectively suppressed the production of reactive oxygen species and damages of sensory perceptions induced by the six insecticides, indicating that the activation of oxidative stress can act as an important cellular contributor to the observed damage of the examined insecticides in affecting sensory perceptions. Our data highlighted the potential toxicity of the six insecticides at low concentrations in inducing sensory disturbance to environmental organisms.

Keywords: neurotoxicity, sensory perception, insecticides, *Caenorhabditis elegans*, oxidative stress

OPEN ACCESS

Edited by:
Liangang Mao,
Institute of Plant Protection (CAAS), China

Reviewed by:
Neha Vijay Kalmankar,
National Centre for Biological Sciences, India
Qi Rui,
Nanjing Agricultural University, China

***Correspondence:**
Yuanqing Bu
byq@nies.org

†These authors have contributed equally to this work and share first authorship

Specialty section:
This article was submitted to Toxicology, Pollution and the Environment, a section of the journal Frontiers in Environmental Science

Received: *21 January 2022*
Accepted: *17 February 2022*
Published: *24 March 2022*

Citation:
Zhou R, Yu Y, Zhang W, Wang D, Bai Y, Wang Y and Bu Y (2022) Sensory Disturbance by Six Insecticides in the Range of μg/L in Caenorhabditis elegans. Front. Environ. Sci. 10:859356. doi: 10.3389/fenvs.2022.859356

INTRODUCTION

The application of insecticides has made great contributions to the development of agriculture around the world. Among insecticides, most of the neonicotinoid insecticides are considered as classic neurotoxins since they can irreversibly target to nicotinic acetylcholine receptors and cause paralysis and eventual death in most arthropods rather than in vertebrates (Matsuda et al., 2005; Bradford et al., 2020). Moreover, diamide insecticides could damage muscle contraction *via* activating ryanodine receptors and releasing stored calcium from the sarcoendoplasmic reticulum, which is an important mechanism to control lepidopteran pests (Cordova et al., 2006). Sulfoximine insecticides (such as sulfoxaflor) could kill insects by damaging Ca^{2+} homeostasis in muscle cells (Guo et al., 2019).

After release into the environment, insecticides potentially cause toxicity to environmental organisms. As reported in previous studies, organochlorines, organophosphates, carbamates,

pyrethroids, and neonicotinoid insecticides could cause damage on reproduction, feeding, and avoidance of predation in poultry populations (Walker, 2003). In addition, exposure to insecticides also poses a great threat to some soil organisms—for example, cycloxaprid, a novel neonicotinoid insecticide, could induce neurotoxicity in earthworms, such as neurological dysfunctions, stress responses, and damage on calcium binding (Qi et al., 2018).

Due to the properties of short lifespan, small size, short life cycle, and high sensitivity to pollutants (Leung et al., 2008; Haegerbaeumer et al., 2018; Queirós et al., 2019; Wang, 2020; Zhang et al., 2022), *Caenorhabditis elegans* has been used as an ideal model for examining the response to environmental toxicants or stresses (Wang et al., 2021a; Liu et al., 2021c; Sun et al., 2021). Recently, it was reported that some neonicotinoid insecticides could cause a dysfunction in the development, reproduction, and locomotion behaviors of *C. elegans* (Bradford et al., 2020). Moreover, *C. elegans* is an important animal model for the developmental study of nervous systems because of its simple nervous system structure composed of 302 neurons in adult hermaphrodite (Bargmann, 1998; Corsi et al., 2015). *C. elegans* is helpful for investigating different functions of the nervous system, such as learning and memory (Ardiel and Rankin, 2010; Bargmann et al., 1993). In addition, *C. elegans* is a powerful animal model for assessing neurotoxicity induced by different toxicants (Wang, 2019; Liu et al., 2021a)—for example, in *C. elegans*, the development of dopaminergic nervous systems and their functions (such as sensory perception behaviors) were found to be affected by exposure to nanoparticles (Qu and Wang, 2020). Considering the fact that ~80% of *C. elegans* proteome has human homologous genes, specifically neurodevelopmental genes (Riddle et al., 1997), *C. elegans* is an important animal model for both biomedical and environmental toxicology. Due to the availability of some disease models (Moy et al., 2009; Griffin et al., 2017), *C. elegans* is also useful for pharmaceutical screening.

Sensory perception is an important function for organisms to sense and detect the existence and alteration of environmental stimuli. Nevertheless, the possible toxic mode of action on sensory perception behaviors induced by exposure to insecticides remains largely unclear in organisms. Thus, the aim of this study is to compare the possible damage of six insecticides (acetamiprid, nitenpyram, thiacloprid, thiamethoxam, dinotefuran, and sulfoxaflor) on the sensory perception behaviors of *C. elegans* as representative for other nematodes. Among them, acetamiprid, nitenpyram, thiacloprid, thiamethoxam, and dinotefuran are neonicotinoid insecticides. Sulfoxaflor belongs to sulfoximine insecticides. *C. elegans* has been widely used for the assessment of pesticide toxicity (Gomez-Eyles et al., 2009; Roh and Choi, 2011; Ruan et al., 2012; Du et al., 2015; Yu et al., 2020). The well-described backgrounds of development and functions of the nervous system of *C. elegans* provide a strong support for this research. The sensory perception behaviors of thermotaxis, avoidance to copper ion, chemotaxis to NaCl, and chemotaxis to diacetyl were examined in this study. Thermotaxis reflects a sensory perception to physical stimuli. The chemotaxis to NaCl and avoidance to copper reflect a gustatory perception to soluble chemicals. The chemotaxis to diacetyl indicates an olfactory perception to volatile chemicals. Our results demonstrated the potential of exposure to the examined insecticides in the range of micrograms per liter (μg/L) in causing damage on sensory perceptions to different degrees in nematodes. The obtained data highlights the toxicity of long-term exposure to the examined insecticides at low concentrations in inducing damage on sensory perceptions in environmental organisms.

MATERIALS AND METHODS

Reagents

The standards for six insecticides (**Figure 1**) were obtained from Shanghai Pesticide Research Institute Co. (Shanghai, China). Acetamiprid (purity, 98.0%), nitenpyram (purity, 99.1%), thiacloprid (purity, 99.4%), thiamethoxam (purity, 98.0%), dinotefuran (purity, 99.0%), and sulfoxaflor (purity, 99.7%) were dissolved in distilled water to obtain stock solutions (1 g/L). The working concentrations of the examined insecticides are shown in **Supplementary Table S1**.

Strains and Maintenance

The wild-type (N2) nematodes were obtained from *Caenorhabditis* Genetics Center. Nematode growth medium (NGM) plates seeded with *Escherichia coli* OP50 were used to maintain the examined worms (Brenner, 1974). To obtain age-synchronous L1-larvae nematodes, the gravid worms were lysed using a bleaching mixture solution containing 2% HOCl and 0.45 M NaOH to release enough eggs from the body (Yang et al., 2021b). After that, the eggs were allowed to develop into L1-larvae on new NGM plates.

Exposure

Nematodes were exposed to six insecticides with the addition of OP50 (4×10^6 colony-forming units, CFUs) from L1-larvae to adult stage (adult day-1, approximately 4.5 days). The age-synchronous L1-larvae were used for the exposure. Insecticides were diluted into the examined concentrations using K-medium to determine their effects on different sensory perception behaviors.

Thermotaxis Assay

Radial temperature gradient was employed to perform the thermotaxis assay as described by Ye *et al.* (2008). A steeper temperature gradient in the range from 17°C (at the center) to 25°C (at the periphery) was prepared. To generate this radial temperature gradient, a vial containing frozen acetic acid was put on the bottom of 9-cm culture plates, and the culture plates were incubated at 26°C (the preferred temperature for nematodes) for 90 min. After exposure to

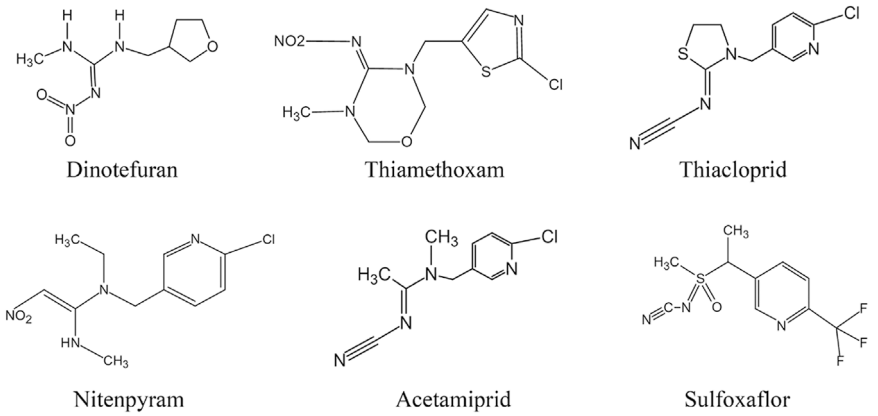

FIGURE 1 | Structures of the six insecticides examined.

insecticides and the following washing with M9 buffer, the individual worms were transferred on the agar surface of the prepared 9-cm culture plates having a thermal gradient. On the agar surface, the worms were allowed to move for 2 h. After removing the worms, the traces of movement that the examined worms left on the agar surface were captured by camera. The percentages of worms performing isothermal tracking (IT) were counted. Approximately 30 nematodes were examined for each exposure. Three replicates were performed.

Avoidance of Copper

Under normal conditions, the nematodes will avoid the copper on the NGM assay plate (Sambongi et al., 2000). An assay of avoidance of Cu^{2+} was performed as described previously (Sambongi et al., 2000). A 9-cm culture plate was divided into four equal parts. Among these four equal parts, normal NGM medium was added into two opposite sides. Meanwhile, NGM medium containing 100 μM Cu^{2+} was added into the other two opposite sides. After exposure to the insecticides and the following washing with M9 buffer, the worms were transferred onto the surface of Cu^{2+}-free parts for 1 h. The avoidance index was calculated as the value of the number of worms on NGM containing Cu^{2+}/total number of worms. Approximately 100 nematodes were examined for each exposure. Three replicates were performed.

Chemotaxis to NaCl

Chemotaxis to NaCl (a water-soluble chemoattractant) was performed as described previously (Saeki et al., 2001). An agar plug containing NaCl (100 mM) was placed on the off-center surface of an agar plate prepared with agar (20 g/L), potassium phosphate (5 mM, pH 6.0), $CaCl_2$ (1 mM), and $MgSO_4$ (1 mM). After overnight treatment, the NaCl plug was removed. In order to anesthetize the nematodes, 1 μl sodium azide (0.5 M) was added on position 4 cm away from NaCl plug position (control) and NaCl plug position. After 1 h, the chemotaxis index (CI) was calculated as the value of (number of worms within 1.5 cm of center of NaCl spot — number of worms within 1.5 cm of the control spot) / (total number of worms). Approximately 100 nematodes were examined for each exposure. Three replicates were performed.

Chemotaxis to Diacetyl

Chemotaxis to diacetyl was performed as described previously (Li et al., 2011). One microliter of diacetyl (10^{-2}) was added on the surface of the assay plates. Meanwhile, 1 μl sodium azide (0.5 M) was added on diacetyl position and the position 4 cm away from the diacetyl position (control). After 1 h, the CI was calculated as the value of (number of worms within 1.5 cm of the center of the diacetyl spot—number of worms within 1.5 cm of the control spot) / (total number of worms). Approximately 100 nematodes were examined for each exposure. Three replicates were performed.

Reactive Oxygen Species Production

Reactive oxygen species (ROS) production was used to reflect the activation of oxidative stress (Liu et al., 2021b). To detect the production of ROS, the control and exposed nematodes were labeled with CM-H_2DCFDA (1 μM) in the dark for 3 h (Yang et al., 2021a). After that, the nematodes were washed with M9 buffer three times. *C. elegans* was then mounted on a 2% agar pad and analyzed for their fluorescence signals at 510 nm (emission filter)/488 nm (excitation wavelength) using laser scanning confocal microscopy. The intestinal fluorescent intensities were determined by normalization against the autofluorescence. For each treatment, 50 nematodes were used. Three replicates were performed.

Pharmacological Assay

The nematodes were first exposed to six insecticides (100 μg/L) with the addition of OP50 (4×10^6 CFUs) from L1-larvae to adult day-1. After that, the nematodes were treated with 10 mM ascorbate (an antioxidant) for 24 h. Three replicates were performed.

Lethality Assay

For the lethality assay, 100 worms were added into each well in a 24-well plate with 250 μl insecticide at concentrations of 0.1, 1, 10,

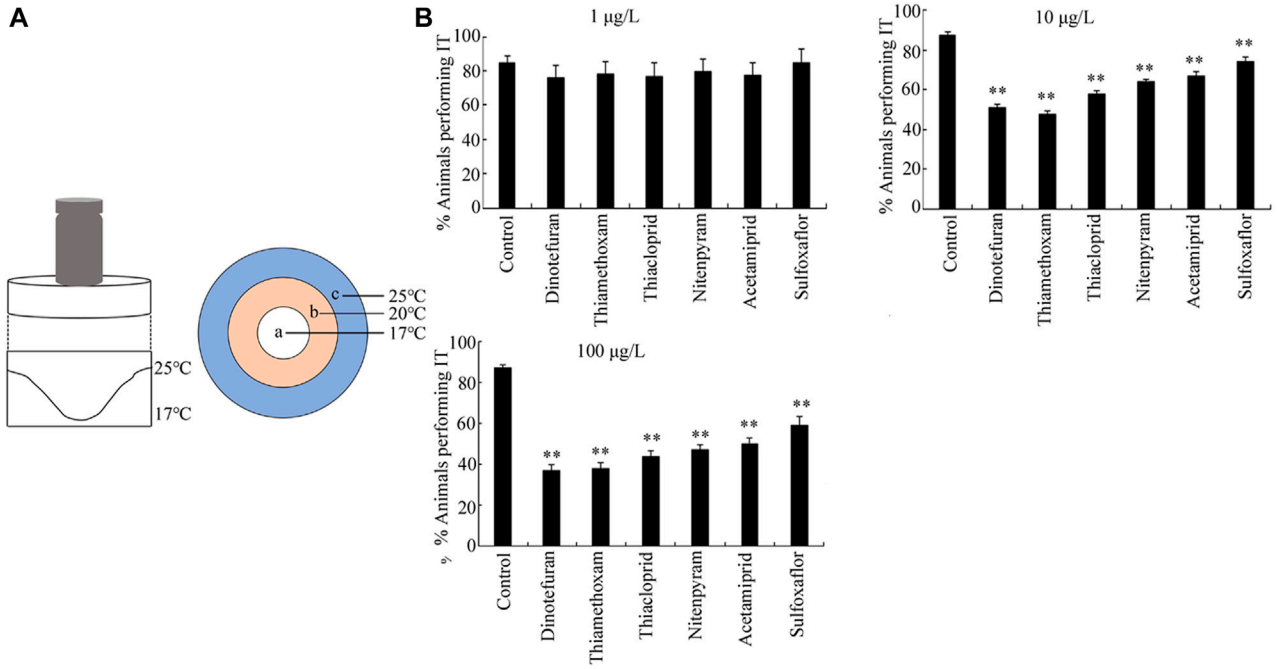

FIGURE 2 | Toxicity of insecticides in affecting thermotaxis. **(A)** Assay model for thermotaxis. **(B)** Toxicity of the six insecticides examined in affecting thermotaxis ability. IT, isothermal tracking. Nematodes were exposed to insecticide with the addition of OP50 from L1-larvae to adult day-1. Bars represent means ± SD. $^{**}p < 0.01$ *vs*. control.

or 100 mg/L. After exposure, the nematodes were transferred to a fresh NGM plate. After gently touching with a needle, the nematodes showing immobilization without recovery were considered dead. Three replicates were performed in each exposure.

The LC_{50} and 95% confidence interval of the examined insecticides were analyzed using SPSS 13.0 software. The LC_{50} and 95% confidence interval of the examined insecticides are shown in **Supplementary Table S2**.

Body Bend Assay

Body bend refers to the alteration in bending direction at the mid-body as described by Wang *et al.* (2021b). Forty nematodes were analyzed per treatment. Three replicates were performed.

Statistical Analysis

Statistical analysis was performed using SPSS 12.0 software. The probability level of 0.01 (**) was considered to be statistically significant. The one-way analysis of variance, followed by *post-hoc* Bonferroni test, was performed for group comparisons.

RESULTS

Toxicity Comparison of Six Insecticides in Affecting Thermotaxis

The first sensory perception response to the exposure of six insecticides examined was thermotaxis (**Figure 2A**). At the concentration of 1 μg/L, none of the six insecticides induced significant changes in thermotaxis in nematodes. However, after exposure to all the examined insecticides at concentrations of 10–100 μg/L, the thermotaxis ability of nematodes decreased significantly compared to the control ($p < 0.01$) (**Figure 2B**), and the order for the toxicity of the six insecticides in reducing thermotaxis was dinotefuran > thiamethoxam > thiacloprid > nitenpyram > acetamiprid > sulfoxaflor (**Figure 2B**).

Toxicity Comparison of Six Insecticides in Affecting Avoidance of Copper Ion

The second sensory perception response to the exposure of six insecticides examined was avoidance of copper ion (**Figure 3A**). Exposure to the six insecticides examined at the concentration of 1 μg/L did not significantly affect the avoidance index (**Figure 3B**). However, after exposure at concentrations of 10–100 μg/L, all the six insecticides examined could cause a significant increase in the avoidance index compared to the control ($p < 0.01$) (**Figure 3B**). At concentrations of 10–100 μg/L, the order for the toxicity of the six insecticides in reducing ability to avoid copper ion was dinotefuran > thiamethoxam > thiacloprid > nitenpyram > acetamiprid > sulfoxaflor (**Figure 3B**).

Toxicity Comparison of Six Insecticides in Affecting Chemotaxis to NaCl

The third sensory perception response to the exposure of six insecticides examined was chemotaxis to NaCl (**Figure 4A**). After

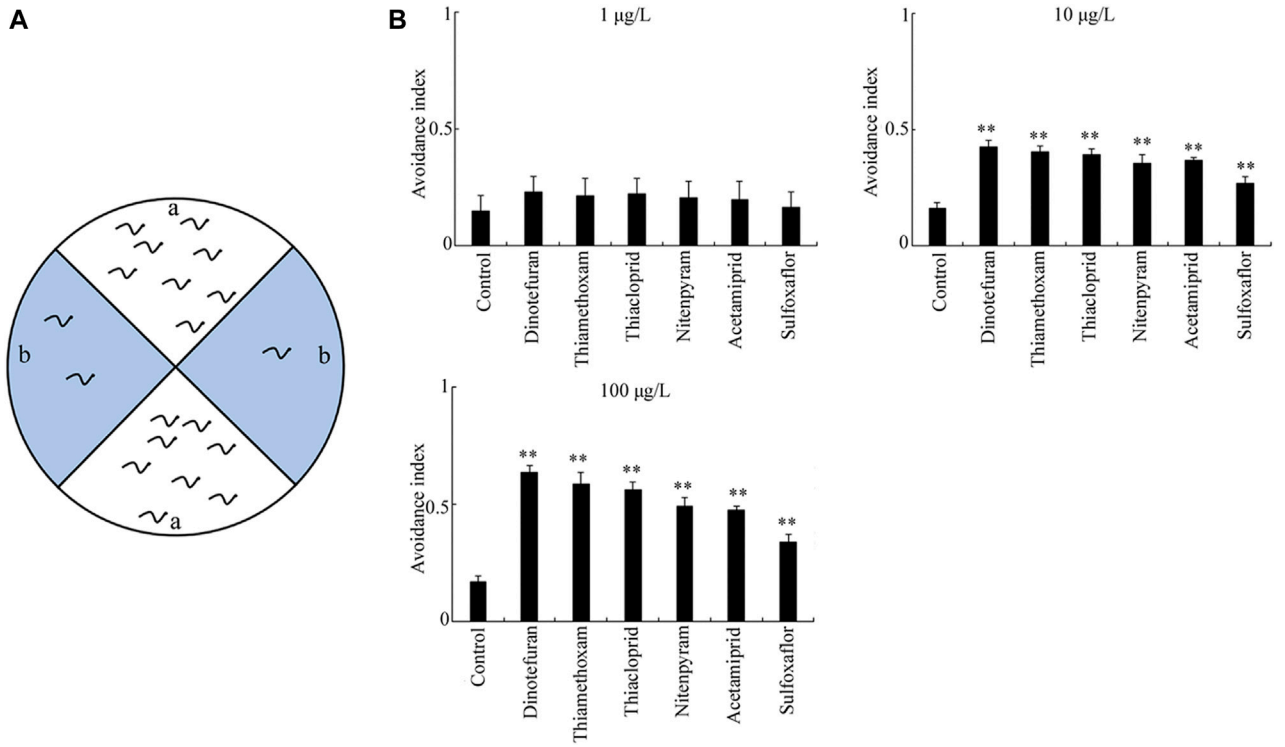

FIGURE 3 | Toxicity of insecticides in affecting avoidance of copper ion. **(A)** Assay model for avoidance of copper ion. **(B)** Toxicity of the six insecticides examined in affecting the avoidance of copper ion. Nematodes were exposed to insecticide with the addition of OP50 from L1-larvae to adult day-1. Bars represent means ± SD. $^{**}p < 0.01$ *vs.* control.

exposure at the concentration of 1 μg/L, dinotefuran, thiamethoxam, thiacloprid, nitenpyram, acetamiprid, and sulfoxaflor did not alter chemotaxis to NaCl obviously (**Figure 4B**). However, after exposure at concentrations of 10–100 μg/L, all the examined insecticides significantly decreased the chemotaxis to NaCl compared to the control ($p < 0.01$) (**Figure 4B**). Additionally, after exposure at concentrations of 10–100 μg/L, the order for the toxicity of the six insecticides in inhibiting chemotaxis to NaCl was dinotefuran > thiamethoxam > thiacloprid > nitenpyram > acetamiprid > sulfoxaflor (**Figure 4B**).

Toxicity Comparison of Six Insecticides in Affecting Chemotaxis to Diacetyl

The fourth sensory perception response to the exposure of six insecticides determined was chemotaxis to diacetyl (**Figure 5A**). After exposure at the concentration of 1 μg/L, dinotefuran, thiamethoxam, thiacloprid, nitenpyram, acetamiprid, and sulfoxaflor did not remarkably influence chemotaxis to diacetyl (**Figure 5B**). Differently from this, the exposure to all the examined insecticides at concentrations of 10–100 μg/L significantly inhibited chemotaxis to diacetyl compared to the control ($p < 0.01$) (**Figure 5B**). Moreover, in the concentration range of 10–100 μg/L, the order for the toxicity of the six insecticides in suppressing chemotaxis to diacetyl was dinotefuran > thiamethoxam > thiacloprid > nitenpyram > acetamiprid > sulfoxaflor (**Figure 5B**).

Treatment With Antioxidant Suppressed the Damage of Insecticides on Sensory Behaviors

Exposure to the six insecticides (100 μg/L) examined from L1-larvae to adult day-1 caused significant ROS production ($p < 0.01$) (**Figure 6A**). In contrast, treatment with 10 mM ascorbate from adult day-1 for 24 h could not induce obvious ROS production. Moreover, after exposure to insecticides, post-treatment with 10 mM ascorbate could obviously suppress ROS production in nematodes exposed to the six insecticides examined ($p < 0.01$) (**Figure 6A**).

In nematodes, treatment with 10 mM ascorbate alone could not alter the sensory perception of thermotaxis, avoidance of copper ion, chemotaxis to NaCl, and chemotaxis to diacetyl (**Figures 6B–E**). Moreover, after exposure to insecticides, post-treatment with 10 mM ascorbate could further significantly inhibit the damage induced by exposure to the six insecticides examined in reducing thermotaxis, suppressing avoidance of copper ion, decreasing chemotaxis to NaCl, and reducing chemotaxis to diacetyl (**Figures 6B–E**).

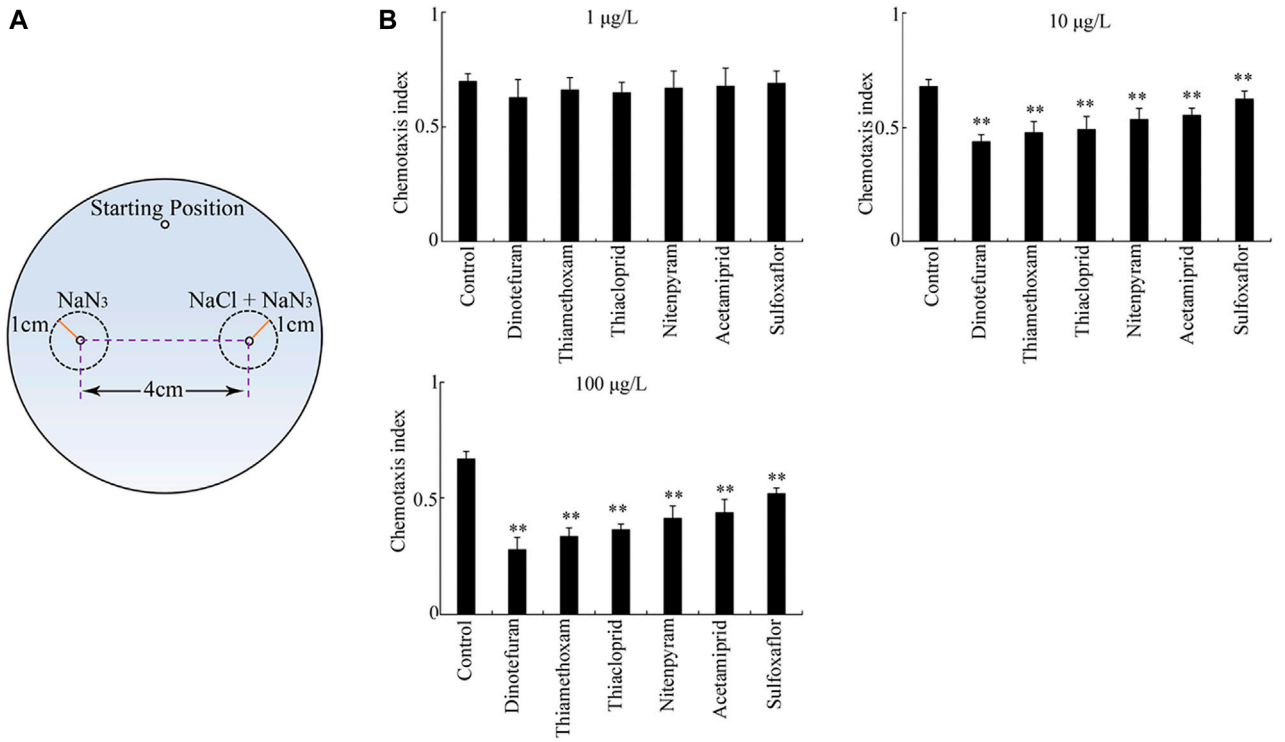

FIGURE 4 | Toxicity of insecticides in affecting chemotaxis to NaCl. **(A)** Assay model for chemotaxis to NaCl. **(B)** Toxicity of the six insecticides examined in affecting chemotaxis to NaCl. Nematodes were exposed to insecticide with the addition of OP50 from L1-larvae to adult day-1. Bars represent means ± SD. $^{**}p < 0.01$ *vs*. control.

DISCUSSION

Normally, the environmental concentrations of insecticides in surface water were in the range of microgram or nanogram per liter (μg/L or ng/L) (Faria et al., 2020). This is one of the important reasons for our focus on insecticide concentrations in the range of μg/L—to determine the effect of insecticide exposure on sensory perception in this study. Besides this, according to our study, exposure to the six insecticides examined at a concentration of 1–100 mg/L caused significant lethality, but exposure to the six insecticides (0.1 mg/L) examined did not induce significant lethality (**Supplementary Figure S1**). Thus, the observed damage on sensory perceptions in nematodes exposed to the six insecticides examined at a concentration of ≤100 μg/L might be largely not due to the lethal effect. This is another reason for our focus on insecticide concentrations in the range of μg/L—to determine the effect of insecticide exposure on sensory perception in nematodes.

Using *C. elegans* as an animal model, it has been shown that exposure to certain insecticides (such as neonicotinoid insecticides) could result in oxidative stress and damage on reproduction, locomotion behaviors, and growth (Rajini et al., 2008; Han et al., 2017; Kudelska et al., 2017; Zeng et al., 2017; Bradford et al., 2020). In this study, we found that prolonged exposure to insecticides in the range of μg/L potentially caused damage on multiple aspects of sensory perception in nematodes.

Temperature is an important environmental factor for the survival of organisms. Meanwhile, temperature is also an important environmental stimulus for environmental animals to sense. *C. elegans* has highly sensitive and sophisticated thermosensory mechanisms to detect environmental temperatures (Takeishi et al., 2020). As shown in **Figure 2**, exposure to neonicotinoid insecticides potentially noticeably affected thermotaxis behavior in nematodes. Sulfoxaflor had the weakest toxic effect on thermotaxis behavior among the six insecticides examined.

Avoidance of copper ion reflects a form of gustatory perception of worms, and this form of gustatory perception is controlled by ASH sensory neurons (Wang, 2019). All the six insecticides examined (10–100 μg/L) suppressed the avoidance of copper and showed the following toxicity order: dinotefuran > thiamethoxam > thiacloprid > nitenpyram > acetamiprid > sulfoxaflor (**Figure 3**). The heavy metal Cu is neurotoxic for worms (Wang and Xing, 2009; Zhang et al., 2010). These observations suggested that exposure to the examined insecticides in the range of μg/L may cause the difficulty for organisms to avoid harmful compounds or noxious stimuli in the environment. It was also reported that exposure to some insecticides might adversely influence the avoidance of predation in the poultry populations (Walker, 2003).

Chemotaxis towards NaCl is another form of gustatory perception of worms, and ASE sensory neurons controlled this form of gustatory perception (Bargmann and Horvitz, 1991).

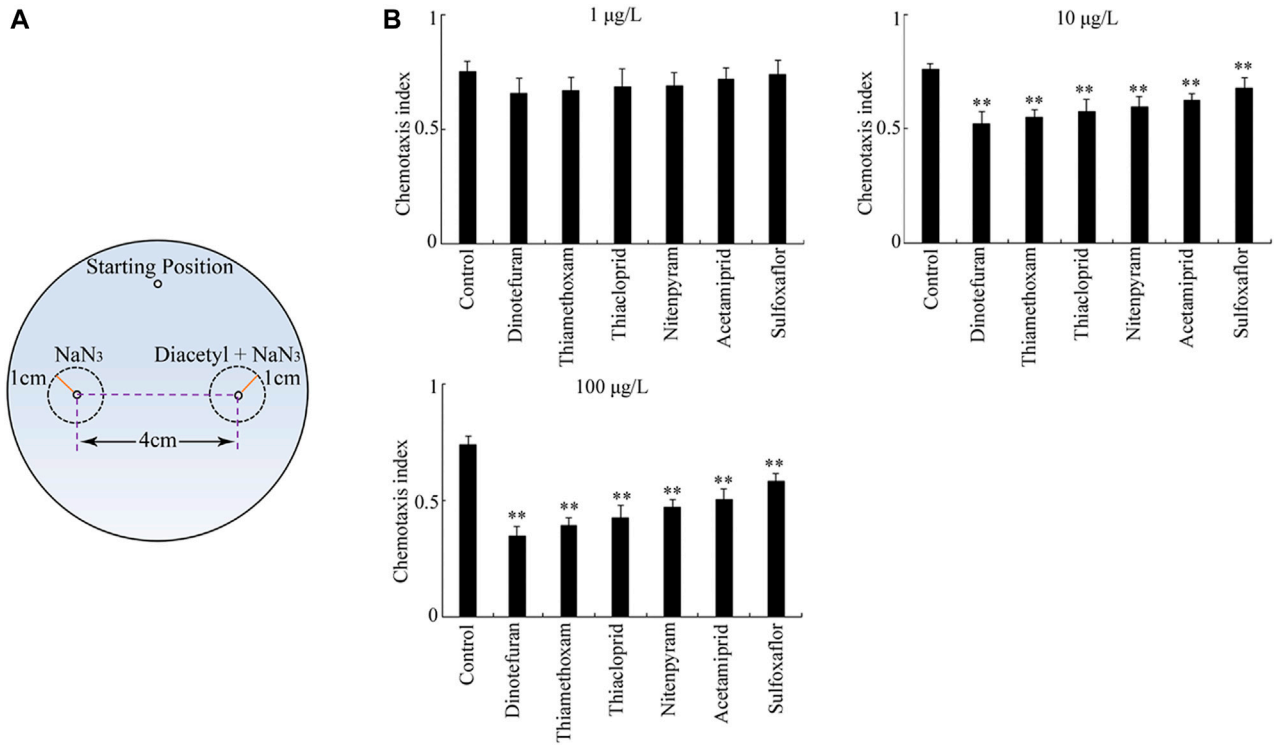

FIGURE 5 | Toxicity of insecticides in affecting chemotaxis to diacetyl. **(A)** Assay model for chemotaxis to diacetyl. **(B)** Toxicity of the six insecticides examined in affecting chemotaxis to diacetyl. Nematodes were exposed to insecticide with the addition of OP50 from L1-larvae to adult day-1. Bars represent means ± SD. $^{**}p < 0.01$ *vs.* control.

Similar to the observations on thermotaxis behavior and avoidance of copper ion, these six insecticides at concentrations of 10–100 μg/L caused a remarkable deficit in chemotaxis to NaCl and exhibited the following toxicity order: dinotefuran > thiamethoxam > thiacloprid > nitenpyram > acetamiprid > sulfoxaflor (**Figure 4**). In honeybees, exposure to thiamethoxam also caused a deficit in sensory perception of sugar (Aliouane et al., 2009).

Chemotaxis to diacetyl reflects the ability of olfactory perception in worm, and this sensory perception is mainly controlled by AWA sensory neurons (Metaxakis et al., 2018). After exposure at concentrations of 10–100 μg/L, the toxicity order for the six insecticides examined in affecting chemotaxis to diacetyl was dinotefuran > thiamethoxam > thiacloprid > nitenpyram > acetamiprid > sulfoxaflor (**Figure 5**). These observations demonstrated that, in worms exposed to the examined insecticides in the range of μg/L, both gustatory perception and olfactory perception would be noticeably damaged. Besides the four forms of sensory perceptions examined, there are also some other forms of sensory perceptions in *C. elegans* (Metaxakis et al., 2018). The possible effects of exposure to the examined insecticides on other forms of sensory perceptions still remain unclear in nematodes.

After exposure, 100 μg/L of the six insecticides examined obviously decreased the locomotion behavior as reflected by the endpoint of body bend (**Supplementary Figure S2**). In contrast, dinotefuran, thiamethoxam, thiacloprid, nitenpyram, acetamiprid, and sulfoxaflor at concentrations of ≤100 μg/L did not affect the locomotion behavior (**Supplementary Figure S2**). Therefore, the observed damage of the six insecticides examined at concentrations ≤100 μg/L on sensory perceptions was not due to the deficit in locomotion behavior.

In nematodes, exposure to insecticides (such as lindane) could induce oxidative stress (Yu et al., 2021). Ascorbate is a normally used antioxidant against oxidative stress in nematodes (Li et al., 2012). We further found that post-treatment with the antioxidant ascorbate could effectively suppress damage by the six insecticides examined in reducing themotaxis, in suppressing avoidance of copper ion, in decreasing chemotaxis toward NaCl, and in reducing chemotaxis toward diacetyl (**Figures 6B–E**). Meanwhile, post-treatment with the antioxidant ascorbate could also obviously suppress the ROS production induced by exposure to the six insecticides examined (**Figure 6A**). Therefore, the activation of oxidative stress can act as an important cellular contributor to the observed damage of the examined insecticides in affecting sensory perceptions. In nematodes, the ROS signals are mainly detected in the pharynx and the intestinal cells (Yang et al., 2021a). This implied that the examined insecticides might potentially bind to certain group(s) of biomolecules so as to induce oxidative damage in primary biological barriers, such as pharynx barrier, in nematodes. After that, neurotoxicity on sensory perceptions

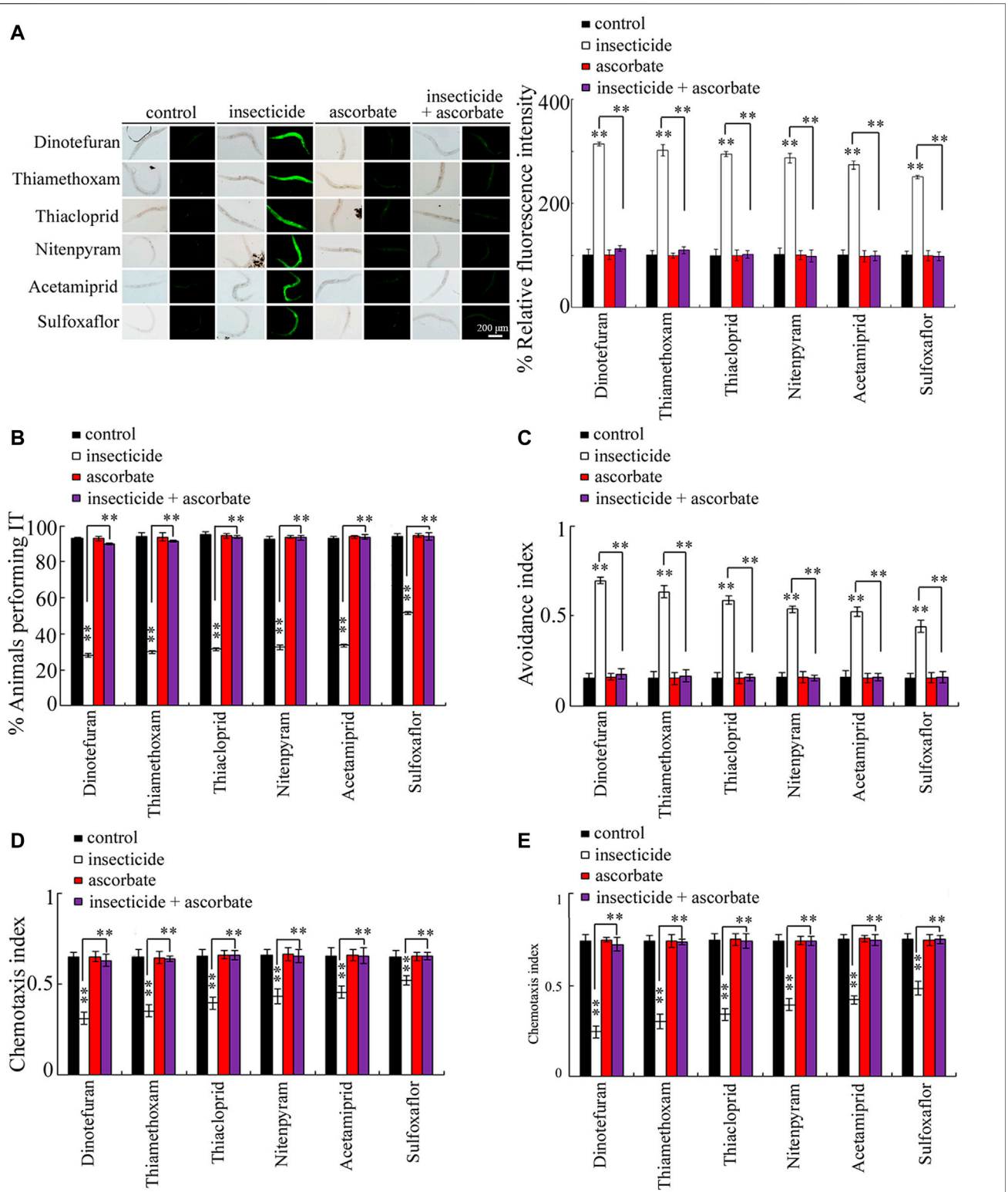

FIGURE 6 | Effect of treatment with ascorbate on the toxicity of the examined insecticides in affecting sensory behaviors. **(A)** Effect of treatment with ascorbate on the toxicity of the examined insecticides in inducing reactive oxygen species production. **(B)** Effect of treatment with ascorbate on the toxicity of the examined insecticides in affecting thermotaxis ability. **(C)** Effect of treatment with ascorbate on the toxicity of the examined insecticides in affecting the avoidance of copper ion. **(D)** Effect of treatment with ascorbate on the toxicity of the examined insecticides in affecting chemotaxis to NaCl. **(E)** Effect of treatment with ascorbate on the toxicity of the examined insecticides in affecting chemotaxis to diacetyl. Nematodes were first exposed to 100 μg/L insecticides with the addition of OP50 from L1-larvae to adult day-1. After that, the nematodes were treated with 10 mM ascorbate (an antioxidant) for 24 h. Bars represent means ± SD. $^{**}p < 0.01$ *vs.* control (if not specifically indicated).

will be further induced after insecticide exposure—that is, the damage on the examined four forms of sensory perceptions might be largely due to the fact that both sulfoxaflor and neonicotinoid insecticides could cause the activation of oxidative stress. This is also helpful to explain the fact that the sensory perceptions were affected in the same way by the examined insecticides.

The possible adverse effects of insecticides at various aspects have also been determined with other organisms, such as *Daphnia magna* and *Ceriodaphnia dubia* (Sheets et al., 2016; Raby et al., 2018). Moreover, it was observed that exposure to neonicotinoid insecticides could result in developmental neurotoxicity (Sheets et al., 2016)—that is, at least at high concentrations, the observed damage on sensory perceptions to temperature, copper ion, NaCl, and diacetyl might also be possibly due to the developmental deficits in related neurons and/or neuronal circuit(s) governing these sensory perceptions in nematodes.

CONCLUSION

The potential damage on sensory perceptions by exposure to six insecticides (dinotefuran, thiamethoxam, thiacloprid, nitenpyram, acetamiprid, and sulfoxaflor) was compared in *C. elegans*. Exposure to these insecticides at concentrations of 10–100 μg/L caused severe deficits in sensory perceptions to temperature, copper ion, NaCl, and diacetyl. Activation of oxidative stress acted as an important cellular mechanism for the observed damage of the six insecticides examined in affecting sensory perceptions. Therefore, our results suggested the potential of long-term exposure to the examined insecticides in the range of μg/L in inducing damage on sensory perceptions in organisms.

DATA AVAILABILITY STATEMENT

The original contributions presented in the study are included in the article/**Supplementary Material**, further inquiries can be directed to the corresponding author.

AUTHOR CONTRIBUTIONS

RZ and YY contributed to study design, experimentation, and initial draft writing. WZ and DW contributed to experimentation. YB and YW contributed to data analysis and result visualization. YB took charge of funding acquisition. All authors reviewed the final version of the manuscript and approve it for publication.

FUNDING

This study was funded by the National Key Research and Development Program of China (No. 2018YFC1801105), the Fundamental Research Fund of Central Public Welfare Research Institutions in 2019 (Innovative Team Research Project of New Approach and Application on Substitution Toxicology of Environmental Hormone Substance), and the Open Project of State Environmental Protection Key Laboratory of Pesticide Environmental Assessment and Pollution Control. All sources of funding received for the research have been submitted.

SUPPLEMENTARY MATERIAL

The Supplementary Material for this article can be found online at: https://www.frontiersin.org/articles/10.3389/fenvs.2022.859356/full#supplementary-material

REFERENCES

Aliouane, Y., El Hassani, A. K., Gary, V., Armengaud, C., Lambin, M., and Gauthier, M. (2009). Subchronic Exposure of Honeybees to Sublethal Doses of Pesticides: Effects on Behavior. *Environ. Toxicol. Chem.* 28, 113–122. doi:10.1897/08-110.1

Ardiel, E. L., and Rankin, C. H. (2010). An Elegant Mind: Learning and Memory in *Caenorhabditis Elegans*. *Learn. Mem.* 17, 191–201. doi:10.1101/lm.960510

Bargmann, C. I., and Horvitz, H. R. (1991). Chemosensory Neurons with Overlapping Functions Direct Chemotaxis to Multiple Chemicals in *C. Elegans*. *Neuron* 7, 729–742. doi:10.1016/0896-6273(91)90276-6

Bargmann, C. I., Hartwieg, E., and Horvitz, H. R. (1993). Odorant-selective Genes and Neurons Mediate Olfaction in *C. Elegans*. *Cell* 74, 515–527. doi:10.1016/0092-8674(93)80053-h

Bargmann, C. I. (1998). Neurobiology of the *Caenorhabditis E* Genome. *Science* 282, 2028–2033. doi:10.1126/science.282.5396.2028

Bradford, B. R., Whidden, E., Gervasio, E. D., Checchi, P. M., and Raley-Susman, K. M. (2020). Neonicotinoid-Containing Insecticide Disruption of Growth, Locomotion, and Fertility in *Caenorhabditis E. PLoS One* 15, e0238637. doi:10.1371/journal.pone.0238637

Brenner, S. (1974). The Genetics of *Caenorhabditis Elegans*. *Genetics* 77, 71–94. doi:10.1093/genetics/77.1.71

Cordova, D., Benner, E. A., Sacher, M. D., Rauh, J. J., Sopa, J. S., Lahm, G. P., et al. (2006). Anthranilic Diamides: A New Class of Insecticides with a Novel Mode of Action, Ryanodine Receptor Activation. *Pestic. Biochem. Physiol.* 84, 196–214. doi:10.1016/j.pestbp.2005.07.005

Corsi, A. K., Wightman, B., and Chalfie, M. (2015). A Transparent Window into Biology: A Primer on *Caenorhabditis Elegans*. *Genetics* 200, 387–407. doi:10.1534/genetics.115.176099

Du, H., Wang, M., Wang, L., Dai, H., Wang, M., Hong, W., et al. (2015). Reproductive Toxicity of Endosulfan: Implication from Germ Cell Apoptosis Modulated by Mitochondrial Dysfunction and Genotoxic Response Genes in *Caenorhabditis Elegans*. *Toxicol. Sci.* 145, 118–127. doi:10.1093/toxsci/kfv035

Faria, M., Wu, X., Luja-Mondragón, M., Prats, E., Gómez-Oliván, L. M., Piña, B., et al. (2020). Screening Anti-predator Behaviour in Fish Larvae Exposed to Environmental Pollutants. *Sci. Total Environ.* 714, 136759. doi:10.1016/j.scitotenv.2020.136759

Gomez-Eyles, J. L., Svendsen, C., Lister, L., Martin, H., Hodson, M. E., and Spurgeon, D. J. (2009). Measuring and Modelling Mixture Toxicity of Imidacloprid and Thiacloprid on *Caenorhabditis Elegans* and *Eisenia F. Ecotoxicology Environ. Saf.* 72, 71–79. doi:10.1016/j.ecoenv.2008.07.006

Griffin, E. F., Caldwell, K. A., and Caldwell, G. A. (2017). Genetic and Pharmacological Discovery for Alzheimer's Disease Using *Caenorhabditis E. ACS Chem. Neurosci.* 8, 2596–2606. doi:10.1021/acschemneuro.7b00361

Guo, L., Li, C., Liang, P., and Chu, D. (2019). Cloning and Functional Analysis of Two Ca^{2+}-Binding Proteins (CaBPs) in Response to Cyantraniliprole Exposure in Bemisia Tabaci (Hemiptera: Aleyrodidae). *J. Agric. Food Chem.* 67, 11035–11043. doi:10.1021/acs.jafc.9b04028

Haegerbaeumer, A., Höss, S., Heininger, P., and Traunspurger, W. (2018). Is *Caenorhabditis Elegans* Representative of Freshwater Nematode Species in Toxicity Testing? *Environ. Sci. Pollut. Res.* 25, 2879–2888. doi:10.1007/s11356-017-0714-7

Han, Y., Song, S., Wu, H., Zhang, J., and Ma, E. (2017). Antioxidant Enzymes and Their Role in Phoxim and Carbaryl Stress in *Caenorhabditis E. Pestic. Biochem. Physiol.* 138, 43–50. doi:10.1016/j.pestbp.2017.02.005

Kudelska, M. M., Holden-Dye, L., O'Connor, V., and Doyle, D. A. (2017). Concentration-dependent Effects of Acute and Chronic Neonicotinoid Exposure on the Behaviour and Development of the nematodeCaenorhabditis Elegans. *Pest Manag. Sci.* 73, 1345–1351. doi:10.1002/ps.4564

Leung, M. C. K., Williams, P. L., Benedetto, A., Au, C., Helmcke, K. J., Aschner, M., et al. (2008). *Caenorhabditis Elegans*: An Emerging Model in Biomedical and Environmental Toxicology. *Toxicol. Sci.* 106, 5–28. doi:10.1093/toxsci/kfn121

Li, Y.-X., Wang, Y., Hu, Y.-O., Zhong, J.-X., and Wang, D.-Y. (2011). Modulation of the Assay System for the Sensory Integration of 2 Sensory Stimuli that Inhibit Each Other in Nematode *Caenorhabditis Elegans*. *Neurosci. Bull.* 27, 69–82. doi:10.1007/s12264-011-1152-z

Li, Y., Yu, S., Wu, Q., Tang, M., Pu, Y., and Wang, D. (2012). Chronic Al2O3-Nanoparticle Exposure Causes Neurotoxic Effects on Locomotion Behaviors by Inducing Severe ROS Production and Disruption of ROS Defense Mechanisms in Nematode *Caenorhabditis E. J. Hazard. Mater.* 219-220, 221–230. doi:10.1016/j.jhazmat.2012.03.083

Liu, H., Tian, L., Wang, S., and Wang, D. (2021a). Size-Dependent Transgenerational Toxicity Induced by Nanoplastics in Nematode *Caenorhabditis Elegans*. *Sci. Total Environ.* 790, 148217. doi:10.1016/j.scitotenv.2021.148217

Liu, H., Qiu, Y., and Wang, D. (2021b). Alteration in Expressions of Ion Channels in *Caenorhabditis Elegans* Exposed to Polystyrene Nanoparticles. *Chemosphere* 273, 129686. doi:10.1016/j.chemosphere.2021.129686

Liu, H., Zhao, Y., Bi, K., Rui, Q., and Wang, D. (2021c). Dysregulated *Mir-76* Mediated a Protective Response to Nanopolystyrene by Modulating Heme Homeostasis Related Molecular Signaling in Nematode *Caenorhabditis Elegans*. *Ecotoxicology Environ. Saf.* 212, 112018. doi:10.1016/j.ecoenv.2021.112018

Matsuda, K., Shimomura, M., Ihara, M., Akamatsu, M., and Sattelle, D. B. (2005). Neonicotinoids Show Selective and Diverse Actions on Their Nicotinic Receptor Targets: Electrophysiology, Molecular Biology, and Receptor Modeling Studies. *Biosci. Biotechnol. Biochem.* 69, 1442–1452. doi:10.1271/bbb.69.1442

Metaxakis, A., Petratou, D., and Tavernarakis, N. (2018). Multimodal Sensory Processing in *Caenorhabditis Elegans*. *Open Biol.* 8, 180049. doi:10.1098/rsob.180049

Moy, T. I., Conery, A. L., Larkins-Ford, J., Wu, G., Mazitschek, R., Casadei, G., et al. (2009). High-Throughput Screen for Novel Antimicrobials Using a Whole Animal Infection Model. *ACS Chem. Biol.* 4, 527–533. doi:10.1021/cb900084v

Qi, S., Wang, D., Zhu, L., Teng, M., Wang, C., Xue, X., et al. (2018). Effects of a Novel Neonicotinoid Insecticide Cycloxaprid on Earthworm, *Eisenia F. Environ. Sci. Pollut. Res.* 25, 14138–14147. doi:10.1007/s11356-018-1624-z

Qu, M., and Wang, D. (2020). Toxicity Comparison between Pristine and Sulfonate Modified Nanopolystyrene Particles in Affecting Locomotion Behavior, Sensory Perception, and Neuronal Development in *Caenorhabditis Elegans*. *Sci. Total Environ.* 703, 134817. doi:10.1016/j.scitotenv.2019.134817

Queirós, L., Pereira, J. L., Gonçalves, F. J. M., Pacheco, M., Aschner, M., and Pereira, P. (2019). Caenorhabditis Elegansas a Tool for Environmental Risk Assessment: Emerging and Promising Applications for a "Nobelized Worm". *Crit. Rev. Toxicol.* 49, 411–429. doi:10.1080/10408444.2019.1626801

Raby, M., Nowierski, M., Perlov, D., Zhao, X., Hao, C., Poirier, D. G., et al. (2018). Acute Toxicity of 6 Neonicotinoid Insecticides to Freshwater Invertebrates. *Environ. Toxicol. Chem.* 37, 1430–1445. doi:10.1002/etc.4088

Rajini, P. S., Melstrom, P., and Williams, P. L. (2008). A Comparative Study on the Relationship between Various Toxicological Endpoints inCaenorhabditis elegansExposed to Organophosphorus Insecticides. *J. Toxicol. Environ. Health A* 71, 1043–1050. doi:10.1080/15287390801989002

Riddle, D. L., Blumenthal, T., Meyer, B. J., and Priess, J. R. (1997). C. E *II*. 2nd edition. Cold Spring Harbor (NY): Cold Spring Harbor Laboratory Press.

Roh, J.-Y., and Choi, J. (2011). Cyp35a2 Gene Expression Is Involved in Toxicity of Fenitrothion in the Soil Nematode *Caenorhabditis Elegans*. *Chemosphere* 84, 1356–1361. doi:10.1016/j.chemosphere.2011.05.010

Ruan, Q.-L., Ju, J.-J., Li, Y.-H., Li, X.-B., Liu, R., Liang, G.-Y., et al. (2012). Chlorpyrifos Exposure Reduces Reproductive Capacity Owing to a Damaging Effect on Gametogenesis in the Nematode *Caenorhabditis Elegans*. *J. Appl. Toxicol.* 32, 527–535. doi:10.1002/jat.1783

Saeki, S., Yamamoto, M., and Iino, Y. (2001). Plasticity of Chemotaxis Revealed by Paired Presentation of a Chemoattractant and Starvation in the Nematode *Caenorhabditis Elegans*. *J. Exp. Biol.* 204, 1757–1764. doi:10.1242/jeb.204.10.1757

Sambongi, Y., Takeda, K., Wakabayashi, T., Ueda, I., Wada, Y., and Futai, M. (2000). *Caenorhabditis E* Senses Protons through Amphid Chemosensory Neurons. *Neuroreport* 11, 2229–2232. doi:10.1097/00001756-200007140-00033

Sheets, L. P., Li, A. A., Minnema, D. J., Collier, R. H., Creek, M. R., and Peffer, R. C. (2016). A Critical Review of Neonicotinoid Insecticides for Developmental Neurotoxicity. *Crit. Rev. Toxicol.* 46, 153–190. doi:10.3109/10408444.2015.1090948

Sun, L., Li, D., Yuan, Y., and Wang, D. (2021). Intestinal Long Non-coding RNAs in Response to Simulated Microgravity Stress in *Caenorhabditis Elegans*. *Sci. Rep.* 11, 1997. doi:10.1038/s41598-021-81619-4

Takeishi, A., Takagaki, N., and Kuhara, A. (2020). Temperature Signaling Underlying Thermotaxis and Cold Tolerance in *Caenorhabditis Elegans*. *J. Neurogenet.* 34, 351–362. doi:10.1080/01677063.2020.1734001

Walker, C. H. (2003). Neurotoxic Pesticides and Behavioural Effects upon Birds. *Ecotoxicology* 12, 307–316. doi:10.1023/a:1022523331343

Wang, D., and Xing, X. (2009). Pre-Treatment with Mild Metal Exposure Suppresses the Neurotoxicity on Locomotion Behavior Induced by the Subsequent Severe Metal Exposure in *Caenorhabditis Elegans*. *Environ. Toxicol. Pharmacol.* 28, 459–464. doi:10.1016/j.etap.2009.07.008

Wang, S., Zhang, R., and Wang, D. (2021a). Induction of Protective Response to Polystyrene Nanoparticles Associated with Methylation Regulation in *Caenorhabditis Elegans*. *Chemosphere* 271, 129589. doi:10.1016/j.chemosphere.2021.129589

Wang, S., Liu, H., Qu, M., and Wang, D. (2021b). Response of Tyramine and Glutamate Related Signals to Nanoplastic Exposure in *Caenorhabditis Elegans*. *Ecotoxicology Environ. Saf.* 217, 112239. doi:10.1016/j.ecoenv.2021.112239

Wang, D. Y. (2019). *Target Organ Toxicology in* Caenorhabditis E. Singapore: Springer Nature Singapore Pte Ltd.

Wang, D. Y. (2020). *Exposure Toxicology in* Caenorhabditis E. Singapore: Springer Nature Singapore Pte Ltd.

Yang, Y., Wu, Q., and Wang, D. (2021a). Dysregulation of G Protein-Coupled Receptors in the Intestine by Nanoplastic Exposure in *Caenorhabditis E. Environ. Sci. Nano* 8, 1019–1028. doi:10.1039/d0en00991a

Yang, Y., Dong, W., Wu, Q., and Wang, D. (2021b). Induction of Protective Response Associated with Expressional Alterations in Neuronal G Protein-Coupled Receptors in Polystyrene Nanoparticle Exposed *Caenorhabditis Elegans*. *Chem. Res. Toxicol.* 34, 1308–1318. doi:10.1021/acs.chemrestox.0c00501

Ye, H.-Y., Ye, B.-P., and Wang, D.-Y. (2008). Evaluation of the Long-Term Memory for Thermosensation Regulated by Neuronal Calcium Sensor-1 in *Caenorhabditis Elegans*. *Neurosci. Bull.* 24, 1–6. doi:10.1007/s12264-008-0920-x

Yu, Y., Hua, X., Chen, H., Wang, Y. e., Li, Z., Han, Y., et al. (2020). Toxicity of Lindane Induced by Oxidative Stress and Intestinal Damage in *Caenorhabditis Elegans*. *Environ. Pollut.* 264, 114731. doi:10.1016/j.envpol.2020.114731

Yu, Y., Chen, H., Hua, X., Wang, Z., Li, L., Li, Z., et al. (2021). Long-Term Toxicity of Lindane through Oxidative Stress and Cell Apoptosis in *Caenorhabditis Elegans*. *Environ. Pollut.* 272, 116036. doi:10.1016/j.envpol.2020.116036

Zeng, R., Yu, X., Tan, X., Ye, S., and Ding, Z. (2017). Deltamethrin Affects the Expression of Voltage-Gated Calcium Channel α1 Subunits and the

Locomotion, Egg-Laying, Foraging Behavior of *Caenorhabditis E. Pestic. Biochem. Physiol.* 138, 84–90. doi:10.1016/j.pestbp.2017.03.005

Zhang, Y., Ye, B., and Wang, D. (2010). Effects of Metal Exposure on Associative Learning Behavior in Nematode *Caenorhabditis E. Arch. Environ. Contam. Toxicol.* 59, 129–136. doi:10.1007/s00244-009-9456-y

Zhang, L., Wang, S., Zhao, Y., Bi, K., and Wang, D. (2022). Increase in Germline Methyltransferases Governing the Methylation of Histone H3K9 Is Associated with Transgenerational Nanoplastic Toxicity in *Caenorhabditis E. Environ. Sci. Nano* 9, 265–274. doi:10.1039/d1en00835h

Conflict of Interest: The authors declare that the research was conducted in the absence of any commercial or financial relationships that could be construed as a potential conflict of interest.

Publisher's Note: All claims expressed in this article are solely those of the authors and do not necessarily represent those of their affiliated organizations or those of the publisher, the editors and the reviewers. Any product that may be evaluated in this article or claim that may be made by its manufacturer is not guaranteed or endorsed by the publisher.

frontiers | Frontiers in Environmental Science

ORIGINAL RESEARCH
published: 04 May 2022
doi: 10.3389/fenvs.2022.888252

Characterization of Montmorillonite–Biochar Composite and Its Application in the Removal of Atrazine in Aqueous Solution and Soil

*Pingping Wang[1], Marianne Stenrød[2], Liang Wang[3], Shankui Yuan[4], Liangang Mao[1], Lizhen Zhu[1], Lan Zhang[1], Yanning Zhang[1], Hongyun Jiang[1], Yongquan Zheng[1] and Xingang Liu[1]**

[1]State Key Laboratory for Biology of Plant Disease and Insect Pests, Institute of Plant Protection, Chinese Academy of Agricultural Sciences, Beijing, China, [2]Norwegian Institute of Bioeconomy Research (NIBIO), Høgskoleveien, Norway, [3]SINTEF Energy Research, Trondheim, Norway, [4]Environment Division, Institute for the Control of Agrochemicals, Ministry of Agriculture and Rural Affairs, Beijing, China

Atrazine is a widely used triazine herbicide, which poses a serious threat to human health and aquatic ecosystem. A montmorillonite–biochar composite (MMT/BC) was prepared for atrazine remediation. Biochar samples were characterized by using scanning electron microscope (SEM), transmission electron microscopy (TEM), Fourier transform infrared spectroscopy (FTIR), and X-ray photoelectron spectrometer (XPS). Structural and morphological analysis of raw biochar (BC) and MMT/BC showed that MMT particles have been successfully coated on the surface of biochar. Sorption experiments in aqueous solution indicated that the MMT/BC has higher removal capacity of atrazine compared to BC (about 3.2 times). The sorption of atrazine on the MMT/BC was primarily controlled by both physisorption and chemisorption mechanisms. The amendment of MMT/BC increased the sorption capacity of soils and delayed the degradation of atrazine. Findings from this work indicate that the MMT/BC composite can effectively improve the sorption capacity of atrazine in aquatic environment and farmland soil and reduce the environmental risk.

Keywords: montmorillonite–biochar composite, atrazine, sorption, degradation, soil

OPEN ACCESS

Edited by:
Oladele Ogunseitan, University of California, Irvine, United States

Reviewed by:
Kassio Ferreira Mendes, Federal University of Viçosa, Brazil
Huacheng Xu, Nanjing Institute of Geography and Limnology (CAS), China

****Correspondence:***
Xingang Liu
liuxingang@caas.cn

Specialty section:
This article was submitted to Toxicology, Pollution and the Environment, a section of the journal Frontiers in Environmental Science

Received: *02 March 2022*
Accepted: *08 April 2022*
Published: *04 May 2022*

Citation:
Wang P, Stenrød M, Wang L, Yuan S, Mao L, Zhu L, Zhang L, Zhang Y, Jiang H, Zheng Y and Liu X (2022) Characterization of Montmorillonite–Biochar Composite and Its Application in the Removal of Atrazine in Aqueous Solution and Soil. Front. Environ. Sci. 10:888252. doi: 10.3389/fenvs.2022.888252

INTRODUCTION

Atrazine, 6-chloro-N2-ethyl-N4-isopropyl-1,3,5-triazine-2,4-diamine, is a widely used triazine herbicide used for controlling annual grasses and broadleaf weeds (Solomon et al., 1996). Due to its persistence, moderate aqueous solubility (35 mg/L), high mobility, and long half-life, atrazine has a high detection rate in surface water, groundwater, and soil (Tappe et al., 2002; Qu et al., 2017; Zheng et al., 2019). In the Hubei Province of central China, atrazine was detected in the sediments of six eutrophic lakes, and the highest concentration of atrazine was found to be 0.171 mg/kg in Honghu Lake (Qu et al., 2017). Atrazine was also detected in two soils in Belgium and Germany (8.3 and 15.2 μg/kg, respectively), even in soils not treated with atrazine (Jablonowski et al., 2010). In addition, atrazine has been categorized as an endocrine disruptor and a probable human carcinogen, which may affect the central nervous system and immune systems and even affect human semen quality and fertility (Hayes et al., 2003; Swan et al., 2003; Chen et al., 2009). Atrazine has been banned

in some European countries, but it is still widely used in China. Therefore, it is necessary to develop a reliable and effective treatment to remove or sequester atrazine from aquatic environment and farmland soil to reduce the environmental and health risk of atrazine.

Biochar, a carbon-rich solid material, is produced by pyrolysis of biomass with limited or without oxygen (Novak et al., 2009). As an excellent remediation agent, biochar has been widely used in wastewater and soil to immobilize or sequester pesticides, such as herbicides and insecticides, through sorption, partition, and pore diffusion (Zheng et al., 2010; Yu et al., 2011; Li et al., 2018). Liu et al. (2015) reported that soybean biochar has much higher atrazine removal ability in aqueous solution. Jin et al. (2016) indicated that biochar would be helpful to stabilize soil contaminated with imidacloprid, isoproturon, and atrazine. Our previous research found that peanut shell biochar also had a good sorption effect on atrazine (Wang et al., 2020). Therefore, biochar can effectively reduce the environmental risk of atrazine. Many studies have shown that the degradation degree of pesticides in soil is different after adding biochar. Generally, biochar-amended soil increases sorption of pesticides and reduces bioavailability of soil to microorganisms, which reduces the biodegradation of pesticides and prolongs the half-life of pesticides (Yang et al., 2010; Yu et al., 2011; Li et al., 2017b). However, some studies have found that the organic matter of biochar can enhance the biological activity of microorganisms by providing nutrients so as to accelerate the degradation of pesticides (Fang et al., 2016; Wu et al., 2019). Singh et al. (2022) found that the addition of biochar to the soils increased the half-life of atrazine and significantly improved the recovery process of soil biological activities under atrazine stress.

Recently, the combination of biochar and clay has been widely used for pollutant removal in order to improve the structure and sorption characteristics of biochar (Zhang and Gao, 2013; Yao et al., 2014; Tang et al., 2015). Clay minerals are abundant natural resources with inexpensive, high surface area, cation exchange capacity, and structural properties. Montmorillonite (MMT) is the most commonly studied clay material, which is an irregular lamellar crystal composed of layers of one octahedral and two tetrahedral sheets (Zhu et al., 2019). The fine particles of MMT are unsuitable for water treatment, but in a composite form, biochar has a good porous structure to support MMT (Chen et al., 2017). In addition, MMT could provide exogenous metal atoms (i.e., aluminum and magnesium), which may be embedded to react with biochar, forming a high-performance biochar complex (Song et al., 2020). The composite makes full use of the good sorption capacity of biochar and MMT to become a low-cost and effective sorbent. However, research on the effect of MMT/BC on sorption and degradation of contaminants, as well as on the removal of contamination from aqueous solution and soil, was scarce.

Therefore, the aims of this study were to (1) develop a low-cost and effective MMT–biochar composite by using a simple and low-cost method, (2) assess the ability and mechanisms of atrazine removal from aqueous solutions, and (3) evaluate the effects of MMT–biochar composite on the sorption and degradation of atrazine in different soil. This study provides useful information for better evaluation of the potential of biochar–clay composite in reducing pesticide residues.

MATERIALS AND METHODS

Reagents and Chemicals

Standard atrazine (purity 99.2%) was obtained from Shenyang Research Institute of Chemical Industry (Shenyang, China). HPLC-grade acetonitrile, formic acid, and sodium azide (NaN_3) were purchased from Sigma-Aldrich (Steinheim, Germany). All analytical reagents including calcium chloride ($CaCl_2$), sodium chloride (NaCl), anhydrous magnesium sulfate ($MgSO_4$), sodium hydroxide (NaOH), and hydrochloric acid (HCl) were obtained from Sinopharm Chemical Reagent Co., Ltd (Beijing, China). MMT was purchased from Shanghai Macklin Biochemical Co., Ltd (Shanghai, China). Ultrapure water was prepared using a Milli-Q reagent water system (Bedford, MA, United States).

Biochar and Soil Preparation and Characterization

Peanut shells were collected from the Shandong Province of China, washed with tap water to remove the surface dust and soil, dried at 70°C, and then crushed by using a high-speed pulverizer and passed through an 18-mesh sieve. A stable MMT suspension was prepared by adding MMT powder to 100 ml ultrapure water and mixed with ultrasound for 30 min. Then, 20 g peanut shells were immersed in MMT suspensions, stirred by magnetic stirrer for 2 h, and dried in oven at 105°C for 12 h. The impregnated samples were placed in a quartz boat of a tubular furnace (Zhonghuan Experimental Furnace Co., Ltd., Tianjin, China), pyrolyzed in a continuous flow of N_2, heated at a rate of 5°C/min, and maintained for 1 h when the pyrolysis temperature reached 600°C. The produced biochar samples were crushed, passed through an 80-mesh sieve, stored in a brown ground glass bottle, and sealed in a dryer. In total, five types of MMT–biochar composites were prepared by changing the mass ratio of MMT to BC (i.e., 20, 25, 30, 40, and 50%), and the resulting products were designated as 20% MMT/BC, 25% MMT/BC, 30% MMT/BC, 40% MMT/BC, and 50% MMT/BC, respectively. At the same time, peanut shells were treated with the same method to prepare BC as control. Unless otherwise specified, the MMT/BC mentioned later is 25% MMT/BC. By changing the pyrolysis temperature, MMT/BC under different temperature conditions was prepared, and the pyrolysis temperature was set to 400, 500, and 600 °C, respectively.

Elemental analysis using surface structure, scanning electron microscope (SEM), Fourier transform infrared spectroscopy (FTIR), and X-ray photoelectron spectrometer (XPS) was based on our previous analysis methods (Wang et al., 2020). Transmission electron microscopy (TEM) (FEI, Thermo Fisher Scientific, United States) was used to observe the microstructure of the biochar. Zeta potential of biochar was determined using a Zetasizer Nano ZS90 (Malvern Instruments, Malvern,

United Kingdom). The pH value of the solution was measured by using a pH meter (FiveEasy Plus, Mettler Toledo, United States).

Two kinds of agricultural soil without detectable atrazine were collected from Jilin (44°23′52″N, 125°10′2″E) and Shandong provinces (36°12′43″N, 116°41′29″E) of China, denoted as S-DB and S-SD, respectively. The soils were taken at the top 10 cm and screened by using a 2 mm sieve for sorption and degradation experiments. The physicochemical properties of the S-DB showed it to be sandy loam (65.4% sand, 15.1% silt, and 19.5% clay) with pH 7.83, 41.0 g/kg organic matter, 1.15% organic carbon, and 17.2 cmol (+)/kg CEC. The S-SD also belonged to sandy loam (57.9% sand, 17.3% silt, and 24.8% clay) with pH 7.24, 29.2 g/kg organic matter, 0.39% organic carbon, and 21.4 cmol (+)/kg cation exchange capacity (CEC).

Sorption Experiments of Biochar in Aqueous Solution

To determine the effect of MMT dosage (0, 20, 25, 30, 40, and 50%) and pyrolysis temperature (400, 500, and 600°C) on the removal of atrazine, 100 mg biochar and 40 ml of 10 mg/L atrazine aqueous solution (contained 0.01 mol/L $CaCl_2$ and 200 mg/L NaN_3) were introduced into 50 ml brown sample bottles. The bottles were then sealed and shaken in the dark on a reciprocating shaker at 180 rpm and 25 ± 1°C for 72 h. The pH of the mixtures was adjusted to 7.0 ± 0.2 using 0.1 M HCl/NaOH and monitored during and after sorption. The same conditions were used to test the effects of initial pH in the range of 2–9 on MMT/BC sorption. After the experiments, the bottles were put to rest for 10 min to make the biochar samples sink into the bottom by gravity to achieve solid–liquid separation, and the supernatant was filtered using a 0.22 μm membrane filter. The filtered solutions were then stored at −20°C until analysis.

The sorption kinetic and isotherm of atrazine were carried out on BC and MMT/BC using the same conditions and procedures, as described before. The kinetic tests were conducted with an initial atrazine concentration of 10 mg/L, 150 mg of BC, or 50 mg of MMT/BC per 40 ml atrazine solution. Duplicate bottles were sampled at predetermined times (1, 2, 4, 6, 8, 10, 12, 24, 48, and 72 h) and analyzed for atrazine concentration in the solution. In the sorption isotherm experiment, 150 mg BC or 50 mg MMT/BC was mixed with 40 ml atrazine solution with the concentration of 0.25–30 mg/L for 72 h.

Under the same conditions, the solutions without biochar were set for the control test. The loss of atrazine was negligible, including hydrolysis and sorption on the bottle wall. Based on the initial and final concentration of atrazine in solution and the dosage of biochar, the sorption capacity of atrazine on biochar was calculated.

Sorption Experiments on Soil and Biochar–Soil Mixtures

The sorption isotherms of atrazine on biochar and biochar–soil mixtures were determined by three repeated batch sorption experiments under eight initial concentrations of atrazine (0.25–30 mg/L). A 5 g aliquot of soil with or without 50 mg BC or MMT/BC was weighed into a 50 ml centrifuge tube. Then, 25 ml of the background solution containing 0.01 M $CaCl_2$ and 200 mg/L NaN_3 was added. According to the initial concentration, a certain amount of atrazine stock solution was added to the centrifuge tube, the cover was tightened, and then shaken for 72 h at 180 rpm and 25 ± 1°C in the dark. At the end of the experiment, the tubes were centrifuged at 4,000 rpm for 10 min, and 1.5 ml of supernatant was filtered into the injection vial through 0.22 μm membrane filter. The filtered solutions were stored at −20°C until analysis.

Degradation Experiments

Before the degradation experiments, a part of the collected soil was pre-cultured with a moisture content of 60% of the water holding capacity in the dark incubator (25 ± 1°C) for 2 weeks, and the other part was sterilized at 121°C for 30 min in an autoclave (Lead-Tech Scientific Instruments Co., Ltd, Shanghai, China). MMT/BC was chosen to investigate the impacts on atrazine degradation in the two soils. First, an aliquot of 20 g soil (dry weight) or the biochar–soil mixture (4 g of MMT/BC) was weighed into a 500 ml glass bottle, and then 100 μL of the atrazine acetone stock solution (10,000 mg/L) was added into the bottle. The soil samples were kept for 10 min until the acetone volatilized completely and then vortexed for 5 min. Next, another 180 g soil was weighed into the bottle, vortexed for 30 min, and mixed well with the spiked soil; the final concentration of atrazine in soil was 5 mg/kg (dry weight). After that, 15 g of spiked soil was weighted into 50 ml pre-cleaned glass bottle, and the soil moisture content was adjusted with ultrapure water to 60% of the saturated soil moisture content. In the same operation, the sterilized ultrapure water containing 200 mg/L NaN_3 was added into the sterilized soil to inhibit the growth of microorganisms. The bottles were stoppered with cotton and cultured in the dark in an incubator under constant temperature (25 ± 1°C) and humidity (70%). The water content was monitored regularly during soil incubation to maintain the initial state of soil moisture. Triplicate sample bottles of each treatment were removed after predetermined incubation times (0, 1, 3, 5, 7, 14, 21, 30, 40, 60, 90, and 120 days), and the soil samples were freeze-dried and stored at −20°C until extraction. Details of the soil sample treatment are shown in **Supplementary Text S1**.

Data Analysis

Different mathematical models including first-order, second-order, and Elovich models were used to fit the kinetics data (Inyang et al., 2014; Yao et al., 2014; Liu et al., 2015):

$$\text{First} - \text{order}: \ q_t = q_e\left(1 - e^{-k_1 t}\right), \tag{1}$$

$$\text{Second} - \text{order}: \ q_t = \frac{k_2 q_e^2 t}{1 + k_2 q_e^2 t}, \tag{2}$$

$$\text{Elovich}: \ q_t = \frac{1}{\beta}\ln(\alpha\beta t + 1), \tag{3}$$

TABLE 1 | Physical and chemical characteristics of BC and MMT/BC.

Biochar	Elemental composition (%)				Atomic ratio			SA[a] (m^2/g)	PV[b] (cm^3/g)	PD[c] (nm)
	C	H	N	O	H/C	O/C	(O + N)/C			
BC	87.35	3.61	0.81	6.53	0.50	0.06	0.06	262.86	0.014	4.4438
MMT/BC	50.91	2.61	0.50	6.33	0.62	0.09	0.10	233.16	0.066	12.0242

[a]*SA, surface area determined by the BET adsorption method.*
[b]*PV, pore volume.*
[c]*PD, pore diameter.*

where q_t and q_e represent the amount of atrazine removed at time t and at equilibrium, respectively (mg/kg); k_1 and k_2 are the sorption rate constants (1/h); α represents the initial sorption rate (mg/kg); and β represents the desorption constant (kg/mg).

Three models (Freundlich, Langmuir, and dual-mode) were used to fit the isotherm experimental data (Uchimiya et al., 2010; Zhang et al., 2011; Suo et al., 2019):

$$\text{Freundlich}: \ q_e = K_f C_e^n, \tag{4}$$

$$\text{Langmuir}: \ q_e = \frac{q_m K C_e}{1 + K C_e}, \tag{5}$$

$$\text{Dual} - \text{mode}: \ q_e = \frac{bQC_e}{1 + bC_e} + K_D C_e, \tag{6}$$

where q_e represents the atrazine concentration on the solid-phase at equilibrium (mg/kg), C_e represents the solution concentration of atrazine at equilibrium (mg/L), K_f [(mg/kg)/(mg/L)^n] and K (L/mg) represent affinity coefficient, n represents the Freundlich linearity constant, b represents the affinity constant (L/mg), K_D represents the partition domain coefficient (L/kg), and q_m and Q represents the maximum capacity (mg/kg).

The first-order reaction kinetic model was used to fit the data of atrazine degradation kinetics in soil and biochar–soil mixtures (Zhang et al., 2018):

$$C_t = C_0 e^{-kt}, \tag{7}$$

where C_0 is the initial concentration of atrazine (mg/kg), C_t is the concentration of atrazine (mg/kg) at sampling time t (d), k is the degradation rate constant (d^{-1}), and the half-life ($t_{1/2}$) was ln2/k.

The experimental data were fitted by Origin 9.1. The statistical analyses were analyzed by SPSS 25.0 one-way analysis of variance (ANOVA).

RESULTS AND DISCUSSION

Characterization of Biochar

The properties of biochar varied greatly between BC and MMT/BC. The elemental composition (C, N, H, and O) of BC and MMT/BC, presented in **Table 1**, suggested that the addition of MMT reduced the content of C, N, H, and O, especially the carbon content, from 87.35% to 50.91%. The surface area of MMT/BC was slightly decreased from 262.86 to 233.16 m^2/g, which may be related to the pore coating or plugging caused by the existence of MMT minerals (Yao et al., 2014). The total pore volume and the average pore diameter of the MMT/BC were increased from 0.014 to 0.066 cm^3/g and 4.44–12.02 nm in comparison with BC. This is probably because MMT is layered silicate mineral, which contains mineral elements with small surface areas and abundant transitional pores (Li et al., 2015; Li et al., 2017a; Yao et al., 2014). The N_2 adsorption–desorption isotherms and pore size distribution of MMT/BC and BC are shown in **Supplementary Figure S1**. As described by the International Union of Pure and Applied Chemistry (IUPAC), the isotherms of BC evolved to type I, which shows the characteristic of a microporous material (Jing et al., 2014). The N_2 isotherms of MMT/BC resemble those of type II, and the observed hysteresis curves of MMT/BC is of type H4, indicating the narrow cracks and pores in the sorbent materials (Jing et al., 2014). In the pore size distribution curve (**Supplementary Figure S1B**), BC and MMT/BC exhibited heterogenous pore structures, and mesopore (2–50 nm) was the main pore structure.

The SEM images of BC and MMT/BC are shown in **Figures 1A,B**. Surface and pore filling mechanisms may be responsible for the removal of atrazine as the pores were observed on biochar surfaces. The SEM images of MMT/BC clearly showed that MMT particles adhered to the biochar surface and completely coated the pure biochar, changing the surface morphologies and providing more sorption sites (Liang et al., 2019; Premarathna et al., 2019). Also, the MMT did not block the pores of biochar, which ensures the accessible to the adsorbate molecules (Premarathna et al., 2019). TEM imaging of the MMT/BC (**Figure 1D**) showed that the biochar surface was widely covered by the layered structures compared with BC (**Figure 1C**). In addition, it is reported that the structure is a common clay structural morphology (Tyagi et al., 2006; Zhou et al., 2009).

As shown in FTIR (**Figure 2**), the spectrum at ~3,400 cm^{-1} showed stretching vibrations of O-H, ~1,580 cm^{-1} was related to stretching vibration of C=C of the aromatic ring (Chen et al., 2008; Keiluweit et al., 2010). The band observed around 1,050 cm^{-1} was related to the Si-O functional groups on the MMT/BC surface (Tyagi et al., 2006; Chen et al., 2017). The bands appearing below 800 cm^{-1} of MMT/BC could be attributed to Si-O stretching, Si-O-Mg bending, Si-O-Al bending, and Si-O-Si bending (Zhou et al., 2009; Chen et al., 2017).

Raman spectra (**Supplementary Figure S2**) showed two prominent peaks at ~1,350 cm^{-1} and ~1,600 cm^{-1}, representing D-band originated from sp^3 hybridization with disordered mode and G-band induced by crystalline

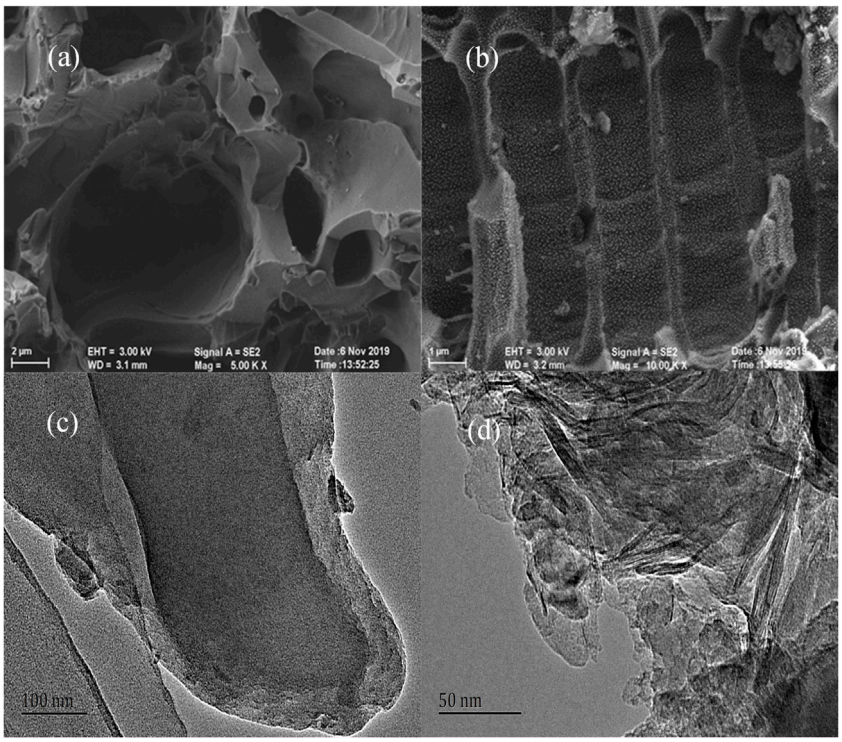

FIGURE 1 | SEM images of BC **(A)** and MMT/BC **(B)**; TEM images of BC **(C)** and MMT/BC **(D)**.

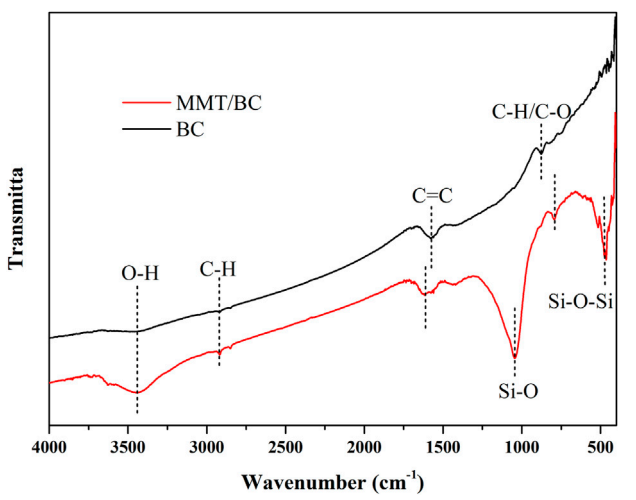

FIGURE 2 | FTIR spectra of BC and MMT/BC.

graphitic/sp^2 carbon stretching vibrations with the tangential mode, respectively (Ferrari and Robertson, 2000; Akhavan, 2010). The higher ratio of I_D/I_G peak intensity means higher defect concentration and increased functional groups on the sorbents surface. The I_D/I_G decrease from 1.04 for BC to 1.00 for MMT/BC, which was not a significant change.

Zeta potentials of MMT/BC are depicted in **Supplementary Figure S3**. In the pH range between 2 and 9, the MMT/BC resulted in a zeta potential drop of 35 mV. The MMT/BC surface was negatively charged at pH values greater than the point of zero charge pH (pH_{pzc}, 2.7) and was positively charged at pH values lower than pH_{pzc} (Nandi et al., 2009).

The full XPS spectra representing the chemical composition and crystalline states are displayed in **Figures 3A,E**. For MMT/BC, the six peaks at 285.0, 400.0, 532.6, 74.0, 103.2, and 1,304.3 eV were attributed to the element of C, N, O, Al, Si, and Mg on the surface, respectively, while there are no obvious peaks corresponds to Al, Si, and Mg on the surface of BC. The high-resolution C 1s spectra (**Figures 3B,F**) could be deconvoluted into four peaks: C-C/C-H (~284.8 eV), C-O (~286.4 eV), C=O (~288.0 eV), and O-C=O (~289.5 eV) (Gao et al., 2018; Liu et al., 2015). The O 1s spectra (**Figures 3C,G**) could be attributed into three groups: C=O (~531.6 eV), -OH (~532.5 eV), and C-O (~534.1 eV) (Lyu et al., 2017b; Zhou et al., 2007). The N 1s spectra of BC (**Figure 3D**) can be deconvoluted into two peaks at 398.7 and 400.6 eV, which can be assigned to the pyridinic N (C-N=C) and pyrrolic N (C-N). A new peak corresponding to graphitic N can be found at 402.0 eV for MMT/BC (**Figure 3H**) (Jansen and Van Bekkum, 1995; Lyu et al., 2017a; Mueller et al., 2015). **Supplementary Table S1** listed their relative percentages on BC and MMT/BC. For C 1s, the C-O ratio of biochar increased from 8.74% to 12.09% after MMT was added, and the C=O ratio increased from 4.52% to 4.98%, indicating the participation of oxygen-containing functional groups (Liang et al., 2019). For O

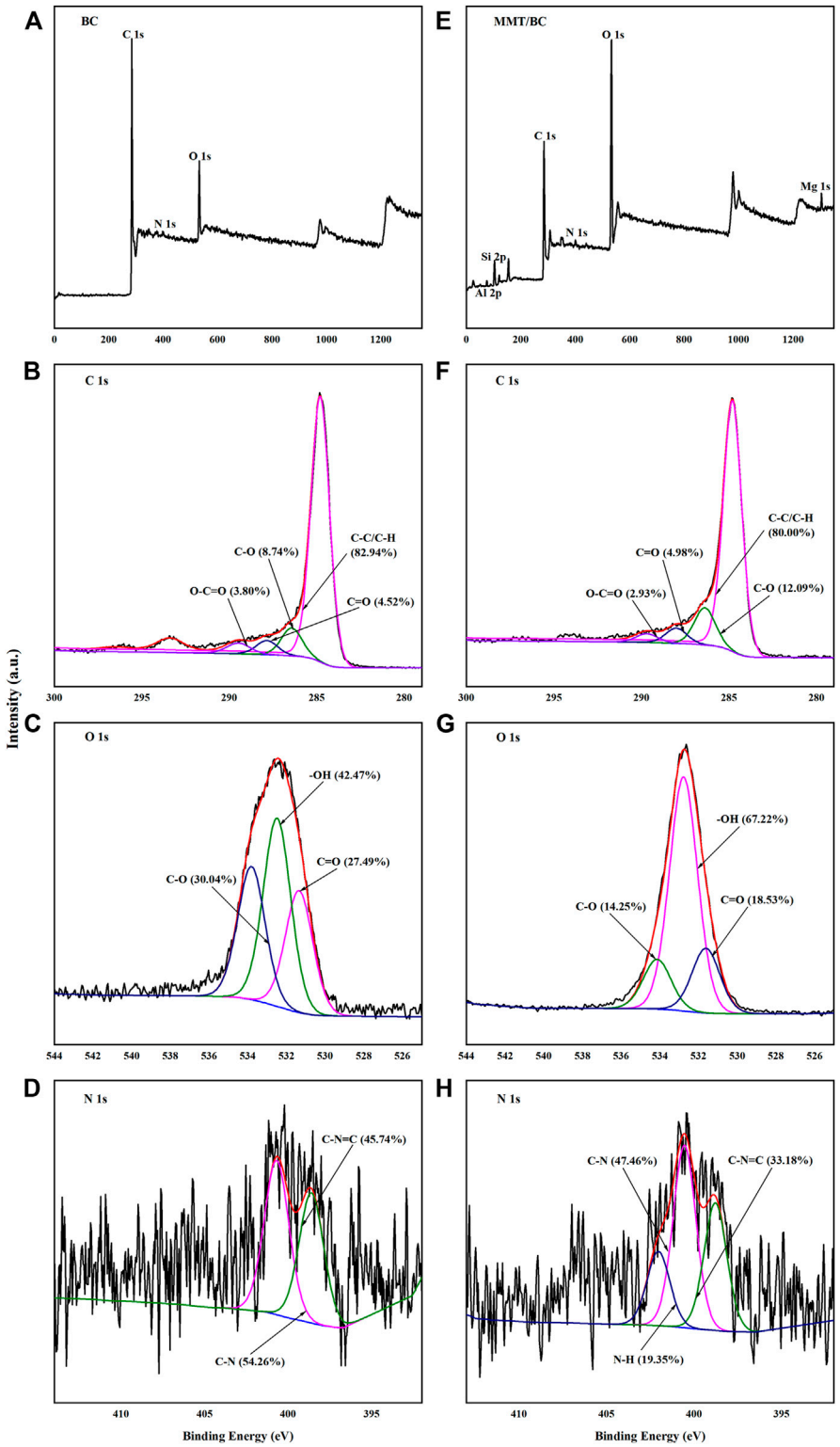

FIGURE 3 | XPS spectra of BC **(A–D)** and MMT/BC **(E–H)**. **(A,E)** Wide survey scan, **(B,F)** C 1s, **(C,G)** O 1s, **(D,H)** N 1s.

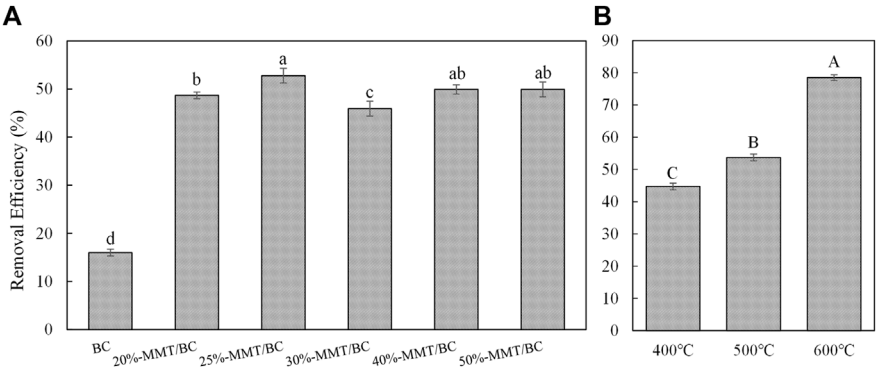

FIGURE 4 | Effects of MMT dosage during biochar preparation **(A)** and pyrolysis temperature of MMT/BC **(B)** on atrazine removal efficiency. Values with lowercase letters are different from each other ($p < 0.05$), and values with capital letters are significantly different from each other ($p < 0.01$).

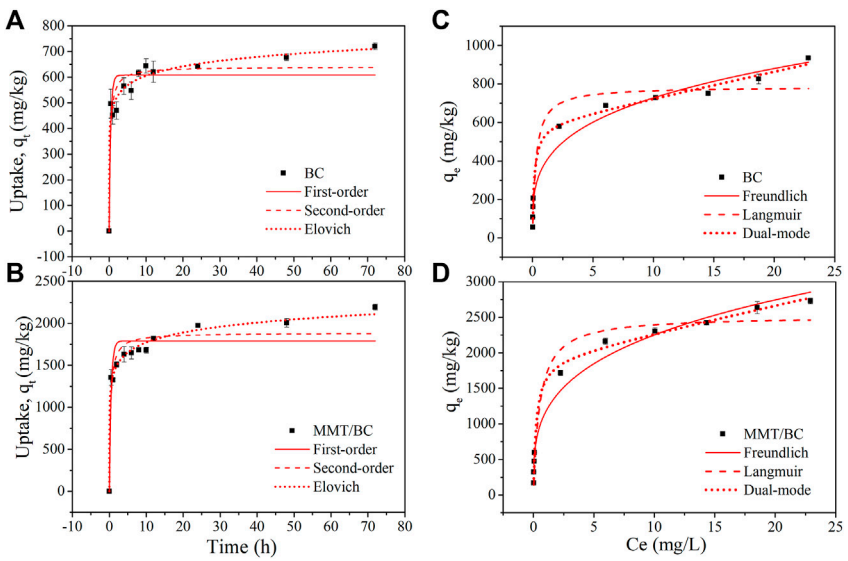

FIGURE 5 | Sorption kinetics **(A,B)** and sorption isotherms **(C,D)** of atrazine on BC and MMT/BC. Kinetic data were fitted to first-order, second-order, and Elovich models. Isotherm data were fitted to Freundlich, Langmuir, and dual-mode models. Error bars indicate SD.

1s, the -OH ratio of biochar increased from 42.47% to 67.22% after MMT was added, and the effect of MMT/BC on atrazine had hydrogen bond involvement.

Sorption of Atrazine on Biochar

Effects of MMT Dosage

The effects of MMT rate during biochar preparation on the removal efficiency of atrazine were investigated. As shown in **Figure 4A**, the removal efficiency of atrazine significantly ($p < 0.05$) increased from 16.01% (BC) to 52.78% (25% MMT/BC) with an increase of the MMT contents from 0 to 25%, suggesting a 36.77% increase. However, relatively lower removal efficiencies were obtained by other dosage (20, 30, 40, and 50%), suggesting 29.89%–33.90% increase compared to the control (BC). The surface of BC coated with MMT led to its larger pore size and volume (**Table 1**), especially the reactive surface area and CEC (Yao et al., 2014; Chen et al., 2017); therefore, the combination of MMT and biochar is particularly effective in the removal of atrazine. However, the excessive clay particles could block the pores of biochar, resulting in the decrease of available sorption sites and sorption capacity of the composite (Yao et al., 2014; Fosso-Kankeu et al., 2015). Therefore, 25% MMT was the best ratio of composite materials, and 25% MMT/BC was selected for sorption experiment and identification of sorption mechanism in aqueous solution, as well as sorption and degradation experiments in soils.

Effects of Pyrolysis Temperature

As shown in **Figure 4B**, with the increase of pyrolysis temperature, the removal efficiency of atrazine by

TABLE 2 | Fitting parameters of sorption kinetics and sorption isotherms of atrazine on BC and MMT/BC.

Sorption kinetics	Biochar	First-order			Second-order			Elovich		
		qe (mg/kg)	k1 (1/h)	R2	qe (mg/kg)	k2 (1/h)	R2	α (mg/kg)	β (kg/mg)	R2
	BC	608 ± 26	2.34 ± 0.74	0.836	641 ± 23	(5.34 ± 1.93) × 10–3	0.909	(4.71 ± 5.64) × 105	0.019 ± 0.0022	0.974
	MMT/BC	1791 ± 73	2.02 ± 0.57	0.848	1887 ± 67	(1.61 ± 0.54) × 10–3	0.914	(5.47 ± 3.61) × 105	(5.85 ± 0.42) × 10–3	0.988

Sorption isotherms	Biochar	Freundlich			Langmuir			Dual-mode			
		Kf (mg/kg)/(mg/L)n	n	R2	qm (mg/kg)	K (L/mg)	R2	b (L/mg)	Q (mg/kg)	KD (L/kg)	R2
	BC	386 ± 28	0.28 ± 0.028	0.967	786 ± 38	3.55 ± 1.49	0.940	6.46 ± 1.08	593 ± 29	13.76 ± 1.89	0.992
	MMT/BC	1,164 ± 80	0.29 ± 0.026	0.974	2,518 ± 111	1.93 ± 0.74	0.961	4.37 ± 0.55	1920 ± 66	38.20 ± 4.28	0.996

± represents the SE of the fitting parameter.

MMT–biochar composites increased from 44.72% (400°C) to 53.71% (500°C) and 78.50% (600°C). Our previous study (Wang et al., 2020) found that in the low concentration (about <15 mg/L) the sorption capacity of peanut shell biochar for atrazine increased with the increase of pyrolysis temperature. The results showed that biochar composites are also affected by pyrolysis temperature, 600°C was taken as the pyrolysis temperature of MMT/BC. This temperature was also used to prepare clay–biochar composite materials by Yao et al. (2014).

Sorption Kinetics of Atrazine on Biochar

Sorption kinetics of atrazine on BC and MMT/BC are shown in **Figures 5A,B**. The kinetics experiment data showed that the uptake of atrazine by BC and MMT/BC increased rapidly from 0 to 496.00 and 1,353.49 mg/kg in the first half hour, respectively, and increased steadily after 12 h (620.75 mg/kg for BC and 1819.39 mg/kg for MMT/BC). In order to determine the atrazine sorption equilibrium, the next experiment time was determined as 72 h.

The corresponding fitting parameters and the coefficient of determination (R^2) values are shown in **Table 2**. Compared with the first-order and second-order sorption kinetic models, the Elovich models fit the experimental data better with $R^2 >$ 0.97 (0.974 for BC and 0.988 for MMT/BC); the second was second-order (0.909 for BC and 0.914 for MMT/BC), and the worst was first-order (0.836 for BC and 0.848 for MMT/BC). The results revealed that atrazine sorption to the BC and MMT/BC was controlled by multiple mechanisms (Yao et al., 2014).

Sorption Isotherms of Atrazine on Biochar

Sorption isotherms of atrazine on BC and MMT/BC are shown in **Figures 5C,D**. All three isotherm models fit the data well, and the parameters are shown in **Table 2**. The dual-mode model has better fitting performance than Freundlich and Langmuir, with R^2 of 0.992 for BC and 0.996 for MMT/BC. The results revealed that sorption of atrazine on BC and MMT/BC was mainly partition and surface adsorption (Tang et al., 2015). Compared to BC, the Q value of atrazine on MMT/BC was increased from 592.99 to 1920.18 mg/kg. Therefore, the maximum capacity of MMT/BC on atrazine was about 3.2 times greater than that of BC. Hence, the modification method of MMT in this study could effectively improve the performance of biochar.

Effects of Solution pH

The effects of pH on atrazine sorption by MMT/BC are presented in **Supplementary Figure S4**. The sorption capacity was strongly affected by the initial pH of the aqueous solution. In brief, the uptake of atrazine decreased from 2,337.98 (pH = 2) to 1,292.89 mg/kg (pH = 9), with the increase of the pH value. It has been reported that the solution pH may change the degree of ionization of pesticide molecule, surface charge, and extent of dissociation of functional groups on the active sites of the biochar (Nandi et al., 2009). Atrazine is a weak alkaline pesticide with pKa value of 1.7, mainly exists as neutral molecule in the environment of pH 5–9, and promotes the formation of triazine cation at very low pH (Zheng et al., 2010). The MMT/BC surface was negatively charged at pH > 2.7, and it was combined with the triazine cations of atrazine by electrostatic interaction. Moreover, triazine cation could be exchanged with interlayer hydrated cations (Na^+ and Ca^{2+}) to enter the interlayer space of MMT (Premarathna et al., 2019). Therefore, the sorption capacity of MMT/BC to atrazine under low pH was high. At high pH, sorption was barely influenced by pH; this was similar to the result of Tan et al. (2016). Although, physisorption dominated, chemical sorption by chemical bonding and the increase of effective binding area caused by MMT deposition on the surface of biochar also promoted the sorption (Premarathna et al., 2019).

Sorption Mechanism Analysis

For both the BC and MMT/BC, the aromatic carbon on the surface of biochar can used as both an electron acceptor and an electron donor. The heterocyclic ring in atrazine is a π electron donor, so atrazine can interact with biochar through π-π electron donor–acceptor interactions (Sun et al., 2010; Zhao et al., 2013). Atrazine could also be used as hydrogen donors and acceptors to form hydrogen bonds with H, N, or O on the surface of biochar, further enhancing the sorption affinity of biochar. For both BC and MMT/BC, the sorption of atrazine is mainly chemical interactions, such as π–π interaction, hydrogen bonding, ion exchange, and electrostatic interactions. Due to the porosity of biochar, physical sorption may also be carried out *via* pore filling mechanism. In addition, the high surface activity and interlayer spaces of MMT improved the sorption

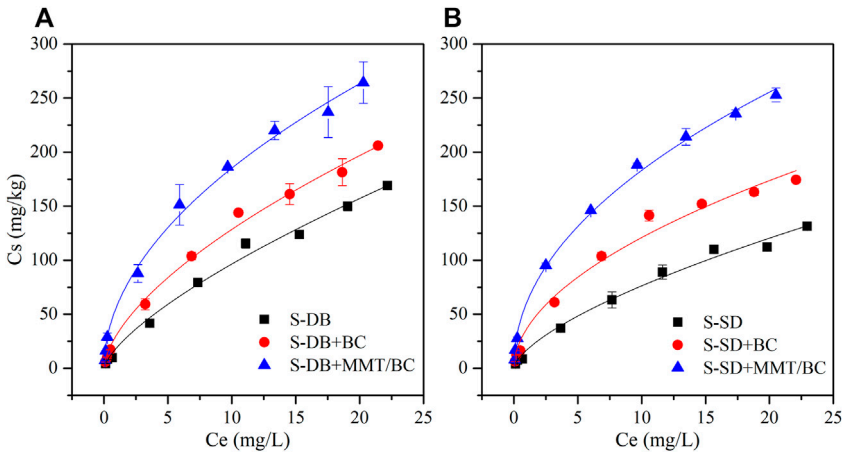

FIGURE 6 | Sorption isotherms of atrazine onto soil, BC-soil mixtures, and MMT/BC-soil mixtures [**(A)**: S-DB; **(B)**: S-SD). Isotherm data were fitted to Freundlich model.

TABLE 3 | Freundlich model of sorption isotherms of atrazine on soils and biochar–soil mixtures.

	Freundlich			K_d (L/kg)[a]		
	K_f (mg/kg)/(mg/L)^{nb}	n[c]	R^2	C_e = 0.05	C_e = 0.5	C_e = 5
S-DB	19.01 ± 2.31	0.70 ± 0.043	0.992	46.70	23.40	11.73
S-DB + BC	31.08 ± 2.62	0.62 ± 0.030	0.990	97.02	40.45	16.86
S-DB + MMT/BC	57.35 ± 3.75	0.51 ± 0.025	0.995	248.91	80.54	26.06
S-SD	16.71 ± 2.05	0.66 ± 0.043	0.991	46.27	21.15	9.67
S-SD + BC	36.32 ± 4.46	0.52 ± 0.045	0.983	152.98	50.66	16.77
S-SD + MMT/BC	60.48 ± 3.11	0.48 ± 0.019	0.996	287.18	86.73	26.19

[a]*Kd (L/kg) is the sorption coefficient estimated from the Freundlich sorption isotherms using Kd = Cs/Ce at Ce = 0.05, 0.5, and 5 mg/L.*
[b]*K_f [(mg/kg)/(mg/L)^n] is the Freundlich affinities related to sorption capacity.*
[c]*n is the isotherm nonlinearity factors of sorption.*

capacity of MMT/BC for atrazine through both surface sorption and intercalation interactions. So, MMT/BC was an effective adsorbent to remove atrazine from aqueous solution compared with BC.

Sorption of Atrazine on Soils and Biochar–Soil Mixtures

The sorption isotherms (**Figure 6**) were fitted using the Freundlich model (**Eq. 4**), and the parameters of the atrazine in two agricultural soils and biochar–soil mixtures are shown in **Table 3**. The Freundlich model can well describe the sorption data of atrazine (R^2 > 0.98). It was well documented that organic matter affects the sorption potential of soils, and higher organic matter content leads to more contaminants sorption (Fenoll et al., 2011). The organic matter contents of S-DB and S-SD were 41.0 and 29.2 g/kg, respectively, so the K_f of S-DB [19.01 (mg/kg)/(mg/L)^n] was higher than that of S-SD [16.71 (mg/kg)/(mg/L)^n]. The addition of biochar increased the sorption affinity of atrazine in soil, and the effect of MMT/BC is more obvious. For S-DB, the addition of BC increased K_f to 31.08 (mg/kg)/(mg/L)^n and the addition of MMT/BC increased to 57.35 (mg/kg)/(mg/L)^n; for S-SD, the addition of BC increased K_f to 36.32 (mg/kg)/(mg/L)^n and the addition of MMT/BC increased to 60.48 (mg/kg)/(mg/L)^n. The n values for biochar-amended soils were less than that of unamended soils, which indicated that the degree of isotherm non-linearity increased after biochar amendment, especially MMT/BC. Due to the non-linearity of the isotherms, the distribution coefficients (K_d) of three equilibrium concentrations (C_e = 0.05, 0.5, and 5 mg/L) were calculated (**Table 3**). Similar to K_f, the K_d of the soil was also increased with biochar amendment, and the K_d values of all the soils and biochar–soil mixtures decreased with increasing atrazine concentration. Previous studies have shown that water-soluble organic matters could be sorbed by biochar and compete with the added organic matter for limited sorption site or pores of biochar, thus reducing the sorption capacity of biochar (Cornelissen et al., 2005; Koelmans et al., 2009). However, organic substances may diffuse through the humic layer into biochar micropores overtime (Pignatello et al., 2006). Obviously, in the current research, atrazine may reach the micropores of biochar through the humic layer, thus improving the sorption capacity of atrazine.

Degradation of Atrazine in Soil and Biochar–Soil Mixtures

The degradation parameters of atrazine in soils and biochar–soil mixtures for 120 days under sterilized and non-sterilized conditions are shown in **Table 4**. The degradation curves of atrazine in non-

TABLE 4 | Degradation of atrazine in soils and biochar–soil mixtures during 120 days of incubation.

Soils		k (day^{-1})	R^2	$t_{1/2}$ (days)	Total removal (%)
S-DB	Unsterilized	0.024 ± 0.0022	0.9643	29.1	89.39[a]
	Sterilized	0.0020 ± 0.00046	0.6272	341.5	26.49[e]
S-DB + 2% MMT/BC	Unsterilized	0.0071 ± 0.0022	0.3765	97.8	60.54[c]
	Sterilized	0.0058 ± 0.0013	0.7554	119.7	58.05[c]
S-SD	Unsterilized	0.017 ± 0.0014	0.9650	40.5	81.69[b]
	Sterilized	0.0013 ± 0.00043	0.4087	521.2	21.10[f]
S-SD + 2% MMT/BC	Unsterilized	0.0055 ± 0.0019	0.4167	126.7	59.13[c]
	Sterilized	0.0042 ± 0.00035	0.9360	166.6	40.00[d]

Values represent the mean ± SD (n = 3). Values with the different letter (a–f) in the column indicate a statistically significant difference ($p < 0.05$).

sterilized S-DB and S-SD were fitted well with the first-order reaction kinetics model ($R^2 > 0.96$), and the half-lives were 29.1 and 40.5 days, respectively. The degradation of atrazine in S-DB was faster than that in S-SD; the main reason could be the high content of organic matter in S-DB, which can serve as an energy source to stimulate microbial activities and accelerate the degradation of pesticides (Gavrilescu, 2005; Briceño et al., 2007). However, in sterilized soils, the half-lives increased to 341.5 and 521.2 days, indicating that soil microbial was the main reason for atrazine degradation. After MMT/BC addition, the half-lives of atrazine in the non-sterilized soils increased (from 29.1 to 97.8 days for S-DB and 40.5 days to 126.7 for S-SD) and the degradation amount decreased (from 89.39% to 60.54% for S-DB and 81.69%–59.13% for S-SD). Previous studies have shown that biochar application in soil could reduce the biodegradation of pesticides (such as atrazine, acetochlor, diuron, and acetamiprid) by enhancing its sorption to the soil (Yang et al., 2006; Loganathan et al., 2009; Yu et al., 2011; Li et al., 2018) because the sorbed pesticides can only be biodegraded after being desorbed by the soil and diffused into the soil solution (Yu et al., 2011). The strong sorption of atrazine by MMT/BC made atrazine difficult to desorb, and atrazine was not easy to be degraded by microorganism; therefore, the degradation of atrazine was delayed. For sterilization treatment, the addition of MMT/BC accelerated the degradation of atrazine, indicating that biochar promoted the chemical degradation. It has been proved that biochar can also affect the chemical degradation of pesticides; Zhang et al. (2018) reported that the active groups on the biochar mineral surface played an important role in the chemical degradation of thiacloprid in biochar–soil mixtures. However, the mechanism of atrazine chemical degradation by MMT/BC remains to be further studied.

CONCLUSION

In this study, a montmorillonite–biochar composite (MMT/BC) was prepared *via* slow pyrolysis of MMT pretreated peanut shells for atrazine remediation. Structure and morphology analysis of raw biochar (BC) and MMT/BC showed that MMT particles have been successfully coated on the surface of biochar. However, excessive MMT particles will reduce the sorption capacity of biochar; 25% MMT was the best ratio of composite materials. MMT/BC was also affected by pyrolysis temperature; the higher the temperature (600°C), the better the sorption effect. Sorption experiments indicated that MMT/BC has higher removal capacity of atrazine than that of BC. The sorption of atrazine to MMT/BC was depended on pore-filling, π–π interaction, hydrogen bonding, ion exchange, and electrostatic interactions, and the high surface activity and interlayer spaces of MMT also improved the sorption capacity of MMT/BC through both surface sorption and intercalation interactions. In addition, the amendment of MMT/BC in soil improved the sorption capacity and delayed the degradation of atrazine. The results showed that MMT-modified biochar was a promising soil amendment to control atrazine contamination. According to the sorption and degradation mechanism of biochar and soil properties, it provided a basis for the selection of an effective biochar sorbent.

DATA AVAILABILITY STATEMENT

The original contributions presented in the study are included in the article/**Supplementary Material**, further inquiries can be directed to the corresponding author.

AUTHOR CONTRIBUTIONS

PW: conceptualization, methodology, data curation, formal analysis, investigation, validation, and writing—original draft. MS, LW, SY, LM, LZZ, LZ, YZ, and HJ: supervision. YZ: conceptualization, resources, supervision, and project administration. XL: supervision. resources, project administration, writing—review and editing, and funding acquisition.

FUNDING

This work was supported by the National Natural Science Foundation of China (32102269 and 31861133021).

SUPPLEMENTARY MATERIAL

The Supplementary Material for this article can be found online at: https://www.frontiersin.org/articles/10.3389/fenvs.2022.888252/full#supplementary-material

REFERENCES

Akhavan, O. (2010). Graphene Nanomesh by ZnO Nanorod Photocatalysts. *ACS nano* 4, 4174–4180. doi:10.1021/nn1007429

Briceño, G., Palma, G., and Durán, N. (2007). Influence of Organic Amendment on the Biodegradation and Movement of Pesticides. *Crit. Rev. Environ. Sci. Technol.* 37, 233–271. doi:10.1080/10643380600987406

Chen, B., Zhou, D., and Zhu, L. (2008). Transitional Adsorption and Partition of Nonpolar and Polar Aromatic Contaminants by Biochars of pine needles with Different Pyrolytic Temperatures. *Environ. Sci. Technol.* 42, 5137–5143. doi:10.1021/es8002684

Chen, C., Yang, S., Guo, Y., Sun, C., Gu, C., and Xu, B. (2009). Photolytic Destruction of Endocrine Disruptor Atrazine in Aqueous Solution under UV Irradiation: Products and Pathways. *J. Hazard. Mater.* 172, 675–684. doi:10.1016/j.jhazmat.2009.07.050

Chen, L., Chen, X. L., Zhou, C. H., Yang, H. M., Ji, S. F., Tong, D. S., et al. (2017). Environmental-friendly Montmorillonite-Biochar Composites: Facile Production and Tunable Adsorption-Release of Ammonium and Phosphate. *J. Clean. Prod.* 156, 648–659. doi:10.1016/j.jclepro.2017.04.050

Cornelissen, G., Gustafsson, Ö., Bucheli, T. D., Jonker, M. T. O., Koelmans, A. A., and Van Noort, P. C. M. (2005). Extensive Sorption of Organic Compounds to Black Carbon, Coal, and Kerogen in Sediments and Soils: Mechanisms and Consequences for Distribution, Bioaccumulation, and Biodegradation. *Environ. Sci. Technol.* 39, 6881–6895. doi:10.1021/es050191b

Fang, W., Wang, Q., Han, D., Liu, P., Huang, B., Yan, D., et al. (2016). The Effects and Mode of Action of Biochar on the Degradation of Methyl Isothiocyanate in Soil. *Sci. Total Environ.* 565, 339–345. doi:10.1016/j.scitotenv.2016.04.166

Fenoll, J., Ruiz, E., Flores, P., Hellín, P., and Navarro, S. (2011). Reduction of the Movement and Persistence of Pesticides in Soil through Common Agronomic Practices. *Chemosphere* 85, 1375–1382. doi:10.1016/j.chemosphere.2011.07.063

Ferrari, A. C., and Robertson, J. (2000). Interpretation of Raman Spectra of Disordered and Amorphous Carbon. *Phys. Rev. B* 61, 14095–14107. doi:10.1103/PhysRevB.61.14095

Fosso-Kankeu, E., Waanders, F. B., and Steyn, F. W. (2015). "The Preparation and Characterization of clay-biochar Composites for the Removal of Metal Pollutants," in 7th International Conference on latest Trends in Engineering and Technology (ICLTET'2015), Irene Pretoria South Africa, 54–57.

Gao, X., Wu, L., Li, Z., Xu, Q., Tian, W., and Wang, R. (2018). Preparation and Characterization of High Surface Area Activated Carbon from pine wood Sawdust by Fast Activation with H3PO4 in a Spouted Bed. *J. Mater. Cycles Waste Manag.* 20, 925–936. doi:10.1007/s10163-017-0653-x

Gavrilescu, M. (2005). Fate of Pesticides in the Environment and its Bioremediation. *Eng. Life Sci.* 5, 497–526. doi:10.1002/elsc.200520098

Hayes, T., Haston, K., Tsui, M., Hoang, A., Haeffele, C., and Vonk, A. (2003). Atrazine-induced Hermaphroditism at 0.1 Ppb in American Leopard Frogs (Rana pipiens): Laboratory and Field Evidence. *Environ. Health Perspect.* 111, 568–575. doi:10.1289/ehp.5932

Inyang, M., Gao, B., Zimmerman, A., Zhang, M., and Chen, H. (2014). Synthesis, Characterization, and Dye Sorption Ability of Carbon Nanotube-Biochar Nanocomposites. *Chem. Eng. J.* 236, 39–46. doi:10.1016/j.cej.2013.09.074

Jablonowski, N. D., Hamacher, G., Martinazzo, R., Langen, U., Köppchen, S., Hofmann, D., et al. (2010). Metabolism and Persistence of Atrazine in Several Field Soils with Different Atrazine Application Histories. *J. Agric. Food Chem.* 58, 12869–12877. doi:10.1021/jf103577j

Jansen, R. J. J., and Van Bekkum, H. (1995). XPS of Nitrogen-Containing Functional Groups on Activated Carbon. *Carbon* 33, 1021–1027. doi:10.1016/0008-6223(95)00030-H

Jin, J., Kang, M., Sun, K., Pan, Z., Wu, F., and Xing, B. (2016). Properties of Biochar-Amended Soils and Their Sorption of Imidacloprid, Isoproturon, and Atrazine. *Sci. Total Environ.* 550, 504–513. doi:10.1016/j.scitotenv.2016.01.117

Jing, X.-R., Wang, Y.-Y., Liu, W.-J., Wang, Y.-K., and Jiang, H. (2014). Enhanced Adsorption Performance of Tetracycline in Aqueous Solutions by Methanol-Modified Biochar. *Chem. Eng. J.* 248, 168–174. doi:10.1016/j.cej.2014.03.006

Keiluweit, M., Nico, P. S., Johnson, M. G., and Kleber, M. (2010). Dynamic Molecular Structure of Plant Biomass-Derived Black Carbon (Biochar). *Environ. Sci. Technol.* 44, 1247–1253. doi:10.1021/es9031419

Koelmans, A. A., Meulman, B., Meijer, T., and Jonker, M. T. O. (2009). Attenuation of Polychlorinated Biphenyl Sorption to Charcoal by Humic Acids. *Environ. Sci. Technol.* 43, 736–742. doi:10.1021/es802862b

Li, J., Li, S., Dong, H., Yang, S., Li, Y., and Zhong, J. (2015). Role of Alumina and Montmorillonite in Changing the Sorption of Herbicides to Biochars. *J. Agric. Food Chem.* 63, 5740–5746. doi:10.1021/acs.jafc.5b01654

Li, Y., Liu, X., Wu, X., Dong, F., Xu, J., Pan, X., et al. (2018). Effects of Biochars on the Fate of Acetochlor in Soil and on its Uptake in maize Seedling. *Environ. Pollut.* 241, 710–719. doi:10.1016/j.envpol.2018.05.079

Li, Y., Wang, Z., Xie, X., Zhu, J., Li, R., and Qin, T. (2017a). Removal of Norfloxacin from Aqueous Solution by clay-biochar Composite Prepared from Potato Stem and Natural Attapulgite. *Colloids Surf. A: Physicochemical Eng. Aspects* 514, 126–136. doi:10.1016/j.colsurfa.2016.11.064

Li, Y., Zhu, Y., Liu, X., Wu, X., Dong, F., Xu, J., et al. (2017b). Bioavailability Assessment of Thiacloprid in Soil as Affected by Biochar. *Chemosphere* 171, 185–191. doi:10.1016/j.chemosphere.2016.12.071

Liang, G., Wang, Z., Yang, X., Qin, T., Xie, X., Zhao, J., et al. (2019). Efficient Removal of Oxytetracycline from Aqueous Solution Using Magnetic Montmorillonite-Biochar Composite Prepared by One Step Pyrolysis. *Sci. Total Environ.* 695, 133800. doi:10.1016/j.scitotenv.2019.133800

Liu, N., Charrua, A. B., Weng, C.-H., Yuan, X., and Ding, F. (2015). Characterization of Biochars Derived from Agriculture Wastes and Their Adsorptive Removal of Atrazine from Aqueous Solution: A Comparative Study. *Bioresour. Technology* 198, 55–62. doi:10.1016/j.biortech.2015.08.129

Loganathan, V. A., Feng, Y., Sheng, G. D., and Clement, T. P. (2009). Crop-Residue-Derived Char Influences Sorption, Desorption and Bioavailability of Atrazine in Soils. *Soil Sci. Soc. Am. J.* 73, 967–974. doi:10.2136/sssaj2008.0208

Lyu, H., Gao, B., He, F., Ding, C., Tang, J., and Crittenden, J. C. (2017a). Ball-milled Carbon Nanomaterials for Energy and Environmental Applications. *ACS Sustainable Chem. Eng.* 5, 9568–9585. doi:10.1021/acssuschemeng.7b02170

Lyu, H., Tang, J., Huang, Y., Gai, L., Zeng, E. Y., Liber, K., et al. (2017b). Removal of Hexavalent Chromium from Aqueous Solutions by a Novel Biochar Supported Nanoscale Iron Sulfide Composite. *Chem. Eng. J.* 322, 516–524. doi:10.1016/j.cej.2017.04.058

Mueller, A., Schwab, M. G., Encinas, N., Vollmer, D., Sachdev, H., and Müllen, K. (2015). Generation of Nitrile Groups on Graphites in a Nitrogen RF-Plasma Discharge. *Carbon* 84, 426–433. doi:10.1016/j.carbon.2014.11.054

Nandi, B. K., Goswami, A., and Purkait, M. K. (2009). Adsorption Characteristics of Brilliant green Dye on Kaolin. *J. Hazard. Mater.* 161, 387–395. doi:10.1016/j.jhazmat.2008.03.110

Novak, J. M., Lima, I., Xing, B. S., Gaskin, J. W., Steiner, C., Das, K. C., et al. (2009). Characterization of Designer Biochar Produced at Different Temperatures and Their Effects on a Loamy Sand. *Ann. Environ. Sci.* 3, 195–206.

Pignatello, J. J., Kwon, S., and Lu, Y. (2006). Effect of Natural Organic Substances on the Surface and Adsorptive Properties of Environmental Black Carbon (Char): Attenuation of Surface Activity by Humic and Fulvic Acids. *Environ. Sci. Technol.* 40, 7757–7763. doi:10.1021/es061307m

Premarathna, K. S. D., Rajapaksha, A. U., Adassoriya, N., Sarkar, B., Sirimuthu, N. M. S., Cooray, A., et al. (2019). Clay-biochar Composites for Sorptive Removal of Tetracycline Antibiotic in Aqueous media. *J. Environ. Manag.* 238, 315–322. doi:10.1016/j.jenvman.2019.02.069

Qu, M., Li, H., Li, N., Liu, G., Zhao, J., Hua, Y., et al. (2017). Distribution of Atrazine and its Phytoremediation by Submerged Macrophytes in lake Sediments. *Chemosphere* 168, 1515–1522. doi:10.1016/j.chemosphere.2016.11.164

Singh, R. P., Ahsan, M., Mishra, D., Pandey, V., AnupamaYadav, A., Yadav, A., et al. (2022). Ameliorative Effects of Biochar on Persistency, Dissipation, and Toxicity of Atrazine in Three Contrasting Soils. *J. Environ. Manage.* 303, 114146. doi:10.1016/j.jenvman.2021.114146

Solomon, K. R., Baker, D. B., Richards, R. P., Dixon, K. R., Klaine, S. J., La Point, T. W., et al. (1996). Ecological Risk Assessment of Atrazine in North American Surface Waters. *Environ. Toxicol. Chem.* 15, 31–76. doi:10.1002/etc.205010.1002/etc.5620150105

Song, J., Zhang, S., Li, G., Du, Q., and Yang, F. (2020). Preparation of Montmorillonite Modified Biochar with Various Temperatures and Their Mechanism for Zn Ion Removal. *J. Hazard. Mater.* 391, 121692. doi:10.1016/j.jhazmat.2019.121692

Sun, K., Gao, B., Zhang, Z., Zhang, G., Zhao, Y., and Xing, B. (2010). Sorption of Atrazine and Phenanthrene by Organic Matter Fractions in Soil and Sediment. *Environ. Pollut.* 158, 3520–3526. doi:10.1016/j.envpol.2010.08.022

Suo, F., You, X., Ma, Y., and Li, Y. (2019). Rapid Removal of Triazine Pesticides by P Doped Biochar and the Adsorption Mechanism. *Chemosphere* 235, 918–925. doi:10.1016/j.chemosphere.2019.06.158

Swan, S. H., Kruse, R. L., Liu, F., Barr, D. B., Drobnis, E. Z., Redmon, J. B., et al. (2003). Study Future Families Res, GSemen Quality in Relation to Biomarkers of Pesticide Exposure. *Environ. Health Perspect.* 111, 1478–1484. doi:10.1289/ehp.6417

Tan, G., Sun, W., Xu, Y., Wang, H., and Xu, N. (2016). Sorption of Mercury (II) and Atrazine by Biochar, Modified Biochars and Biochar Based Activated Carbon in Aqueous Solution. *Bioresour. Technol.* 211, 727–735. doi:10.1016/j.biortech.2016.03.147

Tang, J., Lv, H., Gong, Y., and Huang, Y. (2015). Preparation and Characterization of a Novel Graphene/biochar Composite for Aqueous Phenanthrene and Mercury Removal. *Bioresour. Technology* 196, 355–363. doi:10.1016/j.biortech.2015.07.047

Tappe, W., Groeneweg, J., and Jantsch, B. (2002). Diffuse Atrazine Pollution in German Aquifers. *Biodegradation* 13, 3–10. doi:10.1023/a:1016325527709

Tyagi, B., Chudasama, C. D., and Jasra, R. V. (2006). Determination of Structural Modification in Acid Activated Montmorillonite clay by FT-IR Spectroscopy. *Spectrochimica Acta A: Mol. Biomol. Spectrosc.* 64, 273–278. doi:10.1016/j.saa.2005.07.018

Uchimiya, M., Wartelle, L. H., Lima, I. M., and Klasson, K. T. (2010). Sorption of Deisopropylatrazine on Broiler Litter Biochars. *J. Agric. Food Chem.* 58, 12350–12356. doi:10.1021/jf102152q

Wang, P., Liu, X., Yu, B., Wu, X., Xu, J., Dong, F., et al. (2020). Characterization of Peanut-Shell Biochar and the Mechanisms Underlying its Sorption for Atrazine and Nicosulfuron in Aqueous Solution. *Sci. Total Environ.* 702, 134767. doi:10.1016/j.scitotenv.2019.134767

Wu, C., Liu, X., Wu, X., Dong, F., Xu, J., and Zheng, Y. (2019). Sorption, Degradation and Bioavailability of Oxyfluorfen in Biochar-Amended Soils. *Sci. Total Environ.* 658, 87–94. doi:10.1016/j.scitotenv.2018.12.059

Yang, X.-B., Ying, G.-G., Peng, P.-A., Wang, L., Zhao, J.-L., Zhang, L.-J., et al. (2010). Influence of Biochars on Plant Uptake and Dissipation of Two Pesticides in an Agricultural Soil. *J. Agric. Food Chem.* 58, 7915–7921. doi:10.1021/jf1011352

Yang, Y., Sheng, G., and Huang, M. (2006). Bioavailability of Diuron in Soil Containing Wheat-Straw-Derived Char. *Sci. Total Environ.* 354, 170–178. doi:10.1016/j.scitotenv.2005.01.026

Yao, Y., Gao, B., Fang, J., Zhang, M., Chen, H., Zhou, Y., et al. (2014). Characterization and Environmental Applications of clay-biochar Composites. *Chem. Eng. J.* 242, 136–143. doi:10.1016/j.cej.2013.12.062

Yu, X.-Y., Mu, C.-L., Gu, C., Liu, C., and Liu, X.-J. (2011). Impact of Woodchip Biochar Amendment on the Sorption and Dissipation of Pesticide Acetamiprid in Agricultural Soils. *Chemosphere* 85, 1284–1289. doi:10.1016/j.chemosphere.2011.07.031

Zhang, G., Zhang, Q., Sun, K., Liu, X., Zheng, W., and Zhao, Y. (2011). Sorption of Simazine to Corn Straw Biochars Prepared at Different Pyrolytic Temperatures. *Environ. Pollut.* 159, 2594–2601. doi:10.1016/j.envpol.2011.06.012

Zhang, M., and Gao, B. (2013). Removal of Arsenic, Methylene Blue, and Phosphate by biochar/AlOOH Nanocomposite. *Chem. Eng. J.* 226, 286–292. doi:10.1016/j.cej.2013.04.077

Zhang, P., Sun, H., Min, L., and Ren, C. (2018). Biochars Change the Sorption and Degradation of Thiacloprid in Soil: Insights into Chemical and Biological Mechanisms. *Environ. Pollut.* 236, 158–167. doi:10.1016/j.envpol.2018.01.030

Zhao, X., Ouyang, W., Hao, F., Lin, C., Wang, F., Han, S., et al. (2013). Properties Comparison of Biochars from Corn Straw with Different Pretreatment and Sorption Behaviour of Atrazine. *Bioresour. Technology* 147, 338–344. doi:10.1016/j.biortech.2013.08.042

Zheng, H., Bao, J., Huang, Y., Xiang, L., Faheem, B., Ren, B., et al. (2019). Efficient Degradation of Atrazine with Porous Sulfurized Fe2O3 as Catalyst for Peroxymonosulfate Activation. *Appl. Catal. B: Environ.* 259, 118056. doi:10.1016/j.apcatb.2019.118056

Zheng, W., Guo, M., Chow, T., Bennett, D. N., and Rajagopalan, N. (2010). Sorption Properties of Greenwaste Biochar for Two Triazine Pesticides. *J. Hazard. Mater.* 181, 121–126. doi:10.1016/j.jhazmat.2010.04.103

Zhou, J.-H., Sui, Z.-J., Zhu, J., Li, P., Chen, D., Dai, Y.-C., et al. (2007). Characterization of Surface Oxygen Complexes on Carbon Nanofibers by TPD, XPS and FT-IR. *Carbon* 45, 785–796. doi:10.1016/j.carbon.2006.11.019

Zhou, L., Chen, H., Jiang, X., Lu, F., Zhou, Y., Yin, W., et al. (2009). Modification of Montmorillonite Surfaces Using a Novel Class of Cationic Gemini Surfactants. *J. Colloid Interf. Sci.* 332, 16–21. doi:10.1016/j.jcis.2008.12.051

Zhu, L., Yang, H., Zhao, Y., Kang, K., Liu, Y., He, P., et al. (2019). Biochar Combined with Montmorillonite Amendments Increase Bioavailable Organic Nitrogen and Reduce Nitrogen Loss during Composting. *Bioresour. Technol.* 294, 122224. doi:10.1016/j.biortech.2019.122224

Conflict of Interest: The authors declare that the research was conducted in the absence of any commercial or financial relationships that could be construed as a potential conflict of interest.

frontiers | Frontiers in Environmental Science

ORIGINAL RESEARCH
published: 10 May 2022
doi: 10.3389/fenvs.2022.853033

The Disappearance Behavior, Residue Distribution, and Risk Assessment of Kresoxim-Methyl in Banana (*Musa nana* Lour.) Based on a Modified QuEChERS Procedure Using HPLC-MS/MS

Siwei Wang, Haibin Sun, Yanping Liu*, Xiaonan Wang and Hong Chang*

Plant Protection Research Institute Guangdong Academy of Agricultural Sciences, Provincial Key Laboratory of High Technology for Plant Protection, Guangzhou, China

OPEN ACCESS

Edited by:
Liangang Mao,
Institute of Plant Protection, Chinese (CAAS), China

Reviewed by:
Bining Jiao,
Southwest University, China
Yiqiang Li,
Tobacco Research Institute (CAAS), China

***Correspondence:**
Haibin Sun
sunhb@gdppri.cn
Yanping Liu
liuliuyp@tom.com

Specialty section:
This article was submitted to Toxicology, Pollution and the Environment, a section of the journal Frontiers in Environmental Science

Received: *12 January 2022*
Accepted: *22 February 2022*
Published: *10 May 2022*

Citation:
Wang S, Sun H, Liu Y, Wang X and Chang H (2022) The Disappearance Behavior, Residue Distribution, and Risk Assessment of Kresoxim-Methyl in Banana (Musa nana Lour.) Based on a Modified QuEChERS Procedure Using HPLC-MS/MS. Front. Environ. Sci. 10:853033. doi: 10.3389/fenvs.2022.853033

A modified-QuEChERS method to determine kresoxim-methyl in banana and soil was developed and validated *via* high-performance liquid chromatography–tandem mass spectrometry (HPLC-MS/MS). The dissipation behavior, residue distribution, and risk assessment of kresoxim-methyl in banana were further investigated based on this method. The dissipation behavior of kresoxim-methyl in banana and soil was described by using first-order kinetics and its half-life, 4.8–5.7 days and 5.5–6.5 days, respectively. The concentrations of kresoxim-methyl were 0.03–0.08 mg kg^{-1}, 0.06–0.17 mg kg^{-1}, and <0.01 mg kg^{-1} for a whole banana, peel, and pulp, respectively, on the basis of spraying three times the recommended dosage and pre-harvest interval (PHI, 42 days). The results showed that the risk quotient of kresoxim-methyl in banana to people exhibited an acceptable low dietary risk. This current study could help in guiding the scientific and proper usage of this formulation.

Keywords: kresoxim-methyl, banana and soil, dissipation behavior, residue distribution, risk assessment

INTRODUCTION

Banana is one of the most popular fruits worldwide. It has high nutritional content such as dietary fibers, mineral, vitamins, and phenolic compounds (Facundo et al., 2015; Pereira and Maraschin, 2015; Vu et al., 2018). It has been reported that banana contains bioactive compounds that contribute to physiological defense against oxidative and free-radical-mediated reactions in the biological system (Singh et al., 2016). Hence, banana has great antioxidant potentials. However, diseases are among the most important factors in banana production. Black Sigatoka, which is known for its widespread destruction, could cause significant reductions in leaf area, with yield losses of more than 50% (Castelan et al., 2013; Cook et al., 2013). At present, the use of chemicals remains the main method for plant disease management. Strobilurin fungicides are widely used for disease control in most fruits due to their high efficiency, low toxicity, and broad spectrum.

Kresoxim-methyl (**Figure 1**) was released by BASF in 1992, which belonged to the first generation of strobilurins (Kolosova et al., 2017). It inhibited mitochondrial respiration by blocking electron transfer between cytochrome b and cytochrome c1, at the ubiquinol oxidizing site (Chen et al., 2015;

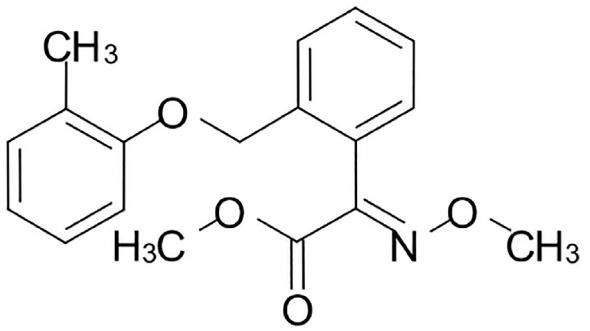

FIGURE 1 | Chemical structures of kresoxim-methyl.

Li et al., 2016; Lee et al., 2017). As a protective and curative fungicide, kresoxim-methyl shows an obvious effect in controlling black Sigatoka in banana, powdery mildew in apples, and mildew in vegetables (Reuveni et al., 2017).

Previous studies commonly used gas chromatography (GC), high-performance liquid chromatography (HPLC), and GC-mass spectrometry (MS) to determine kresoxim-methyl residues (Abreu et al., 2006; Aguilera et al., 2012; Lefrancq et al., 2013; Liang et al., 2013; Aguilera et al., 2014; Celeiro et al., 2014; Khandelwal et al., 2014; Xue et al., 2015). Few studies have shown the dissipation rates and half-lives of kresoxim-methyl in different crops regarding the dissipation behavior and distribution of kresoxim-methyl in banana. Therefore, this research will be provide an important outlook towards food safety to evaluate the risk of residues to consumers. The maximum residue limit (MRL) in banana has been legislated in some organizations and countries: 0.01 mg kg^{-1} (temporary limit, European Union, http://ec.europa.eu/sanco_pesticides/public/index.cfm?event=substance.resultat&s=1) and 5 mg kg^{-1} (Japan, http://www.m5.ws001.squarestart.ne.jp/foundation/agrdtl.php?a_inq=19000). The main objectives of the present study were to (1) establish an effective and sensitive method of kresoxim-methyl based on the LC-ESI-MS/MS technique in banana and soil samples; (2) investigate the dissipation dynamics and terminal residues of kresoxim-methyl in banana and soil by field trial and distribution in a whole banana, pulp, and peel; and (3) evaluate the dietary risk probability of kresoxim-methyl in banana by the value of *RQ* based on the terminal residue data after spraying three and four times the recommended dosage.

MATERIALS AND METHODS

Chemicals and Reagents

Standard kresoxim-methyl (98.0% purity) was purchased from Dr. Ehrenstorfer GmbH (Augsburg, Germany). A suspension emulsion (SE) containing 40% kresoxim-methyl was obtained from Shanxi Biaozheng Crop Science Co. Ltd (Shanxi, China). HPLC-grade acetonitrile was purchased from J. T. Baker (Phillipsburg, NJ, United States). MS-grade formic acid was obtained from Aladdin Industrial Corporation (Shanghai, China). Analytical grade activated anhydrous magnesium sulfate and sodium chloride were obtained from Merck (Darmstadt, Germany). Primary secondary amine (PSA; 40–60 μm in size) and octadecylsilane (C_{18}; 40–60 μm in size) were purchased from Agela Technologies Company (Tianjin, China). Wahaha pure water was used (Wahaha Group Co., Ltd., Hangzhou, China).

Field Experiment Design and Sample Collection

Field trials to investigate the dissipation of kresoxim-methyl and residues in banana and soil were carried out in Guangzhou (GZ: 113°E, 22°N, oceanic subtropical monsoon climate) in Guangdong Province, and Fangchenggang (FCG: 108°E, 21°N, oceanic monsoon climate) in Guangxi Province in 2016 according to the "Guidelines for Pesticide Residue Field Trials" (NY/T 788-2004) issued by the Ministry of Agriculture of China. Plots where kresoxim-methyl had never been previously applied were selected. The average rainfall in GZ and FCG was 291 mm and 465 mm, respectively; the average temperature was 23°C and 33°C, respectively, and the average relative humidity was 69% and 78%, respectively. Trials were conducted from September 9 to December 14 in GZ and from May 12 to July 19 in FCG. The characteristic properties of the soil in the fields were as follows: sandy loam in GZ with an organic matter content of 23.0 g kg^{-1} and a pH of 6.71, and clay in FCG with an organic matter content of 19.9 g kg^{-1} and a pH of 5.83.

Dissipation Trials

Forty percent kresoxim-methyl suspension emulsion (SE) dissolved in water was sprayed to banana plots and soil plots once, at a dosage of 750 mg/kg (1.5 times the recommended dosage) when the banana reached 50% of the size of a ripe banana. Each banana plot contained three banana trees, and the soil plot measured 30 m^2. In addition, there was a 1-m buffer zone between plots, each plot was set in triplicate, and no-pesticide application was treated with clear water. Representative banana and soil samples were randomly collected from each plot to evaluate dissipation at 2 h (calculated as the original concentration) and 1, 3, 7, 10, 14, 21, 28, 35, and 42 days after spraying.

Terminal Trials

The kresoxim-methyl formulation (40% SE) was applied to the final residual experimental plots at a low-dose level of 500 mg/kg (the recommended dosage) and a high-dose level of 750 mg/kg (1.5 times the recommended dosage) three and four times for two treatments. The re-treatment interval was 7 days, which was the recommended minimum re-treatment interval. Terminal residue samples were randomly collected from each plot at different pre-harvest intervals (PHIs; 35 and 42 days) to investigate its distribution in the whole banana, pulp, and peel. Twelve bananas were randomly collected with a knife from each treatment plot.

Sample Preparation

Representative banana samples were cut into smaller pieces according to the four-point method. Samples of 0.5 kg were

homogenized in a food processor (Hobart FP-400, United States). Soil samples were thoroughly mixed, and 200 g of subsample was used for kresoxim-methyl analyses. All collected samples were stored in a freezer at −20°C until analysis. There was no need to consider the storage stability problem of analytical samples, because the kresoxim-methyl was stable at −20°C at least 18 months according to the JMPR report 1999.

Pretreatment Procedure

The sample (5 g) was weighed in a 50-ml centrifuge tube, 20 ml of acetonitrile was added, and the screw cap was closed and vigorously shaken for 1 min using a vortex mixer at maximum speed. Next, 1 g of NaCl and 4 g of anhydrous $MgSO_4$ were added, vortexed for 1 min, and centrifuged for 2 min at 5,000 rpm. An aliquot of 2 ml was drawn from the supernatant and added in a pre-prepared 5-ml tube with 50 mg of PSA and 50 mg of C_{18}; then, this tube was immediately shaken by hand, vortexed for 10 s, and centrifuged for 2 min at 5,000 rpm. Finally, the extract was filtered through a filter membrane (0.22 μm, Millex-GV, Millipore, Bedford, MA, United States) and then analyzed by HPLC-MS/MS. A blank sample was collected and subjected to pretreatment using the same procedure described above.

LC-MS/MS Analysis

A high-performance liquid chromatography system (Agilent 1,200, United States) tandem triple quadrupole mass spectrometer (AB SCIEX 4000Q TRAP, United States) was employed to separate and quantify kresoxim-methyl. The analyses were separated by a poroshell-120 EC-C_{18} column (150 mm × 3.0 mm, 2.7 μm, Agilent, United States). The oven temperature was set at 35°C; the flow rate and injection volume were 0.35 ml/min and 5 μl. The mobile phase consisted of (A) acetonitrile and (B) 0.1% (v/v) formic acid aqueous solution, and the ratio of solvent A to solvent B was 75:25. This current speed was kept constant throughout the 7-min analysis time.

Electrospray ionization was carried out using the positive ion mode (ESI^+). The capillary voltage was set at 5.0 kV. The temperature of the source was 550°C. Nitrogen was used as the nebulizer and drying gas at 50 psi and 350°C. Multiple reaction monitoring (MRM) was selected. The selected precursor ion was m/z 314.0 with product quantitative and qualitative ions of m/z 116.1, m/z 222.0, and m/z 235.4, respectively, when the corresponding collision energy levels were set at 17.3 V, 18.9 V, and 24.3 V. Under the above conditions, the kresoxim-methyl retention time was approximately 3.9 min (total run time = 7 min).

Calculations

Dissipation Kinetics

The dissipation rates of kresoxim-methyl were evaluated using the first-order kinetics equations $C_t = C_0 e^{-kt}$, where C_t and C_0 denote the concentration of the pesticide residue (mg kg^{-1}) and initial concentration (mg kg^{-1}) at time t (days), and k is the rate constant derived from In (C_0/C_t) versus t plots by regression analysis. The half-lives of dissipation (DT_{50}) were equal to In2/k.

Risk Evaluation

National estimated daily intake (NEDI), expressed as mg kg^{-1}, is obtained as follows:

$$NEDI = \left(\sum (STMRi \times Fi)\right)/bw,$$

Where $STMRi$ (mg kg^{-1}) is the supervised trial median residue in the collected samples, Fi (kg) is the dietary reference intake for a certain kind of food used to assess nutrient intakes of healthy Chinese people, and bw (kg) is the body weight. Based on the report by the China Health and Nutrition Survey, the average body weight for a Chinese adult is 63 kg (Chen et al., 2018).

Risk quotient is calculated for pesticide by dividing the $NEDI$ by the acceptable daily intake (ADI) (mg kg^{-1} bw) for pesticide.

$$RQ = NEDI/ADI,$$

The ADI of kresoxim-methyl is 0.4 mg kg^{-1} bw based on the National Food Safety Standard of China (http://www.fao.org/fileadmin/templates/agphome/documents/Pests_Pesticides/JMPR/Evaluation01/11_Kesoxim-methyl.pdf).

The RQ is a measurement of the potential risk of adverse health effects from chemical constituents. A RQ of less than 100% indicates that the exposure does not exceed the level considered to be "acceptable". In contrast, if it exceeds one, there is a possibility of suffering from adverse effects (Wang et al., 2015).

RESULTS AND DISCUSSION

Method Performance

The matrix effect is usually considered to be a major drawback in trace-level analysis. Matrix-matched calibration is an efficient method to avoid matrix effects (ME) (Utture et al., 2011; Wiest et al., 2011; Rahman et al., 2015). ME were calculated using the following equation:

$$\mathrm{ME}\,(\%) = ((m_{matrix}/m_{solvent})\text{-}1) \times 100\%$$

Where m_{matrix} and $m_{solvent}$ are the slope of the calibration curves in the matrix and in the pure solvent, respectively. An ME with a positive (negative) value indicates that the analyte response is enhanced (suppressed) by the matrix; a zero value indicates that the analyte response is removed by the matrix. The result showed that the ME of the whole banana and peel were all negative values (−3.9% and −36%), which indicated that they caused signal suppression. In contrast, the ME of the pulp caused signal enhancement. The calibration curves were constructed by plotting standard concentrations against the response of the chromatographic peak, and the correlation coefficients for all the calibration curves were greater than 0.999 (**Supplementary Table S1**).

Recoveries were determined to evaluate the accuracy and precision of this method. Banana and soil samples spiked at three levels of fortification (0.01, 0.1, and 1.0 mg kg^{-1}), with five replicates for each level (**Table 1**), and the selectivity of the method is illustrated in **Figure 2**. The average recoveries ranged from 90.3% to 97.7% with RSDs of 2.29%–4.14% in

TABLE 1 | Average recovery, LODs, and LOQs of kresoxim-methyl in banana and soil.

Sample	Spiking level[a](mg kg^{-1})	Recovery ±SD[b] (%)	RSD[c] (%)	LOD (μg kg^{-1})	LOQ (μg kg^{-1})
Whole banana	0.01	90.3 ± 3.7	4.14	0.04	0.12
	0.1	94.1 ± 3.2	3.42		
	1	97.7 ± 2.2	2.29		
Pulp	0.01	90.6 ± 2.5	2.74		
	0.1	91.6 ± 2.8	3.03		
	1	96.4 ± 2.9	2.95		
Peel	0.01	85.9 ± 3.1	3.64		
	0.1	91.4 ± 4.2	4.56		
	1	96.3 ± 2.9	3.03		
Soil	0.01	94.2 ± 4.5	4.75		
	0.1	95.1 ± 5.5	5.77		
	1	99.7 ± 1.9	1.89		

[a]*The standard fungicide was spiked before the sample grinding.*

[b]*The recovery was calculated by the formula: Recovery = $C_d/C_s \times 100\%$, where C_d represents the detected concentration and C_s represents the spiked concentration. Results were expressed as mean ± standard deviation (SD) with 95% confidence intervals.*

[c]*Mean value of five determinations.*

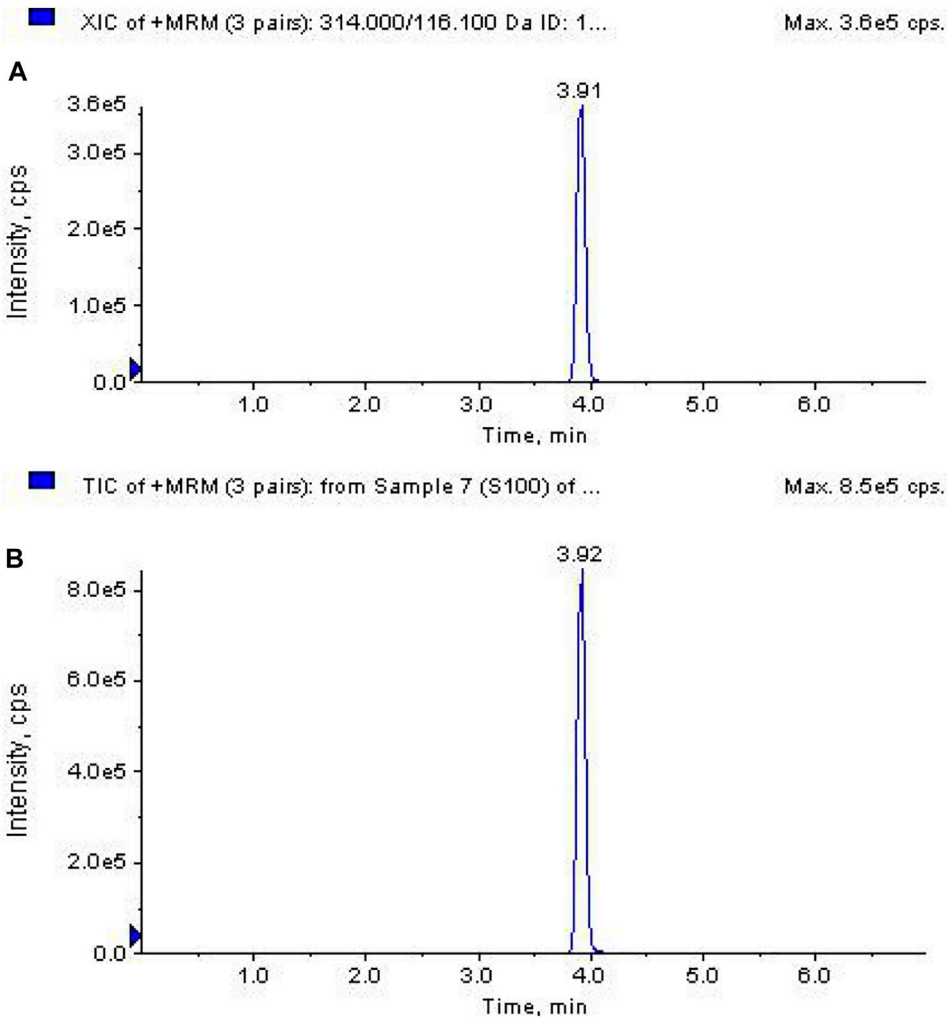

FIGURE 2 | The typical chromatograms of standard kresoxim-methyl at 0.1 mg/L **(A)** and banana sample spiked with fungicides at 0.1 mg/L **(B)**.

TABLE 2 | Dissipation dynamics parameters of kresoxim-methyl in banana and soil.

Experiment spots	Sample	Regression equation	Half-life (days)	Initial deposits (mg kg^{-1})	Correlation coefficient
Guangdong	Banana	$C_t = 4.6485\exp^{-0.122x}$	5.7	3.33	0.9074
Guangxi		$C_t = 4.4873\exp^{-0.144x}$	4.8	2.84	0.871
Guangdong	Soil	$C_t = 1.7318\exp^{-0.106x}$	6.5	1.43	0.9191
Guangxi		$C_t = 1.3673\exp^{-0.127x}$	5.5	1.23	0.9591

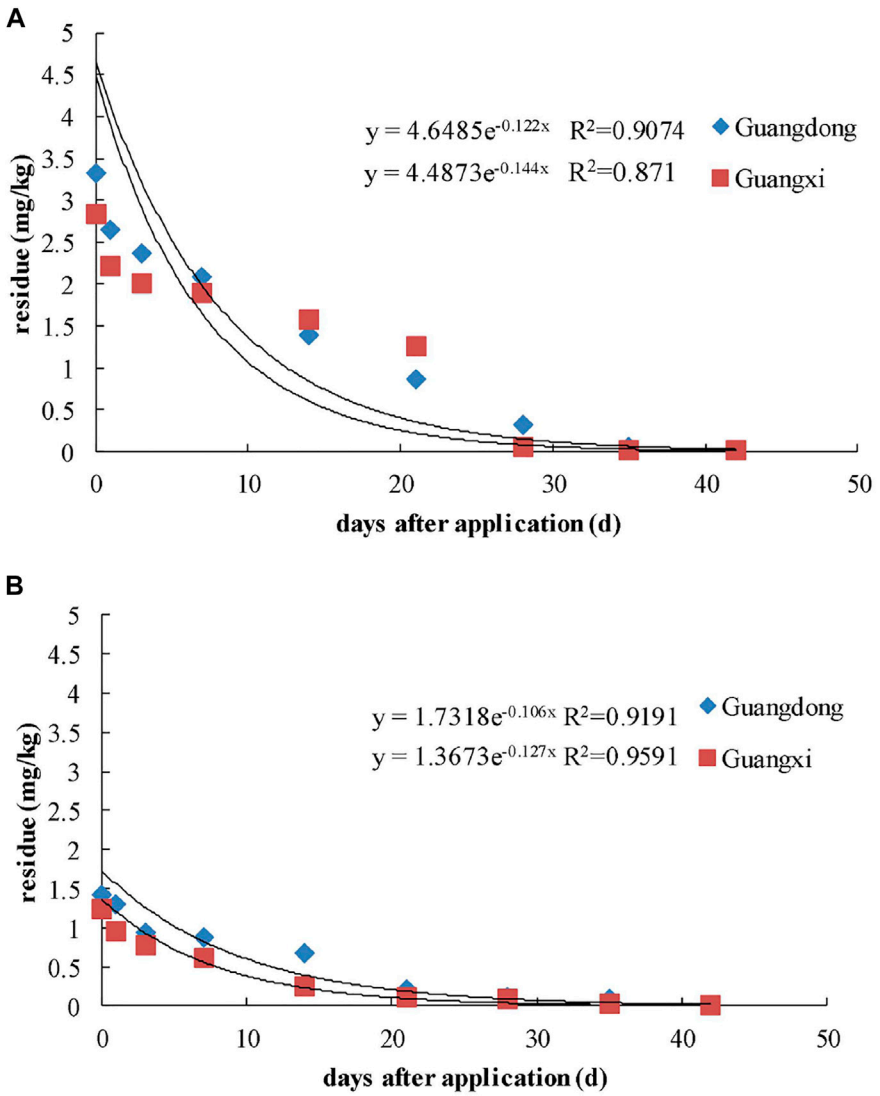

FIGURE 3 | Dissipation curve of kresoxim-methyl in banana **(A)** and soil **(B)**.

the whole banana, from 90.6% to 96.4% with RSDs of 2.74%–3.03% in pulp, from 85.9% to 96.3% with RSDs of 3.03%–4.56% in peel, and from 94.2% to 99.7% with RSDs of 1.89%–5.77% in soil, respectively. LOQs were defined as the minimum fortified concentrations of analyte in the matrix with a signal-to-noise ratio of 10, which was 0.12 μg kg^{-1} for the whole banana, pulp, peel, and soil. LODs were 0.04 μg kg^{-1}, which could be calculated at a signal-to-noise ratio of 3.

Dissipation of Kresoxim-Methyl in Banana and Soil

The initial concentrations of kresoxim-methyl residues in the whole banana were 3.33 mg kg^{-1} in GZ and 2.84 mg kg^{-1} in FCG. The half-lives were 5.7 and 4.8 days in GZ and FCG. The degradation rate was gradually decreased with the time elapsed, and the concentrations of kresoxim-methyl reached more than 55% of the initial concentration after 14 days. These

values are lower than those observed in other studies, where the half-lives of kresoxim-methyl were 10.6–14.5 days in greenhouse strawberry (Chen et al., 2018) and 5–10 days in wheat (Yu and Cai, 2010). The half-lives of kresoxim-methyl in banana were higher than cucumber (1.5–2.1 days) (Liu et al., 2012) and were similar to the half-lives of 4.58–4.77 days in apple (Malhat et al., 2013). The dissipation rate of kresoxim-methyl in GZ was slower than in FCG. The experiment in GZ was conducted from September to December, and from May to July in FCG; thus, the variety of banana and growth dilution may be major factors during the dissipation. The precipitation could not be an important factor due to the low water solubility of kresoxim-methyl (2 mg/L, 20°C). The temperature and humidity in GZ (15.6°C, 64%) were lower than those in FCG (26.5°C, 78%); hence, it may cause the lower initial concentration and short half-lives in FCG. Some chemical and physical factors like experiment plot, growth speed, chemical properties of pesticide, and light could play a significant role in the degradation of fungicide. The half-life ($t_{1/2}$) and other statistical parameters of dissipation were calculated from the experimental data, and the results are summarized in **Table 2** and **Figure 3**.

The initial kresoxim-methyl residues in soil were 1.43 mg kg^{-1} in GZ and 1.23 mg kg^{-1} in FCG. The half-lives of kresoxim-methyl in soil were 5.5 and 6.5 days in GZ and FCG, respectively. The dissipation rate of kresoxim-methyl in soil was faster than in apple soil (12–13 days) (Zhang et al., 2008), strawberry soil (8–12 days) (Li et al., 2009), and wheat soil (7–13 days) (Yu and Cai, 2010). The results showed that different chemical and physical factors of soil like pH, cation exchange capacity, and microorganism might influence the adsorption and leaching of kresoxim-methyl in soil, which led to different dissipation rates in soil.

Terminal Residues of Kresoxim-Methyl in Banana

The terminal residue concentrations of kresoxim-methyl in bananas at 35 and 42 days after the last application were investigated. When kresoxim-methyl formulation was applied 3 times and 1.5 times the recommended dosage, the residues were 0.12–0.54 mg kg^{-1} and 0.13–0.79 mg kg^{-1}, respectively, based on PHI (35 days). It was easily observed that the concentrations under different dosages followed the trend that residues increased with the increase in the applied dosage. When kresoxim-methyl was applied three and four times the recommended dosage based on PHI (42 days), the concentrations of kresoxim-methyl were 0.03–0.08 mg kg^{-1} and 0.12–0.25 mg kg^{-1}, respectively. There were positive relations between residues and application times. When kresoxim-methyl was applied three times the recommended dosage based on different PHI (35 days and 42 days), the kresoxim-methyl residues were 0.12–0.54 mg kg^{-1} and 0.03–0.08 mg kg^{-1}, respectively. It revealed that the residues were lower with a longer harvest interval.

Residue Distributions of Kresoxim-Methyl in the Whole Banana, Peel, and Pulp

The terminal residues were 0.03–0.08 mg kg^{-1}, 0.06–0.17 mg kg^{-1}, and <0.01 mg kg^{-1} in the whole banana, peel, and pulp, respectively, when kresoxim-methyl was applied three times the recommended dosage based on PHI (42 days). The residues in peel were much more than the whole banana, in which the concentration in peel was about 2 times that of the whole banana. It revealed that most of the residues were concentrated in the peel (**Table 3**). The peel accounts for about 35% of the whole fruit weight (Vu et al., 2017). The peel has been traditionally used for the treatment of burns, inflammation, and so on (Pereira and Maraschin, 2015). Thus, high levels of residue in the peel should be paid attention due to its broad use in the medical field and animal forage.

The residues of kresoxim-methyl in the whole banana ranged from 0.03 to 0.08 mg kg^{-1} (high residue, HR) when kresoxim-methyl was applied three times the recommended dosage based on PHI (42 days), which was higher than the MRL value of EU (0.01 mg kg^{-1}) and lower than Japan (5 mg kg^{-1}). In China, the principle of pesticide maximum residue limit standard is based on at least double the HR value with rounding up; thus, the MRL value for kresoxim-methyl in banana is 0.5 mg kg^{-1}.

The surface of the pulp was covered with peel, and kresoxim-methyl SE was applied to the peel, so the pulp is not directly exposed to the fungicide. First, the fungicide needs to pass through a wax layer of banana before slowly entering the pulp. The kresoxim-methyl is a fat-soluble fungicide due to its *Kow* logP (3.4, pH 7, 25°C) (the e-pesticide manual, Version 5.0), which indicated that it is adsorbed in the peel. Other factors like wax thickness, rainfall, and temperature will also influence the residue levels in the peel. Hence, the residues that permeated into the pulp were very low. The above results showed that the kresoxim-methyl residues were all below 0.01 mg kg^{-1} in pulp, which was far below the MRL value in China.

Risk Assessment

The measure of the potential risk to humans due to the presence of pesticide in banana is assessed through the estimation of the risk quotient (*RQ*) (**Tables 4** and **5**). The Chinese dietary structure, registered crops in China, and the corresponding MRLs recommended by various countries and organizations were taken into account to accurately assess the *NEDI*. If there was no *STMRi*, the corresponding MRLs would be adopted for risk assessment. The selection standards of residue limits followed the principle of China first, CAC second, United States third, Australia fourth, Korea fifth, EU sixth, and Japan last, and at the same time, the selection standards of residue limits needed to satisfy the value with the greatest risk. The *STMR* of kresoxim-methyl in banana at the PHI of 35 and 42 days were 0.22 mg kg^{-1} and 0.10 mg kg^{-1}, respectively (**Supplementary Table S2**). The total *NEDI* was 0.6232 mg (PHI 35) and 0.6178 mg (PHI 42) in various food classifications, and the RQ was 2.47% and 2.45%. The results showed that the *RQ* values of kresoxim-methyl in banana were all below 100% of the recommended dosage after being applied three and four times, which indicated that the residual amounts of kresoxim-methyl in banana were not hazardous to people.

CONCLUSION

A sensitive and efficient HPLC–MS/MS method for the analysis of kresoxim-methyl residues in banana and soil was established.

TABLE 3 | Distribution of kresoxim-methyl in pulp, the whole banana, and peel.

Experiment spot	Spraying time	Time after application (days)	Residue (mg kg^{-1})		
			Pulp	Whole banana	Peel
Guangdong	3	35	<0.01	0.19–0.54	0.41–1.19
		42	<0.01	0.04–0.08	0.08–0.17
	4	35	<0.01	0.25–0.50	0.54–1.10
		42	<0.01	0.14–0.25	0.30–0.54
Guangxi	3	35	<0.01	0.12–0.18	0.27–0.41
		42	<0.01	0.03–0.07	0.06–0.15
	4	35	<0.01–0.01	0.13–0.32	0.29–0.73
		42	<0.01–0.01	0.12–0.18	0.27–0.41

TABLE 4 | Corresponding MRLs of kresoxim-methyl registered by various countries and organizations.

Register crops	Food classification	MRLs						
		China	CAC	United States	Australia	Korea	European Union	Japan
Rice	Rice and its products	1			0.02		0.01[a]	
Wheat	Flour and its products	0.05	0.05[a]		0.1		0.01[a]	0.1
Cucumber	Light vegetables	0.5	0.05[a]		0.6		0.05[a]	0.5
Tomato	Dark vegetables				1	3	0.6	3
Pepper (Fresh)	Dark vegetables					2		
Strawberry	Fruits	2				1	1.5	5
Apple	Fruits	0.2		1			0.2	5
Melon	Fruits						0.3	1
Grape	Fruits		1	1			1	15
Watermelon	Fruits					0.2	0.3	1
Banana	Fruits	0.5					0.01[a]	5

[a]*Represents the temporary limit.*

TABLE 5 | Risk probability of kresoxim-methyl in banana.

Food classification	Fi (kg)	References residue limits (mg kg^{-1})	Sources	NEDI (mg)	ADI (mg)	Risk probability (%)
Rice and its products	0.2399	1	China	0.2399	0.4 × 63	
Flour and its products	0.1385	0.05	China	0.0069		
Other cereals	0.0233					
Tubers	0.0495					
Dried beans and their products	0.016					
Dark vegetables	0.0915	3	Korea	0.2745		
Light vegetables	0.1837	0.5	China	0.0919		
Pickles	0.0103					
Fruits	0.0457	0.22	STMR	0.0101		
Nuts	0.0039					
Livestock and poultry	0.0795					
Milk and its products	0.0263					
Egg and its products	0.0236					
Fish and shrimp	0.0301					
Vegetable oil	0.0327					
Animal oil	0.0087					
Sugar, starch	0.0044					
Salt	0.012					
Soy sauce	0.009					
Total	1.0286			0.6232	25.2	2.47

The dissipation and terminal residues of kresoxim-methyl in banana were investigated to ensure the reasonable and safe use of kresoxim-methyl. The results showed that the half-lives of kresoxim-methyl in banana and soil were 4.8–5.7 days and 5.5–6.5 days, respectively. The terminal residues of kresoxim-methyl in banana were below 0.08 mg kg^{-1} based on spraying

three times the recommended dosage, PHI (42 days). The potential dietary risk induced by kresoxim-methyl was negligible for banana consumers. The results of this work with regard to the development of analytical methods and evaluation of residue levels of kresoxim-methyl in banana fields will be useful in keeping agricultural products safe.

DATA AVAILABILITY STATEMENT

The original contributions presented in the study are included in the article/**Supplementary Material**, further inquiries can be directed to the corresponding authors.

AUTHOR CONTRIBUTIONS

SW: Methodology, Data curation, and Writing—Original draft preparation. XW: Validation and Data Curation. HC: Investigation and Software. HS: Funding acquisition. YL: Supervision and Data Curation.

SUPPLEMENTARY MATERIAL

The Supplementary Material for this article can be found online at: https://www.frontiersin.org/articles/10.3389/fenvs.2022.853033/full#supplementary-material

REFERENCES

Abreu, S. M., Caboni, P., Cabras, P., Garau, V. L., and Alves, A. (2006). Validation and Global Uncertainty of a Liquid Chromatographic with Diode Array Detection Method for the Screening of Azoxystrobin, Kresoxim-Methyl, Trifloxystrobin, Famoxadone, Pyraclostrobin and Fenamidone in Grapes and Wine. *Analytica Chim. Acta* 573-574, 291–297. doi:10.1016/j.aca.2006.01.090

Aguilera, A., Valverde, A., Camacho, F., Boulaid, M., and García-Fuentes, L. (2012). Effect of Household Processing and Unit to Unit Variability of Azoxystrobin, Acrinathrin and Kresoxim Methyl Residues in Zucchini. *Food Control* 25, 594–600. doi:10.1016/j.foodcont.2011.11.038

Aguilera, A., Valverde, A., Camacho, F., Boulaid, M., and García-Fuentes, L. (2014). Household Processing Factors of Acrinathrin, Fipronil, Kresoxim-Methyl and Pyridaben Residues in green Beans. *Food Control* 35, 146–152. doi:10.1016/j.foodcont.2013.06.038

Castelan, F. P., Abadie, C., Hubert, O., Chilin-Charles, Y., de Lapeyre de Bellaire, L., and Chillet, M. (2013). Relation between the Severity of Sigatoka Disease and Banana Quality Characterized by Pomological Traits and Fruit green Life. *Crop Prot.* 50, 61–65. doi:10.1016/j.cropro.2013.02.019

Celeiro, M., Llompart, M., Lamas, J. P., Lores, M., Garcia-Jares, C., and Dagnac, T. (2014). Determination of Fungicides in white Grape Bagasse by Pressurized Liquid Extraction and Gas Chromatography Tandem Mass Spectrometry. *J. Chroma A.* 1343, 18–25. doi:10.1016/j.chroma.2014.03.057

Chen, L., Song, Y., Tang, B., Song, X., Yang, H., Li, B., et al. (2015). Aquatic Risk Assessment of a Novel Strobilurin Fungicide: A Microcosm Study Compared with the Species Sensitivity Distribution Approach. *Ecotoxicol Environ. Saf.* 120, 418–427. doi:10.1016/j.ecoenv.2015.06.027

Chen, X., Fan, X., Ma, Y., and Hu, J. (2018). Dissipation Behaviour, Residue Distribution and Dietary Risk Assessment of Tetraconazole and Kresoxim-Methyl in Greenhouse Strawberry via RRLC-QqQ-MS/MS Technique. *Ecotoxicology Environ. Saf.* 148, 799–804. doi:10.1016/j.ecoenv.2017.11.019

Cook, D. C., Liu, S., Edwards, J., Villalta, O. N., Aurambout, J.-P., Kriticos, D. J., et al. (2013). Predicted Economic Impact of Black Sigatoka on the Australian Banana Industry. *Crop Prot.* 51, 48–56. doi:10.1016/j.cropro.2013.03.016

Facundo, H. V. D. V., Gurak, P. D., Mercadante, A. Z., Lajolo, F. M., and Cordenunsi, B. R. (2015). Storage at Low Temperature Differentially Affects the Colour and Carotenoid Composition of Two Cultivars of Banana. *Food Chem.* 170, 102–109. doi:10.1016/j.foodchem.2014.08.069

Khandelwal, A., Gupta, S., Gajbhiye, V. T., and Varghese, E. (2014). Degradation of Kresoxim-Methyl in Soil: Impact of Varying Moisture, Organic Matter, Soil Sterilization, Soil Type, Light and Atmospheric CO_2 Level. *Chemosphere* 111, 209–217. doi:10.1016/j.chemosphere.2014.03.044

Kolosova, A., Maximova, K., Eremin, S. A., Zherdev, A. V., Mercader, J. V., Abad-Fuentes, A., et al. (2017). Fluorescence Polarisation Immunoassays for Strobilurin Fungicides Kresoxim-Methyl, Trifloxystrobin and Picoxystrobin. *Talanta* 162, 495–504. doi:10.1016/j.talanta.2016.10.063

Lee, S., Kwon, O. S., Lee, C.-S., Won, M., Ban, H. S., and Ra, C. S. (2017). Synthesis and Biological Evaluation of Kresoxim-Methyl Analogues as Novel Inhibitors of Hypoxia-Inducible Factor (HIF) -1 Accumulation in Cancer Cells. *Bioorg. Med. Chem. Lett.* 27, 3026–3029. doi:10.1016/j.bmcl.2017.05.024

Lefrancq, M., Imfeld, G., Payraudeau, S., and Millet, M. (2013). Kresoxim Methyl Deposition, Drift and Runoff in a Vineyard Catchment. *Sci. Total Environ.* 442, 503–508. doi:10.1016/j.scitotenv.2012.09.082

Li, H., Zhang, Y. T., Guo, Y. Z., Shao, H., Liu, L., and Li, S. R. (2009). Residual Dynamics of Dry 50%kresoxim-Methyl Suspending Agent in Strawberry and Soil. *Anhui Agric. Sci.* 37, 9596–9597. doi:10.13989/j.cnki.0517-6611.2009.20.070

Li, L., Li, M., Chi, H., Yang, J., Li, Z., and Liu, C. (2016). Discovery of Flufenoxystrobin: Novel Fluorine-Containing Strobilurin Fungicide and Acaricide. *J. Fluorine Chem.* 185, 173–180. doi:10.1016/j.jfluchem.2016.03.013

Liang, P., Liu, G., Wang, F., and Wang, W. (2013). Ultrasound-assisted Surfactant-Enhanced Emulsification Microextraction with Solidification of Floating Organic Droplet Followed by High Performance Liquid Chromatography for the Determination of Strobilurin Fungicides in Fruit Juice Samples. *J. Chromatogr. B* 926, 62–67. doi:10.1016/j.jchromb.2013.02.011

Liu, C. Y., Wang, Y. C., Wan, K., Huang, J. X., and Wang, F. H. (2012). Residue and Risk Assessment of Kresoxim-Methyl in Cucumber under Field Conditions. *Chin. J. Pes Sci.* 14, 685–688. doi:10.3969/j.issn.1008-7303.2012.06.18

Malhat, F., Kamel, E., Saber, A., Hassan, E., Youssef, A., Almaz, M., et al. (2013). Residues and Dissipation of Kresoxim Methyl in Apple under Field Condition. *Food Chem.* 140, 371–374. doi:10.1016/j.foodchem.2013.02.050

Pereira, A., and Maraschin, M. (2015). Banana (Musa Spp) from Peel to Pulp: Ethnopharmacology, Source of Bioactive Compounds and its Relevance for Human Health. *J. Ethnopharmacology* 160, 149–163. doi:10.1016/j.jep.2014.11.008

Rahman, M. M., Abd El-Aty, A. M., Choi, J.-H., Kim, S.-W., Shin, S. C., and Shim, J.-H. (2015). Consequences of the Matrix Effect on Recovery of Dinotefuran and its Metabolites in green tea during Tandem Mass Spectrometry Analysis. *Food Chem.* 168, 445–453. doi:10.1016/j.foodchem.2014.07.095

Rahman, M. M., Jang, J., Park, J.-H., Abd El-Aty, A. M., Ko, A.-Y., Choi, J.-H., et al. (2014). Determination of Kresoxim-Methyl and its Thermolabile Metabolites in Pear Utilizing Pepper Leaf Matrix as a Protectant Using Gas Chromatography. *J. Adv. Res.* 5, 329–335. doi:10.1016/j.jare.2013.05.003

Reuveni, M., Gur, L., and Farber, A. (2017). Development of Improved Disease Management of Powdery Mildew on Mango Trees in Israel. *Crop Prot.* 110, 221–228. doi:10.1016/j.cropro.2017.07.017

Singh, B., Singh, J. P., Kaur, A., and Singh, N. (2016). Bioactive Compounds in Banana and Their Associated Health Benefits - A Review. *Food Chem.* 206, 1–11. doi:10.1016/j.foodchem.2016.03.033

Utture, S. C., Banerjee, K., Dasgupta, S., Patil, S. H., Jadhav, M. R., Wagh, S. S., et al. (2011). Dissipation and Distribution Behavior of Azoxystrobin, Carbendazim, and Difenoconazole in Pomegranate Fruits. *J. Agric. Food Chem.* 59, 7866–7873. doi:10.1021/jf200525d

Vu, H. T., Scarlett, C. J., and Vuong, Q. V. (2017). Optimization of Ultrasound-Assisted Extraction Conditions for Recovery of Phenolic Compounds and Antioxidant Capacity from Banana (*Musa* Cavendish) Peel. *J. Food Process. Preservation* 41, e13148. doi:10.1111/jfpp.13148

Vu, H. T., Scarlett, C. J., and Vuong, Q. V. (2018). Phenolic Compounds within Banana Peel and Their Potential Uses: A Review. *J. Funct. Foods* 40, 238–248. doi:10.1016/j.jff.2017.11.006

Wang, Z., Cang, T., Qi, P., Zhao, X., Xu, H., Wang, X., et al. (2015). Dissipation of Four Fungicides on Greenhouse Strawberries and an Assessment of Their Risks. *Food Control* 55, 215–220. doi:10.1016/j.foodcont.2015.02.050

Wiest, L., Buleté, A., Giroud, B., Fratta, C., Amic, S., Lambert, O., et al. (2011). Multi-Residue Analysis of 80 Environmental Contaminants in Honeys, Honeybees and Pollens by One Extraction Procedure Followed by Liquid and Gas Chromatography Coupled with Mass Spectrometric Detection. *J. Chromatogr. A* 1218, 5743–5756. doi:10.1016/j.chroma.2011.06.079

Xue, J., Chen, X., Jiang, W., Liu, F., and Li, H. (2015). Rapid and Sensitive Analysis of Nine Fungicide Residues in chrysanthemum by Matrix Extraction-Vortex-Assisted Dispersive Liquid-Liquid Microextraction. *J. Chromatogr. B* 975, 9–17. doi:10.1016/j.jchromb.2014.10.029

Yu, X. L., and Cai, L. M. (2010). Residues Dynamics of Kresoxim-Methyl 30%SC in Wheat and Soil. *Agrichemicals* 4, 361–362. doi:10.16820/j.cnki.1006-0413.2010.05.018

Zhang, Y. T., Guo, Y. Z., Shao, H., Liu, L., Li, H., and Song, S. R. (2008). Residue Dynamics of Kresoxim-Methyl in Apple and Soil. *Agrochemicals* 47, 668–610. doi:10.16820/j.cnki.1006-0413.2008.09.018

Zhu, X., Jia, C., Duan, L., Zhang, W., Yu, P., He, M., et al. (2016). Residue Behavior and Dietary Intake Risk Assessment of Three Fungicides in Tomatoes (*Lycopersicon Esculentum* Mill.) under Greenhouse Conditions. *Regul. Toxicol. Pharmacol.* 81, 284–287. doi:10.1016/j.yrtph.2016.09.015

Conflict of Interest: The authors declare that the research was conducted in the absence of any commercial or financial relationships that could be construed as a potential conflict of interest.

Publisher's Note: All claims expressed in this article are solely those of the authors and do not necessarily represent those of their affiliated organizations, or those of the publisher, the editors, and the reviewers. Any product that may be evaluated in this article, or claim that may be made by its manufacturer, is not guaranteed or endorsed by the publisher.

frontiers | Frontiers in Environmental Science

ORIGINAL RESEARCH
published: 11 May 2022
doi: 10.3389/fenvs.2022.860359

Toxicological Effects of Malathion at Low Dose on Wister Male Rats With Respect to Biochemical and Histopathological Alterations

Ahmed Massoud[1], *Moustafa SaadAllah*[1], *Naief A. Dahran*[2], *Nasr Elsayed Nasr*[3], *Ismael El-Fkharany*[1], *Mohamed S. Ahmed*[4], *Khalaf F. Alsharif*[5], *Ehab Kotb Elmahallawy*[6]* *and Aly Derbalah*[1]

[1]*Pesticides Chemistry and Toxicology Department, Faculty of Agriculture, Kafrelsheikh University, Kafrelsheikh, Egypt,* [2]*Department of Anatomy, Faculty of Medicine, University of Jeddah, Jeddah, Saudi Arabia,* [3]*Department of Biochemistry and Clinical Biochemistry, Faculty of Veterinary Medicine, Kafrelsheikh University, Kafrelsheikh, Egypt,* [4]*Department of Pathology, Faculty of Veterinary Medicine, Kafrelsheikh University, Kafrelsheikh, Egypt,* [5]*Department of Clinical Laboratory Sciences, College of Applied Medical Sciences, Taif University, Taif, Saudi Arabia,* [6]*Department of Zoonoses, Faculty of Veterinary Medicine, Sohag University, Sohag, Egypt*

OPEN ACCESS

Edited by:
Jiehong Guo,
University of Minnesota Twin Cities, United States

Reviewed by:
Muhammad Adeel,
Beijing Normal University, China
Wu Dong,
Inner Mongolia University for Nationalities, China

***Correspondence:**
Ehab Kotb Elmahallawy
eehaa@unileon.es

Specialty section:
This article was submitted to Toxicology, Pollution and the Environment, a section of the journal Frontiers in Environmental Science

Received: *22 January 2022*
Accepted: *13 April 2022*
Published: *11 May 2022*

Citation:
Massoud A, SaadAllah M, Dahran NA, Nasr NE, El-Fkharany I, Ahmed MS, Alsharif KF, Elmahallawy EK and Derbalah A (2022) Toxicological Effects of Malathion at Low Dose on Wister Male Rats With Respect to Biochemical and Histopathological Alterations. Front. Environ. Sci. 10:860359. doi: 10.3389/fenvs.2022.860359

The toxicity of organophosphorus insecticides is considered a major global health problem, and the target of the toxic action of these compounds in humans and pests is the same. Malathion is the most commonly used organophosphate, and its danger lies in prolonged exposure to low doses. Based on a review of the literature, little is known about the toxicological and clinicopathological effects of low doses of malathion on animal enzyme activity, such as acetylcholinesterase (AChE), alkaline phosphatase (ALP), glutamic-pyruvic transaminase (GPT), glutamic-oxaloacetic transaminase (GOT), and glutathione S-transferase (GST). Furthermore, the histopathological changes in the organs being studied (liver, kidney, brain, and lung) in treated rats were described. Three groups of experimental animals were created (each with eight rats): two experimental groups and one control group. The first group of rats received a dose of 5 mg/kg malathion orally for 24 h, the second received a dose of 5 mg/kg malathion for 21 days, and the third served as a control. Surprisingly, ALP, GPT, GOT, and GST enzymatic activities increased significantly in both malathion-treated groups (24 h or 21 days), while those of AChE significantly decreased. The histopathological changes were minimal and almost negligible in rats treated with malathion for 24 h. However, multiple histopathological changes were reported in rats treated with malathion for 21 days, including focal hepatocellular necrosis, chronic pyelonephritis, cerebral malaria, interstitial pneumonia, and testicular degeneration. Interestingly, there was a direct correlation between the alterations in biochemical parameters and histopathological lesions with the prolonged time of low malathion dose administration in rats. The study highlights the importance of research involving malathion's chronic toxicity by non-lethal low concentrations of malathion to which most people and animals are exposed, whether as residues in water, air, or food.

Keywords: malathion, biochemical parameters, toxicity, histopathology, rats

1 INTRODUCTION

Pesticides have been used for several decades to improve agricultural productivity, reduce economic losses caused by controlling unwanted insects, worms, and animals, and eradicate disease vectors (Bhardwaj and Saraf, 2014). However, pesticides are not entirely beneficial since they are considered a significant source of pollution and have negative health consequences, some of which are irreversible (LaVerda et al., 2015; Navarrete-Meneses et al., 2017; Zhou et al., 2022). Therefore, the long-term effects of low doses of pesticides on human health, non-target species, and the environment raise serious concerns (Massoud et al., 2010; Ahmed et al., 2020). It is, therefore, not surprising to mention that many researchers are interested in implementing advanced methods for detoxification of these insecticides from their major resources, primarily aquatic media (Derbalah et al., 2021; Massoud et al., 2021; Massoud et al., 2022).

Pesticides, even at sub-lethal doses, are among the major hazards for humans and environments (Ahmed et al., 2020). Malathion is an insecticide that is widely used worldwide because of its effectiveness in controlling insects in field crops, fruits, vegetables, and livestock (Rettich, 1980; Chamber, 1992; Barlas, 1996; Tchounwou et al., 2015). Organophosphates (malathion, diazinon, and chlorpyrifos) have been detected in samples of water collected from vegetable and paddy fields in Bangladesh (Chowdhury et al., 2012). Similarly, another previous study conducted in Punjab, Pakistan (Ahmad et al., 2008), showed several pesticide residues in different rice samples, including karate, padan, malathion, and novacran. In addition, Hamid et al. (2020) reported that the concentration of malathion was 18.26 mg/kg in rice from India, which is higher than the maximum limit, suggesting a significant health risk for rice consumers. Therefore, the United States Environmental Protection Agency (USEPA and other studies; US Department of Health and Human Services, 1999; Zheng and Hwang, 2006) classified malathion as a very hazardous compound in Group 2A. Despite its low environmental persistence, high-level exposure to malathion toward animals and other higher vertebrates is considered neurotoxic in animals (US Department of Health and Human Services, 1999; Gurushankara et al., 2007; Budischak et al., 2009; Kumar et al., 2010; International Agency for Research on Cancer, 2015). Several international organizations, notably the Food and Drug Administration and USEPA, have established maximum residual concentrations of malathion in various food crops, such as 8 mg/kg in rice (US Department of Health and Human Services, 1999). In addition, the toxicity of several organophosphorus insecticides, for example, malathion, is increased by their breakdown products, such as oxygen analogs (oxons), which can be bio-activated within an organism or when exposed to sunlight (Derbalah and Ismail, 2013). The influence of pesticides on biochemical parameters, tissues, and organs is commonly used to assess their toxicity toward humans and animals (Enan et al., 1982; Ghanem et al., 2006). Measuring the enzymatic activity in the blood is commonly carried out to measure pesticide toxicity because of its high sensitivity and it is less time consuming. Furthermore, investigating the histopathological changes is considered a reliable diagnostic measure of the toxic effects of pesticides (Cornelius et al., 1959; Adeel et al., 2020; Adeel et al., 2021). The liver is the primary target of xenobiotic toxicity and is an essential organ for metabolizing many chemicals by biotransformation. The kidneys participate in the disposal of toxic metabolites (Neal, 1972). Hepatocytes secrete transaminases (glutamic-pyruvic transaminase [GPT] and glutamic-oxaloacetic transaminase [GOT]), which play an important role in amino acid biosynthesis and are, thus, specific indicators of liver injury. GPT and GOT are normally found in hepatocytes; however, when liver tissue is damaged, they leak into the bloodstream, leading to an increase in their level and activity in the plasma (Banaee et al., 2011). The alkaline phosphatase enzyme degrades different phosphorous esters in an alkaline medium, and its increased activity has been associated with liver cell damage (Sayim, 2007). Collectively, these organs, liver and kidney, are considered the target for malathion toxins (Yang et al., 2000). These organs are frequently used as a key indicator of the toxicity of various substances (Massoud et al., 2010). Although humans and animals are mostly exposed to pesticides at low doses for long-term periods, most of the previous studies evaluated the toxicity of pesticides at high doses, and very limited information is available regarding the effects of low doses (Derbalah and Ismail, 2013; Ahmed et al., 2020). Given the aforementioned information, this study evaluated the toxic effects of malathion at a low dose (5 mg/kg) in rats. Malathion toxicity was determined by examining its effects on numerous biochemical parameters combined with an assessment of the histopathological changes in some organs (liver, kidney, brain, lung, and testes) 24 h and 21 days after treatment versus the untreated control.

2 MATERIALS AND METHODS

2.1 Chemicals

Malathion (purity = 99.9%) was purchased from Kafr El-Zayat Company for chemicals and pesticides, (Kafr El-Zayat, Egypt). All chemical kits used for the determination of some biochemical parameters were bought from Biogenic Co., Ltd. (United States).

2.2 Toxicity Experiments

2.2.1 Ethical Statement

This study's experimental protocol and animal care followed the ethical standards of the Faculty of Veterinary Medicine, Kafrelsheikh University, Egypt. The study's ethical approval code number is KFS-2019/3.

2.2.2 Animals

In this study, adult Wister male rats (*Rattus norvegicus*) were procured from the Animal House of the High Institute of Public Health, Tanta, Egypt, at 8 weeks of age and weighing 100–120 g. The animals were kept in wire cages under standard conditions, with unrestricted access to food and water. The rats were kept in a temperature-controlled room with 14 h of light and 10 h of dark cycles, standard temperature of 24 ± 4 °C, and relative humidity of 60 ± 10%. The animals were acclimatized for 2 weeks under these conditions before starting the treatment (Korsrud et al., 1972).

2.2.3 Animal Treatment

This experiment was performed in the Department of Pesticide Chemistry and Toxicology, Faculty of Agriculture, Kafrelsheikh University, Egypt. The experimental animals were divided into three groups (eight animals per group). The first and second groups were used to test the pesticide's effects after 24 h (G1: Group 1) and 21 days (G2: Group 2), respectively, while the third group (G3: Group 3) served as a control (no malathion administered). Malathion was given to the rats at a dose of 5 mg/kg (volume, 1 ml) (1/316 LD_{50} for malathion). The rats were checked daily for any clinical signs of toxicity, moribund status, and mortality throughout the testing period (Ahmed et al., 2020).

2.2.4 Biochemical Assays

Blood samples were collected from each treatment group (one sample per animal), centrifuged at 4,500 rpm for 20 min, and serum was extracted and stored at −20°C until the enzymatic activities were measured. Colorimetric methods were performed as described previously (Waber and Dtsch, 1966; Gornal AC and David., 1949; Belfield A, 1971; Reitman and Frankel, 1957; and; Rose and Wallbank, 1986) to determine the activity of AChE, total protein, ALP, GPT, GOT, and GST. A spectrophotometer (SPECTRO MASTER Model 415; Fisher Scientific) was used to determine the level of enzymes after treatment with malathion. The specific activity of the selected enzymes was calculated by dividing the number of units/mL by the protein concentration in mg/mL to obtain μmol/min/mg (Manole et al., 2008).

2.2.5 Histopathological Examination

Animals were sacrificed under anesthesia and all lesions were recorded after the post-mortem examination. To investigate possible histopathological changes, specimens from the liver, kidneys, brain, lungs, and testes were collected and preserved in neutral buffered 10% formalin. Later on, the samples were dehydrated in ascending concentrations of alcohol, cleared in xylene, embedded in paraffin wax, cut at a thickness of 4 μm, stained with hematoxylin and eosin, and examined under a light microscope (Bancroft and Stevens, 1996). Histopathological lesions were scored according to the set criteria: marked [massive] (41–100% of tissue involved), moderate (21–40% of tissue involved), mild [slight] (11–20% of tissue involved), and minimal (0–10% of tissue involved) by recording the nature and extent of the lesion and its frequency of occurrence in randomly selected sites in the tissue (Shackelford et al., 2002).

2.3 Statistical Analysis

One-way analysis of variance (ANOVA) was used to analyze the biochemical data using the SPSS statistical software package for Windows version 11.0. Duncan's multiple range test (Duncan, 1955) was also used to determine significant differences between the means. The significance level was set at $p \leq 0.05$ (Duncan, 1955).

3 RESULTS

3.1 Biochemical Effects in Rats Treated With Malathion

Figure 1 shows that the ALP, GPT, GOT, and GST activities were significantly increased after 24 h of treatment with malathion, whereas those of AChE were significantly decreased compared with those of the untreated rats. After 21 days of treatment, the assessed enzymes (ALP, GPT, GOT, and GST) showed the same trend and were significantly increased, while the activity of the AChE enzyme was significantly decreased (**Figure 2**).

3.2 Histopathological Changes in Rats Treated With Malathion

3.2.1 Histopathological Changes in the Liver

As shown in **Figure 3**, there was slight sinusoidal cell activation, mainly with macrophages and the presence of single hepatocytes cell necrosis among rats treated with malathion for 24 h. Meanwhile, the livers of rats which received the same dose of malathion for 21 days showed congestion and dilatation of the hepatic sinusoids, moderate inflammatory reaction in the form of periportal mononuclear cell infiltration, and focal hepatocellular necrosis.

3.2.2. Histopathological Changes in the Kidney

The kidneys of rats treated with malathion for 24 h showed no histopathological changes and had normal renal tubules and glomeruli. However, those rats treated for 21 days had moderate vacuolar degeneration in the renal tubules lining the epithelium, presence of proteinaceous casts in the lumens of renal tubules, massive pyelonephritis with mononuclear cell infiltration in the pelvis, and squamous metaplasia of the renal pelvis lining epithelium and tubular basophilia (**Figure 4**).

3.2.3 Histopathological Changes in the Brain

There were few changes in the brain of rats treated with malathion for 24 h in the form of a slight perivascular cuff. However, there was focal cerebral malacia with infiltration of many glial cells in rats treated with malathion for 21 days (**Figure 5**).

3.2.4. Histopathological Changes in the Lungs

There were few microscopic changes noticed in the lungs of rats treated with malathion for 24 h in the form of congestion of the inter-alveolar blood vessels with perivascular eosinophilic infiltration. The lungs of rats treated with malathion for 21 days showed moderate interstitial pneumonia with thickened inter-alveolar septa and infiltration of numerous mononuclear inflammatory cells (**Figure 6**).

3.2.5. Histopathological Changes in the Testes

In this work, no microscopic changes in the testes of rats treated with malathion for 24 h were noticed and the testes appeared similar to those of the control rats. However, rats treated with malathion for 21 days showed testicular degeneration with

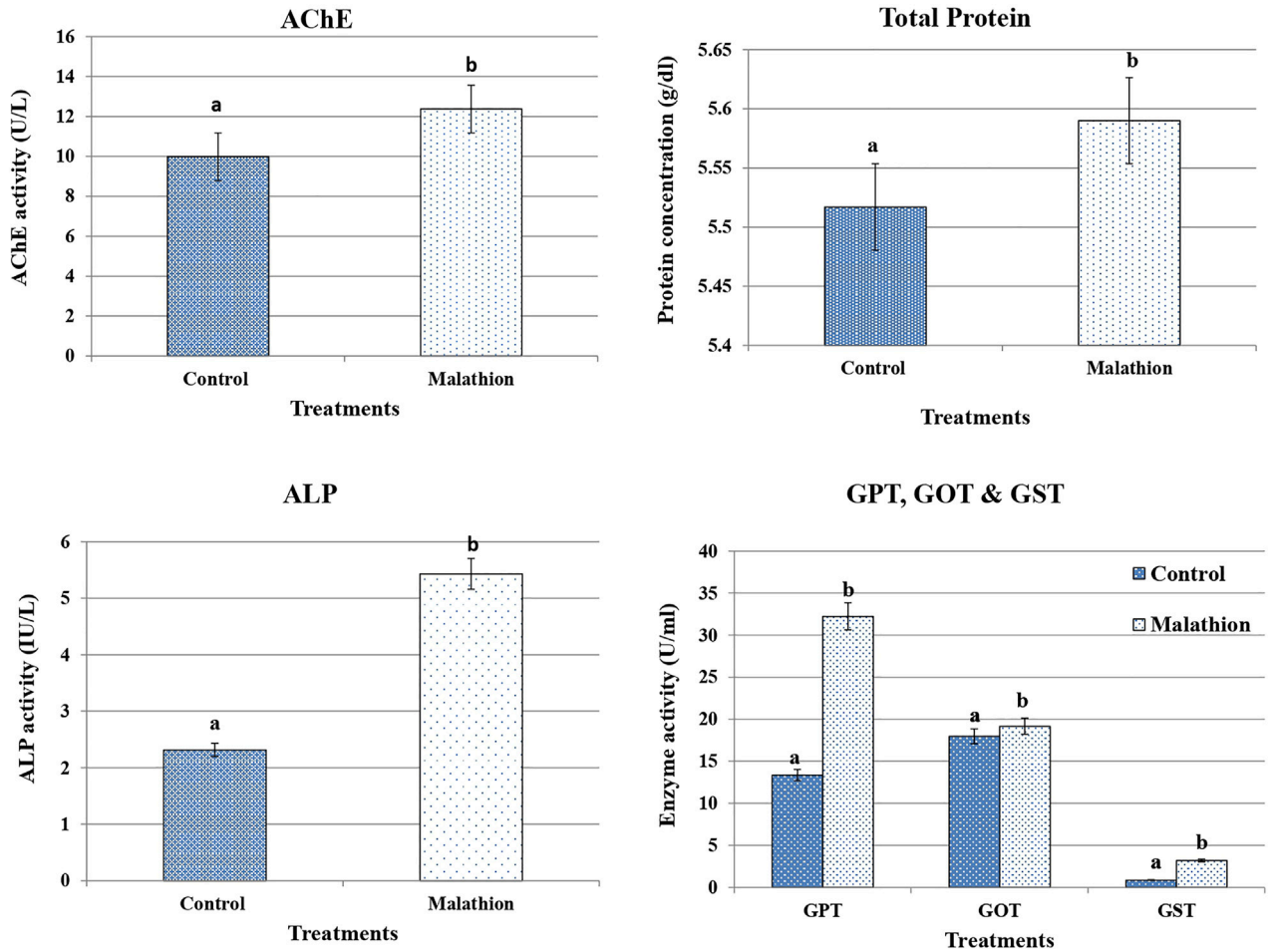

FIGURE 1 | Effect of malathion on AChE, total protein, ALP GPT, GOT, and GST in male rats after 24 h of treatment compared to control. Bars represent means ± SD. *$p < 0.05$ versus control. Different letters **(A,B)** indicate the significant differences between means according to Duncan's multiple range test.

complete necrosis of the germinal lining epithelium of some seminiferous tubules and massive interstitial edema (**Figure 7**).

3.2.6 Quantification of Histopathological Changes in Rats Treated With Malathion

The quantification and scores of histopathological lesions recorded for the liver, kidneys, brain, lungs and testis in rats treated with malathion are shown in **Table 1**.

4 DISCUSSION

This study reveals interesting biochemical and histopathological findings evaluating the toxic effects of malathion at a low dose (5 mg/kg) in rats after 24 h and 21 days of treatment. The study measured several biochemical enzymes followed by assessing the histopathological changes in the liver, kidney, brain, lung, and testes. In the present work, we observed a significant increase in the activity of liver enzymes (GOT and GPT) after treatment with malathion, which is in agreement with previous reports (Bogusz, 1968; Menratha et al., 1973; and Abdel-Rahman et al., 1985). Notably, the elevated levels of the GPT and GOT enzymes indicate the damage of hepatic tissue (Massoud et al., 2010; Banaee et al., 2011).

It should be stressed that the liver is considered one of the most important organs affected by malathion toxicity, resulting in hepatocellular damage and increased liver enzymatic activity (Badr, 2020). In the present work, high levels of ALT and AST were reported in the treated groups compared with the control animals, which is in harmony with the histological changes found in liver tissue and is in agreement with previous studies (Agrahari et al., 2007). The reported alteration in the activity of hepatic enzymes in malathion-treated mice could be attributed to early hepatocyte damage induced by malathion (Banaee et al., 2011) (Ncibi et al., 2008). It is noteworthy to mention that ALT, AST, and ALP are considered markers of liver damage (Gokcimen et al., 2007). In addition, it has been shown that organophosphorus insecticides can elevate the enzymatic activities of ALT, AST, and ALP (Khan et al., 2005; Rezg et al., 2007; Ncibi et al., 2008; Ogutcu et al., 2008; Celik et al.,

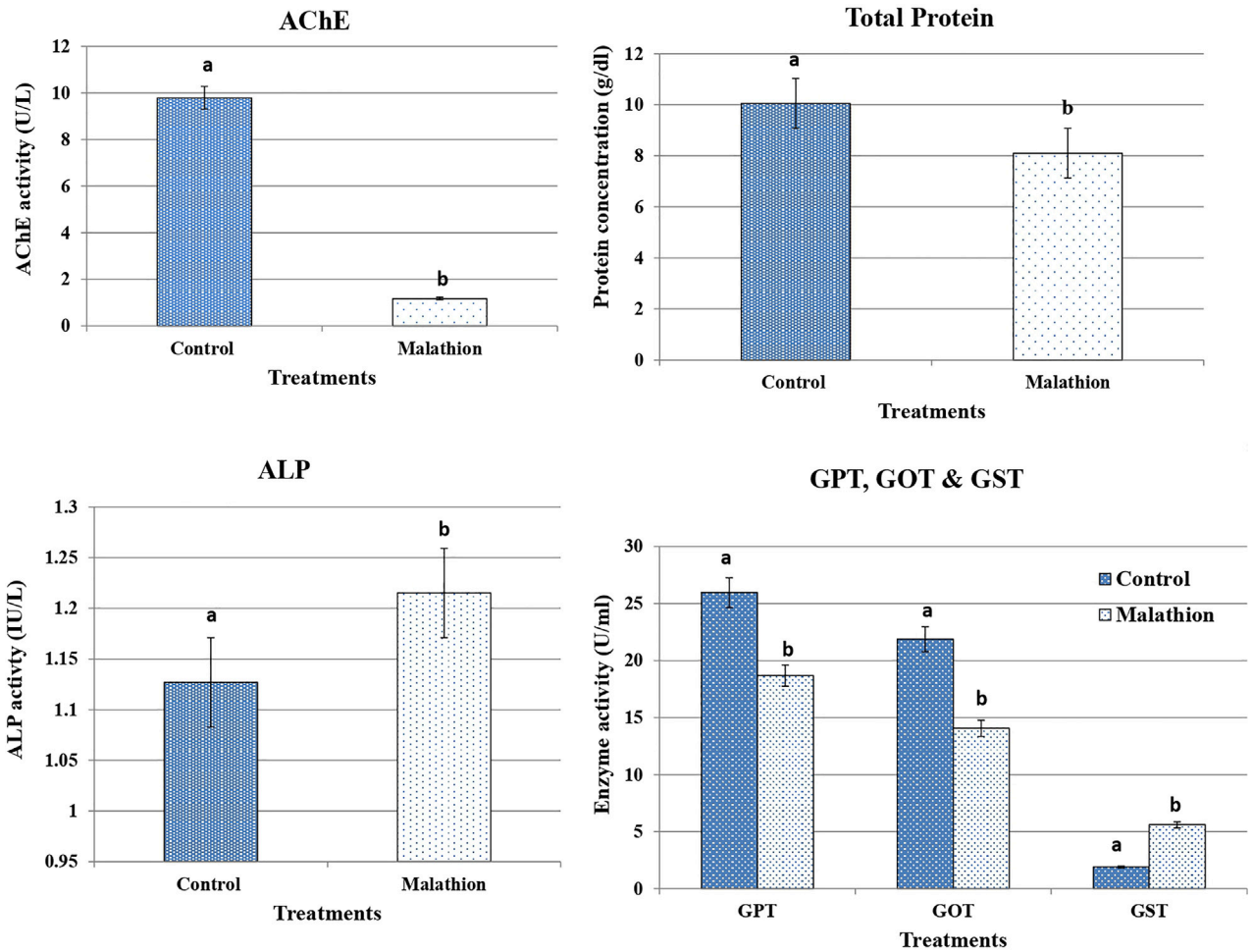

FIGURE 2 | Effect of malathion on AChE, total protein, ALP GPT, GOT, and GST in male rats after 21 days of treatment compared to control. Bars represent means ± SD. *$p < 0.05$ versus control. Different letters **(A,B)** indicate the significant differences between means according to Duncan's multiple range test.

2009). The ALP enzyme is involved in various biological processes, including the removal of toxic compounds, metabolism, and biosynthesis, all required for cell function. As a result, any disruption in this enzyme contributes to tissue and cell function disruption (Rezg et al., 2007). In the present study, there was an increase in the activity of this enzyme in rats treated with malathion compared with the control group which might be attributed to the damage that occurred in liver tissues with the disturbance of the normal liver function. This interpretation is consistent with several previous studies showing that the damage of the cell membrane of the liver is followed by the release of many enzymes into the blood, including ALT, AST, and ALP (Abdel-Rahman et al., 1985; Rezg et al., 2007; Ncibi et al., 2008).

Taken into account, the GST enzyme targets the detoxification of organophosphate insecticides. This enzyme acts by either rapidly metabolizing the insecticide into non-toxic products or rapid binding to the insecticide (Hemingway et al., 1998; Kostaropoulos et al., 2001). In this work, rats treated with malathion after 24 h had reduced hepatic GSH activity, which is in agreement with previous reports (Lasram et al., 2014; Selmi et al., 2015). In stark contrast, rats treated with malathion for 21 days exhibited an increase in GST activity, which was also observed in a previous study (Hazarika et al., 2003).

Furthermore, the amount of GSH present in the cell as a co-substrate of GST appears adequate to cope with the enzyme's increased activity (data not shown). Importantly, the inhibition of AChE remains among the main mechanisms of malathion toxicity (Esen and Uysal, 2018); AChE activity could be used as a surrogate marker of oxidative stress in health monitoring and, therefore, is considered an indicator of brain function. In this work, the activity of the cholinesterase enzyme decreased in rats treated with malathion compared with the control group. The present findings agree with many researchers who revealed that poisoning with organophosphorus pesticides, such as malathion, inhibits the enzyme cholinesterase in the blood (Hazarika et al., 2003; Timur et al., 2003). In a previous study, workers exposed to organophosphorus pesticides had significantly lower AChE activity (Hernández et al., 2013). The significant decrease in acetylcholinesterase activity after malathion administration can be explained because organophosphate insecticides inhibit AChE

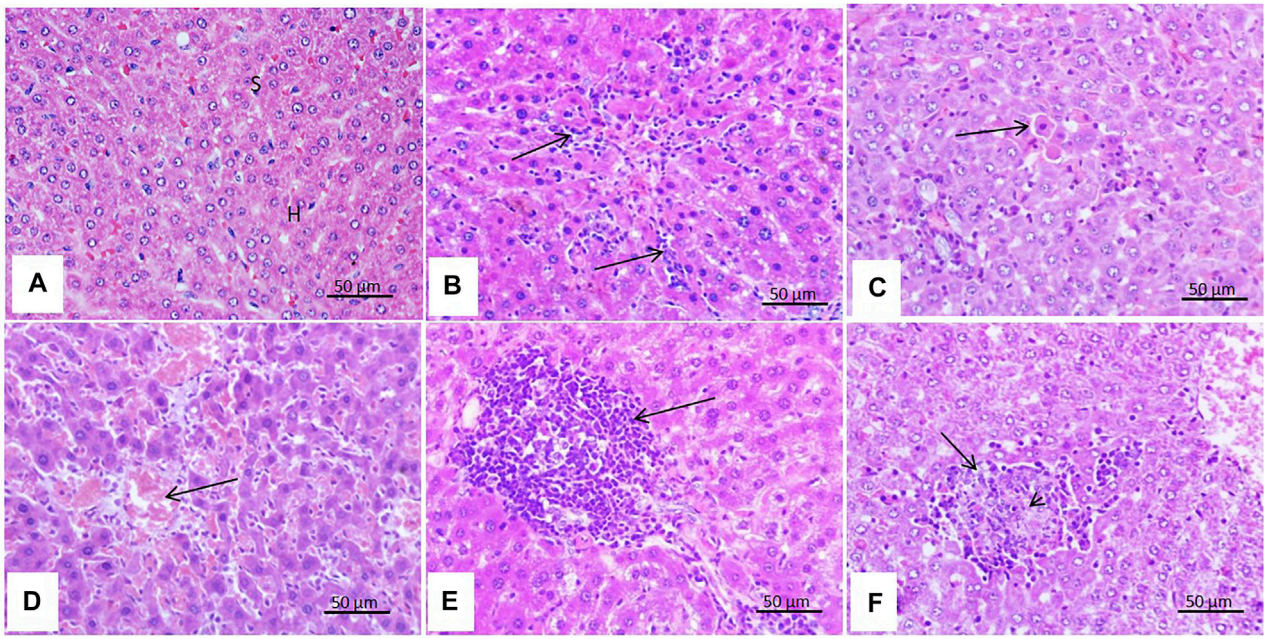

FIGURE 3 | Effect of malathion on the liver. **(A)** Liver of the control rats showing intact hepatic parenchyma with normal arrangement of hepatocytes (H), sinusoids (S), and central vein (C). **(B)** Liver of rats treated with malathion for 24 h showing mild sinusoidal cell activation (arrow) and **(C)** single cell necrosis of hepatocytes (arrow). **(D)** Liver of rats treated with malathion for 21 days showing severe congestion (arrow), **(E)** massive periportal mononuclear cell infiltration (arrow), and **(F)** focal hepatocytic necrosis (arrow) with the infiltration of mononuclear cells within and at the margin of the necrosis areas (arrow head).

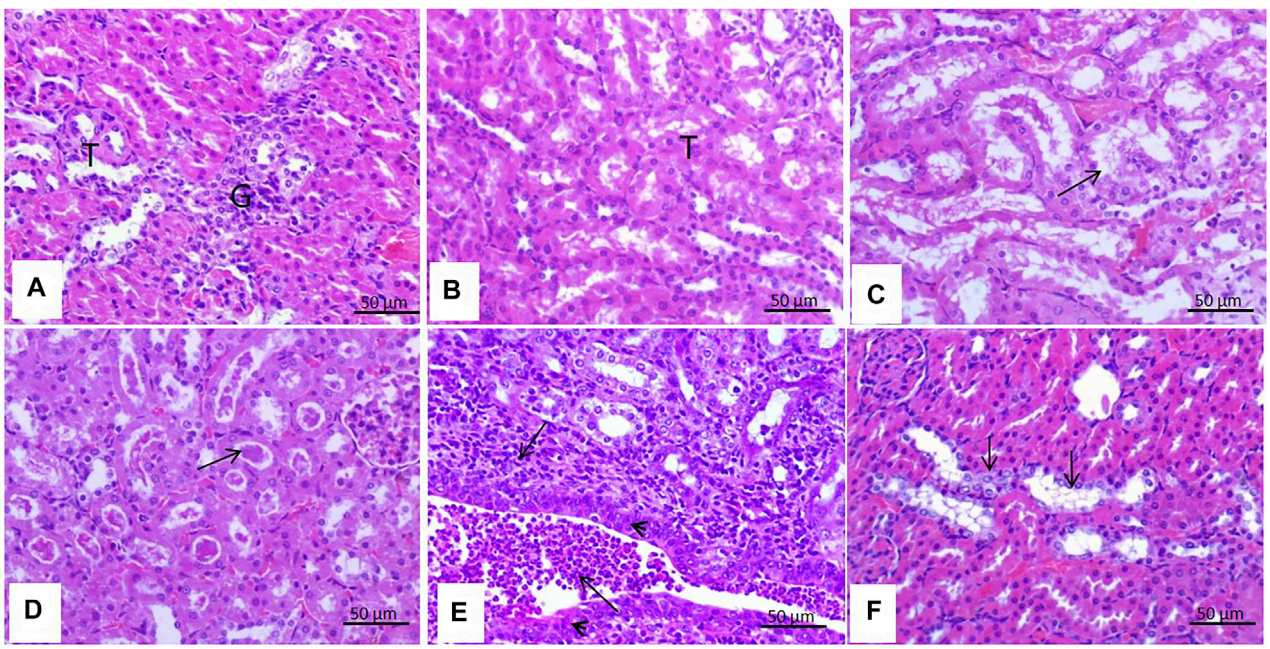

FIGURE 4 | Effect of malathion on the kidneys. **(A,B)** Kidneys of control rats and those treated with malathion for 24 h appeared with normal renal tubules (T) and glomeruli (G). **(C)** Rats treated with malathion for 21 days showing a moderate degree of vacuolar degeneration (arrow) in the lining epithelium of the renal tubules, **(D)** presence of proteinaceous casts (arrow) in the lumens of renal tubules, **(E)** massive pyelonephritis with mononuclear cell infiltration (arrow) in the pelvis and squamous metaplasia (arrow head) of the renal pelvis lining epithelium, and **(F)** tubular basophilia (arrow) of the tubular lining epithelium.

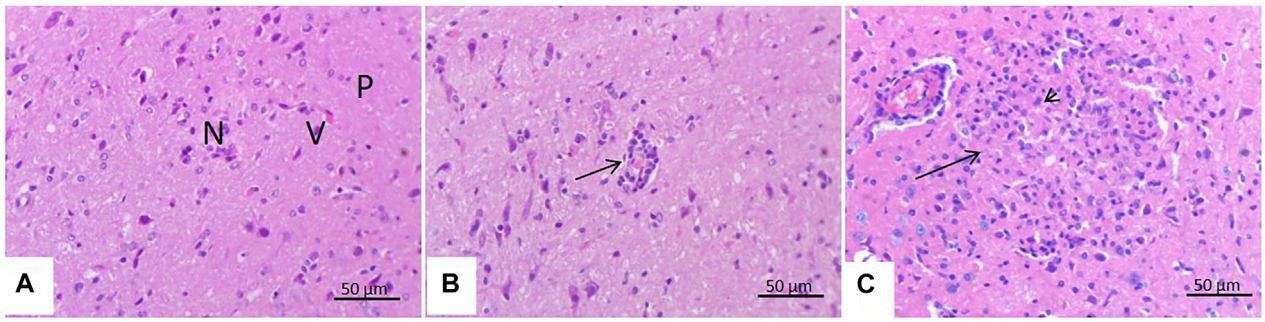

FIGURE 5 | Effect of malathion on the brain. **(A)** Brain of control rats showing intact neuronal cells (N) and blood vessels (V) in the neuropil (P) of the cerebrum. **(B)** Brain of rats treated with malathion for 24 h showing a slight perivascular cuff (arrows). **(C)** Brain of rats treated with malathion for 21 days showing cerebral malacia (arrow) with the infiltration of large number of glial cells (arrow head).

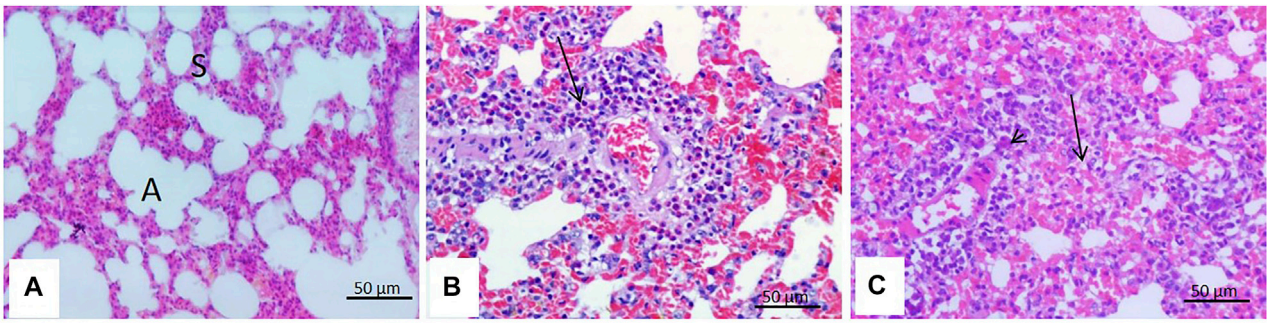

FIGURE 6 | Effect of malathion on the lungs. **(A)** Lungs of control rats with clear and intact alveoli **(A)** with thin inter-alveolar septa (S). **(B)** Lungs of rats treated with malathion for 24 h showing congestion of the inter-alveolar blood vessels and perivascular eosinophilic infiltration (arrow). **(C)** Lungs of rats treated with malathion for 21 days showing thickening of the inter-alveolar septa infiltration of a large number of mononuclear inflammatory cells (arrow).

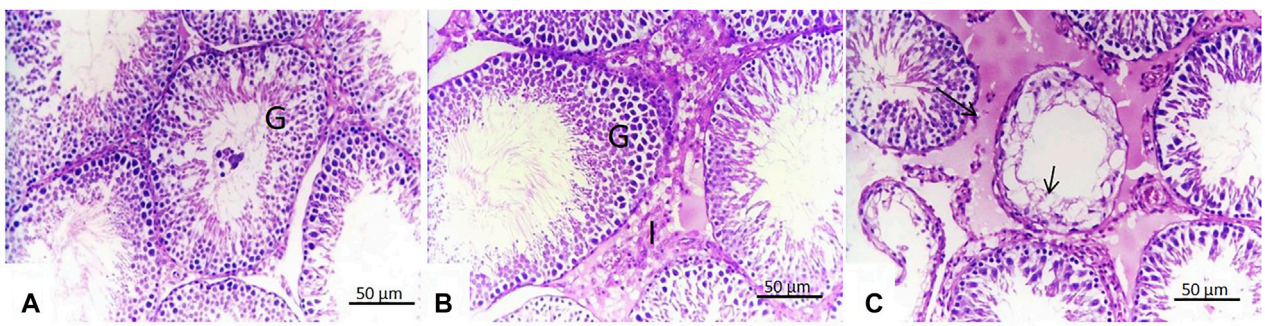

FIGURE 7 | Effect of malathion on the testis. **(A,B)** Testis of control rats and those treated with malathion for 24 h showing normal testicular structures with germinal epithelium (G) in the seminiferous tubules and interstitial (Leydig) cells (L). **(C)** Testis of rats treated with malathion for 21 days showed testicular degeneration with complete necrosis of the germinal lining epithelium (arrow) of some seminiferous tubules and massive interstitial edema (short arrow).

irreversibly by the phosphorylation of the enzyme's serine-OH group (Dumschat et al., 1991; Mortensen et al., 1998).

Regarding the histopathological changes in this work, a slight inflammatory reaction was observed in the liver tissue of rats treated with malathion as a single dose. In contrast, an advanced inflammatory reaction was represented by focal hepatic necrosis with periportal infiltration of mononuclear cells in the rats treated with malathion for 21 days. These later lesions might arise from the toxic effects of malathion and their influence on the liver's detoxification mechanisms and inflammatory response (Gokcimen et al., 2007; Yehia et al., 2007). As mentioned previously, the liver is a well-known detoxifying organ which

TABLE 1 | Lesions and scoring criteria for reported histopathological lesions of the liver, kidneys, brain, lung, and testis scored in the rats treated with malathion.

Organ	Lesion	Treatment with malathion for 24 h	Treatment with malathion for 21 days
Liver	Sinusoidal cell activation	11–20% of the tissue involved	11–20% of the tissue involved
	Single necrosis	11–20% of the tissue involved	11–20% of the tissue involved
	Congestion	<10% of tissue involved	<10% of tissue involved
	Periportal mononuclear cell infiltration	<10% of tissue involved	Between 21 and 40% of tissue parts affected
	Focal necrosis	<10% of tissue involved	Between 21 and 40% of tissue parts affected
Kidneys	Vacuolar degeneration	0–10% of tissue involved	Between 21 and 40% of tissue parts affected
	Proteinaceous casts	0–10% of tissue involved	11–20% of the tissue involved
	Pyelonephritis	0–10% of tissue involved	Between 41 and 100% of tissue parts affected
	Squamous metaplasia	0–10% of tissue involved	<10% of tissue involved
	Tubular basophilia	0–10% of tissue involved	<10% of tissue involved
Brain	Perivascular cuff	<10% of tissue involved	11–20% of the tissue involved
	Focal cerebral malacia	0–10% of tissue involved	11–20% of the tissue involved
Lung	Congestion	11–20% of the tissue involved	11–20% of the tissue involved
	Perivascular eosinophilic infiltration	<10% of tissue involved	11–20% of the tissue involved
	Interstitial pneumonia	<10% of tissue involved	Between 21 and 40% of tissue parts affected
Testis	Testicular degeneration	0–10% of tissue involved	Between 21 and 40% of tissue parts affected
	Interstitial oedema	0–10% of tissue involved	Between 41 and 100% of tissue parts affected

mainly performs through p450-mediated enzymatic catalysis (Ahmed et al., 2020). In this study, it seems that prolonged treatment with malathion inhibited p450-mediated biostimulants or negatively affected the mitochondrial membrane transport system of hepatocytes of treated rats, resulting in hepatocyte damage and death, and these findings are consistent with several previous studies (Guengerich and Avadhani, 2018; He et al., 2020). The observed mild degenerative changes in the liver of rats after 24 h of treatment are consistent with previous studies (Toś-Luty et al., 2003). It was discovered that exposure of male Wister rats to a single dose of malathion caused degenerative changes in the liver and induced parenchymatous degeneration. Similarly, after 21 days of treatment, the observed hepatic changes were correlated with increased levels of liver enzymes that rendered to subchronic liver damage. These later findings are consistent with those reported previously (Sayim, 2007; Kim et al., 2008; Singh et al., 2013).

Organophosphorus pesticides induce various histopathological changes in the liver and kidneys (Zidan, 2015). These induced histopathological changes include bleeding, infiltration of inflammatory cells, and necrosis (Kalender et al., 2006) and were consistent with several previous reports (Kerem et al., 2007; Afshar et al., 2008). In this work, the kidneys of rats which received malathion for 24 h did not show any microscopic abnormalities. However, marked renal changes were observed in rats sacrificed after 21 days of treatment. It seems that the long time exposure of kidneys to malathion resulted in subchronic toxicity and a series of degenerative changes in the glomerular tufts and peritubular renal capillaries, chronic pyelonephritis with infiltration of numerous mononuclear cells, and squamous metaplasia of the lining epithelium of the renal pelvis (Yun et al., 2015; Iavicoli et al., 2016). The proximal tubules are the main site for xenobiotic biotransformation, making them more susceptible to chemical insult, and therefore, all reported lesions were confined mainly to the renal cortex (Lock and Reed, 1998).

The brain is a highly sensitive organ to toxicity and highly susceptible to oxidative processes (Savolainen, 1978). As observed in this work, the brain showed slight histopathological changes in rats treated with malathion for 24 h, but these histopathological changes became more severe after treatment for 21 days, indicating the stress condition of these rats, which was reported in previous studies (Cheng et al., 2020). As mentioned previously, some pesticides, such as organophosphorus compounds, are neurotoxic (Ahmed et al., 2011). Malathion is considered one of the compounds that interfere with the chemical neurotransmission or ion channels and cause reversible neurotoxic effects such as neuritis and gliosis, consistent with previous research (Eddleston et al., 2002; Gunnell et al., 2007).

Regarding the lungs, as shown, malathion was not toxic to the lungs after 24 h. However, after a long period (21 days) of exposure to malathion, the lungs showed more severe pulmonary changes. The resulting pulmonary lesions might be attributed to the breakdown of the alveolar epithelial/endothelial barrier and the release of exudative inflammatory infiltrate into the lungs (Hussain and Sultan, 2005). However, a previous study (Adamis et al., 1999) mentioned that the pathophysiological processes leading to these inflammatory reactions are unclear, but pulmonary toxicity can induce acute inflammatory reactions with different features.

Examination of the male reproductive organs after exposure to malathion is of great importance (Bustos-Obregon et al., 2001). In this study, rats treated with malathion for 24 h showed the same histological structure as the control group. This result is in agreement with that reported previously (Recena et al., 2006). Meanwhile, malathion-treated rats showed evident testicular changes after 21 days. Previous reports have shown that malathion affects the testes' germinal and somatic cells, decreases testosterone activity, and consequently inhibits spermatogenesis through damage and vacuolation of Sertoli's cells and germ cells (Steger et al., 1999; Farag et al., 2000; Mahgoub and El-Medany, 2001). In this work, necrosis and

edema in the seminiferous tubules and interstitial tissue were similar to those noticed in several previous studies (Farag et al., 2000; Khan et al., 2001; Uzunhisarcikli et al., 2007). Taken together, the study concluded that low or sub-lethal doses of malathion have toxic effects on the treated rats, particularly after 21 days of treatment reflected in a series of biochemical and histopathological changes. This shows that exposure to malathion residues in food or water can have serious long-term toxic effects on human and animal health, particularly at low doses.

CONCLUSION

According to the present findings, malathion pesticide induced several biochemical alterations combined with a series of histopathological changes and damage in the liver, kidneys, brain, lung, and testes after a short time of exposure to a dose of 5 mg/kg. Considering this, the toxic effects of malathion on human health cannot be overlooked, especially when long-term exposure and low doses of the pesticide are considered. Our study suggests future research to investigate the toxicological effects of malathion at low concentrations close to the environmental level and over longer periods of time.

DATA AVAILABILITY STATEMENT

The original contributions presented in the study are included in the article/Supplementary Material; further inquiries can be directed to the corresponding author.

ETHICS STATEMENT

Animal care and experimental protocols used in the present study followed relevant guidelines and regulations of the ethical standards of Veterinary Medicine, Kafrelsheikh University, Egypt. The ethical approval code number of the study is KFS-2019/3.

AUTHOR CONTRIBUTIONS

Conceptualization: AM, MS, IE-F, MA, KA, EE, and AD; data curation: MS and MA; formal analysis: IE-F, MS, AA, and MA; funding acquisition: MS and MA; investigation: AM, AD, IE-F, MS, and EE; methodology: AM, MS, and AD; project administration: AM and IE-F; resources: MS and MA; software: EE; supervision: AM, AD, NN, ND, KA, and EE; validation: AM, AD, and EE; visualization: AM, EE, and AD; writing—original draft: NN, MS, MA, ND, KA, EE, and AD; and writing—review and editing: AM, MS, MA, EE, and AD. All authors have read and approved of the published version of the manuscript.

FUNDING

This work was supported in part by the Taif University Researchers Supporting Program (Project Number TURSP-2020/153), Taif University, Saudi Arabia.

REFERENCES

Abdel-Rahman, M. S., Lechner, D. W., and Klein, K. M. (1985). Combination Effect of Carbaryl and Malathion in Rats. *Arch. Environ. Contam. Toxicol.* 14 (4), 459–464. doi:10.1007/bf01055532

Adamis, Z., Tátrai, E., Honma, K., and Ungváry, G. (1999). Effects of Lead(II) Nitrate and a Dithiocarbamate Fungicide on the Rat Lung. *J. Appl. Toxicol.* 19 (5), 347–350. doi:10.1002/(sici)1099-1263(199909/10)19:5<347::aid-jat587>3.0.co;2-3

Adeel, M., Shakoor, N., Hussain, T., Azeem, I., Zhou, P., Zhang, P., et al. (2021). Bio-interaction of Nano and Bulk Lanthanum and Ytterbium Oxides in Soil System: Biochemical, Genetic, and Histopathological Effects on *Eisenia fetida*. *J. Hazard. Mater.* 415, 125574. doi:10.1016/j.jhazmat.2021.125574

Adeel, M., Tingting, J., Hussain, T., He, X., Ahmad, M. A., Irshad, M. K., et al. (2020). Bioaccumulation of Ytterbium Oxide Nanoparticles Insinuate Oxidative Stress, Inflammatory, and Pathological Lesions in ICR Mice. *Environ. Sci. Pollut. Res.* 27 (26), 32944–32953. doi:10.1007/s11356-020-09565-8

Afshar, S., Farshid, A., Heidari, R., and Ilkhanipour, M. (2008). Histopathological Changes in the Liver and Kidney Tissues of Wistar Albino Rat Exposed to Fenitrothion. *Toxicol. Ind. Health* 24 (9), 581–586. doi:10.1177/0748233708100090

Agrahari, S., Pandey, K. C., and Gopal, K. (2007). Biochemical Alteration Induced by Monocrotophos in the Blood Plasma of Fish, Channa Punctatus (Bloch). *Pesticide Biochem. Physiology* 88 (3), 268–272. doi:10.1016/j.pestbp.2007.01.001

Ahmad, S., Zia-Ul-Haq, M., Imran, M., Iqbal, S., Iqbal, J., and Ahmad, M. (2008). Determination of Residual Contents of Pesticides in Rice (Oryza Sativa L) Crop from Different Regions of Pakistan. *Pak. J. Bot.* 40 (3), 1253–1257.

Ahmed, M. S., Massoud, A. H., Derbalah, A. S., Al-Brakati, A., Al-Abdawani, M. A., Eltahir, H. A., et al. (2020). Biochemical and Histopathological Alterations in Different Tissues of Rats Due to Repeated Oral Dose Toxicity of Cymoxanil. *Anim. (Basel)* 10 (12), E2205. doi:10.3390/ani10122205

Ahmed, M. S., Massoud, A. H., Derbalah, A. S., and Ismail, A. A. (2011). Pathological and Biochemical Assesment of the Fungicide (Metalaxyl) on Rats. *Egypt. J. Comp. Pathol. Clin. Pathol.* 24, 136–154.

Badr, A. M. (2020). Organophosphate Toxicity: Updates of Malathion Potential Toxic Effects in Mammals and Potential Treatments. *Environ. Sci. Pollut. Res.* 27 (21), 26036–26057. [pii]. doi:10.1007/s11356-020-08937-410.1007/s11356-020-08937-4

Banaee, M., Sureda, A., Mirvaghefi, A. R., and Ahmadi, K. (2011). Effects of Diazinon on Biochemical Parameters of Blood in Rainbow Trout (*Oncorhynchus mykiss*). *Pesticide Biochem. physiology* 99 (1), 1–6. doi:10.1016/j.pestbp.2010.09.001

Bancroft, J., and Stevens, A. (1996). *Theory and Practice of Histological Techniques*. 4th ed. New York/London/San Francisco/Tokyo: Churchill Livingstone.

Barlas, N. E. (1996). Toxicological Assessment of Biodegraded Malathion in Albino Mice. *Bull. Environ. Contam. Toxicol.* 57 (5), 705–712. doi:10.1007/s001289900247

Belfield, A., and Goldberg, D. M. (1971). Revised Assay for Serum Phenyl Phosphatase Activity Using 4- Amino - Antipyrine. *Enzyme* 12, 561–573. doi:10.1159/000459586

Bhardwaj, J. K., and Saraf, P. (2014). Malathion-Induced Granulosa Cell Apoptosis in Caprine Antral Follicles: An Ultrastructural and Flow Cytometric Analysis. *Microsc. Microanal.* 20, 1861–1868. doi:10.1017/s1431927614013452

Bogusz, M. (1968). Influence of Insecticides on the Activity of Some Enzymes Contained in Human Serum. *Clin. Chim. Acta* 19 (3), 367–369. doi:10.1016/0009-8981(68)90260-x

Budischak, S. A., Belden, L. K., and Hopkins, W. A. (2009). Relative Toxicity of Malathion to Trematode-Infected and Noninfected *Rana palustris* Tadpoles. *Arch. Environ. Contam. Toxicol.* 56 (1), 123–128. doi:10.1007/s00244-008-9167-9

Bustos-Obregón, E., Díaz, O., and Sobarzo, C. (2001). Parathion Induces Mouse Germ Cells Apoptosis. *Ital. J. Anat. Embryol.* 106 (2 Suppl. 2), 199–204.

Celik, I., Yilmaz, Z., and Turkoglu, V. (2009). Hematotoxic and Hepatotoxic Effects of Dichlorvos at Sublethal Dosages in Rats. *Environ. Toxicol.* 24 (2), 128–132. doi:10.1002/tox.20390

Chamber, H. (1992). Organophosphorus Compounds: an Overview. *Organophosphates Chem. fate Eff.* 3–17. doi:10.1016/b978-0-08-091726-9.50005-7

Cheng, B., Zhang, H., Hu, J., Peng, Y., Yang, J., Liao, X., et al. (2020). The Immunotoxicity and Neurobehavioral Toxicity of Zebrafish Induced by Famoxadone-Cymoxanil. *Chemosphere* 247, 125870. doi:10.1016/j.chemosphere.2020.125870

Chowdhury, M. A. Z., Banik, S., Uddin, B., Moniruzzaman, M., Karim, N., Gan, S. H., et al. (2012). Organophosphorus and Carbamate Pesticide Residues Detected in Water Samples Collected from Paddy and Vegetable Fields of the Savar and Dhamrai Upazilas in Bangladesh. *Ijerph* 9 (9), 3318–3329. doi:10.3390/ijerph9093318

Cornelius, C. E., Bishop, J., Switzer, J., and Rhode, E. A. (1959). Serum and Tissue Transaminase Activities in Domestic Animals. *Cornell Vet.* 49 (1), 116–126.

Derbalah, A., and Ismail, A. (2013). Remediation Technologies of Diazinon and Malathion Residues in Aquatic System. *Environ. Prot. Eng.* 39 (3). doi:10.37190/epe130310

Derbalah, A., Massoud, A., El-Mehasseb, I., Allah, M. S., Ahmed, M. S., Al-Brakati, A., et al. (2021). Microbial Detoxification of Dimethoate and Methomyl Residues in Aqueous Media. *Water* 13 (8), 1117. doi:10.3390/w13081117

Dumschat, C., Müller, H., Stein, K., and Schwedt, G. (1991). Pesticide-sensitive ISFET Based on Enzyme Inhibition. *Anal. Chim. acta* 252 (1-2), 7–9. doi:10.1016/0003-2670(91)87189-e

Duncan, D. B. (1955). Multiple Range and Multiple F Tests. *Biometrics* 11 (1), 1–42. doi:10.2307/3001478

Eddleston, M., Szinicz, L., Eyer, P., and Buckley, N. (2002). Oximes in Acute Organophosphorus Pesticide Poisoning: a Systematic Review of Clinical Trials. *Qjm* 95 (5), 275–283. doi:10.1093/qjmed/95.5.275

Enan, E. E., El-Sebae, A. H., Enan, O. H., and El-Fiki, S. (1982). In-vivo Interaction of Some Organophosphorus Insecticides with Different Biochemical Targets in White Rats. *J. Environ. Sci. Health, Part B* 17 (5), 549–570. doi:10.1080/03601238209372341

Esen, M., and Uysal, M. (2018). Protective Effects of Intravenous Lipid Emulsion on Malathion-Induced Hepatotoxicity. *Bratisl. Lek. Listy* 119 (6), 373–378. doi:10.4149/BLL_2018_069

Farag, A., Eweidah, M., and El-Okazy, A. (2000). Reproductive Toxicology of Acephate in Male Mice. *Reprod. Toxicol.* 14 (5), 457–462. doi:10.1016/s0890-6238(00)00094-0

Ghanem, N. F., Hassan, N. A., and Ismail, A. A. (2006). Biochemical and Histopathological Changes Induced in Rats Fed on Diets and Byproducts of Fumigated Wheat Grains with Phostoxin. *Pro. 4th Int. Con. Biol.Sc. (zool)*, 259–268.

Gokcimen, A., Gulle, K., Demirin, H., Bayram, D., Kocak, A., and Altuntas, I. (2007). Effects of Diazinon at Different Doses on Rat Liver and Pancreas Tissues. *Pesticide Biochem. physiology* 87 (2), 103–108. doi:10.1016/j.pestbp.2006.06.011

Gornal Ac, B. C., and David, M. M. (1949). Protein–Biuret Colorimetric Method. *J. Biol. Chem.* 177, 751.

Gunnell, D., Fernando, R., Hewagama, M., Priyangika, W. D. D., Konradsen, F., and Eddleston, M. (2007). The Impact of Pesticide Regulations on Suicide in Sri Lanka. *Int. J. Epidemiol.* 36 (6), 1235–1242. doi:10.1093/ije/dym164

Gurushankara, H. P., Krishnamurthy, S. V., and Vasudev, V. (2007). Effect of Malathion on Survival, Growth, and Food Consumption of Indian Cricket Frog (Limnonectus Limnocharis) Tadpoles. *Arch. Environ. Contam. Toxicol.* 52 (2), 251–256. doi:10.1007/s00244-006-0015-5

Hamid, A., Yaqub, G., Ayub, M., and Naeem, M. (2020). Determination of Malathion, Chlorpyrifos, λ-cyhalothrin and Arsenic in Rice. *Food Sci. Technol.* 41, 461–466. doi:10.1590/fst.01020

Hazarika, A., Sarkar, S. N., Hajare, S., Kataria, M., and Malik, J. K. (2003). Influence of Malathion Pretreatment on the Toxicity of Anilofos in Male Rats: a Biochemical Interaction Study. *Toxicology* 185 (1-2), 1–8. doi:10.1016/s0300-483x(02)00574-7

He, B., Ni, Y., Jin, Y., and Fu, Z. (2020). Pesticides-induced Energy Metabolic Disorders. *Sci. Total Environ.* 729, 139033. doi:10.1016/j.scitotenv.2020.139033

Hemingway, J., Hawkes, N., Prapanthadara, L., Jayawardenal, K. G. I., and Ranson, H. (1998). The Role of Gene Splicing, Gene Amplification and Regulation in Mosquito Insecticide Resistance. *Phil. Trans. R. Soc. Lond. B* 353 (1376), 1695–1699. doi:10.1098/rstb.1998.0320

Hernández, A. F., Gil, F., Lacasaña, M., Rodríguez-Barranco, M., Gómez-Martin, A., Lozano, D., et al. (2013). Modulation of the Endogenous Antioxidants Paraoxonase-1 and Urate by Pesticide Exposure and Genetic Variants of Xenobiotic-Metabolizing Enzymes. *Food Chem. Toxicol.* 61, 164–170. doi:10.1016/j.fct.2013.05.039

Hussain, A. M., and Sultan, S. T. (2005). Organophosphorus Insecticide Poisoning: Management in Surgical Intensive Care Unit. *J. Coll. Physicians Surg. Pak* 15 (2), 100–102. doi:10.2005/JCPSP.100102

Iavicoli, I., Fontana, L., and Nordberg, G. (2016). The Effects of Nanoparticles on the Renal System. *Crit. Rev. Toxicol.* 46 (6), 490–560. doi:10.1080/10408444.2016.1181047

International Agency for Research on Cancer, I (2015). *Evaluation of Fve Organophosphate Insecticides and Herbicides (WHO), 20 March*. Monographs 112. Lyon, France: IARC

Kalender, Y., Uzunhisarcikli, M., Ogutcu, A., Acikgoz, F., and Kalender, S. (2006). Effects of Diazinon on Pseudocholinesterase Activity and Haematological Indices in Rats: the Protective Role of Vitamin E. *Environ. Toxicol. Pharmacol.* 22 (1), 46–51. doi:10.1016/j.etap.2005.11.007

Kerem, M., Bedirli, N., Guerbuez, N., Ekinci, O., Bedirli, A., Akkaya, T., et al. (2007). Effects of Acute Fenthion Toxicity on Liver and Kidney Function and Histology in Rats. *Turkish J. Med. Sci.* 37 (5), 281–288.

Khan, I. A., Reddy, B. V., Mahboob, M., Rahman, M. F., and Jamil, K. (2001). Effects of Phosphorothionate on the Reproductive System of Male Rats. *J. Environ. Sci. Health, Part B* 36 (4), 445–456. doi:10.1081/pfc-100104188

Khan, S. M., Sobti, R. C., and Kataria, L. (2005). Pesticide-induced Alteration in Mice Hepato-Oxidative Status and Protective Effects of Black Tea Extract. *Clin. Chim. Acta* 358 (1-2), 131–138. doi:10.1016/j.cccn.2005.02.015

Kim, Y. S., Kim, J. S., Cho, H. S., Rha, D. S., Kim, J. M., Park, J. D., et al. (2008). Twenty-eight-day Oral Toxicity, Genotoxicity, and Gender-Related Tissue Distribution of Silver Nanoparticles in Sprague-Dawley Rats. *Inhal. Toxicol.* 20 (6), 575–583. doi:10.1080/08958370701874663

Korsrud, G. O., Grice, H. C., and McLaughlan, J. M. (1972). Sensitivity of Several Serum Enzymes in Detecting Carbon Tetrachloride-Induced Liver Damage in Rats. *Toxicol. Appl. Pharmacol.* 22 (3), 474–483. doi:10.1016/0041-008x(72)90255-4

Kostaropoulos, I., Papadopoulos, A. I., Metaxakis, A., Boukouvala, E., and Papadopoulou-Mourkidou, E. (2001). The Role of glutathioneS-Transferases in the Detoxification of Some Organophosphorus Insecticides in Larvae and Pupae of the Yellow Mealworm,*Tenebrio molitor* (Coleoptera: Tenebrionidae). *Pest. Manag. Sci.* 57 (6), 501–508. doi:10.1002/ps.323

Kumar, R., Nagpure, N. S., Kushwaha, B., Srivastava, S. K., and Lakra, W. S. (2010). Investigation of the Genotoxicity of Malathion to Freshwater Teleost Fish Channa Punctatus (Bloch) Using the Micronucleus Test and Comet Assay. *Arch. Environ. Contam. Toxicol.* 58 (1), 123–130. doi:10.1007/s00244-009-9354-3

Lasram, M. M., Dhouib, I. B., Bouzid, K., Lamine, A. J., Annabi, A., Belhadjhmida, N., et al. (2014). Association of Inflammatory Response and Oxidative Injury in the Pathogenesis of Liver Steatosis and Insulin Resistance Following Subchronic Exposure to Malathion in Rats. *Environ. Toxicol. Pharmacol.* 38 (2), 542–553. doi:10.1016/j.etap.2014.08.007

LaVerda, N. L., Goldsmith, D. F., Alavanja, M. C. R., and Hunting, K. L. (2015). Pesticide Exposures and Body Mass Index (BMI) of Pesticide Applicators from the Agricultural Health Study. *J. Toxicol. Environ. Health, Part A* 78 (20), 1255–1276. doi:10.1080/15287394.2015.1074844

Lock, E. A., and Reed, C. J. (1998). Xenobiotic Metabolizing Enzymes of the Kidney. *Toxicol. Pathol.* 26 (1), 18–25. doi:10.1177/019262339802600102

Mahgoub, A. A., and El-Medany, A. H. (2001). Evaluation of Chronic Exposure of the Male Rat Reproductive System to the Insecticide Methomyl. *Pharmacol. Res.* 44 (2), 73–80. doi:10.1006/phrs.2001.0816

Manole, A., Herea, D., Chiriac, H., and Melnig, V. (2008). *Laccase Activity Determination*. Scientific Annals of Alexandru Ioan Cuza din Iași University, 17–24.

Massoud, A., Derbalah, A., El-Mehasseb, I., Allah, M. S., Ahmed, M. S., Albrakati, A., et al. (2021). Photocatalytic Detoxification of Some Insecticides in Aqueous Media Using TiO2 Nanocatalyst. *Ijerph* 18 (17), 9278. doi:10.3390/ijerph18179278

Massoud, A., Derbalah, A. S., Iman, A., Abd-Elaziz, I., and Ahmed, M. (2010). Oral Toxicity of Malathion at Low Doses in Sprague-Dawley Rats: A Biochemical and Histopathological Study. *Monofyia Vet. J.* 7 (1), 183–196.

Massoud, A., El-Mehasseb, I., Saad Allah, M., Elmahallawy, E. K., Alsharif, K. F., S. Ahmed, M. M., et al. (2022). Advanced Oxidation Processes Using Zinc Oxide Nanocatalyst for Detoxification of Some Highly Toxic Insecticides in an Aquatic System Combined with Improving Water Quality Parameters. *Front. Environ. Sci.* 10, 807290. doi:10.3389/fenvs.2022.807290

Menrath, R. L. E., Gray, K. W., and Cameron, C. W. (1973). Toxicity of Bunamidine. *N. Z. Veterinary J.* 21, 212–215. doi:10.1080/00480169.1973.34109

Mortensen, S. R., Hooper, M. J., and Padilla, S. (1998). Rat Brain Acetylcholinesterase Activity: Developmental Profile and Maturational Sensitivity to Carbamate and Organophosphorus Inhibitors. *Toxicology* 125 (1), 13–19. doi:10.1016/s0300-483x(97)00157-1

Navarrete-Meneses, M. P., Salas-Labadía, C., Sanabrais-Jiménez, M., Santana-Hernández, J., Serrano-Cuevas, A., Juárez-Velázquez, R., et al. (2017). "Exposure to the Insecticides Permethrin and Malathion Induces Leukemia and Lymphoma-Associated Gene Aberrations *In Vitro* ". *Toxicol. Vitro* 44, 17–26. doi:10.1016/j.tiv.2017.06.013

Ncibi, S., Ben Othman, M., Akacha, A., Krifi, M. N., and Zourgui, L. (2008). Opuntia ficus Indica Extract Protects against Chlorpyrifos-Induced Damage on Mice Liver. *Food Chem. Toxicol.* 46 (2), 797–802. doi:10.1016/j.fct.2007.08.047

Neal, R. A. (1972). A Comparison of the *In Vitro* Metabolism of Parathion in the Lung and Liver of the Rabbit. *Toxicol. Appl. Pharmacol.* 23 (1), 123–130. doi:10.1016/0041-008x(72)90211-6

Ogutcu, A., Suludere, Z., and Kalender, Y. (2008). Dichlorvos-induced Hepatotoxicity in Rats and the Protective Effects of Vitamins C and E. *Environ. Toxicol. Pharmacol.* 26 (3), 355–361. doi:10.1016/j.etap.2008.07.005

Peter Guengerich, F., and Avadhani, N. G. (2018). Roles of Cytochrome P450 in Metabolism of Ethanol and Carcinogens. *Alcohol Cancer*, 15–35. doi:10.1007/978-3-319-98788-0_2

Recena, M. C., Pires, D. X., and Caldas, E. D. (2006). Acute Poisoning with Pesticides in the State of Mato Grosso Do Sul, Brazil. *Sci. Total Environ.* 357 (1-3), 88–95. doi:10.1016/j.scitotenv.2005.04.029

Reitman, S., and Frankel, S. (1957). A Colorimetric Method for the Determination of Serum Glutamic Oxalacetic and Glutamic Pyruvic Transaminases. *Am. J. Clin. Pathol.* 28 (1), 56–63. doi:10.1093/ajcp/28.1.56

Rettich, F. (1980). Residual Toxicity of Wall-Sprayed Organophosphates, Carbamates and Pyrethroids to Mosquito *Culex pipiens* Molestus Forskal. *J. Hyg. Epidemiol. Microbiol. Immunol.* 24 (1), 110–117.

Rezg, R., Mornagui, B., Kamoun, A., El-Fazaa, S., and Gharbi, N. (2007). Effect of Subchronic Exposure to Malathion on Metabolic Parameters in the Rat. *Comptes rendus Biol.* 330 (2), 143–147. doi:10.1016/j.crvi.2006.11.002

Rose, H. A., and Wallbank, B. E. (1986). Mixed-function Oxidase and Glutathione S-Transferase Activity in a Susceptible and a Fenitrothion-Resistant Strain of Oryzaephilus Surinamensis (Coleoptera: Cucujidae). *J. Econ. entomology* 79 (4), 896–899. doi:10.1093/jee/79.4.896

Savolainen, H. (1978). Superoxide Dismutase and Glutathione Peroxidase Activities in Rat Brain. *Res. Commun. Chem. Pathol. Pharmacol.* 21 (1), 173–176.

Sayim, F. (2007). Dimethoate-induced Biochemical and Histopathological Changes in the Liver of Rats. *Exp. Toxicol. Pathol.* 59 (3-4), 237–243. doi:10.1016/j.etp.2007.05.008

Selmi, S., El-Fazaa, S., and Gharbi, N. (2015). Oxidative Stress and Alteration of Biochemical Markers in Liver and Kidney by Malathion in Rat Pups. *Toxicol. industrial health* 31 (9), 783–788. doi:10.1177/0748233713475507

Shackelford, C., Long, G., Wolf, J., Okerberg, C., and Herbert, R. (2002). Qualitative and Quantitative Analysis of Nonneoplastic Lesions in Toxicology Studies. *Toxicol. Pathol.* 30 (1), 93–96. doi:10.1080/01926230252824761

Singh, S. P., Kumari, M., Kumari, S. I., Rahman, M. F., Mahboob, M., and Grover, P. (2013). Toxicity Assessment of Manganese Oxide Micro and Nanoparticles in Wistar Rats after 28 Days of Repeated Oral Exposure. *J. Appl. Toxicol.* 33 (10), 1165–1179. doi:10.1002/jat.2887

Steger, K., Rey, R., Louis, F., Kliesch, S., Behre, H., Nieschlag, E., et al. (1999). Reversion of the Differentiated Phenotype and Maturation Block in Sertoli Cells in Pathological Human Testis. *Hum. Reprod.* 14 (1), 136–143. doi:10.1093/humrep/14.1.136

Tchounwou, P. B., Patlolla, A. K., Yedjou, C. G., and Moore, P. D. (2015). Environmental Exposure and Health Effects Associated with Malathion Toxicity. *Toxic. Hazard Agrochem.* 51, 2145–2149. doi:10.5772/60911

Timur, S., Önal, S., Karabay, N. Ü., Sayim, F., and Zĭhnĭoğlu, F. (2003). *In Vivo* effects of Malathion on Glutathione-S-Transferase and Acetylcholinesterase Activities in Various Tissues of Neonatal Rats. *Turkish J. Zoology* 27 (3), 247–252. doi:10.3906/zoo-0212-1

Toś-Luty, S., Obuchowska-Przebirowska, D., Latuszyńska, J., Tokarska-Rodak, M., and Haratym-Maj, A. (2003). Dermal and Oral Toxicity of Malathion in Rats. *Ann. Agric. Environ. Med.* 10, 101–106.

US Department of Health and Human Services (1999). *Agency for Toxic Substances and Disease RegistryToxicological Profle for Asbestos (Update)*. Atlanta: Agency for Toxic Substances and Disease Registry.

Uzunhisarcikli, M., Kalender, Y., Dirican, K., Kalender, S., Ogutcu, A., and Buyukkomurcu, F. (2007). Acute, Subacute and Subchronic Administration of Methyl Parathion-Induced Testicular Damage in Male Rats and Protective Role of Vitamins C and E. *Pesticide Biochem. physiology* 87 (2), 115–122. doi:10.1016/j.pestbp.2006.06.010

Waber, H., and Dtsch, M. (1966). Cholinestrase Kinetic Colorimetric Method. *Dtsch. Med. Wschr* 91, 1927.

Yang, M. C., McLean, A. J., Rivory, L. P., and Le Couteur, D. G. (2000). Hepatic Disposition of Neurotoxins and Pesticides. *Pharmacol. Toxicol.* 87 (6), 286–291. doi:10.1034/j.1600-0773.2000.pto870608.x

Yehia, M. A., El-Banna, S. G., and Okab, A. B. (2007). Diazinon Toxicity Affects Histophysiological and Biochemical Parameters in Rabbits. *Exp. Toxicol. Pathol.* 59 (3-4), 215–225. doi:10.1016/j.etp.2007.09.003

Yun, J.-W., Kim, S.-H., You, J.-R., Kim, W. H., Jang, J.-J., Min, S.-K., et al. (2015). Comparative Toxicity of Silicon Dioxide, Silver and Iron Oxide Nanoparticles after Repeated Oral Administration to Rats. *J. Appl. Toxicol.* 35 (6), 681–693. doi:10.1002/jat.3125

Zheng, Y., and Hwang, H.-M. (2006). Effects of Temperature and Microorganisms on Malathion Transformation in River Water. *Bull. Environ. Contam. Toxicol.* 76 (4), 712–719. doi:10.1007/s00128-006-0978-y

Zhou, R., Yu, Y., Zhang, W., Wang, D., Bai, Y., Wang, Y., et al. (2022). Sensory Disturbance by Six Insecticides in the Range of μg/L in *Caenorhabditis elegans*. *Front. Environ. Sci.* 10, 859356. doi:10.3389/fenvs.2022.859356

Zidan, N. E.-H. A. (2015). Hepato- and Nephrotoxicity in Male Albino Rats Exposed to Malathion and Spinosad in Stored Wheat Grains. *Acta Biol. Hung.* 66 (2), 133–148. doi:10.1556/018.66.2015.2.1

Conflict of Interest: The authors declare that the research was conducted in the absence of any commercial or financial relationships that could be construed as a potential conflict of interest.

frontiers | Frontiers in Environmental Science

ORIGINAL RESEARCH
published: 26 May 2022
doi: 10.3389/fenvs.2022.880807

Bioremediation Potential of Plant-Bacterial Consortia for Chlorpyrifos Removal Using Constructed Wetland

Tahira Aziz[1], *Sajida Rasheed*[1]*, *Asad Hussain Shah*[1], *Habib Nasir*[2], *Anila Fariq*[1], *Asma Jamil*[3] *and Sammyia Jannat*[1]

[1]Department of Biotechnology, University of Kotli Azad Jammu and Kashmir, Kotli, Pakistan, [2]School of Natural Sciences, National University of Sciences and Technology, Islamabad, Pakistan, [3]Department of Earth and Environmental Sciences, Bahria University, Islamabad, Pakistan

The extensive and unchecked application of chlorpyrifos against crop insects has caused contamination of various ecosystems, such as soil, sediments, and water, posing harm to plants, animals, useful arthropods, and humans. The present study aimed at evaluating the ability of proto-type constructed wetland to biodegrade chlorpyrifos and its major metabolites especially 2-hydroxy-3, 5, 6-trichloropyridine/ol (TCP) using chlorpyrifos-degrading indigenous bacterial strains, namely, *Acinetobacter baumanni* and *Bacillus cibi* with *Canna* spps. and indigenous *Mentha* spps. as a bacterial–plant consortium. Soil and plant samples were collected at regular time intervals for 12 weeks; analytes were extracted using the toluene method and evaluated through gas chromatography–mass spectrometry (GC-MS). In case of wetland vegetation with *Canna* and *Mentha*, 2-hydroxy-3, 5, 6-trichloropyridine (TCP, m/z = 198) and 2- hydroxypyridine (m/z = 97) with deprotonated molecular ions at m/z = 69 $(M\text{-}H)^-$were detected as the intermediate metabolites, while in the bacterial–plant consortium, instead of TCP, 3, 5, 6-trichloro-2-methoxypyridine (TMP, m/z = 212) was formed along with di-ethylthiophosphate (DETP, m/z = 169). Based on the metabolite analysis using GC-MS, the biodegradation pathway for chlorpyrifos degradation through bacterial–plant consortia is predicted. The constructed wetland with the bacterial–plant consortium showed its potential to either bypass TCP generation, or TCP may have been immediately biodegraded by the plant part of the consortium. The designed constructed wetland provided a novel remedial measure to biodegrade chlorpyrifos without producing harmful metabolites.

Keywords: chlorpyrifos, bioremediation, crop insects, constructed wetland, biodegradation pathway

OPEN ACCESS

Edited by:
Mazhar Iqbal Zafar,
Quaid-i-Azam University, Pakistan

Reviewed by:
Muhammad Afzal,
King Saud University, Saudi Arabia
Vineet Kumar,
National Environmental Engineering Research Institute (CSIR), India
Muhammad Saqib Nawaz,
King Abdullah University of Science and Technology, Saudi Arabia

***Correspondence:**
Sajida Rasheed
drsajida142@gmail.com

Specialty section:
This article was submitted to Toxicology, Pollution and the Environment, a section of the journal Frontiers in Environmental Science

Received: *21 February 2022*
Accepted: *07 April 2022*
Published: *26 May 2022*

Citation:
Aziz T, Rasheed S, Shah AH, Nasir H, Fariq A, Jamil A and Jannat S (2022) Bioremediation Potential of Plant-Bacterial Consortia for Chlorpyrifos Removal Using Constructed Wetland. Front. Environ. Sci. 10:880807. doi: 10.3389/fenvs.2022.880807

1 INTRODUCTION

Chlorpyrifos is a broad-spectrum pesticide, extensively used against pests in agricultural (cotton, grains, and fruits) and urban (lawns, commercial, and domestic buildings) settings. It belongs to the organo-phosphate class, under the chemical name O, O-diethyl O-(3, 5, 6-trichloro-2- pyridinyl)-phosphorothioate ($C_9H_{11}C_{l3}NO_3PS$) having low water solubility (2 mg/L) but soluble in organic solvents (Tariq et al., 2007).

Less than 1% of chlorpyrifos (CP) is applied to the target organisms, and most of the remaining chlorpyrifos ends up contaminating the atmosphere, soil, and water (Shi et al., 2019). Therefore,

long-term and irregular applications of chlorpyrifos have resulted in large-scale pollution of soil, groundwater, sediment, and air. It eradicates non-targeted organisms along with the targeted ones including fish, useful arthropods, plants, animals, and humans. Its exposure leads to acetylcholine accumulation leading to high irritation and nerve compression (Gilani et al., 2016). This nerve compression leads to seizures and finally death of insects and mammals. Furthermore, CP and its metabolites are associated with endocrine disruption (Ur-Rehman et al., 2021; Ramos et al., 2019). This non-targeted biocidal activity on these organisms may also be responsible for the loss of biodiversity and overall environmental quality deterioration (Eskenazi et al., 1999; Matthews, 2006; Benachour et al., 2007).

The half-life of CP in water is 50 days (Dores & De-Lamonica-Freire, 2001), while in soil it varies from 60 to 120 days, although it can deviate from 2 weeks to over 1 year, depending on the soil type, climate, and other environmental conditions (Uniyal et al., 2021). Therefore, it has been detected as the second most common pesticide in food and water (John and Shaika, 2015). In aquatic environments, its metabolites, for e.g., 3, 5, 6-trichloropyridinol (TCP) and diethyl chlorpyrifos (DEC) are found, among which TCP has been documented as more toxic, persistent, and mobile than its parent compound CP, by the US-EPA with a half-life ranging from 65 to 360 days in soil (El-Hellow et al., 2013; Sud et al., 2020). The long half-life and antimicrobial nature pose a hurdle for the complete remediation of CP through microorganisms, leading to the accumulation of TCP which results in the loss of soil biodiversity.

There are numerous methods available for detoxification of chlorpyrifos including chemical treatment (Rayment and Higginson, 1992), photodecomposition, volatilization, and incineration, but most of them are not applicable for complete removal of contamination at low concentration due to their inefficiency, expensive, and environmentally unfriendly nature (Abraham et al., 2013). In the past few years, physicochemical (advanced oxidation process) and biological treatment approaches have been widely employed for pesticide removal. Being a cost-effective and eco-friendly method (Walkley and Black, 1934), bioremediation (microbial and phyto-degradation) of environmental pollutants, especially pesticides have been a focus to improve environmental quality in general and soil quality in particular (Nandhini et al., 2021). Chlorpyrifos, previously shown to be resistant to enhanced degradation, has now been proved to undergo enhanced microbe-mediated decay (John and Shaike, 2015). Several bacterial genera, especially *Bacillus* and *Acinetobacter*, *Pseudomonas*, *Flavobacterium*, *Sphingomonas*, and *Agrobacterium* sp. have been reported to biodegrade CP (Alizadeh et al., 2018; Anwar et al., 2009; Pino and Peñuela, 2011; Maya et al., 2011; Fulekar & Geetha, 2008; Yang et al., 2006). Among these reported bacterial species, *Acinetobacter* is reported as an efficient biodegrader of various organophosphates and is able to use those organophosphates as a sole carbon and energy source (Sabit et al., 2011). Therefore, microbial degradation is proven as a major factor determining the fate of organophosphate pesticides in the environment. In addition to microbial degradation, indigenous vegetation is reported to be involved in the degradation of CP. Plants may serve as a means to enhance the bioremediation process of contaminated soils as they can absorb and accumulate a variety of xenobiotics and metals from polluted soils and even degrade them, but the uptake process of organic pollutants and metals by plant roots is affected by several factors (Chandra et al., 2021). The herbaceous plants derived from local wetland species showed good growth when used to biodegrade chlorinated perchloro-ethylene (PCE) or its by-products (Avsar et al., 2007). Sometimes, the extended root system of plants in the soil apparently sustains microbial communities which are responsible for both anaerobic and aerobic biodegradative activity against such contaminants (Amon et al., 2007). These plants enhance the bioremediation process by release of exudates and enzymes such as carbohydrates, carboxylic acid, and amino acids that stimulate both microbial and biochemical activity in surrounding soil and mineralization of pollutants in rhizosphere soil (Tarla et al., 2020). The constant supply of carbon compounds from plant roots to rhizosphere microbes acts as fuels for complex interactions among rhizosphere organisms including those between microorganisms and plants (Daane et al., 2001). This consortium when exists as a land transition between terrestrial and aquatic systems, termed as wetland, plays an important role in the environment rehabilitation through natural decomposition or degradation (Terry and Bañuelos, 1999; Mejáre and Bülow, 2001). In addition to natural wetlands, lab-scale constructed wetland offers an option for *ex situ* bioremediation of contaminants, displaying a considerable potential to mitigate pesticide load including CP (Schulz and Peall, 2001). Plants in constructed wetlands also serve to stabilize the bed surface, increases porosity throughout the wetland volume for aerobic bacteria thriving in the soil, thus contributing toward the biodegradation process. Approximately, 92% removal of different pesticides from wastewater has been reported by Cooper et al. (2016) when a three-stage bio-bed was used as wetland. Retention capability was assessed by Schulz and Peall (2001) when no pesticide was detected in the outlet of a constructed wetland, while Gregoire et al. (2009) mentioned almost 80% removal efficiency for pesticide flux. Tang et al. (2019) reported a 98% CP removal with *Cyperus alternifolius*, *Canna indica*, *Iris pseudacorus*, *Juncus effusus*, and *Typha orientalis* in recirculating vertical flow constructed wetland systems. In a similar study, a constructed wetland (CW) cultivated with *Polygonum punctatum*, *Cynodon* spp., and *Mentha aquatic* showed approximately 98% removal efficiency of CP by Souza et al. (2017).

It has been shown that multiple bacterial species co-exist, not as isolated pockets of pure cultures, but as complex communities known as biofilms, which are capable of maximizing nutrient utilization and redox environments, etc., for example, some members of a community may convert plant exudates into a form available to other member of the community (Nottingham and Messer, 2021). Bacteria were isolated from the rhizosphere of *Phragmites australis* growing in the distillery effluent contaminated site mostly present in the lower region of roots, capable for the bioremediation of distillery wastewater contaminated sites (Chandra & Chaturvedi, 2002).

Taking into account the CP biodegradation process, the major CP metabolite, TCP, being antimicrobial and having a higher

water-soluble nature, makes it more mobile in various environmental matrices (Bose et al., 2021). Furthermore, the produced TCP, as a result of microbial biodegradation, in turn proves lethal for the biodegrading microorganisms resulting not only in decline in the biodegradation efficiency but also in the loss of diversity of soil microbial fauna (Abraham et al., 2013). In addition, studies concerning its fate and degradation in the soil are very limited. So, its further degradation is crucial to alleviate its concentration to prevent its magnification in the environment, thus mitigating the pollution and toxicity posed by TCP in particular and other metabolites of CP in general.

The CP biodegradation efficiency in a proto-type CW is influenced by many independent environmental factors such as bacterial species, nature of the pesticide, hydraulic retention time (HRT), and the plant species (deMatos et al., 2009; Tu et al., 2018). As reported by Romos et al. (2019) for pesticides with short aquatic half-lives, wetland systems require to exhibit much longer residence times (RTs). So, in the present study, the bacterial–plant consortium was used to 1) observe the potential of constructed wetland for bioremediation of CP and its major metabolites, especially TCP using the indigenous plant–bacterial consortium; 2) compare the biodegradation of chlorpyrifos (CP) and its metabolites using wetland vegetation alone and plant–bacterial consortium for possible biodegradation pathway analysis.

2 MATERIALS AND METHODS

2.1 Chemicals and Reagents

Analytical-grade chemicals and reagents were purchased from Sigma-Aldrich, while commercial chlorpyrifos (48% w/v) was purchased from standard commercial suppliers. Minimal salt medium (MSM; pH 6.8–7.0) was prepared using the chemicals as described: dextrose, 1.0 g/L; K_2HPO_4, 7.0 g/L; KH_2PO_4, 2.0 g/L; sodium citrate, 0.5 g/L; $MgSO_4.7H_2O$, 0.1 g/L; and $(NH_4)_2SO_4$, 1.0 g/L (Parmar et al., 2014).

2.1.1 Soil Parameter Analysis

Different parameters of soil such as pH, soil nutrients, soil texture, and soil nitrogen contents were analyzed as described in the following sections.

2.1.2 pH Measurement

In a 100-ml bottle, about 10 g of air-dried soil was weighed, and 25 ml of distilled water was added and shaken for about 1 h. After shaking, the glass electrode was dipped in soil suspension and pH of soil was recorded (Ohtsu et al., 1994).

2.1.3 Organic Matter Determination

To the air-dried and sieved 1 g soil, 10 ml of $k_2Cr_2O_7$ solution (1 N) was added. Then, 20 ml of concentrated H_2SO_4 was added and mixed well, and the mixture was allowed to stand for about half an hour. On the other hand, 25–30 drops of diphenylamine indicator and 0.2 g of sodium fluoride were added to distilled water, and the solution was titrated with ferrous ammonium sulfate solution. A color change from dull green to brilliant green was noticed. A blank sample (without soil) was also run in the same way (Walkely–Black method).

2.1.4 Total Nitrogen

One gram of dried soil was shifted to a digestion tube along with 10 ml of H_2SO_4 and 5 g of catalyst mixture and heated to 100°C with an increase in temperature up to 400°C. The sample was noted, and the cooled sample was shifted into a distillation unit with 40 ml NaOH (40%) and 20 ml boric acid (4%) as an indicator, and any color change was noted. The distillate was titrated with sulfuric acid (0.02 N). A blank sample was also run using the same method (AOAC, 1995).

2.1.5 Total Phosphorous

Dried soil (2.5 g) was added to 0.5 g activated charcoal. To this mixture, 50 ml $NaHCO_3$ (0.5 M) solution was added and shaken for almost half an hour and filtered through the Whatman filter paper. The filtrate was acidified by adding H_2SO_4 (5N) and ascorbic acid with distilled water as an added solvent. A blank sample was also run with the similar conditions and compared with the test sample (Koenig & Johnson, 1942).

2.1.6 Determination of Potassium

Five gram of soil was weighed with 25 ml of ammonium acetate (NH_4OAc) solution, then shaken for five minutes, and filtered through the Whatman filter paper. Potassium extract was measured (Black, 1965).

2.2 Screening and Isolation of Chlorpyrifos-Degrading Bacteria

To isolate the potential bacterial strains, soil samples from selected chlorpyrifos-infested sites were collected from Kotli, Azad Jammu, and Kashmir-Pakistan (33.2896 oN 73.7414 oE). This particular field of choice has been exposed to continuous applications of chlorpyrifos for a considerable period of time. The soil samples were obtained from 5 to 10 cm layers below soil surface as described by Wang et al. (2021). One gram soil sample was mixed in distilled water (10 ml), and 1 ml of the solution was spread on the nutrient agar media through the spread plate method. The plates were incubated at 37°C for 24 h. Morphologically distinct colonies were selected and purified through the streak plate method.

2.2.1 Enrichment of the Bacterial Strains

Isolated strains were selected by subjecting them to the increasing concentrations of chlorpyrifos (250, 500, 750, and 1,000 ug/L). For this purpose, the isolated strains were grown in MSM medium (pH 7.0) on a shaker (IRMECO, I 3000, Germany) at 200 rpm for a period of 72 h as described by Abraham et al. (2013) with some modification. CP degradation was observed in the first set of experiments by bacterial isolates in minimal salt media (MSM) in different concentrations and combinations with CP as the sole carbon source along with positive and negative controls.

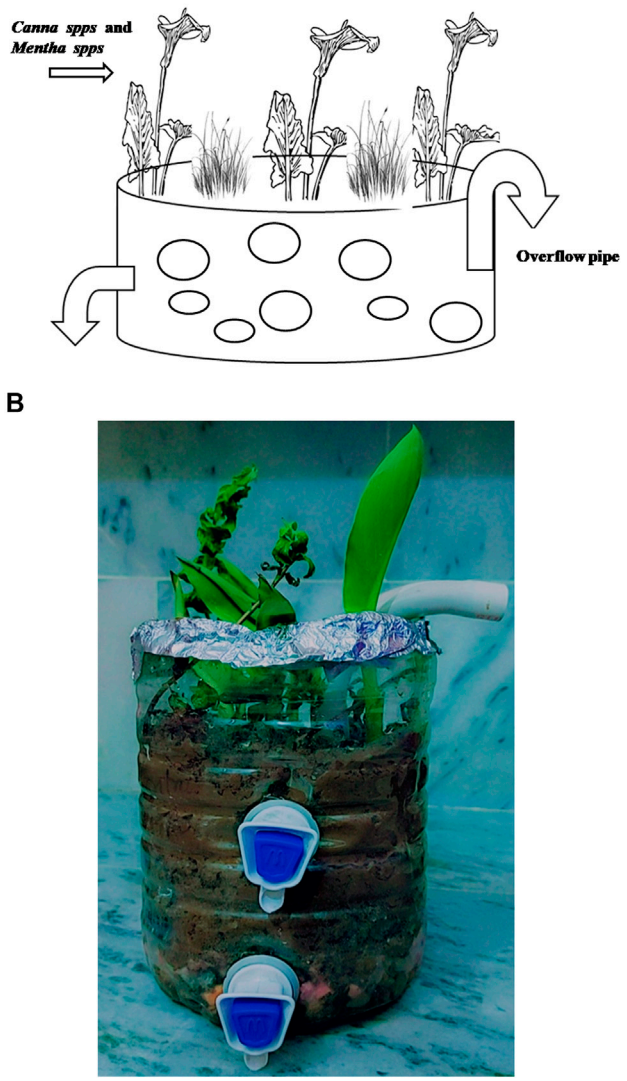

FIGURE 1 | (A) Proto-type constructed wetland. **(B)**. Execution of the prototype constructed wetland.

2.3 Proto-Type Constructed Wetland

A prototype wetland was constructed using pots filled with coarse and fine gravel, coarse gravel (20–30 mm diameter), fine gravel (2–10 mm diameter), sand, and soil from a specific site (**Figures 1A,B**). Prior to hand milling, soil was air-dried and screened through a sieve (2 mm pore size). The local plants, namely, *Canna* spps. and *Mentha* spps. (indigenous mint), were selected for constructed wetland (CW) establishment due to their ubiquitous abundance in the region, especially on the sampling site and along the river. The use of indigenous species is preferred as they do not pose any negative impact on micro-flora and has better survival chance (Farhan et al., 2021). A total of twelve (12) CW arrangements were maintained under different experimental conditions, namely, control, with isolated bacterial strains in soil alone, with plant and soil alone, and with a mix bacterial–plant consortium, and spiked with predefined CP concentrations.

2.3.1 Extraction of Chlorpyrifos From Soil

After a set retention time, the remaining chlorpyrifos was extracted from the CW soils using the toluene method as described by Reddy et al. (2013). A measured quantity of soil (12.5 g) was added to 20 ml toluene in 50-ml Teflon centrifuge tubes and kept on a horizontal shaker (IRMECO, OS 10, Germany) at 150 rpm for 4 h at 25°C. The tubes were then centrifuged at 4000 rpm for 10 min (Reddy et al., 2013). The resultant extract was filtered through anhydrous sodium sulfate (Na_2SO_4). For GC-MS analysis, 1 ml of toluene was added to the filtrate.

2.3.2 GC-MS Analysis for Chlorpyrifos Biodegradation

Degradation of chlorpyrifos to its metabolites was confirmed by GC-MS (Perkin Elmer, MS Claurus SQ 8S, GC Claurus 590, USA) equipped with a HP-5MS capillary column (30 m, 0.025 mm i.d) in helium carrier gas (1 ml per min) and with a splitless injection system. Initially, the column was maintained for 5 min at 90°C and then increased to 290°C at a rate of 8°C per min and held at 290°C for 5 min (Reddy et al., 2013). The injector and interface temperature were kept at 280°C and the source temperature at 250°C. A mass spectrum was obtained by the electron impact (EI) at 70 eV.

3 RESULTS AND DISCUSSION

3.1 Soil Analysis

Soil used in the constructed wetland was analyzed for different parameters such as saturation, pH, texture, organic matter, nitrogen content, phosphorous, and potassium. Soil saturation was 51% with basic pH (8.12) with a texture of clayey loam with 0.059%, 16, and 131 ppm of nitrogen, phosphorous, and potassium contents, respectively.

3.2 Isolation and Identification of Pesticide-Degrading Bacteria

In the present study, a bioremediation system was developed by isolating CP-degrading indigenous bacterial cultures, and their subsequent application in the indigenous plants using constructed wetland (CW). A total of two morphologically distinct CP-tolerant bacterial strains MBT035 and MBT037 were isolated and identified through ribotyping (16s rRNA) by Macrogen (Macrogen Inc., South Korea) as *Acinetobacter baumanni* and *Bacillus cibi*, respectively.

The CW establishment was applied in two combinations: a) soil and plants only and b) soil, plant, and bacterial consortium, to observe the effect of the bacterial isolate alone, plants alone, and in consortium. The CP removal efficiency in constructed wetland was analyzed by GC-MS, in which MS spectra of the extracted samples showed an effective biodegradation using constructed wetland when cultivated with indigenous *Canna* spps. and

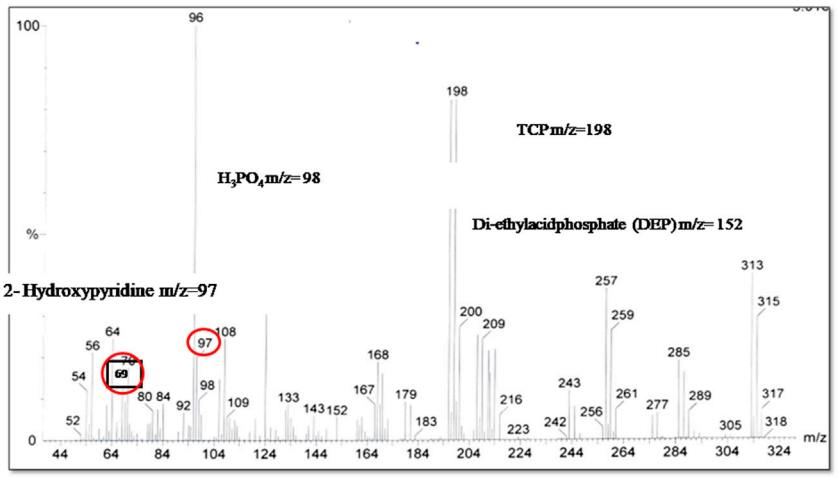

FIGURE 2 | GC-MS chromatograph for wetland with indigenous *Canna* spps. and *Mentha* spps.

Mentha spps. and bioaugmented with *Acinetobacter baumanni* and *Bacillus cibi* (CP-degrading bacterial isolates). By observing the chromatograph, it is evident that chlorpyrifos was metabolized to produce various intermediates of different m/z in various combinations of CWs, that is, plant alone and in the bacterial–plant consortium. The results are described in the following sections:

3.2.1 Wetland With Indigenous Plants

The wetland vegetation, *Cannas* spps. and *Mentha* spps., in a CW was used to monitor the biodegradation of CP through the phyto-degradation process. Several characteristic peaks of different metabolites of chlorpyrifos's biodegradation were observed in the GC-MS chromatogram. Among them, the most documented intermediate and degradation product, TCP (3, 5, 6-tricloro-2-piridinol) was detected, which was confirmed by the m/z peak of m/z = 198 (**Figure 2**).This product has already been documented in case of bacterial biodegradation by various researchers (Abraham et al., 2013; Zhu et al., 2019). But, it is also reported as a more toxic pollutant than the parent compound CP in the environment, especially for the microbes in the soil (antimicrobial agent). This may be a possible reason for resistance to enhanced microbial biodegradation for CP biodegradation. In the current study, TCP was also reported when indigenous plant vegetation was used. But, a good growth response to this toxic TCP was shown by the wetland vegetation. This toxic antimicrobial compound seemed either non-toxic to the indigenous plants or the plants might have coped with the toxicity posed by this particular intermediate of CP biodegradation. The study endorses the hypothesis of plant degradation potential for TCP.

Further degradative product, diethyl acid phosphate (DEP) with a molecular ion at m/z 152.98 $[M - 1]^-$ was also detected which was further metabolized into a molecule of m/z = 98, identified as H_3PO_4. These results were found in accordance with Shi et al. (2019).

TCP was further degraded to form 2-hydroxypyridine (m/z = 97) with deprotonated molecular ions at m/z = 69 (M-H)− as described by Uniyal et al. (2021).The results were found in accordance with Tang et al. (2019) who reported a decrease in the half-life of TCP when *Canna indica* was used as wetland vegetation with approximately 33 percent removal. These results showed efficient biodegradation of CP and its metabolites, especially TCP in proto-type constructed wetland when *Canna* and *Mentha* spps. were used.

3.2.2 Soil, Plant, and Bacterial Consortium

In the second phase of the experimentation setup of the plant–bacterial consortium, when wetland vegetation, i.e., *Canna* spps. and *Mint* spps., was used along with the indigenous bacterial strains, a CP metabolite with m/z = 212 was detected corresponding to TMP (3, 5, 6-trichloro-2-methoxypyridine). In addition to TMP, another metabolite (m/z = 169) was also detected and found out to be diethyl-thio-phosphate (DETP) a CP hydrolysis product mentioned by Bicker et al. (2005) in his studies (**Figure 3**). As described by Chen et al. (2012), the degrading microorganisms tend to metabolize chlorpyrifos by hydrolysis to form diethyl-thio-phosphoric acid (DETP) along with TCP. On the other hand, the bacterial–plant consortium showed good growth performance, depicting a good consortium establishment between plants and isolated strains (**Figure 4**). When metabolites of the biodegradation in both the experimental designs, i.e., wetland vegetation alone and plant–bacterial consortium, were compared, this TCP was not detected in plant–bacterial association rather TMP was detected. It is already described by Shi et al. (2019) that TCP can further generate TMP. The transient appearance of TCP and its subsequent degradation to TMP may be attributed to the mutual interaction and biodegradation ability of the plant–bacterial consortium. It may further be inferred from the GC-MS chromatogram that the formation of TCP may be either bypassed, or it was synthesized for a very short period of time and immediately biodegraded by the plant part of the

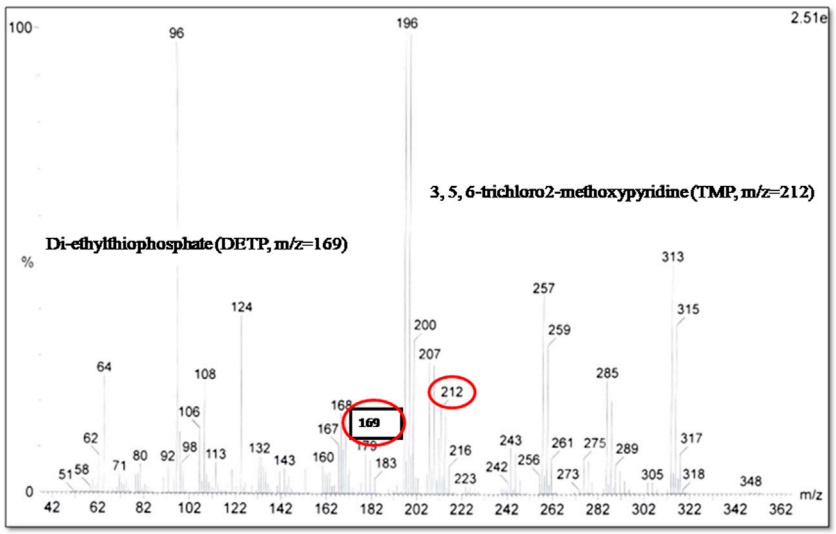

FIGURE 3 | GC chromatogram of the chlorpyrifos metabolites formed in the microbial–plant consortium.

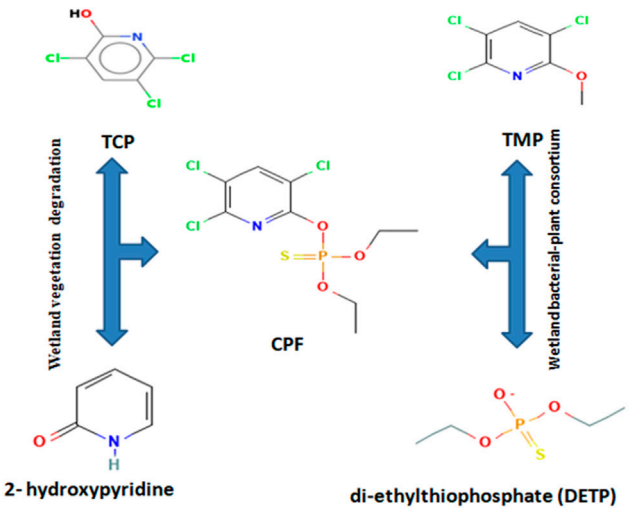

FIGURE 4 | Proto-type constructed wetland with indigenous bacterial strains and *Canna* and *Mentha* spps.

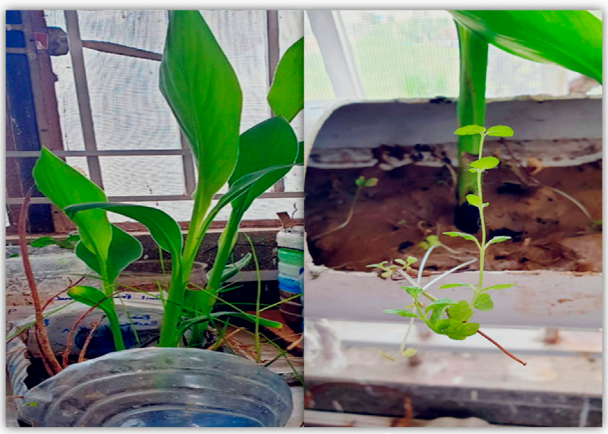

FIGURE 5 | Proposed biodegradative pathway for chlorpyrifos in wetland vegetation and bacterial–plant association.

consortium. The synthesis of TMP in place of TCP was found against the findings of Chen et al. (2012) as in most of the cases reported to date, the bacterial isolates tended to transform chlorpyrifos to yield TCP, which in turn accumulated in the batch cultures or soils and posed toxic effects on the microbial culture. So, the enhanced microbial degradation could not occur owing to its antimicrobial properties (Chen et al., 2012).

During the study, a good adaptation of the bacterial isolates to the applied CP was observed in the plant–bacterial consortium, since the bacterial number increased with increasing concentration of the pesticide to the soil. This could be reasoned to the absence of TCP in the bacterial–plant consortium which may be the reason for prolonged survival and good growth of the bacterial–plant consortium. An overall 96% of CP removal was observed in the bacterial–plant consortium. These results were found against the findings of Chen et al. (2012) who reported formation of TCP along with DETP.

Thus, the bacterial augmentation in the experimental soil with wetland vegetation eventually caused higher degradation, suggesting the compatibility of the augmented culture with the indigenous wetland vegetation. The dominant removal process was reported to occur through microbial degradation in wetland technology as described by Liu et al. (2019). In a similar study, Singh et al. (2003) observed maximum biodegradation of CP using *Pseudomonas putida* after 90 days in basic soils. These

results were also found in accordance with Souza et al. (2017) and Uniyal et al. (2021).

3.3 Proposed Biodegradation Pathway for CP

The insecticide CPF mostly undergoes hydrolysis to 3, 5, 6-trichloro-2-pyridinol (TCP), diethyl-thio-phosphoric acid (DETP), and negligible amounts of other intermediate products (Das and Adhya, 2015).TCP is a major metabolite of CP, and under all pathways, it is observed to undergo ring cleavage to form smaller organic and inorganic molecules as described by Sud et al. (2020). The degradation pathway of chlorpyrifos begins with cleavage of the phosphorus ester bond to yield 3, 5, 6-trichloro-2-pyridinol (TCP) (Lee et al., 2012). Based on the GC-MS analysis, the possible degradation pathway in case of wetland vegetation is proposed via hydrolysis as: CP (m/z = 358 > TCP (m/z = 198) >2- hydroxypyridine (m/z = **198)** > 69. While in case of bacterial–plant association, CP (m/z = 358)>TMP (m/z = 212>TCP-2H (m/z = 196) > DETP (m/z = 169) is suggested (**Figure 5**).

4 CONCLUSION

The present study was designed to observe the potential of constructed wetland using indigenous bacterial–plant association for the chlorpyrifos biodegradation. Therefore, a bioremediation system was developed by isolating CP-degrading indigenous bacterial cultures and their subsequent application in couple with indigenous plants using constructed wetland.

1. Two morphologically distinct CP-biodegrading bacterial strains *Acinetobacter baumanni* (MBT035) and *Bacillus cibi* (MBT037) were isolated and purified.
2. A pro-type constructed wetland (CW) with indigenous *Canna* spps. and *Mentha* spps. and bioaugmented with *Acinetobacter baumanni* and *Bacillus cibi* showed enhanced biodegradation of chlorpyrifos (CP) up to 96%.
3. TCP (3, 5, 6-tricloro-2-piridinol, m/z = 198) was observed when indigenous plant vegetation was used in CW which was further degraded to form 2-hydroxypyridine (m/z = 97) with de-protonated molecular ions at m/z = 69 (M-H)–.
4. In case of the bacterial–plant consortium, instead of TCP, a 3, 5, 6-trichloro-2-methoxypyridine (TMP, m/z = 212) was detected along with diethyl-thio-phosphate (DETP, m/z = 169).
5. The results of the present study showed good potential constructed wetland with *Canna* spps. and *Mentha* spps. and bioaugmented with *Acinetobacter baumanni* and *Bacillus cibi.*

5 FUTURE PROSPECTS

The current study promotes further research on plant–microbe joint combined remediation and examines the different behaviors. Following future prospects may be considered:

1. The fate of the other metabolites of CP and their toxicity may be monitored in the plants and animal species thriving in soil or environment.
2. Attempts could be made to optimize the bacterial–plant consortium for maximum and efficient bioremediation of the CP as well other environmental contaminants.

DATA AVAILABILITY STATEMENT

The original contributions presented in the study are included in the article/Supplementary Materials, further inquiries can be directed to the corresponding author.

AUTHOR CONTRIBUTIONS

TA performed the experiments and wrote the manuscript. SR designed the experiments, administered the project, and wrote the manuscript. AS conceived the idea and designed the experiments. HN assisted in metabolite analysis. AF assisted in manuscript writing and editing. AJ assisted in the analysis of the results and review of the manuscript. SJ reviewed the manuscript.

ACKNOWLEDGMENTS

The authors are thankful to the technical support provided by the National University of Sciences and Technology (NUST), Islamabad, Pakistan.

REFERENCES

Abraham, J., Shanker, A., and Silambarasan, S. (2013). Role of Gordonia Sp JAAS1 in Biodegradation of Chlorpyrifos and its Hydrolysing Metabolite 3,5,6-Trichloro-2-Pyridinol. *Lett. Appl. Microbiol.* 57, 510–516. doi:10.1111/lam.12141

Amon, J. P., Agrawal, A., Shelley, M. L., Opperman, B. C., Enright, M. P., Clemmer, N. D., et al. (2007). Development of a Wetland Constructed for the Treatment of Groundwater Contaminated by Chlorinated Ethenes. *Ecol. Eng.* 30, 51–66. doi:10.1016/j.ecoleng.2007.01.008

Anwar, S., Liaquat, F., Khan, Q. M., Khalid, Z. M., and Iqbal, S. (2009). Biodegradation of Chlorpyrifos and its Hydrolysis Product 3,5,6-Trichloro-2-Pyridinol by Bacillus Pumilus Strain C2A1. *J. Hazard. Mater.* 168, 400–405. doi:10.1016/j.jhazmat.2009.02.059

Aoac, A. (1995). *Official Methods of Analysis*. 16th Ed. Washington DC, USA: Association of official analytical chemists. Sci. Educ.

Avsar, Y., Tarabeah, H., Kimchie, S., and Ozturk, I. (2007). Rehabilitation by Constructed Wetlands of Available Wastewater Treatment Plant in Sakhnin. *Ecol. Eng.* 29, 27–32. doi:10.1016/j.ecoleng.2006.07.008

Benachour, N., Moslemi, S., Sipahutar, H., and Seralini, G. (2007). Cytotoxic Effects and Aromatase Inhibition by Xenobiotic Endocrine Disrupters Alone and in

Combination☆. *Toxicol. Appl. Pharmacol.* 222, 129–140. doi:10.1016/j.taap.2007.03.033

Bicker, W., Lämmerhofer, M., and Lindner, W. (2005). Determination of Chlorpyrifos Metabolites in Human Urine by Reversed-Phase/weak Anion Exchange Liquid Chromatography-Electrospray Ionisation-Tandem Mass Spectrometry. *J. Chromatogr. B* 822, 160–169. doi:10.1016/j.jchromb.2005.06.003

Black, C. A. (1965). *Methods of Soil Analysis Part I Am. Soc.* Madison, Wis.: American Society of Agronomy.

Bose, S., Kumar, P. S., and Vo, D.-V. N. (2021). A Review on the Microbial Degradation of Chlorpyrifos and its Metabolite TCP. *Chemosphere* 283, 131447. doi:10.1016/j.chemosphere.2021.131447

Chandra, R., Bharagava, R. N., and Yadav, S. (2021). Wetland Rhizosphere Bacteria: An Eco-Friendly Tool for Bioremediation of Environmental Pollutants.

Chandra, R., and Chaturvedi, S. (2002). "Isolation and Characterization of Bacterial Population from Rhizosphere of *Cyperus Papyrus* Growing in Distillery Effluent Contaminated Site," in 2 nd International conference on plants and environmental pollution held on 2002 at NBRI (India: Lucknow). Abstract no. SIII/P-5.

Chen, S., Liu, C., Peng, C., Liu, H., Hu, M., and Zhong, G. (2012). Biodegradation of Chlorpyrifos and its Hydrolysis Product 3,5,6-Trichloro-2-Pyridinol by a New Fungal Strain Cladosporium Cladosporioides Hu-01. *PLoS One* 7, e47205. doi:10.1371/journal.pone.0047205

Cooper, R. J., Fitt, P., Hiscock, K. M., Lovett, A. A., Gumm, L., Dugdale, S. J., et al. (2016). Assessing the Effectiveness of a Three-Stage On-Farm Biobed in Treating Pesticide Contaminated Wastewater. *J. Environ. Manage.* 181, 874–882. doi:10.1016/j.jenvman.2016.06.047

Daane, L. L., Harjono, I., Zylstra, G. J., and Häggblom, M. M. (2001). Isolation and Characterization of Polycyclic Aromatic Hydrocarbon-Degrading Bacteria Associated with the Rhizosphere of Salt Marsh Plants. *Appl. Environ. Microbiol.* 67, 2683–2691. doi:10.1128/aem.67.6.2683-2691.2001

Das, S., and Adhya, T. K. (2015). Degradation of Chlorpyrifos in Tropical rice Soils. *J. Environ. Manage.* 152, 36–42. doi:10.1016/j.jenvman.2015.01.025

Dores, E. F. G. d. C., and De-Lamonica-Freire, E. M. (2001). Contaminação Do ambiente aquático por pesticidas. Estudo de caso: águas usadas para consumo humano em Primavera Do Leste, Mato Grosso - análise preliminar. *Quím. Nova* 24, 27–36. doi:10.1590/S0100-40422001000100007

El-Helow, E. R., Badawy, M. E. I., Mabrouk, M. E. M., Mohamed, E. A. H., and El-Beshlawy, Y. M. (2013). Biodegradation of Chlorpyrifos by a Newly IsolatedBacillus subtilisStrain, Y242. *Bioremediation J.* 17, 113–123. doi:10.1080/10889868.2013.786019

Eskenazi, B., Bradman, A., and Castorina, R. (1999). Exposures of Children to Organophosphate Pesticides and Their Potential Adverse Health Effects. *Environ. Health Perspect.* 107, 409–419. doi:10.1289/ehp.99107s3409

Farhan, M., Ahmad, M., Kanwal, A., Butt, Z. A., Khan, Q. F., Raza, S. A., et al. (2021). Biodegradation of Chlorpyrifos Using Isolates from Contaminated Agricultural Soil, its Kinetic Studies. *Sci. Rep.* 11, 1–14. doi:10.1038/s41598-021-88264-x

Fulekar, M. H., and Geetha, M. (2008). Bioremediation of Chlorpyrifos by *Pseudomonas aeruginosa* Using Scale up Technique. *J. Appl. Biosci.* 12, 657–660.

Gilani, R. A., Rafique, M., Rehman, A., Munis, M. F. H., Rehman, S. U., and Chaudhary, H. J. (2016). Biodegradation of Chlorpyrifos by Bacterial genusPseudomonas. *J. Basic Microbiol.* 56, 105–119. doi:10.1002/jobm.201500336

Gregoire, C., Elsaesser, D., Huguenot, D., Lange, J., Lebeau, T., Merli, A., et al. (2009). Mitigation of Agricultural Nonpoint-Source Pesticide Pollution in Artificial Wetland Ecosystems - A Review. *Clim. Change Intercropping, Pest Control. Beneficial Microorg.*, 293–338. doi:10.1007/978-90-481-2716-0_11

John, E. M., and Shaike, J. M. (2015). Chlorpyrifos: Pollution and Remediation. *Environ. Chem. Lett.* 13, 269–291. doi:10.1007/s10311-015-0513-7

Koenig, R., and Johnson, C. (1942). Colorimetric Determination of Phosphorus in Biological Materials. *Ind. Eng. Chem. Anal. Ed.* 14, 155–156. doi:10.1021/i560102a026

Lee, K. Y., Strand, S. E., and Doty, S. L. (2012). Phytoremediation of Chlorpyrifos byPopulusandSalix. *Int. J. Phytoremediation* 14, 48–61. doi:10.1080/15226514.2011.560213

Liu, T., Xu, S., Lu, S., Qin, P., Bi, B., Ding, H., et al. (2019). A Review on Removal of Organophosphorus Pesticides in Constructed Wetland: Performance, Mechanism and Influencing Factors. *Sci. Total Environ.* 651, 2247–2268. doi:10.1016/j.scitotenv.2018.10.087

Matos, A., Freitas, W., and Lo Monaco, P. (2009). Capacidade extratora de diferentes espécies vegetais cultivadas em sistemas alagados utilizados no tratamento de águas residuárias da suinocultura. *Ambi-Agua* 4, 31–45. doi:10.4136/ambi-agua.84

Matthews, G. A. (2006). *Pesticides: Health, Safety and the Environment*. Chichester, UK: Blackwell Publishing.

Maya, K., Singh, R. S., Upadhyay, S. N., and Dubey, S. K. (2011). Kinetic Analysis Reveals Bacterial Efficacy for Biodegradation of Chlorpyrifos and its Hydrolyzing Metabolite TCP. *Process Biochem.* 46, 2130–2136. doi:10.1016/j.procbio.2011.08.012

Mejáre, M., and Bülow, L. (2001). Metal-binding Proteins and Peptides in Bioremediation and Phytoremediation of Heavy Metals. *Trends Biotechnol.* 19, 67–73. doi:10.1016/S0167-7799(00)01534-1

Nandhini, A. R., Muthukumar, H., and Gummadi, S. N. (2021). Chlorpyrifos in Environment and Foods: A Critical Review of Detection Methods and Degradation Pathways. *Environ. Sci. Process. Impacts*. doi:10.1039/D1EM00178G

Nottingham, E. R., and Messer, T. L. (2021). A Literature Review of Wetland Treatment Systems Used to Treat Runoff Mixtures Containing Antibiotics and Pesticides from Urban and Agricultural Landscapes. *Water* 13, 3631. doi:10.3390/w13243631

Parmar, K. J., Tomar, R. S., Parakhia, M. V., Malviya, B. J., Rathod, V. M., Thakkar, J. R., et al. (2014). Isolation and Bio-Analytical Characterization of Chloropyrifos Degrading Bacteria. *J.Cell Tissue Res.* 14, 4641.

Pino, N., and Peñuela, G. (2011). Simultaneous Degradation of the Pesticides Methyl Parathion and Chlorpyrifos by an Isolated Bacterial Consortium from a Contaminated Site. *Int. Biodeterioration Biodegradation* 65, 827–831. doi:10.1016/j.ibiod.2011.06.001

Ramos, A., Whelan, M. J., Guymer, I., Villa, R., and Jefferson, B. (2019). On the Potential of On-Line Free-Surface Constructed Wetlands for Attenuating Pesticide Losses from Agricultural Land to Surface Waters. *Environ. Chem.* 16, 563–576. doi:10.1071/en19026

Rayment, G. E., and Higginson, F. R. (1992). *Australian Laboratory Handbook of Soil and Water Chemical Methods*. c1992 xvii, 330 p.. Melbourne: Inkata press.

Reddy, A., Madhavi, V., Reddy, K. G., and Madhavi, G. (2013). Remediation of Chlorpyrifos Contaminated Soils by Laboratory-Synthesized Zero-Valent Nano Iron Particles: Effect of pH and Aluminium Salts. *J. Chem.* 2013, 1–7. doi:10.1155/2013/521045

Sabit, H. H., Said, O. A., Shamseldin, A. F., and &Elsayed, K. (2011). Molecular Identification of Acinetobacter Isolated from Egyptian Dumpsite as Potential Bacteria to Degrade Malathion. *Int. J. Acad. Res.* 3, 84–90.

Schulz, R., and Peall, S. K. C. (2001). Effectiveness of a Constructed Wetland for Retention of Nonpoint-Source Pesticide Pollution in the Lourens River Catchment, South Africa. *Environ. Sci. Technol.* 35, 422–426. doi:10.1021/es0001198

Shi, T., Fang, L., Qin, H., Chen, Y., Wu, X., and Hua, R. (2019). Rapid Biodegradation of the Organophosphorus Insecticide Chlorpyrifos by Cupriavidus Nantongensis X1T. *Ijerph* 16, 4593. doi:10.3390/ijerph16234593

Singh, B. K., Walker, A., Morgan, J. A. W., and Wright, D. J. (2003). Effects of Soil pH on the Biodegradation of Chlorpyrifos and Isolation of a Chlorpyrifos-Degrading Bacterium. *Appl. Environ. Microbiol.* 69, 5198–5206. doi:10.1128/AEM.69.9.5198-5206.2003

Souza, T. D. D., Borges, A. C., Matos, A. T. D., Mounteer, A. H., and Queiroz, M. E. L. R. d. (2017). Removal of Chlorpyrifos Insecticide in Constructed Wetlands with Different Plant Species. *Rev. Bras. Eng. Agríc. Ambient.* 21, 878–883. doi:10.1590/1807-1929/agriambi.v21n12p878-883

Sud, D., Kumar, J., Kaur, P., and Bansal, P. (2020). Toxicity, Natural and Induced Degradation of Chlorpyrifos. *J. Chil. Chem. Soc.* 65, 4807–4816. doi:10.4067/S0717-97072020000204807

Tang, X.-Y., Yang, Y., McBride, M. B., Tao, R., Dai, Y.-N., and Zhang, X.-M. (2019). Removal of Chlorpyrifos in Recirculating Vertical Flow Constructed Wetlands

with Five Wetland Plant Species. *Chemosphere* 216, 195–202. doi:10.1016/j.chemosphere.2018.10.150

Tariq, M. I., Afzal, S., Hussain, I., and Sultana, N. (2007). Pesticides Exposure in Pakistan: a Review. *Environ. Int.* 33, 1107–1122. doi:10.1016/j.envint.2007.07.012

Tarla, D. N., Erickson, L. E., Hettiarachchi, G. M., Amadi, S. I., Galkaduwa, M., Davis, L. C., ..Nurzhanova, A., and Pidlisnyuk, V. (2020). Phytoremediation and Bioremediation of Pesticide-Contaminated Soil. *Appl. Sci.* 10 (4), 1217. doi:10.3390/app10041217

Terry, N., and Bañuelos, G. (1999). *Phytoremediation of Contaminated Soil and Water*. Lewis Publishers is an imprint of CRC Press LLC. Printed in the United States of Florida, America. doi:10.1201/9780367803148

Tu, Y., Jiang, L., and Li, H. (2018). Non-persistent Pesticides Removal in Constructed Wetlands. *AIP Conf. Proc.* 1944, 020045. AIP Publishing LLC. doi:10.1063/1.5029761

Ubaid Ur Rahman, H., Asghar, W., Nazir, W., Sandhu, M. A., Ahmed, A., and Khalid, N. (2021). A Comprehensive Review on Chlorpyrifos Toxicity with Special Reference to Endocrine Disruption: Evidence of Mechanisms, Exposures and Mitigation Strategies. *Sci. Total Environ.* 755, 142649–649. doi:10.1016/j.scitotenv.2020.142649

Uniyal, S., Sharma, R. K., and Kondakal, V. (2021). New Insights into the Biodegradation of Chlorpyrifos by a Novel Bacterial Consortium: Process Optimization Using General Factorial Experimental Design. *Ecotoxicology Environ. Saf.* 209, 111799–799. doi:10.1016/j.ecoenv.2020.111799

Walkley, A., and Black, I. A. (1934). An Examination of the Degtjareff Method for Determining Soil Organic Matter, and a Proposed Modification of the Chromic Acid Titration Method. *Soil Sci.* 37, 29–38. doi:10.1097/00010694-193401000-00003

Wang, Y., Zhang, W., Zhang, Z., Wang, W., Xu, S., and He, X. (2021). Isolation, Identification and Characterization of Phenolic Acid-degrading Bacteria from Soil. *J. Appl. Microbiol.* 131 (1), 208–220. doi:10.1111/jam.14956

Yang, C., Liu, N., Guo, X., and Qiao, C. (2006). Cloning of Mpd Gene from a Chlorpyrifos-Degrading Bacterium and Use of This Strain in Bioremediation of Contaminated Soil. *FEMS Microbiol. Lett.* 265, 118–125. doi:10.1111/j.1574-6968.2006.00478.x

Zhu, J., Zhao, Y., and Ruan, H. (2019). Comparative Study on the Biodegradation of Chlorpyrifos-Methyl by *Bacillus Megaterium* CM-Z19 and *Pseudomonas syringae* CM-Z6. *Acad. Bras. Ciênc.* 91, e20180694. doi:10.1590/0001-3765201920180694

Conflict of Interest: The authors declare that the research was conducted in the absence of any commercial or financial relationships that could be construed as a potential conflict of interest.

Publisher's Note: All claims expressed in this article are solely those of the authors and do not necessarily represent those of their affiliated organizations, or those of the publisher, the editors, and the reviewers. Any product that may be evaluated in this article, or claim that may be made by its manufacturer, is not guaranteed or endorsed by the publisher.

frontiers | Frontiers in Environmental Science

ORIGINAL RESEARCH
published: 01 June 2022
doi: 10.3389/fenvs.2022.830589

Pesticides are Substantially Transported in Particulate Phase, Driven by Land use, Rainfall Event and Pesticide Characteristics—A Runoff and Erosion Study in a Small Agricultural Catchment

Meindert C. Commelin[1], Jantiene E. M. Baartman[1], Paul Zomer[2], Michel Riksen[1] and Violette Geissen[1]*

[1]Soil Physics and Land Management Group, Wageningen University, Wageningen, Netherlands, [2]Wageningen Food Safety Research, Wageningen University and Research, Wageningen, Netherlands

OPEN ACCESS

Edited by:
Jiehong Guo,
University of Minnesota Twin Cities,
United States

Reviewed by:
Cláudio Ernesto Taveira Parente,
Federal University of Rio de Janeiro,
Brazil
Rafael Muñoz-Carpena,
University of Florida, United States

***Correspondence:**
Meindert C. Commelin
meindert.commelin@wur.nl

Specialty section:
This article was submitted to Toxicology, Pollution and the Environment, a section of the journal Frontiers in Environmental Science

Received: 07 December 2021
Accepted: 09 May 2022
Published: 01 June 2022

Citation:
Commelin MC, Baartman JEM, Zomer P, Riksen M and Geissen V (2022) Pesticides are Substantially Transported in Particulate Phase, Driven by Land use, Rainfall Event and Pesticide Characteristics—A Runoff and Erosion Study in a Small Agricultural Catchment. Front. Environ. Sci. 10:830589. doi: 10.3389/fenvs.2022.830589

Agriculture on sloping lands is prone to processes of overland flow and associated soil detachment, transportation, and deposition. The transport of pesticides to off-target areas related to runoff processes and soil erosion poses a threat of pollution to the downstream environment. This study aimed to quantify transport of pesticides both dissolved in water and in the particulate phase in transported sediments. Particulate phase transport of pesticides on short temporal time scales from agricultural fields is scarcely studied. During two growing seasons (2019 and 2020) rainfall—runoff events were monitored in a catchment of 38.5 ha. We selected 30 different pesticides and one metabolite based on interviews with the farmers on the application pattern. Concentrations for these 31 residues were analyzed in runoff water (dissolved phase–DP) and sediment (particulate phase–PP) and in soil samples taken in the agricultural fields. In all runoff events active substances (AS) were detected. There was a clear difference between DP and PP with 0–5 and 8–18 different AS detected in the events, respectively. Concentrations in PP were higher than in DP, with factors ranging from 12 to 3,700 times. DP transport mainly occurs in the first days after application (69% within 10 days), and PP transport occurs over the long term with 90% of transported mass within 100 days after application. Potato cultivation was the main source of runoff, erosion, and pesticide transport. Cereals and apples with grassed inter-rows both have a very low risk of pesticide transport during overland flow. We conclude that for arable farming on sloping lands overland transport of pesticide in the particulate phase is a substantial transport pathway, which can contribute to pollution over longer time periods compared to transport in water. This process needs to be considered in future assessments for pesticide fate and environmental risk.

Keywords: erosion, pesticide transport, particulate phase, event-based monitoring, runoff

1 INTRODUCTION

The use of pesticides in agriculture is one of the key components in the rapid increase of food production in the past decades. In the coming decades, sustaining food security for the growing world population is one of the main global challenges (FAO, IFAD, UNICEF, WFP, WHO 2020). Aktar et al. (2009) stated that without pesticide use, the current quantity and quality of global food production cannot be sustained. However, the downside of the extensive use of pesticides is that it poses threats to human health and the environment (Bevan et al., 2017; Casado et al., 2019; Silva et al., 2019), including significant biodiversity loss (Geiger et al., 2010; Lanz et al., 2018). On average 3.14 kg ha^{-1} of pesticides was applied on cropland in the EU-28 in 2018 (FAO 2020). Beside reaching the target pest, these pesticides can be pollutants to other parts of on- and offsite ecosystems (Boivin and Poulsen 2017; Topping et al., 2020). Although many improvements in pesticide type, application efficiency and mitigation are made, still uncertainties and threats exist on off-target effects of pesticide use (Sattler et al., 2007; Lechenet et al., 2017), especially in cases of farming on sloping land.

Agriculture on sloping lands is prone to processes of overland flow and associated soil detachment, transportation, and deposition. For the EU the average soil loss on arable land, which covers 28% of the surface area, has been estimated at 2.46 t/ha per year (Panagos et al., 2015), but locally it can exceed 50 t/ha depending on rainfall erosivity, slope, erodibility of the soil, land use and land management. Soil erosion itself is a threat due to the loss of fertile topsoil which is needed for crop cultivation. However, the transport of pesticides to off-target areas related to runoff processes and soil erosion poses another threat of pollution to the downstream environment (Tang et al., 2012). Runoff and erosion events are often characterized by short high intensity peaks (Lefrancq et al., 2017) which can contain high concentrations of pesticides in both runoff water and transported sediment (Peruzzo, Porta, and Ronco 2008; Climent et al., 2019). Multiple studies investigating the pesticide pollution of headwaters and rivers show increased concentrations of pesticides in water after runoff events (Peruzzo et al., 2008; Lefrancq et al., 2017; Casado et al., 2019; Climent et al., 2019; Halbach et al., 2021), often exceeding the regulatory limits. In the current legal framework in the EU, the limits in water are 0.1 μg L^{-1} for single substances and 0.5 μg L^{-1} for combined mixtures (European directive 2013/39/EC). However, threshold values for soils and eroding sediments as well as sediment in surface water bodies are not set and are complex to derive due to the wide diversity in active substances, toxicity and possible degradation (Silva et al., 2019; Geissen et al., 2021).

In sloping areas, soil erosion occurs alongside runoff, and beside the dissolved phase (DP) the particulate phase (PP) is a transport pathway for pesticides. The contribution of particulate phase transport to total transport of pesticides, and the potential risk this could pose for off-site locations, is currently not well understood. Payraudeau and Gregoire (2012) concluded that dissolved and particulate transport of pesticides in rapid flow processes, mainly via overland flow, can function as a main transport pathway for pesticides to open water. Enrichment processes during rainfall events and erosion cause the transported sediment to contain higher amounts of pollutants than the surrounding soils (Ghadiri and Rose, 1991a) which increases off-site pollution risk (Ghadiri and Rose, 1991b). In a review of the transport characteristics of pesticides (Wauchope 1978), erosion related transport of pesticides was stated to be relevant only for strongly sorbing pesticides and main transport risk was by water. Less water-soluble pesticides with a higher sorption coefficient were introduced into the market to avoid leaching to groundwater and overland transport. Several widely used pesticides adsorb strongly to sediment and organic materials (Tang et al., 2012) and are thus classified as slightly mobile or non-mobile substances (McCall et al., 1980).

Synthesizing the results presented in multiple studies in the past decade, reveals that the contribution of pesticide transport in PP versus DP is unclear and various studies are contradicting. On the one hand, several studies on field scale conclude that PP transport is of minor importance (often <5% of the total load) (Maillard et al., 2011; Oliver et al., 2012; Todorovic et al., 2014; Napoli et al., 2016). However, other plot scale and flume experiments show potentially high transport of pesticides in PP (Yang, et al., 2015; Melland et al., 2016; Bento et al., 2018). Yang et al. (2015a) observed a natural rainfall event 2 days after pesticide application and detected DP concentrations of 0.7–1.3 μg L^{-1} and PP content of 40–60 μg L^{-1}. The contribution of PP to total observed pesticide transport was 71%. At larger scales, concentrations of pesticides in total suspended solids (TSS) in rivers, and in river or stream sediments are often much higher than in water (Masiá et al., 2013; Cruzeiro et al., 2016; Climent et al., 2019), which is related to significant transport in the particulate phase.

Within the mentioned studies there is variation in design how the process of overland transport of pesticides is studied. On small plot scale, experiments are usually done within several days after pesticide applications. These experiments are on arable soils comparing tillage (Todorovic et al., 2014) or residue cover effects on transport (Melland et al., 2016; Bento et al., 2018). Field scale studies include vineyard or fruit tree orchards (Oliver et al., 2012; Maillard and Imfeld 2014; Napoli et al., 2016), but no results for arable land on field scale are known to the authors. Lastly several studies investigated pesticide transport dissolved in water and in TSS of river systems throughout the growing season (Masiá et al., 2013; Cruzeiro et al., 2016; Climent et al., 2019). However, runoff, erosion and related pesticide transport processes occur on short temporal scale and evaluation on annual basis is not sufficient to understand the exact scope of this transport (Tang et al., 2012; Lefrancq et al., 2017). On the other hand, the spatial scale of erosion processes demands to be analyzed on field and small catchment scale (Cerdan et al., 2004). Plot experiments can indicate effects but cannot include larger scale connectivity, heterogeneity and topography effects (Boardman and Evans 2020). To gain a further understanding of PP and DP transport of pesticides, field observations that include different land use types are needed.

In this study multiple season field scale observations were done to quantify the contribution of PP transport of pesticides in a small agricultural catchment. Observations were done for multiple land uses and active substances (AS). We hypothesize that PP pesticide transport will contribute substantially to total overland transport of pesticides from small agricultural

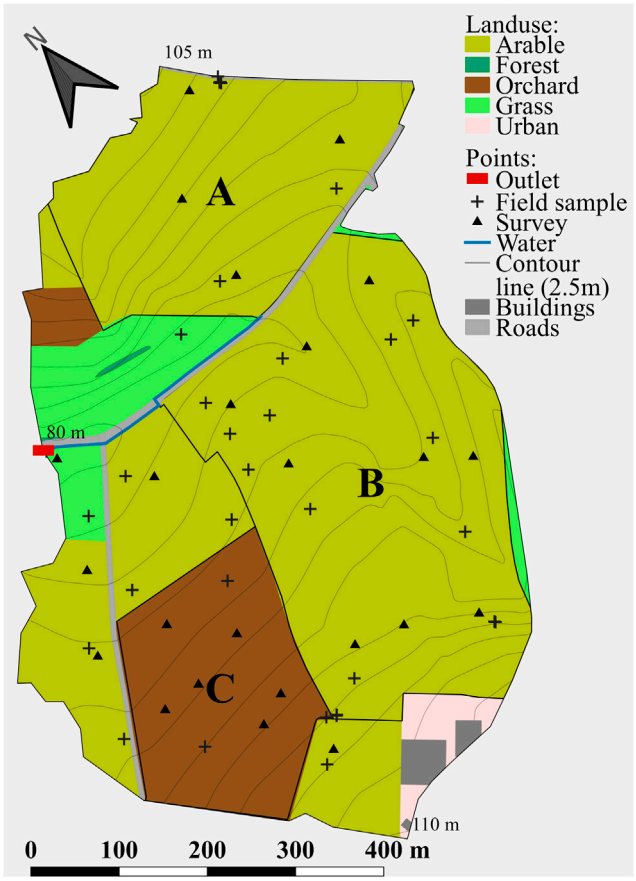

FIGURE 1 | Map of the study area in South-Limburg, the Netherlands indicating sampling points. The letters **(A,B and C)** indicate the three fields of main interest in this study.

catchments in sloping areas during erosive rainstorm events. To verify this hypothesis, this study quantified the contribution of particulate phase transport to the total off-site transport of pesticides during and after rainfall events. For this purpose, a measurement campaign was set up in which we sampled rainfall-runoff events at high temporal resolution at the catchment outlet and performed multiple field sampling surveys within the catchment during 2019 and 2020.

2 METHODS

2.1 Study Area

Sampling and field observations were done in a small agricultural catchment (38.6 ha) in the hilly area of South-Limburg, Netherlands (**Figure 1**). The catchment has a typical land use pattern for the loess belt covering parts of Belgium and the south of Limburg in the Netherlands. Arable agriculture was the main land use covering 25.2 ha, consisting of a crop rotation of winter cereals and intensive crops like potatoes, sugar beet and chicory. An apple orchard covered 5.3 and 5.0 ha was extensively managed grassland. The remaining area consisted of roads, urban area, and a small tree nursery. All agricultural fields were under conventional crop management, including pesticide applications, with apple and potato cultivation having the highest annual application rates.

The catchment has an elevation difference of 30 m (80–110 m. a.s.l.) and an average slope of 6.3% (sd ± 4.0%, range 0.1–30%). The catchment borders were calculated with QGIS 3.16 (QGIS 2021), based on the AHN3 DTM with a 0.5 m resolution (AHN 2019). The borders were adjusted if field observations showed different flow lines. The soil type is loess soil, a homogenous, fertile, but erosion sensitive Luvisol with a silt loam texture. Soil characteristics are (mean ± SE): sand 45.6 ± 2.2%, silt 51.0 ± 2.1%, clay 3.5 ± 0.2%, OM 3.6 ± 0.3%, pH 6.5 ± 0.10. The catchment is located in a temperate climate (Cfb) with a mean annual temperature of 10.7°C (±0.7°C) (KNMI 2021b) and mean annual precipitation of 757 mm (±108 mm) (KNMI 2021a), based on measurements from 1991–2020 at a weather station 2.5 km from the catchment. A dry ditch connects the fields to the catchment outlet, in which only for short periods after intensive rainfall events discharge occurs.

2.2 Measurement Design

To relate measured pesticide concentrations at the outlet to application and management on the fields, samples were collected throughout the catchment after five runoff events (+ in **Figure 1**). A baseline soil survey (04 March 2020), consisting of 30 samples covering the whole catchment through a structured random design, was done before the growing season of 2020 (▲ in **Figure 1**). A total of 68 samples from the top 1 cm of the soil was collected. These samples were stored in a freezer and used for analysis of pesticides, texture, organic matter content, and pH. The concentrations of different pesticides in the upper layer of the fields indicates potential transport risk by runoff and erosion. In addition, pesticide application data (date, pesticide type, application concentration) were obtained from the landowners of the three main agricultural fields in the catchment (A, B and C in **Figure 1**).

Other data on climate, land use and soil conditions were monitored to investigate the dynamics and processes driving the pesticide transport during the rainfall events. Data was collected for rainfall, crop type, crop cover and soil moisture content of fields. Rainfall was measured at the outlet with a 0.2 mm tipping bucket (ARG100, Campbell Sci.) on a 1 min resolution. Crop height and cover was measured during surveys, soil moisture content was measured using a Time Domain Reflectometer (TDR) during surveys after events. Finally, radar precipitation data (5 min, 1 km^2) from KNMI was used (KNMI 2021c) to obtain a spatial coverage of rainfall in the catchment and to fill gaps in the timeseries of the tipping bucket.

At the outlet of the catchment the water and sediment discharge was measured by a two feet Parshall flume, with an accurate measurement range between 12 and 650 L s^{-1} (See **Supplementary Figure S1**). Data was collected during runoff events and independent of pesticide application pattern. When free flow conditions in the channel were met, the accuracy of the Parshall flume is ±3% (Parshall 1926; Bos 1989). Water level readings were collected every minute at two locations in the flume. Automated sampling at the outlet, with an ISCO 3700 (Teledyne Isco, Inc. United States), was activated when the discharge would exceed 12 L s^{-1}. Then, a runoff sample was

pumped from the stream every 6 min. This was done using an inlet device, optimized for sampling of sediment and water samples, adapted from Gettel et al. (2011) and Eads and Thomas (1983). All details on the flume measurement set-up are given in **Supplementary Material S1.1**. A maximum of 12 samples could be taken by the sampler, resulting in 72 min of sampled event duration, which covered 80% of the runoff peaks occurring in this catchment in 2019 and 2020.

During the measurement years 2019 and 2020, based on the discharge data from the flume, 39 runoff events occurred. Due to temporarily malfunctioning of the equipment or because of insufficient sample coverage during some events, the analysis in this study is based on 14 events (see **Supplementary Material S1.2** for further details). The analyzed events do not show significant ($p < 0.05$) differences with the not analyzed events, when comparing runoff and erosion characteristics. However, due to limitations in event duration for sample collection and minimal erosion for pesticide analysis, the analyzed subset shows a tendency for shorter events with higher runoff and erosion rates (see **Supplementary Figure S2**).

2.3 Analysis of Soil, Runoff Water and TSS Samples

Each sample during a runoff event consisted of two bottles with identical content. One was used for analysis of pesticides in sediment and water, the other was used to derive total suspended solids (TSS) in water and other parameters of interest (OM, pH, and texture).

The soil and sediment analysis was done at the Soil Hydro Physics laboratory at Wageningen University. For TSS determination the samples were weighed and dried at 105°C for 24 h. For runoff TSS samples and soil samples in the catchment, dried sediment was collected and used to determine pH (suspension in 0.01 M CaCl), OM (loss on ignition) (Roper et al., 2019) and texture. For the determination of texture, 1 g of dried sediment was sieved on 500 µm, and analyzed with laser diffraction (Mastersizer S, Malvern Panalytical) in triplicate on wet samples by the department of Earth and Environmental Sciences, KU Leuven, Belgium.

To investigate pesticide concentrations for both components of the runoff (water and TSS), the samples were separated using a centrifuge (30 min at 3,600 rpm). The water part was transferred to a new tube and both samples were stored in a freezer until further analysis. During this stage samples were combined when the sediment content was too low for individual analysis; sediments from the 6 min timesteps were combined until a minimum of 7 g dry material was obtained for analysis.

2.4 Pesticide Applications, Selection, and Analysis

The selection of pesticides for analysis was based on the application of pesticides in the growing season of 2019. The applications by the two landowners managing the 3 largest fields (A, B and C in **Figure 1**) of the area, where used as initial pesticide list. A selection of these compounds was analyzed, based on analysis possibilities within the limited mass of TSS samples (often <10 gr) and financial budget. Compounds were selected that could be analyzed with a multi-residue method (LC- MS/MS positive). Prior studies (Bento et al., 2018; Yang et al., 2015a, 2015b) indicated particulate phase (PP) transport for glyphosate and AMPA to be important, so these compounds were also selected for this research, and a single residue method was used for determination. These two analyses covered 31 compounds: 20 fungicides, five herbicides and five insecticides, and amino-methyl phosphonic acid (AMPA) as metabolite of glyphosate. The chemical characteristics of the selected AS range for adsorption (k_{oc}) from 1.6–4.2 10^6 ml g^{-1} and for degradation (DT_{50}) from 0.8–419 days, according to data retrieved from the Public Pesticide Database (PPDB) (Lewis et al., 2016).

2.4.1 Chemical Determinations and Response Analysis

The list of chemicals and reagents used for the analysis is identical to Silva et al. (2019). The glyphosate and AMPA analysis was done several weeks earlier than the multi-residue analysis. To minimize sample disturbances, aliquots for both analyses were prepared at the same moment and stored in a freezer until further analysis. Because TSS sediment samples did not always provide enough material for the standard analysis, adapted masses (1/4 or 1/2 of the standard weight) were used if needed. Analysis for glyphosate and AMPA was done following the procedure described by Bento et al., 2016 and Bento et al., 2018. The multi residue analysis was done according the QuEChERS approach for soil and sediment samples (Anastassiades et al., 2003; Mol et al., 2008).

The quality control and chemical determination of the samples was done according to the guidance document for pesticide residues in food and feed (European Commission 2019). Calibration standards were prepared and injected at the start and end of each sampling sequence. The standards consisted of 1.25, 3.125, 6.25, 12.5 and 50 ng ml^{-1}; 0.625 and 25 ng ml^{-1} were added during analyses of diluted samples. The glyphosate/AMPA standards were 5, 10, 20, 50, 100, 200, 500, 1,000 and ng ml^{-1}. See **Supplementary Material S2.1** for further details.

Since all analyzed soil and sediment samples contained soil moisture, and in varying amounts, the measured concentrations had to be adjusted for the volumetric water content (VWC). This was done by drying the sample material after the extraction to derive the dry weight of the soil or sediment. The concentration was corrected for VWC and the concentration of the compound in the relating water sample. All final concentrations were adjusted for the recovery of the compound. The recovery was detected based on 9 quality control (QC) samples, with a known concentration for each compound.

2.5 Data Analysis and Accuracy

All data analysis, calculations and statistics were done using R software (R Core Team 2021), including the "drc" package for

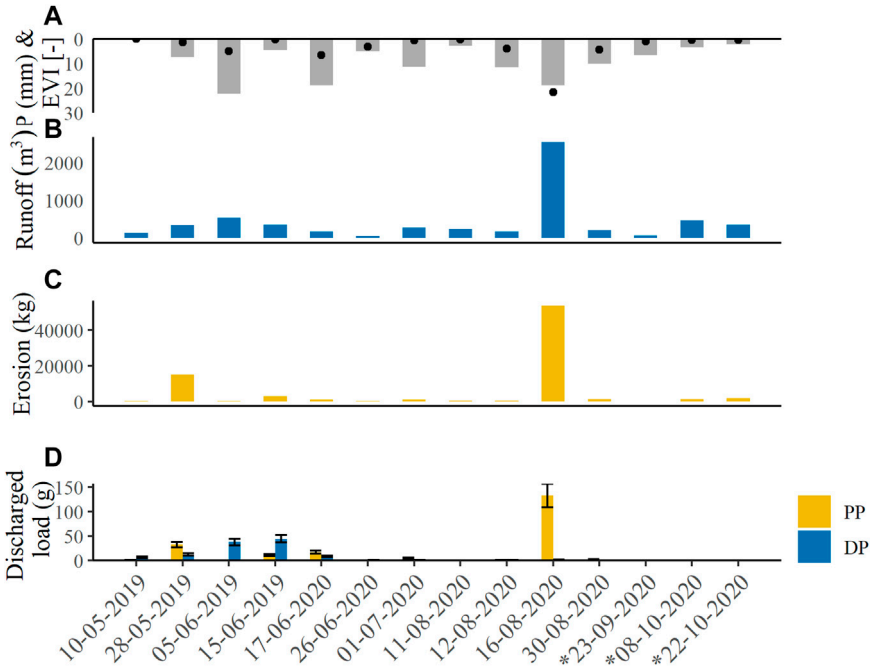

FIGURE 2 | Overview of rainfall **(A)**, runoff **(B)**, related erosion **(C)** and total pesticides transported (g) by particulate (PP) and dissolved phase (DP) **(D)** for the 14 events measured in 2019 and 2020. Error bars indicate uncertainty of total value (±18% PP and ±17% DP, see **Section 2.5**).

first order decay analysis (Ritz et al., 2015). To compare rainfall events with each other the event index (EVI) was calculated (Baartman et al., 2013).

The discharge was calculated based on the water height measured in the Parshall flume. Discharge was calculated based on the empirical formulas given by Parshall (1926). When submergence exceeded 50%, free flow conditions were not met and the discharge was corrected (Parshall 1926), for more details see **Supplementary Material S1.1**.

The calculations of the total pesticide loads in particulate (PP) and dissolved phase (DP) were based on variables that each introduce uncertainty towards the final quantification. Propagation of uncertainty was calculated with the standard deviation expressed as relative error for each variable (Taylor and Thompson 1998). The uncertainty for each variable is presented in more detail in **Supplementary Material S3**. While uncertainty of primary measurements (e.g., rainfall or water discharge) is still low, the propagation of the error during calculations results in uncertainty of 18% for pesticide loads in TSS.

3 RESULTS AND DISCUSSION

Synthesizing the results obtained in this study, we found that transport of pesticides during erosive runoff events is determined by three main aspects. Both the quantity as well as the main mode of transport are influenced by 1) the precipitation events and related runoff, 2) the chemical characteristics of the transported active substances as well as by 3) the land use and managements on the fields. The findings and dynamics of each of these processes in relation to pesticide transport are discussed in detail below.

3.1 Runoff and Erosion as Transport Modes for Pesticides

3.1.1 Rainfall Events, Runoff and Erosion

The 14 events included in this study cover a wide range in terms of rainfall intensity, total precipitation and related runoff and erosion (**Figure 2**). Two events (28 May 2019 and 16 August 2020) had high erosion rates, with mean total suspended solids (TSS) concentrations of 44 and 21 g L^{-1}, respectively, while the mean TSS concentration for all events was 7.5 g L^{-1}. The total water discharged from the catchment during the selected events was 5,800 (±290) m^3 and the total soil loss was 79 (±5) ton dry soil, resulting in a ratio Q_{sed}: Q_{wat} of 1–73. This sediment loss equals 3.1 t ha^{-1} for the arable fields in the catchment. Although not all events that occurred in these two seasons (39) are included, the observed erosion rates are in line with the estimated average of 2.46 t ha^{-1} y^{-1} for arable lands in Europe (Panagos et al., 2015).

There is no significant relation between rainfall characteristics and runoff or erosion. Linear regression was applied on the total discharge of water and sediment, with total rainfall and event duration as explanatory variables. This results in an r^2 of 0.68 for total amount of runoff. No direct relationship between the event characteristics and the amount of erosion could be found. This

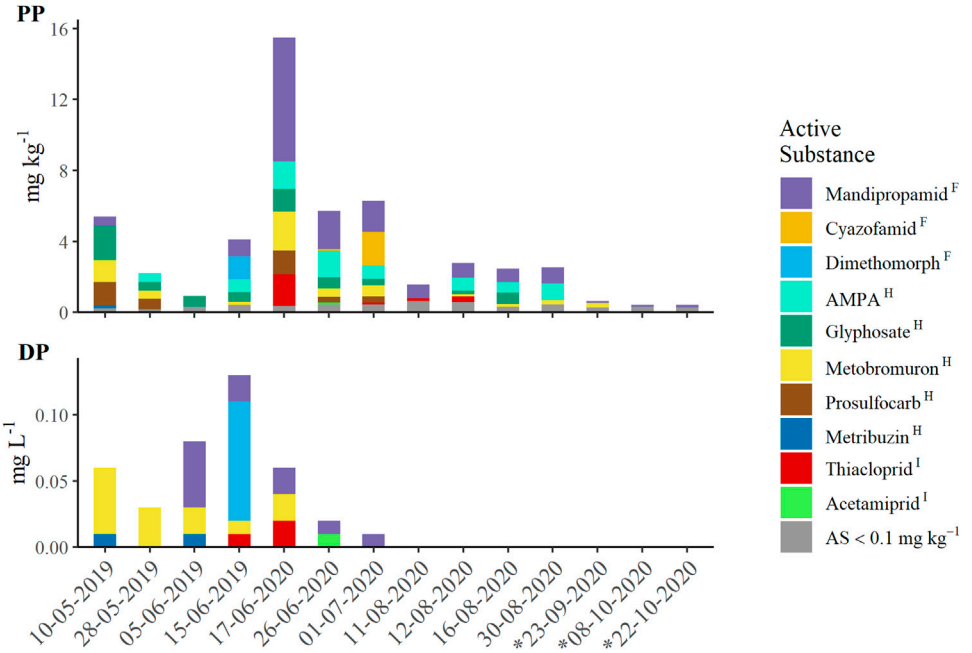

FIGURE 3 | Concentrations of active substances (AS) detected in runoff during each event in the particulate (PP) and dissolved (DP) phase. Superscript in legend denotes: [F] Fungicides, [H] Herbicides, and [I] Insecticides. All AS in a specific event with a content in the PP below 0.1 mg kg^{-1} are grouped for visualization. * For the events after 23-09-2020, Glyphosate and AMPA are excluded due to point source pollution.

can be related to other variables like crop cover and soil moisture which varied between events and influence erosion rates and runoff (Morgan et al., 1984; Zambon et al., 2021). Because of the event-based nature of overland flow, longer term monitoring is needed to understand the variability between rainfall events, cultivated crops and seasons within the year (Borrelli et al., 2021). The events included in this study, show the different mechanisms that affect transport and partitioning between phases of AS during overland flow. However, the high variability does not allow for generalizations, because adding or subtracting several events can influence general findings to a large extent.

3.1.2 Pesticides Transported During Rainfall—Runoff Events

The Glyphosate and AMPA results for the three events from 23-09-2020 are excluded from further analysis, due to occurrence of point source pollution. The glyphosate concentration on 23-09-2020, which is a small event in terms of runoff and erosion, is 550 mg kg^{-1} in PP and 2.2 mg L^{-1} in DP. These values are a factor 20–50 higher than all other detected levels in the discharge as well as on the fields in the catchment. Point source pollution which reaches the outlet at the first rainfall event can explain these extreme peaks (Reichenberger et al., 2007; Syafrudin et al., 2021). Because this study aims to investigate diffuse source transport, these results are not taken into account. A detailed description and further discussion is given in the **Supplementary Material S2.2**.

Within the analyzed events, six events occurred with substantial transport (>5 g) of pesticides in DP and PP combined, in the other events the transported load was small (see **Figure 2D**). The pesticide concentrations (PP and PD combined) during the 14 events ranged from 0.2 (±0.04) to 160 (±30) µg L^{-1}. The contribution of PP transport to total overland transport shows high variability between events, ranging from 0.1% to 99%. When comparing the transport for each event with the characteristics of rainfall, runoff and erosion, the concentrations of pesticides were not related to the intensity of rainfall or runoff. Both the quantity of runoff as well as the concentrations of active substances transported could result in high total mass transported from the catchment. The event of 16-08-2020 had a high discharge of water and sediment (**Figures 2B,C**), but the concentrations of AS were not high (**Figure 3**). Opposingly, the event of 17-06-2020 was relatively small in terms of runoff, but had high concentrations, resulting in substantial amounts of transported pesticides.

The high concentrations of pesticides detected in the particulate phase (PP) of runoff, caused increased transport of pesticides in PP when total erosion during a runoff event increased (r^2 = 0.60). The two events with TSS above 10 g L^{-1} had most transport in PP. In events with TSS concentrations between 3 and 10 g L^{-1} the dominant transport mode can vary, and with lower concentrations the PP share drops towards zero. The partitioning between DP and PP in terms of concentration varied through the events. In all events the PP concentration was higher than DP, with factors ranging from 12 to 3,700 for the 9 events in which DP was

detected, for six events no DP concentration was measured. Other studies taking both PP and DP into account report factors ranging from 10–1,000 times higher PP concentrations compared to DP (Todorovic et al., 2014; Maillard and Imfeld 2014; Cruzeiro et al., 2016; Yang et al., 2015b).

The mean concentrations were always cocktails of multiple active substances (AS). **Figure 3** shows the composition of AS for each event in both phases of the runoff. The number of detected AS in PP ranged from 8–18, compared to 0–5 different AS in the DP. During the whole observation period 8 different AS were measured in DP against 24 (including AMPA) in the PP. However the LOQ for water samples in this study was 2.5 $\mu g\,L^{-1}$, which corresponds with analysis in other studies (Peruzzo et al., 2008; Melland et al., 2016). This limits the detection of lower concentrations of AS in water.

The difference in measured concentrations, and related evaluation of environmental risks, between short term local events and larger temporal scales was emphasized by Lefrancq et al. (2017). During peaks in runoff, pesticide concentrations up to 387 $\mu g\,L^{-1}$ were detected in runoff water by Lefrancq et al. (2017); in the present study the maximal concentration during an event was 128 $\mu g\,L^{-1}$. Concentrations, in both PP and DP, increased a lot during the main application period when rainfall events occurred shortly after pesticide applications (see **Figure 3**). In 9 of the 14 events observed during our study the single substance as well as combined concentrations exceeded the regulatory limits, 0.1 and 0.5 $\mu g\,L^{-1}$, respectively, set by the EU (European directive 2013/39/EC). When the pesticides enter the headwater streams they are also easily transported over longer distances, and pesticides are detected in many smaller streams throughout Europe (Casado et al., 2019).

Increased PP transport related to higher erosion rates corresponds with other studies investigating the PP and DP transport of pesticides. Melland et al. (2016), found that the PP could be significant (up to 47% of total load) with TSS concentrations ranging from 1.4–10.3 $g\,L^{-1}$. Yang et al. (2015a) also reports high (70–80%) PP transport in a study with erosion rates of 7–10 tons ha^{-1}. Several studies that conclude PP transport is not substantial (Maillard et al., 2011; Oliver et al., 2012; Napoli et al., 2016) all observed low TSS concentrations. The erosion rates in the region of the catchment of this study were assessed to be between 1–2 t ha^{-1} y^{-1} (Panagos et al., 2015), while observed erosion rates during the seasons 2019 and 2020 were slightly higher in this study. However the estimated mean of 2.46 t ha^{-1} y^{-1} for erosion prone lands in Europe (Panagos et al., 2015), stresses the need to take particulate phase transport of pesticides into account in further assessments for pesticide fate and environmental risk.

3.2 Influence of Pesticide Characteristics on Transport

Whether pesticides are transported to off-site areas also depends on the behavior of the specific active substance after application on the field. Biodegradability (DT_{50}), adsorption (k_{oc}) to soil particles and solubility in water (S_w) are the main characteristics that prescribe this behavior (Leonard 1990). During the observations in this study, dissolved phase (DP) transport occurred mainly shortly after the applications of AS to the field: 62% of total DP transport occurred within 5 days after field application, 69% within 10 days and 98% within 50 days. In contrast, PP transport occurred over a much longer period, with 9% of the total transported mass within 5 days, 10% within 10 days, 31% in 50 days and 90% within 100 days after application. All AS which were transported in high loads in DP shortly after applications, were transported for longer periods in PP afterwards. The field plot studies on differences in DP and PP transport from arable fields (Todorovic et al., 2014; Melland et al., 2016), have analyzed transport rates for events occurring shortly (<3 days) after pesticide application, concluding that DP transport is dominant. The data from the current study also shows that shortly after application DP transport occurs in substantial amounts. However, for rainfall events longer after application, pesticides are still detected in PP and can be transported during events with runoff and erosion.

3.2.1 Adsorption and Water Solubility

Table 1 compares the amount of applied AS for each chemical characteristic with the amount of transported AS. Statistical analysis, including regression, correlation and multivariate analysis did not show a relation between k_{oc} or S_w of AS and transport in either DP or PP. The transport in "high" as well as "low" solubility classes occurs more in PP than in DP, and no relation with transport can be found in this study. However, the mass transported for each class of adsorption does show a trend. The ratio of transport in DP to PP shifts from mainly DP for "mobile" AS to mainly PP for AS classified as "mobile." This result corresponds with the expected behavior of pesticides, in relation to this adsorption coefficient (Wauchope et al., 2002; Leonard 1990). However, not all individual AS follow this pattern. The AS which were detected in DP have k_{oc} values ranging from 48 up to 1.6 10^4 ml g^{-1}, according to the PPDB, which covers the classes "mobile" up to "non-mobile." Moreover, nine AS were detected in PP but not in DP, which were applied within 10 days before an occurring rainfall event. K_{oc} values for these AS range from 1.6 up to 1.6 10^4 ml g^{-1} (PPDB, Lewis et al., 2016). Based on the chemical classification at least Flonicamid (very mobile) and Cymoxanil (mobile) would be expected to be detected in DP.

These findings correspond with analysis in other studies, where some AS were found to follow the theoretical classification well, but other AS were transported more in an unexpected phase. Oliver et al. (2012) reported that the AS with highest solubility was transported proportionally less in DP compared to AS with lower solubility properties. In a field experiment with runoff 2 days after the application of pesticides, the AS with higher adsorption to soil particles were also transported most in PP (Melland et al., 2016). On larger scales, also no significant correlation was found between adsorption characteristics of AS and partitioning between DP and PP (Climent et al., 2019), although more different AS and in higher frequency where detected in PP (Cruzeiro et al., 2016). These results from other studies as well as the observations in the

TABLE 1 | Overview of application and transport of AS in relation to chemical characteristics.

Class	Range of class	Application in catchment			Transport at outlet			
		AS applied (n)	Mass applied (kg)	% of applied mass	AS detected (n)	PP mass (g)	DP mass (g)	% of transported mass
Solubility in water (S_w, mg L^{-1})								
Low	<50	20	111	46%	16	89	70	57%
Moderate	50–500	3	29	12%	2	26	39	23%
High	>500	7	104	42%	5	47	8	20%
Soil adsorption (k_{oc}, mL g^{-1})								
Very mobile	<15	1	3	1%	1	0	0	0%
Mobile	15–75	2	8	3%	2	1	7	3%
Moderately mobile	75–500	7	35	14%	5	25	65	32%
Slightly mobile	500–4,000	15	131	54%	12	90	45	48%
Non-mobile	>4,000	5	67	28%	3	46	1	17%
Biodegradability (DT_{50}, days)								
Non-persistent	<30	14	121	50%	8	24	12	13%
Moderately persistent	30–100	9	52	21%	8	85	104	68%
Persistent	100–365	7	70	29%	7	53	1	19%

Note: the biodegradability class "very persistent" (>365 days) did not occur in this study. AMPA, as metabolite is excluded from this overview. Characteristics of chemicals (class and range) are obtained from the PPDB (Lewis et al., 2016).

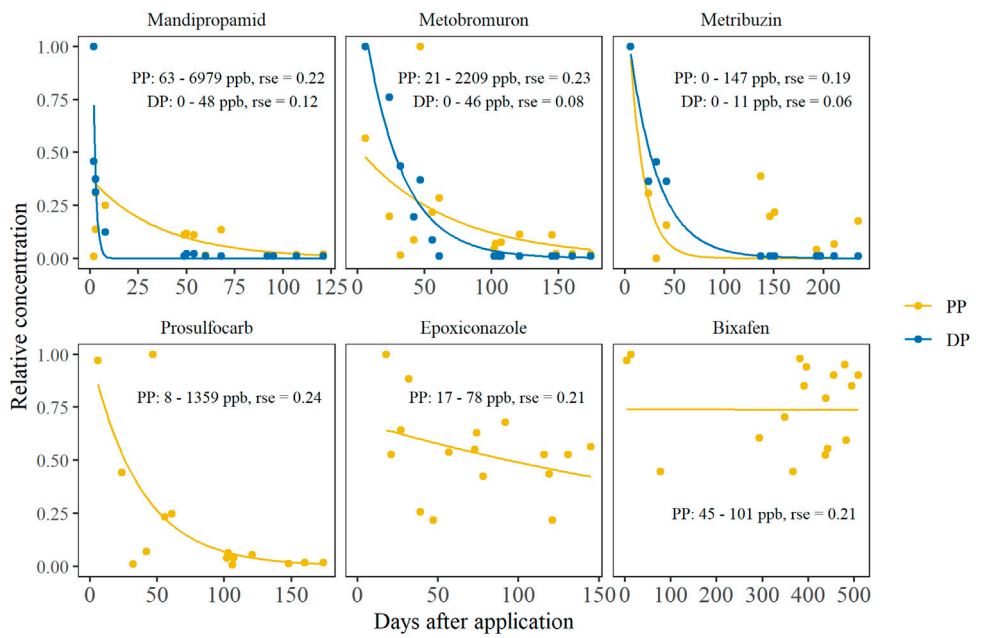

FIGURE 4 | Decrease of the relative concentrations in DP and PP for six AS. The concentration range (min—max) of the AS detected in runoff is given, ppb in PP is µg kg^{-1}, and in DP µg L^{-1}, rse is the residual standard error.

present study indicate that solubility and adsorption characteristics may not suffice to predict the dominant transport mode and related environmental fate of pesticides.

Mandipropamid, Glyphosate, Metobromuron and Prosulfocarb were the main transported AS in PP. Prosulfocarb has a high k_{oc} and low solubility, and it is only detected in PP. Glyphosate is detected in both phases although the majority of transport occurred in PP (97%). The other two AS have more affinity for dissolved transport and were also transported in DP, mandipropamid for 41% and metobromuron for 63% of total mass. During the growing seasons a total of 52 different AS were applied. Due to limitations in the analysis, several AS that might be interesting for analysis, had to be excluded. This were mancozeb, diquat and captan among others, of which some were applied in high frequency or had chemical characteristics that suggested high potential for PP transport (Chiovarou and Siewicki 2008). Therefor the transported loads in this study cannot be used as a mass balance, because including or excluding several AS from the analysis can influence the quantities that are reported.

3.2.2 Transport in Relation to Persistence and Application Frequency

The persistence of an AS is of major influence for the transport by runoff. Of the 30 analyzed AS, seven where not detected in any runoff event, these are characterized by a fast degradation (DT_{50} < 32 days). Two of these AS were applied during potato cultivation and 5 on the apple orchard. **Table 1** shows that persistence influences the risk of transport. Of total applied AS mass, 50% is non-persistent, and 50% is moderately persistent or persistent. However, in the runoff, these ratios change, and only 13% of transported AS belong to the "non-persistent" class, compared to 87% of transported mass belonging to the moderately-persistent and persistent class.

In **Figure 4**, a comparison of the decrease of transported concentration over time since application is shown for six AS that were detected on a regular basis. Three of these were transported in both phases. The data shows that after 60 days no transport in DP is detected, while transport in PP lasts much longer. In addition, the concentrations transported in DP drop faster over time; even for metribuzin where the fitted 1st order decay curves have nearly the same slope for DP and PP. After 150 days significant concentrations were still detected in PP. The fitted curves show a reasonably good fit for DP with residual standard errors (RSE) between 0.06 and 0.12. This confirms the overall observation that in the 14 events of this dataset, 69% of all DP transport occurs within 10 days after application on the field. This finding corresponds with other studies, which report DP transport mainly close to application (Boithias et al., 2014; Cruzeiro et al., 2016; Melland et al., 2016). PP concentrations have a higher RSE, meaning that the time between application and event alone cannot explain concentration or transported load in PP. Differences in reported degradation rates (e.g., PPDB) with observed degradation in the field can be caused by the high variability in environmental degradation of AS (Arias-Estévez et al., 2008; Bento et al., 2016).

The three AS shown in **Figure 4**, that were transported in both phases, were all applied frequently, which increases the chance for a runoff event to occur close to the application date. Epoxiconazole and Bixafen both show low or no decrease in transported concentration over time: both compounds have slow biodegradation (98 and 203 days DT_{50}, respectively) and originate from applications of the previous growing season. Bixafen was applied one time in 2019 and once in 2018 but was detected on stable levels around 50 $\mu g\ kg^{-1}$ on arable fields in this study. The concentrations in which these AS were transported are low compared to, e.g., Prosulfocarb, however these AS were transported with every erosive runoff event and in this way formed a constant source of pollution. No studies were found that relate the transported load of different AS to the varying biodegradation rate in the environment. However studies on concentrations and detection of AS in rivers, clearly show increased levels and numbers of different AS during periods with intensive pesticide use, often spring and summer (Peruzzo et al., 2008; Cruzeiro et al., 2016; Climent et al., 2019).

The three chemical characteristics of interest; biodegradation, water solubility and adsorption coefficient alone cannot explain the transported concentrations or the partitioning between dissolved and particulate phase. The transported mass during an event, both in DP and PP, depends not only on concentration, but also on runoff and erosion quantity and related variables, which are strongly event specific. The transport dynamics on field scale are also influenced by runoff generation processes and sediment connectivity (Heckmann et al., 2018; Bracken and Jacky. 2007), which takes into account factors like upstream area, spatial land use distribution and field specific land management (see **Section 3.3**.), distance to the outlet (Borselli et al., 2008; Cavalli et al., 2013) and rainfall amounts and intensity (López-Vicente and Ben-Salem 2019).

3.3 Land Use Effect on Transport in PP and DP

Based on the application data for each field and the concentrations of AS during field surveys in the soil, the source field and associated land use type can be derived for the AS detected at the catchment outlet during the events (a full table with AS, detection, field concentration and application data is supplied in **Supplementary Table S9**). Land use and management of agricultural fields affect runoff, erosion, and thus the potential transport of AS to off-site locations. The number of detected AS in runoff is the highest in the main cropping season (June—August), which corresponds with the frequency of applications on the fields.

3.3.1 Apples

On the apple orchard the highest total amount of pesticides was applied, with a mean of 21 $kg\ ha^{-1}$ active ingredients (**Supplementary Table S8**), and the frequency of applications throughout the growing season is high. This does however not result in high discharges of pesticides at the catchment outlet. Six AS were detected in the runoff, of which four were fungicides, one herbicide and one insecticide. Four of these (Fluxapyroxad, Pyraclostrobin, Chlorantraniliprole and Difenoconazole) where only applied on apples and were not transported in DP, only in PP and contributed 1% to total PP load. Besides that, Boscalid and Glyphosate were applied, which are also used in potato cultivation, the exact source field could not be derived based on this dataset. These compounds contribute 1% and 23% tot total DP and PP transport, respectively. The borders and interrow area of the orchard were covered with grass, which has a reducing effect on soil erosion and a filtering and buffering effect on the transport of pesticides (Muñoz-Carpena et al., 2018; Reichenberger et al., 2019; Yu et al., 2019). During field observation, no signs of erosion were recorded from the apples. These findings correspond with studies on orchards and vineyards with grassed rows, also reporting low AS transport (Oliver et al., 2012; Napoli et al., 2016).

3.3.2 Cereals

None of the transported AS can be directly associated with the cereal cultivation. This corresponds with the low erosion risk associated with cereals in summer (Prasuhn 2020) and the low

total amount of applied pesticides (0.4 kg ha^{-1}, **Supplementary Table S8**). However, during cereal cultivation persistent AS were applied (Epoxiconazole, Bixafen and Isopyrazam), which were still detected in the soil in the next growing season, when a different crop was grown on the field (i.e., the next crop in the rotation). These three AS were detected in 100%, 100% and 93% of all runoff events, respectively. They were transported from the field in the rotation after the cereals, when potatoes were cultivated, which caused the runoff and erosion. The transport of these AS 1 year after application contributes for 4% of the PP transported mass from the catchment. To the authors no other studies are known presenting results of delayed transport of pesticides in overland transport, however persistent AS were shown to be a risk for leaching to groundwater (Reichenberger et al., 2007; Schuhmann et al., 2019).

3.3.3 Potatoes

The main source of pesticide transport in this study was the field cultivated with potatoes. 21 of all detected AS (including AMPA) where related to this cultivation, this also included persistent AS which were applied in previous cropping seasons (see previous section). At least 72% of PP and 99% of DP transport originates from the potato cultivation. As discussed above, Glyphosate and Boscalid can originate from apples as well as potato cultivation. Based on the observations of major runoff and erosion the potato field is likely to also be the main source area for these AS. Potato cultivation on sloping lands is a combination of erosion prone land use (Olivier et al., 2014) with high amount of pesticide applications (11 kg ha^{-1}, **Supplementary Table S8**). During field observations potato cultivation was identified as the main source of runoff and erosion (see **Supplementary Figures S3–S5**), which corresponds with the detected AS in the runoff and TSS. These results show that erosion prone and pesticide intensive cultivations form the main risk for both DP and PP transport of pesticides during runoff events. In the currently available literature of PP transport of pesticide only plot scale simulations on arable fields are available, comparing either tillage practices or crop and mulch cover (Todorovic et al., 2014; Yang et al., 2015a; Melland et al., 2016; Bento et al., 2018). These studies show the effect of increased transport with erosion prone land management types. However, the smaller scale and often short time between application and runoff event of these studies, did not suffice to understand the extent of potential PP transport from arable fields with an erosion prone cultivation.

The large difference in observed transport between the potato cultivation and the cereals or apple orchard, emphasize that preventing erosion and runoff will also reduce the overland transport of pesticide. Implementation of on-site measure like vegetated filter strips (Muñoz-Carpena, Ritter, and Fox 2019) or micro-dams between the potato ridges (Olivier et al., 2014) can reduce runoff and erosion from the specific fields. Moreover off-site erosion measures like riparian buffers and wetlands are shown to mitigate further transport of pesticides in to the environment (Imfeld et al., 2021).

4 CONCLUSION AND RECOMMENDATIONS

This study confirmed our hypothesis that particulate phase transport contributes to total overland transport of pesticides on field scale on sloping land. Based on observations in two growing seasons (2019 and 2020) in which 14 rainfall-runoff events were sampled we can conclude that in a small agricultural catchment with intensive arable farming, PP transport contributed substantially to total overland transport of pesticides.

Event specific contributions of PP show high variability, which is the result of interacting factors, including hydrological and sediment dynamics during the event, chemical characteristics of the transported active substances and land management on the fields. This results in high variability in quantity, phase and type of the transported pesticides. Land use types which are pesticide intensive and erosion prone, pose a threat for high discharges of pesticides via runoff, both in dissolved and particulate phase.

Transport in DP occurred mainly shortly after application of the pesticide (69% within 10 days). Opposingly, the transport of pesticides in PP occurs over much longer time spans, where 90% of the total transport is reached within 100 days after application in this study.

Biodegradability (DT_{50}), adsorption to soil (k_{oc}) and solubility in water ($S_{w)}$ of AS alone cannot explain the transport mode and related fate of individual pesticides after application. However, the biodegradability (DT_{50}) of an active substance determines how long it will be available for overland transport either in PP or DP. Most non-persistent AS were not transported or only shortly after application, where several persistent AS were transported year-round during erosive runoff events.

Considering the extent of erosion from arable land, significantly more transport occurs than is predicted when PP transport during runoff events is not taken into account. Our results imply that event-scale dynamics are important for pesticide transport and that interactions between management, event characteristics and applied active substances can cause events that contribute disproportionally high to total transport. Because most transport of pesticides occurred from erosion prone land use, this study emphasizes the need for on-site and off-site erosion mitigation to prevent off-site transport of pesticides in the environment.

For further generalization and understanding of the findings in the study, additional observational data will be valuable. Transport behavior in different pedoclimatic and geomorphic environments as well as under different land management practices, will further increase our understanding of these dynamics. The current study is limited to three land use types, on erosion prone loess soils. Moreover the observation period of 2 years, results in a variety of rainfall events, but longer term observations are needed to be able to derive

generalized conclusions. Other research methods, such as modelling studies that investigate the relevant variables and that can explicitly simulate the dynamics within the catchment, might add to our ability to assess the pollution risk of currently used pesticides.

DATA AVAILABILITY STATEMENT

The datasets presented in this article are available at https://doi.org/10.4121/19690684. The code for analysis is available at https://doi.org/10.4121/19690840 or https://github.com/mcommelin/pesticide_transport_runoff_erosion

AUTHOR CONTRIBUTIONS

MC, JB, MR, and VG designed the field research, MC did the data collection. Together with PZ the chemical analysis and interpretation was performed. MC wrote the draft manuscript and JB, PZ, MR, and VG edited and reviewed for the final version.

FUNDING

This research has received funding from the European Union's Horizon 2020 research and innovation program under grant agreement No. 727984.

ACKNOWLEDGMENTS

The authors thank Piet Peters for his help with the fieldwork, the waterboard of Limburg for the kind sharing of data and assistance during field observations, and the landowners for cooperation by sharing data and giving access to their fields. We would like to thank the reviewers for their helpful comments on an earlier draft of this paper.

SUPPLEMENTARY MATERIAL

The Supplementary Material for this article can be found online at: https://www.frontiersin.org/articles/10.3389/fenvs.2022.830589/full#supplementary-material

REFERENCES

AHN (2019). AHN3 DTM. Available at: https://www.ahn.nl/ahn-3.

Aktar, M. W., Sengupta, D., and Chowdhury, A. (2009). Interdisciplinary toxicology, and undefined 2009. "Impact of Pesticides Use in Agriculture: Their Benefits and Hazards". *Sciendo. Com.* doi:10.2478/v10102-009-0001-7

Anastassiades, M., Lehotay, S. J., Štajnbaher, D., and Schenck, F. J. (2003). Fast and Easy Multiresidue Method Employing Acetonitrile Extraction/Partitioning and "Dispersive Solid-phase Extraction" for the Determination of Pesticide Residues in Produce. *J. AOAC Int.* 86 (2), 412–431. doi:10.1093/jaoac/86.2.412

Arias-Estévez, M., López-Periago, E., Martínez-Carballo, E., Simal-Gándara, J., Mejuto, J.-C., and García-Río, L. (2008). The Mobility and Degradation of Pesticides in Soils and the Pollution of Groundwater Resources. *Agric. Ecosyst. Environ.* 123, 247–260. doi:10.1016/j.agee.2007.07.011

Baartman, J. E. M., Temme, A. J. A. M., Veldkamp, T., Jetten, V. G., and Schoorl, J. M. (2013). Exploring the Role of Rainfall Variability and Extreme Events in Long-Term Landscape Development. *Catena* 109 (October), 25–38. doi:10.1016/j.catena.2013.05.003

Bento, C. P. M., CommelinCommelin, M. C., Baartman, J. E. M., Yang, X., Peters, P., Mol, H. G. J., et al. (2018). Spatial Glyphosate and AMPA Redistribution on the Soil Surface Driven by Sediment Transport Processes - A Flume Experiment. *Environ. Pollut.* 234 (March), 1011–1020. doi:10.1016/j.envpol.2017.12.003

Bento, C. P. M., Yang, X., Gort, G., Xue, S., van Dam, R., Zomer, P., et al. (2016). Persistence of Glyphosate and Aminomethylphosphonic Acid in Loess Soil under Different Combinations of Temperature, Soil Moisture and Light/Darkness. *Sci. Total Environ.* 572 (December), 301–311. doi:10.1016/j.scitotenv.2016.07.215

Bevan, R., Brown, T., Matthies, F., Sams, C., Jones, K., Hanlon, J., et al. (2017). Human Biomonitoring Data Collection from Occupational Exposure to Pesticides. *EFSA Support. Publ.* 14 (3), 1185E. doi:10.2903/SP.EFSA.2017.EN-1185

Boardman, J., and Evans, R. (2020). The Measurement, Estimation and Monitoring of Soil Erosion by Runoff at the Field Scale: Challenges and Possibilities with Particular Reference to Britain. *Prog. Phys. Geogr. Earth Environ.* 44 (1), 31–49. doi:10.1177/0309133319861833

Boithias, L., Sauvage, S., Srinivasan, R., Leccia, O., and Sánchez-Pérez, J.-M. (2014). Application Date as a Controlling Factor of Pesticide Transfers to Surface Water during Runoff Events. *Catena* 119 (August), 97–103. doi:10.1016/j.catena.2014.03.013

Boivin, A., and Poulsen, V. (2017). Environmental Risk Assessment of Pesticides: State of the Art and Prospective Improvement from Science. *Environ. Sci. Pollut. Res.* 24 (8), 6889–6894. doi:10.1007/s11356-016-8289-2

Borrelli, P., Alewell, C., Alvarez, P., Anache, J. A. A., Baartman, J., Ballabio, C., et al. (2021). Soil Erosion Modelling: A Global Review and Statistical Analysis. *Sci. Total Environ.* 780 (August), 146494. doi:10.1016/j.scitotenv.2021.146494

Borselli, L., Cassi, P., and Torri, D. (2008). Prolegomena to Sediment and Flow Connectivity in the Landscape: A GIS and Field Numerical Assessment. *CATENA* 75 (3), 268–277. doi:10.1016/J.CATENA.2008.07.006

Bos, M. G. G. (1989). *Discharge Measurement Structures*. 3rd ed. Delft, The Netherlands: Delft Hydraul. Lab. doi:10.1201/9781315141343-2

Bracken, L. J., and Croke, J. (2007). The Concept of Hydrological Connectivity and its Contribution to Understanding Runoff-Dominated Geomorphic Systems. *Hydrol. Process.* 21 (13), 1749–1763. doi:10.1002/HYP.6313

Casado, J., Brigden, K., Santillo, D., and Johnston, P. (2019). Screening of Pesticides and Veterinary Drugs in Small Streams in the European Union by Liquid Chromatography High Resolution Mass Spectrometry. *Sci. Total Environ.* 670 (June), 1204–1225. doi:10.1016/j.scitotenv.2019.03.207

Cavalli, M., Trevisani, S., Comiti, F., and Marchi, L. (2013). Geomorphometric Assessment of Spatial Sediment Connectivity in Small Alpine Catchments. *Geomorphology* 188 (April), 31–41. doi:10.1016/J.GEOMORPH.2012.05.007

Cerdan, O., Le Bissonnais, Y., Govers, G., Lecomte, V., Van Oost, K., Couturier, A., et al. (2004). Scale Effect on Runoff from Experimental Plots to Catchments in Agricultural Areas in Normandy. *J. Hydrology* 299 (1–2), 4–14. doi:10.1016/j.jhydrol.2004.02.017

Chiovarou, E. D., and Siewicki, T. C. (2008). Comparison of Storm Intensity and Application Timing on Modeled Transport and Fate of Six Contaminants. *Sci. Total Environ.* 389 (1), 87–100. doi:10.1016/J.SCITOTENV.2007.08.029

Climent, M. J., Herrero-Hernández, E., Sánchez-Martín, M. J., Rodríguez-Cruz, M. S., Pedreros, P., and Urrutia, R. (2019). Residues of Pesticides and Some Metabolites in Dissolved and Particulate Phase in Surface Stream Water of Cachapoal River Basin, Central Chile. *Environ. Pollut.* 251 (August), 90–101. doi:10.1016/j.envpol.2019.04.117

Cruzeiro, C., Pardal, M. Â., Rodrigues-Oliveira, N., Castro, L. F. C., Rocha, E., and Rocha, M. J. (2016). Multi-Matrix Quantification and Risk Assessment of Pesticides in the Longest River of the Iberian Peninsula. *Sci. Total Environ.* 572 (December), 263–272. doi:10.1016/j.scitotenv.2016.07.203

Eads, R. E., and Thomas, R. B. (1983). Evaluation of a Depth Proportional Intake Device for Automatic Pumping Samplers. *J. Am. Water Resour. Assoc.* 19 (2), 289–292. doi:10.1111/j.1752-1688.1983.tb05328.x

European Commission (2019). Analytical Quality Control and Method Validation for Pesticide Residues Analysis in Food and Feed(SANTE/12682/2019). *Sante/12682/2019* Available at: https://www.eurl-pesticides.eu/docs/public/tmplt_article.asp?CntID=727.

FAO (2020). FaoStat. Available at: http://www.fao.org/faostat/en/#data/EPData.

FAO, IFAD, UNICEF, WFP, WHO (2020). *The State of Food Security and Nutrition in the World 2020*. doi:10.4060/ca9692en

Geiger, F., Bengtsson, J., Berendse, F., Weisser, W. W., Emmerson, M., Morales, M. B., et al. (2010). Persistent Negative Effects of Pesticides on Biodiversity and Biological Control Potential on European Farmland. *Basic Appl. Ecol.* 11 (2), 97–105. doi:10.1016/j.baae.2009.12.001

Geissen, V., Silva, V., Lwanga, E. H., Beriot, N., Oostindie, K., Bin, Z., et al. (2021). Cocktails of Pesticide Residues in Conventional and Organic Farming Systems in Europe - Legacy of the Past and Turning Point for the Future. *Environ. Pollut.* 278 (June), 116827. doi:10.1016/j.envpol.2021.116827

Gettel, M., Gulliver, J. S., Kayhanian, M., Degroot, G., Brand, J., Mohseni, O., et al. (2011). Improving Suspended Sediment Measurements by Automatic Samplers. *J. Environ. Monit.* 13 (10), 2703–2709. doi:10.1039/c1em10258c

Ghadiri, H., and Rose, C. W. (1991a). Sorbed Chemical Transport in Overland Flow: I. A Nutrient and Pesticide Enrichment Mechanism. *J. Environ. Qual.* 20 (3), 628–33. doi:10.2134/jeq1991.00472425002000030020x

Ghadiri, H., and Rose, C. W. (1991b). Sorbed Chemical Transport in Overland Flow: II. Enrichment Ratio Variation with Erosion Processes. *J. Environ. Qual.* 20 (3), 628–41. doi:10.2134/jeq1991.00472425002000030021x

Halbach, K., Möder, M., Schrader, S., Liebmann, L., Schäfer, R. B., Schneeweiss, A., et al. (2021). Small Streams-Large Concentrations? Pesticide Monitoring in Small Agricultural Streams in Germany during Dry Weather and Rainfall. *Water Res.* 203 (August), 117535. doi:10.1016/j.watres.2021.117535

Heckmann, T., Cavalli, M., Cerdan, O., Foerster, S., Javaux, M., Lode, E., et al. (2018). Indices of Sediment Connectivity: Opportunities, Challenges and Limitations. *Earth-Science Rev.* 187 (December), 77–108. doi:10.1016/J.EARSCIREV.2018.08.004

Imfeld, G., Payraudeau, S., Tournebize, J., Sauvage, S., Macary, F., Chaumont, C., et al. (2021). The Role of Ponds in Pesticide Dissipation at the Agricultural Catchment Scale: A Critical Review. *Water* 13, 1202. doi:10.3390/w13091202

KNMI (2021a). Monthly and Yearly Amount of Precipitation. Available at: https://cdn.knmi.nl/knmi/map/page/klimatologie/gegevens/maandgegevens/mndgeg_380_rh24.txt.

KNMI (2021b). Monthly and Yearly Mean Temperatures. Available at: https://cdn.knmi.nl/knmi/map/page/klimatologie/gegevens/maandgegevens/mndgeg_380_tg.txt.

KNMI (2021c). Precipitation - Radar/Gauge 5 minute Final Reanalysis Accumulations over the Netherlands. https://dataplatform.knmi.nl/dataset/nl-rdr-data-rfcor-5m-1-0.

Lanz, B., Dietz, S., and Swanson, T. (2018). The Expansion of Modern Agriculture and Global Biodiversity Decline: An Integrated Assessment. *Ecol. Econ.* 144 (February), 260–277. doi:10.1016/j.ecolecon.2017.07.018

Lechenet, M., Dessaint, F., Py, G., Makowski, D., and Munier-Jolain, N. (2017). Reducing Pesticide Use while Preserving Crop Productivity and Profitability on Arable Farms. *Nat. Plants* 3 (3), 2017. doi:10.1038/nplants.2017.8

Lefrancq, M., Jadas-Hécart, A., La Jeunesse, I., Landry, D., and Payraudeau, S. (2017). High Frequency Monitoring of Pesticides in Runoff Water to Improve Understanding of Their Transport and Environmental Impacts. *Sci. Total Environ.* 587-588 (June), 75–86. doi:10.1016/j.scitotenv.2017.02.022

Leonard, R. A. (1990). "Movement of Pesticides into Surface Waters," in *Pesticides in the Soil Environment: Processes, Impacts, and Modeling* (John Wiley & Sons), 303–49, 303–349. doi:10.2136/sssabookser2.c9

Lewis, K. A., Tzilivakis, J., Warner, D. J., and Green., A. (2016). An International Database for Pesticide Risk Assessments and Management. *Hum. Ecol. Risk Assess. Int. J.* 22 (4), 1050–1064. doi:10.1080/10807039.2015.1133242

López-Vicente, M., and Ben-Salem, N. (2019). Computing Structural and Functional Flow and Sediment Connectivity with a New Aggregated Index: A Case Study in a Large Mediterranean Catchment. *Sci. Total Environ.* 651 (February), 179–191. doi:10.1016/J.SCITOTENV.2018.09.170

Maillard, E., and Imfeld, G. (2014). Pesticide Mass Budget in a Stormwater Wetland. *Environ. Sci. Technol.* 48 (15), 8603–8611. doi:10.1021/es500586x

Maillard, E., Payraudeau, S., Faivre, E., Grégoire, C., Gangloff, S., and Imfeld, G. (2011). Removal of Pesticide Mixtures in a Stormwater Wetland Collecting Runoff from a Vineyard Catchment. *Sci. Total Environ.* 409 (11), 2317–2324. doi:10.1016/j.scitotenv.2011.01.057

Masiá, A., Campo, J., Vázquez-Roig, P., Blasco, C., and Picó, Y. (2013). Screening of Currently Used Pesticides in Water, Sediments and Biota of the Guadalquivir River Basin (Spain). *J. Hazard. Mater.* 263 (December), 95–104. doi:10.1016/j.jhazmat.2013.09.035

McCall, P. J., Laskowski, D. A., Swann, R. L., and Dishburger, H. J. (1980). "Measurement of Sorption Coefficients of Organic Chemicals and Their Use in Environmental Fate Analysis Test Protocols for Environ.mental Fate and Movement of Toxicants," in Proceedings of the 94th Annual Meeting of the American Association of Official Analytical Chemists (AOAC).

Melland, A. R., Silburn, D. M., McHugh, A. D., Fillols, E., Rojas-Ponce, S., Baillie, C., et al. (2016). Spot Spraying Reduces Herbicide Concentrations in Runoff. *J. Agric. Food Chem.* 64 (20), 4009–4020. doi:10.1021/acs.jafc.5b03688

Mol, H. G. J., Plaza-Bolaños, P., Zomer, P., De Rijk, T. C., Stolker, A. A. M., and Mulder, P. P. J. (2008). Toward a Generic Extraction Method for Simultaneous Determination of Pesticides, Mycotoxins, Plant Toxins, and Veterinary Drugs in Feed and Food Matrixes. *Anal. Chem.* 80 (24), 9450–9459. doi:10.1021/ac801557f

Morgan, R. P. C., Morgan, D. D. V., and Finney, H. J. (1984). A Predictive Model for the Assessment of Soil Erosion Risk. *J. Agric. Eng. Res.* 30 (C), 245–253. doi:10.1016/S0021-8634(84)80025-6

Muñoz-Carpena, R., Fox, G. A., Ritter, A., Perez-Ovilla, O., and Rodea-Palomares, I. (2018). Effect of Vegetative Filter Strip Pesticide Residue Degradation Assumptions for Environmental Exposure Assessments. *Sci. Total Environ.* 619-620, 977–987. doi:10.1016/j.scitotenv.2017.11.093

Muñoz-Carpena, R., Ritter, A., and Fox, G. A. (2019). Comparison of Empirical and Mechanistic Equations for Vegetative Filter Strip Pesticide Mitigation in Long-Term Environmental Exposure Assessments. *Water Res.* 165, 114983. doi:10.1016/j.watres.2019.114983

Napoli, M., Marta, A. D., Zanchi, C. A., Orlandini, S., Anna Dalla Ad Marta, Ad., et al. (2016). Transport of Glyphosate and Aminomethylphosphonic Acid under Two Soil Management Practices in an Italian Vineyard. *J. Environ. Qual.* 45 (5), 1713–1721. doi:10.2134/jeq2016.02.0061

Oliver, D. P., Kookana, R. S., Anderson, J. S., Cox, J. W., Waller, N., and Smith, L. H. (2012). Off-Site Transport of Pesticides in Dissolved and Particulate Forms from Two Land Uses in the Mt. Lofty Ranges, South Australia. *Agric. Water Manag.* 106 (April), 78–85. doi:10.1016/j.agwat.2011.11.001

Olivier, C., Goffart, J. P., Baets, D., Xanthoulis, D., Fonder, N., Lognay, G., et al. (2014). Use of Micro-dams in Potato Furrows to Reduce Erosion and Runoff and Minimise Surface Water Contamination through Pesticides. *Commun. Agric. Appl. Biol. Sci.* 79 (3), 513

Panagos, P., Borrelli, P., Poesen, J., Ballabio, C., Lugato, E., Meusburger, K., et al. (2015). The New Assessment of Soil Loss by Water Erosion in Europe. *Environ. Sci. Policy* 54 (December), 438–447. doi:10.1016/j.envsci.2015.08.012

Parshall, R. L. (1926). The Improved Venturi Flume. *T. Am. Soc. Civ. Eng.* 89 (1), 841–851. doi:10.1061/taceat.0003626

Peruzzo, P. J., Porta, A. A., and Ronco, A. E. (2008). Levels of Glyphosate in Surface Waters, Sediments and Soils Associated with Direct Sowing Soybean Cultivation in North Pampasic Region of Argentina. *Environ. Pollut.* 156 (1), 61–66. doi:10.1016/j.envpol.2008.01.015

Prasuhn, V. (2020). Twenty Years of Soil Erosion On-farm Measurement: Annual Variation, Spatial Distribution and the Impact of Conservation Programmes for Soil Loss Rates in Switzerland. *Earth Surf. Process. Landforms* 45 (7), 1539–1554. doi:10.1002/ESP.4829

QGIS (2021). *QGIS Geographic Information System, 3.16*. Hannover QGIS Assosaction. http://www.qgis.org.

R Core Team (2021). *R: A Language and Environment for Statistical Computing*. Vienna: R Foundation for Statistical Computing. https://www.r-project.org/.

Reichenberger, S., Bach, M., Skitschak, A., and Frede, H.-G. (2007). Mitigation Strategies to Reduce Pesticide Inputs into Ground- and Surface Water and Their Effectiveness; A Review. *Sci. Total Environ.* 384 (1–3), 1–35. doi:10.1016/j.scitotenv.2007.04.046

Reichenberger, S., Sur, R., Kley, C., Sittig, S., and Multsch, S. (2019). Recalibration and Cross-Validation of Pesticide Trapping Equations for Vegetative Filter Strips (VFS) Using Additional Experimental Data. *Sci. Total Environ.* 647, 534–550. doi:10.1016/j.scitotenv.2018.07.429

Ritz, C., Baty, F., Streibig, J. C., and Gerhard, D. (2015). Dose-Response Analysis Using R. *PLoS ONE* 10 (12), e0146021. doi:10.1371/journal.pone.0146021

Roper, W. R., Robarge, W. P., Osmond, D. L., and Heitman, J. L. (2019). Comparing Four Methods of Measuring Soil Organic Matter in North Carolina Soils. *Soil Sci. Soc. Am. J.* 83 (2), 466–474. doi:10.2136/sssaj2018.03.0105

Sattler, C., Kächele, H., and Verch, G. (2007). Assessing the Intensity of Pesticide Use in Agriculture. *Agric. Ecosyst. Environ.* 119 (3–4), 299–304. doi:10.1016/j.agee.2006.07.017

Schuhmann, A., Klammler, G., Weiss, S., Gans, O., Fank, J., Haberhauer, G., et al. (2019). Degradation and Leaching of Bentazone, Terbuthylazine and S-Metolachlor and Some of Their Metabolites: A Long-Term Lysimeter Experiment. *Plant Soil Environ.* 65 (No. 5), 273–281. doi:10.17221/803/2018-PSE

Silva, V., Mol, H. G. J., Zomer, P., Tienstra, M., Ritsema, C. J., and Geissen, V. (2019). Pesticide Residues in European Agricultural Soils - A Hidden Reality Unfolded. *Sci. Total Environ.* 653 (February), 1532–1545. doi:10.1016/j.scitotenv.2018.10.441

Syafrudin, M., Kristanti, R. A., Yuniarto, A., Hadibarata, T., Rhee, J., Al-Onazi, W. A., et al. (2021). Pesticides in Drinking Water-A Review. *Int. J. Environ. Res. Public. Health.* 18, 468. doi:10.3390/IJERPH18020468

Tang, X., Zhu, B., and Katou, H. (2012). A Review of Rapid Transport of Pesticides from Sloping Farmland to Surface Waters: Processes and Mitigation Strategies. *J. Environ. Sci.* 24 (3), 351–361. doi:10.1016/S1001-0742(11)60753-5

Taylor, J. R., and Thompson., W. (1998). An Introduction to Error Analysis: The Study of Uncertainties in Physical Measurements. *Phys. Today* 51 (1), 57–58. doi:10.1063/1.882103

Todorovic, G. R., Rampazzo, N., Mentler, A., Blum, W. E. H., Eder, A., Strauss, P., et al. (2014). Influence of Soil Tillage and Erosion on the Dispersion of Glyphosate and Aminomethylphosphonic Acid in Agricultural Soils. *Int. Agrophysics* 28 (1), 93–100. doi:10.2478/intag-2013-0031

Topping, C. J., Aldrich, A., and Berny, P. (2020). Overhaul Environmental Risk Assessment for Pesticides. *Science* 367, 360–363. doi:10.1126/science.aay1144

Wauchope, R. D. (1978). The Pesticide Content of Surface Water Draining from Agricultural Fields-A Review. *J. Environ. Qual.* 7 (4), 459–472. doi:10.2134/jeq1978.00472425000700040001x

Wauchope, R. D., Yeh, S., Linders, J. B. H. J., Kloskowski, R., Tanaka, K., Rubin, B., et al. (2002). Pesticide Soil Sorption Parameters: Theory, Measurement, Uses, Limitations and Reliability. *Pest. Manag. Sci.* 58, 419–445. doi:10.1002/ps.489

Yang, X., Wang, F., Bento, C. P. M., Meng, L., van Dam, R., Mol, H., et al. (2015a). Decay Characteristics and Erosion-Related Transport of Glyphosate in Chinese Loess Soil under Field Conditions. *Sci. Total Environ.* 530-531 (October), 53087–53195. doi:10.1016/j.scitotenv.2015.05.082

Yang, X., Wang, F., Bento, C. P. M., Xue, S., Gai, L., van Dam, R., et al. (2015b). Short-Term Transport of Glyphosate with Erosion in Chinese Loess Soil - A Flume Experiment. *Sci. Total Environ.* 512-513513 (April), 406–414. doi:10.1016/j.scitotenv.2015.01.071

Yu, C., Duan, P., Yu, Z., and Gao, B. (2019). Experimental and Model Investigations of Vegetative Filter Strips for Contaminant Removal: A Review. *Ecol. Eng.* 126 (October 2018), 25–36. doi:10.1016/j.ecoleng.2018.10.020

Zambon, N., Johannsen, L. L., Strauss, P., Dostal, T., Zumr, D., Cochrane, T. A., et al. (2021). Cochrane, and Andreas KlikSplash Erosion Affected by Initial Soil Moisture and Surface Conditions under Simulated Rainfall. *Catena* 196 (January), 104827. doi:10.1016/j.catena.2020.104827

Conflict of Interest: The authors declare that the research was conducted in the absence of any commercial or financial relationships that could be construed as a potential conflict of interest.

Publisher's Note: All claims expressed in this article are solely those of the authors and do not necessarily represent those of their affiliated organizations, or those of the publisher, the editors and the reviewers. Any product that may be evaluated in this article, or claim that may be made by its manufacturer, is not guaranteed or endorsed by the publisher.

frontiers | Frontiers in Environmental Science

ORIGINAL RESEARCH
published: 13 June 2022
doi: 10.3389/fenvs.2022.914636

Identification and Detection of CYP4G68 Overexpression Associated With Cyantraniliprole Resistance in *Bemisia tabaci* From China

Ran Wang[1*†], *Wunan Che*[2†], *Cheng Qu*[1], *Jinda Wang*[3] *and Chen Luo*[1*]

[1]Institute of Plant Protection, Beijing Academy of Agriculture and Forestry Sciences, Beijing, China, [2]Department of Pesticide Sciences, Shenyang Agricultural University, Shenyang, China, [3]National Engineering Research Center of Sugarcane, Fujian Agricultural and Forestry University, Fuzhou, China

Bemisia tabaci, the tobacco whitefly, is one of the most notorious agricultural sucking insect pests that severely damage a series of crops worldwide. Throughout China, *B. tabaci* threatens agricultural production with increasing cases of resistance to commonly used insecticides, prompting the widespread use of cyantraniliprole as an alternative to control hemipteran pests. Here, we found overexpression of the *CYP4G68* gene conferring cyantraniliprole resistance using quantitative real-time PCR (qPCR) and RNA interference (RNAi) in one lab-selected resistant strain CYAN-R (to about 80-fold higher than control). Furthermore, we measured levels of resistance to cyantraniliprole in whiteflies with 18 field-sampled populations across China and then confirmed that, among them, 14 field-sampled populations showed low-to-high resistance to cyantraniliprole compared with the susceptible strain. We measured *CYP4G68* expression in the 14 field populations, and the results of qPCR and RNAi indicated that in two of these populations, Haikou and Wuhan, significant overexpression of *CYP4G68* contributed to the development of field-evolved resistance to cyantraniliprole. These results indicate the need to facilitate strategies of management to delay the evolution of resistance to cyantraniliprole and control of whiteflies more sustainably, and to prevent overuse of insecticides in the environment through rational application practices.

Keywords: *Bemisia tabaci*, cyantraniliprole, resistance management, field-evolved resistance, P450s, overexpression, RNA interference

OPEN ACCESS

Edited by:
Liangang Mao,
Institute of Plant Protection (CAAS), China

Reviewed by:
Yu-Zhou Du,
Yangzhou University, China
Zhaojiang Guo,
Institute of Vegetables and Flowers (CAAS), China

***Correspondence:**
Chen Luo
luochen@ipepbaafs.cn
Ran Wang
rwang1105@126.com

†These authors have contributed equally to this work

Specialty section:
This article was submitted to Toxicology, Pollution and the Environment, a section of the journal Frontiers in Environmental Science

Received: *07 April 2022*
Accepted: *09 May 2022*
Published: *13 June 2022*

Citation:
Wang R, Che W, Qu C, Wang J and Luo C (2022) Identification and Detection of CYP4G68 Overexpression Associated With Cyantraniliprole Resistance in Bemisia tabaci From China. Front. Environ. Sci. 10:914636. doi: 10.3389/fenvs.2022.914636

INTRODUCTION

Bemisia tabaci, the tobacco whitefly, is a destructive sucking pest that devastates the production of economically important and horticultural crops worldwide. The tobacco whitefly is invasive in many locations and reported to infect over 700 species of plants (Wang et al., 2017; Horowitz et al., 2020). In addition to damaging plants by sucking, *B. tabaci* transmits over 200 plant viruses in the process of feeding (Wei et al., 2017). In recent decades, *B. tabaci* has been controlled *via* the application of various widely used chemical agents including organophosphates, carbamates, pyrethroids, insect growth regulators (pyriproxyfen and buprofezin), and neonicotinoids. However, the management of whiteflies rests primarily on the extensive usage of chemical agents over the long-term, which has

caused *B. tabaci* to develop a high or exceedingly high level of resistance to various popular chemical agents (Horowitz et al., 2020). Therefore, widely and heavily applied insecticides will not be effective for controlling *B. tabaci* in China.

It has been shown that anthranilic diamides can be used against a variety of agricultural insect pests efficiently since they have been introduced to markets around the world (Jeanguenat, 2013). Apart from excellent insecticidal functions with lethal concentrations of anthranilic diamides, they also exert influences on target insect pests at sublethal concentrations and then result in biological and physiological alterations in the pests (Huang et al., 2016; Nozad-Bonab et al., 2017; Meng et al., 2020). Among commercialized insecticides of anthranilic diamide, cyantraniliprole is a second-generation product and targets a wide range of agricultural pests from various orders of insects by acting on their ryanodine receptors (Lahm et al., 2005; Sattelle et al., 2008; Jeanguenat, 2013). Considering that cyantraniliprole can be absorbed via roots and stems of the plants, this chemical agent displays significant insecticidal effects against various orders of insects such as sucking and chewing pests, in comparison with first-generation products like flubendiamide and chlorantraniliprole, which are largely useful for controlling caterpillars (Foster et al., 2012; Barry et al., 2015; Bielza and Guillén, 2015; Grávalos et al., 2015; Moreno et al., 2018). Moreover, it was demonstrated to successfully manage immature stages and adults of *B. tabaci* and reduce the efficiency of transmitting plant viruses (Portillo et al., 2009; Schuster et al., 2009; (Stansly et al., 2010).

Due to long-term and excessive applications of insecticides, it has been well indicated that among most conventional chemical agents, a growing number of them became inefficacious for controlling agricultural insect pests (Palumbo et al., 2001). In the field applications in China, the heavy dependence on chemical agents for controlling insect pests contributed to more and more resistance cases to various classes of chemical agents that were significantly effective against *B. tabaci*. In particular, neonicotinoids are highly effective for whitefly control, but resistance to neonicotinoids has been widely reported in whiteflies from several geographic regions across China, which has led to serious control failures (Wang et al., 2010; Yang et al., 2013; Zheng et al., 2017; Zheng et al., 2021). Based on this situation, resistance to neonicotinoids has been investigated, and mechanisms of resistance were demonstrated gradually in China (Yang et al., 2020; Yang et al., 2021; Du et al., 2021; Liang et al., 2022). Not surprisingly, although it has been shown that cyantraniliprole could be one powerful alternative to popular chemical agents, field-evolved cyantraniliprole resistance in *B. tabaci* has been reported in China (Wang et al., 2018), and it has been reported that in *Aphis gossypii*, UGTs and P450s are possibly related with resistance to cyantraniliprole (Zeng et al., 2021).

In our previous work, a baseline of susceptibility to cyantraniliprole in China was established and five field-collected populations with moderate cyantraniliprole resistance were detected (Wang et al., 2018). Based on the above results, high cyantraniliprole resistance was observed in the SX population (138.4-fold) after successive selection (Wang et al., 2019). By crossing and successive backcrossing between SX and the susceptible population, one near-isogenic line of the CYAN-R strain was developed that showed 63.317-fold cyantraniliprole resistance compared to the control (Wang et al., 2020a). In the current work, we carried out lab experiments to select the CYAN-R strains with cyantraniliprole, generation by generation, to obtain stable cyantraniliprole resistance (80.8-fold) and found overexpression of the *CYP4G68* gene conferring cyantraniliprole resistance in the use of qPCR and RNAi in the CYAN-R strain. Then, in 2021, we established the baseline of susceptibilities to cyantraniliprole in 18 field-sampled populations from China and demonstrated that most of the field-sampled populations of *B. tabaci* showed various levels of cyantraniliprole resistance. Furthermore, expression levels of *CYP4G68* were measured in 14 field populations, and the results of qPCR and RNAi indicated that in two of the populations, Haikou and Wuhan, significant overexpression of *CYP4G68* contributed to the development of field-evolved resistance to cyantraniliprole. These results provide new insights for the cognition of P450-associated insecticide resistance and are solid evidence for putting forward appropriate tactics for the sustainable management of whiteflies without the overuse of insecticides.

MATERIALS AND METHODS

Insects and Chemicals

The CYAN-R strain of *B. tabaci* with cyantraniliprole resistance and the MED-S susceptible strain were recorded previously (Wang et al., 2020a), and all field-collected populations used in this work were recorded before (Wang et al., 2022). All used populations were raised on a plant of cotton without exposure to insecticides in the chamber with a temperature of 26 ± 1°C, relative humidity of 55 ± 5%, and photoperiod of 16 h light: 8 h dark. About 300 adults of *B. tabaci* were collected at random from each of the lab-reared and field-collected populations for identification of cryptic species according to the reported approach (Luo et al., 2002), and all of the tested ones were confirmed as Mediterranean cryptic species. All chemical agents utilized were analytically standardized, and cyantraniliprole (Sigma Aldrich, CAS# 736994-63-1, catalog# 32372-25MG), triton X-100 (Sigma Aldrich, CAS# 9002-93-1, catalog# 93443-100 ML), and dimethyl sulfoxide (Sigma Aldrich, CAS# 67-68-5, catalog# D8418-500 ML) were bought from Sigma Aldrich, Shanghai, China.

Bioassays

Based on our previously reported approach (Wang et al., 2018), leaf-dipping bioassays were carried out with whitefly adults from each of the tested populations. Cotton discs with a 2-cm diameter were soaked for about 20 s in the water (control) or the specific working concentration, and after air-drying, they were moved into test tubes with plug caps, respectively. After that, 25–35 whitefly adults were sampled and moved into each of the test tubes at random, and all the test tubes were kept in the chamber for 48 h and then mortality was checked. The CYAN-R cyantraniliprole resistance strain was screened with cyantraniliprole for 15 successive generations, every generation

TABLE 1 | Selection of cyantraniliprole resistance in the CYAN-R strain of *Bemisia tabaci*.

G[a]	N[b]	LC_{50} (95%CL)[c] (mg L^{-1})	Slope (±SE)	X^2 (Df)	RR[d]
0	599	85.487 (70.805–101.269)	1.484 ± 0.138	1.985 (3)	55.0
1	601	73.004 (60.288–90.682)	1.288 ± 0.133	1.211 (3)	47.0
2	593	83.420 (69.848–97.928)	1.587 ± 0.142	2.282 (3)	53.7
3	588	80.207 (66.186–100.322)	1.321 ± 0.136	2.072 (3)	51.6
4	579	94.274 (80.982–108.744)	1.820 ± 0.149	2.446 (3)	48.5
5	594	83.251 (70.446–100.754)	1.559 ± 0.142	1.192 (3)	53.6
6	590	89.523 (72.782–109.232)	1.239 ± 0.133	1.614 (3)	57.6
7	582	92.885 (75.775–110.078)	1.668 ± 0.153	1.879 (3)	59.8
8	603	105.144 (84.521–126.335)	1.435 ± 0.138	1.089 (3)	67.7
9	593	109.064 (83.600–135.258)	1.199 ± 0.134	2.141 (3)	70.2
10	596	117.425 (90.397–145.688)	1.169 ± 0.132	2.050 (3)	75.6
11	594	128.392 (100.653–158.165)	1.187 ± 0.132	1.277 (3)	82.6
12	598	120.752 (94.639–148.269)	1.222 ± 0.132	1.473 (3)	77.7
13	597	126.814 (101.082–153.085)	1.419 ± 0.140	2.348 (3)	81.6
14	599	132.184 (97.337–167.897)	1.069 ± 0.131	2.567 (3)	85.1
15	599	125.566 (93.133–158.609)	1.112 ± 0.132	2.187 (3)	80.8

[a]*Generation of adults used in the bioassay.*
[b]*Number of tested adults.*
[c]*CL, confidence limits.*
[d]*RR (resistance ratio) = LC_{50} of selected generation/LC_{50} of MED-S (1.554 mg L^{-1}).*

of *B. tabaci* adults were put through the selection with a median lethal concentration of cyantraniliprole. F_1 offspring adults of 18 field-sampled populations from nine provinces of China were used for bioassay to monitor the levels of resistance to cyantraniliprole in China.

Expression Patterns of Detoxification-Related P450s

Based on previous publications concerning insecticide resistance associated with P450 genes in *B. tabaci* (Wang Q et al., 2020; Zhou et al., 2020), 12 candidate P450s (*CYP6DZ4*, *CYP6CM1*, *CYP4G68*, *CYP6CX4*, *CYP6DW2*, *CYP303A1*, *CYP4C64*, *CYP6DZ7*, *CYP6CX1v1*, *CYP6CX3*, *CYP6CX5*, and *CYP6DW3*) were picked out and set as candidates for the analysis of gene expression. For each tested population, total RNA was extracted from 100 adults of *B. tabaci* collected at random from each tested populations, and on the basis of our reported approach (Wang et al., 2020c), qPCR was carried out, and two reference genes, EF-1α and TUB1α, were selected for the normalization. All sequences of primers are listed in **Supplementary Table S1**.

Silencing of *CYP6DW2* and *CYP4G68*

Silencing of *CYP6DW2* and *CYP4G68* was conducted, respectively, to confirm the function of *CYP6DW2* and *CYP4G68* in whiteflies via RNA interference (RNAi) based on the method recorded before (Wei et al., 2018). The double-stranded RNA (dsRNA) was synthesized using a T7 RiboMAX Express RNAi kit (Promega, Madison, WI, United States), and the primer sequences are listed in **Supplementary Table S1**. Adult *B. tabaci* were fed dsRNAs targeting enhanced green fluorescent protein (dsEGFP), or *CYP6DW2* (dsCYP6DW2), or *CYP4G68* (dsCYP4G68) for 48 h, and concentrations of dsCYP6DW2, dsCYP4G68, and dsEGFP were 0.5 μg μL^{-1}, and the artificial diet solution contained 30% sucrose (w/v) and 5% yeast extract.

Data Analysis

Data of bioassays were analyzed using PoloPlus software (2003). Resistance ratio (RR) of each of the tested chemical agents was determined by dividing the median lethal concentration of the tested field-sampled population by the median lethal concentration of the susceptible population. Values of RR were utilized to display grades of insecticide resistance, and Student's t-test and one-way ANOVA followed by Tukey's HSD for multiple comparisons were performed to analyze statistical significance ($p < 0.05$) in SPSS software (SPSS Inc., Chicago, IL, United States).

RESULTS

Cyantraniliprole Resistance Selection

Cyantraniliprole resistance in the resistant CYAN-R strain of *B. tabaci* was continuously selected for 15 generations. According to the values of LC_{50}, there was no considerable increase from G_0 to G_{15} (**Table 1**), but the resistance ratio (RR) was increased from 50.0-fold at G_0 to 80.8-fold at G_{15}. Specifically, the resistant strain of *B. tabaci* developed resistance rapidly from G_0 to G_9 (RR from 55.0- to 70.2-fold) and then remained steady after G_9, with RRs around 80-fold.

Monitoring Resistance to Cyantraniliprole in China

Baseline of susceptibilities to cyantraniliprole was constructed in the basis of 18 field-sampled populations from nine provinces across China in the year of 2021 (**Table 2**). Compared to the susceptible population MED-S, 14 of the 18 field-collected populations displayed low-to-high levels of resistance to cyantraniliprole with RRs ranging from 5.0- to 59.6-fold (LC_{50} from 8.521 to 101.474 mg L^{-1}).

Expression Profiles of the Selected P450s and RNA Interference

Compared to the susceptible ones, expression patterns of the 12 candidates (*CYP6DZ4*, *CYP6CM1*, *CYP4G68*, *CYP6CX4*, *CYP6DW2*, *CYP303A1*, *CYP4C64*, *CYP6DZ7*, *CYP6CX1v1*, *CYP6CX3*, *CYP6CX5*, and *CYP6DW3*) in CYAN-R were measured using qPCR. Expressions of *CYP6DW2* (increased 4.50-fold) and *CYP4G68* (increased 6.52-fold) in CYAN-R were significantly elevated in comparison with the susceptible ones (**Figure 1**). To explore the functions of *CYP6DW2* and *CYP4G68* further, dsCYP6DW2 and dsCYP4G68 were made and fed to adult *B. tabaci* from the CYAN-R strain to knockdown the expression of *CYP6DW2* and *CYP4G68*, respectively. After 48 h of feeding on dsCYP6DW2 and dsCYP4G68, the expression of *CYP6DW2* and *CYP4G68* in adult *B. tabaci* decreased by 41% (**Figure 2A**) and 47% (**Figure 2C**), respectively. After

TABLE 2 | Bioassays of 18 field populations and one susceptible strain of *B. tabaci* to cyantraniliprole.

Population	N[a]	Slope ±SE	LC_{50} (95%FL)[b] (mg L^{-1})	X^2 (Df)	RR[b]
MED-S	590	1.337 ± 0.137	1.703 (1.381–2.051)	2.559 (3)	—
LY	558	1.421 ± 0.142	7.070 (5.771–8.478)	1.986 (3)	4.2
CY	558	1.295 ± 0.139	4.849 (3.939–6.273)	1.617 (3)	2.8
HD	607	1.913 ± 0.148	4.706 (4.105–5.387)	2.555 (3)	2.8
TZ	600	1.048 ± 0.134	38.052 (25.899–50.023)	1.038 (3)	22.4
WQ	574	1.047 ± 0.133	15.871 (12.521–21.105)	1.207 (3)	9.3
JH	569	1.451 ± 0.142	29.108 (23.397–35.013)	1.600 (3)	17.1
ZJK	566	1.152 ± 0.137	4.848 (3.576–6.135)	1.248 (3)	2.8
BD	582	1.427 ± 0.138	30.835 (25.865–37.205)	2.487 (3)	18.1
ZZ	602	1.261 ± 0.135	22.026 (17.194–27.004)	2.196 (3)	12.9
XZ	596	1.194 ± 0.134	9.034 (7.292–11.750)	1.058 (3)	5.3
JN	584	1.409 ± 0.140	16.186 (13.197–19.381)	1.930 (3)	9.5
TA	593	1.782 ± 0.146	8.521 (7.345–9.844)	1.471 (3)	5.0
WH	592	1.378 ± 0.137	76.642 (63.818–94.437)	1.935 (3)	45.0
XY	583	1.082 ± 0.131	62.890 (50.203–80.686)	1.157 (3)	36.9
CS	573	1.218 ± 0.133	52.089 (42.353–64.292)	1.374 (3)	30.6
YY	593	1.140 ± 0.131	70.357 (56.804–89.825)	1.225 (3)	41.3
HK	597	1.335 ± 0.134	87.995 (72.632–105.840)	2.169 (3)	51.7
SY	577	1.922 ± 0.155	101.474 (87.203–116.694)	1.640 (3)	59.6

[a]*Number of insects used.*
[b]*RR (resistance ratio) = LC_{50} (field-collected population)/LC_{50} (MED-S).*

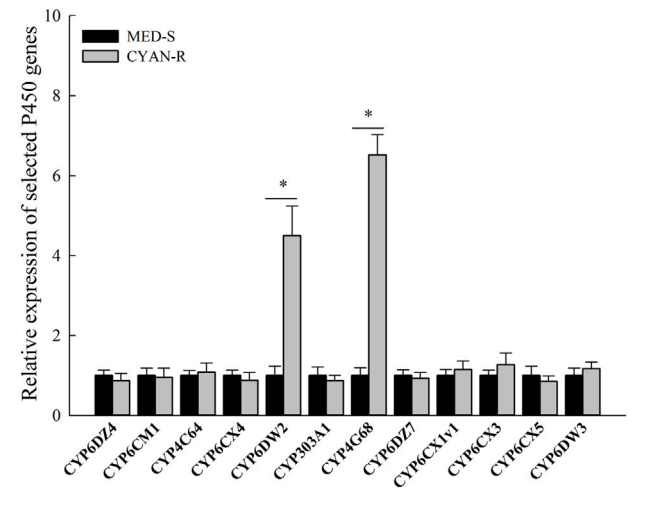

FIGURE 1 | Expression profiles of 12 candidate P450 genes.

cyantraniliprole selection, feeding on dsCYP4G68 by adults resulted in considerably higher death rate compared to that of the dsEGFP control (**Figure 2D**), and little remarkable increase in death rate was found with the feeding on dsCYP6DW2 compared with the control (**Figure 2B**).

Expression Patterns of *CYP4G68* in the Fourteen Field-Resistant Populations

Relative expression profiles of *CYP4G68* in 14 field-collected cyantraniliprole-resistant populations were established and compared to MED-S (**Figure 3**). Among the field-collected population and the susceptible strain, significant overexpression of *CYP4G68* was observed in WH (3.52-fold), CS (3.41-fold), HK (4.55-fold), and SY (3.98-fold). In other field-resistant populations, significant overexpression of *CYP4G68* was not observed.

Confirmation of the Role of *CYP4G68* in the Four Field-Resistant Populations

Based on the above results, to further investigate the functions of *CYP4G68* in the four field-resistant populations, dsCYP4G68 was synthesized and fed to the WH, CS, HK, and SY populations of adults to silence *CYP4G68* in each of the populations. After 48 h of ingestion of dsCYP4G68, adult *B. tabaci* displayed decreased expression of *CYP4G68* from 42 to 49% in the four tested populations (**Figures 4A–D**). After the cyantraniliprole treatment, feeding on dsCYP4G68 by adults resulted in a considerably elevated death rate compared to the dsEGFP control in WH and HK populations (**Figure 4E** and **Figure 4G**), but little remarkable increase in death rate was found with the feeding on dsCYP4G68 compared to that of the control in CS and SY populations (**Figure 4F** and **Figure 4H**).

DISCUSSION

Cyantraniliprole has shown excellent efficacy against sucking insect pests worldwide, but field-evolved cyantraniliprole resistance in whiteflies has been recorded in China after several years of extensive application (Wang et al., 2019). Previously, we established the CYAN-R strain of *B. tabaci* on the basis of a field-developed cyantraniliprole-resistant

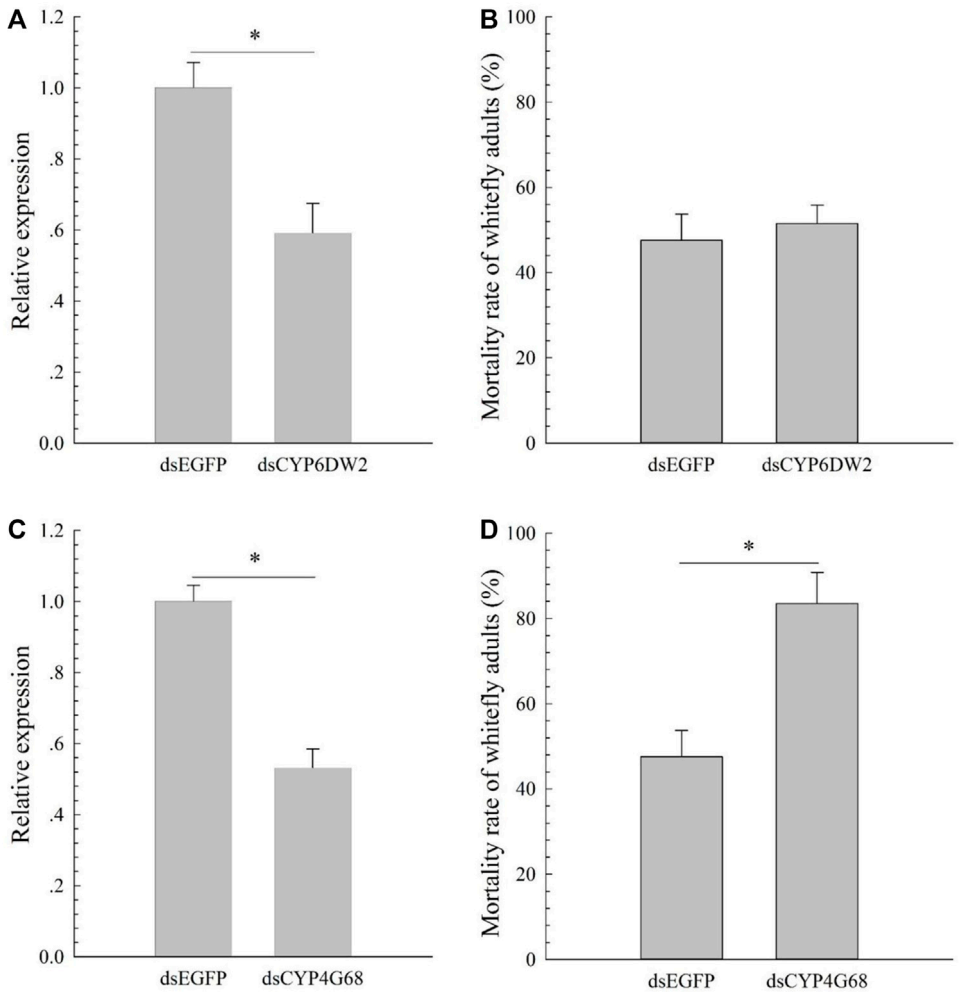

FIGURE 2 | Effects of dsCYP6DW2 on the expression of *CYP6DW2* **(A)** and effects of silencing *CYP6DW2* **(B)** on resistance to cyantraniliprole, and effects of dsCYP4G68 on the expression of *CYP4G68* **(C)** and effects of silencing *CYP4G68* **(D)** on resistance to cyantraniliprole.

population. After that, a series of biochemical assays were performed, and the results demonstrated that enhanced P450 activities functioned directly in the cyantraniliprole resistance of the CYAN-R strain (Wang et al., 2020a). Insect pests have been demonstrated to develop some resistance to other classes of chemical agents under chronic exposure of selection, prompting studies to explore mechanisms of resistance (Wang et al., 2020b; Wang et al., 2020d; Yang et al., 2020; Zeng et al., 2021). In the current work, continuous cyantraniliprole selections for 15 generations increased resistance from 55.0-fold to 80.9-fold in the CYAN-R strain.

The overexpression of P450s mediating metabolic resistance to various insecticides has been indicated in many species of insect pests worldwide (Nauen et al., 2022). In recent reports of insecticide resistance in *B. tabaci*, P450-mediated resistance was one of the most reported mechanisms underlying resistance to several insecticides including imidacloprid, thiamethoxam, acetamiprid, and flupyradifurone (Wang et al., 2020c; Wang Q et al., 2020; Yang et al., 2020; Zhou et al., 2020; Liang et al., 2022). In the current study, overexpression was detected for two P450 genes, *CYP6DW2* and *CYP4G68*, in the CYAN-R strain compared with the susceptible strain. Similarly, a previous report showed that various levels of resistance to imidacloprid in field populations of *B. tabaci* resulted from the overexpression of *CYP4C64* and *CYP6CM1*, two P450 genes (Yang et al., 2013). Furthermore, we found that silencing *CYP4G68* resulted in a considerably increased death rate in adults treated with cyantraniliprole in the CYAN-R strain, yet silencing *CYP6DW2* did not significantly increase the death rate of adults treated with cyantraniliprole in the CYAN-R strain. All the findings demonstrated that *CYP4G68* can contribute to increased cyantraniliprole resistance in whiteflies. In addition to P450-mediated cyantraniliprole resistance, it has been demonstrated that the expression of calmodulin and 1,4,5-trisphosphate receptor can be associated with changed susceptibility to cyantraniliprole (Guo et al., 2017; Guo

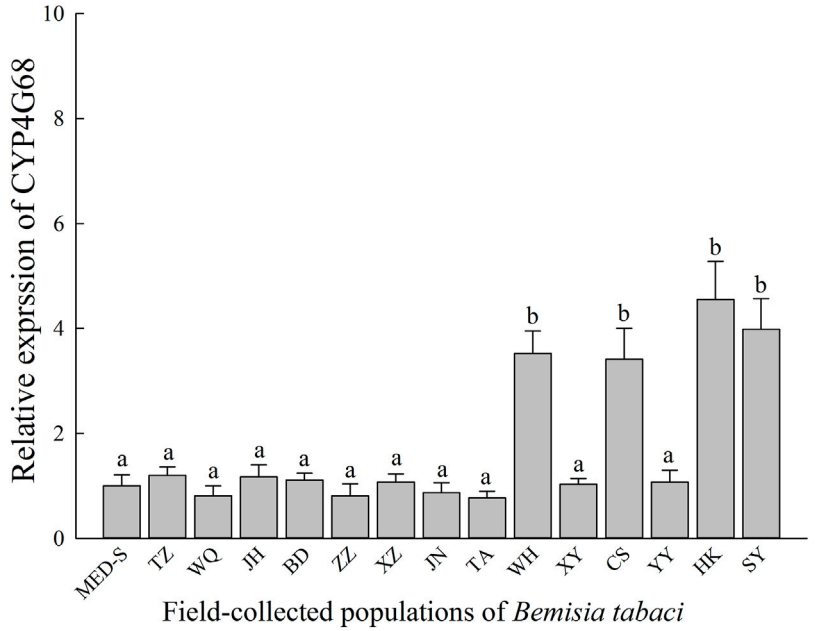

FIGURE 3 | Expression profiles of *CYP4G68* in 14 field-evolved cyantraniliprole-resistant *B. tabaci* populations from China.

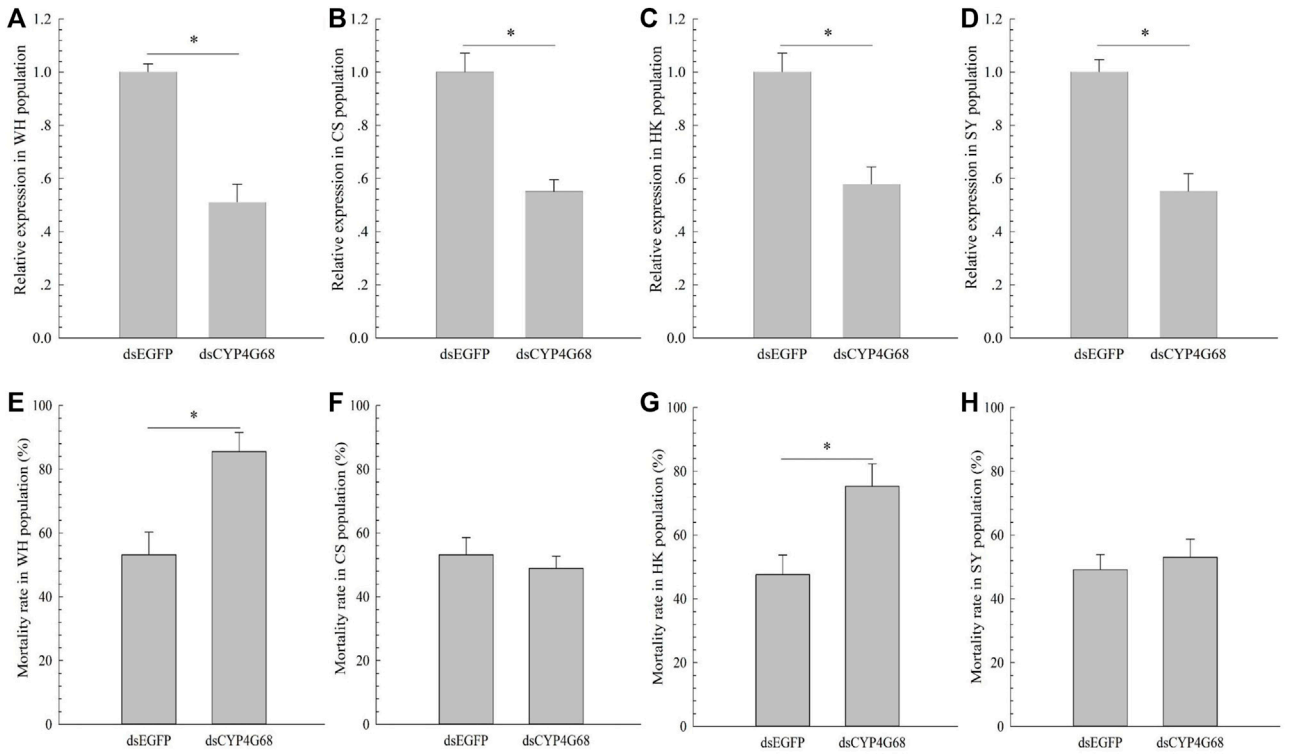

FIGURE 4 | Effects of dsCYP4G68 on the expression of *CYP4G68* in populations WH **(A)**, CS **(B)**, HK **(C)**, and SY **(D)**. Effects of silencing *CYP4G68* on resistance to cyantraniliprole in populations WH **(E)**, CS **(F)**, HK **(G)**, and SY **(H)**.

et al., 2021) and Ca^{2+}-binding protein function in response to cyantraniliprole exposure through the stabilization of Ca^{2+} concentration (Guo et al., 2019).

Considering that the use of cyantraniliprole across China has facilitated reasonable solutions for solving underlying problems of resistance to popular chemical agent against *B. tabaci*, it is essential to understand whether whiteflies have already developed resistance to cyantraniliprole in the field. Previously, we monitored the resistance levels of cyantraniliprole against whiteflies throughout China from 2015 to 2016 and found only a few field-collected populations showing low resistance (Wang et al., 2018). In our current work, we monitored the levels of cyantraniliprole resistance in 18 field-sampled populations from nine provinces across China in 2021, and found that 14 of the populations showed low-to-high resistance to cyantraniliprole, which means field-evolved cyantraniliprole resistance has escalated in China. Furthermore, we found the overexpression of *CYP4G68* in the cyantraniliprole-resistant populations, WH, CS, HK, and SY, and confirmed that this overexpression contributed to resistance in the WH and HK populations but not in the CS and SY populations. Considering that *CYP4G68* functions in thiamethoxam and imidacloprid resistance in *B. tabaci* (Wang Q et al., 2020; Liang et al., 2022), we surmise that overuse and the long-term application of neonicotinoids and cyantraniliprole in China may give rise to the rapid development of resistance associated with overexpression of *CYP4G68*. Hence, *CYP4G68* can be utilized for monitoring and managing cyantraniliprole resistance in field-developed resistant populations. Our current findings supply novel opinions and understandings concerning possible functions of P450 genes in cyantraniliprole resistance and provide more evidence for the further studies of P450s-associated resistance. Besides, our results could be instrumental in formulating strategies of pest management for controlling insect pests sustainably with more environment-friendly approaches.

DATA AVAILABILITY STATEMENT

The raw data supporting the conclusions of this article will be made available by the authors, without undue reservation.

AUTHOR CONTRIBUTIONS

RW, WC, and CL conceived and designed the study. RW and WC performed the experiments and analyzed the data with the help of CQ, JW, and CL. RW wrote the first draft of the manuscript. RW, WC, CQ, JW, and CL participated in manuscript drafting and modification.

FUNDING

This work was supported by the National Natural Science Foundation of China (31972266, 32172438, 31801743).

SUPPLEMENTARY MATERIAL

The Supplementary Material for this article can be found online at: https://www.frontiersin.org/articles/10.3389/fenvs.2022.914636/full#supplementary-material

REFERENCES

Barry, J. D., Portillo, H. E., Annan, I. B., Cameron, R. A., Clagg, D. G., Dietrich, R. F., et al. (2015). Movement of Cyantraniliprole in Plants after Foliar Applications and its Impact on the Control of Sucking and Chewing Insects. *Pest. Manag. Sci.* 71 (3), 395–403. doi:10.1002/ps.3816

Bielza, P., and Guillén, J. (2015). Cyantraniliprole: A Valuable Tool for *Frankliniella occidentalis*(Pergande) Management. *Pest. Manag. Sci.* 71 (8), 1068–1074. doi:10.1002/ps.3886

Du, T., Fu, B., Wei, X., Yin, C., Yang, J., Huang, M., et al. (2021). Knockdown of UGT352A5 Decreases the Thiamethoxam Resistance in *Bemisia tabaci* (Hemiptera: Gennadius). *Int. J. Biol. Macromol.* 186, 100–108. doi:10.1016/j.ijbiomac.2021.07.040

Foster, S. P., Denholm, I., Rison, J. L., Portillo, H. E., Margaritopoulis, J., and Slater, R. (2012). Susceptibility of Standard Clones and European Field Populations of the Green Peach Aphid, *Myzus persicae*, and the Cotton Aphid, *Aphis gossypii* (Hemiptera: Aphididae), to the Novel Anthranilic Diamide Insecticide Cyantraniliprole. *Pest. Manag. Sci.* 68 (4), 629–633. doi:10.1002/ps.2306

Grávalos, C., Fernández, E., Belando, A., Moreno, I., Ros, C., and Bielza, P. (2015). Cross-resistance and Baseline Susceptibility of Mediterranean Strains of *Bemisia tabaci* Cyantraniliprole. *Pest. Manag. Sci.* 71 (7), 1030–1036. doi:10.1002/ps.3885

Guo, L., Liang, P., Fang, K., and Chu, D. (2017). Silence of Inositol 1,4,5-trisphosphate Receptor Expression Decreases Cyantraniliprole Susceptibility in *Bemisia tabaci*. *Pesticide Biochem. Physiol.* 142, 162–169. doi:10.1016/j.pestbp.2017.07.005

Guo, L., Li, C., Liang, P., and Chu, D. (2019). Cloning and Functional Analysis of Two Ca^{2+}-Binding Proteins (CaBPs) in Response to Cyantraniliprole Exposure in *Bemisia tabaci* (Hemiptera: Aleyrodidae). *J. Agric. Food Chem.* 67 (40), 11035–11043. doi:10.1021/acs.jafc.9b04028

Guo, L., Li, C., Coupland, G., Liang, P., and Chu, D. (2021). Up-regulation of Calmodulin Involved in the Stress Response to Cyantraniliprole in the Whitefly, *Bemisia tabaci* (Hemiptera: Aleyrodidae). *Insect Sci.* 28 (6), 1745–1755. doi:10.1111/1744-7917.12887

Horowitz, A. R., Ghanim, M., Roditakis, E., Nauen, R., and Ishaaya, I. (2020). Insecticide Resistance and its Management in *Bemisia tabaci* Species. *J. Pest Sci.* 93, 893–910. doi:10.1007/s10340-020-01210-0

Huang, L., Lu, M., Han, G., Du, Y., and Wang, J. (2016). Sublethal Effects of Chlorantraniliprole on Development, Reproduction and Vitellogenin Gene (CsVg) Expression in the Rice Stem borer, *Chilo suppressalis*. *Pest. Manag. Sci.* 72 (12), 2280–2286. doi:10.1002/ps.4271

Jeanguenat, A. (2013). The Story of a New Insecticidal Chemistry Class: the Diamides. *Pest. Manag. Sci.* 69 (1), 7–14. doi:10.1002/ps.3406

Lahm, G. P., Selby, T. P., Freudenberger, J. H., Stevenson, T. M., Myers, B. J., Seburyamo, G., et al. (2005). Insecticidal Anthranilic Diamides: A New Class of Potent Ryanodine Receptor Activators. *Bioorg. Med. Chem. Lett.* 15 (22), 4898–4906. doi:10.1016/j.bmcl.2005.08.034

Liang, J., Yang, J., Hu, J., Fu, B., Gong, P., Du, T., et al. (2022). Cytpchrome P450 CYP4G68 is Associated with Imidacloprid and Thiamethoxam Resistance in Field Whitefly, *Bemisia tabaci* (Hemiptera: Gennadius). *Agriculture* 12 (4), 473. doi:10.3390/agriculture12040473

Luo, C., Yao, Y., Wang, R. J., Yan, F. M., Hu, D. X., and Zhang, Z. L. (2002). The Use of Mitochondrial Cytochrome Oxidase mt COI Gene Sequences for the Identification of Biotypes of *Bemisia tabaci* (Gennadius) in China. *Acta Entomol. Sin.* 45, 759–763.

Meng, X., Zhang, N., Yang, X., Miao, L., Jiang, H., Ji, C., et al. (2020). Sublethal Effects of Chlorantraniliprole on Molting Hormone Levels and mRNA Expressions of Three Halloween Genes in the Rice Stem Borer, *Chilo suppressalis*. *Chemosphere* 238, 124676. doi:10.1016/j.chemosphere.2019.124676

Moreno, I., Belando, A., Grávalos, C., and Bielza, P. (2018). Baseline Susceptibility of Mediterranean Strains of *Trialeurodes vaporariorum* (Westwood) to Cyantraniliprole. *Pest. Manag. Sci.* 74 (7), 1552–1557. doi:10.1002/ps.4869

Nauen, R., Bass, C., Feyereisen, R., and Vontas, J. (2022). The Role of Cytochrome P450s in Insect Toxicology and Resistance. *Annu. Rev. Entomol.* 67, 105–124. doi:10.1146/annurev-ento-070621-061328

Nozad-Bonab, Z., Hejazi, M. J., Iranipour, S., and Arzanlou, M. (2017). Lethal and Sublethal Effects of Some Chemical and Biological Insecticides on *Tuta absoluta* (Lepidoptera: Gelechiidae) Eggs and Neonates. *J. Econ. Entomol.* 110 (3), 1138–1144. doi:10.1093/jee/tox079

Palumbo, J. C., Horowitz, A. R., and Prabhaker, N. (2001). Insecticidal Control and Resistance Management for *Bemisia tabaci*. *Crop Prot.* 20 (9), 739–765. doi:10.1016/S0261-2194(01)00117-X

Portillo, H. E., Annan, I. B., and Marçon, G. Z. (2009). "Cyazypyr (DPX-HGW86, Cyantraniliprole): A Novel Anthranilic Diamide Insecticide for Control of Whiteflies and Other Important Arthropod Pests," in 5th International Bemisia Workshop Abstracts, 60, Guangzhou, China. Available at: http://invasivespecies.org.cn/uploadfile/20091207/ 20091207104910715.pdf (Accessed September 8, 2011).

Sattelle, D. B., Cordova, D., and Cheek, T. R. (2008). Insect Ryanodine Receptors: Molecular Targets for Novel Pest Control Chemicals. *Invert. Neurosci.* 8 (3), 107–119. doi:10.1007/s10158-008-0076-4

Schuster, D. J., Perez, N. A., Portillo, H. E., Marçon, G. Z., and Annan, I. B. (2009). "Cyazypyr (DPX6HGW86, Cyantraniliprole): A Novel Anthranilic Diamide Insecticide for Managing *Bemisia tabaci* and Interfering With Transmission of Tomato Yellow Leaf Curl Virus on Tomato Transplants," in 5th International Bemisia Workshop Abstracts, 59, Guangzhou, China. Available at: http://invasivespecies.org.cn/uploadfile/20091207/ 20091207104910715.pdf (Accessed September 8, 2011).

Stansly, P. A., Kostyk, B., and Riefer, R. (2010). Effect of Rate and Application Method of Cyazypyr (HGW86) on Control of Silverleaf Whitefly and Southern Armyworm in Staked Tomato. *Arthropod. Manag. Tests* 35, 1–3.

Wang, Z., Yan, H., Yang, Y., and Wu, Y. (2010). Biotype and Insecticide Resistance Status of the Whitefly *Bemisia tabaci* from China. *Pest. Manag. Sci.* 66 (12), 1360–1366. doi:10.1002/ps.2023

Wang, X. W., Li, P., and Liu, S. S. (2017). Whitefly Interactions with Plants. *Curr. Opin. Insect Sci.* 19, 70–75. doi:10.1016/j.cois.2017.02.001

Wang, R., Wang, J. D., Che, W. N., and Luo, C. (2018). First Report of Field Resistance to Cyantraniliprole, a New Anthranilic Diamide Insecticide, on *Bemisia tabaci* MED in China. *J. Integr. Agric.* 17 (1), 158–163. doi:10.1016/S2095-3119(16)61613-1

Wang, R., Wang, J. D., Che, W. N., Sun, Y., Li, W. X., and Luo, C. (2019). Characterization of Field-Evolved Resistance to Cyantraniliprole in *Bemisia tabaci* MED from China. *J. Integr. Agric.* 18 (11), 2571–2578. doi:10.1016/S2095-3119(19)62557-8

Wang, R., Che, W., Wang, J., Qu, C., and Luo, C. (2020a). Cross-resistance and Biochemical Mechanism of Resistance to Cyantraniliprole in a Near-Isogenic Line of Whitefly *Bemisia tabaci* Mediterranean (Q Biotype). *Pesticide Biochem. Physiol.* 167, 104590. doi:10.1016/j.pestbp.2020.104590

Wang, R., Qu, C., Wang, Z., and Yang, G. (2020b). Cross-resistance, Biochemical Mechanism and Fitness Costs of Laboratory-Selected Resistance to Pyridalyl in Diamondback Moth, *Plutella xylostella*. *Pesticide Biochem. Physiol.* 163, 8–13. doi:10.1016/j.pestbp.2019.10.008

Wang, R., Wang, J., Zhang, J., Che, W., Feng, H., and Luo, C. (2020c). Characterization of Flupyradifurone Resistance in the Whitefly *Bemisia tabaci* Mediterranean (Q Biotype). *Pest Manag. Sci.* 76 (12), 4286–4292. doi:10.1002/ps.5995

Wang, R., Wang, Z., Luo, C., and Yang, G. (2020d). Characterization of Pyridalyl Resistance in a Laboratory-Selected Strain of *Frankliniella occidentalis*. *Pesticide Biochem. Physiol.* 166, 104564. doi:10.1016/j.pestbp.2020.104564

Wang, R., Gao, B., Che, W., Qu, C., Zhou, X., and Luo, C. (2022). First Report of Field Resistance to Afidopyropen, the Novel Pyropene Insecticide, on *Bemisia tabaci* Mediterranean (Q Biotype) from China. *Agronomy* 12 (3), 724. doi:10.3390/agronomy12030724

Wang, Q., Wang, M. N., Jia, Z. Z., Ahmat, T., Xie, L. J., and Jiang, W. H. (2020). Resistance to Neonicotinoid Insecticides and Expression Changes of Eighteen Cytochrome P450 Genes in Field Populations of *Bemisia tabaci* from Xinjiang, China. *Entomol. Res.* 50 (4), 205–211. doi:10.1111/1748-5967.12427

Wei, J., He, Y. Z., Guo, Q., Guo, T., Liu, Y. Q., Zhou, X. P., et al. (2017). Vector Development and Vitellogenin Determine the Transovarial Transmission of Begomoviruses. *Proc. Natl. Acad. Sci. U.S.A.* 114 (26), 6746–6751. doi:10.1073/pnas.1701720114

Wei, P., Che, W., Wang, J., Xiao, D., Wang, R., and Luo, C. (2018). RNA Interference of Glutamate-Gated Chloride Channel Decreases Abamectin Susceptibility in *Bemisia tabaci*. *Pesticide Biochem. Physiol.* 145, 1–7. doi:10.1016/j.pestbp.2017.12.004

Yang, X., Xie, W., Wang, S. L., Wu, Q. J., Pan, H. P., Li, R. M., et al. (2013). Two Cytochrome P450 Genes are Involved in Imidacloprid Resistance in Field Populations of the Whitefly, *Bemisia tabaci*, in China. *Pesticide Biochem. Physiol.* 107 (3), 343–350. doi:10.1016/j.pestbp.2013.10.002

Yang, X., Deng, S., Wei, X., Yang, J., Zhao, Q., Yin, C., et al. (2020). MAPK-directed Activation of the Whitefly Transcription Factor CREB Leads to P450-Mediated Imidacloprid Resistance. *Proc. Natl. Acad. Sci. U.S.A.* 117 (19), 10246–10253. doi:10.1073/pnas.1913603117

Yang, X., Wei, X., Yang, J., Du, T., Yin, C., Fu, B., et al. (2021). Epitranscriptomic Regulation of Insecticide Resistance. *Sci. Adv.* 7 (19), eabe5903. doi:10.1126/sciadv.abe5903

Zeng, X., Pan, Y., Tian, F., Li, J., Xu, H., Liu, X., et al. (2021). Functional Validation of Key Cytochrome P450 Monooxygenase and UDP-Glycosyltransferase Genes Conferring Cyantraniliprole Resistance in *Aphis gossypii* Glover. *Pesticide Biochem. Physiol.* 176, 104879. doi:10.1016/j.pestbp.2021.104879

Zheng, H., Xie, W., Wang, S., Wu, Q., Zhou, X., and Zhang, Y. (2017). Dynamic Monitoring (B versus Q) and Further Resistance Status of Q-type *Bemisia tabaci* in China. *Crop Prot.* 94, 115–122. doi:10.1016/j.cropro.2016.11.035

Zheng, H., Xie, W., Fu, B., Xiao, S., Tan, X., Ji, Y., et al. (2021). Annual Analysis of Field-evolved Insecticide Resistance in *Bemisia tabaci* across China. *Pest Manag. Sci.* 77 (6), 2990–3001. doi:10.1002/ps.6338

Zhou, C. S., Cao, Q., Li, G. Z., and Ma, D. Y. (2020). Role of Several Cytochrome P450s in the Resistance and Cross-Resistance against Imidacloprid and Acetamiprid of *Bemisia tabaci* (Hemiptera: Aleyrodidae) MEAM1 Cryptic Species in Xinjiang, China. *Pesticide Biochem. Physiol.* 163, 209–215. doi:10.1016/j.pestbp.2019.11.017

Conflict of Interest: The authors declare that the research was conducted in the absence of any commercial or financial relationships that could be construed as a potential conflict of interest.

frontiers | Frontiers in Environmental Science

ORIGINAL RESEARCH
published: 14 June 2022
doi: 10.3389/fenvs.2022.888394

Sewage Sludge-Induced Effect on Growth, Enzyme Inhibition, and Genotoxicity can be Ameliorated Using Wheat Straw and Biochar in *Pheretima posthuma* Earthworms

Hira Khalid[1], *Muhammad Kashif Zahoor*[1]*, *Danish Riaz*[2], *Madeeha Arshad*[2], *Rabia Yaqoob*[2] *and Kanwal Ranian*[1]*

[1]*Department of Zoology, Government College University, Faisalabad, Pakistan,* [2]*Division of Science and Technology, University of Education Lahore, Lahore, Pakistan*

OPEN ACCESS

Edited by:
Mazhar Iqbal Zafar,
Quaid-i-Azam University, Pakistan

Reviewed by:
Sajida Rasheed,
University of Kotli Azad Jammu and Kashmir, Pakistan
Sartaj Ahmad Bhat,
Gifu University, Japan

***Correspondence:**
Muhammad Kashif Zahoor
kashif.zahoor@gcuf.edu.pk
Kanwal Ranian
kanwalranian22@gcuf.edu.pk

Specialty section:
This article was submitted to Toxicology, Pollution and the Environment, a section of the journal Frontiers in Environmental Science

Received: *02 March 2022*
Accepted: *25 April 2022*
Published: *14 June 2022*

Citation:
Khalid H, Kashif Zahoor M, Riaz D, Arshad M, Yaqoob R and Ranian K (2022) Sewage Sludge-Induced Effect on Growth, Enzyme Inhibition, and Genotoxicity can be Ameliorated Using Wheat Straw and Biochar in Pheretima posthuma Earthworms. Front. Environ. Sci. 10:888394. doi: 10.3389/fenvs.2022.888394

Sewage sludge, rich in organic matter and nutrients, is widely used as a fertilizer to increase the fertility of soil. The direct application of sewage sludge without any treatment causes soil contamination as well as significantly affects the earthworm population. In the present study, the effect of sewage sludge-amended soil on growth, enzyme activities, and the DNA damage in *Pheretima posthuma* earthworms was studied under wheat straw and biochar treatment of 30-day laboratory incubation. Wheat straw, biochar, and sewage sludge were applied at 0 (control), 5, 10, and 25% w/w along with combined treatment of sewage sludge with biochar and wheat straw, respectively at 25% each. After the incubation period, the percentage change in mean weight and length was measured and esterase and phosphatase enzyme activities were quantitatively determined. RAPD-PCR and the comet assay were performed to assess the genotoxicity. A significant weight loss was observed (26%) at a 25% rate of sewage sludge and biochar (11%). Similarly, a maximum decrease in length was observed with sewage sludge (2.5%) followed by biochar (0.80%) at a 25% application rate. Mean weight and length both decreased by increasing the rate of sewage sludge and biochar. In addition, no change was observed in the weight and length of *P. posthuma* in the treatment consisting of sewage sludge and wheat straw. Moreover, sewage sludge caused inhibition of esterase and phosphatase activities as well as induced DNA damage. The comet parameters showed that wheat straw and biochar ameliorated the toxic effects of sewage sludge. It is, therefore, concluded that sewage sludge has a tangible impact on earthworms which ultimately disrupts ecosystem functions and wheat straw and biochar can thus be utilized to reduce the toxicity of sewage sludge in *Pheretima posthuma* earthworms.

Keywords: biochar, sewage sludge, vermicompost, earthworm, comet assay, esterases and phosphatases, genotoxicity

INTRODUCTION

Earthworms are commonly defined as "ecosystem engineers" and are considered as the largest element of animal biomass. They take part in many ecosystem services such as soil structure formation, pedogenesis and nutrient cycle in soil, and regulation and movement of water where they make it more available for plants (Valckx et al., 2010; Blouin et al., 2013; Li et al., 2018). They aid in soil formation and stabilization by mixing material present in the soil, reconditioning the soil with the help of various microbes, improving soil structure and aeration, increasing soil porosity, facilitating decomposition of organic matter, and helping to develop vermicompost (Ansari and Ismail, 2012; He et al., 2016). There are more than 3,000 species of earthworm in the natural environment which turnover large quantities of organic matter. Detailed scientific knowledge is only known for about five percent. Two tons per hectare of earthworm populations have been recorded in the natural environment which can be potentially increased up to 10 times under controlled laboratory conditions. The principle function of earthworms in vermicomposting is to increase the surface area available for micro and macro-organisms involved in the decomposition and stabilization of organic matter (Murtaza et al., 2016; Murtaza, 2015).

The *Pheretima posthuma* earthworm belongs to the order Oligochaeta and class Clitella which includes all segmented worms with clitella. The structure of the clitella appears as a modification of the epidermal layer (Martin et al., 2007; Ansari and Saywack 2011). Adult *P. posthuma* is generally brownish in color due to the presence of porphyrin pigment and has a 15–30 cm body length. They are usually terrestrial and also found in the moist soil of agricultural areas, near plantations, and soil near ponds and other water bodies (Elmer et al., 2015). Earthworms are usually classified into three categories on the basis of feeding, burrowing, and the ecological niches they inhabit, i.e., aneic, endogeic, and epigeic. *P. posthuma* are endogeic worms with shallow burrowing only up to 30–45 cm deep in the soil. They generally feed on soil organic matter which is decomposed by microbial decomposers present in their guts (Van Groenigen et al., 2014). The gut, in fact, harbors a wide diversity of microorganisms including bacteria, algae, fungi, protozoa, actinomycetes, and even nematodes (Birkas et al., 2010). Earthworm species are tolerable to a range of contaminants such as herbicides, heavy metals, and the organic pollutants emerging from industries, factories, and hospitals *via* wastewater and sewage sludge (Murtaza et al., 2016; Murtaza, 2015). They reduce the concentrations and toxicity of soil contaminants by accumulating them in their body tissues (Dabke 2013; Ibrahim et al., 2016).

Sewage sludge is a byproduct of wastewater treatment plants rich in organic matter, nutrients (e.g., nitrogen, phosphorus, sodium, potassium, magnesium, and sulfur), and heavy metals including copper, zinc, cadmium, and many others (Singh and Agrawal 2008). Sewage sludge has high organic matter (40–70%) and can manipulate the physical, chemical, and biological properties of soil; thus potentially increasing the crop yield. Approximately 50% of all sludge produced in the United Kingdom and human waste-based sludge imported from the Netherlands is used in agriculture. Approximately 25% of all the sludge disposed to agriculture in the United Kingdom is raw sludge derived from small rural works (Charlton et al., 2016; Murtaza et al., 2016; Edwards and Arancon, 2004). In Pakistan, about 6.75 million tons of solid waste is being formed on a daily basis, and 50–70% of this total is either transported to open dumps or landfills. The remaining 30–50% is left as masses in populous regions that cause numerous health-related issues in dwellers (Pak-Epa, 2005; Ali and Hasan, 2001). In Pakistan, wastewater treatment plants (WWTPs) have been installed on different industrial and municipal sites and remain functional throughout the year (Haydar et al., 2015) and generate huge amounts of sewage sludge on a daily basis (Bareen and Tahira, 2011; Afzal et al., 2016). These WWTPs generate sewage sludge in large volume on a daily basis which is then used by some farmers owing to their nutritious value.

Sewage sludge is considered an inexpensive source of plant nutrients to increase soil fertility; however, the presence of heavy metals and persistent organic pollutants (POPs) in sewage sludge poses a serious threat to soil biota earthworms. The number of earthworms in soil is continuously declining due to the application of raw sewage sludge as fertilizer (Kızılkaya and Hepş;en 2004). Many studies have reported negative effects of sewage sludge on the physiology, activity, and diversity of earthworms (e.g., Kızılkaya and Hepş;en 2004; Liu et al., 2005; Stöven and Schnug 2009; Karimi e al. 2020). The addition of wheat straw to soil is of great importance as it increases the production and heat in the soil. The application of wheat straw with sewage sludge in the soil is greatly degraded by earthworms (Wanga et al., 2014). Wheat straw is an efficient culture medium for large scale production of vermicompost for sustainable land restoration practices at low input. Biochar is an organic amendment developed from pyrolysis of biomass waste in the absence of oxygen which generally consists of recalcitrant organic carbon and improves the soil physio-chemical environment (Riaz et al., 2017; Gul et al., 2015). Biochar has been shown to reduce the toxicity of both organic and inorganic pollutants in the soil environment by reducing their bioavailability to soil organisms (Park et al., 2011; Zhang et al., 2013; Zhang et al., 2017). Subsequently, biochar reduces the negative effects of pollutants on earthworms (e.g., Malińska et al., 2016; Sanchez-Hernandez et al., 2019).

Despite the handful of benefits associated with land application of sewage sludge, the presence of potentially toxic elements in these amendments could be a serious threat to soil, soil fauna, and also, to a certain extent, to food health and quality (Murtaza et al., 2016; Murtaza, 2015). Since, very limited data are available on the toxicity and overall effect of sewage sludge on the growth and enzyme activities in earthworms, the present study was conducted wherein we hypothesized that wheat straw and biochar would decrease the toxic effect of sewage sludge on growth and enzyme activities in *Pheretima posthuma* earthworms. Whereas the addition of wheat straw and biochar would also improve earthworm activities by providing them with food and reducing the negative effects of sewage sludge, and these

effects would largely depend upon the rate of amendment applications. The objectives of this study, therefore, were to investigate the deleterious effects of different concentrations of sewage sludge on the growth, enzyme activities, and genotoxicity in *P. posthuma* earthworms under laboratory conditions.

MATERIAL AND METHODS

Collection of Earthworms and Soil Samples

The samples of *P. posthuma* earthworms with well-defined clitella were collected by hand digging from agricultural field plots in Faisalabad as they are one of the most abundantly found earthworms in the soil of Pakistan. Soil samples were also collected from the area where the earthworms were collected. The soil was dried in air and sieved through a 2.0 mm mesh to remove any vegetation litter and stones. The soil was alkaline calcareous clay loam with pH 8.02, EC 1.34 dS m^{-1}, total organic C 9.21 g $kg^{-1,}$ and total N 0.54 g kg^{-1} (Riaz et al., 2017). Earthworms were kept in plastic buckets containing soil moistened to a 60% water holding capacity (WHC) and mixed with leaf litter (Ali et al., 2019). Simultaneously, the soil was brought to 60% WHC and pre-incubated to recondition the earthworms with optimum microbial activities before the start of the experiment.

Collection of Sewage Sludge, Wheat Straw, and Biochar

Sewage sludge was collected from Water and Sanitation Agency Faisalabad, air-dried, and sieved with 2.0 mm mesh for uniform particle size. It had a pH of 7.06, EC 12.46 dS m^{-1}, total organic C 146 g kg^{-1}, total N 1.19 g kg^{-1} and total P 1.02 g kg^{-1}, and heavy metals including Cd (0.86 mg kg^{-1}), Cr (50 mg kg^{-1}), Ni (56 mg kg^{-1}), and Pb (47 mg kg^{-1}) (Riaz et al., 2020). Wheat straw was collected from an agriculture field in Faisalabad and was crushed in a sieve from a 2.0 mm mesh. It had a total organic C of 427 g kg^{-1}, a total N of 6.6 g kg^{-1}, and a C/N ratio of 65 (Riaz et al., 2017). Biochar was collected from the Department of Environmental Sciences and Engineering, Government College University Faisalabad. Biochar was developed from corncob biomass at 400°C and contained 733 and 10.3 g kg^{-1} of total organic C and total N contents, respectively (Riaz et al., 2017).

Laboratory Incubation Experiment

A microcosm experimental setup was developed in 1 L glass Mason jars filled with 700 g of pre-incubated moist soils mixed with treatments in a completely randomized experimental design. Treatments consisted of control (soil only), wheat straw, and biochar at 5, 10, and 25% w/w basis rates where wheat straw plus biochar received 25% each of wheat straw and biochar. Each treatment was replicated three times. Earthworms were pre-starved by being placed on petri plates on a moistened paper towel overnight to ensure their guts were free of any food before introducing them into the microcosms. After starvation, the body weight and length of each group of earthworms (consisting of three biological replicates) were measured before introducing them into the treatment jars. During the 30 day incubation period, the jars were partially closed with their lids, and moisture contents were maintained on a daily basis by adding distilled water. After 30 days of exposure, at the end of the incubation period, the soil was removed from incubation jars to remove earthworms which were gently washed in tap water, partially dried with paper towels, and their body weights (g) and lengths (cm) were measured. Changes in body weight and length were measured with the following formulae (Givaudan et al., 2014).

$$\text{Change in weight } (\%) = \left(\frac{\text{Final weight} - \text{Initial weight}}{\text{Final weight}}\right) \times 100 \quad (1)$$

$$\text{Change in length } (\%) = \left(\frac{\text{Final length} - \text{Initial length}}{\text{Final length}}\right) \times 100 \quad (2)$$

The worms were preserved in 70% alcohol for further biochemical and molecular assays.

Quantitative Analysis of Esterases and Phosphatases in *Pheretima posthuma* Earthworms

A body extract of earthworm was prepared by following a modified protocol of Hrzenjak et al. (1992). The adult clitellate earthworms (1.35 g/per worm) were washed with running tap water and kept in 0.65% NaCl solution at room temperature for 2 h to ensure their guts were empty. Worms were minced and homogenized in sodium phosphate buffer, centrifuged at 8,000 rpm, and the supernatant was used for the estimation of esterase and phosphatase activities (Callaham et al., 2002; Younes et al., 2011). The percentage inhibition of the enzyme activity in test extracts was calculated as follows:

$$\text{Enzyme Inhibition } (\%) = \left(\frac{\text{OD of control worm} - \text{OD of treated orm}}{\text{OD of control worm}}\right) \times 100 \quad (3)$$

DNA Extraction

Genomic DNA was extracted from earthworms by the TNE (Tris-HCL-NaCl-EDTA) buffer method (Zulhussnain et al., 2020). Earthworms (prostomium, clitella, gut, and tail) were separately homogenized in 400 µl of TNE buffer (0.45 M NaCl, 3 mM EDTA, and 10 mM Tris-HCl; pH: 8.0). The mixture was vortexed and centrifuged at 10,000 rpm for 10 min before the supernatant was collected. After the addition of 50 µl of 20% SDS and 100 µl of 20 mg/ml of proteinase-K to the supernatants, samples were incubated in a water bath at 54°C for 1.5 h. After incubation, 300 µl of 5 M NaCl was added and DNA was precipitated using 350–400 µl of ice-cold 100% ethanol and resuspended in 50 µl of sterile water (D_3H_2O). The concentration of DNA was quantified by measuring the absorption of samples at 260 nm on a UV Spectrophotometer (Dynamic DB-20, United Kingdom).

Random Amplified Polymerase DNA Polymerase Chain Reaction

DNA variations of earthworms were determined by employing the RAPD-PCR assay (Zulhussnain et al., 2020). Six oligomer primers of Gene Link-A series were used for the amplification of DNA (**Supplementary Table S1**). The PCR products were run on 1.5% agarose gel electrophoresis at 80 voltages for 1 h and the gel was observed under UV light. The size of DNA bands was observed with respect to the ladder.

Comet Assay

A comet assay was performed for the detection of DNA damage by following the methodology of Singh et al. (1988). Different parts of dissected earthworms (head, tail, clitellum, prostomium, and gut) were homogenized in 400 µl of buffer (0.07 M NaCl and 0.24 M EDTA). The mixture was centrifugated at 13,000 rpm for 10 min and the palette was resuspended in 1,000 µl of ice-cold homogenizing buffer for nuclei preparation. The earthworm body mixture (100 µl) was mixed with 200 µl of 1% LMPA and evenly distributed on a slide precoated with NMPA. Slides were dipped in freshly prepared cold lysing solution (100 mM EDTA, 3 M NaCL, 12 mM Tris-HCl, pH 10). Then, 10% dimethyl sulphoxide (DMSO) and 1% X-100 Triton were added to the lysing solution 20 min before use. After lysing, the slides were dipped in alkaline buffer (1 mM EDTA, 400 mM NaOH; pH 12.5) for 20 min for DNA unwinding. Electrophoresis was done in electrophoresis buffer (0.18 EDTA, 400 mM NaOH, pH 13) for 20 min, 25 min on 25 V and 300 mA. Slides were neutralized by washing for 5 min with neutralizing buffer (Tris-Base, pH 7.5) and left overnight on a clean dust-free area. Slides were evenly stained with 20 mg ml^{-1} of 75 µl ethidium bromide (EB), with cover slips. After staining, slides were examined at ×400 magnification with Komet 5.5 Image Analysis Systems (Kinetic Imaging, Liverpool, United Kingdom). A total of 100 cells were selected randomly from each slide and were analyzed for damages in DNA showing a definite tail and comet-like shape whereas the cells with no tail and round shape were considered normal.

The actual number of comet cells was scored with the following formula:

$$\text{Total DNA Damage Score} = (0 \times n_0 + 1 \times n_1 + 2 \times n_2 + 3 \times n_3 + 4 \times n_4)$$

Where 0–4 is the number of comet classes, and n_0–n_4 is the number of comet scores in each class.

Arbitrary unit damage is classified into five levels (0–4). 0 indicates no damage while four represents maximum damage. The other three levels are intermediate between 0 and 4. Computer image analysis ($Casp^R$ software) was used to measure head length, tail length, comet length, head DNA, tail DNA, and tail movement. Cells with maximum damage showed the highest value for tail DNA and minimum value of head DNA (Attullah et al., 2020; Zulhussnain et al., 2020).

Statistical Analysis

The data were subjected to the analysis of variance (ANOVA) test to find significance of treatment effects on experimental variables using Statistica 13.0 for Windows software. The means were separated using Tukey's HSD post-hoc test at the significance level of 0.05. PCR products were analyzed using gel electrophoresis and the genetic data were analyzed using POPGENE software (Ashraf et al., 2016). For the comet assay, the DNA damage in the earthworm cells was assessed following the assumptions of Dua et al. (2013) and reported by Zulhussnain et al. (2020) and Attullah et al. (2020).

RESULTS

Changes in Weight and Length of *Pheretima posthuma*

The respective change in weight and length of *P. posthuma* after exposing them to sewage sludge, wheat straw, biochar, sewage sludge + wheat straw, and sewage sludge + biochar is shown in **Table 1**. The mean weight was found to decrease significantly with increased concentration of sewage sludge and biochar. The highest weight loss of 26% was observed under sewage sludge at a 25% application rate followed by 11% in 25% biochar-treated soil. Weight loss with the treatment of 5 and 10% of sewage sludge was 2% and 16% respectively, followed by biochar treatment as 1% and 6%, respectively at the same application. However, the decrease in body weight following the sewage sludge + wheat straw treatment was not significant compared to the control and biochar and wheat straw treatments alone. The highest decrease in body weight was observed at a 25% concentration of sewage sludge while the lowest decrease in weight was recorded after the addition of sewage sludge and wheat straw combined (**Table 1**).

Similarly, it was observed that mean length decreased significantly with the increase in rate of sewage sludge application. A maximum decrease in length (3%) was observed at a 25% rate of sewage sludge followed by biochar (1%). At 5 and 10% concentrations of sewage sludge, the decrease in mean length was found to be 1% and 2%, respectively followed by biochar at the same rate. There was a slight change in mean length (0.14%) with the treatment of 25% sewage sludge in combination with the same rate of biochar. No change in length was observed with the combined treatment of sewage sludge + wheat straw (**Table 1**).

Enzymatic Activities in *Pheretima posthuma*

The effects of treatments and application rates on the activities of acetylcholinesterase (AChE), acid phosphate (ACP), and alkaline phosphatase (AKP) in earthworms are presented in **Table 2**. The inhibition in acetylcholinesterase activity was increased significantly with the increase in concentrations of soil amendments. The maximum inhibition in acetylcholinesterase activity was found at 25% sewage sludge (40%) followed by biochar and wheat straw at the same rate. At 5% and 10% sewage sludge, the inhibition in acetylcholinesterase activity was 7 and 28%, respectively. However, biochar amendment at

TABLE 1 | Percentage decrease in mean weight and length after exposure to different concentrations of soil amendments in *Pheretima posthuma*.

Treatments	Rate (%, w/w)	F values; d.f; *p* Value	Percent mean weight decrease after 30 days of exposure	F Value; d.f; *p* Value	Percentage mean length decrease after 30 days of exposure
Control	0	70.669 (df = 2; *p*=<0.05)	0.2 ± 0.05f	0.800 (df = 2; *p*=<0.05)<	0.001 ± 0.05d
WS	5% 10% 25%	70.669 (df = 2; *p*=<0.05)	0.1 ± 0.03f 0.01 ± 0.003f 0.1 ± 0.003f	0.800 (df = 2; *p*=<0.05)	0.02 ± 0.02c 0.01 ± 0.00b 0.01 ± 0.00b
B	5% 10% 25%	1022 (df = 2; *p*=<0.05)	1.3 ± 0.03ef 6.4 ± 0.03d 11.00 ± 0.5c	1594.158 (df = 2; *p*=<0.05)	0.13 ± 0.03a 0.53 ± 0.04a 0.80 ± 0.01c
SS	5% 10% 25%	969.73 (df = 2; *p*=<0.05)	2.3 ± 0.06e 16.07 ± 0.51b 25.75 ± 0.58a	276.117 (df = 2; *p*=<0.05)	0.64 ± 0.01d 1.74 ± 0.05b 2.5 ± 0.00a
SS + WS SS + B	25% + 25% 25% + 25%	1022.323 (df = 2; *p*=<0.05)	0.00 ± 0.005f 0.16 ± 0.03f	0.180 (df = 2; *p*=<0.05)	0.00 ± 0.00d 0.14 ± 0.029c

p < *0.01 = highly significant,* p < *0.001 = highly significant,* p > *0.05 = non-significant,* p < *0.05 = significant. WS, wheat straw; B, biochar; SS, sewage sludge.*

TABLE 2 | Percentage inhibition of different enzyme activities after exposure to different concentrations of soil amendments in *Pheretima posthuma*.

Treatments	Rate (%)	F Value; d.f; *p* Value	Acetylcholinesterase (AChE) activity	F Value; d.f; *p* Value	Acid Phosphatase (ACP) activity	F Value; d.f; *p* Value	Alkaline Phosphatase (AKP) activity
Control	0	0.642 (df = 2; *p*=<0.05)	0.2 ± 0.05F	1.647 (df = 2; *p*=<0.05)	0.0 ± 0.05D	3.250 (df = 2; *p*=<0.05)	0.00 ± 0.05D
WS	5% 10% 25%	0.642 (df = 2; *p*=<0.05)	0.01 ± 0.01b 0.01 ± 0.03b 0.1 ± 0.003a	1.647 (df = 2; *p*=<0.05)	0.006 ± 0.00b 0.01 ± 0.00a 0.003 ± 0.00c	3.250 (df = 2; *p*=<0.05)	0.013 ± 0.01a 0.00 ± 0.00b 0.01 ± 0.00b
B	5% 10% 25%	458 (df = 2; *p*=<0.05)	4.6 ± 0.08c 8.6 ± 0.29b 15.83 ± 1.4a	133.5 (df = 2; *p*=<0.05)	9.0 ± 0.10c 10.8 ± 0.91b 22.70 ± 0.63a	41.98 (df = 2; *p*=<0.05)	8.66 ± 0.21c 16.18 ± 0.83b 20.40 ± 1.33a
SS	5% 10% 25%	209 (df = 2; *p*=<0.05)	6.70 ± 0.32c 27.7 ± 0.6b 39.83 ± 1.8a	267.5 (df = 2; *p*=<0.05)	9.36 ± 0.42c 33.07 ± 1.5b 47.60 ± 1.2a	37.85 (df = 2; *p*=<0.05)	4.70 ± 0.29c 18.03 ± 2.5b 23.05 ± 2.23b
SS + WS SS + B	25% + 25% 25% + 25%	176 (df = 2; *p*=<0.05)	0.00 ± 0.01c 2.96 ± 0.2a	296 (df = 2; *p*=<0.05)	0.003 ± 0.0015c 11.03 ± 0.6a	620 (df = 2; *p*=<0.05)	0.02 ± 0.01c 7.06 ± 0.08a

p < *0.01 = highly significant,* p < *0.001 = highly significant,* p > *0.05 = non-significant,* p < *0.05 = significant. W, wheat straw; B, biochar; SS, sewage sludge.*

5% and 10% rate caused inhibition of 5% and 9%, respectively. A very low inhibition in acetylcholinesterase activity was found with the treatment of sewage sludge and wheat straw combined; while an inhibition of 3% in the acetylcholinesterase activity was observed in the combined addition of sewage sludge and biochar (**Table 2**).

Maximum and significant inhibition in acid phosphatase activity in *P. posthuma* was observed at a 25% application of sewage sludge (50%) followed by biochar (23%) at the same application rate (**Table 2**). At 5% and 10% sewage sludge rates, the decrease in acid phosphatase activity was 9 and 33%, respectively and the inhibition at 5 and 10% biochar rates was 9 and 11%, respectively. The combination of 25% sewage sludge with the same concentration of wheat straw reduced the negative effects of sewage sludge on acid phosphatase activity and resulted in <1% inhibition. Similarly, wheat biochar with sewage sludge also reduced inhibition in acid phosphatase activity (11%; **Table 2**).

The highest percentage inhibition of alkaline-phosphatase activity was found at 25% sewage sludge (23%) followed by biochar (21%) (**Table 2**). At a 10% rate of sewage sludge and biochar separately, the inhibition was found to be 18% and 16%, respectively. However, at a 5% rate, biochar more strongly reduced alkaline-phosphatase activity than that of sewage sludge. In the combined application of sewage sludge and biochar, a 7% inhibition of alkaline-phosphatase activity was found. Whereas, the combination of wheat straw and sewage sludge reduced the negative effects of sewage sludge on alkaline-phosphatase activity and resulted in <1% inhibition (**Table 2**).

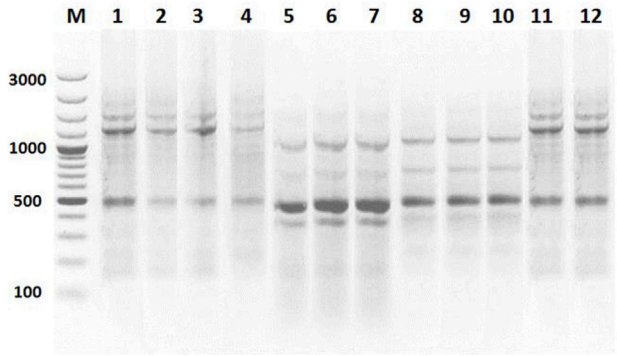

FIGURE 1 | Comparison of RAPD profile for genotoxicity in *Pheretima posthuma* with primer A-05. Lane M = DNA marker (size 100 bp). L_1 = Control; L_2 = Wheat straw (5%); L_3 = Wheat straw (10%); L_4 = Wheat straw (25%), L_5 = Biochar (5%), L_6 = Biochar (10%), L_7 = Biochar (25%), L_8 = Sewage sludge (5%), L_9 = Sewage sludge (10%), L_{10} = Sewage sludge (25%), L_{11} = Sewage sludge + wheat straw, and L_{12} = Sewage sludge + Biochar.

DNA Damage Detection Through Random Amplified Polymerase DNA Polymerase Chain Reaction

DNA damage in *P. posthuma* under various treatments of sewage sludge, biochar, and wheat straw was assessed through RAPD-PCR to evaluate the genotoxic effects. The size of amplified fragments of DNA was analyzed using a 1 kb DNA marker. The lowest size of the band of DNA maker was 100 base pairs (bp) and the band with highest size was of 5,000 bp. A different banding profile was observed in earthworms under treatments than control (**Figure 1**). The maximum number of bands was observed in sewage sludge treatment at all tested concentrations which showed fragmentation in DNA. A similar banding pattern was also observed with biochar. The number of bands was increased with the increase of the concentration of sewage sludge and biochar. No change in banding profile was observed in treatment with wheat straw similar to control. The number of DNA bands also remained similar for control and

TABLE 3 | Comet parameters after exposure to different concentrations of soil amendments in *Pheretima posthuma*.

Comet Parameters	Treatment	F Value; d.f; *p* Value	Rate (%, w/w)			
			Control	5%	10%	25%
Tail length (μm)	WS	(F = 9.50); d.f = 3; *p* (0.005)	3.47 ± 0.28c	4.82 ± 0.20a	3.85 ± 0.10bc	4.39 ± 0.11ab
	B	(F = 448.55); d.f = 3; *p* (0.000)		7.75 ± 0.24b	8.47 ± 0.36b	19.36 ± 0.35a
	SS	(F = 51.51); d.f = 3; *p* (0.000)		8.34 ± 0.34b	10.63 ± 0.20a	9.49 ± 0.72ab
	SS + WS	(F = 52.18); d.f = 3; *p* (0.002)		(SS + WS 25% + 25%) 6.67 ± 0.44a		
	SS + B	(F = 146.3); d.f = 3; *p* (<0.05)		(SS + B 25% + 25%) 10.77 ± 0.23a		
Comet length (μm)	WS	(F = 53.29); d.f = 3; *p* (0.000)	9.29 ± 0.51b	15.74 ± 0.73a	16.30 ± 0.32a	17.73 ± 0.49a
	B	(F = 306.65); d.f = 3; *p* (0.000)		18.82 ± 0.48c	23.37 ± 0.41b	27.49 ± 0.35a
	SS	(F = 181.41); d.f = 3; *p* (0.000)		19.04 ± 0.37c	24.88 ± 0.97b	27.85 ± 0.34a
	SS + WS	(F = 118.16); d.f = 3; *p* (0.000)		(SS + WS 25% + 25%) 18.24 ± 0.64a		
	SS + B	(F = 102.6); d.f = 3; *p* (<0.05)		(SS + B 25% + 25%) 25.21 ± 0.42b		
Tail DNA (%)	WS	(F = 10.46); d.f = 3; *p* (0.004)	1.34 ± 0.08d	2.9 ± 0.17ab	2.91 ± 0.14ab	4.57 ± 0.78a
	B	(F = 43.55); d.f = 3; *p* (<0.000)		11.76 ± 0.29c	28.73 ± 4.14b	44.80 ± 3.66a
	SS	(F = 1596); d.f = 3; *p* (0.000)		46.32 ± 0.88c	76.10 ± 0.88b	80.72 ± 0.67a
	SS + WS	(F = 606.9); d.f = 3; *p* (0.000)		(SS + WS 25% + 25%) 60.86 ± 0.76a		
	SS + B	(F = 128.7); d.f = 3; *p* (<0.05)		(SS + B 25% + 25%) 78.82 ± 0.12b		
Tail movement (μm)	WS	(F = 25.67); d.f = 3; *p* (0.000)	0.13 ± 0.07c	0.4 ± 0.04a	0.27 ± 0.03b	0.42 ± 0.00a
	B	(F = 26.75); d.f = 3; *p* (0.000)		4.89 ± 2.15b	15.10 ± 1.76a	18.66 ± 1.84a
	SS	(F = 5.519); d.f = 3; *p* (0.024)		9.6 ± 0.68ab	9.7 ± 4.2ab	11.63 ± 0.31a
	SS + WS	(F = 166.3); d.f = 3; *p* (0.000)		(SS + WS 25% + 25%) 11.56 ± 0.80a		
	SS + B	(F = 328.72); d.f = 3; *p* (<0.05)		(SS + B 25% + 25%) 12.22 ± 0.18a		
Head length (μm)	WS	(F = 22.12); d.f = 3; *p* (0.000)	8.43 ± 0.37b	10.46 ± 0.95b	14.81 ± 0.59a	16.64 ± 1.09a
	B	(F = 7.285); d.f = 3; *p* (0.011)		13.74 ± 7.0c	18.60 ± 0.30b	30.76 ± 0.79a
	SS	(F = 31.71); d.f = 3; *p* (0.000)		18.47 ± 0.93a	20.11 ± 0.94a	22.70 ± 1.73a
	SS + WS	(F = 153.10); d.f = 3; *p* (<0.000)		(SS + WS 25% + 25%) 17.16 ± 0.60a		
	SS + B	(F = 498.18); d.f = 1; *p* (<0.05)		(SS + B 25% + 25%) 19.87 ± 0.12a		
Head DNA (%)	WS	(F = 21.80); d.f = 3; *p* (0.000)	92.35 ± 1.21a	89.77 ± 1.27a	85.12 ± 0.66b	82.46 ± 0.31b
	B	(F = 155.32); d.f = 3; *p* (0.000)		63.44 ± 2.7b	57.07 ± 1.9b	36.74 ± 0.90c
	SS	(F = 752.73); d.f = 3; *p* (0.000)		49.94 ± 1.32b	21.61 ± 1.64c	18.32 ± 0.5c
	SS + WS	(F = 502.1); d.f = 3; *p* (0.000)		(SS + WS 25% + 25%) 38.56 ± 0.47a		
	SS + B	(F = 262.4); d.f = 3; *p* (<0.05)		(SS + B 25% + 25%) 32.24 ± 0.24c		

p < *0.01 = highly significant,* p < *0.001 = highly significant,* p > *0.05 = non-significant,* p < *0.05 = significant. WS, wheat straw; B, biochar; SS, sewage sludge.*

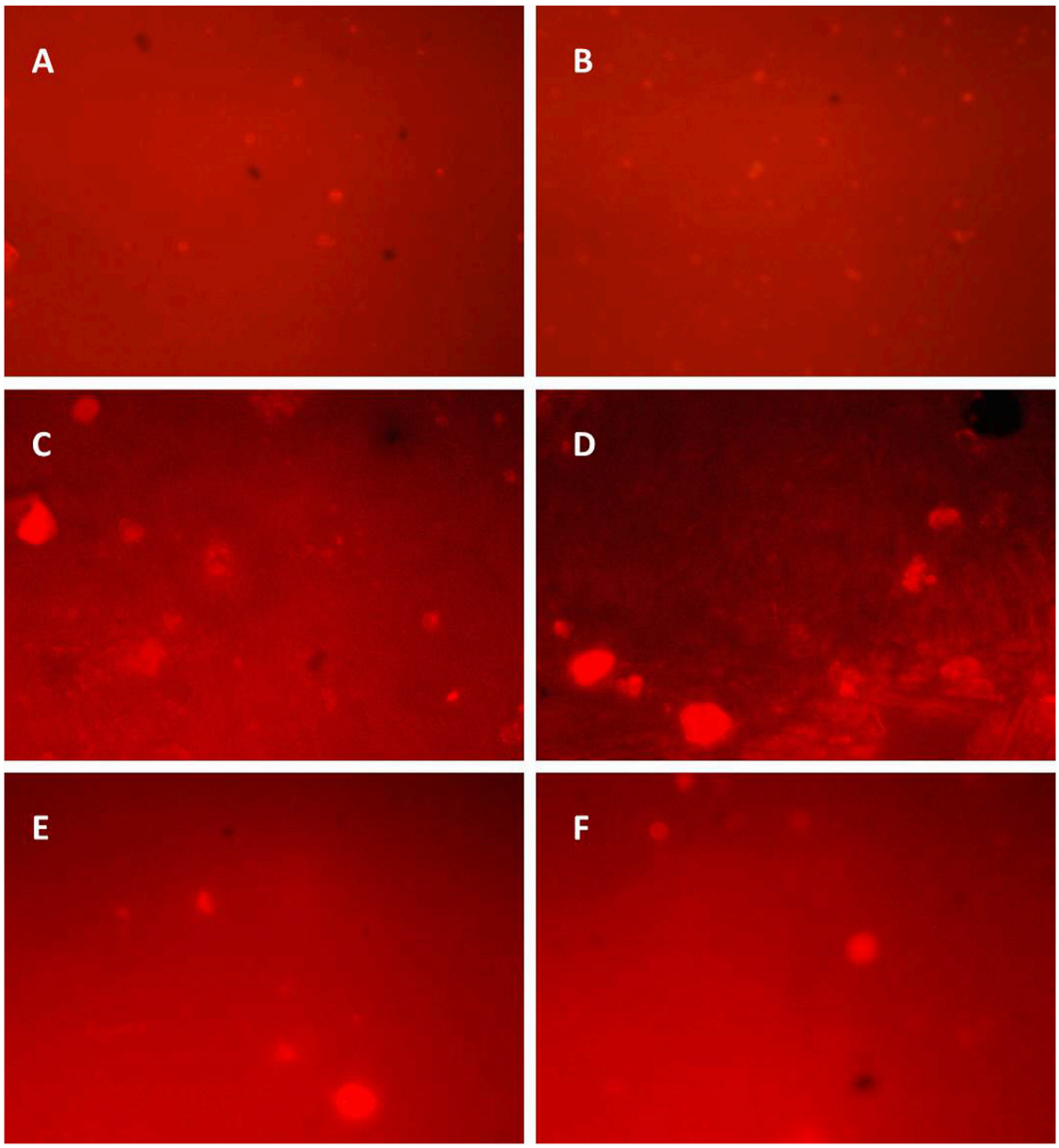

FIGURE 2 | Comet assay profile for genotoxicity in *Pheretima posthuma.* **(A)** = Control; **(B)** = Wheat straw; **(C)** = Biochar; **(D)** = Sewage sludge; **(E)** = Sewage sludge 25% + Biochar 25%; **(F)** = Sewage sludge 25% + Wheat straw 25%.

wheat straw + sewage sludge treatments in *P. posthuma*; meaning thereby, that DNA damage occurred in this combined treatment (**Figure 1**).

Comet Assay

The comet parameters, i.e., head and the tail length of DNA and head and tail movement, were measured to identify the DNA damage. A very minor increase in tail length was observed in earthworms treated with wheat straw at 5, 10, and 25% rates as compared to control. However, under biochar treatment, tail and head lengths increased with an increase in the rate of application. A similar trend was also observed with the treatment of different concentrations of sewage sludge wherein tail DNA (%), head DNA (%), tail length, and head length increased with increasing concentrations. In combined treatments of sewage sludge against wheat straw and biochar, a change in head and tail length was obtained as compared to treatment with wheat straw alone (**Table 3**). The tail length value was found significantly low in treatments with wheat straw at all the concentrations. Cells with maximum damage show the highest value for tail DNA. Hence, the highest value of tail DNA% (46, 76, and 81%, at 5, 10, and 25%, respectively) due to sewage sludge showed high DNA damage which was reduced (18 at 25%) when combined with wheat straw (**Figure 2**).

DISCUSSION

Earthworms assist soil. To regulate water within the soil, their presence influences the presence of nutrients and minerals within soil and the availability of these nutrients for animals and plants. They increase the microbial activity in the soil. They perform vermicomposting of sewage sludge and other pollutants within the soil (Wang et al., 2019). But the application of sewage sludge and heavy metals bioaccumulate in the earthworm's body and cause physiological and biochemical damage (Babic et al., 2016; Kooch and Jalil 2008; Ahmad et al., 2021).

Earthworms cause the fragmentation of sewage sludge, thus converting it into castings and increasing the surface area available for drying and microbial decomposition; improving aeration due to the tunnelling action of worms. In the United Kingdom and mostly in Europe, human waste-based sewage sludge is being used which is high yielding towards crops. In Pakistan, wastewater treatment plants (WWTPs) have been installed on different industrial and municipal sites and remain functional throughout the year to generate huge amounts of sewage sludge on a daily basis (Haydar et al., 2015). Particularly, this sewage sludge potentially causes a negative effect in earthworms. It produces growth defects and induces enzyme inhibition and toxicity potentially at the genetic level. The land application of sewage sludge can damage soil, water, and plants since it contains variable levels of organic and inorganic pollutants, salts, and pathogens (Singh and Agrawal, 2008 and 2010; Latare et al., 2014; Qadir et al., 2015). Despite being considered fertilizer in the farming community, it has been reported that the sewage sludge affects the soil fauna and resulted in low crop yield. The yield reduction could be due to the heavy metal accumulation in the soil which is in line with previous studies reported on maize, pea, and mustard. In fact, the higher contents of metal in sewage sludge like Cd and Pb can lead to a toxic effect on the soil fauna (Liu et al., 2005). Singh and Agrawal (2010) reported that the application of sewage sludge increased the straw yield of rice but at higher rates negatively affected the yield due to higher accumulation of metals in soil fauna presumably earthworms and ultimately resulted in a decreased yield.

The *P. posthuma* earthworm, being abundantly found across Pakistan, plays an important role in our ecosystem, food chain, and soil. Thus, the present study was performed to assess the toxic effects of sewage sludge on *P. posthuma* earthworms and how biochar and wheat straw can ameliorate the toxicity in terms of growth and weight of worms before and after treatment. In addition, the damage at the biochemical and molecular levels in earthworms was also studied (Khan et al., 2017; Wang et al., 2019). Application of sewage sludge alone is toxic for normal growth and reproduction of earthworms as compared to combining treatment with wheat straw and biochar. Growth parameters were suppressed with an increase in the rate of sewage sludge. A decrease in mean weight was observed and a similar rate-dependent decrease in length was also observed. The very low mean decrease in length was observed in lower concentrations of sewage sludge. For a 5% concentration of sewage sludge, the decrease in length was only 0.65%, but when increasing the concentration, a decrease in length was also seen (Dominguez et al., 2012). These results are supported by the study of Zaltauskaite and Sodiene (2010) who reported a smaller decrease in weight at lower concentrations of sewage sludge. However, a higher decrease in weight of earthworms at higher sewage sludge rates have been shown earlier (Yang et al., 2014). The reduction in the length of earthworms after exposure to sewage sludge has been attributed to the poor development of earthworms (Lemtiri et al., 2015; Babic et al., 2016).

The addition of wheat straw with sewage sludge is of great importance for bioremediation of sludge, soil fertility, earthworm growth, functioning to facilitate organic matter turnover, and nutrient availability for all soil life. Wheat straw also facilitated fast and efficient bioremediation of sewage sludge-amended soil by earthworms without genetically and physiologically affecting the earthworms (Yang et al., 2014; Elyamine and AU 2020). In the present study, we found that little or no changes in length and weight of earthworms were observed in the mixed treatment consisting of 25% sewage sludge and wheat straw (Sizmur et al., 2017). The normal growth rates and development of earthworms in wheat straw and sewage sludge-mixed treatments showed a positive correlation between sewage sludge and wheat straw. The results of the present study are in accordance to the findings of Yang et al. (2014) who reported similar positive effects of wheat straw on earthworm growth and functions in sewage sludge applied to soil to enhance active remediation of sewage sludge without affecting the population of earthworms. Wheat straw is a natural organic fertilizer and its combined application with sewage sludge enhances the microbial activity of soil, hence decontamination of sewage sludge containing heavy metals also increases without affecting the population of *Pheretima posthuma* in soils.

The current results showed that the excessive use of sewage sludge as a fertilizer resulted in the accumulation of heavy metals in soils and earthworm bodies and a decrease in percentage weight and length was also reported if worms were treated solely with biochar, and the weight and length decreased with increasing biochar rate. A maximum decrease in weight was observed at a 25% biochar rate followed by 10%. However, when earthworms were treated with sewage sludge and biochar combined, the negative effects of sewage sludge were significantly reduced as was evident from the minor decrease in weight and length. The addition of biochar along with sewage sludge could rescue the negative effect on growth (Zhang et al., 2017; Sanchez-Hernandez et al., 2019). Biochar alone has been shown to have little effect on earthworms which was reflected in recent studies in the low reduction in length and weight in some of the earthworms after biochar application; however, combined application of sewage sludge and biochar moderated their toxic effects as shown by minor changes in length and weight of earthworms. So, the disposal of sewage sludge with biochar is the best and safe way to reuse sludge in an environmentally friendly way (Li et al., 2011).

Sewage sludge, wheat straw, and biochar were also tested for their effects on the enzyme activity of *P. posthuma* for acetylcholinesterases, acid phosphatases, and alkaline

phosphatases; as enzymes are important indicators of toxicant accumulation at the molecular level in worms. The acid phosphatases group of enzymes is related to the class of enzyme hydrolases and the enzyme in acidic conditions catalyzes the hydrolysis of monoester (orthophosphate) (Tewari et al., 2016). Alkaline phosphatase is an enzyme that phosphorylates molecules under alkaline conditions which are present throughout the body of earthworms but occur most excessively within the gizzard/crop and intestine of earthworms. Acetylcholinesterase is a serine group that belongs to the class of hydrolases and is reported to target sites of many toxicants. Alkaline and acidic phosphatases are involved in the detoxification of many toxicants containing heavy metals. The addition of contaminants to soil-inhabiting earthworms directly affects the enzyme activity of earthworms (Wang et al., 2016). Our study showed that the sewage sludge induces changes in the activity of crucial enzymes of earthworms responsible for the metabolism of the energy, neurotransmission, and oxidation systems. The dose-dependent response was observed by increasing the concentration of sewage sludge enzyme inhibition (Sanchez-Hernandez et al., 2020). In the case of sewage sludge, acid phosphatase activity was affected by sewage sludge followed by biochar and at the same concentrations of these amendments also caused inhibition of acetylcholinesterase activity within earthworms. However, alkaline phosphates seemed less influenced by the same concentrations of sewage sludge and biochar. The results further demonstrated that the inhibition in enzyme activities increased with increasing rates of sewage sludge and biochar. However, when wheat straw and biochar were applied in combination with sewage, inhibition in enzymatic activities was significantly reduced suggesting that both wheat straw and biochar salvaged the negative effects of sewage sludge which caused physiological abnormalities in earthworms (Song et al., 2009; Yasmin 2010).

PCR-based molecular approaches are considered to provide a reliable estimation of DNA damage in earthworms exposed to contaminants, as earthworms are bioindicators of toxicant contamination. This technique is relatively inexpensive and technically simple yet provides robust estimates of DNA damages. The RAPD DNA primer marker is commonly used to assess the damage caused by sewage sludge and other contaminants present in soil (Sharma et al., 2011). We found that the maximum number of bands (fragmented DNA; damaged) were observed at a 25% sewage sludge application rate followed by biochar treatment at the same rate. Fewer bands were observed in treatments with sewage sludge applied in combination with biochar and wheat straw. The sewage sludge caused DNA damage in *P. posthuma* which can be diminished by using wheat straw and biochar. It has been reported that sewage sludge applied to soils without any pre-treatment causes lower development and reproduction and genotoxicity to earthworms which can be reduced by applying other organic amendments such as wheat straw and biochar along with sewage sludge (Yadhav and Mullah 2017; Fouche et al., 2022). However, there can be unintended negative effects of the application of biochar alone in soil on DNA and enzymatic activities in earthworms as were evident from our study and also suggested by Kim et al. (2014). The application of biochar (black carbon) alone on soil influences earthworm behavior, growth, and reproduction and also causes damage at the molecular level. The number of castings by earthworms is also declined in soils with biochar which indicate a change in the feeding habitat of earthworms under the influence of biochar (Weyears et al., 2011).

The comet assay is considered as a very reliable technique used for detecting damage and repairing DNA to assess the genotoxicity caused by the application of chemicals and pesticides (Attullah et al., 2020; Zulhussnain et al., 2020). Hence, in the present study, a comet assay was performed to assess the genotoxicity in *P. posthuma* caused by the application of sewage sludge. It was observed that DNA damage increased as observed with DNA tail length and tail movement increases with the increasing concentration of sewage sludge (25%) followed by biochar (25%) as compared to control which showed damage at the DNA level of *P. posthuma*. There was a much smaller increase in DNA head length and movement in the case of control and wheat straw-treated *P. posthuma* at all the concentrations. The sewage sludge when combined with wheat straw and biochar resulted in a change in DNA head and tail length compared to treatment with wheat straw and biochar alone. The high value of tail DNA in the comet assay showed maximum damage; thus, the high value of tail DNA% due to sewage sludge revealed high DNA damage which was reduced with treatment of wheat straw (Button et al., 2010; Fouche et al., 2022).

CONCLUSION

The present study revealed the negative effects of sewage sludge on growth, enzyme inhibitory activity, and genotoxicity in *P. posthuma* earthworms. It was found that sewage sludge showed more toxic effects individually, which caused a decrease in length and body weight as well as inhibition of enzyme activity and induced DNA damage. Being a good fertilizer for crops, sewage sludge should be used only after the addition of proper soil amendments like wheat straw and biochar, otherwise it causes severe damage to growth, development, and functioning of earthworms. Wheat straw can rescue the negative effects produced in *P. posthuma* earthworms and helps increase the production of vermicompost. Based on the current work, it is suggested that the use of wheat straw and biochar can rescue the negative effects of sewage sludge in *P. posthuma* earthworms. The research work needs to be extended to examine sewage sludge for the presence of heavy metals. The study can also be further extended for other industrial wastes: effluents normally used for irrigation purpose and herbicides frequently used in agriculture. We also emphasize that these effects need to be tested on other species of earthworms under field conditions for better risk assessment.

DATA AVAILABILITY STATEMENT

The original contributions presented in the study are included in the article/**Supplementary Material**, further inquiries can be directed to the corresponding authors.

AUTHOR CONTRIBUTIONS

MKZ designed and supervised the work. HK and KR performed the work. DR helped during sampling and experimentation. MA and RY provided help during the biochemical assay and data analyses. All authors read and approved the manuscript.

ACKNOWLEDGMENTS

The facilities provided by Department of Zoology and Environmental Sciences and Engineering, GCUF are highly acknowledged.

SUPPLEMENTARY MATERIAL

The Supplementary Material for this article can be found online at: https://www.frontiersin.org/articles/10.3389/fenvs.2022.888394/full#supplementary-material

REFERENCES

Afzal, M. Z., Ikram, M., and Israr, S. (2016). Study of the Pollutants in Wastewater from Edible Oil/ghee Industries and Their Impacts on Plant Life, Islamabad, Pakistan. *Environ. Sci.* 12, 112–117.

Ahmad, A., Aslam, Z., Bellitürk, K., Iqbal, N., Idrees, M., Nawaz, M., et al. (2021). Earth Worms and Vermicomposting: A Review on the Story of Black Gold. *J. Innovative Sci.* 7 (1), 167–173. doi:10.17582/journal.jis/2021/7.1.167.173

Ali, K., Wang, X., Riaz, M., Islam, B., Khan, Z. H., Shah, F., et al. (2019). Biochar: an Eco-Friendly Approach to Improve Wheat Yield and Associated Soil Properties on Sustainable Basis. *Pak. J. Bot.* 51 (4), 1255–1261. doi:10.30848/pjb2019-4(7)

Ali, M., and Hasan, A. (2001). *Integrating Recycling and Disposal System for Solid Waste Management in Karachi*. Karachi, Pakistan: Report Urban Resource Center.

Ansari, A. A., and Saywack, P. (2011). Identification and Classification of Earthworm Species in Guyana. *Int. J. Zoological Res.* 7, 93–99. doi:10.3923/ijp.2011.212.216

Ansari, A., and Ismail, S. (2012). Earthworms and Vermiculture Biotechnology Management of Organic Waste. *Soil Biol. Biochem.* 41 (5), 905–909. doi:10.5772/30957

Ashraf, H. M., Zahoor, M. K., Nasir, S., Majeed, H. N., and Zahoor, S. (2016). Genetic Analysis of Aedes aegypti Using Random Amplified Polymorphic DNA (RAPD) Markers from Dengue Outbreaks in Pakistan. *J. Arthropod Borne Dis.* 10 (4), 546–559.

Attaullah, Zahoor, M. K., Zahoor, M. A., Mubarik, M. S., Rizvi, H., Majeed, H. N., et al. (2020). Insecticidal, Biological and Biochemical Response of *Musca domestica* (Diptera: Muscidae) to Some Indigenous Weed Plant Extracts. *Saudi J. Biol. Sci.* 27 (1), 106–116. doi:10.1016/j.sjbs.2019.05.009

Babić, S., Barišić, J., Malev, O., Klobučar, G., Popović, N. T., Strunjak-Perović, I., et al. (2016). Sewage Sludge Toxicity Assessment Using Earthworm Eisenia fetida: Can Biochemical and Histopathological Analysis Provide Fast and Accurate Insight? *Environ. Sci. Pollut. Res. Int.* 23 (12), 12150–12163. doi:10.1007/s11356-016-6097-3

Bareen, F.-e., and Tahira, S. A. (2011). Metal Accumulation Potential of Wild Plants in Tannery Effluent Contaminated Soil of Kasur, Pakistan: Field Trials for Toxic Metal Cleanup Using Suaeda Fruticosa. *J. Hazard. Mater.* 186, 443–450. doi:10.1016/j.jhazmat.2010.11.022

Birkas, M., Bottlik, L., Stingli, A., Gyuricza, C., and Jolánkai, M. (2010). Effect of Soil Physical State on the Earthworms in Hungary. *Appl. Environ. Soil Sci.* 20 (8). doi:10.1155/2010/830853

Blouin, M., Hodson, M. E., Delgado, E. A., Baker, G., Brussaard, L., Butt, K. R., et al. (2013). A Review of Earthworm Impact on Soil Function and Ecosystem Services. *Eur. J. Soil Sci.* 64 (2), 161–182. doi:10.1111/ejss.12025

Button, M., Jenkin, G. R. T., Bowman, K. J., Harrington, C. F., Brewer, T. S., Jones, G. D. D., et al. (2010). DNA Damage in Earthworms from Highly Contaminated Soils: Assessing Resistance to Arsenic Toxicity by Use of the Comet Assay. *Mutat. Research/Genetic Toxicol. Environ. Mutagen.* 696 (2), 95–100. doi:10.1016/j.mrgentox.2009.12.009

Callaham, M. A., Stewart, A. J., Alarcón, C., and McMillen, S. J. (2002). Effects of Earthworm (Eisenia Fetida) and Wheat (Triticum Aestivum) Straw Additions on Selected Properties of Petroleum-Contaminated Soils. *Environ. Toxicol. Chem.* 21 (8), 1658–1663. doi:10.1897/1551-5028(2002)021<1658:eoeefa>2.0.co;2

Charlton, A., Sakrabani, R., Tyrrel, S., Rivas Casado, M., McGrath, S. P., Crooks, B., et al. (2016). Long-term Impact of Sewage Sludge Application on Soil Microbial Biomass: An Evaluation Using Meta-Analysis. *Environ. Pollut.* 219, 1021–1035. doi:10.1016/j.envpol.2016.07.050

Dabke, S. V. (2013). Vermi-remediation of Heavy Metal-Contaminated Soil. *J. Health Pollut.* 3 (4), 4–10. doi:10.5696/2156-9614-3.4.4

Domínguez-Crespo, M. A., Sánchez-Hernández, Z. E., Torres-Huerta, A. M., Negrete-Rodríguez, M., de la Luz, X., Conde-Barajas, E., et al. (2012). Effect of the Heavy Metals Cu, Ni, Cd and Zn on the Growth and Reproduction of Epigeic Earthworms (E. Fetida) during the Vermistabilization of Municipal Sewage Sludge. *Water, Air Soil Pollut.* 223 (2), 915–931. doi:10.1007/s11270-011-0913-7

Dua, V. K., Kumar, A., Pandey, A. C., and Kumar, S. (2013). Insecticidal and Genotoxic Activity of Psoralea Corylifolia Linn. (Fabaceae) against Culex quinquefasciatus Say, 1823. *Parasites Vectors* 6 (1), 30. doi:10.1186/1756-3305-6-30

Edwards, C. A., and Arancon, N. Q. (2004). The Use of Earthworms in the Breakdown of Organic Wastes to Produce Vermicomposts and Animal Feed Protein. *Earthworm Ecol.* 2, 345–380.

Elmer, W. H., Lattao, C. V., and Pignatello, J. J. (2015). Active Removal of Biochar by Earthworms (Lumbricus Terrestris). *Pedobiologia* 58 (1), 1–6. doi:10.1016/j.pedobi.2014.11.001

Elyamine, A. M., and Hu, C. (2020). Earthworms and Rice Straw Enhanced Soil Bacterial Diversity and Promoted the Degradation of Phenanthrene. *Environ. Sci. Eur.* 32 (1), 1–12. doi:10.1186/s12302-020-00400-y

Fouché, T., Claassens, S., and Maboeta, M. S. (2022). Ecotoxicological Effects of Aflatoxins on Earthworms under Different Temperature and Moisture Conditions. *Toxins* 14 (2), 75. doi:10.3390/toxins14020075

Givaudan, N., Wiegand, C., Le Bot, B., Renault, D., Pallois, F., Llopis, S., et al. (2014). Acclimation of Earthworms to Chemicals in Anthropogenic Landscapes, Physiological Mechanisms and Soil Ecological Implications. *Soil Biol. Biochem.* 73, 49–58. doi:10.1016/j.soilbio.2014.01.032

Gul, S., Whalen, J. K., Thomas, B. W., Sachdeva, V., and Deng, H. (2015). Physico-chemical Properties and Microbial Responses in Biochar-Amended Soils: Mechanisms and Future Directions. *Agric. Ecosyst. Environ.* 206, 46–59. doi:10.1016/j.agee.2015.03.015

Haydar, S., Hussain, G., Nadeem, O., Aziz, J. A., Bari, A. J., and Asif, M. (2015). Water Conservation Initiatives and Performance Evaluation of Wastewater Treatment Facility in a Local Beverage Industry in Lahore. *Pak. J. Engg. Appl. Sci.* 16, 100–109.

He, X., Zhang, Y., Shen, M., Zeng, G., Zhou, M., and Li, M. (2016). Effect of Vermicomposting on Concentration and Speciation of Heavy Metals in Sewage Sludge with Additive Materials. *Bioresour. Technol.* 218, 867–873. doi:10.1016/j.biortech.2016.07.045

Hrzenjak, T., Hrzenjak, M., Kasuba, V., Efenberger-Marinculić, P., and Levanat, S. (1992). A New Source of Biologically Active Compounds-Eearthworm Tissue (Eisenia Foetida, Lumbricus Rubelus). *Comp. Biochem. Physiol. Comp. Physiol.* 102, 441–447. doi:10.1016/0300-9629(92)90191-r

Ibrahim, M. H., Quaik, S., and Ismail, S. A. (2016). "General Introduction to Earthworms, Their Classifications, and Biology," in *Prospects of Organic Waste Management and the Significance of Earthworms*(Springer, Cham) 22 (69–103).

Karimi, F., Rahimi, G., and Kolahchi, Z. (2020). Interaction Effects of Salinity, Sewage Sludge, and Earthworms on the Fractionations of Zn and Cu, and the Metals Uptake by the Earthworms in a Zn- and Cu-Contaminated Calcareous Soil. *Environ. Sci. Pollut. Res.* 27, 10565–10580. doi:10.1007/s11356-020-07719-2

Khan, M. U., Ahmed, M., and Nazim, K. (2017). The Population Behavior of Earth Worm (*Pheritema Posthuma Kinberg*) under the Influence of Industrial Waste. *Fuuast J. Biol.* 7 (1), 1–8.

Kim, W. I., Kunhikrishnan, A., Go, W. R., Jeong, S. H., Kim, G. J., Lee, S., et al. (2014). Influence of Various Biochars on the Survival, Growth, and Oxidative DNA Damage in the Earthworm *Eisenia Fetida*. *Korean J. Environ. Agric.* 33, 231–238. doi:10.5338/kjea.2014.33.4.231

Kızılkaya, R., and Hepşen, S. (2004). Effect of Biosolid Amendment on Enzyme Activities in Earthworm (*Lumbricus Terrestris*) Casts. *J. Plant Nutr. Soil Sci.* 167, 202–208. doi:10.1002/jpln.200321263

Kooch, Y., and Jalilvand, H. (2008). Earthworms as Ecosystem Engineers and the Most Important Detritivors in Forest Soils. *Pak. J. Biol. Sci.* 11 (6), 819–825. doi:10.3923/pjbs.2008.819.825

Latare, A. M., Kumar, O., Singh, S. K., and Gupta, A. (2014). Direct and Residual Effect of Sewage Sludge on Yield, Heavy Metals Content and Soil Fertility under Rice-Wheat System. *Ecol. Eng.* 69, 17–24. doi:10.1016/j.ecoleng.2014.03.066

Lemtiri, A., Liénarda, A., Alabib, T., Brostauxc, Y., Cluzeaud, D., Francisb, F., et al. (2015). Earthworms Eisenia fetida Affect the Uptake of Heavy Metals by Plants Vicia faba and Zea mays in Metal-Contaminated Soils. *Appl. Soil Ecol.* 11 (6), 819–825. doi:10.1016/j.apsoil.2015.11.021

Li, D., Hockaday, W. C., Masiello, C. A., and Alvarez, P. J. J. (2011). Earthworm Avoidance of Biochar Can Be Mitigated by Wetting. *Soil Biol. Biochem.* 43 (8), 1732–1737. doi:10.1016/j.soilbio.2011.04.019

Li, Y., Luo, J., Yu, J., Xia, L., Zhou, C., Cai, L., et al. (2018). Improvement of the Phytoremediation Efficiency of *Neyraudia Reynaudiana* for Lead-Zinc Mine-Contaminated Soil under the Interactive Effect of Earthworms and EDTA. *Sci. Rep.* 8 (1), 6417. doi:10.1038/s41598-018-24715-2

Liu, X., Hu, C., and Zhang, S. (2005). Effects of Earthworm Activity on Fertility and Heavy Metal Bioavailability in Sewage Sludge. *Environ. Int.* 31, 874–879. doi:10.1016/j.envint.2005.05.033

Malińska, K., Zabochnicka-Świątek, M., Cáceres, R., and Marfà, O. (2016). The Effect of Precomposted Sewage Sludge Mixture Amended with Biochar on the Growth and Reproduction of *Eisenia fetida* during Laboratory Vermicomposting. *Ecol. Eng.* 90, 35–41. doi:10.1016/j.ecoleng.2016.01.042

Martin, P., Martinez-Ansemil, E., Pinder, A., Timm, T., and Wetzel, M. J. (2007). Global Diversity of Oligochaetous Clitellates ("Oligochaeta"; Clitellata) in Freshwater. *Hydrobiologia* 595, 117–127. doi:10.1007/s10750-007-9009-1

Murtaza, B., Murtaza, G., Sabir, M., Owens, G., Abbas, G., Imran, M., et al. (2016). Amelioration of Saline-Sodic Soil with Gypsum Can Increase Yield and Nitrogen Use Efficiency in Rice-Wheat Cropping System. *Arch. Agron. Soil Sci.* 63, 1267–1280. doi:10.1080/03650340.2016.1276285

Murtaza, G. (2015). "Evaluation and Management of Sludge and Compost from Different Sources for Sustainable Agriculture," in Proceedings of the First Annual Technical Progress Report for Higher Education Commission (HEC) funded project (April 2014 to March 2017). (Inst. Soil Environ. Sci., Univ. Agric., Faisalabad, Pakistan)

Pak-Epa (2005). *Guidelines for Soil Waste Management*. Islamabad, Pakistan: Pakistan Environmental Protection Agency Pakistan.

Park, J. H., Choppala, G. K., Bolan, N. S., Chung, J. W., and Chuasavathi, T. (2011). Biochar Reduces the Bioavailability and Phytotoxicity of Heavy Metals. *Plant Soil* 348, 439–451. doi:10.1007/s11104-011-0948-y

Qadir, M., Mateo-Sagasta, J., Jiménez, B., Siebe, C., Siemens, J., and Hanjra, M. A. (2015). "Environmental Risks and Cost-Effective Risk Management in Wastewater Use Systems," in *Wastewater* (Springer, Netherlands), 55–72. doi:10.1007/978-94-017-9545-6_4

Riaz, M., Roohi, M., Arif, M. S., Hussain, Q., Yasmeen, T., Shahzad, T., et al. (2017). Corncob-derived Biochar Decelerates Mineralization of Native and Added Organic Matter (AOM) in Organic Matter Depleted Alkaline Soil. *Geoderma* 294, 19–28. doi:10.1016/j.geoderma.2017.02.002

Riaz, U., Murtaza, G., SaifullahFarooq, M., Farooq, M., Aziz, H., Qadir, A. A., et al. (2020). Chemical Fractionation and Risk Assessment of Trace Elements in Sewage Sludge Generated from Various States of Pakistan. *Environ. Sci. Pollut. Res.* 27, 39742–39752. In press. doi:10.1007/s11356-020-07795-4

Sanchez-Hernandez, J. C., Ro, K. S., and Díaz, F. J. (2019). Biochar and Earthworms Working in Tandem: Research Opportunities for Soil Bioremediation. *Sci. Total Environ.* 688, 574–583. doi:10.1016/j.scitotenv.2019.06.212

Sanchez-Hernandez, J. C., Sáez, J. A., Vico, A., Moreno, J., and Moral, R. (2020). Evaluating Earthworms' Potential for Remediating Soils Contaminated with Olive Mill Waste Sediments. *Appl. Sci.* 10 (7), 2624. doi:10.3390/app10072624

Sharma, A., Sonah, H., Deshmukh, R. K., Gupta, N. K., Singh, N. K., and Sharma, T. R. (2011). Analysis of Genetic Diversity in Earthworms Using DNA Markers. *Zoological Sci.* 28 (1), 25–31. doi:10.2108/zsj.28.25

Singh, N. P., McCoy, M. T., Tice, R. R., and Schneider, E. L. (1988). A Simple Technique for Quantitation of Low Levels of DNA Damage in Individual Cells. *Exp. Cell. Res.* 175, 184–191. doi:10.1016/0014-4827(88)90265-0

Singh, R. P., and Agrawal, M. (2010). Effect of Different Sewage Sludge Applications on Growth and Yield of Vigna Radiata L. Field Crop: Metal Uptake by Plant. *Ecol. Eng.* 36, 969–972. doi:10.1016/j.ecoleng.2010.03.008

Singh, R. P., and Agrawal, M. (2008). Potential Benefits and Risks of Land Application of Sewage Sludge. *Waste Manag.* 28, 347–358. doi:10.1016/j.wasman.2006.12.010

Sizmur, T., Martin, E., Wagner, K., Parmentier, E., Watts, C., and Whitmore, A. P. (2017). Milled Cereal Straw Accelerates Earthworm (Lumbricus Terrestris) Growth More Than Selected Organic Amendments. *Appl. Soil Ecol.* 113, 166–177. doi:10.1016/j.apsoil.2016.12.006

Song, Y., Zhu, L. S., Wang, J., Wang, J. H., Liu, W., and Xie, H. (2009). DNA Damage and Effects on Antioxidative Enzymes in Earthworm (Eisenia Foetida) Induced by Atrazine. *Soil Biol. Biochem.* 41 (5), 905–909. doi:10.1016/j.soilbio.2008.09.009

Stövenm, K., and Schnug, E. (2009). Long Term Effects of Heavy Metal Enriched Sewage Sludge Disposal in Agriculture on Soil Biota. *Agric. For. Res.* 2 (59), 131–138.

Tiwari, R. K., Singh, S., Pandey, R. S., and Sharma, B. (2016). Enzymes of Earthworm as Indicators of Pesticide Pollution in Soil. *Aer* 4 (4), 113–124. doi:10.4236/aer.2016.44011

Valckx, J., Govers, G., Hermy, M., and Muys, B. (2010). Manipulated Earthworm Populations Decrease Runoff and Erosion Rates in Arable Land with Distinct Soil Tillage Treatments. *Soil Biol. Biochem.* 41 (5), 905–909. doi:10.1007/978-3-642-14636-7_2

Van Groenigen, J. W., Lubbers, I. M., Vos, H. M. J., Brown, G. G., De Deyn, G. B., and Van Groenigen, K. J. (2014). Earthworms Increase Plant Production: a Meta-Analysis. *Sci. Rep.* 4, 6365. doi:10.1038/srep06365

Wang, F., Wang, H., Li, S., and Diao, X. (2019). Effects of Earthworms and Effective Microorganisms on the Composting of Sewage Sludge with Cassava Dregs in the Tropics. *J. Air Waste Manag. Assoc.* 69 (6), 710–716. doi:10.1080/10962247.2018.1552215

Wang, Z., Cui, Z., Liu, L., Ma, Q., and Xu, X. (2016). Toxicological and Biochemical Responses of the Earthworm *Eisenia fetida* Exposed to Contaminated Soil: Effects of Arsenic Species. *Chemosphere* 154, 161–170. doi:10.1016/j.chemosphere.2016.03.070

Wanga, L., Løvåsb, T., and Houshfarb, E. (2014). Effect of Sewage Sludge Addition on Potassium Release and Ash Transformation during Wheat Straw Combustion. *Chem. Eng.* 37, 7–12. doi:10.3303/CET1437002

Weyers, S. L., and Spokas, K. A. (2011). Impact of Biochar on Earthworm Populations: A Review. *Appl. Environ. Soil. Sci.* doi:10.1155/2011/541592

Yadav, S., and Mullah, M. (2017). A Review on Molecular Markers as Tools to Study Earthworm Diversity. *Int. J. Pure Appl. Zoology* 5 (1), 62–69.

Yang, J., Lv, B., Zhang, J., and Xing, M. (2014). Insight into the Roles of Earthworm in Vermicomposting of Sewage Sludge by Determining the Water-Extracts through Chemical and Spectroscopic Methods. *Bioresour. Technol.* 154, 94–100. doi:10.1016/j.biortech.2013.12.023

Yasmin, S., and D'Souza, D. (2010). Effects of Pesticides on the Growth and Reproduction of Earthworm: A Review. *Appl. Environ. Soil. Sci.* doi:10.1155/2010/678360

Younes, M., Othman, S. E., Elkersh, M. A., Youssef, N. S., and Omar, G. A. (2011). Effect of Seven Plant Oils on Some Biochemical Parameters in Khapra Beetle

Trogoderma Granarium Everts (Coleoptera: Dermestidae). *Egypt. J. Exp. Biol.* 7 (1), 53–61.

Zaltauskaitė, J., and Sodienė, I. (2010). Effects of Total Cadmium and Lead Concentrations in Soil on the Growth, Reproduction and Survival of Earthworm Eisenia fetida. *Ekologija* 56 (1-2), 10–16. doi:10.2478/v10055-010-0002-z

Zhang, R. H., Li, Z. G., Liu, X. D., Wang, B., Zhou, G. L., Huang, X. X., et al. (2017). Immobilization and Bioavailability of Heavy Metals in Greenhouse Soils Amended with Rice Straw-Derived Biochar. *Ecol. Eng.* 98, 183–188. doi:10.1016/j.ecoleng.2016.10.057

Zhang, X., Wang, H., He, L., Lu, K., Sarmah, A., Li, J., et al. (2013). Using Biochar for Remediation of Soils Contaminated with Heavy Metals and Organic Pollutants. *Environ. Sci. Pollut. Res.* 20, 8472–8483. doi:10.1007/s11356-013-1659-0

Zulhussnain, M., Zahoor, M. K., Rizvi, H., Zahoor, M. A., Rasul, A., Ahmad, A., et al. (2020). Insecticidal and Genotoxic Effects of Some Indigenous Plant Extracts in Culex quinquefasciatus Say Mosquitoes. *Sci. Rep.* 10 (1), 6826. doi:10.1038/s41598-020-63815-w

Conflict of Interest: The authors declare that the research was conducted in the absence of any commercial or financial relationships that could be construed as a potential conflict of interest.

Publisher's Note: All claims expressed in this article are solely those of the authors and do not necessarily represent those of their affiliated organizations, or those of the publisher, the editors and the reviewers. Any product that may be evaluated in this article, or claim that may be made by its manufacturer, is not guaranteed or endorsed by the publisher.

frontiers | Frontiers in Environmental Science

TYPE Original Research
PUBLISHED 02 September 2022
DOI 10.3389/fenvs.2022.917334

OPEN ACCESS

EDITED BY
Liangang Mao,
Institute of Plant Protection (CAAS), China

REVIEWED BY
Shuying Li,
Zhejiang University, China
Miguel Ángel González-Curbelo,
EAN University, Colombia
Kankan Zhang,
Guizhou University, China

*CORRESPONDENCE
Li Li,
sxaulili@sxau.edu.cn

SPECIALTY SECTION
This article was submitted to Toxicology, Pollution and the Environment, a section of the journal Frontiers in Environmental Science

RECEIVED 11 April 2022
ACCEPTED 28 July 2022
PUBLISHED 02 September 2022

CITATION
Fan J and Li L (2022), Residues, dissipation, and dietary risk assessment of oxadixyl and cymoxanil in cucumber. *Front. Environ. Sci.* 10:917334. doi: 10.3389/fenvs.2022.917334

Residues, dissipation, and dietary risk assessment of oxadixyl and cymoxanil in cucumber

Jiqiao Fan and Li Li*

College of Plant Protection, Shanxi Agricultural University, Taiyuan, China

Oxadixyl and cymoxanil are widely used for controlling downy mildew in cucumber; however, there are few systematic studies on monitoring residue levels of these two pesticides in cucumber under greenhouse and open field conditions. In this study, a simplified quick, easy, cheap, effective, rugged, and safe (QuEChERS) method was applied to analyze target compounds in cucumber. The average recoveries of oxadixyl and cymoxanil in cucumber ranged from 96% to 102%, with relative standard deviations (RSDs) of 1.8%–4.0%. The limits of quantification (LOQs) for two pesticides were both 0.01 mg/kg. The dissipation of oxadixyl was in accordance with a first-order kinetics equation, with half-lives ranging from 1.8 to 3.1 days. At the pre-harvest interval (PHI) of 3 or 5 days, the residue levels of oxadixyl in cucumber under open field conditions were higher than those under greenhouse conditions. Compared to oxadixyl, the cymoxanil degraded quickly, and its residues were below LOQ on the 3rd or 5th day after the last application. The terminal residues of oxadixyl and cymoxanil in the cucumber were both lower than the maximum residue limits (MRLs) in China. The risk quotient (RQ) used for dietary risk assessment was 1.8%–3.5% and 0.26%–0.51% for oxadixyl and cymoxanil, respectively. The results showed that the risks of these two pesticides used on cucumber at the experimental dosages are comparably acceptable for Chinese consumers of different gender and age groups. This study provides a reference data to use oxadixyl and cymoxanil scientifically and rationally.

KEYWORDS

oxadixyl, cymoxanil, cucumber, residue, dietary risk assessment

Introduction

Cucumber (*Cucumis sativus* L.), one of the most popular and widely cultivated fruiting vegetables in China, is rich in nutrients such as minerals, vitamins, and sugars, which are beneficial for human health (Shi et al., 2015; Li et al., 2021). Cucumber can be eaten raw or processed, which increases people's preference for it (Feng et al., 2021). As one of the most economically valuable vegetables, the output of cucumber reached 56 million tons in 2018 (Bian et al., 2020; FAOSTAT, 2020). However, cucumbers are susceptible to a variety of fungal diseases during their cultivation, such as gray mold, downy mildew, and powdery mildew, among which cucumber downy mildew is one of the most serious epidemic and devastating diseases (Granke et al., 2014; Wang et al., 2015;

Shirley et al., 2021). Consequently, fungicides are commonly used during cucumber cultivation for increasing cucumber output and improving quality. The unreasonable and excessive application of fungicides resulted in pesticide residues in agricultural products and threatened human health, which have been widely concerned and repeatedly reported (Benbrook and Davis, 2020; Heshmati et al., 2020; Chai et al., 2021; Wang et al., 2021). Hence, it is necessary to study the residues and dissipation of fungicides in cucumbers to ensure food safety as well as human health.

It is well known that the use of a single fungicide may cause resistance to the target, and mixed use of two or three pesticides with different modes of action has been developed in production. Oxadixyl is a systemic phenylamide fungicide with fungistatic and fungitoxic functions and is often applied to control diseases caused by downy mildew and phytophthora on many crops (Mirzoian and Ammann, 2014; Kwon et al., 2015; Liu et al., 2022), while cymoxanil is a new systemic fungicide with the characteristics of high efficiency (to Peronosporales fungi, especially Phytophthora and Peronospora) and low toxicity and is registered to control downy mildew and late blight in tomatoes, cucumbers, potatoes, and grapes (Gisi and Sierotzki, 2008; Cespedes et al., 2013; D'Arcangelo et al., 2021). Cymoxanil is often mixed with other protective fungicides to achieve better control effects. As one of these mixtures, a combination of oxadixyl and cymoxanil is used to control the cucumber downy mildew with good effects. They are both systematic fungicides with protective and curative functions, which could be absorbed by plants through roots and leaves after application, transferred to the edible parts (Pullagurala et al., 2018), and enriched in the food chains (Pirsaheb et al., 2019). However, few studies have been conducted on the residual behavior and dissipation of oxadixyl and cymoxanil in cucumber, which is insufficient to comprehensively evaluate the dietary risk.

In this study, an analytical method was developed for the determination of oxadixyl and cymoxanil, and the terminal residues and dissipation of these two pesticides in cucumbers under field or greenhouse conditions were obtained at 12 sites in China. Combined with the dietary data of different genders and ages and toxicological data, the risks were assessed. The results of this study would be helpful in providing guidance for the rational and safe use of oxadixyl and cymoxanil in cucumber.

Materials and methods

Chemicals and reagents

Standards of oxadixyl (97.69%) and cymoxanil (99.60%) were purchased from Dr. Ehrenstorfer GmbH (Augsburg, Germany). Acetonitrile (HPLC grade) and mass spectrometry-grade formic acid were obtained from Fisher Chemical Co., Ltd. (Waltham, MA, United States). Analytical-grade sodium chloride (NaCl) was purchased from Beijing Tongguang Fine Chemical Co. (Beijing, China). The pesticides 38% oxadixyl + cymoxanil water-dispersible granule (oxadixyl 8% and cymoxanil 30%) was used. The centrifuge tube (50 mL) and syringe filter (0.22 μm) were provided by ANPEL Laboratory Technologies Inc. (Shanghai, China). In addition, ultrapure water was prepared using a Milli-Q Advantage AW system (Millipore, United States).

Solution preparation

The stock solutions were prepared by accurately weighing the standards of oxadixyl (24.5 mg) and cymoxanil (25.0 mg) in 25-mL flasks separately and dissolving them in acetonitrile. A volume of 100 mg/L mixed standard solutions of oxadixyl and cymoxanil was prepared by diluting stock solutions with acetonitrile. All standard solutions were kept at 4°C in the dark before use. The working and matrix-matched standard solutions were prepared freshly when used at the

TABLE 1 Latitude and longitude, climate type, and growing practices of 12 sites.

Experimental location	Latitude and longitude	Climate type	Growing practice
Huhhot, Inner Mongolia	40.70N, 111.83E	Mid-temperate continental monsoon climate	Greenhouse
Changchun, Jilin	44.00N, 125.62E	Temperate continental humid climate	Greenhouse
Taiyuan, Shanxi	37.68N, 112.53E	Warm temperate continental monsoon climate	Greenhouse
Changping, Beijing	40.14N, 116.35E	Continental monsoon climate	Greenhouse
Taian, Shandong	36.07N, 116.94E	Temperate continental subhumid monsoon climate zone	Open field
Zhengzhou, Henan	34.35N, 113.57E	Temperate continental monsoon climate	Greenhouse
Hefei, Anhui	31.85N, 117.04E	Subtropical humid monsoon climate	Open field
Songjiang, Shanghai	30.93N, 121.07E	Subtropical maritime monsoon climate	Greenhouse
Ezhou, Hubei	30.45N, 114.63E	Subtropical monsoon climate	Open field
Changsha, Hunan	28.31N, 113.30E	Subtropical monsoon climate	Open field
Nanning, Guangxi	22.84N, 108.30E	Humid subtropical monsoon climate	Open field
Foshan, Guangdong	23.08N, 113.02E	Humid subtropical monsoon climate	Open field

TABLE 2 Gradient elution procedure.

Time (min)	Flow rate (mL/min)	Acetonitrile (%)	0.05% formic acid aqueous solution (%)
0	0.30	10.0	90.0
1.40	0.30	10.0	90.0
1.50	0.30	90.0	10.0
3.00	0.30	90.0	10.0
3.10	0.30	10.0	90.0
5.00	0.30	10.0	90.0

TABLE 3 LC-MS/MS (ESI) characteristics of oxadixyl and cymoxanil.

Compound	T_R (min)	Precursor ion	Quantitation ion	Collision energy (eV)	Confirmatory ion	Collision energy (eV)	Fragmentor voltage (V)	Polarity
Oxadixyl	3.61	279.286	219.192	15	132.969	22	22	Positive
Cymoxanil	3.55	199.171	128.082	6	111.095	18	16	Positive

concentrations of 0.005, 0.01, 0.025, 0.05, 0.1, 0.25, 0.50, 1.0, and 2.5 mg/L using acetonitrile or blank sample extracts.

Field trials and sample collection

The field experiments were designed according to the pesticide registration information and the Guideline on Pesticide Residue Trials (NY/T 788-2018) issued by the Ministry of Agriculture and Rural Affairs, P. R. of China (Ministry of Agriculture and Rural Affairs of the People's Republic of China, 2018). Field trials were conducted on 12 different production areas, which represented different climates and environmental conditions in China, while six sites were under open field conditions and the others in greenhouses. The latitude and longitude, climate type, and growing practices of 12 locations are shown in Table 1.

In order to test the dissipation and terminal residues of oxadixyl and cymoxanil in cucumber, a treatment area and a control area were set up in the experiment, and each plot was 50 m^2 with a 2 m separated area between plots. In the terminal residue experiments, the cucumber plants were sprayed with the recommended high dosage (342 g a.i.·ha^{-1}) three times with an interval of 7 days. Cucumber samples were randomly collected from each plot at 3 and 5 days after the last application. At least 12 normally growing cucumbers with a total weight of at least 2 kg were collected from each plot, and the sample collection was carried out in duplicate according to the guidelines. The cucumber samples from the field trials were cut into small pieces and put into plastic bags.

The dissipation tests were conducted on four sites, including Inner Mongolia, Beijing, Anhui, and Guangxi, under open field or greenhouse conditions, respectively. For the dissipation tests, cucumber samples were collected from treatment plot on 0, 1, 3, 5, and 7 days after the last application using the same sampling method. All test samples were transported to the laboratory within 8 h and kept at −20°C until analysis.

Storage stability test

In our study, the storage stability of oxadixyl and cymoxanil was tested according to the Guideline for the Stability Testing of Pesticide Residues in Stored Commodities of Plant Origin (NY/T 3094-2017, issued by the Ministry of Agriculture and Rural Affairs of the People's Republic of China, 2017). Aliquots of 10 g blank cucumber samples were accurately weighed into a 50-mL centrifuge tube, then a 100 μL standard solution of oxadixyl or cymoxanil was added individually into the tubes with a spiked level of 0.10 mg/kg, and the samples were quickly mixed and stored at ≤ −18°C. The samples were analyzed at the intervals of 0, 30, 66, and 130 days.

Sample preparation

A volume of 10 g homogenized cucumber sample was accurately weighed into a 50-mL centrifuge tube, and then 10 mL of chromatographic-grade acetonitrile was added and

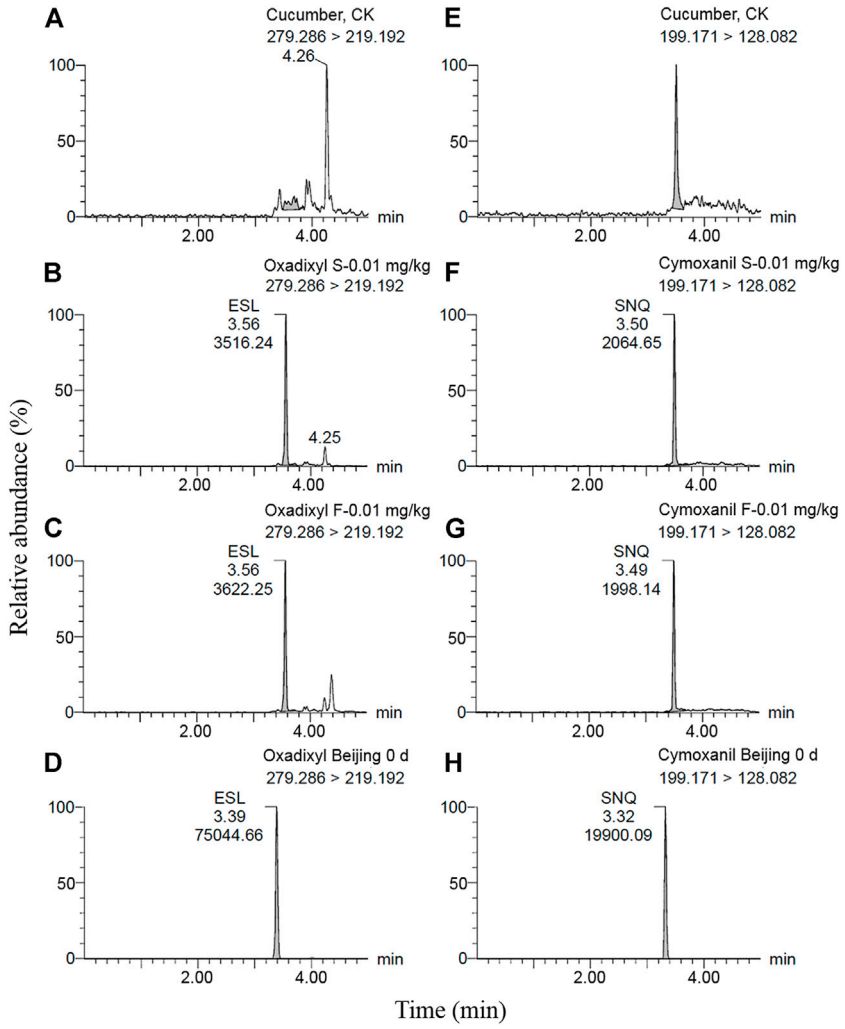

FIGURE 1
LC-MS/MS chromatograms of oxadixyl **(A–D)** and cymoxanil **(E–H)** in cucumber, control sample, matrix-matched standard solution (0.01 mg/kg), fortified level (0.01 mg/kg), and cucumber sample (S indicates matrix-matched standard solution, and F indicates the fortified level).

TABLE 4 Method validation results for oxadixyl and cymoxanil in cucumber.

Fungicide	Fortified level (mg/kg)	Recovery (%, n = 5)	RSD (%, n = 5)	Linearity range (mg/L)	Solvent calibration curve (correlation coefficient, r)	Matrix-matched calibration curve (correlation coefficient, r)	ME (%)
Oxadixyl	0.010	100	3.7	0.005-1	y = 2139x + 1611 (r = 0.9960)	y = 2404x + 6247 (0.9968)	12
	0.50	98	1.8				
	5.0	102	3.6				
Cymoxanil	0.010	99	4.0	0.005-1	y = 1994x + 717.2 (r = 0.9999)	y = 1591x + 1931 (0.9998)	−20
	0.50	96	3.0				
	5.0	101	3.9				

TABLE 5 Storage stability results of oxadixyl and cymoxanil in cucumber under frozen conditions.

Storage interval (d)	Oxadixyl		Cymoxanil	
	Residue (mg/kg)	Degradation rate (%)	Residue (mg/kg)	Degradation rate (%)
0	0.11	—	0.11	—
30	0.11	0	0.098	11
66	0.098	11	0.096	13
130	0.099	10	0.10	9

well mixed. After ultrasonic extraction for 15 min, 6 g (± 0.05 g) of NaCl was added and then shaken vigorously for 1 min. It was centrifuged at 3,000 rpm for 5 min, and 1 mL of the supernatant was passed through a 0.22-μm membrane and put into the sample vial for UPLC-MS/MS analysis.

UPLC-MS/MS analysis

Oxadixyl and cymoxanil were analyzed by ultra-high performance liquid chromatography (Waters ACQUITY UPLC H-Class, Milford, MA, United States) and tandem triple quadrupole mass spectrometry (Waters Corp., Milford, MA, United States) with an electrospray ionization (ESI) source operated in the positive ion mode (ESI+). An ACQUITY UPLC BEH C18 column (100 mm × 2.1 mm, 1.7 μm) was used for chromatographic separation at a temperature of 30°C. The mobile phases consisted of A: acetonitrile and B: 0.05% formic acid in aqueous solution. The gradient elution procedure is shown in Table 2. The flow rate was 0.30 mL/min, and the injection volume was 1 μL. The analysis was finished within 5 min. The capillary voltages were 3,500 V, the taper hole voltages were 15 V, and the ion source temperature was set at 150°C under the positive ion detection mode. For MS detection working conditions, the desolvent gas temperature was set at 500°C, the desolvent gas flow rate at 1,000 L/h, and cone hole gas flow was 5 L/h. Analytes were determined in the multiple reaction monitoring (MRM) mode. The MS/MS parameters of oxadixyl and cymoxanil are listed in Table 3. The representative spectrums of oxadixyl and cymoxanil are shown in Figure 1. MassLynx version 4.1 SCN 9.4 (Waters Corp., Milford, MA, United States) was used for data acquisition and processing.

Method validation

According to the EU guidelines (European Commission, 2020), the analytical method was validated by the linearity, matrix effect, limit of quantification (LOQ), recovery, and relative standard deviations (RSDs). The linearity of this method was studied using the solvent standard solution and matrix-matched calibration. The ME was evaluated using the following equation (Ferrer et al., 2011):

$$ME(\%) = \left(\frac{the\ slope\ of\ matrix\ standard}{the\ slope\ of\ solvent\ standard} - 1 \right) \times 100\%.$$

A percentage of the matrix effect (ME) between −20% and 20% was considered no matrix effect. A medium matrix effect occurred when the values were between −50% and −20% or 20% and 50%, and a strong matrix effect would be below −50% or above 50%. The LOQ was defined as the lowest spiked level of oxadixyl and cymoxanil in cucumber (Vial et al., 2003; Burns and Valdivia, 2008). According to NY/T 788-2018, the accuracy and precision of this method were evaluated through recovery studies at three spiked levels with five replicates.

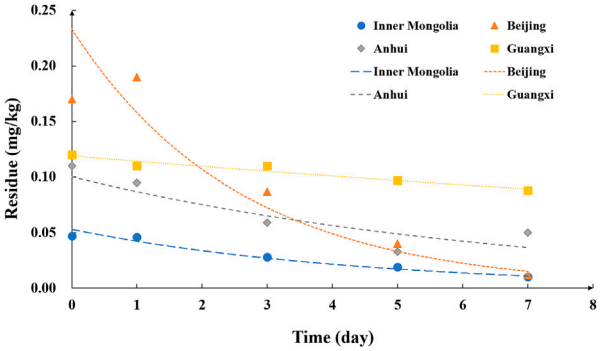

FIGURE 2
Dissipation of oxadixyl in cucumber samples in Inner Mongolia, Beijing, Anhui, and Guangxi.

Dissipation study

Based on the previous reports, the dissipation rates of oxadixyl and cymoxanil were expressed using the first-order

TABLE 6 Terminal residues, median residues, highest residues, and their corresponding MRLs on cucumbers at different intervals.

Fungicide	Interval (day)	Residue (mg/kg)	STMR (mg/kg)	HR (mg/kg)	MRL (mg/kg)
Oxadixyl	3	<0.01–0.11	0.053	0.11	5.0 (China) and 0.01(European Union)
	5	<0.01–0.097	0.036	0.097	
Cymoxanil	3	<0.01–0.032	<0.01	0.032	0.5 (China) and 0.08(European Union)
	5	<0.01	<0.01	<0.01	

Notes: STMR is the median of the surveillance test of the pesticide residues, and HR is the highest residues; MRL is the maximum residue limit.

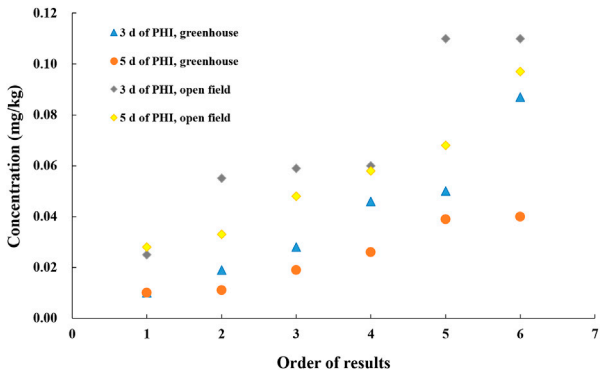

FIGURE 3
Residue levels of oxadixyl in greenhouse and open field cucumbers on different PHI (12 samples from different experiment sites, in the order of smallest to largest in the residue level).

kinetic model and half-life values (Xie et al., 2019). The calculation formulas were as follows:

$$C_t = C_0 e^{-kt},$$

$$t_{1/2} = \frac{ln\,2}{k},$$

where C_t (mg/kg) is the residual concentration of the compound at time t (d), C_0 (mg/kg) is the initial concentration of the compound, k is the dissipation rate constant, and $t_{1/2}$ is the half-time of compound degradation.

Chronic dietary risk assessment

The national estimated daily intake (NEDI) and risk quotient (RQ) were used to evaluate chronic dietary risk and calculated using the following formulas:

$$NEDI = \sum STMR_i \times F_i,$$

$$RQ = NEDI / (ADI \times bw) \times 100\%,$$

where $STMR_i$ (mg/kg) is the the supervised trials median residue, Fi (kg) is the average daily intake of a certain food in the general population, and bw is the average body weight of the population subgroups. ADI (mg/kg bw) is the acceptable daily intake, and the values were derived from GB 2763-2021 (National Health and Family Planning Commission, Ministry of Agriculture and Rural Affairs of the People's Republic of China, 2021). The corresponding MRLs can be used for NEDI calculation if there is no $STMR_i$ data. If the RQ value is ≥100%, the risk would be considered unacceptable; otherwise, the risk was acceptable.

Results and discussion

Method validation

A simplified QuEChERS method was developed for the determination of oxadixyl and cymoxanil in cucumber. The linearity, limits of quantification (LOQs), matrix effect, precision, and accuracy were assessed to validate the performance of this method according to the EU guidelines (European Commission, 2020) and the NY/T 788-2018 (Ministry of Agriculture and Rural Affairs of the People's Republic of China, 2018). As shown in Table 4, the linearity was obtained for two analytes in cucumber (r = 0.9968 for oxadixyl and cymoxanil r = 0.9998). The average recoveries of oxadixyl and cymoxanil in cucumber were 98%–102% and 96%–101% at spiked levels of 0.010, 0.50, and 5.0 mg/kg with RSDs of 1.8%–3.7% and 3.0%–4.0%, respectively. According to this definition and the recovery experiments, the LOQs of oxadixyl and cymoxanil in cucumber are both 0.01 mg/kg under the aforementioned analysis conditions. The ME values of oxadixyl and cymoxanil in cucumber were 12% and 20%, respectively, indicating that there existed matrix effect for these two pesticides. Hence, to eliminate the matrix effect, the matrix-matched calibration curves of oxadixyl and cymoxanil were implemented for quantitative analysis of test samples in this study.

Overall, these results indicated that the accuracy and precision of the method were acceptable and that it is suitable for the analysis of the residues oxadixyl and cymoxanil in cucumber.

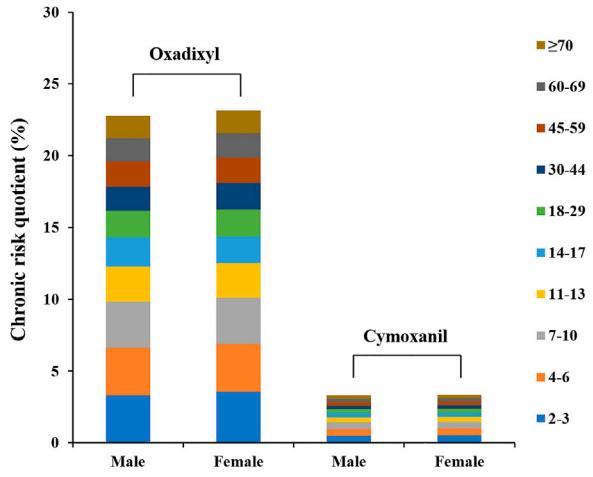

FIGURE 4
Chronic dietary risk assessment of oxadixyl and cymoxanil in cucumber.

Storage stability test

Field samples were stored in the laboratory for several weeks or even longer before analysis. The target compounds might change or degrade during storage, which might affect the accuracy of the detection. Therefore, the storage stability of pesticides is closely related to the reliability of pesticide residue detection results. In our study, the storage stability of oxadixyl and cymoxanil was evaluated under frozen conditions (≤−18°C) for 130 days. The results of the storage stability test are shown in Table 5. The degradation rates of oxadixyl and cymoxanil in the stored fortified samples were 11% and 13%, respectively, at 130 days of ≤ −18°C frozen storage. According to the Chinese standard NY/T 3094–2017 (Industrial Standard of the People's Republic of China, 2017) and FAO regulations (Food and Agriculture Organization of the United Nations, 2016), the degradation rate was less than 30% during the storage before analysis, indicating that the target compounds were comparably stable.

Dissipation kinetics in cucumber

In our study, the residue level in the sample 2 h after application was defined as the initial residue level. According to the experimental results, the dissipation curve of oxadixyl in cucumbers from Inner Mongolia (greenhouse), Beijing (greenhouse), Anhui (open field), and Guangxi (open field) are shown in Figure 2. The initial residue of oxadixyl in cucumbers from Inner Mongolia, Beijing, Anhui, and Guangxi were 0.047, 0.17, 0.11, and 0.12 mg/kg after 2 h of spraying. The dissipation dynamics equations of oxadixyl were C_t = 0.0528 $e^{-0.224x}$ (Inner Mongolia), C_t = 0.2333 $e^{-0.390x}$ (Beijing), C_t = 0.1003 $e^{-0.145x}$ (Anhui), and C_t = 0.1191 $e^{-0.041x}$ (Beijing) in cucumber, with half-lives ($t_{1/2}$) of 3.1, 1.8, 4.8, and 16.9 days, respectively. The maximum initial deposition (0.17 mg/kg) and the fastest dissipation rate (93% after 7 days) both occurred in the samples of Beijing. The minimum initial deposition (0.047 mg/kg) occurred in the samples of Inner Mongolia, and the slowest dissipation rate (27% after 7 days) occurred in the samples of Guangxi, with a half-life of 16.9 days.

In contrast to oxadixyl, cymoxanil dissipated rapidly in cucumber, and the kinetic equation was not available. The initial concentrations were 0.059, 0.27, 0.25, and 0.14 mg/kg in cucumbers from Inner Mongolia, Beijing, Anhui, and Guangxi, respectively. After 3 days, the residue of cymoxanil in samples of Beijing was 0.032 and <0.01 mg/kg than those in other three places. The initial residue level of oxadixyl and cymoxanil in cucumber was both below MRL in China, whether in open field or greenhouse. Until now, studies on the dissipation of oxadixyl were limited, while the half-lives of cymoxanil in different crops were reported previously, which were 6.3–6.7 days in the plant of ginseng, 0.5–0.7 days in grape, and 2.26 days in potato (He et al., 2007; Yan et al., 2016; Huang et al., 2019). In our study, cymoxanil dissipated rapidly in cucumber at three field sites, and the kinetic equation was not available for cymoxanil residues, which was consistent with the previous studies (Hong et al., 2018). The dissipation of pesticides in plants is usually related to the physicochemical properties of the pesticide, the climate and experimental conditions, and the growth dilution factor (Zhao et al., 2011). In our study, the environmental parameters, the crop, and the growth factor were all the same for oxadixyl and cymoxanil, and the difference in dissipation was correlated with the physical–chemical properties of these two pesticides.

Terminal residues in cucumber

The pesticide was sprayed three times with a dosage of 342 g a.i./ha at an interval of 7 days, and the terminal residue data of oxadixyl and cymoxanil in cucumber are shown in Table 6. The terminal residue levels of target compounds decreased with the increasing pre-harvest interval time. The PHI was 3 and 5 days; the terminal residues of oxadixyl in cucumber at harvest were <0.01–0.11 and <0.01–0.097 mg/kg, and the terminal residues of cymoxanil in cucumber at harvest were <0.01–0.032 and <0.01 mg/kg, respectively. Therefore, no matter on third or fifth day, the terminal residues of oxadixyl and cymoxanil in cucumbers were both lower than MRLs of China, which were 5 mg/kg for oxadixyl and 0.5 mg/kg for cymoxanil, respectively. The results of cymoxanil were consistent with those reported by Huang et al. (2019). The EU sets the MRL of oxadixyl at 0.01 mg/kg in vegetables (EFSA, 2021), which is much stricter than the limits in China.

Effects of cultivation conditions on residues

According to the data of the National Bureau of Statistics, the planting scale of greenhouse vegetables in China is approximately 3.86 million hectares. Cucumber is mainly cultivated in greenhouses in northern China and open fields in southern China. The residue behavior of fungicides in greenhouse-cultivated vegetables is different from those in the open field (Bojac´a et al., 2013; Angioni et al., 2012). Residue levels of oxadixyl and cymoxanil in cucumber were determined in the greenhouse planting process, and the obtained results were compared with those in the open field conditions. Cymoxanil residues are not further considered in our study because the residue levels of cymoxanil were all <0.01 mg/kg except in Beijing (the residue value was 0.032 mg/kg with the PHI of 3 days). The comparison results of oxadixyl are presented in Figure 3 in the order of the smallest to largest in the residue level (residue levels below 0.01 mg/kg were expressed as 0.01 mg/kg). As shown in Figure 3, on PHI of 3 or 5 days, the residue levels of oxadixyl in cucumbers grown in open field are higher than those in greenhouse. This result showed that the greenhouse accelerated the dissipation of oxadixyl in cucumbers. Cultivation conditions and environmental factors could greatly influence the dissipation rate of fungicides in plants. Due to the better water and fertilizer conditions in the greenhouse, cucumbers grow faster than those in the open field, coupled with the fast growth dilution property of cucumbers (Wang et al., 2014), which may result in the quicker dissipation of oxadixyl in greenhouse cucumber than that in the open field.

Chronic dietary risk assessment

To evaluate the long-term dietary intake risk of oxadixyl and cymoxanil, the NEDI and RQ were used as important parameters. According to the experimental results, the STMR values of oxadixyl and cymoxanil were 0.053 and <0.01 mg/kg for the PHI of 3 days, respectively. The ADI values of oxadixyl and cymoxanil were 0.01 and 0.013 mg/kg bw, respectively. Combined with different dietary patterns of Chinese populations, the NEDI values of oxadixyl and cymoxanil across different age groups and different genders were estimated to be 0.0044–0.011 and 0.00082–0.0021 mg (kg bw·day)$^{-1}$, while the RQ values were 1.8%–3.5% and 0.26%–0.51%, respectively. It can be seen intuitively from Figure 4 that the dietary risks of the two pesticides generally show a downward trend with age, and females had a greater risk than males with no significant difference. The RQ values were both less than 100%, indicating that the long-term dietary risk of oxadixyl and cymoxanil for Chinese residents of different age groups was low and acceptable.

Conclusion

In this study, the dissipation and terminal residues of oxadixyl and cymoxanil were analyzed in cucumber, and the long-term dietary intake risk was evaluated. In the dissipation study, cymoxanil dissipated faster than oxadixyl in cucumber. The terminal residues of oxadixyl and cymoxanil in cucumber were both lower than the maximum residue limit in China. The RQs of oxadixyl and cymoxanil in cucumber were both less than 100% in the dietary risk assessment, indicating that the long-term dietary risk for Chinese residents of different age groups was acceptable. Up to the present, there has been limited literature on the safety evaluation of oxadixyl, and the results will provide an important reference for the proper use of it in cucumbers.

Data availability statement

The original contributions presented in the study are included in the article/Supplementary Material; further inquiries can be directed to the corresponding author.

Author contributions

Investigation, LL; methodology, JF; supervision, LL; writing–original draft, JF and LL; and writing–review and editing, LL.

Funding

This work was supported by the Fundamental Research Program of Shanxi Province (No. 20210302124131).

Conflict of interest

The authors declare that the research was conducted in the absence of any commercial or financial relationships that could be construed as a potential conflict of interest.

Publisher's note

References

Angioni, A., Porcu, L., and Dedola, F. (2012). Determination of famoxadone, fenamidone, fenhexamid and iprodione residues in greenhouse tomatoes. *Pest Manag. Sci.* 68, 543–547. doi:10.1002/ps.2287

Benbrook, C. M., and Davis, D. R. (2020). The dietary risk index system: A tool to track pesticide dietary risks. *Environ. Health* 19, 103. doi:10.1186/s12940-020-00657-z

Bian, Y., Guo, G., Liu, F., Chen, X., Wang, Z., and Hou, T. (2020). Meptyldinocap and azoxystrobin residue behaviors in different ecosystems under open field conditions and distribution on processed cucumber. *J. Sci. Food Agric.* 100, 648–655. doi:10.1002/jsfa.10059

Bojac´a, C. R., Arias, L. A., Ahumada, D. A., Casilimas, H. A., and Schrevens, E. (2013). Evaluation of pesticide residues in open field and greenhouse tomatoes from Colombia. *Food control.* 30, 400–403. doi:10.1016/j.foodcont.2012.08.015

Burns, M., and Valdivia, H. (2008). Modelling the limit of detection in real-time quantitative PCR. *Eur. Food Res. Technol.* 226, 1513–1524. doi:10.1007/s00217-007-0683-z

Cespedes, M. C., Cardenas, M. E., Vargas, A. M., Rojas, A., Morales, J. G., Jimenez, P., et al. (2013). Physiological and molecular characterization of phytophthora infestans isolates from the central Colombian andean region. *Rev. Iberoam. Micol.* 30, 81–87. doi:10.1016/j.riam.2012.09.005

Chai, Y. D., Liu, R., He, W., Xu, F. L., Chen, Z. L., Li, L., et al. (2021). Dissipation behavior, residue, and risk assessment of benziothiazolinone in apples. *Int. J. Environ. Res. Public Health* 18, 4478. doi:10.3390/ijerph18094478

D'arcangelo, K. N., Adams, M. L., Kerns, J. P., and Quesada-Ocampo, L. M. (2021). *Assessment of fungicide product applications and program approaches for control of downy mildew on pickling cucumber in North Carolina*, 140, 105412. doi:10.1016/j.cropro.2020.105412*Crop Prot.*

European Commission (2020). Guidance document on analytical quality control and method validation procedures for pesticide residues and analysis in food and feed (SANTE/12682/2019). Available at: https://www.eurl-pesticides.eu/userfiles/file/Eurl ALL/AqcGuidance_SANTE_2019_12682.pdf (Accessed August 20, 2021).

Faostat (2020). The FAO (food and agriculture organization of the united Nations) compare data. Available at: http://www.fao.org/faostat/zh/#compare (Accessed August 5, 2021).

Feng, X., Pan, L., Jing, J., Zhang, J., Zhuang, M., Zhang, Y., et al. (2021). Dynamics and risk assessment of pesticides in cucumber through field experiments and model simulation. *Sci. Total Environ.* 773, 145615. doi:10.1016/j.scitotenv.2021.145615

Ferrer, C., Lozano, A., Aguera, A., Jiménez, G. A., and Fernández-Alba, A. R. (2011). Overcoming matrix effects using the dilution approach in multiresidue methods for fruits and vegetables. *J. Chromatogr. A* 1218 (42), 7634–7639. doi:10.1016/j.chroma.2011.07.033

Food and Agriculture Organization of the United Nations (2016). *Manual on the submission and evaluation of pesticide residues data for the estimation of maximum residue limits in food and feed*. Rome: FAO.

Gisi, U., and Sierotzki, H. (2008). Fungicide modes of action and resistance in downy mildews. *Eur. J. Plant Pathol.* 122, 157–167. doi:10.1007/s10658-008-9290-5

Granke, L. L., Morrice, J. J., and Hausbeck, M. K. (2014). Relationships between airborne pseudoperonospora cubensis sporangia, environmental conditions, and cucumber downy mildew severity. *Plant Dis.* 98, 674–681. doi:10.1094/pdis-05-13-0567-re

He, L., Sun, Y., Huang, Y., Pei, R., and Zheng, S. (2007). Residue dynamics of cymoxanil in mixed formulation in potatoes and soil. *J. Agro-Environment* 2007, 322–325.

Heshmati, A., Nili-Ahmadabadi, A., Rahimi, A., Vahidinia, A., and Taheri, M. (2020). Dissipation behavior and risk assessment of fungicide and insecticide residues in grape under open-field, storage and washing conditions. *J. Clean. Prod.* 270, 122287. doi:10.1016/j.jclepro.2020.122287

Hong, S., S, Y., Zhang, C., Cao, X., Zheng, L., Wang, S., et al. (2018). Simultaneous detection and degradation of pyraclostrobin and cymoxanil in cucumber and soil. *Food Sci. Biotechnol.* 29, 262–266.

Huang, J., Ye, Q., Wan, K., and Wang, F. (2019). Residue behavior and risk assessment of cymoxanil in grape under field conditions and survey of market samples in Guangzhou. *Environ. Sci. Pollut. Res.* 26, 3465–3472. doi:10.1007/s11356-018-3890-1

Kwon, H., Kim, T. K., Hong, S. M., Se, E. K., Cho, N. J., and Kyung, K. S. (2015). Effect of household processing on pesticide residues in field-sprayed tomatoes. *Food Sci. Biotechnol.* 24, 1–6. doi:10.1007/s10068-015-0001-7

Li, C., Zhou, J., Yue, N., Wang, Y., Wang, J., and Jin, F. (2021). Dissipation and dietary risk assessment of tristyrylphenol ethoxylate homologues in cucumber after field application. *Food Chem. x.* 338, 127988. doi:10.1016/j.foodchem.2020.127988

Liu, J., X, X., Wu, A., Song, S., Kuang, H., Liu, L., et al. (2022). An immunochromatographic assay for the rapid detection of oxadixyl in cucumber, tomato and wine samples. *Food Chem.* 379, 132131. doi:10.1016/j.foodchem.2022.132131

EFSA (European Food Safety Authority) (2021). The 2019 European Union report on pesticide residues in food. *EFSA J.* 19 (4), e06491. doi:10.2903/j.efsa.2021.6491

Ministry of Agriculture and Rural Affairs of the People's Republic of China (2017). *NY/T 3094-2017, guideline for the stability testing of pesticide residues in stored Commodities of plant Origin*. Beijing: China agriculture press.

Ministry of Agriculture and Rural Affairs of the People's Republic of China (2018). *NY/T 788-2018, guideline for the testing of pesticide residues in crops*. China: Agricultural Industry Standard of the People's Republic of China.

Mirzoian, A., and Ammann, J. R. (2014). Determination of oxadixyl in wines by liquid chromatography-tandem mass spectrometry: Single-laboratory and interlaboratory validation study. *J. Aoac Int.* 97, 1701–1706. doi:10.5740/jaoacint.13-359

National Health and Family Planning CommissionMinistry of Agriculture of the People's Republic of China (2021). National food safety standard–maximum residue limits for pesticides in food (GB 2763–2019). Available at: http://www.nhc.gov.cn/sps/s7891/201702/ed7b47492d7a42359f839daf3f70eb4b.shtml (Accessed August 20, 2021).

Pirsaheb, M., Fakhri, Y., Karami, M., Akbarzadeh, R., Safaei, Z., Fatahi, N., et al. (2019). Measurement of permethrin, deltamethrin and malathion pesticide residues in the wheat flour and breads and probabilistic health risk assessment: A case study in kermanshah, Iran. *Int. J. Environ. Anal. Chem.* 99, 1353–1364. doi:10.1080/03067319.2019.1622009

Pullagurala, V. L. R., Rawat, S., Adisa, I. O., Hernandez-Viezcas, J. A., Peralta-Videa, J. R., and Gardea-Torresdey, J. L. (2018). Plant uptake and translocation of contaminants of emerging concern in soil. *Sci. Total Environ.* 636, 1585–1596. doi:10.1016/j.scitotenv.2018.04.375

Shi, J., Wang, J., Li, R., Li, D., Xu, F., Sun, Q., et al. (2015). Expression patterns of genes encoding plasma membrane aquaporins during fruit development in cucumber (Cucumis sativus L.). *Plant Physiol. biochem.* 96, 329–336. doi:10.1016/j.plaphy.2015.08.018

Shirley, A., Vallad, G. E., Dufault, N. S., Raid, R., and Quesada-Ocampo, L. (2021). Duration of downy mildew control achieved with fungicides on cucumber under Florida field conditions. *Plant Dis.* 106, 1167–1174. doi:10.1094/PDIS-03-21-0507-RE

Vial, J., Le Mapihan, K., and Jardy, A. (2003). What is the best means of estimating the detection and quantification limits of a chromatographic method? *Chromatographia* 57, 303–306. doi:10.1007/bf02492120

Wang, H., Li, M., Xu, J., Chen, M., Li, W., and Li, M. (2015). An early warning method of cucumber downy mildew in solar greenhouse based on canopy temperature and humidity modeling. *Ying Yong Sheng Tai Xue Bao* 26, 3027–3034.

Wang, M., Zhang, Q., Cong, L., Yin, W., and Wang, M. (2014). Enantioselective degradation of metalaxyl in cucumber, cabbage, spinach and pakchoi. *Chemosphere* 95, 241–246. doi:10.1016/j.chemosphere.2013.08.084

Wang, W., Gao, Z., Qiao, C., Liu, F., and Peng, Q. (2021). Residue analysis and removal of procymidone in cucumber after field application. *Food control.* 128, 108168. doi:10.1016/j.foodcont.2021.108168

Xie, J., Zheng, Y., Liu, X., Dong, F., Xu, J., Wu, X., et al. (2019). Human health safety studies of a new insecticide: Dissipation kinetics and dietary risk assessment of afidopyropen and one of its metabolites in cucumber and nectarine. *Regul. Toxicol. Pharmacol.* 103, 150–157. doi:10.1016/j.yrtph.2019.01.025

Yan, J., W, R., Xu, Y., Sun, G., Lu, B., Wang, Y., et al. (2016). The residual dynamics and final residue of cymoxanil in ginseng with the application of cymoxanil·mancozeb 72% WP. *Agrochemicals* 55, 275–277.

Zhao, P., Wang, L., Chen, L., and Pan, C. (2011). Residue dynamics of clopyralid and picloram in rape plant rapeseed and field soil. *Bull. Environ. Contam. Toxicol.* 86, 78–82. doi:10.1007/s00128-010-0184-9

frontiers | Frontiers in Environmental Science

TYPE Original Research
PUBLISHED 23 September 2022
DOI 10.3389/fenvs.2022.991494

OPEN ACCESS

EDITED BY
Liangang Mao,
Institute of Plant Protection (CAAS), China

REVIEWED BY
Andrey S. Zaitsev,
University of Giessen, Germany
Qingming Zhang,
Qingdao Agricultural University, China

*CORRESPONDENCE
Sharon T Pochron,
Sharon.pochron@stonybrook.edu

†These authors have contributed equally to this work and share second authorship

SPECIALTY SECTION
This article was submitted to Toxicology, Pollution and the Environment, a section of the journal Frontiers in Environmental Science

RECEIVED 11 July 2022
ACCEPTED 07 September 2022
PUBLISHED 23 September 2022

CITATION
Pochron ST, Mezic M, Byrne S, Sasoun S, Casamassima A, Kilic M, Nuzzo A and Beaudet C-E (2022), Exposure to Roundup increases movement speed and decreases body mass in earthworms.
Front. Environ. Sci. 10:991494.
doi: 10.3389/fenvs.2022.991494

Exposure to Roundup increases movement speed and decreases body mass in earthworms

Sharon T Pochron[1]*, Mateo Mezic[1†], Samantha Byrne[1†], Samy Sasoun[1], Alex Casamassima[1], Melisa Kilic[1], Amanda Nuzzo[1] and Charles-Edouard Beaudet[2]

[1]Sustainability Studies Program, School of Marine and Atmospheric Sciences, Stony Brook University, Stony Brook, NY, United States, [2]Département d'Informatique et de Génie Logiciel, Université Laval, Ville de Québec, QC, Canada

Glyphosate, the herbicidal ingredient in Roundup products, can persist in soil for months or years, allowing soil invertebrates ample time to encounter and respond to contamination. While Roundup products can negatively impact earthworm (*Eisenia fetida*) health, they may also provide a direct or indirect food source. In a set of three experiments, we aimed to determine if Roundup Ready-to-Use III provides a nutritional benefit, damages earthworm health, or both. We used cameras and ant-farm-style enclosures to measure how exposure to a commonly used Roundup formulation impacted earthworm foraging speed as measured by the amount of soil displaced per minute. We also assessed whether contamination drove changes in earthworm body mass and stress test survival time. We found that earthworms living in contaminated soil decreased body mass and displaced more soil per minute relative to earthworms living in non-contaminated soil, suggesting that contamination offered no nutritional benefit. Exposure to contamination did not significantly impact earthworm survival time during a stress test, suggesting weak direct toxicity. Exposure to this contaminant drove a decrease in body mass and increase in movement, which outside of the lab might increase the speed of tunnel formation and microbial dispersal, at a cost to the earthworms. The results of these experiments highlight the need to understand the relationship between Roundup formulations, earthworm behavior and health, and the interplay between earthworm behavior and soil health.

KEYWORDS

glyphosate, roundup, optimal foraging theory, movement speed, compost worm, body mass, resilience

Introduction

Humans depend heavily on the hundreds of glyphosate-based herbicides marketed under the Roundup name. Because of their effectiveness, price, and safety, Roundup herbicides are currently the most frequently used pesticide in the agricultural sector, and the second most frequently used pesticide in urban settings (Battaglin et al., 2014; Myers

et al., 2016; Benbrook 2018). They are also commonly used in forestry and in horticulture (Sihtmae et al., 2013; Botten et al., 2021). They have been considered safe because under laboratory conditions, glyphosate can degrade quickly (Moore et al., 1983; Balthazor and Hallas, 1986; Jacob et al., 1988; McAuliffe et al., 1990; Barrett and McBride, 2005; Paudel et al., 2015; Li et al., 2016; la Cecilia et al., 2018), thus posing a low risk for persistence. Glyphosate strongly adsorbs onto soil particles (Al-Rajab and Hakami, 2014; Sidoli et al., 2016), lowering the likelihood of leaching, and glyphosate is less toxic than other herbicides (Gill et al., 2018).

Despite its presumed lack of persistence, Roundup formulations, glyphosate itself, and AMPA (aminomethylphosphonic acid), its major metabolite, occur ubiquitously in our environment. Researchers find glyphosate in our precipitates, streams, and groundwater (Battaglin et al., 2014; Lefrancq et al., 2017; Alonso et al., 2018; la Cecilia et al., 2018; Andrade et al., 2021), our soil (Lane et al., 2012; Aparicio et al., 2013; Battaglin et al., 2014; Alonso et al., 2018; Niemeyer et al., 2018; Silva et al., 2018; Schogl et al., 2022) and our food (Mesnage and Antoniou, 2017; Conrad et al., 2017; Mertens et al., 2018; Gillezeau et al., 2019). Glyphosate remains in forest plant tissues for a decade or more (Botten et al., 2021), glyphosate can persist in soil for months or years, and AMPA degrades even slower (Laitinen et al., 2009; Mertens et al., 2018; Nguyen et al., 2018). Plants translocate glyphosate and its associated surfactants into soil via their root systems where it adsorbs to minerals and becomes available to soil invertebrates (Kremer et al., 2005; Lane et al., 2012; Maqueda et al., 2017; Niemeyer et al., 2018; Silva et al., 2018).

Understanding the impact of Roundup formulations, glyphosate, and AMPA contamination on earthworms and on soil health is critically important since soil ecosystem services are estimated at 11.4 trillion dollars globally, or an average of $867 per hectare across all land uses and soil types (Schon and Dominati, 2020). The contribution of earthworms to soil quality is widely documented in the literature (Edwards and Bohlen, 1996; Brown et al., 2004). They play a critical role in soil formation and nutrient cycling (Van Groenigen et al., 2014), decomposition (Schimel and Schaeffer 2012; Creamer et al., 2015), the recovery of soil carbon pools after natural and anthropogenic disturbance (Angst et al., 2019), maintaining soil microbial diversity (Liu et al., 2019; Liu et al., 2020), controlling plant pathogens (Li et al., 2016; Euteneuer et al., 2019; Plaas et al., 2019), and maintenance of soil porosity (Edwards and Bohlen, 1996; Brown et al., 2004). Earthworms increase the value of land by improving pasture production, increasing the value by $222–1,265 per hectare per year depending on whether dairy cows or sheep were using the pasture. Removing dung from soil improved pasture production, increasing the value by an average of $28-$29 per hectare per year, depending on whether dairy cows or sheep were using the land. Earthworms improve net carbon storage and increase drainage, thereby decreasing flood risks and increasing land value by up to $329 per hectare per year (Schon and Dominati, 2020). One of the biggest threats to soil biological activity as grasslands intensify is the physical degradation of soil which can make it a difficult enclosure for the soil biology to function and contribute to ecosystem services (Greenwood and McKenzie, 2001; Schon et al., 2012). This is why Bender et al. (1984) acknowledged the need to maintain or enhance soil biodiversity to enable proper ecosystem functioning.

The ubiquity of this suite of contaminants—Roundup formulations, glyphosate, and AMPA—may impair the ability of soil invertebrates to deliver their ecosystem services. Earthworms, common soil invertebrates, play an important role in temperate ecosystems, influencing nutrient cycling and ecosystem functioning (Edwards and Bohlen, 1996; Zaller et al., 2014). They shred and redistribute organic material in soil, increase soil penetrability for roots, and improve soil health (Zaller et al., 2014; Gaupp-Berghausen et al., 2015). They also help convert plant-derived lipids and ligands into sugar-based microbial necromass; this conversion increases soil stability, making it denser and gluier in texture (Angst et al., 2019). Earthworms' contributions to soil health are so critical that the European Union (EU), the Organization for Economic Co-operation and Development (OECD), the International Organization for Standards (ISO), and the Food and Agriculture Organization of the United Nations (FAO) all use compost worms (*Eisenia fetida*) as an indicator organism for ecotoxicological testing (Piola et al., 2013; Santadino et al., 2014).

Because earthworms possess both highly permeable skin and a highly permeable alimentary tract, they are permanently in close contact with soil contaminants (Jager et al., 2003; Drake and Horn, 2007; Roubalova et al., 2015), and therefore, soil pollutants can significantly impair their health (Jager et al., 2003; Drake and Horn, 2007; Roubalova et al., 2015). Despite a robust and complex immune system (Ghosh 2018), exposure to glyphosate-based herbicides causes tissue damage, lysosomal damage, and cell death in earthworms (Morowati, 2000; Casabé et al., 2007; Correia and Moreira, 2010; Piola et al., 2013; Muangphra et al., 2014; Stanley and Joy, 2014). However, exposure to Roundup formulations, glyphosate and AMPA have a less predictable impact on enzymatic activity, fertility, body mass, and mortality (reviewed in Pochron et al., 2019; Zaller et al., 2021), suggesting that the relationship between exposure to contamination and earthworm health is not always linear or predictable.

Some researchers have suggested that rather than serving as contaminants, Roundup formulations, glyphosate, and/or AMPA may act as a food source for earthworms, either indirectly via the added micronutrients or directly through the addition of fungi or dead plant material to the soil. In an experiment where Roundup exposure led to heavier earthworms, researchers suggested that Roundup application killed soil fungus, providing increased food abundance for the

earthworms (Zaller et al., 2014). Gaupp-Berghausen et al. (2015) reported that exposure to a Roundup contaminant initially stimulated earthworm activity, likely as the consequence of an increased availability of dead leaf material caused by the herbicide. That same study reported a substantial increase in soil nitrate and phosphate concentration with Roundup application, which might also stimulate the growth of microbial populations and thereby provide food for earthworms.

One way to determine whether earthworms experience environmental Roundup as a food source is to investigate their foraging behavior. According to optimal foraging theory (Stephens and Krebs 2019), foraging behavior reflects food availability in predictable ways: in habitats where food availability is low, foragers are predicted to move more quickly than in habitats where food availability is high (Lovette and Holmes 1995; Lyons 2005; Beauchamp 2012; Norberg 2021). For example, male American redstarts (*Setophaga ruticilla*) and semipalmated sandpipers (*Calidris pusilla*) forage faster in food-scarce environments relative to food-rich environments (Lovette and Holmes 1995; Beauchamp 2012).

In this study, we link an assessment of how exposure to Roundup contamination impacts earthworm body mass and stress test survival time with an assessment of earthworm movement speed. We do this by using cameras to observe the speed at which earthworms displace soil during a 7-day period of exposure, and then quantifying how exposure to a Roundup formulation impacts body mass and stress-test survival time. If earthworms move more slowly in a contaminated environment, optimal foraging theory suggests that they are experiencing a food-rich patch of soil; this inference is strengthened if they concurrently gain body mass. Conversely, if earthworms move more quickly in a contaminated environment relative to the un-contaminated control, they may be experiencing a food-scarce patch of soil, especially if they lose body mass. If the primary effect of exposure to contamination is its toxicity, which requires the engagement of the earthworm immune system (Ghosh 2018), then we propose that stress-test survival time will be shorter for earthworms in the contaminated environment relative to those in the uncontaminated and that those in the contaminated environment will lose body mass relative to those in the uncontaminated environments.

Materials and methods

Overview

We built six ant-farm-style enclosures (described below), and we ran the project over nine consecutive weeks. Each week, three enclosures contained clean soil and three contained contaminated soil, as described below, and on a weekly schedule, we measured 1) amount of soil displaced by earthworms per minute in an enclosure during a 7-day period, 2) change in earthworm mass over a 7-day period, and 3) stress-test survival time for earthworms that had been living in the enclosures for a 7-day period. Each enclosure housed one earthworm, preventing density-dependent effects. Each earthworm was weighed before being placed in an enclosure and then again, at the end of the 7-day period.

Earthworm enclosures

We constructed ant-farm-style enclosures using wood and glass. The completed enclosures measured 26.5 cm × 6.9 cm x 24.3 cm, with two viewing areas, front and back, of 18.0 cm × 16.9 cm each. With an internal width of 2.6 cm, earthworms were always visible from at least one side. See Figure 1.

Soil contamination

We filled each enclosure with OMRI listed Black Gold Garden Compost Blend (Sun Gro Horticulture, Agawam, Massachusetts, United States). OMRI-listed materials are certified by the Organic Materials Review Institute. OMRI is accredited to ISO 17,065 standards by the USDA Quality Assessment Division and ensures that materials used in organic food production, such as the compost used in this project, meet organic standards. This means that the compost used in this experiment was free of fertilizer, pesticides, and animal-care products.

The contaminated enclosures received 26.3 mg of glyphosate per kilogram of soil via Roundup Ready-to-Use III (Bayer Corporation, Whippany, New Jersey, United States), which was purchased at the local garden center. This concentration is consistent with the manufacturer's instructions (Bayer, 2016) and with that used by other researchers (e.g., Correia and Moreira, 2010; Buch et al., 2013; García-Torres et al., 2014; Pochron et al., 2019, 2020). Enclosures containing contaminated soil thus received 500 g of composted soil, 3 ml of Roundup Ready-to-Use III, and 1 L of Reverse Osmosis water (RO); enclosures containing non-contaminated soil received 505 g compost, 1 L RO water, and 3 ml additional water to ensure equal moisture levels across treatments. To homogenize the soil, water, and contaminant (for the contaminated enclosures), soil was mixed by gloved hand for 10 minutes before it was added to the enclosures. No plants were grown in these enclosures, and no food beyond that provided by the composted soil and contaminant was provided to the earthworms during the 7-day period of this project.

Earthworm body mass

At the beginning of each of the 9 weeks used to run this experiment, we extracted 15 adult earthworms (*Eisenia fetida*) from the organically raised and maintained stock population

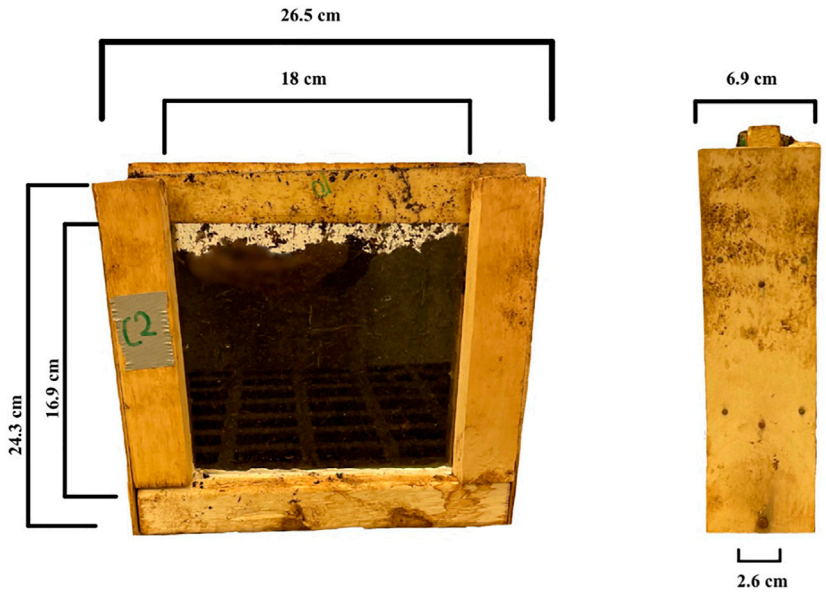

FIGURE 1
The front face of an ant-farm style enclosure used for this experiment. A camera focused on the front face and the back face of each enclosure, and the narrow internal width (2.6 cm) allowed constant visibility within each enclosure.

described in Pochron et al. (2019). We weighed the earthworms using an American Weigh Scales ACP-200 (accurate to 0.01 g) and selected earthworms so that those living in the contaminated enclosures did not differ in mass from those living in the non-contaminated enclosures, using an ANOVA to test for differences (See Supplementary Table S1). Each enclosure received one earthworm, and enclosures were stored in a Conviron CMP6050 (Controlled Environments Limited, Winnipeg, Canada) growth chamber set to a temperature of 24.2 ± 1.6 °C. The growth chamber was set on a 24-h light cycle to support the camera lighting. At the end of each week, we removed the earthworms from the enclosures and weighed them. To calculate change in body mass, we subtracted the initial from the final body mass. We collected initial body mass, final body mass, and calculated the change in body mass for 27 earthworms in each group. We then measured stress-test survival time as described below.

Stress test survival time

Following Pochron et al. (2017, 2018), the growth chamber programmed to a temperature of 35 °C and light intensity (photon flux) of 250 μmol m^2 s^{-1} was used to provide light and heat stress. Petri dishes containing weighed earthworms were placed into the chamber, exposing them to intense heat and intense light. All Petri dishes were inspected at 5-min intervals to determine the time of death for each earthworm. As per Correia and Moreira (2010) and Pochron et al. (2017), earthworms were classified as dead when they failed to respond to gentle mechanical stimulus. While we planned on collecting stress-test data from 27 earthworms in each treatment, a laboratory error forced us to use only 24 earthworms in each group.

Camera setup

Earthworm movement across enclosure faces was caught by a camera (Arducam Lens Board OV5647 Sensor for Raspberry Pi Camera, Adjustable and Interchangeable Lens M12 Module, Focus and Angle Enhancement for Raspberry Pi 4/3/3 B+, RRID:SCR_022325) connected to a single-board Raspberry Pi 3b + computer via a camera cable strip (Arducam Pi Camera Cable, Octoprint Octopi Webcam, Monitor 3D Printer, 3.28 F T/100CM Long Extension Flex Ribbon Cable). We positioned the cameras 70 cm from the enclosures, arranging them to ensure constant in-focus views of both the enclosures' fronts and their backs. We programmed a *Python* script to take photos every 10 min and to store the photos in a one Tb external hard drive attached to each computer. We collected data from January 13th–18 March 2022, producing approximately 1,000 photos per enclosure over each 7-day period. Fluctuations in campus power disrupted the lighting in weeks 4, 5 and 7, reducing the number of images in those weeks.

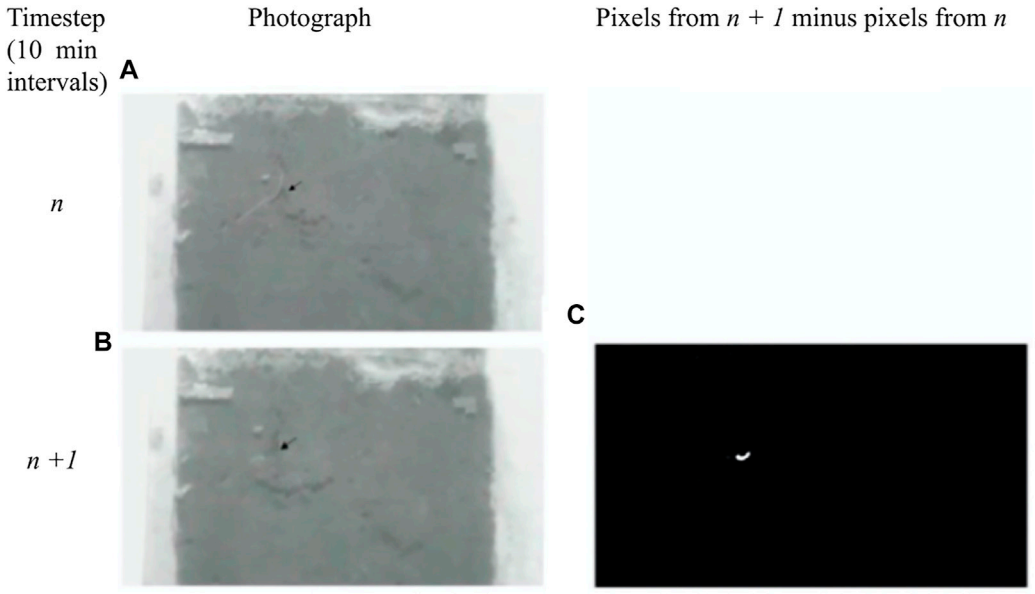

FIGURE 2
Examples of photographs and pixel images generated by this experiment. The cameras photographed enclosure faces once every 10 minutes, as shown in **(A)** and **(B)**. The earthworm seen in image A had changed its location 10 min later, as shown in image **(B)**. Our software translated the photographs into pixel images and subtracted the number of white pixels in newest image from the number of white pixels in the photo proceeding it, as shown in image **(C)**. The 24 white pixels in C cover an area of 15.7 mm^2, showing that earthworms moved 1.57 mm^2 of soil per minute.

Speed of earthworm-driven soil displacement

Cameras recorded the value of individual pixels within the image matrix, and when earthworms moved soil, images from adjacent time steps differed from each other, thereby creating variation in pixel values. When earthworms did not move any soil between one photo and the next, pixel values remained unchanged between 10-min time steps. The software subtracted the pixel values found in the time step *n* from the pixel values in the time step *n*–1.

To describe the process in greater detail: white pixels in a photo represent a change caused by earthworm-driven soil movement, while black pixels show unmoved soil. The software compared the number of white pixels in one image to the number of white pixels in the consecutive image, yielding the change in pixel number over a 10-min period. Since all cameras had identical resolution and were equidistant from each enclosure, we converted number of pixels into area, where 1.0 pixel = 0.6522 mm^2, allowing us to determine how much area earthworms altered per 10-min period. See Figure 2. For each time step, we calculated the area of soil displaced since the previous time step for both the front and the back of the enclosures, and we added those values together.

Initial earthworm size and amount of displaced soil

Variation in initial earthworm body mass, while consistent and small between the two treatments, existed. To ensure that our results were not an artifact of a relationship between body mass and motivation to forage (e.g., smaller earthworms being hungrier and therefore foraging faster), after checking for normality, we ran a regression using initial body mass 7) as the independent variable and total amount of soil displaced on the first day as the dependent variable.

Data analysis

We stored and cleaned data in Microsoft Excel (Version 16.60 RRID:SCR_016137) and conducted statistical tests in StatPlus (StatPlus:mac, AnalystSoft Inc. RRID:SCR_014635) and R. We used a Kolmogorov-Smirnov/Lilliefor Test at the 95% confidence level to check for normality. We used ANOVAs and t-tests to detect differences in means between groups. Means and standard deviations are reported throughout the text. Standard errors of the means are presented in the figures. To further assess the magnitude of

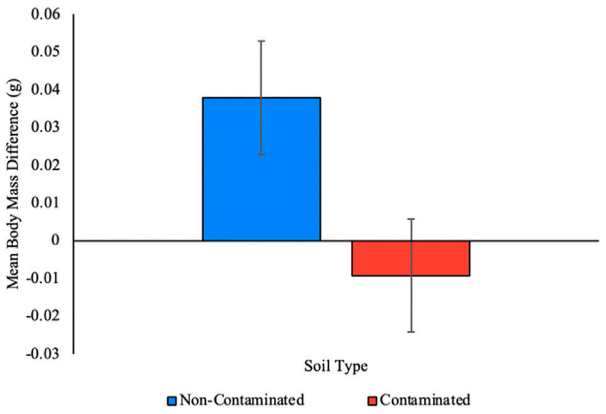

FIGURE 3
The impact of soil contamination on earthworm body mass. Living in contaminated soil for a week causes a slight loss in body mass while living in clean soil causes a slight gain, on average. Error bars represent the standard error of the means. $p < 0.05$.

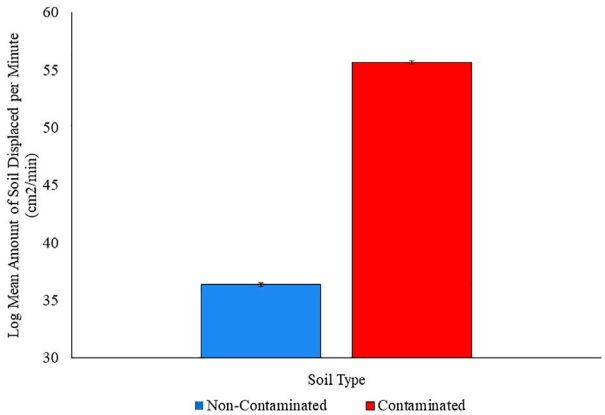

FIGURE 4
Log mean area of soil displaced by earthworms per minute in non-contaminated enclosures and enclosures contaminated with Roundup Ready-to-Use III. Error bars represent the standard error of the means; the standard error of the means is 0.04 for the non-contaminated treatment and 0.12 for the contaminated treatment. $p < 0.000001$.

differences between two groups on a given variable we calculated effect size, via the Cohen's d statistic, which assumes that the standard deviations are roughly equal (Cohen, 1988). We used an effect size calculator to find the Cohen's d (Becker, 2000). To quantify area of soil moved between consecutive photos, we wrote a *Python* image-subtraction script.

Soil testing

We extracted soil samples from both treatment types and sent them to the Cornell Nutritional Analysis Laboratory (CNAL) for analysis. Specifically, while wearing nitrile gloves, we took 250 ml soil prepared for the uncontaminated enclosures, and we placed it into a Ziplock bag, placed that bag into a second Ziplock bag, and labeled it. We repeated this procedure for the contaminated soil. CNAL measured soil pH, soil carbon via Loss On Ignition (LOI), soil organic matter, and soil micronutrient levels. CNAL calculates pH with an electrode in a 1:1 soil:water suspension, and the value is presented in standard pH units. CNAL calculates percent organic matter via LOI, which measures the change in mass after soil samples are exposed to high temperature (500 °C or 932°F) in a furnace. At these temperatures, carbonaceous materials are oxidized to CO_2, while other materials remain. CNAL uses the Modified Morgan extraction procedure for soil testing. The Modified Morgan is a universal extraction procedure used to determine all major nutrients and micronutrients simultaneously. On overview of their methodologies are available in The Cornell Framework (2017).

Results

Change in earthworm body mass

No earthworms in either treatment group died during the 7-days experimental period. To determine the impact of exposure to Roundup Ready-to-Use III on body mass, we assessed change in body mass between the beginning and end of the experiment. Earthworms living in non-contaminated soil for a week slightly increased body mass on average (0.04 g ± 0.08) while earthworms living in soil contaminated with Roundup Ready-to-Use III slightly decreased their body mass on average (-0.01g ± 0.07). (Numbers in parentheses provide means and standard deviations.) In the control group, five of the 27 (18.5%) earthworms lost body mass over the week, while 11 of the 27 earthworms (40.7%) lost body mass over the week in the group exposed to Roundup. Data from both treatments was distributed normally, and an ANOVA reported a significant difference ($F = 5.57$, $DF = 1, 52$, $p = 0.02$). The Cohen's d of 0.64 falls between a "medium" and "high" difference according to Cohen (1988). (See Figure 3.).

Stress-test survival time

Exposure to contamination did not significantly impact stress-test survival time ($F = 0.46$, $DF = 1, 46$, $p = 0.50$). Earthworms that lived in enclosures contaminated with Roundup Ready-to-Use III survived the stress test for a mean of 98.3 ± 21.3 min while earthworms that lived in

TABLE 1 Soil quality analysis for contaminated and non-contaminated soil.

	Contaminated	Non-contaminated
% Moisture	0.34	0.39
pH	4.68	4.57
% LOI	4.14	3.53
% Organic Matter	2.67	2.24
Aluminum	3.15	3.45
Calcium	103.91	98.94
Copper	0.04	0.17
Iron	1.06	1.33
Potassium	75.42	69.73
Magnesium	21.13	19.76
Manganese	2.83	2.66
Molybdenum	0.00	0.00
Sodium	11.25	10.50
Phosphorus	5.70	6.05
Sulfur	21.55	19.92
Zinc	0.55	0.60

non-contaminated enclosures for a week survived for a mean of 102.7 ± 23.7 min.

Speed of earthworm-driven soil displacement

Because the data for this variable was skewed toward the low values and could not go negative, we used a log10 transformation to calculate the means and perform a two-tailed *t*-test. We found that earthworms living in non-contaminated soil displaced less soil per minute (36.4 cm^2/min) than did earthworms living in soil contaminated with Roundup Ready-to-Use III (55.7 cm^2/min). A *t*-test reports a highly significant difference (t = 17.4, DF = 34,991, $p < 2.2e\text{-}16$). Earthworms living in soil contaminated with Roundup Ready-to-Use III increased the amount of soil displaced per minute by 34.7% relative to earthworms living in non-contaminated soil. The Cohen's *d* of 1.6 falls into the "very large" category of difference according to Cohen (1988). (See Figure 4.).

Initial earthworm size and amount of displaced soil

Linear regressions show that initial earthworm body mass did not predict amount of soil displaced in the first 24 h of experiment for earthworms in the contaminated or in the non-contaminated enclosures (Non-contaminated: DF = 1, 16; S = 2,368,928.1; F = 0.08, $p = 0.78$; Contaminated: DF = 1, 16; S = 836,385.8; F = 0.50; $p = 0.49$). Initial body mass also did not predict the amount of soil displace over the totality of the experiment (Non-contaminated: DF = 1, 16; S = 17,084,450.3; F = 0.07, $p = 0.79$; Contaminated: DF = 1, 16; S = 6,585,708.3; F = 0.75; $p = 0.40$).

Soil quality

Adding Roundup Ready-to-Use III at a concentration recommended by the manufacturer and at a concentration used by other researchers does not change the amount of organic matter in soil, soil pH, or soil micronutrients. See Table 1.

Discussion

Understanding the degree to which earthworms experience Roundup-contaminated soil as dangerous or beneficial is an important question because earthworms, which provide a suite of key ecosystem services, live with this contaminant across the globe. This project tested whether contaminated soil could, as proposed by some researchers, benefit earthworms via expansion of the food supply. We did not find support for this hypothesis.

Earthworms living in contaminated soil increased the area of soil displaced per minute by 34.67% relative to earthworms living in un-contaminated soil. This indicates that earthworms moved within contaminated enclosures significantly faster than they did within non-contaminated enclosures. This effect is not driven by initial body mass, and if we interpret this result through the lens of optimal foraging theory (Lovette and Holmes 1995; Lyons 2005; Beauchamp 2012; Stephens and Krebs 2019; Norberg 2021) and assume that natural selection favored earthworms whose behavioral strategies maximized their net energy intake per unit time spent foraging, then increased movement speed indicated that food was scarcer in contaminated than in non-contaminated enclosures (Lovette and Holmes 1995; Lyons 2005; Beauchamp 2012; Norberg 2021). Contaminated and non-contaminated soil did not differ in their percentages of organic material or in micronutrient availability (Table 1), suggesting that food availability was equal in both enclosures, but several researchers have shown that adding glyphosate-based herbicides alters the soil microbial community (Kremer et al., 2005; Schlatter et al., 2018; Meena et al., 2020). Changes in soil microbial communities may change food availability for earthworms, but further studies are needed to verify this hypothesis.

In further support for the hypothesis that adding a glyphosate-based herbicide provided no nutritional benefit to earthworms is the fact that the earthworms in the contaminated enclosures lost body mass while those in the non-contaminated enclosures gained mass, on average. Over a 7-day period, earthworms living in contaminated soil decreased in mass by 2.3% while earthworms living in non-contaminated soil

increased in mass by 10.1%. This is consistent with foraging theory-based expectations: earthworms may have moved more in search of unfindable food, metabolizing body mass in their efforts. Earthworms in the non-contaminated enclosures potentially found more food and spent less energy finding it, resulting in an increase in body mass and the displacement of less soil.

Caveats exist, however. While increased motion and decreased body mass are consistent with optimal-foraging-based hypotheses about organisms in food-scarce environments, foraging speed is not determined exclusively by habitat quality. This is why, for example, the foraging speed of prothonotary warblers (*Protonotaria citrea*) was not associated with food-based habitat quality (Lyons 2005). An ecotoxicology-based explanation may better align with the results.

Coping with environmental contaminants is energetically expensive for invertebrates, and under stress, invertebrates mobilize proteins and lipids as an energy source (Salvio et al., 2016). Internal proteins and lipid concentrations decrease as soil pesticide concentrations increase, indicating high energetic demands under pesticide exposure (Givaudan et al., 2014; Salvio et al., 2016), potentially leading to loss in body mass (Piola et al., 2013). A similar metabolic scenario could be possible for earthworms exposed to soil contaminated with Roundup Ready-to-Use III. A decrease in body mass is a common outcome in ecotoxicological studies (Yasmin 2007; Correia and Moreira 2010; Santos et al., 2011; Garcia-Torres et al., 2014; but see Buch et al., 2013; Piola et al., 2013; Zhou et al., 2013; Santadino et al., 2014; Salvio et al., 2016).

However, earthworms that find themselves needing to pay metabolic costs to cope with contamination can respond via indicators other than body mass. For instance, one earthworm species (*Allolobophora chlorotica*) increased the activities of enzymes associated with oxidative stress as pesticide concentration increased, while a second (*Aporrectodea caliginosa*) responded by losing mass (Givaudan et al., 2014). Similarly, when exposed to crumb-rubber contaminated soil, compost earthworms (*Eisenia fetida*) sometimes maintain growth rates at the cost to resilience as measured by stress-test survival time (Pochron et al., 2017) and sometimes forgo body mass maintenance and invest instead in resilience (Pochron et al., 2018).

In our experiments, living in contaminated soil did not impact earthworm stress-test survival time but did impact earthworm body mass. If Roundup Ready-to-Use III acts as a contaminant that requires metabolic resources to engage immune systems, to remove contaminants, or to repair damaged tissue (Ghosh 2018), then our earthworms might have catabolized body mass for that energy which might then have allowed them to respond to light and heat stress with the same success as the earthworms that did not need to catabolize their body mass.

If the reduced body mass is a response to coping with contamination, then the increase in area of soil displaced per minute might have been driven by attempts to avoid contamination rather than by a need to find food in a resource-scarce environment. Because we homogenized the soil before releasing earthworms into enclosures, earthworms might have not been able to find an uncontaminated position. Researchers frequently report that earthworms actively avoid soil that is contaminated with glyphosate-based herbicides (Verrell, 2004; Casabé et al., 2007; Buch et al., 2013; García-Torres et al., 2014; Salvio et al., 2016; Zaller et al., 2021; but see Santos et al., 2012; Fusilero et al., 2013).

Measures of the impact of glyphosate or glyphosate-based formulations on earthworm behavior are rare. In a series of clever experiments, Zaller and others measured frequency of surface visits as measured by the number of disturbed toothpicks and/or surface castings; they found that application of the herbicide reduced surface visits (Zaller et al., 2014, 2021; Guapp-Bernhausen et al., 2015). However, whether exposure to contamination slowed movement as the contaminant penetrated the soil, or whether the earthworms avoided the surface because it had the highest concentration of contaminant, remains unknown.

Exposure to a common glyphosate-based contaminant both increased the speed with which the earthworms moved through their environment and decreased earthworm body mass. If these results can be extrapolated to behavior outside of a laboratory setting, Roundup contamination might drive an increase in the speed of nutrient cycling, tunnel formation, distribution of organic matter, soil penetrability and the formation of microbial necromasses, at significant cost to the earthworms themselves. If the energy expended in an attempt to escape or metabolize contamination reduces the energy earthworms need to survive and reproduce, the benefit received by the soil will not be sustainable.

Since plants move glyphosate directly into the soil through their roots (Laitinen et al., 2009), and since Roundup use is ubiquitous in agriculture, horticulture, forestry, groundskeeping, and other outdoor industries, many earthworm populations cannot avoid Roundup exposure. Whether earthworms change their behavior and body mass when exposed to this common herbicide due to feeding constraints or in response to pollution, when earthworms could not escape exposure to the herbicide, they increased their movement speed and lost body mass. The glyphosate-based formulation used here, Roundup Ready-to-Use III, did not appear to provide a food source or otherwise increase food availability for earthworms.

If the losses in earthworm body mass discovered here in a laboratory setting scales to a global level, the fact that the majority of our current crops are Roundup Ready and regularly exposed to glyphosate-based herbicides may result in earthworms being decreasingly able to deliver their many ecosystem services and soil biodiversity declining, increasing the challenge of feeding

nearly eight billion people. It is critical that we understand the effects of glyphosate on earthworm populations in order to mitigate the damage as effectively as possible.

Data availability statement

The datasets presented in this study can be found in online repositories. The names of the repository/repositories and accession number(s) can be found below: Reserved DOI: 10.17632/49ptgmbsg9.3.

Author contributions

SP supervised the project. SP, MM, and SB designed the study. SB coordinated the protocol execution and success of the project. MM designed the photo-capturing system. CB, MM, and SB designed and wrote the script for data analysis. SB, SS, AC, MK, and AN performed the data collection, analysis, and organization of data. SP and SB performed the data interpretation. SP, MM, and SB wrote the first draft of the manuscript. SP, SB, and SS performed the statistical analysis, coordinated the write-up of this manuscript, and revised the manuscript. SP performed the final approval of the manuscript to be published. All authors reviewed, read, and approved the submitted version of this manuscript.

Funding

This research was funded in part by Stony Brook University's URECA (Undergraduate Research and Creative Activities) summer Program, which provided a stipend to MM during summer 2019.

Acknowledgments

We thank greenhouse curators Michael Axelrod, John Klumpp, and Sean Halliwell for technical support on this project. We thank Katherine Aubrecht, Director of the Sustainability Studies Program, and Paul Shepson, Dean of the School of Marine and Atmospheric Sciences, for their continued support of undergraduate research opportunities. We thank Kathy Twiss for insightful comments on early drafts of this manuscript. We thank Clara Tucker for statistical support.

Conflict of interest

The authors declare that the research was conducted in the absence of any commercial or financial relationships that could be construed as a potential conflict of interest.

Publisher's note

Supplementary material

The Supplementary Material for this article can be found online at: https://www.frontiersin.org/articles/10.3389/fenvs.2022.991494/full#supplementary-material

References

Al-Rajab, A. J., and Hakami, O. M. (2014). Behavior of the non-selective herbicide glyphosate in agricultural soil. *Am. J. Environ. Sci.* 10 (2), 94–101. doi:10.3844/ajessp.2014.94.101

Alonso, L. L., Demetrio, P. M., Etchegoyen, M. A., and Marino, D. J. (2018). Glyphosate and atrazine in rainfall and soils in agroproductive areas of the pampas region in Argentina. *Sci. Total Environ.* 645, 89–96. doi:10.1016/j.scitotenv.2018.07.134

Andrade, V. S., Gutierrez, M. F., Regaldo, L., Paira, A. R., Repetti, M. R., and Gagneten, A. M. (2021). Influence of rainfall and seasonal crop practices on nutrient and pesticide runoff from soybean dominated agricultural areas in Pampean streams, Argentina. *Sci. Total Environ.* 788, 147676. doi:10.1016/j.scitotenv.2021.147676

Angst, G., Mueller, C. W., Prater, I., Angst, Š., Frouz, J., Jílková, V., et al. (2019). Earthworms act as biochemical reactors to convert labile plant compounds into stabilized soil microbial necromass. *Commun. Biol.* 2 (1), 441–447. doi:10.1038/s42003-019-0684-z

Aparicio, V. C., de Gerónimo, E., Marino, D., Primost, J., Carriquiriborde, P., and Costa, J. L. (2013). Environmental fate of glyphosate and aminomethylphosphonic acid in surface waters and soil of agricultural basins. *Chemosphere* 93 (9), 1866–1873. doi:10.1016/j.chemosphere.2013.06.041

Balthazor, T. M., and Hallas, L. E. (1986). Glyphosate-degrading microorganisms from industrial activated sludge. *Appl. Environ. Microbiol.* 51 (2), 432–434. doi:10.1128/aem.51.2.432-434.1986

Barrett, K., and McBride, M. (2005). Oxidative degradation of glyphosate and aminomethylphosphonate by manganese oxide. *Environ. Sci. Technol.* 39 (23), 9223–9228. doi:10.1021/es051342d

Battaglin, W. A., Meyer, M. T., Kuivila, K. M., and Dietze, J. E. (2014). Glyphosate and its degradation product AMPA occur frequently and widely in U.S. Soils, surface water, groundwater, and precipitation. *J. Am. Water Resour. Assoc.* 50 (2), 275–290. doi:10.1111/jawr.12159

Bayer, S. (2016). Application reminders for Roundup brand glyphosate agricultural herbicide. AvaliableAt: https://www.roundupreadyplus.com/resourcecenter/application-reminders-for-roundup-brand-agricultural-herbicides (Accessed February 15, 2020).

Beauchamp, G. (2012). Foraging speed in staging flocks of semipalmated sandpipers: Evidence for scramble competition. *Oecologia* 169 (4), 975–980. doi:10.1007/s00442-012-2269-0

Becker, L. A. (2000). *Effect Size Calculators*. Available at: https://lbecker.uccs.edu/ (Accessed August 2, 2022).

Benbrook, C. M. (2018). Why regulators lost track and control of pesticide risks: Lessons from the case of glyphosate-based herbicides and genetically engineered-crop technology. *Curr. Environ. Health Rep.* 5 (3), 387–395. doi:10.1007/s40572-018-0207-y

Bender, E. A., Case, T. J., and Gilpin, M. E. (1984). Perturbation experiments in community ecology: Theory and practice. *Ecology* 65 (1), 1–13. doi:10.2307/1939452

Botten, N., Wood, L., and Werner, J. (2021). Glyphosate remains in forest plant tissues for a decade or more. *For. Ecol. Manage.* 493, 119259. doi:10.1016/j.foreco.2021.119259

Brown, G. G., Edwards, C. A., and Brussaard, L. (2004). How earthworms affect plant growth: Burrowing into the mechanisms. *Earthworm Ecol.* 2, 13–49. doi:10.1201/9781420039719-9

Buch, A. C., Brown, G. G., Niva, C. C., Sautter, K. D., and Sousa, J. P. (2013). Toxicity of three pesticides commonly used in Brazil to Pontoscolex corethrurus (Müller, 1857) and *Eisenia andrei* (Bouché, 1972). *Appl. Soil Ecol.* 69, 32–38. doi:10.1016/j.apsoil.2012.12.011

Casabé, N., Piola, L., Fuchs, J., Oneto, M. L., Pamparato, L., Basack, S., et al. (2007). Ecotoxicological assessment of the effects of glyphosate and chlorpyrifos in an Argentine soya field. *J. Soils Sediments* 7 (4), 232–239. doi:10.1065/jss2007.04.224

Cohen, J. (1988). *Statistical power analysis for the behaviors science*. 2nd Edn. Hillsdale, NJ: Laurence Erlbaum Associates, Publishers, Hillsdale.

Conrad, A., Schröter-Kermani, C., Hoppe, H. W., Rüther, M., Pieper, S., and Kolossa-Gehring, M. (2017). Glyphosate in German adults–Time trend (2001–2015) of human exposure to a widely used herbicide. *Int. J. Hyg. Environ. Health*. 220 (1), 8–16.

Correia, F. V., and Moreira, J. C. (2010). Effects of glyphosate and 2, 4-D on earthworms (*Eisenia foetida*) in laboratory tests. *Bull. Environ. Contam. Toxicol.* 85 (3), 264–268. doi:10.1007/s00128-010-0089-7

Creamer, C. A., de Menezes, A. B., Krull, E. S., Sanderman, J., Newton-Walters, R., and Farrell, M. (2015). Microbial community structure mediates response of soil C decomposition to litter addition and warming. *Soil Biol. Biochem.* 80, 175–188. doi:10.1016/j.soilbio.2014.10.008

Drake, H. L., and Horn, M. A. (2007). As the worm turns: The earthworm gut as a transient habitat for soil microbial biomes. *Annu. Rev. Microbiol.* 61 (1), 169–189. doi:10.1146/annurev.micro.61.080706.093139

Edwards, C., and Bohlen, P. (1996). *Biology and ecology of earthworms*. London, U.K: Chapman and Hall Press.

Euteneuer, P., Wagentristl, H., Steinkellner, S., Scheibreithner, C., and Zaller, J. G. (2019). Earthworms affect decomposition of soil-borne plant pathogen *Sclerotinia sclerotiorum* in a cover crop field experiment. *Appl. Soil Ecol.* 138, 88–93. doi:10.1016/j.apsoil.2019.02.020

Fusilero, M. A., Mangubat, J., Ragas, R. E., Baguinon, N., Taya, H., and Rasco, E. (2013). Weed management systems and other factors affecting the earthworm population in a banana plantation. *Eur. J. Soil Biol.* 56, 89–94. doi:10.1016/j.ejsobi.2013.03.002

García-Torres, T., Giuffré, L., Romaniuk, R., Ríos, R. P., and Pagano, E. A. (2014). Exposure assessment to glyphosate of two species of annelids. *Bull. Environ. Contam. Toxicol.* 93 (2), 209–214. doi:10.1007/s00128-014-1312-8

Gaupp-Berghausen, M., Hofer, M., Rewald, B., and Zaller, J. G. (2015). Glyphosate-based herbicides reduce the activity and reproduction of earthworms and lead to increased soil nutrient concentrations. *Sci. Rep.* 5 (1), 12886–12889. doi:10.1038/srep12886

Ghosh, S. (2018). Environmental pollutants, pathogens and immune system in earthworms. *Environ. Sci. Pollut. Res.* 25 (7), 6196–6208. doi:10.1007/s11356-017-1167-8

Gill, J. P. K., Sethi, N., Mohan, A., Datta, S., and Girdhar, M. (2018). Glyphosate toxicity for animals. *Environ. Chem. Lett.* 16 (2), 401–426.

Gillezeau, C., van Gerwen, M., Shaffer, R. M., Rana, I., Zhang, L. P., Sheppard, L., et al. (2019). The evidence of human exposure to glyphosate: A review. *Environ. Health* 18, 2. doi:10.1186/s12940-018-0435-5

Givaudan, N., Binet, F., Le Bot, B., and Wiegand, C. (2014). Earthworm tolerance to residual agricultural pesticide contamination: Field and experimental assessment of detoxification capabilities. *Environ. Pollut.* 192, 9–18. doi:10.1016/j.envpol.2014.05.001

Greenwood, K., and McKenzie, B. (2001). Grazing effects on soil physical properties and the consequences for pastures: A review. *Aust. J. Exp. Agric.* 41 (8), 1231–1250. doi:10.1071/ea00102

Jacob, G., Garbow, J., Hallas, L., Kimack, N., Kishore, G., and Schaefer, J. (1988). Metabolism of glyphosate in Pseudomonas sp. strain LBr. *Appl. Environ. Microbiol.* 54 (12), 2953–2958. doi:10.1128/aem.54.12.2953-2958.1988

Jager, T., Fleuren, R. H., Hogendoorn, E. A., and De Korte, G. (2003). Elucidating the routes of exposure for organic chemicals in the earthworm, *Eisenia andrei* (Oligochaeta). *Environ. Sci. Technol.* 37 (15), 3399–3404. doi:10.1021/es0340578

Kremer, R., Means, N., and Kim, S. (2005). Glyphosate affects soybean root exudation and rhizosphere micro-organisms. *Int. J. Environ. Anal. Chem.* 85 (15), 1165–1174. doi:10.1080/03067310500273146

la Cecilia, D., Tang, F. H., Coleman, N. V., Conoley, C., Vervoort, R. W., and Maggi, F. (2018). Glyphosate dispersion, degradation, and aquifer contamination in vineyards and wheat fields in the Po Valley, Italy. *Water Res.* 146, 37–54. doi:10.1016/j.watres.2018.09.008

Laitinen, P., Rämö, S., Nikunen, U., Jauhiainen, L., Siimes, K., and Turtola, E. (2009). Glyphosate and phosphorus leaching and residues in boreal sandy soil. *Plant Soil* 323 (1-2), 267–283. doi:10.1007/s11104-009-9935-y

Lane, M., Lorenz, N., Saxena, J., Ramsier, C., and Dick, R. P. (2012). The effect of glyphosate on soil microbial activity, microbial community structure, and soil potassium. *Pedobiologia* 55 (6), 335–342. doi:10.1016/j.pedobi.2012.08.001

Lefrancq, M., Jadas-Hécart, A., La Jeunesse, I., Landry, D., and Payraudeau, S. (2017). High frequency monitoring of pesticides in runoff water to improve understanding of their transport and environmental impacts. *Sci. Total Environ.* 587, 75–86. doi:10.1016/j.scitotenv.2017.02.022

Li, H., Joshi, S. R., and Jaisi, D. P. (2016). Degradation and isotope source tracking of glyphosate and aminomethylphosphonic acid. *J. Agric. Food Chem.* 64 (3), 529–538. doi:10.1021/acs.jafc.5b04838

Liu, M., Cao, J., and Wang, C. (2020). Bioremediation by earthworms on soil microbial diversity and partial nitrification processes in oxytetracycline-contaminated soil. *Ecotoxicol. Environ. Saf.* 189, 109996. doi:10.1016/j.ecoenv.2019.109996

Liu, T., Chen, X., Gong, X., Lubbers, I. M., Jiang, Y., Feng, W., et al. (2019). Earthworms coordinate soil biota to improve multiple ecosystem functions. *Curr. Biol.* 29 (20), 3420–3429. e3425. doi:10.1016/j.cub.2019.08.045

Lovette, I. J., and Holmes, R. T. (1995). Foraging behavior of American redstarts in breeding and wintering habitats: Implications for relative food availability. *Condor* 97 (3), 782–791. doi:10.2307/1369186

Lyons, J. E. (2005). Habitat-specific foraging of prothonotary warblers: Deducing habitat quality. *Condor* 107 (1), 41–49. doi:10.1093/condor/107.1.41

Maqueda, C., Undabeytia, T., Villaverde, J., and Morillo, E. (2017). Behaviour of glyphosate in a reservoir and the surrounding agricultural soils. *Sci. Total Environ.* 593-594, 787–795. doi:10.1016/j.scitotenv.2017.03.202

McAuliffe, K. S., Hallas, L. E., and Kulpa, C. F. (1990). Glyphosate degradation byAgrobacterium radiobacter isolated from activated sludge. *J. Ind. Microbiol.* 6 (3), 219–221. doi:10.1007/bf01577700

Meena, R. S., Kumar, S., Datta, R., Lal, R., Vijayakumar, V., Brtnicky, M., et al. (2020). Impact of agrochemicals on soil microbiota and management: A review. *Land* 9 (2), 34. doi:10.3390/land9020034

Mertens, M., Höss, S., Neumann, G., Afzal, J., and Reichenbecher, W. (2018). Glyphosate, a chelating agent—Relevant for ecological risk assessment? *Environ. Sci. Pollut. Res.* 25 (6), 5298–5317. doi:10.1007/s11356-017-1080-1

Mesnage, R., and Antoniou, M. N. (2017). Facts and fallacies in the debate on glyphosate toxicity. *Front. Public Health* 5, 316. doi:10.3389/fpubh.2017.00316

Moore, J. K., Braymer, H. D., and Larson, A. D. (1983). Isolation of a Pseudomonas sp. which utilizes the phosphonate herbicide glyphosate. *Appl. Environ. Microbiol.* 46 (2), 316–320. doi:10.1128/aem.46.2.316-320.1983

Morowati, M. (2000). Histochemical and histopathological study of the intestine of the earthworm (Pheretima elongata) exposed to a field dose of the herbicide glyphosate. *Environmentalist* 20 (2), 105–111. doi:10.1023/A:1006704009184

Muangphra, P., Kwankua, W., and Gooneratne, R. (2014). Genotoxic effects of glyphosate or paraquat on earthworm coelomocytes. *Environ. Toxicol.* 29 (6), 612–620. doi:10.1002/tox.21787

Myers, J. P., Antoniou, M. N., Blumberg, B., Carroll, L., Colborn, T., Everett, L. G., et al. (2016). Concerns over use of glyphosate-based herbicides and risks associated with exposures: A consensus statement. *Environ. Health* 15 (1), 19–13. doi:10.1186/s12940-016-0117-0

Nguyen, N. K., Dörfler, U., Welzl, G., Munch, J. C., Schroll, R., and Suhadolc, M. (2018). Large variation in glyphosate mineralization in 21 different agricultural soils explained by soil properties. *Sci. Total Environ.* 627, 544–552. doi:10.1016/j.scitotenv.2018.01.204

Niemeyer, J. C., de Santo, F. B., Guerra, N., Ricardo Filho, A. M., and Pech, T. M. (2018). Do recommended doses of glyphosate-based herbicides affect soil invertebrates? Field and laboratory screening tests to risk assessment. *Chemosphere* 198, 154–160. doi:10.1016/j.chemosphere.2018.01.127

Norberg, R. Å. (2021). To minimize foraging time, use high-efficiency, energy-expensive search and capture methods when food is abundant but low-efficiency, low-cost methods during food shortages. *Ecol. Evol.* 11 (23), 16537–16546. doi:10.1002/ece3.8204

Paudel, P., Negusse, A., and Jaisi, D. P. (2015). Birnessite-catalyzed degradation of glyphosate: A mechanistic study aided by kinetics batch studies and nmr spectroscopy. *Soil Sci. Soc. Am. J.* 79 (3), 815–825. doi:10.2136/sssaj2014.10.0394

Piola, L., Fuchs, J., Oneto, M. L., Basack, S., Kesten, E., and Casabé, N. (2013). Comparative toxicity of two glyphosate-based formulations to *Eisenia andrei* under laboratory conditions. *Chemosphere* 91 (4), 545–551. doi:10.1016/j.chemosphere.2012.12.036

Plaas, E., Meyer-Wolfarth, F., Banse, M., Bengtsson, J., Bergmann, H., Faber, J., et al. (2019). Towards valuation of biodiversity in agricultural soils: A case for earthworms. *Ecol. Econ.* 159, 291–300. doi:10.1016/j.ecolecon.2019.02.003

Pochron, S., Choudhury, M., Gomez, R., Hussaini, S., Illuzzi, K., Mann, M., et al. (2019). Temperature and body mass drive earthworm (*Eisenia fetida*) sensitivity to a popular glyphosate-based herbicide. *Appl. Soil Ecol.* 139, 32–39. doi:10.1016/j.apsoil.2019.03.015

Pochron, S., Nikakis, J., Illuzzi, K., Baatz, A., Demirciyan, L., Dhillon, A., et al. (2018). Exposure to aged crumb rubber reduces survival time during a stress test in earthworms (*Eisenia fetida*). *Environ. Sci. Pollut. Res.* 25 (12), 11376–11383. doi:10.1007/s11356-018-1433-4

Pochron, S., Simon, L., Mirza, A., Littleton, A., Sahebzada, F., and Yudell, M. (2020). Glyphosate but not Roundup harms earthworms (*Eisenia fetida*). *Chemosphere* 241, 125017. doi:10.1016/j.chemosphere.2019.125017

Pochron, S. T., Fiorenza, A., Sperl, C., Ledda, B., Lawrence Patterson, C., Tucker, C. C., et al. (2017). The response of earthworms (*Eisenia fetida*) and soil microbes to the crumb rubber material used in artificial turf fields. *Chemosphere* 173, 557–562. doi:10.1016/j.chemosphere.2017.01.091

Roubalova, R., Prochazkova, P., Dvorak, J., Skanta, F., and Bilej, M. (2015). The role of earthworm defense mechanisms in ecotoxicity studies. *Invertebr. Surviv. J.* 12, 203–213.

Salvio, C., Menone, M. L., Rafael, S., Iturburu, F. G., and Manetti, P. L. (2016). Survival, reproduction, avoidance behavior and oxidative stress biomarkers in the earthworm *Octolasion cyaneum* exposed to glyphosate. *Bull. Environ. Contam. Toxicol.* 96 (3), 314–319. doi:10.1007/s00128-015-1700-8

Santadino, M., Coviella, C., and Momo, F. (2014). Glyphosate sublethal effects on the population dynamics of the earthworm *Eisenia fetida* (Savigny, 1826). *Water Air Soil Pollut.* 225 (12), 2207. doi:10.1007/s11270-014-2207-3

Santos, M. J. G., Ferreira, M. F. L., Cachada, A., Duarte, A. C., and Sousa, J. P. (2012). Pesticide application to agricultural fields: Effects on the reproduction and avoidance behaviour of *Folsomia candida* and *Eisenia andrei*. *Ecotoxicology* 21 (8), 2113–2122. doi:10.1007/s10646-012-0963-7

Santos, M. J. G., Ferreira, V., Soares, A. M. V. M., and Loureiro, S. (2011). Evaluation of the combined effects of dimethoate and spirodiclofen on plants and earthworms in a designed microcosm experiment. *Appl. Soil Ecol.* 48 (3), 294–300. doi:10.1016/j.apsoil.2011.04.009

Schimel, J., and Schaeffer, S. (2012). Microbial control over carbon cycling in soil. *Front. Microbiol.* 3, 348. doi:10.3389/fmicb.2012.00348

Schlatter, D. C., Yin, C. T., Burke, I., Hulbert, S., and Paulitz, T. (2018). Location, root proximity, and glyphosate-use history modulate the effects of glyphosate on fungal community networks of wheat. *Microb. Ecol.* 76 (1), 240–257. doi:10.1007/s00248-017-1113-9

Schlögl, J., Wimmer, B., Cramaro, L., Wirsching, J., Poll, C., Pagel, H., et al. (2022). Heavy rainfall following a summer drought stimulates soil redox dynamics and facilitates rapid and deep translocation of glyphosate in floodplain soils. *Environ. Sci. Process. Impacts* 24, 825–838. doi:10.1039/d1em00527h

Schon, N., and Dominati, E. (2020). Valuing earthworm contribution to ecosystem services delivery. *Ecosyst. Serv.* 43, 101092. doi:10.1016/j.ecoser.2020.101092

Schon, N., Mackay, A., and Minor, M. (2012). Relationship between food resource, soil physical condition, and invertebrates in pastoral soils. *Soil Sci. Soc. Am. J.* 76 (5), 1644–1654. doi:10.2136/sssaj2011.0375

Sidoli, P., Baran, N., and Angulo-Jaramillo, R. (2016). Glyphosate and AMPA adsorption in soils: Laboratory experiments and pedotransfer rules. *Environ. Sci. Pollut. Res.* 23 (6), 5733–5742. doi:10.1007/s11356-015-5796-5

Sihtmäe, M., Blinova, I., Künnis-Beres, K., Kanarbik, L., Heinlaan, M., and Kahru, A. (2013). Ecotoxicological effects of different glyphosate formulations. *Appl. Soil Ecol.* 72, 215–224. doi:10.1016/j.apsoil.2013.07.005

Silva, V., Montanarella, L., Jones, A., Fernández-Ugalde, O., Mol, H. G., Ritsema, C. J., et al. (2018). Distribution of glyphosate and aminomethylphosphonic acid (AMPA) in agricultural topsoils of the European Union. *Sci. Total Environ.* 621, 1352–1359. doi:10.1016/j.scitotenv.2017.10.093

Stanley, O. N., and Joy, O. A. (2014). Histopathological effects of glyphosate and its toxicity to the earthworm Nsukkadrilus mbae. *Br. Biotechnol. J.* 4 (2), 149–163. doi:10.9734/bbj/2014/6727

Stephens, D. W., and Krebs, J. R. (2019). *Foraging theory*. Foraging theory. Princeton, NJ: Princeton University Press in Princeton.

The Cornell Framework (2017). *Comprehensive assessment of soil health*. 3rd edition. Cornell University. Available at: http://soilhealth.cals.cornell.edu/trainingmanual/ (Accessed August, 2022).

Van Groenigen, J. W., Lubbers, I. M., Vos, H. M., Brown, G. G., De Deyn, G. B., and Van Groenigen, K. J. (2014). Earthworms increase plant production: A meta-analysis. *Sci. Rep.* 4 (1), 6365–6367. doi:10.1038/srep06365

Verrell, P. A. V. B., E., and Van Buskirk, E. (2004). As the worm turns: *Eisenia fetida* avoids soil contaminated by a glyphosate-based herbicide. *Bull. Environ. Contam. Toxicol.* 72219, 219. doi:10.1007/s00128-003-9134-0

Yasmin, S. a. D. S., D., and D'Souza, D. (2007). Effect of pesticides on the reproductive output of *Eisenia fetida*. *Bull. Environ. Contam. Toxicol.* 75 (5), 529–532. doi:10.1007/s00128-007-9269-5

Zaller, J. G., Heigl, F., Ruess, L., and Grabmaier, A. (2014). Glyphosate herbicide affects belowground interactions between earthworms and symbiotic mycorrhizal fungi in a model ecosystem. *Sci. Rep.* 4 (1), 5634–5638. doi:10.1038/srep05634

Zaller, J. G., Weber, M., Maderthaner, M., Gruber, E., Takacs, E., Mortl, M., et al. (2021). Effects of glyphosate-based herbicides and their active ingredients on earthworms, water infiltration and glyphosate leaching are influenced by soil properties. *Environ. Sci. Eur.* 33 (1), 51. doi:10.1186/s12302-021-00492-0

Zhou, C. F., Wang, Y. J., Li, C. C., Sun, R. J., Yu, Y. C., and Zhou, D. M. (2013). Subacute toxicity of copper and glyphosate and their interaction to earthworm (*Eisenia fetida*). *Environ. Pollut.* 180, 71–77. doi:10.1016/j.envpol.2013.05.016

Advantages of publishing in Frontiers

OPEN ACCESS
Articles are free to read for greatest visibility and readership

FAST PUBLICATION
Around 90 days from submission to decision

HIGH QUALITY PEER-REVIEW
Rigorous, collaborative, and constructive peer-review

TRANSPARENT PEER-REVIEW
Editors and reviewers acknowledged by name on published articles

Frontiers
Avenue du Tribunal-Fédéral 34
1005 Lausanne | Switzerland

Visit us: www.frontiersin.org
Contact us: frontiersin.org/about/contact

REPRODUCIBILITY OF RESEARCH
Support open data and methods to enhance research reproducibility

DIGITAL PUBLISHING
Articles designed for optimal readership across devices

FOLLOW US
@frontiersin

IMPACT METRICS
Advanced article metrics track visibility across digital media

EXTENSIVE PROMOTION
Marketing and promotion of impactful research

LOOP RESEARCH NETWORK
Our network increases your article's readership